Department of Civil Engineering

Experimental and Numerical Investigations to Assess the Performance of a Buried Pipe Subjected to Traffic Load / Non-Treated and Cement-Treated Trench

Ahdyeh Mosadegh

This thesis is presented for the Degree of
Doctor of Philosophy
of
Curtin University

January 2018

Declaration

To the best of my knowledge and belief this thesis contains no material previously published by any other person except where due acknowledgment has been made.

This thesis contains no material which has been accepted for the award of any other degree or diploma in any university.

Signature: ..... Mosadegh .....

Date: ... 19.1.2018 .....

DEDICATION

This dissertation is dedicated to

my loving daughter, Ava,

my dear husband, Alireza

my supportive mother, Sima,

my sisters Hedieh and Hoda

and

the memory of my beloved father,

Ali Mosadegh (1941-2017)

You are profoundly appreciated for all of your love, supports and unflinching commitment to my career pursuit!

BIOGRAPHY

Ahdyeh Mosadegh is from Bandar-e Anzali, Iran. She received her bachelor's degree in Civil Engineering from Mazandaran University, Iran in 2003. She graduated with a master's degree in Geotechnical Engineering from Ecole National des Ponts et Chaussées in France 2010. Previously, she attained a master's degree in Road & Transportation from University of Tehran, 2007. She worked as a pavement and civil engineer in various consulting engineers companies for eight years prior moving to Australia to pursue a Ph.D. in Civil Engineering at Curtin University. Her research interests are soil stabilisation, numerical analysis focusing on buried pipe and soil deep mixing stabilisations.

Abstract

The performance of buried pipelines subjected to traffic load is an important engineering consideration and there is a need for further research in this field. The main objective of this research is to investigate the behaviour of a buried pipeline under traffic load through laboratory testing and finite element analysis.

A numerical parametric study was carried out to investigate the influence of different factors on pipe-soil behaviour under live load using ABAQUS. The effect of eight different factors including burial depth of pipe, pressure magnitude, width of loading area, internal pressure, pipe-soil interaction properties, pipe material, wall thickness and boundary condition at the pipeline ends on pipe deflection, surface settlement, maximum stress in pipe wall as well as earth pressure on pipe were investigated. The parametric study was followed by sensitivity analysis to investigate how sensitive the model was to change of each above mentioned parameters and to determine the factors with the most relative contribution on model response. As a result, the impact of surface pressure and burial depth was selected to be investigated in the second phase of this research.

Twenty six laboratory cyclic tests were conducted on a buried pipe to investigate model response during initial and cyclic phase for both non-treated and cement-treated trench materials. For this purpose, a new physical modelling was developed to investigate buried pipe performance comprising a large soil box to apply cyclic load on top of trench soil. A series of nonlinear finite element analyses were also developed to investigate pipe response during initial phase. To get the input material properties, a series of direct shear tests were performed to define material strength taking into consideration the impact of curing time. To find a relationship between measured circumferential strain on pipe and pipe deflection, a compressive loading test was carried out and pipe deflection and strain were investigated using Linear Variable Displacement Transducer (LVDT) and strain gauges. A Finite Element Modelling (FEM) was also developed to predict pipe deflections based on numerical simulations for pipe deflection and strains.

Results were presented in terms of pipe deflection, soil surface settlement and earth pressure on pipe and the impact of burial depth, surface pressure and cycles was investigated. Pipe deformation modes were also investigated based on strain measurements at different points around the pipe circumference. Experimental and numerical analysis revealed that increasing burial depth decreases pipe deflection, increases soil surface settlement and decreases pressure on pipe while increasing

surface pressure increases all mentioned parameters. Results also indicated that cement stabilisation improves pipe behaviour and reduces surface settlement of trench and pipe deflection. The results showed that a good agreement between numerical and experimental test was observed. From all numerical and experimental results, equations were developed to predict soil surface settlement, pipe vertical diametric strain and pressure on pipe using Linear Regression Model (LRM) and Artificial Neural Network (ANN) in MATLAB. While linear regression modelling approach was deficient to predict desired parameters, more accurate results were obtained using artificial neural network method. Cumulative error analysis showed that all predicted parameters using artificial neural network method, have less than 20% error.

Acknowledgements

I would like to express my deepest gratitude to my advisors Prof. Hamid Nikraz for his precious guidance and supports throughout my graduate life at Curtin University. His advice helped me to improve my research skills and complete this research successfully. I would also like to extend my sincere thanks to my research committee members Dr. Omid Khalaj, Dr. Amin Cheginizadeh and Dr. Faiz Shaikh for their valuable advice and supports.

Completing this work was not possible without support and friendship provided by the other members of the Engineering Department of Curtin University in Perth. I am indebted to them for their help. I would like to give my recognition to all civil engineering department staff at Curtin University. I would also acknowledge help of Mark Whittaker, Darren Isaac, Mirzet Sehic and Arne Bredin to run equipment and prepare samples at geotechnical laboratory of Curtin University. I acknowledge the support of my friends Hassan Zehtab, Saeed Amiralian, Farzad Habibbeygi in the laboratory.

I gratefully acknowledge the funding sources that made my Ph.D. work possible. I was the recipient of APPA. This support is highly acknowledged. My work was also supported by the CUPS Scholarship of Curtin University. I would like also to thank the Engineering Department of Curtin University for giving me the opportunity to attend conferences and meet so many academic people.

Lastly, I must express my profound gratitude to thank my family for all their love and encouragement. Special thanks to my loving parents who raised me with a love of science and supported me in all my pursuits. I also would like to thank my supportive, encouraging, and patient husband for his supports during this Ph.D. research.

Ahdyeh Mosadegh
Curtin University
Nov 2017

Table of Contents

Page

List of Figures

List of Tables

List of Equations

Nomenclature

B	Width of loading surface
H	Embedment depth of pipe
D	External pipe diameter
t	Pipe wall thickness
P	Surface pressure
α	Loading area
P’	Internal pressure
W	Width size of trench
VDS	Vertical diametric strain of pipe
SSS	Soil surface settlement
RC	Relative contribution
N	Number of cycles
σ	Vertical stress
SG	Strain gauge
Prefix C	Cement treated cases
Prefix NC	Non-cement treated cases
Prefix PS	Pure sand
E_i	Ratio of quantifying importance of stabilization
X_c	Cement-treated specimen properties
X_p	Pure sand specimen properties
Ep_{exp}	Percentage of error for experimental test
Ep_{NUM}	Percentage of error for numerical test
$A_{exp,}$	Observed experimental values at each test series
A_{Num}	Numerical values at each test series
A_{pr}	Predicted values at each test series
VDS_{exp}	Pipe deflection in experimental study
VDS_{FEM}	Pipe deflection in numerical study
VDS_{Pr}	Predicted pipe deflection
SSS_{exp} /H	Ratio of soil surface settlement to burial depth in experimental study
SSS_{FEM} /H	Ratio soil surface settlement to burial depth in numerical study
SSS_{Pr} /H	Ratio of predicted soil surface settlement to burial depth
σ_{exp} /P	Ratio of vertical stress on pipe to applied surface pressure in experimental study
σ_{Num}/P	Ratio of vertical stress on pipe to applied surface pressure in numerical study
σ_{pr}/P	Ratio of predicted vertical stress on pipe to applied surface pressure

List of Publications

The following is a list of publications resulting from the research undertaken for this degree.

i. **Mosadegh. A**; Nikraz.H , BURIED PIPE RESPONSE SUBJECTED TO TRAFFIC LOAD EXPERIMENTAL AND NUMERICAL INVESTIGATIONS, International Journal of GEOMATE, Nov., 2017, Vol.13, Issue 39, pp.01-08, ISSN:2186-2990, Japan, DOI: https://doi.org/10.21660/2017.39.91957

ii. **Mosadegh A**, SZYMKIEWICZ F, Nikraz H, "Experimental Investigation on the Impact of Specimen Preparation and Curing Condition on Cement-Treated Material Strength (Deep Mixing Method)", Engineers Australia, 2017, http://dx.doi.org/10.1080/14488353.2017.1372685

iii. M. Karami, A. Nega, **A. Mosadegh**, H. Nikraz, "Evaluation of Permanent Deformation of BRA Modified Asphalt Paving Mixtures Based on Dynamic Creep Test Analysis", Advanced Engineering Forum, Vol. 16, pp. 69-81, 2016, doi: https://www.scientific.net/AEF.16.69

iv. **Mosadegh. A**; Nikraz.H, "Finite Element Analyses of Buried Pipeline Subjected to Live Load Using ABAQUS", Geoquebec conference, paper 446 proceeding - 2015, Quebec City, Canada

v. **Mosadegh A**, Nikraz H, "Bearing Capacity Evaluation of Footing on a Layered-Soil using ABAQUS", Journal of Earth Sci Clim Change 2015, http://dx.doi.org/10.4172/2157-7617.1000264

The following is a list of unpublished articles publications resulting from the research undertaken for this degree.

vi. **Mosadegh, A**; Nikraz. H, "Numerical Analysis of a Small Flexible Pipe Subjected to Surface Load / Buried in Non-Treated and Cement Treated Trench", Submitted to Geo-Edmonton 2018

vii. **Mosadegh, A, Nikraz. H,** A Numerical Parametric Study on Buried Piped Performance Subjected to Various Conditions / Real Project Condition, 2018

viii. **Mosadegh.A,** Nikraz.H, Khalaj. O, Experimental Investigations of Buried Pipe Performance Under Cyclic Load, 2018

ix. **Mosadegh.A,** Nikraz.H, Khalaj. O, Evaluating the Impact of Stabilization on Performance of Buried Pipe Under Traffic Load / Experimental Investigations, 2018

x. **Mosadegh A**, Nikraz H **,** "Comparison of Neural network and Regression Model in Developing Equations to Predict Pipe Performance under Traffic Load", 2018

1 INTRODUCTION

1.1 BACKGROUND

Pipelines are essential infrastructure for transmitting water, gas and oil in any society. Their usage has expanded with time during past decades because they are more energy efficient than other means of transportation. Although they require significant initial investment, they have a lifetime of up to 40 years with minor maintenance requirement (Kyriakides & Corona, 2007). Oil and natural gas pipelines often cross country borders and sometimes they require investments of billions of dollars. Any damage due to pipe failure can produce loss of functionality and consequently has economic and social impacts. In addition, in the case of sewerage, any failure of pipeline can cause illness in the affected area (Moser, 2001). Many factors are contributing in pipe failures such as deterioration with time, geometry conditions, external factors, human error, fatigue, ground movement, etc. (Abolmaali & Kararam, 2010; Farhadi Hikooei, 2013; Liu et al., 2010; Parker, 2008; Rojhani et al., 2012; Vazouras et al., 2010; Zheng et al., 2012). Geotechnical engineering has a key role in ensuring satisfactory performance of buried pipelines in installation, construction, and routine operations. The main causes of onshore pipeline failure at road crossings are the overburden pressure due to soil cover as well as cyclic traffic load especially at shallow depths (Kyriakides & Corona, 2007; Moser, 1990; Rajeev et al., 2013). As an example, Figure 1-1 illustrates a pipeline failure under road after a water main burst in Melbourne's inner city. The failure of the pipe can be due to the fact that under traffic load, soil strength decreases when number of cyclic load increases. In other words, with time, both pipe and soil can degrade under cyclic load due to traffic affecting long-term performance of pipe-soil system. However, degradation can be induced by other factors than traffic such as buckling, change in temperature, etc.(Kyriakides & Corona, 2007; Randolph & Gourvenec, 2011).

Figure 1-1 Cars swallowed by a sinkhole caused by flooding in Port Melbourne (Grace, 2014)

To improve pipe behaviour under cyclic load and reduce permanent deformation of road, soil can be stabilized. Road stabilization is classified into two categories: mechanical and chemical (Kestler, 2009; Makusa, 2012; Sétra-LCPC, 2000; Sherwood & Transport Research, 1993). There are numerous researches on the use of mechanical road stabilizers such as compacting and blending of soils, incorporating conventional geosynthetics and their impact on pipe-soil response, i.e. (Moghaddas Tafreshi & Khalaj, 2008). However, there is lack of research on the impact of traditional chemical stabilizers including cement, lime, fly ash and bituminous materials on pipe-soil system.

1.2 PROBLEM STATEMENT

Cyclic loading may result in soil loosening, strength and stiffness degradation and the buried pipe breakage and failure (Cubrinovski et al., 2011; Randolph et al., 2011). Therefore, evaluation of a buried pipe performance subjected to traffic load is an important research focus area and the review of literature indicates that relatively few numerical and experimental investigations have been undertaken on this subject. In addition, limited number of numerical or experimental researches is available on investigating impact of cement stabilization on the behaviour of buried pipe. Thus, an experimental and numerical investigation to study the stabilization impact on performance of buried pipe subjected to traffic load is needed. The contribution of the current research and its significances are summarized as follows:

I. Pipelines have various applications and any failure in pipelines system will have many negative impacts in any society.
II. Research is needed to prevent pipeline failure.

III. It is important to develop the fundamental research on pipeline behaviour to minimise the costs of failed pipeline system.
IV. Research is needed to identify the factors affecting buried pipe behaviour by implementing numerical parametric study and sensitivity analysis.
V. A laboratory facility capable of testing pipes subjected to cyclic load is designed to facilitate simulation of traffic load on the pipe which is the main contribution of the current research work.
VI. A numerical model can also be developed to simulate the relevant aspects of the problem to better understand the model behaviour under various conditions.

1.3 OBJECTIVES OF THE THESIS

In the past few decades, many studies have been performed to investigate the behaviour of buried pipes subjected to different conditions. However, a few studies related to pipe-soil interaction under cyclic load are available. Thus, the main objective of this research program is to determine the performance of a buried pipeline subjected to traffic load. Before that, a numerical parametric study on a buried pipe is carried out using finite element software, ABAQUS. A sensitivity analysis is then performed to investigate how sensitive the model is to any change of different parameters. In the next phase, the impact of the most sensitive factors from parametric study will be investigated on a buried pipe experimentally and numerically. Therefore, a tank allowing measurement of the changes in pipe and surrounding soil under cyclic loads is built. This setup is one of the original contributions of this research. In addition, impact of cement stabilization on the performance of buried pipe is investigated. At the end, equations are developed to predict model response due to change of various factors. In summary, the main objectives of the current research are as follows:

I. To identify the factors that have the highest impact on buried pipe response by implementing numerical parametric study and sensitivity analysis;
II. To study the effects of burial depth and surface pressure on a buried pipe performance during static phase using data from physical modelling supported by numerical simulations;
III. To examine the importance of initial phase on model response and evaluate the impact of cyclic load on the performance of buried pipe taking into consideration change of burial depth and surface pressure;

IV. To investigate the impact of traditional chemical stabilization on buried pipe deflection and on improving model behaviour;
V. To develop a relationship between various variables to predict pipe behaviour under static and cyclic loads;

1.4 SCOPES OF THE THESIS

To accomplish the research objectives as detailed above, the scopes of the current research program are summarised as below:

I. Performing numerical parametric study using ABAQUS on both 2D and 3D models to illustrate the effect of various factors on buried pipe responses. The impact of the most important factors affecting pipeline response from sensitivity analysis will be investigated in the second phase of research;
II. Designing appropriate experimental models to verify and validate the results of numerical analysis;
III. Performing appropriate tests to characterise material properties in the laboratory;
IV. Conducting a series of cyclic loads on a pipe buried in a sandy soil. Stresses and strains in the system are recorded using pressure cells, strain gauges and LVDTs;
V. Performing a series of cyclic loads on a pipe buried in cement-treated sand to evaluate the effect of stabilization on pipe-soil interaction and on soil surface settlement;
VI. Developing of a nonlinear model in ABAQUS based on experimental model to compare the results of numerical analysis with experimental results;
VII. Developing equations using Matlab to predict pipe deflection, soil surface settlement and pressure on pipe under specific burial depth and surface pressure for both untreated and stabilized sands under initial and cyclic loadings;
VIII. Comparing accuracy of two different methods of model prediction using Regression and Neural Network methods;

1.5 STRUCTURE OF THE THESIS

This thesis is organised in eight chapters and a brief outline of each chapter is given and summarised in Figure 1-2.

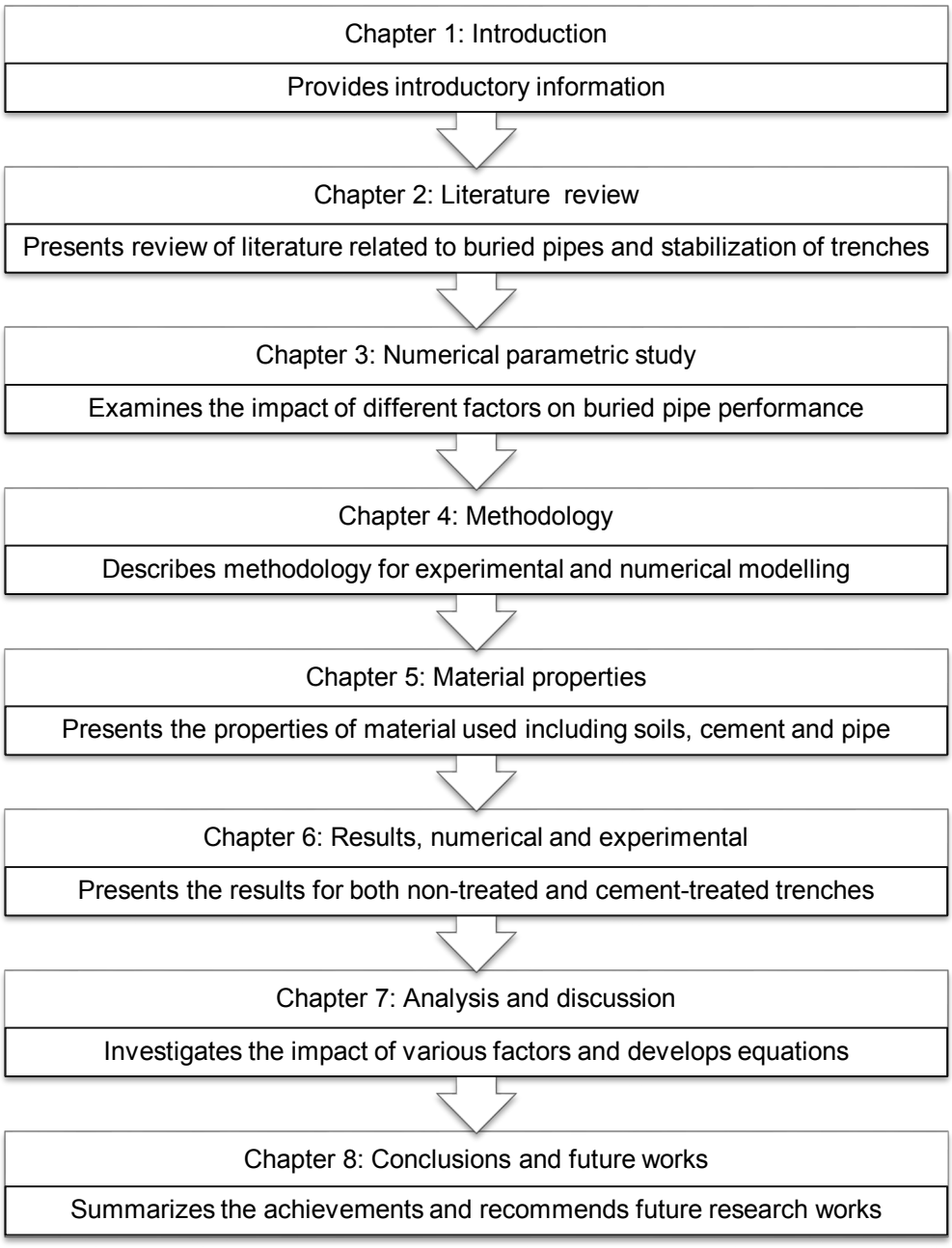

Figure 1-2 Overview of the strategy behind this research

Chapter 1 is an introductory chapter outlining the motivation, objectives and scope of the thesis.

Chapter 2 mainly focuses on literature review. There are numerous publications on buried flexible pipes in literature. However, there are few of experimental and numerical studies dealing with pipe-soil interaction due to cyclic load. In addition, there are limited researches available on the impact of traditional stabilizations on buried pipe response. Based on the reviewed studies, research gaps are identified and the research work to investigate pipe soil behaviour under cyclic load is proposed.

Chapter 3 presents parametric study of the response of buried pipe subjected to traffic load based on the finite-element analysis. This section includes theoretical developments, program description, and comparison of different factors affecting the buried pipe behaviour. Then, the sensitivity analysis is performed to quantify the impact of each parameter on model response and to identify how sensitive the model is to each parameter. The relative contribution of each factor on pipe deflection, soil surface settlement, stress in the pipe wall and earth pressure around pipe is investigated. The most critical parameters are found to be surface pressure, burial depth and loading area.

Chapter 4 describes the methodology and specifications of experimental setup and numerical modelling of buried pipe under live load. Chapter 4 to Chapter 7 focus on the investigation of buried pipe performance both experimentally and numerically under different surface loads and burial depths.

Chapter 5 describes the properties of materials used in this research. To define properties of sandy soil, direct shear tests are carried out at different normal stresses. Soil parameters and constitutive models are developed based on test results. In order to model pipe behaviour, a compressive test is performed on a piece of pipe and the strain and crown deflection are measured. Results are compared with those predicted through finite element and empirical methods.

Chapter 6 presents the results of experimental and numerical analysis of buried pipe subjected to surface load. Before running the tests, bearing capacity of soil under loading plate on non-treated and cement-treated materials is investigated. Then, the impact of various factors including surface pressure, depth of soil layer, and number of cycles for both untreated and cement-treated materials were investigated. The experimental test results are followed by the results of numerical analysis for some cases.

Chapter 7 provides the discussion and analysis of the research results. In addition, the impact of various factors on model response, efficiency of cement stabilization and impact of initial phase are also discussed. Regression models and equations are developed to predict pipe vertical deflection, soil surface settlement and pressure on pipe during initial phase. Results obtained using two methods of Linear Regression Model (LRM) and Artificial Neural Network (ANN) in MATLAB are also compared for cyclic phase.

Chapter 8 summarizes the achievements of the current research project and the recommended future research works.

2 LITERATURE REVIEW

2.1 INTRODUCTION AND CHAPTER OVERVIEW

Underground pipelines have been serving humans life to improve their standard of living since the dawn of civilization. Many ancient civilizations had water and sewerage systems to provide inhabitants with fresh running water. One of the oldest underground systems created by Persian Empire are qanats. The qanat consists of several vertical shafts cut into the soil connected through horizontal pipes at a slight angle. Qanats older than 2700 years are still in use with the use of gravity for moving water in pipes (Takacs & Cline, 2015). Today pipelines infrastructures serve in different applications such as sewer lines, drain lines, water mains, gas lines, oil lines, subway tunnels, electrical distribution lines and etc. Any failure in pipeline can cause malfunctioning of system and lead to economical loss in any society (Moser, 2001). Therefore, a comprehensive research on pipe-soil interaction to minimise the costs of failures is needed. Given the importance of pipeline in any society, research on pipe response is essential. This chapter reviews the buried pipe performance due to various loading conditions with focus on cyclic loading.

The overview of chapter is shown in Figure 2-1 divided into five sections. The first section gives a brief review of the design of buried pipes theories and its development through the past few decades. The design methods are empirical, analytical and numerical. The second section represents different failure modes of pipeline specifically in onshore applications. In this section, the impact of cyclic load on pipe failure which is the main focus of this research will be also identified. In addition, degradation definition and pipe-soil response due to cyclic load are discussed briefly. The third section investigates the methods of reducing pipeline failure under roads. The applications of road stabilization are discussed briefly in this section. This will be followed by representing recent studies dealing with pipe response under different loading conditions. Finally, research gaps will be identified at the end of this chapter based on reviewed studies.

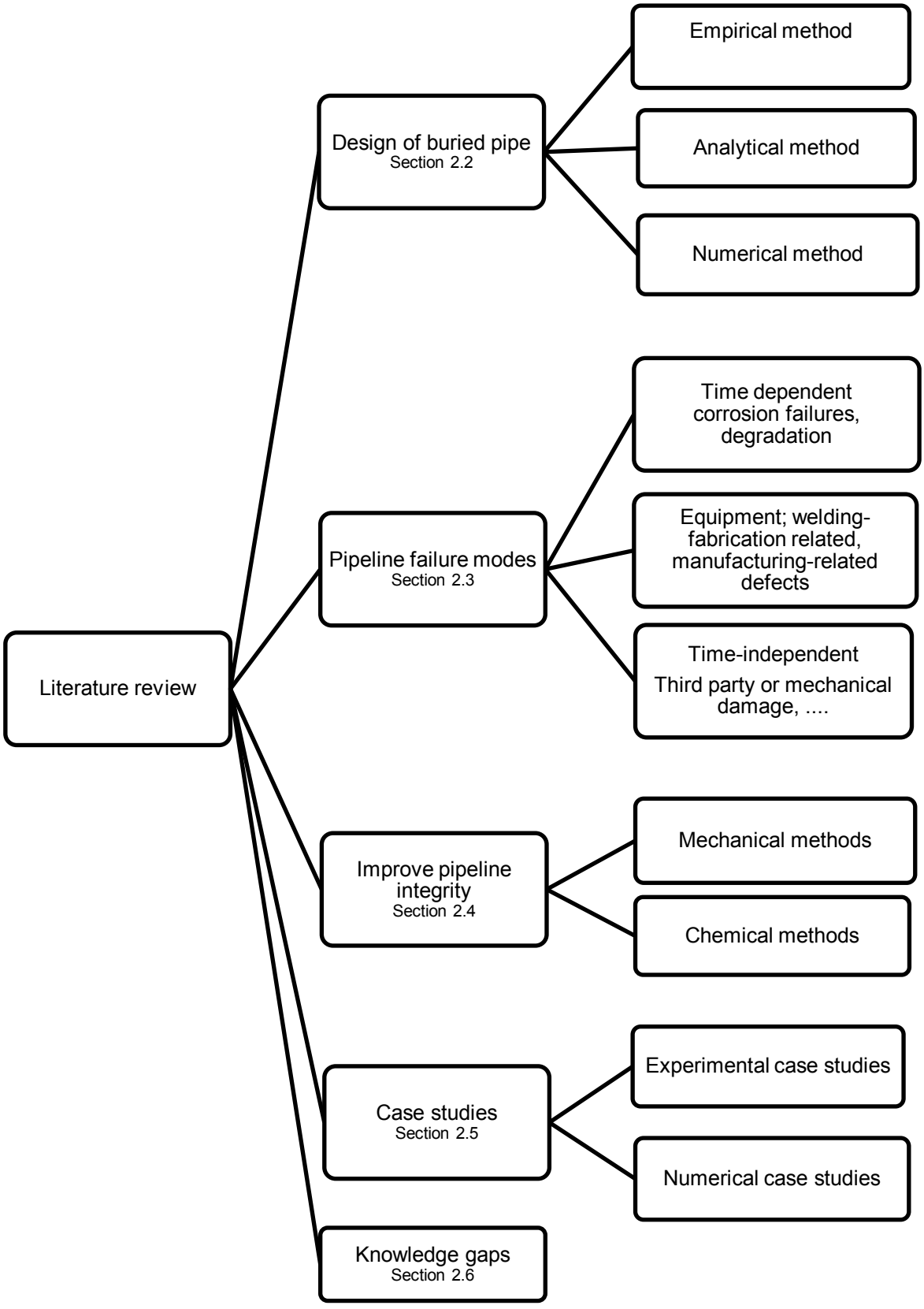

Figure 2-1 Chapter overview

2.2 DESIGN OF BURIED PIPE

Generally the pipes are classified as rigid and flexible. For flexible pipe stiffness is a critical factor while for rigid pipe, strength to resist wall stress is the critical criterion for design. Steel, plastic and ductile iron pipes are generally classified as flexible and concrete and clay pipes are classified as rigid (Moser, 2001). In Figure 2-2 the behaviour of these two types of pipes are illustrated. It should be noted that in Figure 2-2 *S* represents settlement of backfill for the case of rigid pipe and *D* represents vertical deflection of a flexible pipe under earth pressure. Since early 1990s, many researchers have focused on estimating the earth loads on buried pipes as well as stress transmitted to the pipe. Today, different analysis and design methods are available including empirical, analytical and numerical as shown in Figure 2-3. In the following section, a review of commonly used design methods of buried pipes are discussed.

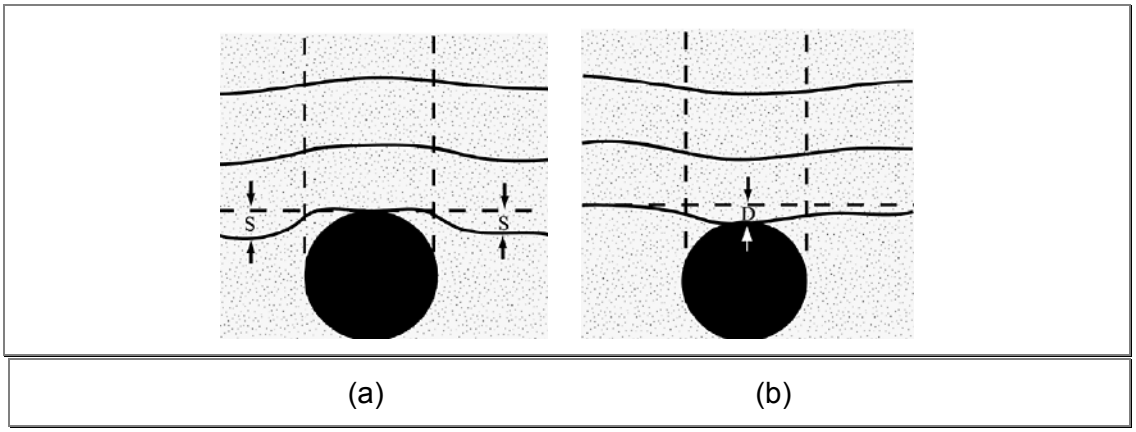

Figure 2-2 Soil settlement of (a) rigid pipe (b) flexible pipe (Järvenkylä, 1989)

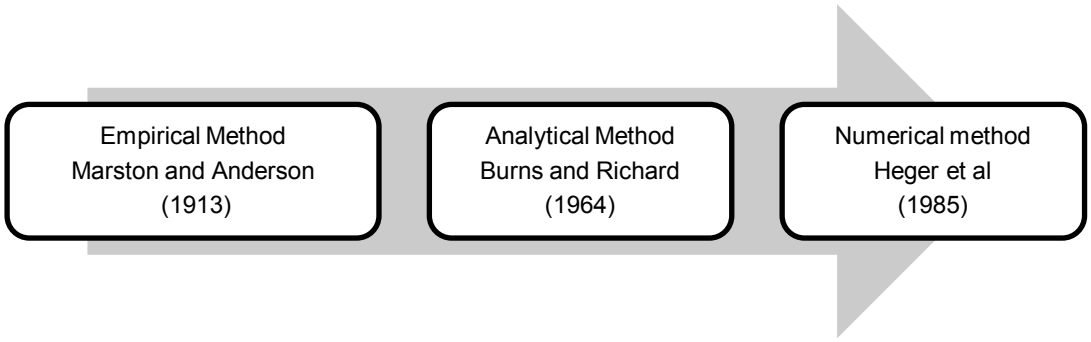

Figure 2-3 History of buried pipe design methods (Kamal, 2012)

2.2.1 Empirical Method

Marston and Anderson (1913) developed a theory for calculating the earth load acting at the top of a buried conduit. It was found that the load on a buried pipe is not the total weight of the soil prism above the conduit, since a portion of this load is transferred to the adjacent soil influenced by the soil arching effect. The load equations were grouped according to the pipe installation procedures. The two common installation methods are: a ditch pipe where the pipe is placed in a trench excavated through existing natural ground, and an embankment pipe where the pipe is laid on the natural ground level above which an embankment is built. For a ditch conduit, the load acting on a buried conduit can be obtained through sum of dead load and live load (Marston & Anderson, 1913).

2.2.1.1 Loads on buried pipes

Any load affecting the buried pipe response must be taken into consideration in the analysis and design of pipeline (ASCE, 2001, 2009; Moser, 2001). As this study considers the impact of live load on buried pipe, the impact of other parameters such as temperature, frost loading, fluid weight, seismic load, wave passage and etc. are not considered in this chapter.

Earth load on rigid pipe

Different parameters affect pipe load sustainability such as relative height of cover, the nature of backfill material, geometry of the trench and relative stiffness of the pipe to the backfill (Marston & Anderson, 1913; Moser, 1990). The theory of Marston which published in 1913 is the beginning of methods for calculating earth loads on buried pipes known as Soil Arching Theory. The theory is based on concept of soil prism in the trench as shown in Figure 2-4. Marston suggested that the weight of the backfill was partly resisted by frictional shear forces on trench walls which are developing in time (Marston & Anderson, 1913; Moser, 2001). He conservatively ignored the apparent cohesion of the soil when enforcing equilibrium of vertical forces to derive his solution. His solution assumes the sum of vertical forces at bottom plus shear force at sides are equal to sum of vertical forces at top plus weight of element for a completely rigid pipe. The vertical force acting on the pipe is shown in Equation 2-1:

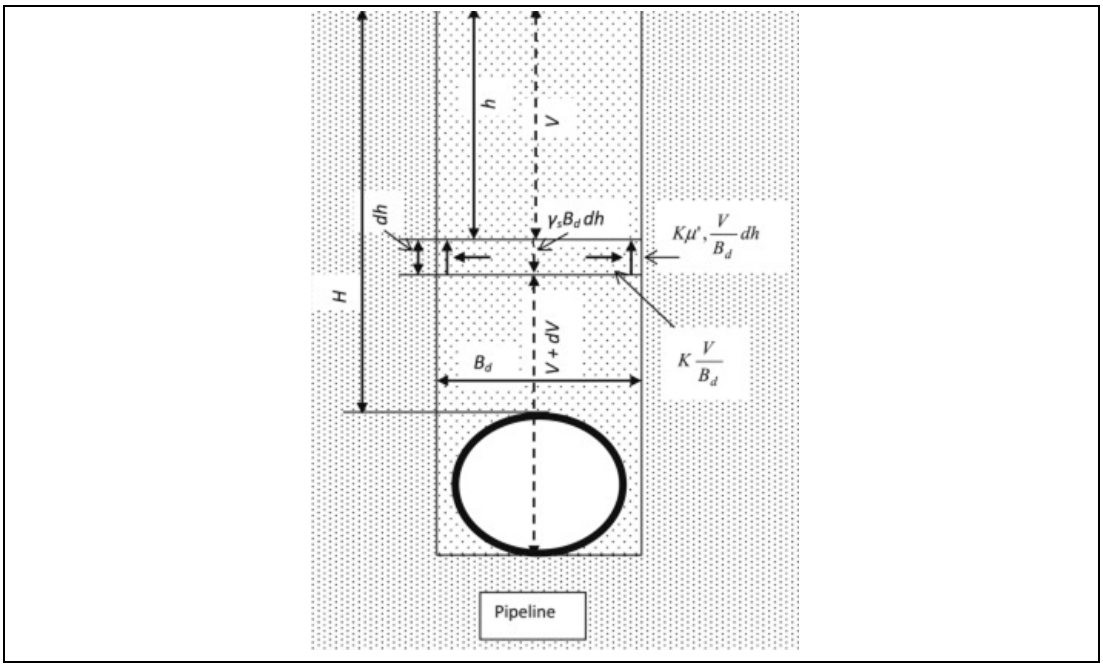

Figure 2-4 Basis of Marston's theory of load on buried pipe (McGowan & Prangnell, 2015)

$$W_d = C_d \Upsilon B^2 \qquad 2\text{-}1$$

Where W_d = load on rigid pipe

C_d = load coefficient

Υ = unit weight of backfill

B = width of trench

C_d or load coefficient is an exponential function of the coefficient of friction ($\mu = tan\delta$) between the natural soil and the backfill. It should be noted that the rigid pipe is not assessed in this research and more details can be found in other references (Moayed et al., 2012; Moser, 2001)

Earth load on flexible pipe

A flexible pipe derives its carrying capacity from its flexibility. Soil can be represented as a spring as shown in Figure 2-5. Under weight of soil above the buried pipe, the pipe tends to deflect. Soil deforms and the majority of load is carried out by pipe. In fact pipe and soil work together to resist the load as shown in Figure 2-5. Deflection of pipe depends on load on pipe, while the load on pipe is function of its deflection. The reduction in load on the buried pipe because of its flexibility is sometimes referred to as arching. However, the overall performance of a flexible pipe is not just due to

this so-called arching, but is also due to the reaction of soil at the sides of the pipe resisting deflection as shown in Figure 2-5-c. Load applied on flexible pipe based on Marston Load Theory is represented in Equation 2-2 (ASCE, 2009; Marston & Anderson, 1913; Moser, 2001)

$$W_c = \frac{C_d \Upsilon {B_d}^2 B_c}{B_d} \; or \; W_c = C_d \Upsilon B_d B_c \qquad 2\text{-}2$$

W_c= load on flexible pipe

C_d =load coefficient

Υ = unit weight of backfill

B_c = pipe outside diameter

B_d=width of trench on top of pipe

As cited by Moser (1990) in Marston load theory the amount of load taken by a pipe is affected by the relative movement between the backfill and the natural soil when settlement of both backfill and pipe occur. It should be noted that in many cases maximum load on pipe is 20 to 25 percent less than the load predicted by Marston and for long – term load applied on buried pipe may be greater than those predicted in Equation 2-2 (Moser, 2001).

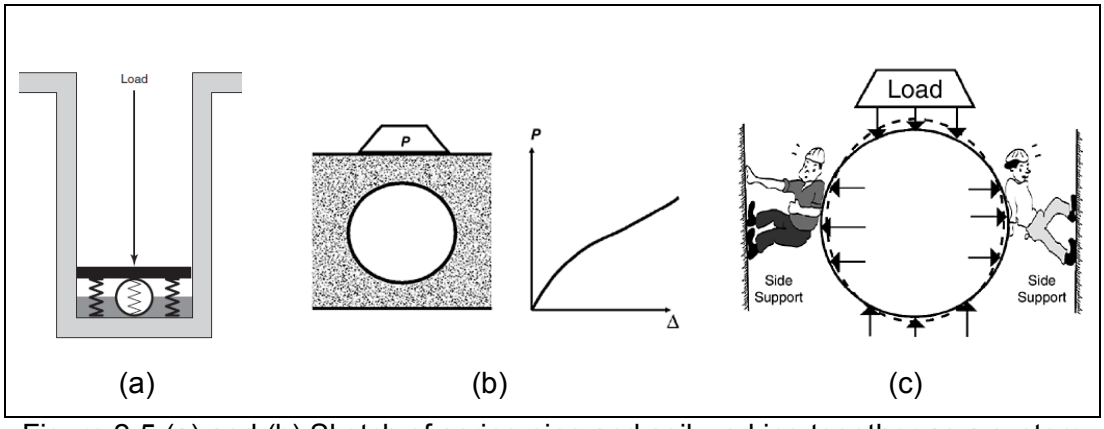

Figure 2-5 (a) and (b) Sketch of spring pipe and soil working together as a system (c) contribution of side support in the performance of flexible pipe (Moser, 2001)

Live load or wheel load on pipes

Live loads can be either static or quasi-static surface loads (Moser, 2001). Buried conduits may be subjected to applied loads by traffic. For the first time the French mathematician Boussinesq calculated the stress distribution in a semi-infinite elastic medium due to a point load on soil surface. Although soil is not an elastic homogenous

isotropic medium, Boussinesq solutions have given reasonable good results so far (Boussinesq, 1885).

Boussinesq and Newmark theory (1885) for calculating live load on buried pipe can be represented as Equation 2-3 in which load is applying on a rectangular surface as shown in Figure 2-6-a.Their assumption is based on elasticity of soil and the pipe should not be placed in a burial depth of less than *D/6*. Figure 2-6-b shows a rectangular area under surface live load representing tire pressure of breadth *B* and length *L* (Austroads, 2012; Moser, 2001). Then, Hall and Newmark developed equations for C_s to be used for calculating concentrated loads as shown in Equation 2-4:

$$P = \frac{W}{(B+H)(L+H)} \qquad 2\text{-}3$$

$$W_{sd} = \frac{C_s P F'}{L} \; or \; W_{sd} = C_s P F' B_c \qquad 2\text{-}4$$

Where:

W_{sd} = load on flexible pipe

C_s = load coefficient

F'= impact factor

L= effective length of conduit

P=Concentrated load

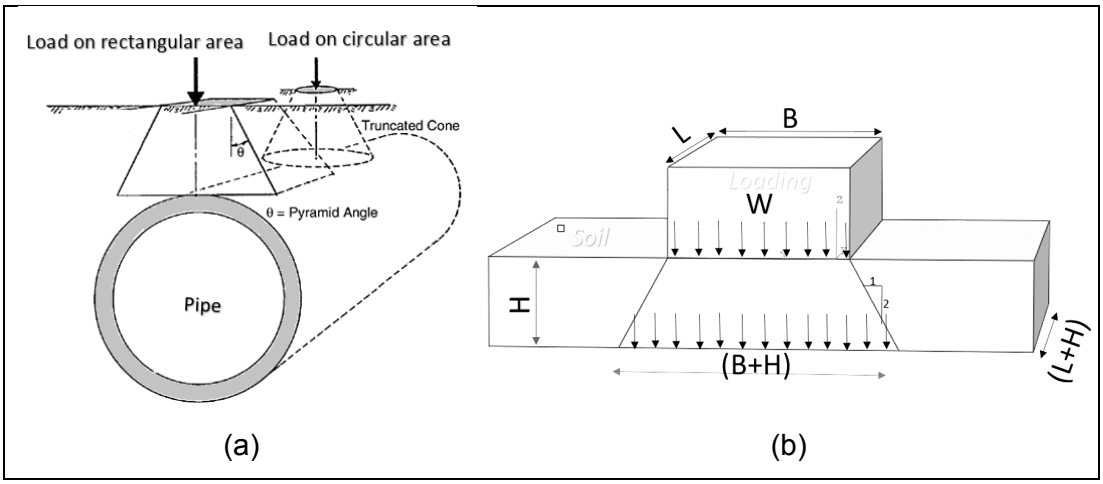

Figure 2-6 (a) Soil stress model for shallow burial depth (Moser, 2001) (b) soil cover *H* by an approaching wheel load *W* causing pressure of approximately P= W/[(B + H) (L + H) according to (Boussinesq,1885)

In practice, buried pipeline can be subjected to live load from sources such as highways, railways or airports which can be caused by truck-wheel loads, railway car, locomotive load or aircraft loads (ASCE, 2001). Depending on the project requirement, design specifications could be based on the live load AASHTO *HS-20* truck, Cooper E-80 railroad or 180 kip airplane gear load. It should be noted for deep burial depths the effect of live load on pipe can be ignored. In addition, the effect of traffic load on buried pipe is important when pipe burial depth is not deep (Uni-Bell, 2012). Parametric studies have shown that the minimum of one foot often is essential for cover heights of pipe or sometimes minimum of *D/6*. For typical granular material however minimum soil cover for flexible pipe is *D/10* (Moser, 2001). Guidelines are available to determine impact factors for specific height of trench cover under different road applications (Moser, 2001).

Vehicular loads are typically *H-20* or *HS-20* configuration which simulates a highway load of a 20-ton truck based on the AASHTO (The American Association of State Highway and Transportation Officials) (AASHTO, 1996). An *H-20* load consists of two 16000-lb or 8 ton concentrated load as shown in Figure 2-7-a. These loads are applied on two 18-in by 20-in area. The Figure 2-7-b is an example of combined load impact on a pipe. In this example, the minimum total load occurs at 4.5 ft or 1.5 m burial depth. It should be noted that live load has a little effect on pipe except for shallow depths. Thus, the design precautions should be taken into consideration for shallow installations under roadways. It is noted under cyclic load, the impact factor should be considered to account for dynamic load effects.

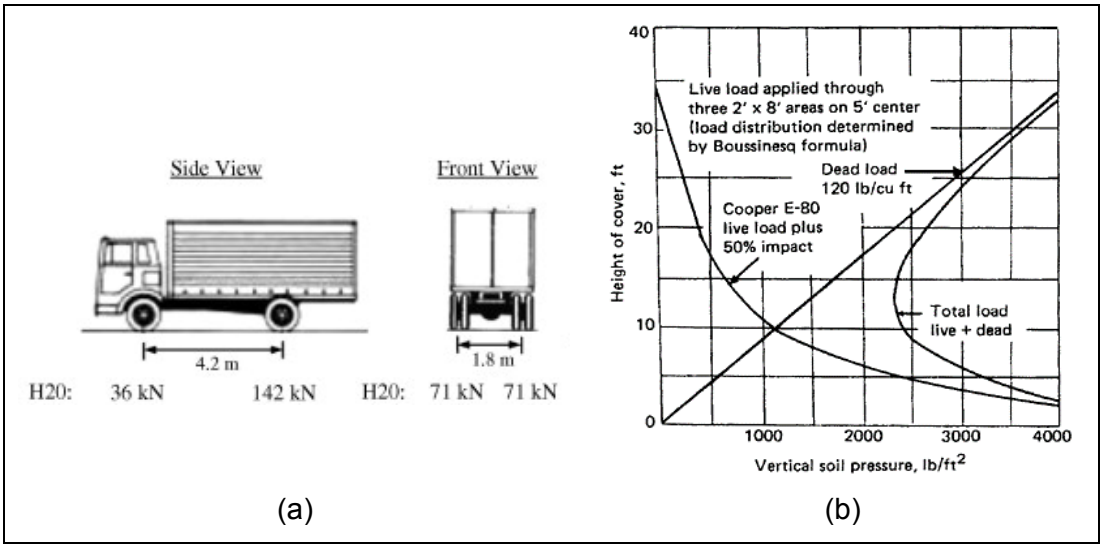

Figure 2-7 (a) AASHTO standard specifications for live loading (b) combined H-20 highway live load and dead load (Kang et al., 2013; Moser, 2001)

2.2.1.2 Pipe design considerations

After a brief review of different types of pipe and investigating load transmitted to the buried pipe in previous sections, design consideration for flexible pipe will be only presented hereafter. It should be noted that in parametric study, experimental and numerical analysis of the current research only flexible pipe performance is investigated.

Performance limit for a flexible pipe is assumed a stage in which pipe cannot perform in an acceptable manner anymore. Performance limit for a flexible pipe is over-deflection, wall buckling and wall crushing. In design of flexible pipe, stiffness is an important design factor and sometimes having a stiffer pipe can be beneficial. Pipe stiffness is related to area, shape and corrugation height. However, a higher stiffness without sufficient wall thickness can cause premature pipe failure. Therefore, for a proper pipe, stiffness considerations should be made to avoid pipe failure. One of these considerations in flexible pipe design is controlling pipe deflection which will be discussed in the following sections (Cameron, 2005; Moser, 2001).

Pipe deflection as shown in Figure 2-8 is a design parameter for flexible pipeline and is expressed as strains relative to the internal diameter of pipe. All flexible pipes should have a design deflection limit which is not a performance limit but performance limit with a safety factor. The deflection of pipe can be expressed shown in Equation 2-5.

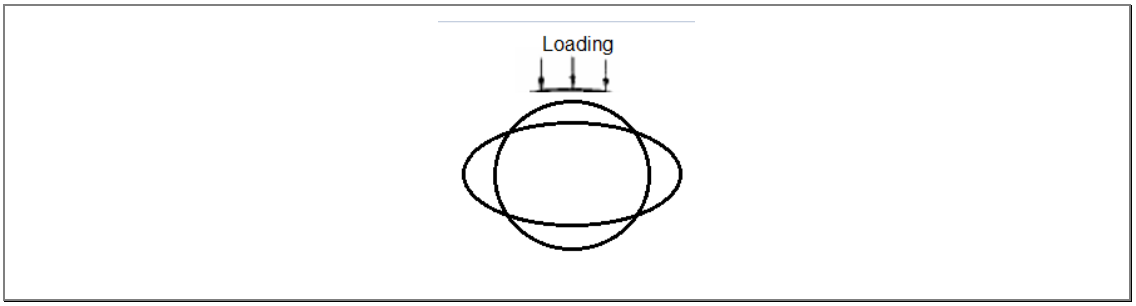

Figure 2-8 Ring deflection of a flexible pipe

$$\Delta_i = \frac{W d_r}{S} \qquad 2\text{-}5$$

In which Δ_i is pipe deflection, W is total transverse load on pipe crown, S is pipe stiffness $=EI/D^3$ and d_r is pipe deflection coefficient in desired direction. The deflection varies with the pressure in the pipe and the direction at which pipe is considered. Equation 2-5 has been developed and results are presented in different references. More details can be found in (Moser, 2001). However, the deflection

criteria can be expressed as strain of pipe wall. The strain of a plastic flexible pipe and HDPE pipe can be calculated through the following equation under combined load (Moser, 2001):

$$\varepsilon = \frac{PD}{2Et} + 6\left(\frac{t}{D}\right) * \left(\frac{\Delta y}{y}\right) \qquad 2\text{-}6$$

In which *P* is internal pressure, *D* is pipe diameter, *E* is Young's modulus of pipe, t is pipe thickness, and *Δy* is total vertical diametric displacement of pipe. A deflection of 5% for flexible pipes is a limit especially for those under construction.

2.2.2 Analytical Method

Burns and Richards (1964) studied the interaction of a circular cylinder buried in the soil and analysed the performance of cylinder, developed different equations through parameters as shown in Figure 2-9 (Burns & Richard, 1964). It produces results such as strain, horizontal deflection, radial load and thrust. It should be noted that this method is not addressed in this research and more details can be found in other references such as (Burns & Richard, 1964; Kamal, 2012; Moser, 2001). However, a weakness of this method is the assumption of linear elastic behaviour of material. This assumption leads to large errors (Moser, 2001).

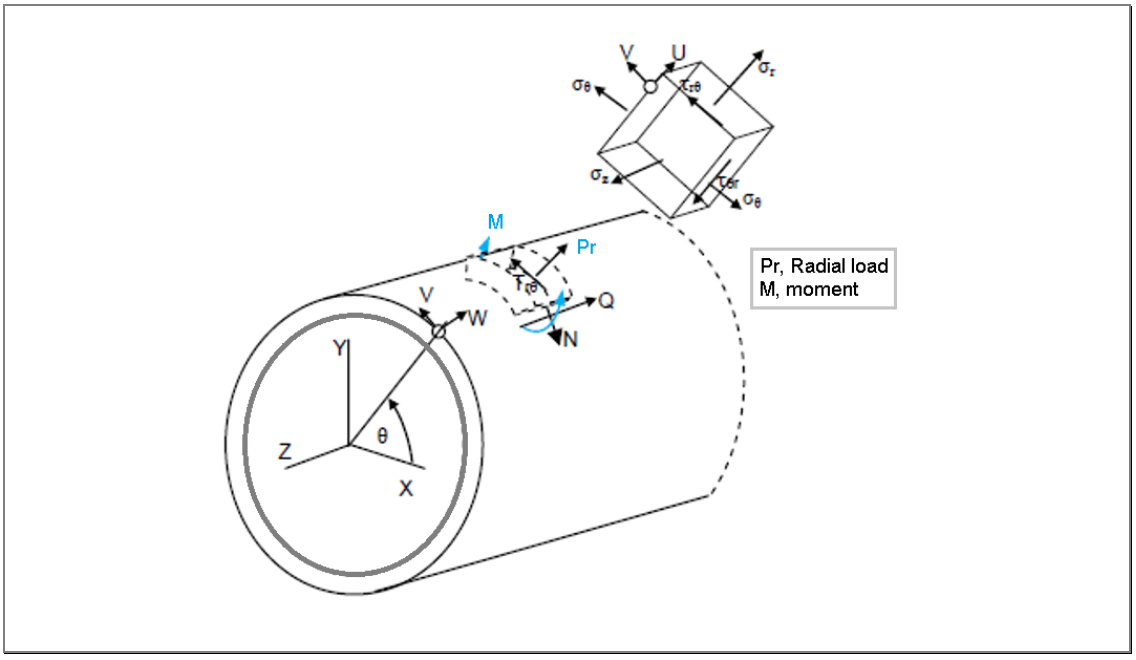

Figure 2-9 Burns and Richard's notation (Burns & Richard, 1964)

2.2.3 Numerical Method

In 1970s, American Concrete Pipe Association (ACPA) initiated a research program to improve and update Marston-Spangler method. In this research program, a design method on pipe soil interaction of buried concrete pipe was introduced as shown in Figure 2-10 (Heger et al., 1985). Later, a finite element method computer programme was introduced for concrete pipe design called SPIDA or Soil-Pipe Interaction Design and Analysis. SPIDA allowed Heger to develop four standards for different levels of installations. Since then many researches have been performed to develop existing numerical models. Since 1981, ABAQUS has become the commercial finite element program capable of comprehensive nonlinear geotechnical analysis. It should be noted that more details and case studies about researches investigating pipe response using ABAQUS and numerical modelling are available in the literature and will be discussed in section 2-4 of this chapter(Abo-Elnor et al., 2004; Abolmaali & Kararam, 2010; Kang et al., 2008; Kunert et al., 2012; J. Lee et al., 2004) .

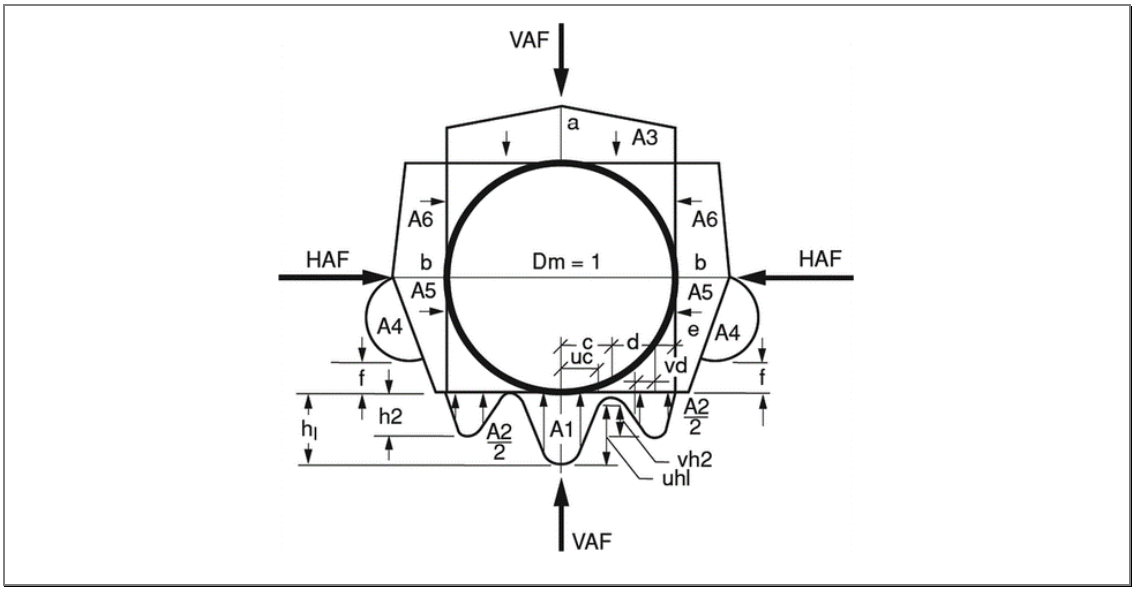

Figure 2-10 Heger pressure distributions (Moncef et al., 2016) .

2.3 PIPELINE FAILURE MODES

Pipelines are reliable modes of transportation and in general they represent a small risk to human life and environment. However, they can be a big threat and represent large capital cost when they fail (Kang et al., 2013; Kyriakides & Corona, 2007). The definition of pipe failure may vary for each project. A newly-installed pipe usually has a high factor of safety, but the load-carrying capacity of a buried pipe decreases gradually over time due to continuous deterioration. In addition, the strength of both

pipe and surrounding soil may decrease over time. As illustrated in Figure 2-11 pipe failure occurs when the two curves (i.e., the curve of deteriorated pipe strength and the curve representing the current stress state of the pipe) meet. Based on available data from the U.S. Pipeline and Hazardous Materials Safety Administration, the average damage costs arising from significant pipeline damage incidents over the past 10 years have been in excess of $400 M/year (PHMSA, 2017).Therefore, it is fundamental to consider different factors causing pipeline failure. The following section will discuss briefly the reasons for pipeline failures and its frequency in some parts of the world.

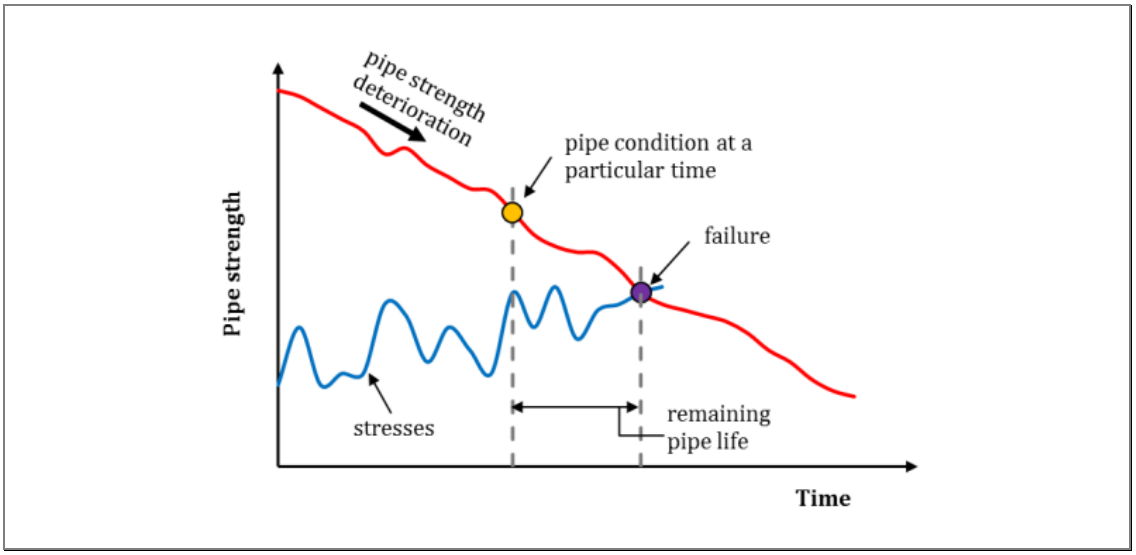

Figure 2-11 A schematic representation of the process leading to pipe failure during the life-time of a pipe (Rathnayaka, 2016)

2.3.1 Case Studies of Pipeline Failure

Pipeline can be used either in offshore or in onshore applications. Offshore structures are placed in locations such as oceans in the forms of platforms and pipelines. Offshore pipelines and flow lines are pipes that are laid on or below the seabed to carry oil, gas or other fluids. They are described as the ‘arteries’ of the oil and gas industry and they can be installed on seafloor or in trench or buried below seafloor. Some hazards which endanger pipeline in offshore applications are: TPD or Third Party Damage due to anchor drop/drag, corrosion, mechanical failure, construction related damage, degradation due to cyclic load and natural hazards. Each year there are hundreds of pipeline failures causing pollution, loss in transportation capacity, loss of gas availability and costly repair expenses. Although failures on offshore lines normally take longer to repair, onshore pipelines have higher number of recorded failures (Randolph & Gourvenec, 2011). As this research is aimed to present pipeline

response due to cyclic load in onshore application no more details regarding offshore pipeline will be discussed here. More details on offshore failures can be found in other resources such as (Dean 2010; Kvalstad et al., 2001; Randolph & Gourvenec, 2011).

In general, onshore pipeline systems can be divided into three major categories: oil, natural gas, and other liquid pipelines (water, chemicals and etc.). The map shown in Figure 2-12 provides an excellent overview of both existing oil and gas pipeline distribution in Australia (ABC-NEWS, 2014). Red and green lines show gas and oil pipeline, respectively. It is noted natural gas industry in Australia represent a substantial energy resource at the national level, and natural gas plays an important role in the Australian energy mix. Australia has also emerged as a significant player in world LNG trades (Department of Resources, 2012). It is noted Australia's shale gas reserves could be as much as 10 times the existing known gas reserves, according to a US government report (Robins, 2013). Now Australia is ranked seventh of the 41 countries reviewed by the EIA for shale gas resources, following Mexico and ahead of South Africa (EIA, 2016). Western Australia alone is estimated to hold one of the most important reserves of shale gas in the world.

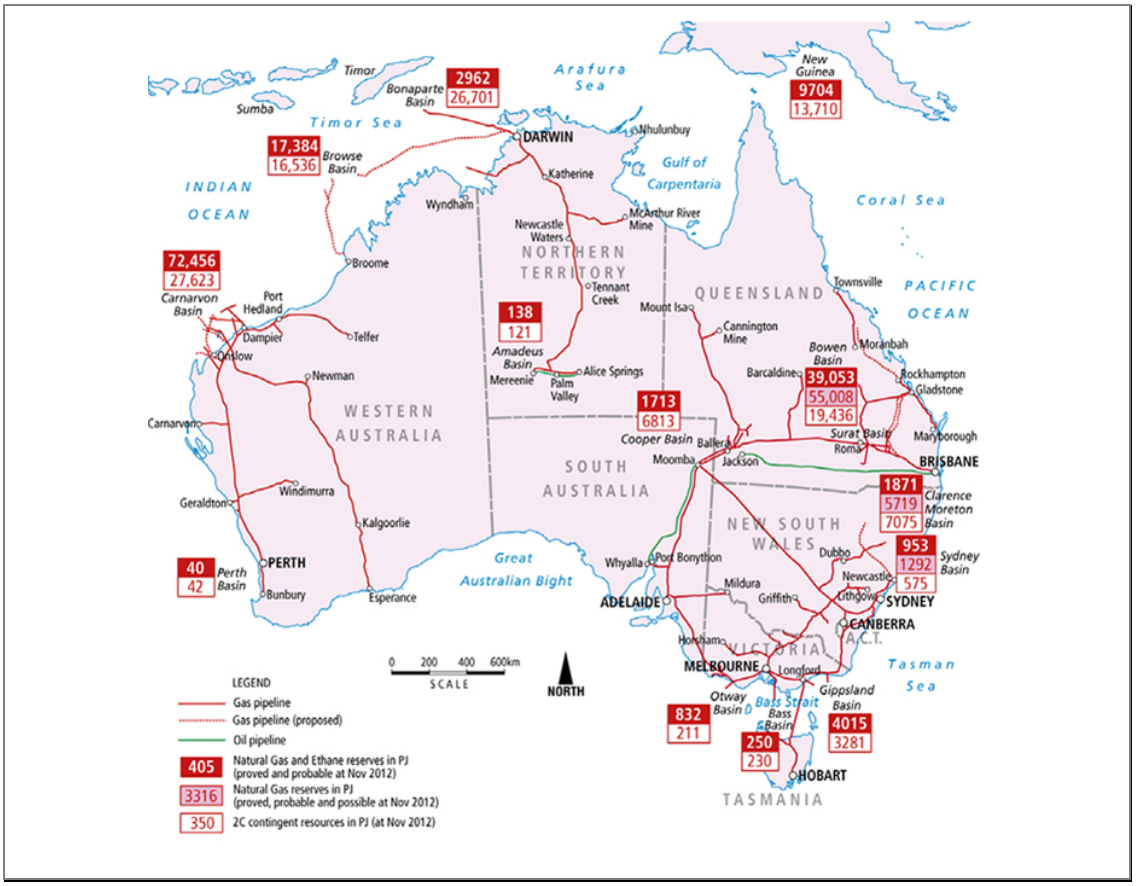

Figure 2-12 Map of major natural gas and oil pipelines in Australia (ABC-NEWS, 2014)

However, over the past few years, a series of incidents have brought pipeline safety to engineering and research field attention. To illustrate global dimensions of onshore pipeline damage, time-lapse maps are created to show the accumulation of fatalities and injuries related to pipeline incidents. For example, Figure 2-13 compares incidents in USA in 1986 and 2016 over 30 years. Red dots indicate failures resulted in fatalities and black dots indicate incidents without fatalities. As illustrated number of incidents and fatalities in US has increased significantly during past 30 years. However, pipelines are still considered as one of the safest means of transportation. In addition, loss of lives and property during pipeline incidents is lower comparing to other modes of transportation such as trucks (NTSB, 2016).

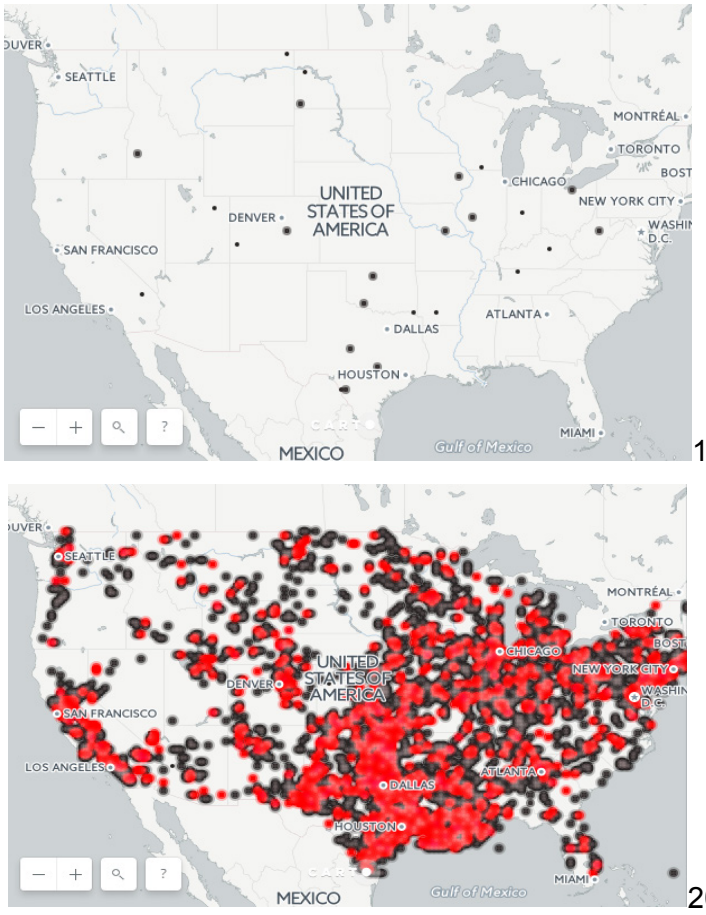

Figure 2-13 Fatalities and injuries associated with pipeline incidents in USA in1986 and 2016 (Joseph, 2016)

In Figure 2-14 three cases of pipeline failure are shown. Figure 2-14-a shows the gas pipeline failure incident in 2014 in Texas. In that explosion, all working area and entire town were evacuated. The reason was due to human error as a crew accidently drilled into the gas pipeline (Gonzales, 2016). In another accident, occurred in 2010 in California, USA, a gas-line was exploded and due to this disaster eight

people were killed and 38 homes were destroyed (NTSB, 2016). Based on FEM analysis and laboratory examination the cause of this explosion was a technical reason which could have been avoided by more accurate engineering design and inspections. Figure 2-14-c shows incident of oil pipeline caused the leakage in Komi-Russia. This incident was one of the worst on record since 1994, resulting in a spill of 100,000 to 350,000 tons of oil-containing fluids that severely affected three rivers and caused environmental issue in the area in 2011 (Enviromental Justice Atlas, 1994).

(a)

(b)

(c)

Figure 2-14 Pipeline failure explosions (a) gas failure in Texas (b) gas failure in California (c) oil pipeline leakage in Komi (Enviromental Justice Atlas, 1994; NTSB, 2016; PHMSA, 2017; The New York Times., 2011)

There are many different reasons for pipeline failure. Onshore pipeline failure can be due to factors such as human action and natural forces, construction and environmental factors, external-force/third-party damage, corrosion, and mechanical failures (materials failure and construction defects). In other words, the threats to pipeline integrity are classified in three main categories: time dependent, stable, and time-independent. The time-dependent threats involve corrosion failures. The stable category covers equipment; welding-fabrication related, as well as manufacturing-related defects. The last category includes third party or mechanical damage, incorrect operational procedure, external force, and weather-related factors. In Figure 2-15, the pie chart provides the statistics about gas pipeline failure in USA between 1993 and 2012 (PHMSA, 2017). It is obvious the largest proportion of failures is due to material, corrosion and excavation damage. The U.S. Department of Transportation (DOT) and Research and Special Programs Administration, Office of Pipeline Safety (RSPA/OPS) reported on gas pipeline incidents and their causes between 2002 and 2003 which are summarised in Table 2-1 (Roberge & Revie, 2007). It can be seen that the cost of pipeline failure just in USA over a 2-year period is more than $ 66 million with significant human life loss.

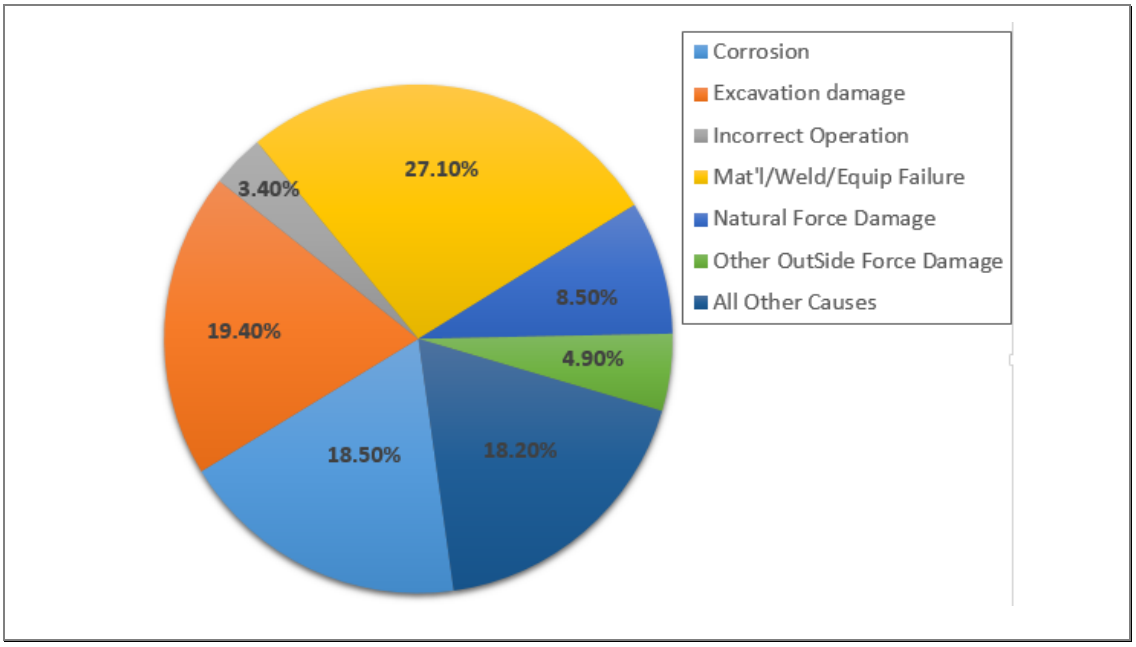

Figure 2-15 Significant onshore incidents cause breakdown in USA between 1993-2012 based on PHMSA (PHMSA, 2017) and (Tudorica, 2014)

Table 2-1 Gas pipeline incidents in USA (Roberge & Revie, 2007)

Reported Cause	Number of Incidents	% of Total Incidents	Property Damages	% of Total Damages	Fatalities	Injuries
Excavation damage	32	17.8	$4,583,379	6.9	2	3
Natural force damage	12	6.7	$8,278,011	12.5	0	0
Other external force damage	16	8.9	$4,688,717	7.1	0	3
Corrosion	46	25.6	$24,273,051	36.6	0	0
Equipment	12	6.7	$5,337,364	8.0	0	5
Materials	36	20.0	$12,130,558	18.3	0	0
Operation	6	3.3	$2,286,455	3.4	0	2
Other	20	11.1	$4,773,647	7.2	0	0
Total	180	-	$66,351,182	-	2	13

Failure in oil and gas has been discussed in the previous sections. Water pipeline failures also have often serious consequences and some individual incident examples from recent years are briefly addressed in this section. Figure 2-16-a shows an incident happened in Adelaide, Australia, in 2015. In this incident water went up to air for 40 metres, the road was closed and nearby homes were damaged (The Advertiser., 2015) . In another incident a sudden collapse in the form of large hole was observed in one of the main roads of Tripoli which was the result of a severe degradation as illustrated in Figure 2-16-b. The original wall thickness of the pipe was reduced and damages in pipe wall caused fluid leakage, cavities in soil and collapse of pavement (Hadi Meilani et al., 2015)

(a)

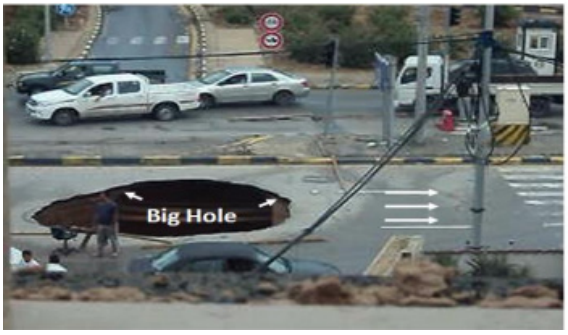

(b)

Figure 2-16 Example cases of water pipe breakage(a) Australia (b) Tripoli (Hadi Meilani et al., 2015; Laffer, 2015) and (Hadi Meilani et al., 2015)

Many factors can affect the performances of a buried water pipeline. In Australia, based on Sydney Water report, major failures are leakage or breakage for a number of reasons. Many parameters can cause leaks, such as: deteriorating joints and fittings; ground movement; changes in water pressure; changes in rainfall and temperature; adjacent features such as trees and poles; soil types and traffic loads. Sydney Water has invested $1 billion in the last decade and will invest $350 million over the next four years to reduce these failures. In a research carried out by Qiao l it was shown that pipe failure modes are basically classified into five categories (Qiao, 2011). These five major failure modes are summarized in the first column of Table 2-2 and the possible causes of these incidents are described in the second column. A schematic diagram of those failure modes are also illustrated in the last column.

Table 2-2 Some causes of water pipeline failure (Qiao, 2011)

Failure mode	Can be caused by:	Schematic illustration
Circumferential breaks	• thermal contraction or expansion • bending stress • inadequate trench and bedding practices • third party interferences such as poor quality repair, maintenance, or replacement practices	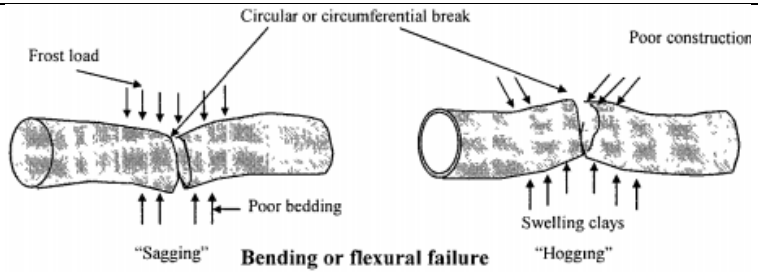
Longitudinal split breaks	• hoop stress due to pressure in the pipe; • ring stress due to soil cover load • live loads caused by traffic • the increase in ring loads when penetrating frost or moisture causes the expansion	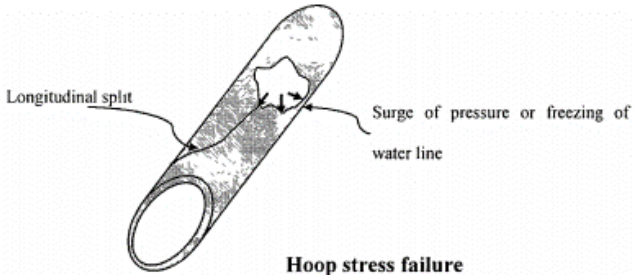
Clamp failures	• fail themselves when clamps are used to repair previous pipe failures	
Pinhole failures due to corrosion	• reduction in pipe wall thickness	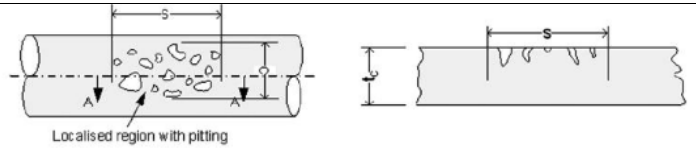
Pipe Joint leaks (including fitting leaks)	• pipe heaving or misaligned connections	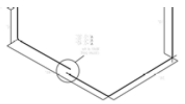

Failure due to cyclic load - degradation

In this section, the definition of degradation which is one of the reasons of pipeline failure is discussed. The main focus of the current research is pipe response due to traffic load and with time, both pipe and soil degrade under cyclic load. Degradation can affect long-term performance of pipe-soil system.

The behaviour of soil is nonlinear from very early loading stages. The degradation of the soil due to cyclic load was examined by Idriss (Idriss et al., 1978). It was concluded that reduction in soil Young's modulus due to the number of cycles is related to the amplitude of the developed shear strain. Different stress-strain models used for nonlinear behaviour are shown in Figure 2-17 and Figure 2-18 . The vertical axis represents shear stress while the horizontal axis represents shear strain in a simple shear test. It can be seen that soil strength decreases when number of cyclic load increases. Different stress–strain models and variations of these models are shown in Figure 2-18.

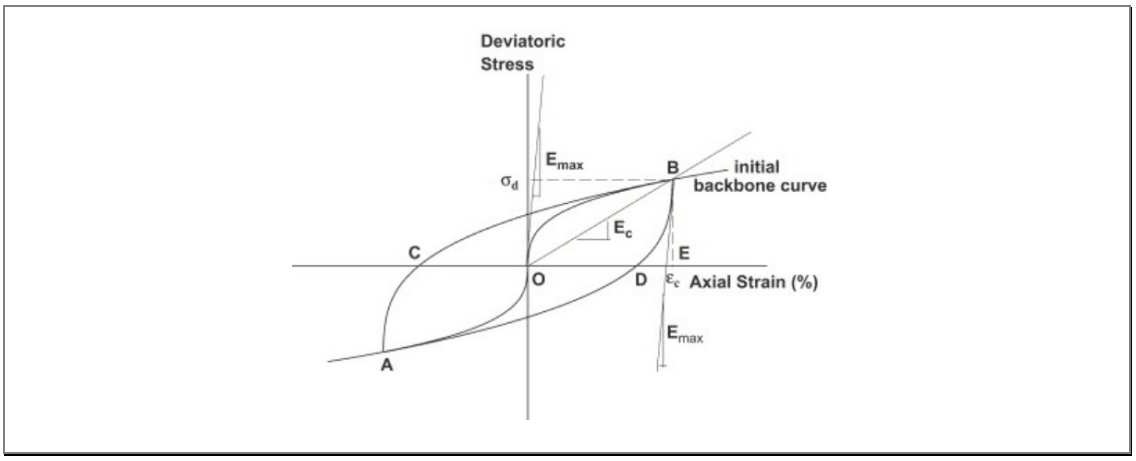

Figure 2-17 Schematic illustration of a symmetric stress–strain loop during the first cycle (Lee & Sheu, 2007)

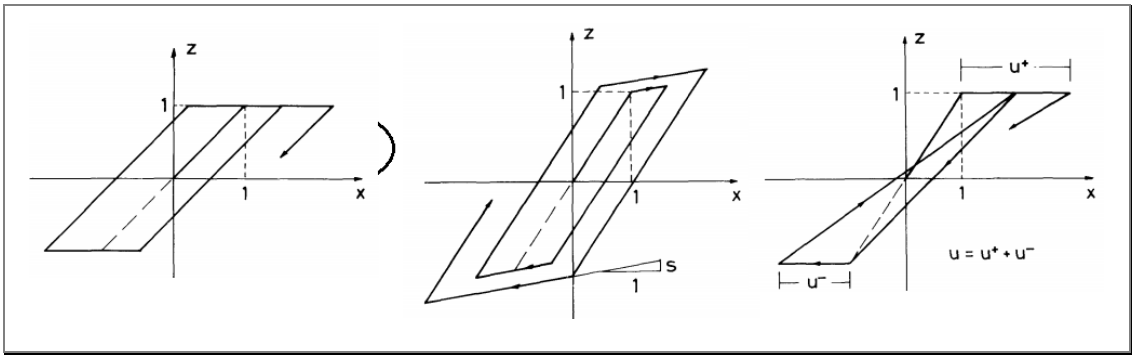

Figure 2-18 Examples of load-deformation hysteretic models, left to right: elastic-perfectly plastic; normalized Kato-Akiyama hysteretic component normalized peak-oriented hysteretic component (Suzuki & Minai, 1988)

Degradation may occur due to either walking or buckling in the pipeline in offshore or traffic in onshore applications. This causes cyclic fatigue, plastic failure in bending, local bending, cracking or tearing, etc. (Bridge et al., 2004; Audibert et al., 1984; Dean 2010). Degradation effect on pipeline is an important issue in offshore geotechnical engineering especially in touchdown zones (TDZ). In those areas when steel catenary risers (SCR) face the seabed, the cyclic load effects are important. More researches in this regard can be found in (Dean 2010; Randolph & Gourvenec, 2011). In onshore applications however, degradation can be induced due to traffic on road. Case studies dealing with degradation impact will be presented later in this chapter.

2.4 IMPROVE PIPELINE INTEGRITY

Previous sections focused on different causes of pipeline failures. However, a combination of structural and geotechnical stabilization such as ground improvement is often considered in the design of buried pipelines.

If soil in trench or base of road is not strong enough, road would deform and crack easily. Therefore, underground infrastructures such as water and sewage pipes, would be threatened due to road damage. With road stabilization, soil will be stronger, incompressible, dry and waterproof and safer to use. Road stabilization techniques can be divided into two categories, mechanical and chemical (Kestler, 2009; Makusa, 2012; Sétra-LCPC, 2000; Sherwood & Transport Research, 1993). Mechanical road stabilization includes various processes such as compacting and blending soils, incorporating conventional geosynthetics or less conventional materials, such as woodchips, sawdust, rubber and woodmats. Traditional chemical stabilizers are cement, lime, fly ash and bituminous materials. Based on properties, such as soil granularity, plasticity, or texture, some stabilizers are more suitable for certain soils than others. Adding cement to soil can increase its bearing capacity and change the mechanism of failure. The function of increasing the bearing capacity is attributed to the “forced” initiation of the potential failure plane along an alternate direction providing a higher total resistance. The stabilization process decreases the shear stresses transferred to the soil and provides vertical confinement on the interface. It also decreases the shear strain near the top layer and limits surface rutting. The bearing failure model of subgrade may change from punching failure without reinforcement to general failure with ideal stabilization. Portland cement is typically used for road stabilization of subgrade or base course, but not for surfacing as the cement-treated material becomes brittle and cracks under traffic loading. The surface

must be cured for at least first 7 days by either periodically applying water or by sealing the surface with a fog seal or similar. Fine-grained and sandy soils can be stabilized with cement while other soils with high organic content, should not be used for cement-stabilizations (Kestler, 2009). Some examples of using mechanical stabilization in pipeline industry are shown in Figure 2-19.

(a)

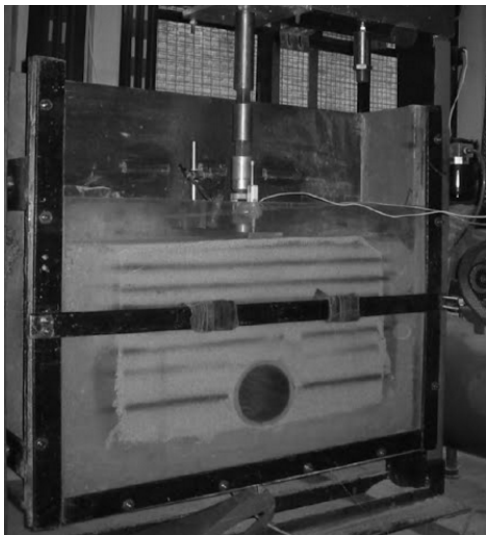

(b)

Figure 2-19 Applications of mechanical stabilization in pipeline industry (a) geocell (Tavakoli Mehrjardi et al., 2012) (b) geosynthetics (Moghaddas Tafreshi & Khalaj, 2008)

2.5 CASE STUDIES

In recent decades, many studies have been performed to investigate the response of buried pipes subjected to different conditions. However, a few studies related to pipe-soil interaction analysis subjected to cyclic load are available. Amongst different methods experimental and finite element analysis used together are the preferred methods for researchers and they produce the most reliable results (Moser, 2011).

The first research work on a buried pipe performance was published in 1913 by Marston and Anderson (Marston & Anderson, 1913). Later, Spangler the student of Marston showed that flexible and rigid pipes behave differently under the load (Spangler, 1941). Marston-Spangler equation then was developed to predict load on pipe and pipe deflection. Since then, different methods of numerical and empirical equations have been used to investigate pipe performance over past decades. However, the usage of finite element methods to simulate pipe soil interaction problems was introduced by CANDE in 1976 and Heger in 1985 (Heger et al., 1985;

Katona, 1978). Since then, many numerical analyses were performed to investigate buried pipe response using finite element methods. In the following sections some recent experimental and numerical case studies of pipe soil interaction are presented. This section is followed by those case studies investigating impact of stabilization on pipe response.

2.5.1 Experimental Case Studies

Large scale testing of buried pipes is a useful method to evaluate the response of pipe and soil under different conditions. Rogers in 1995 designed a laboratory facility to investigate the installation procedure on performance of 100 to 375 mm diameter pipes (Rogers, 1995). After analysing different installation methods, they found that different installation can reduce pipeline costs. Faragher in 1997 performed a full scale controlled field test to analyse the behaviour of embedded flexible pipe under repeated load. Pipe diameter was between 600-1050 mm and the results showed that the impact of cycles is more significant in the beginning of test. In one of the experimental researches the response of buried pipe in granular backfill was investigated by Don. A flexible pipe was subjected to construction traffic as a static load. Results were compared with numerical analysis. They developed a preliminary simple expression for estimating pressure on pipe. In another study, the behaviour of pipe in a large scale soil chamber under cyclic load was investigated. Ko in 2010 investigated the performance of surrounding soil and distribution of acting stress on the pipe was measured using load cells installed on PVC pipe. A schematic diagram of the test tank used in their project is shown in Figure 2-20-a and their results are illustrated in Figure 2-20-b. It was found when pipe was buried in loose sand, it had larger deformation than those in dense backfill. In addition, lateral stress and pipe displacement in the horizontal direction in dense sand is relatively small because of lateral confinement of backfill. The behaviour of a HDPE pipe buried in a sandy soil under cyclic load was investigated using experimental approach by Moghaddas Tafreshi (Moghaddas Tafreshi & Khalaj, 2011). After running the tests, a nonlinear regression model was developed to calculate soil surface settlement and pipe crown displacement based on soil density, burial depth variation and stress. It was found that burial depth, magnitude of surface pressure and soil density dramatically affects pipe behaviour.

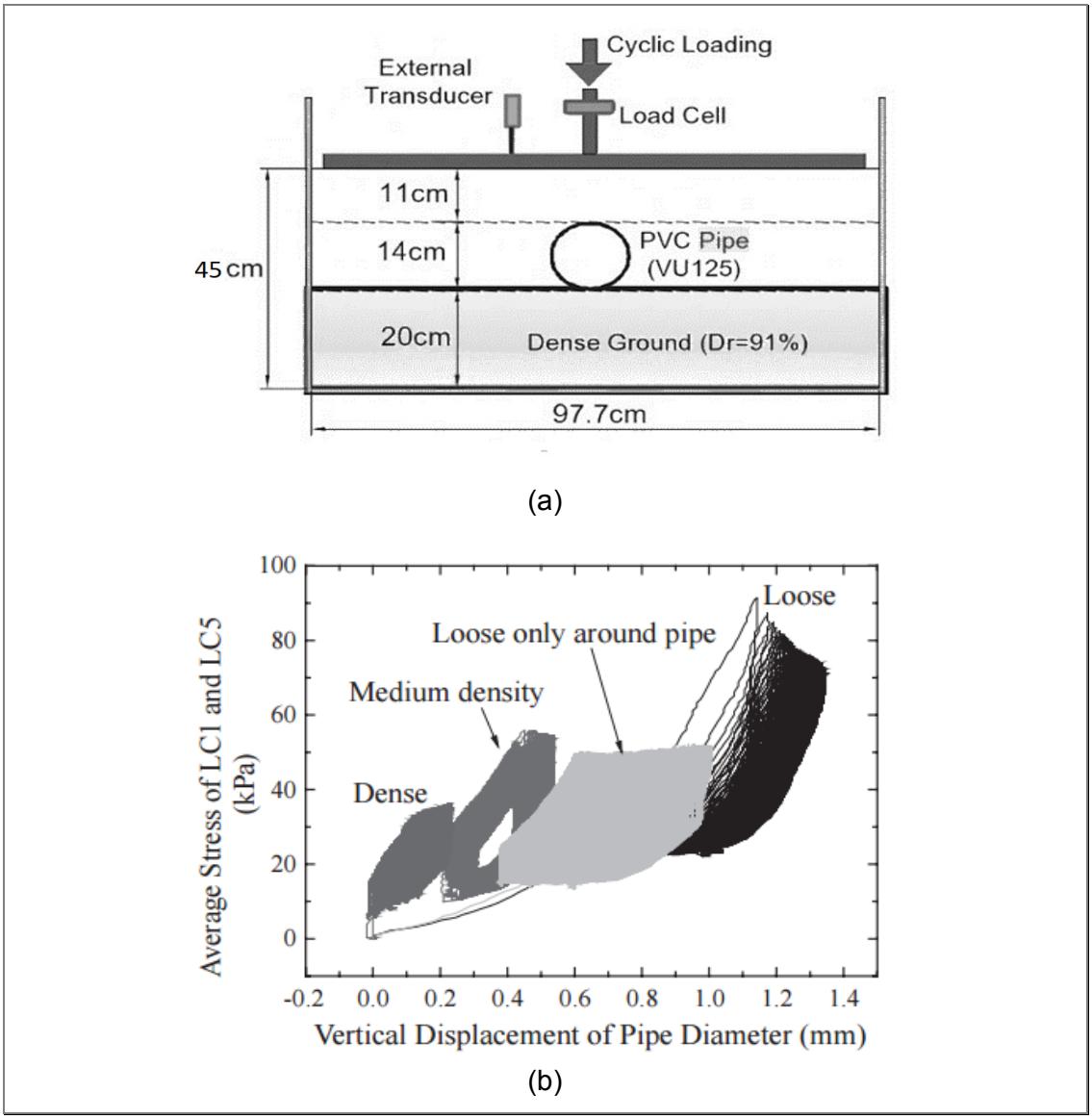

Figure 2-20 (a) Schematic diagram of the test box and loading system of pipe (b) stress distribution on pipe in vertical direction (Ko & Kuwano, 2010)

Figure 2-21-a and b illustrate the results of a research carried out by Moghaddas Tafreshi to investigate the impact of various parameters on buried pipe response. The results from this research showed that increasing the burial depth leads to an increase in Soil Surface Settlement (SSS) and a decrease Vertical Diametral Strain of pipe (VDS). Soil density also had a significant impact on pipe deflection and soil surface settlement. The response of very flexible pipe in an experimental and numerical research was investigated using centrifuge equipment and finite element model. Pipe was buried in a shallow burial depth and impact of surface loading on pipe was investigated. Plaxis was used to simulate three dimensional model and load was applied in a static form in both experimental and numerical model. Results showed that maximum hoop stress decreases with the

height of soil cover. The results obtained through two methods were compared and showed a good agreement (Bryden et al., 2015)

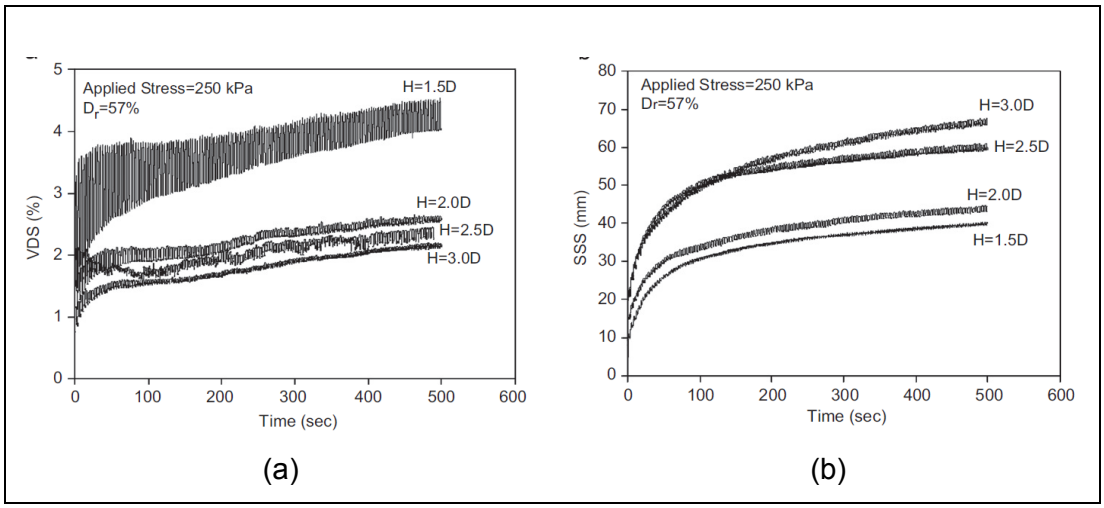

Figure 2-21 (a) Variations of the pipe deflection of buried pipes during repeated load, (b) variations of the soil surface settlement during repeated load (Moghaddas Tafreshi & Khalaj, 2011)

2.5.2 Numerical Case Studies

In general, soil-pipe interaction problems are statically indeterminate and using numerical modelling allows assessing the effect of a wide range of variables efficiently. Many researches have investigated the response of buried flexible pipe under different loading condition during recent years. However, despite numerous researches on buried pipe performance under various conditions, the research effort on pipeline behaviour due to traffic loads is limited. In the research carried out by Leng the effect of cyclic load on characteristics of geogrid-reinforced aggregate was analysed using laboratory testing and finite element analyses using ABAQUS (Leng, 2003). Soil was assumed to behave as an elasto-plastic model, Drucker-Prager with hyperbolic yield surface. In this research degradation was related to base layer thickness and base layer/geogrid interaction. The results of experimental and numerical analysis were found to be consistent. It was also concluded that geosynthetics improves model performance and decreasing stresses at interface and subgrade layer.

In another research carried out by Kang the effect of pipe installation was studied on a deeply buried steel pipe (Kang et al., 2008). They used ABAQUS to model buried pipe and Ducan and Sleig's nonlinear model was used to model clay and sand behaviour. Based on the static analysis results, deflection of pipe was affected by the ratio of depth to pipe diameter, see also (Abo-Elnor et al., 2004;

Calvetti et al., 2004; Chatterjee et al., 2013; Farhadi Hikooei, 2013; Kang et al., 2008; Liu et al., 2010; Rajeev & Kodikara, 2011; Trautmann & O'Rourke, 1985; Zaman et al., 1984). In a research carried out by Abolmaali the effect of various parameters on pipe-soil interaction using ABAQUS was investigated (Abolmaali & Kararam, 2010). Soil and pipe mesh element in a 3D modelling were selected as eight-nodded linear brick (C3D8R) and six-nodded linear triangular prism (C3D6) to model concrete pipe as shown in Figure 2-22. It was concluded that the bedding material stiffness and the compaction levels have higher impact on the induced stresses than bedding thickness, see also (Abolmaali & Kararam, 2010; Jung et al., 2012; Lee., 2010). In a numerical and experimental investigation the impact of moisture on a pipe buried in swelling soil was investigated (Rajeev & Kodikara, 2011). They used FLAC software to model buried pipe model. Soil was modelled as nonlinear material with Mohr Coulomb failure criteria and pipe was assumed to behave linearly. Based on the proposed model the deflection of pipe due to moisture content can be predicted taking into consideration the capillary rise. In another numerical and experimental research the impact of cyclic load on permanent deformation of a road over a buried pipe was investigated (Cao et al., 2016). In this research ABAQUS was used for numerical modelling and a steel reinforced high density polyethylene pipe was used in sandy soil in a large scale tank for experimental investigations. Surface deformation of road was predicted using mechanical empirical model. In addition, results showed that increasing burial depth decreased road permanent surface settlement.

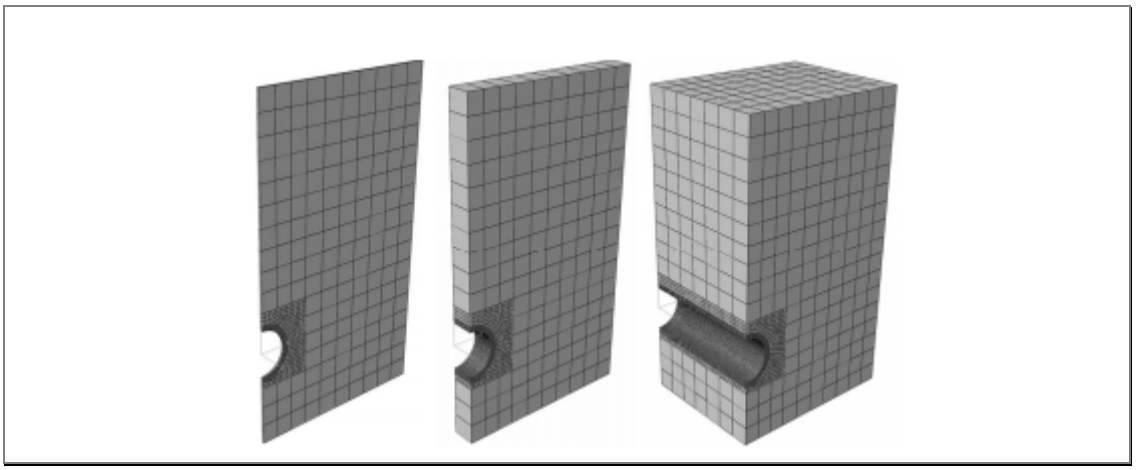

Figure 2-22 Modelling buried pipe in finite element with different pipe lengths in ABAQUS (Abolmaali & Kararam, 2010)

2.5.3 Stabilization Impact on Pipe Performance

Some studies have been carried out to investigate the impact of mechanical stabilization on buried pipe response. Karimian carried out a research to investigate

the response of buried pipe subjected to transverse ground movement as shown in Figure 2-23-a (Karimian, 2006). Both experimental and numerical methods were used to study buried pipe behaviour. The impact of single and dual-geosynthetics lined trench material were investigated in reducing pipeline strain and lateral soil pressure. Large scale test setup and a 2-D plane strain model in FLAC was developed to capture the impact of dilation and soil stress distribution in the model. It was found that the lateral soil pressures in this method were generally lower than those estimated from existing guidelines. In addition to friction between geosynthetics and steel pipe, the relative stiffness between pipe and soil is the major factor in reducing the lateral soil pressure. Tavakoli studied the impact of adding rubber and geocell to soil on buried pipe response (Tavakoli Mehrjardi et al., 2012) as shown in Figure 2-23-b. For the chipped rubber and soil mixture, the pipe has the highest strains under the cyclic loading regardless of the amount of rubber in the soil. According to the results, the minimum soil surface settlement and vertical diametric strain are provided by using 5% of shredded rubber. In another experimental research the impact of adding geosynthetics on buried pipe behaviour under repeated load and soil surface settlement was investigated (Moghaddas Tafreshi & Khalaj, 2008) as shown in Figure 2-23-c. They found adding geosynthetics significantly improved pipe behaviour. The impact of adding geosynthetics and mechanical stabilization of road material was investigated numerically as well. Tavakoli carried out an experimental and numerical research on buried pipe subjected to cyclic load while trench was stabilized with geocell and rubber/soil mixture. They used the finite element software, FLAC-3D for their analysis and pipe was buried in a large scale tank. Pipe material was assumed to be linear elastic and soil was assumed to be elastic perfectly plastic with Mohr Coulomb model criterion. The results showed that combined use of geocell and rubber mixture can reduce soil surface settlement and pipe deflection while providing a secure condition under repeated cyclic load (Tavakoli Mehrjardi et al., 2016). However, there is lack of research in numerical or experimental researches investigating the behaviour of buried pipe under traditionally stabilized soils

.

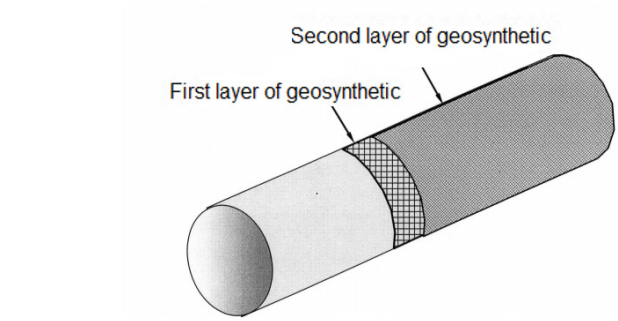

(a)

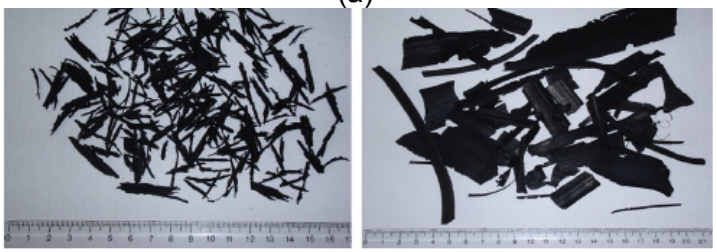

(b)

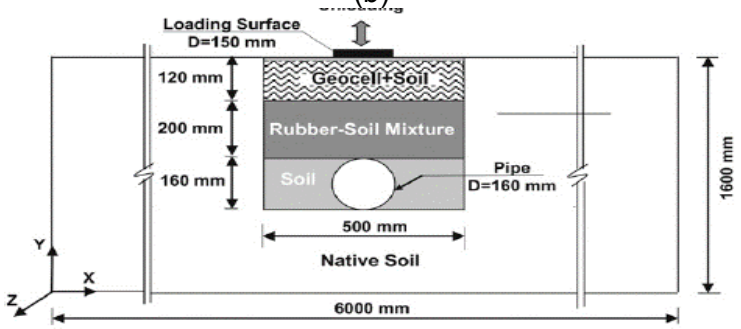

(c)

Figure 2-23 Examples of stabilization to improve buried pipeline behaviour using (a) geosynthetics (b) rubber (c) combined geocell reinforcement and rubber soil mixture (Tavakoli Mehrjardi et al., 2016, Karimian, 2006)(Moghaddas Tafreshi & Khalaj, 2008)

2.6 KNOWLEDGE GAPS AND RESEARCH NEEDS

From the literature review the following conclusions can be made:

- Investigating impact of various design loads on performance of a buried pipe subjected to traffic load to identify the values with highest contribution on buried pipe performance is needed.
- The majority of previous studies are limited to either experimental or numerical analysis. Performing experimental and numerical simulations together to investigate the model response under various conditions needs to be done.

- Fatigue is one of the reasons of buried pipe failure which can result in soil loosening and pipe breakage.
- Design methods of earth pressure acting on pipe do not consider the impact of degradation and strength loss of soil around the pipe.
- Number of numerical or experimental researches investigating behaviour of buried pipe under traditional stabilizations is limited.

From abovementioned remarks, an experimental and numerical study investigating the impact of cyclic load on pipe soil behaviour is needed. The study should include the following aspects:

- A parametric study and sensitivity analysis should be carried out to investigate the impact of various factors on a buried pipe response subjected to traffic load.
- Experimental study has to be done to evaluate the impact of cyclic load on pipe soil interaction. A numerical simulation will be performed to better understand the behaviour of pipe under traffic load
- The impact of cement stabilization of trench material will be investigated on performance of the model.
- Finally, the study should be extended to develop equations to investigate the relationship between various variables.

The methodology of this research is illustrated as a flowchart in Figure 2-24. It can be seen that flowchart initially starts with a numerical parametric study to see how sensitive the model is to any factor. This section will be described in Chapter 3. The impact of the most sensitive factors from sensitivity analysis results will be investigated in the next phase of this research both numerically and experimentally. Suitability of equipment and software to investigate model response due to traffic will be investigated in Chapter 4. The next step is providing correct material properties. Material properties will be investigated through experimentations and presented in Chapter 5. The next part of flowchart shows the experimental and numerical results and the description of possible scenarios for each method which will be discussed in Chapter 6. As shown, flowchart ends with investigating the impact of various factors and developing equations to predict the model response which will be discussed in Chapter 7.

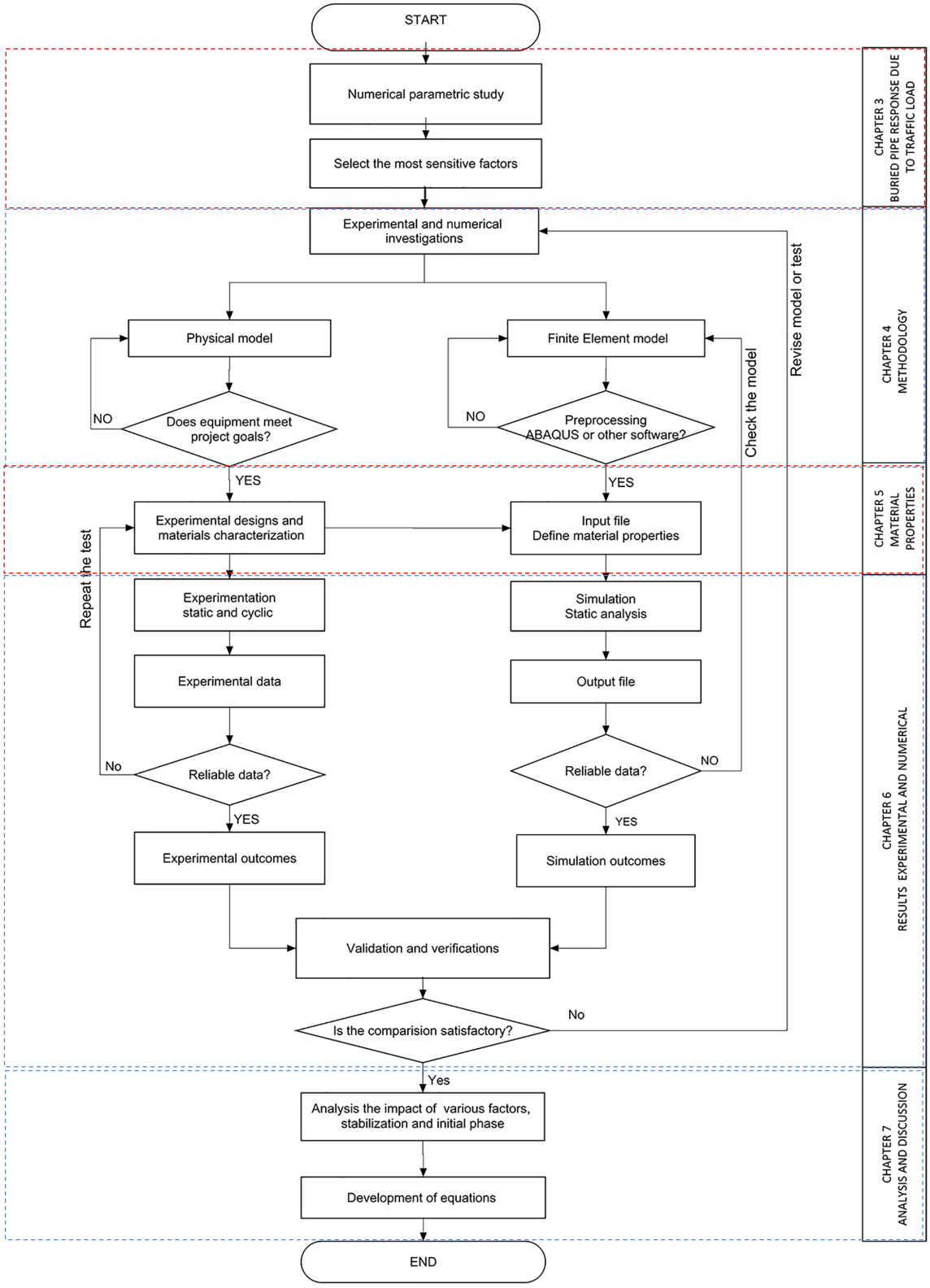

Figure 2-24 Methodology and analysis procedure in the current research

2.7 SUMMARY OF THE CHAPTER

In this chapter literature was reviewed for the studies conducted on pipe soil interaction under cyclic load. In the first section, an introduction and a background about pipeline applications and its significant role in any modern society was explained. In the second section, the theory behind the design of buried pipes and the development through the past few decades were presented. In the third section, different failure modes of pipeline specifically in onshore applications were discussed. In the following section, different methods to reduce pipeline failure under road surfaces such as stabilization application were discussed. Then factors affecting pipe degradation and degradation definition were described briefly. In the fifth section, some of the recent experimental and numerical studies dealing with pipe soil interaction analysis were reviewed. Then, number of case studies investigating impact of either mechanical or traditional stabilization on pipe soil response was presented. In the last section, based on the reviewed studies, research gaps were identified and the proposed study to investigate pipe soil behaviour under cyclic load was presented.

3 A NUMERICAL PARAMETRIC STUDY ON BURIED PIPE PERFORMANCE SUBJECTED TO VARIOUS LOADING CONDITIONS

Some parts of this chapter was published and presented as a conference paper with the title of "*Finite Element Analyses of Buried Pipeline Subjected to Live Load Using ABAQUS"* at Proceedings of the 68th Canadian Geotechnical Conference, GEO Quebec-2015, September 20-23, 2015, Quebec City, Canada; The authors are Ahdyeh Mosadegh, Hamid Nikraz

3.1 INTRODUCTION

In this chapter a numerical parametric study is conducted to investigate the behaviour of buried pipe subjected to traffic load taking into consideration the effect of different factors. These factors include burial depths of pipe, pressure magnitude, width of loading area, internal pressure, pipe-soil interaction properties, pipe material and boundary conditions at the pipeline ends. These factors were selected to be investigated based on literature review which can affect a buried pipe response under roads. The effect of these factors will be analysed due to change in pipe deflection, soil surface settlement, and stress distribution in pipe wall as well as earth pressure on pipe crown. The parametric study will be followed by sensitivity analysis of buried pipe model to investigate how sensitive the model is due to change of each above mentioned factor.

This chapter is presented in four sub-sections. Firstly, following the introduction of parametric study beginning with problem statement, material property and stage of analysis are presented. Then, the results of pipe response due to various parameters are discussed and graphs are presented. In the third section, sensitivity analysis is presented and the effect of each factor on model response is identified and results are presented. In the last section, results and findings from this chapter are discussed and the factors which have the highest impact on model response are identified. An overview of this chapter is presented in Figure 3-1 .

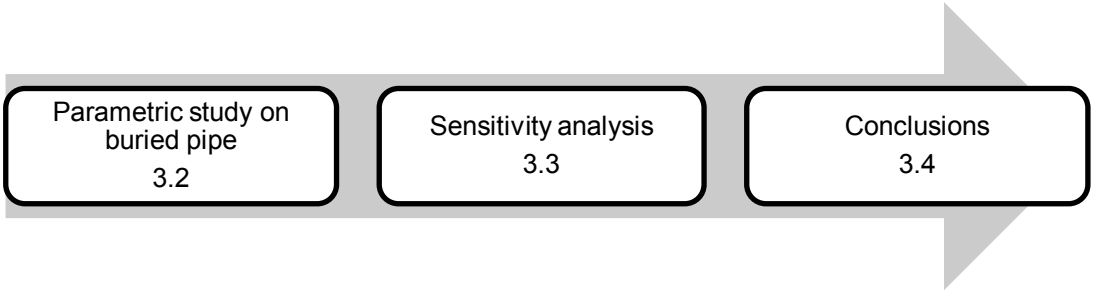

Figure 3-1 Chapter overview

3.2 PARAMETRIC STUDY

In this section a numerical parametric study is performed to investigate the impact of various factors on buried pipe response using nonlinear finite element code ABAQUS (ABAQUS, 2013). The aim of this study is determining the sensitivity of model to each parameter. The chosen parameters are burial depth, surface load, loading area, pipe soil interaction value, internal pressure, pipe wall thickness and boundary condition. Results will be presented in terms of impact on pipe deflection, soil surface settlement, stress in pipe wall and maximum earth pressure on pipe. The reasons of choosing these four factors to be investigated are as follow. The vertical pipe deflection is frequently used as a design criterion in many projects. Soil surface settlement is a good indication of the overall strength of system over the pipeline. Earth pressure and stress in pipe are important factors in pipeline design because they can cause pipe deflection or failure.

3.2.1 Problem Statement

The problem statement involves a 1m diameter pipe buried in sandy backfill material subjected to traffic load. Eight investigating cases consisting of 30 numerical models are investigated and are summarised in Table 3-1. The overview of model is also presented in Figure 3-2 illustrating each term definition. All cases

are categorised into standard and nonstandard cases. The standard case consists a steel pipe with a thickness of 5 cm, burial depth of *H* equal to *D*, surface pressure of 550 kPa and *α* equal to 2D in which α is width of loading area as illustrated in Figure 3-2 . A full- bonded interaction without considering internal pressure was also chosen for this case. For example, Case I investigates the impact of six different burial depths on performance of a steel pipe without any fluid inside. Pipe thickness is 5 cm and loading area is α=2D. It is noted burial depth varies between 1 and 5D. The reason of not considering H >5D is based on Boussinesq bulb curves as shown in Figure 3-3 (Boussinesq, 1885). The contour labels represent percentages of the applied pressure due to footing load. It can be seen that only 5% (0.05p) meets the vertical centre line at a depth of about 5B; and almost the 30% contour (0.3p) is at a depth of just less than 2B which means the impact of the live load is more critical for H<2B. In this figure *B* represents width of loading area. It is noted D and B have the same values in the current research. All results will be presented later and compared with the results published in the existing literature. It is noted soil material property and trench width remain unchanged during analysis.

Table 3-1 Different cases for pipe-soil interaction investigation

Case no.	Investigating factors	Value
Case I	Burial depth, H/D	1, 1.5, 2, 2.5, 3.5, 5
Case II	Surface pressure, P	200, 400, 550, 700 kPa
Case III	Loading area, α/D	0.5, 1, 2
Case IV	Internal pressure, P’	Without fluid, water: 414 kPa, gas: 7500 kPa
Case V	Interaction coefficient	0.1, 0.3, 0.5, 0.7, 0.9, Full bonded
Case VI	Material property type	HDPE, Steel, PVC
Case VII	Wall thickness, t	2, 5, 10 cm
Case VII	Boundary condition	Hinged, roller

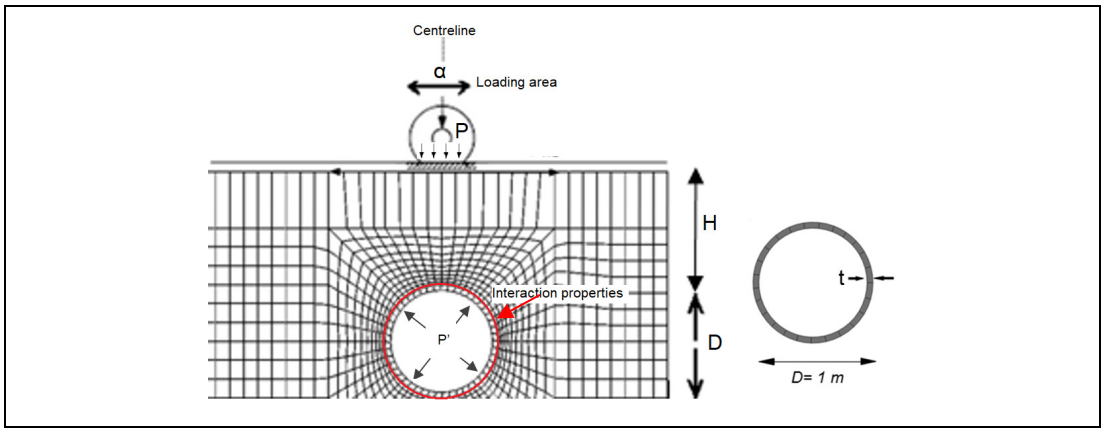

Figure 3-2 Schematic view of model in the current research

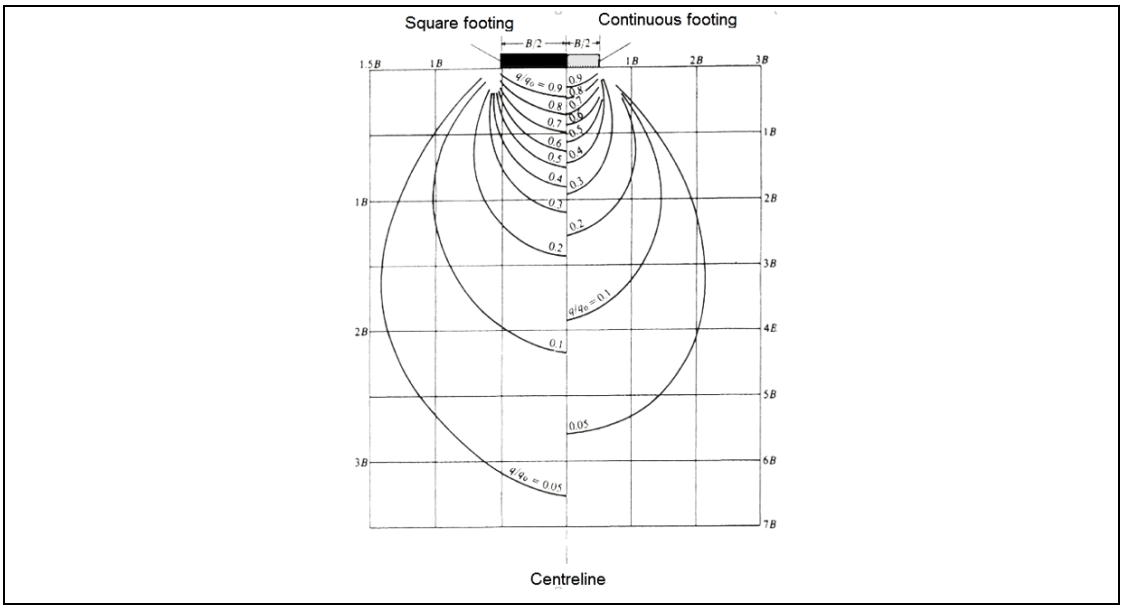

Figure 3-3 Pressure bulb beneath square and strip footing (Boussinesq, 1885; Bowles, 1988)

3.2.1.1 Material properties

Two types of soil and three types of pipe are used to predict live load effects on pipe-soil behaviour. The backfill soil is modelled as an isotropic elasto-plastic material satisfying the Drucker-Prager failure criterion with properties illustrated in Table 3-2. Soil properties are adopted from Helwany (Helwany, 2007).

Table 3-2 Backfill soil properties (Helwany, 2007) and granular soils

Type of soil	Term	Value
Backfill soil	Density (Kg/m^3)	1920
	Young's modulus, E (MPa)	18
	Poisson ratio (v)	0.28
	Cohesion, d, (kPa)	<1
	Friction angle,β (2D) 3-D	48.5^o 55.7^o
	Dilation angle, ψ	12^o
	Flow stress ratio, K	1
Granular soil	Density (Kg/m^3)	2000
	Young's modulus, E (MPa)	3000
	Poisson ratio (v)	0.35

Table 3-3 Material properties of pipes

Parameters	Steel pipe	HDPE pipe	PVC
Density (Kg/m^3)	7850	955	1350
Young's modulus, E (MPa)	200X10^3	816	4000
Poisson ratio (v)	0.3	0.46	0.4
Yielding stress (MPa)	490	23	25

3.2.1.2 Boundary conditions and finite element mesh

Due to the long length of pipe compared to its diameter, the system can be modelled assuming plane strain conditions. The X-Y plane is the area where the soil is subjected to various loads, e.g. positive direction for Y is opposite direction of the weight. For boundary conditions, both vertical sides of the model are fixed in a horizontal direction with vertical displacement, and the bottom of the model is fixed in both vertical and horizontal directions. Due to symmetry, only half of model is created in ABAQUS. In all models, the mesh is refined near the pipe and in areas with stress concentration around the pipe as shown in Figure 3-4.

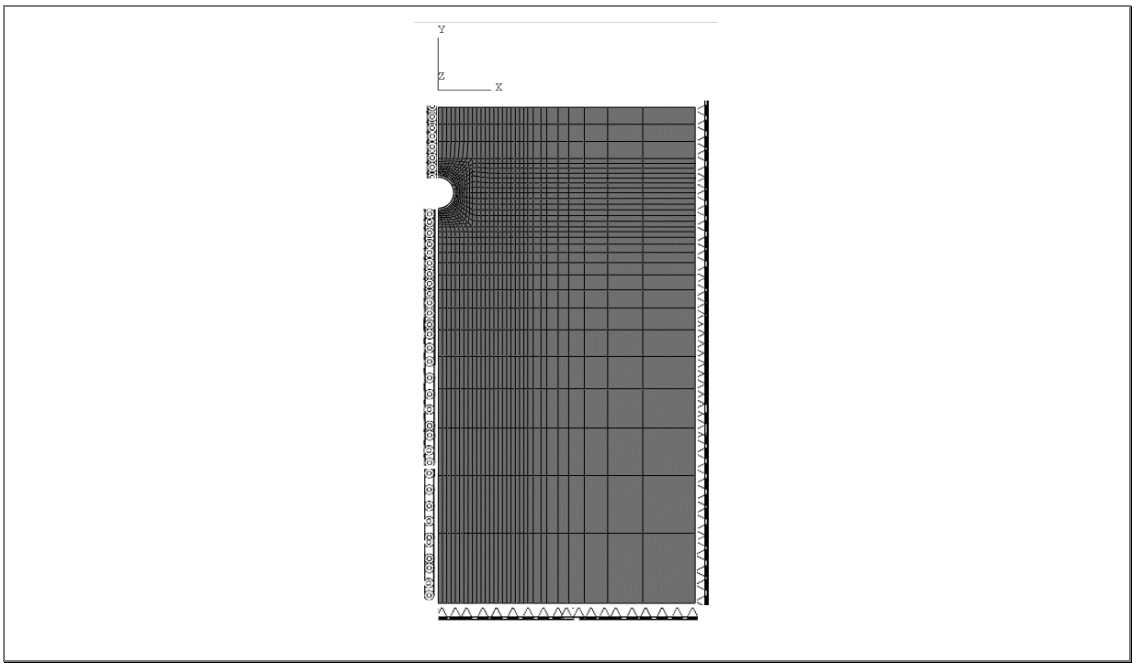

Figure 3-4 Finite element discretization and boundary condition selection of the model (2D)

Trench width should be the greater of 1.5 times of the pipe outside diameter (1 m) plus 305 mm or the pipe outside diameter plus 406 mm (AASHTO, 1998). Trench

width therefore is considered 2 m. Pipe and soil elements are modelled as CPE4R or 4-node bilinear plane strain quadrilateral with reduced integration.

To achieve the reasonable number of meshes, mesh convergence study is carried out and various models consisting of 170, 450, 740, 1100 and 1500 element numbers are created and subjected to the same amount of surface pressure on top of the soil surface. Three of all five investigating models are illustrated graphically in Figure 3-5. Results of mesh convergence study are shown in Figure 3-6. The results illustrate the number of meshes versus various parameters such as soil surface settlement, stress in pipe wall and pressure on pipe crown due to 550 kPa of traffic load on soil surface (standard case condition). It can be seen that the model with 1100 meshes is accurate enough for this study as elements are small enough for the numerical analysis of this research. More number of meshes needs more running time for each model and less number of meshes results in bigger element and less accurate results.

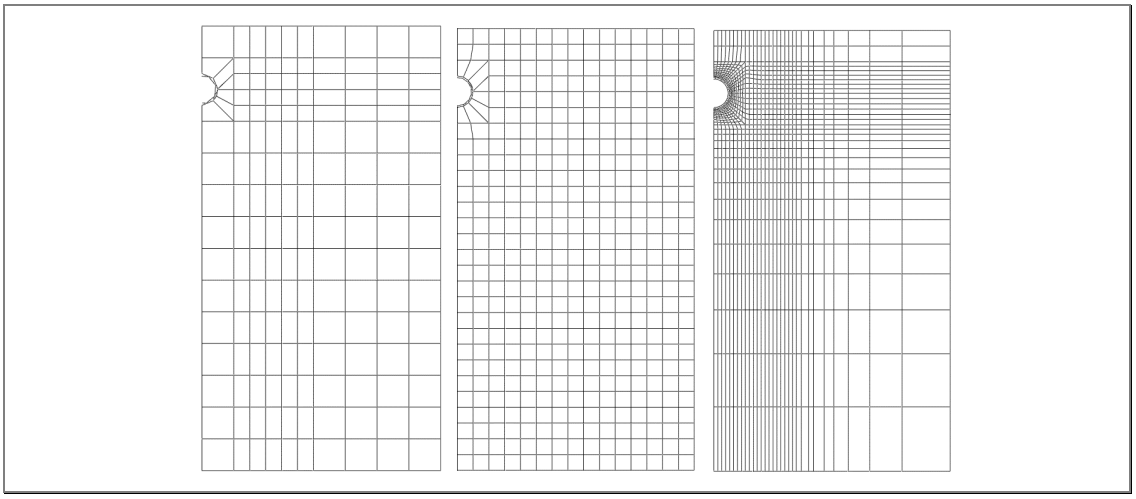

Figure 3-5 Models for mesh convergence study

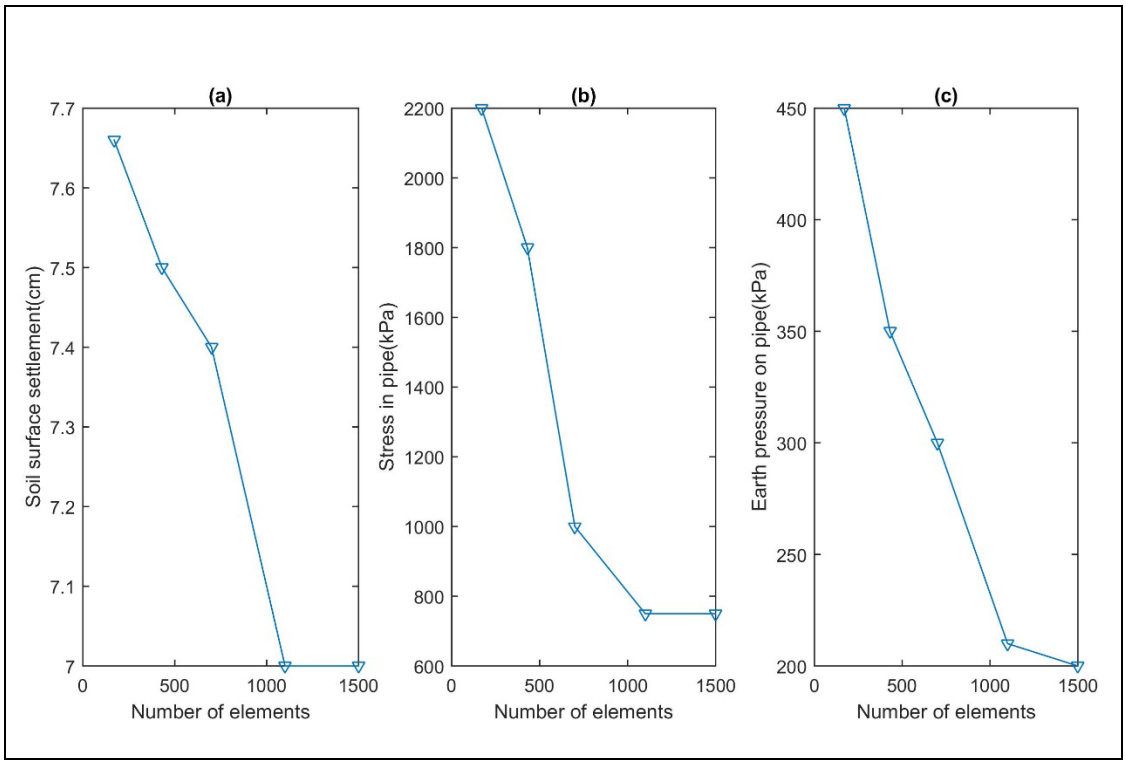

Figure 3-6 Impact of number of meshes on(a) soil surface settlement (b) stress in pipe (c) earth pressure on pipe

It is noted that analysing pipe soil behaviour using plane strain conditions should be carried out with caution as any existing infrastructure along the pipeline path can change the boundary conditions from roller to the hinge causing significant changes in both stress and displacement along the pipeline. For this purpose and to compare the effect of boundary conditions, a 3D model is also built to analyse how boundary conditions affect the stress and displacement distribution along the pipeline. Two types of boundary conditions at the end of pipeline are selected, roller and hinge representing infinite and finite length of the buried pipeline, respectively. As suggested in many standards for three-dimensional analysis, pipe elements are modelled as a series of shell elements. Three-dimensional brick elements are used to simulate the surrounding soil (C3D8R) and four-node reduced-integration shell elements (type S4R) are used for the pipe, as shown in Figure 3-7.

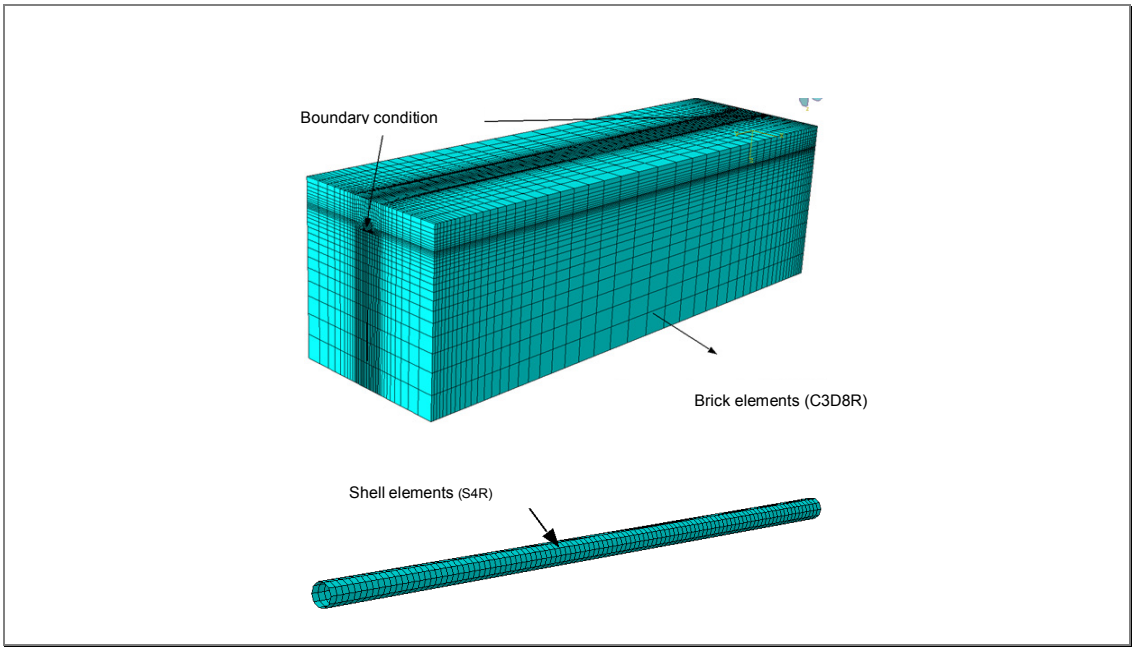

Figure 3-7 Finite element discretization and boundary conditions (3D model) (Mosadegh. & Nikraz., 2015)

3.2.1.3 Interaction

For both 2D and 3D model and from different contact models in ABAQUS, surface-to-surface interaction is chosen to model the interaction between soil and pipe. It is noted that the interaction between pipe and soil has two components, one is perpendicular to the surface and the other is tangential to the surface. The friction coefficient between the pipe and soil is assumed to vary from 0.1 to 1. For this case or for tangential contact, separation is allowed after contact and slipping is allowed during analysis. Hard contact is chosen for the normal direction, meaning there is pressure only when there is contact. To define the interaction in ABAQUS, the pipe element is chosen as the master surface with a stiffer body, and the soil as a slave surface with more refined meshes (King & Richards, 2013). To avoid convergence difficulties, an asymmetric solver matrix is used to solve the problem. To avoid the penetration of the master surface nodes into the slave surface, the slave surface mesh is refined. It is worthy to mention that the benefits of choosing this type of interaction is reducing likelihood of large localized penetrations and snagging, improving accuracy of contact stress. For all models except those investigating the impact of interaction coefficient value on model response, a fully bonded interface between the pipe and wall and the backfill material was assumed. This interface is simulated using surface tie feature in ABAQUS.

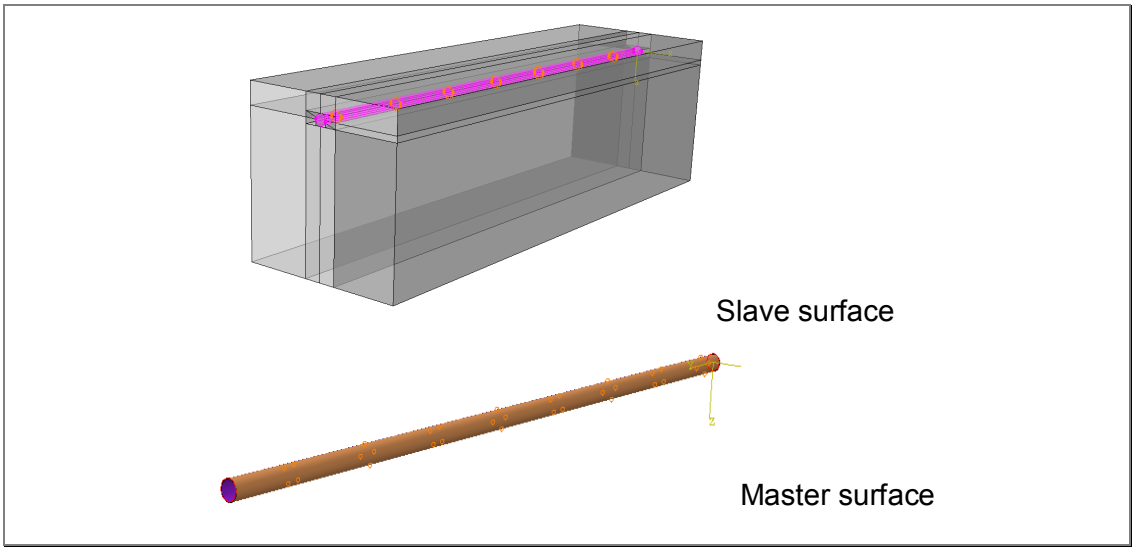

Figure 3-8 Master and slave surface representing pipe-soil interaction

3.2.1.4 Stage of analysis

For both 2D and 3D simulations, the model is created in four steps. In the first step which is the initial condition, all boundary conditions are defined as described previously. In the next step, a geostatic step is applied in which a gravity load is applied to the model. In the third step, pipe and pipe-soil interaction are activated and the pipe weight is applied to the model. Pipe elements are reactivated during this step allowing movement in a vertical direction. In the last step, traffic load is applied to the soil surface in the trench exactly on top of the pipe. In addition, when considering the effect of internal pressure, fluid pressure is applied to the pipe's internal walls during last step as shown in Figure 3-9.

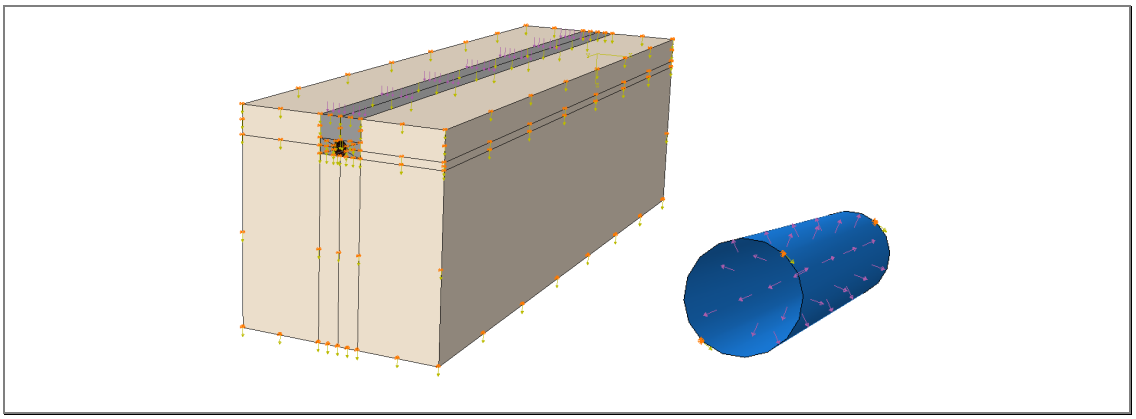

Figure 3-9 Body force, traffic and liquid pressure

3.2.2 Results

The following section presents the results of numerical analysis along with discussions highlighting the effect of different factors on buried pipeline behaviour.

For all cases the study investigates the effect of various factors affecting model response summarized in Table 3-1. All cases are analysed in plane strain condition except for those cases considering impact of boundary condition. One case is considered as standard case and in addition to that case, 29 more cases are investigated with only one parameter different from the standard case. For example, for the case of considering impact of surface pressure, the case consists of a steel pipe at the depth of H=1D, with a full-bond interaction, shell thickness of 5 cm without any fluid inside the pipe. For this investigation, surface pressure changes from 200, 400, 550 to 700 kPa. All results are presented in the following sections and verified against predictions published in the existing literature. Results are presented in terms of impact on pipe deflection, soil surface settlement, stress in pipe wall and maximum earth pressure on pipe.

Validation - Comparison with empirical method

First the finite element model is validated considering vertical stress variation on pipe. The validation of pressure on pipe crown is performed through comparing numerical results with empirical. Based on Marston theory presented in Chapter 2 the pressure on a buried pipe in a semi-infinite elastic medium due to concentrated load at soil surface can be calculated. In addition, Boussinesq developed another equation which is shown in Equations 3-1 to calculate pressure in depth.

$$P_{total} = P_d + P_l = \gamma H + \frac{W}{H^2} \qquad 3\text{-}1$$

In the above equation, P_{total} is sum of the dead load and live load pressures. Dead load pressure, P_d, is a function of the density of the soil and soil depth, *H*. Live load pressure or P_l is a function of W representing wheel load, *H* representing soil depth cover and *L* is the width of loading or the tyre imprint (Moser, 2001). A standard *HS-20* truck is assumed to apply a uniform contact pressure of 750 kPa on a road surface to simulate a highway load of a 20-ton truck (Austroads, 2012). If a 5 cm layer of asphalt is taken into consideration, the maximum applied stress on the soil surface would be reduced to 550 kPa. *W* in above equation is a concentrated load due to soil surface pressure of 550 kPa over the length of B=50 cm considering each wheel has imprint length of 50 cm or 20 inch (AASHTO, 1998). A comparison of two methods, i.e., the empirical and finite element is presented in Figure 3-10. Overall, the results obtained using two methods are consistent and both graphs follow the same pattern. Similar results from literature are also presented in Figure 2-7 in the previous chapter

in which the impact of live load due to truck was calculated using same method. However, results in Figure 3-10 shows that the vertical pressure on the pipe is almost higher using the finite element method for shallower depths, compared to the empirical solution. This difference can be due to the different assumptions made in two methods. For example, in the empirical method soil is assumed to be elastic while in the finite element method, soil shows elasto-plastic behaviour. In addition, the effect of lateral earth pressure is not considered in the empirical method, while in nature and in the finite element method, soil is not classified as an isotropic and homogenous material. In the following section, the impact of each factor on model response is investigated and results are presented in the following sections.

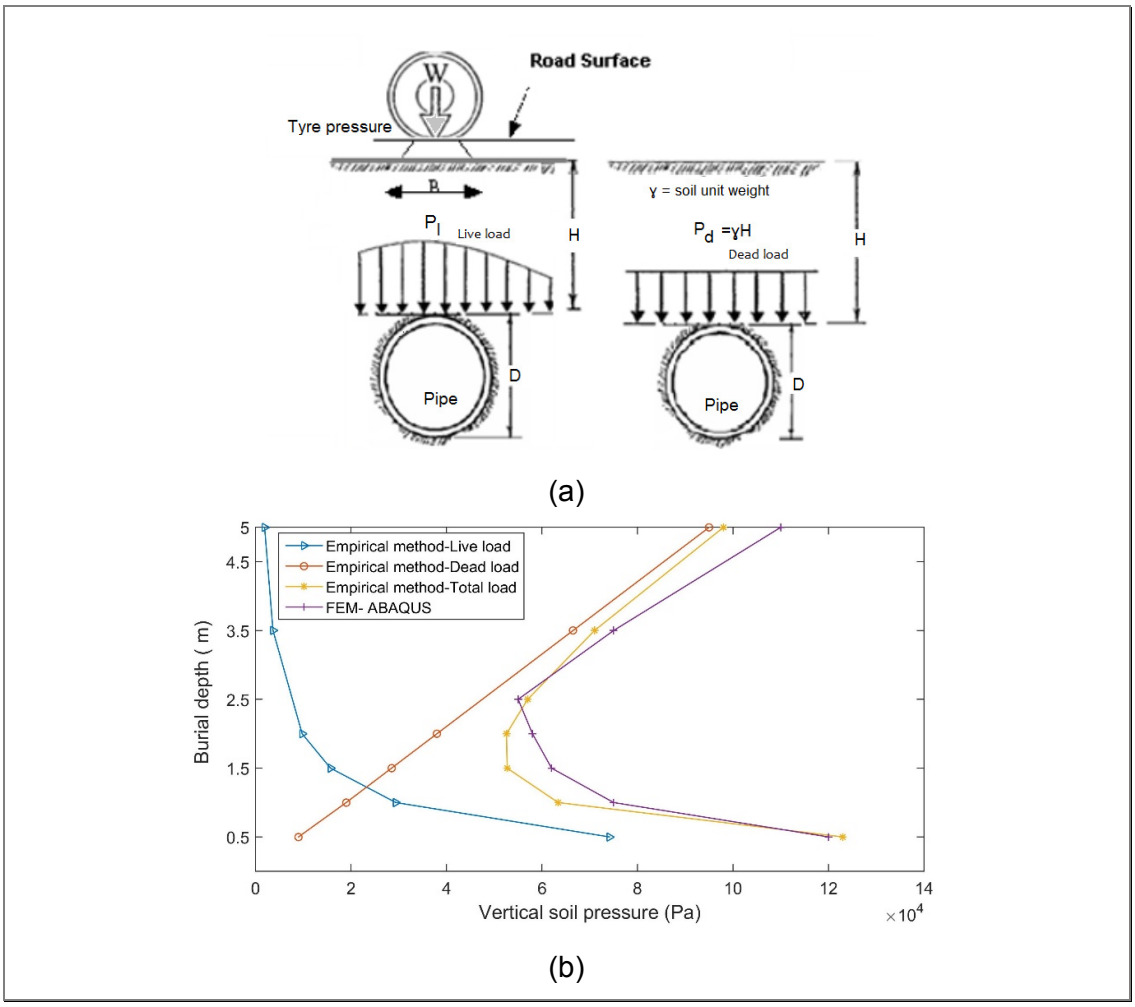

Figure 3-10 (a) Graphic view of pipe and soil subjected to live and dead load based on (ASCE, 2009) (b) comparison of two methods and validation of finite element method

3.2.2.1 Burial depth effect

In this section, the effect of burial depth on a steel buried pipe with surface pressure 550 kPa is investigated. The effect of burial depth variations on pipe deflection, soil surface settlement, stress in pipe wall and pressure on pipe crown is studied. In these

cases, the interaction between pipe and surrounding soil is fully bonded and there is no fluid in the pipe and loading area is at maximum or α=2D. Typical contour plots for predicted model are presented in Figure 3-11. It should be noted that output variable *U* illustrates the displacement of nodes in mm or soil surface settlement. The figures are relevant to burial depths of 1, 1.5 and 3.5 D. It can be seen that increasing burial depth increases soil surface settlement. The reason can be due to compressibility of soil above the pipe crown. With increasing the embedment depth, the thickness of the compressible layer over the pipe would increase. It means that the more the burial depth is, the higher total void above the pipe is. In addition, with increasing burial depth, pipe deflection decreases.

Results of burial depth impact on pipe deflection, soil surface settlement, stress on pipe wall and earth pressure on pipe crown are presented in Figure 3-12-a to d. Overall, for a burial depth of H/D=1, surface settlement is at its minimum, and increasing H/D increases soil surface settlement. Pipe deflection, stress on pipe wall and earth pressure on pipe crown is maximum when burial depth is minimum. In addition, the impact of burial depth in reducing pipe deflection, increasing soil surface settlement, and reducing stress and pressure on pipe is less significant for H>2.5D. Figure 3-12-a illustrates the crown deflection of the pipe at six different burial depths under surface pressure of 550 kPa. It can be seen that increasing burial depth from H/D=1 to H/D=5, decreases pipe deflection from 0.05% to 0.02%. The impact of change in burial depth on soil surface settlement is illustrated in Figure 3-12-b. It is evident when burial depth is minimum, soil surface settlement is minimum. With increasing depth of embedment from 1 to 5, the surface settlement increases from 7 to 10 cm. As mentioned above this can be due to compressibility of soil above the pipe crown and increasing the burial depth, the thickness of the compressible layer over the pipe increases and soil settles more. Change in stress on pipe wall is illustrated in Figure 3-12-c. As illustrated, stress on pipe is maximum when burial depth is minimum. The impact of burial depth on earth pressure on pipe crown is illustrated in Figure 3-12-d. As shown, increasing burial depth from 1 to 5 reduces earth pressure on pipe from 250 to 100 kPa. It means the impact of live load is more important for pipe buried in shallower depths. These results are consistent with results obtained in literature. In the study conducted by Moghaddas the behaviour of a buried pipe was investigated under cyclic load using an experimental approach (Moghaddas Tafreshi & Khalaj, 2011). The result of this research showed that increasing burial depth leads to an increase in soil surface settlement and a decrease in pipe deflection. However, in that research impact of burial depth on other factors such earth pressure on pipe and stress on pipe has not investigated.

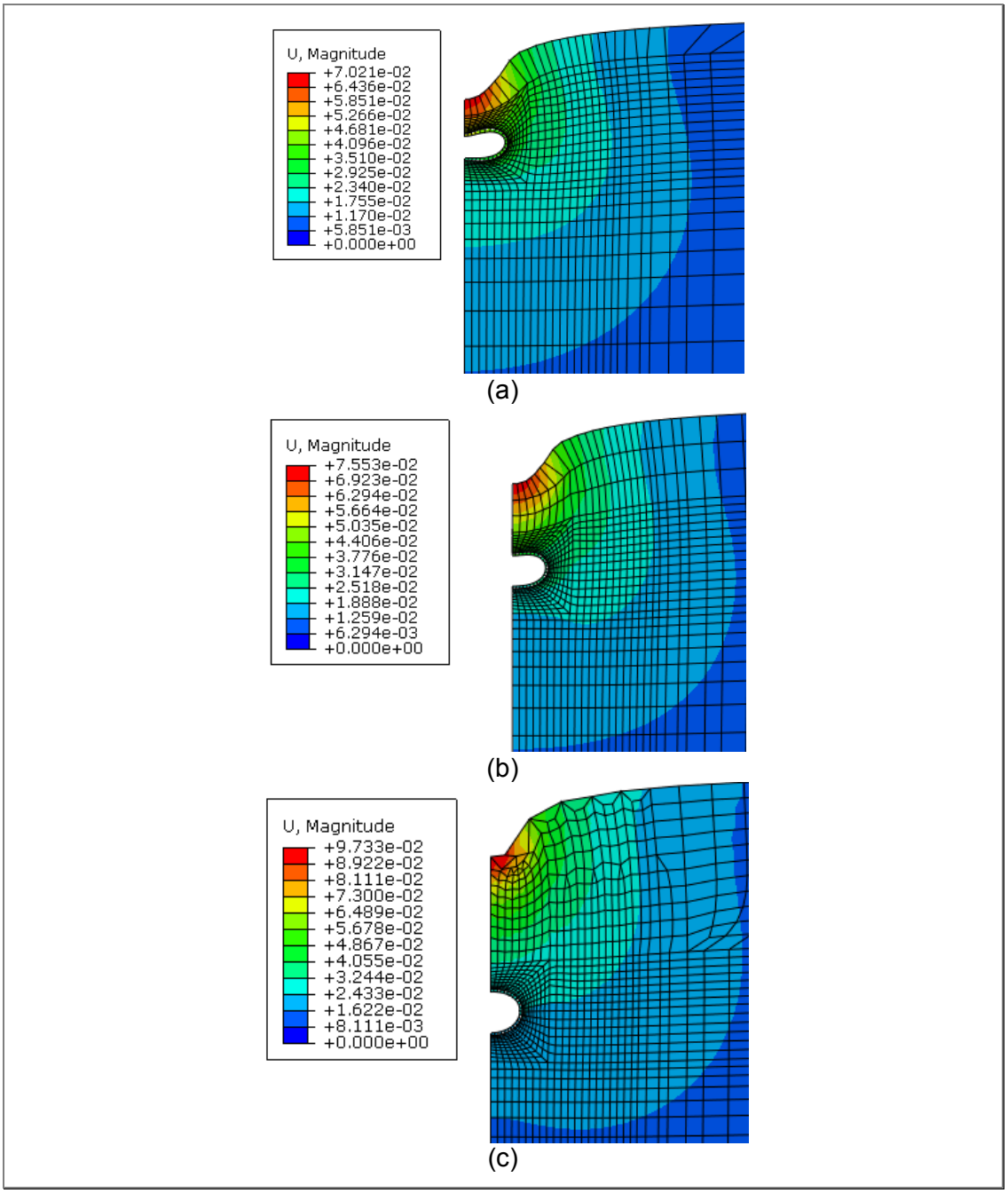

Figure 3-11 Impact of burial depth on soil surface settlement contours (a) H=1D (b) H=1.5D (c) H= 3.5D

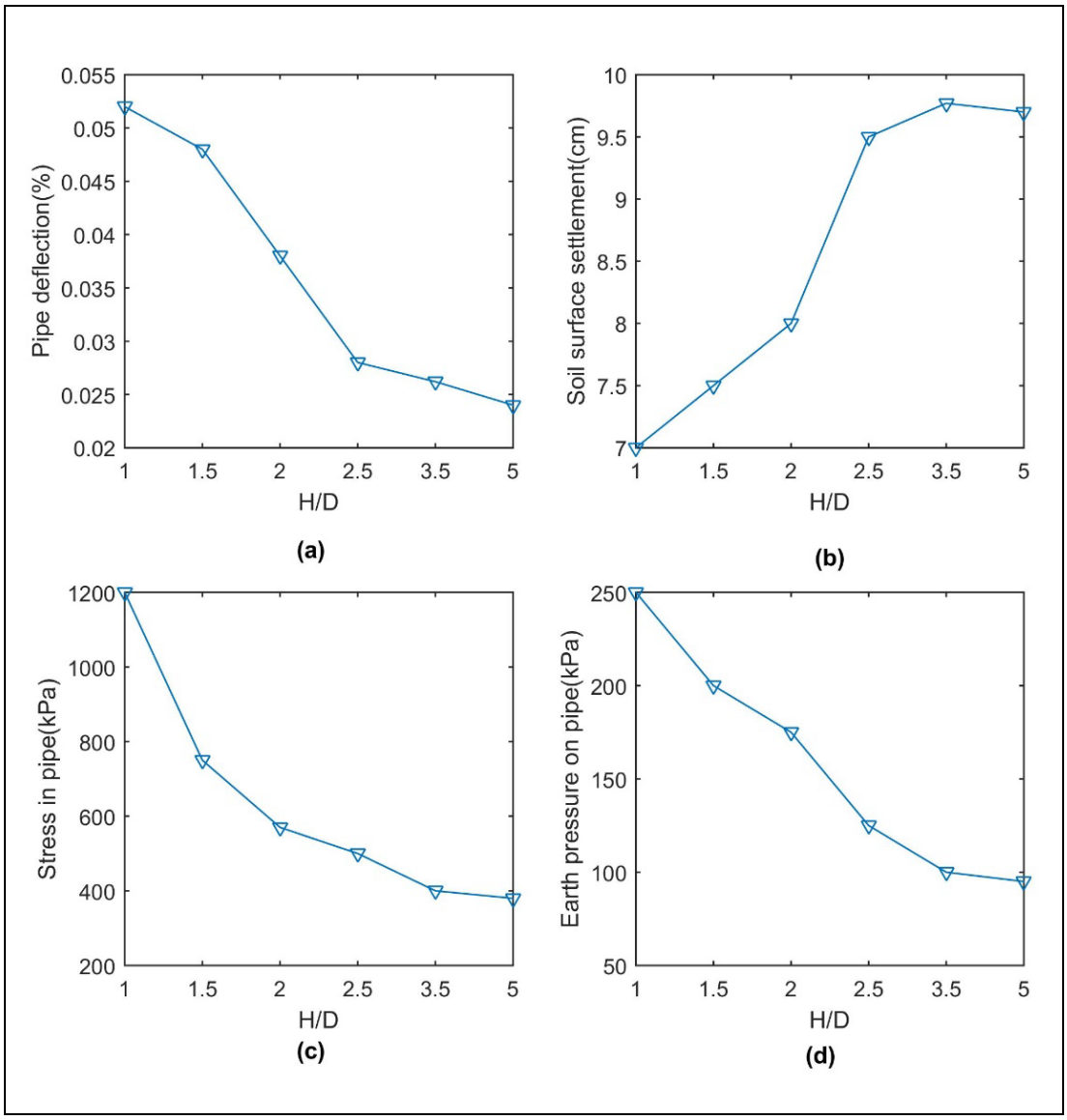

Figure 3-12 Burial depth impact on (a) pipe deflection (b) maximum soil surface settlement (c) maximum stress in pipe (d) maximum earth pressure on pipe

3.2.2.2 Effect of surface pressure

The effect of surface pressure on pipe-soil interaction and soil surface settlement was analysed and results are discussed in this section. To investigate the influence of surface pressure, the numerical model was executed with full-bonded interface and maximum loading area with burial depth of H=1D under surface pressures of 200, 400, 550, and 700 kPa. The results are presented in Figure 3-13.

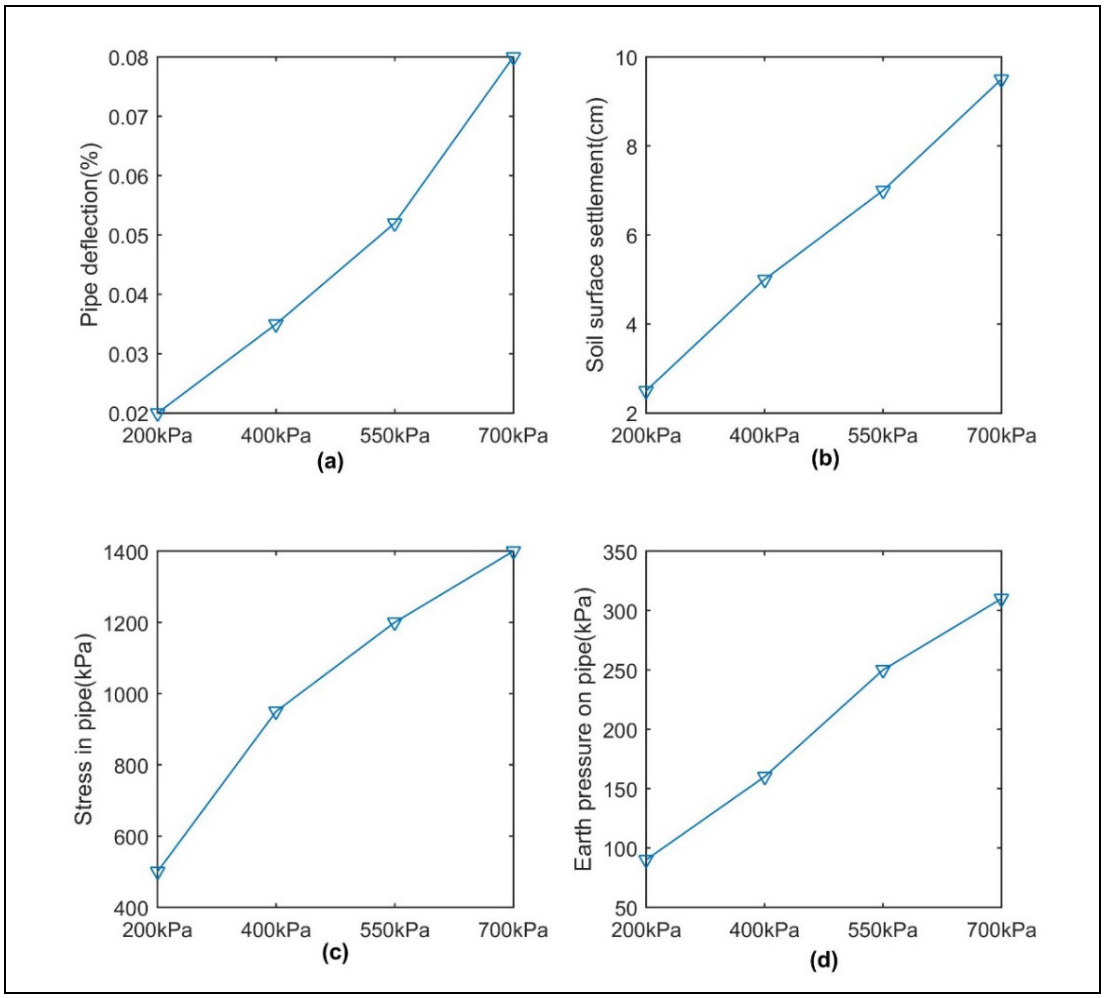

Figure 3-13 Surface pressure impact on (a) pipe deflection (b) maximum soil surface settlement (c) maximum stress in pipe (d) maximum earth pressure on pipe

The results indicate that increasing surface pressure increases pipe deflection, soil surface settlement, stress in pipe wall and pressure on pipe crown as expected. For example, increasing traffic load from 400 to 700 kPa leads to increase in pipe deflection from 0.032 to 0.08; soil surface settlement from 5 to 9.5 cm, stress on pipe wall from 950 to 1400 kPa and increase of earth pressure from 165 to 320 kPa. It means increasing surface pressure by 75%has an important impact on observed value and leads to 150% increase of pipe deflection, 90% increase of soil surface settlement, 47% increase of stress in pipe and 93% increase of earth pressure on pipe. The impact of load on pipe deflection and soil surface settlement was studied in a research performed by Moghaddas (Moghaddas Tafreshi & Khalaj, 2011). The results in this research are consistent with those reported by Moghadas Tafreshi. In this research, impact of loading surface variation on other factors such as stress on pipe and earth pressure variations has not been studied and the pipe type was flexible HDPE.

3.2.2.3 Effect of loading area

The effect of loading area on pipe-soil interaction is analysed in this section. α/D has the value of 0.5, 1 and 2 in which D is diameter of pipe as illustrated earlier in Figure 3-14. Selecting of α is related to the vehicle load for simulating traffic on the road and this factor depends on traffic flow and road usage. For example when an H-20 loading is designed to simulate a highway load of a 20-ton truck, the concentrated load is applied on two 18-in by 20-in areas (45 by 50 cm). This means for a 20-ton truck load over a one-meter diameter pipe, the α/D will be 0.5.

The influence of loading area was analysed and results are illustrated in this section. Increasing loading area from 0.5 to 2 increases pipe deflection from 0.018% to 0.057%, increases soil surface settlement from 3 to 7 cm, increases pipes stress from 680 to 1200 kPa and increases earth pressure from 100 to 250 kPa as shown in Figure 3-14-a to d, respectively. Overall increasing loading area from 0.5 to 2 leads to increase of 217%, 133%, 150% and 76% in the pipe deflection, soil surface settlement, stress in pipe and pressure on pipe respectively.

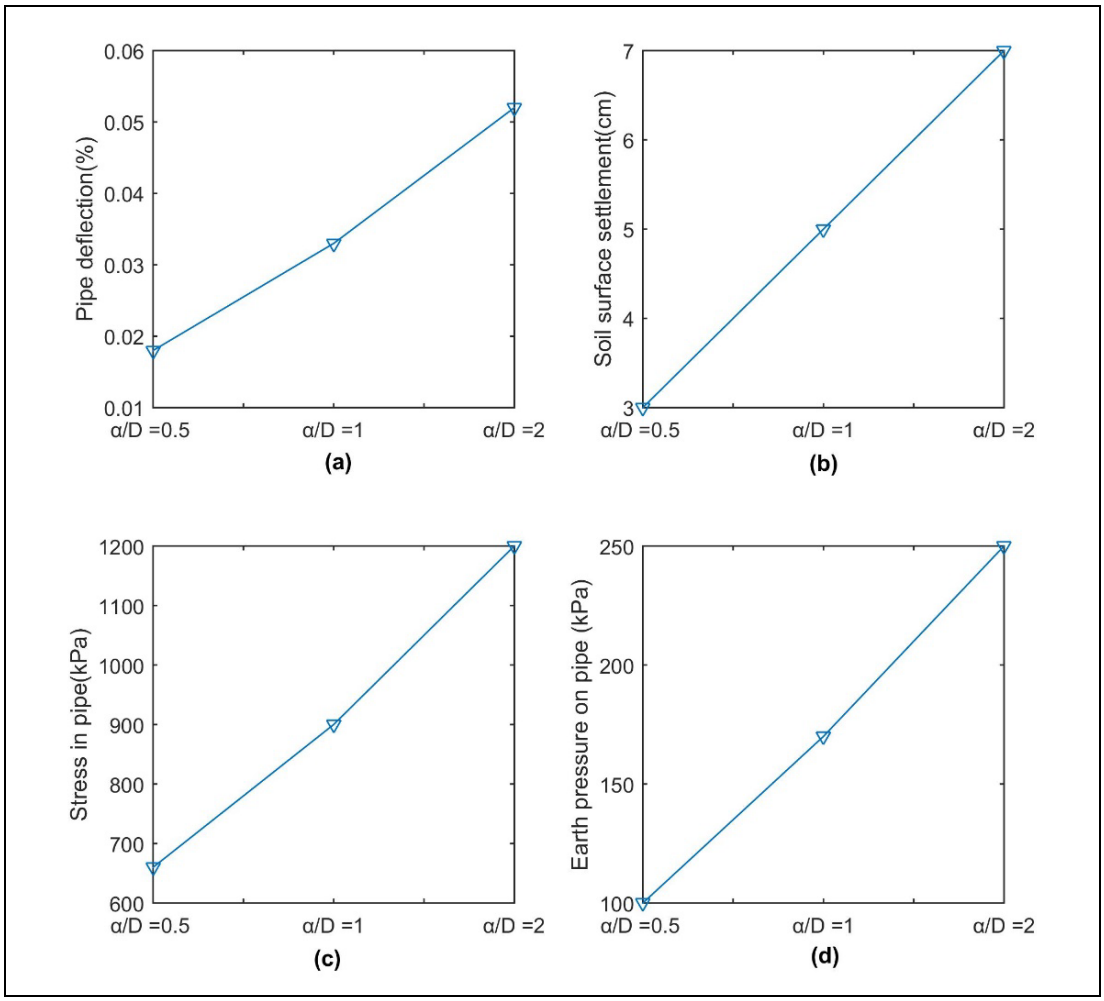

Figure 3-14 Loading area impact on (a) pipe deflection (b) maximum soil surface settlement (c) maximum stress in pipe (d) maximum earth pressure on pipe

3.2.2.4 Effect of internal pressure

This section investigates the performance of buried pipelines subjected to a surface load with regard to internal pressure effect. It was assumed that the same nominal pipe diameter of 1 m is positioned at the shallowest depth of H/D=1 and is subjected to 550 kPa surface pressure. The influence of internal fluid pressure was investigated under a surface pressure of 550 kPa. It was assumed that the fluids in the pipe are water and gas which induce internal pressures of 414 and 7500 kPa, respectively. The effect of three different internal pressures on crown deflection, soil surface settlement, pressure on pipe wall and maximum earth pressure on pipe was investigated. It should be noted that thickness of steel pipe has been increased to 10 cm to apply gas pressure on shallow burial depth because the calculations were stopped due to failure of pipe with thickness of 5 cm. Pipe thickness should be chosen on the basis of internal pressure, and then an engineering analysis is made to ensure the chosen pipe will withstand the external loads (Moser, 2001).

The results of internal pressure impact on pipe deflection variation are illustrated in Figure 3-15-a. It can be seen from the figure that deflection of an empty pipe is 0.047% while after applying internal pressure of water and gas this value decreases to 0.045% and 0.04%, respectively. Applying internal pressure, however, reduces soil surface settlement. The surface settlement drops from 6.85 cm to 6.45 cm as shown in Figure 3-15-b illustrating 6% decrease in surface settlement which means impact of internal pressure on soil surface settlement is not significant. Applying internal pressure in pipe leads to an increase of stress on pipe from 600 to 1200 kPa on pipe crown or 100% increase in stress on pipe wall. According to the diagram, applying internal pressure causes an increase in the maximum stress value in pipe. The higher the internal pressure is, the higher the stress on the pipe occurs as illustrated in Figure 3-15-c. The stress distribution impact of internal pressure on earth pressure on pipe is shown in Figure 3-15-d. As shown in the graph, earth pressure on pipe increases from 350 to 400 kPa or 14% increase in earth pressure on pipe.

These results are consistent with the results found by Shaalan. In their research the effect of three fluid pressures on steel pipeline was investigated using PLAXIS 2D program software (Shaalan, 2014). They concluded that increasing the internal pressure leads to a decrease in pipe crown displacement for shallower burial depths H/D≤3 although this decrease was not significant. In this research, however, impact of internal pressure variations on other factors such as surface settlement or stress on pipe has not been investigated.

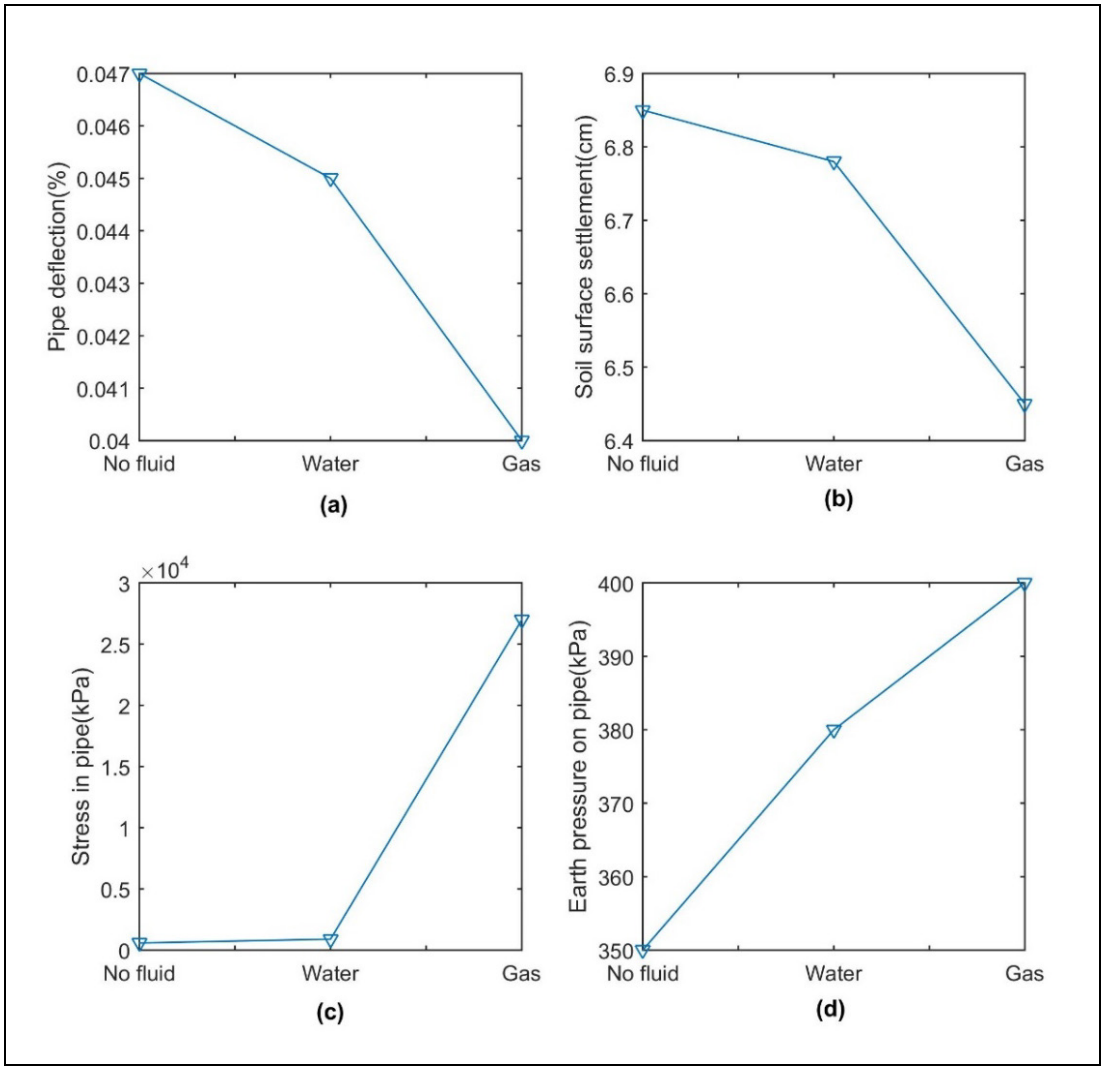

Figure 3-15 Effect of internal pressure on (a) vertical crown deflection (b) soil surface settlement (c) maximum stress in pipe (d) maximum earth pressure on pipe

Impact of internal pressure on stress distribution along pipe is graphically illustrated in Figure 3-16. As shown in Figure 3-16-a, when there is no fluid the maximum stress in pipe is happening at spring-line of pipe. However, maximum stress happens on invert and crown of pipe when considering the impact of internal pressure as illustrated in Figure 3-16-b and c. This shows stress distribution pattern is very different for pipe with or without fluid pressure.

Stress distribution along pipe circumference for two cases of pipe without fluid is illustrated in Figure 3-17. As shown in the graph, the maximum stress happens in the middle part of pipe when there is no fluid. The minimum stress happens in the middle part of pipe when considering the impact of fluid. However maximum stress is happening at pipe invert while there is internal pressure and minimum stress at the same position when there is no internal pressure.

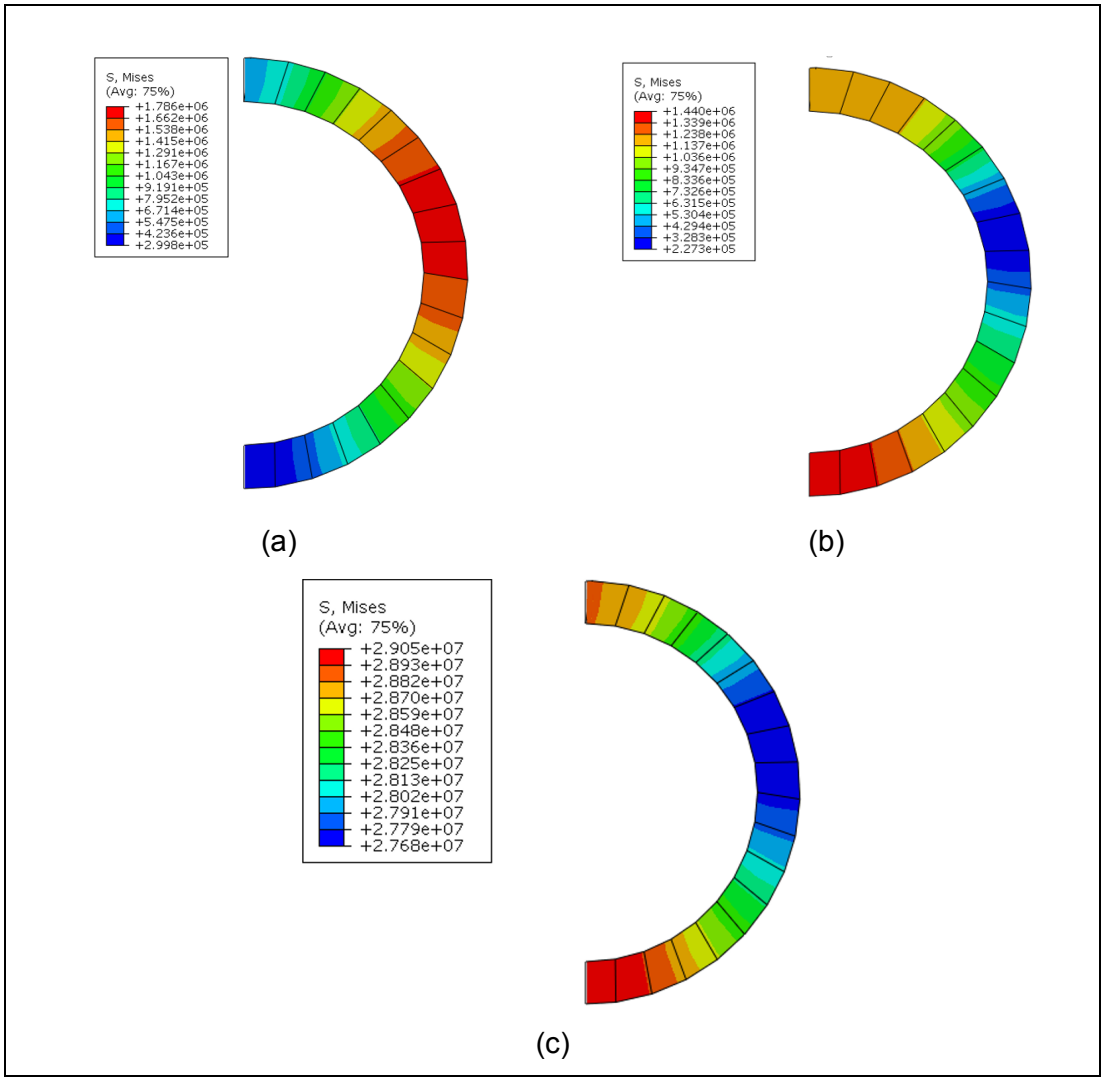

Figure 3-16 Internal pressure effects on pipe displacement (a) without fluid (b) water pressure (c) gas pressure

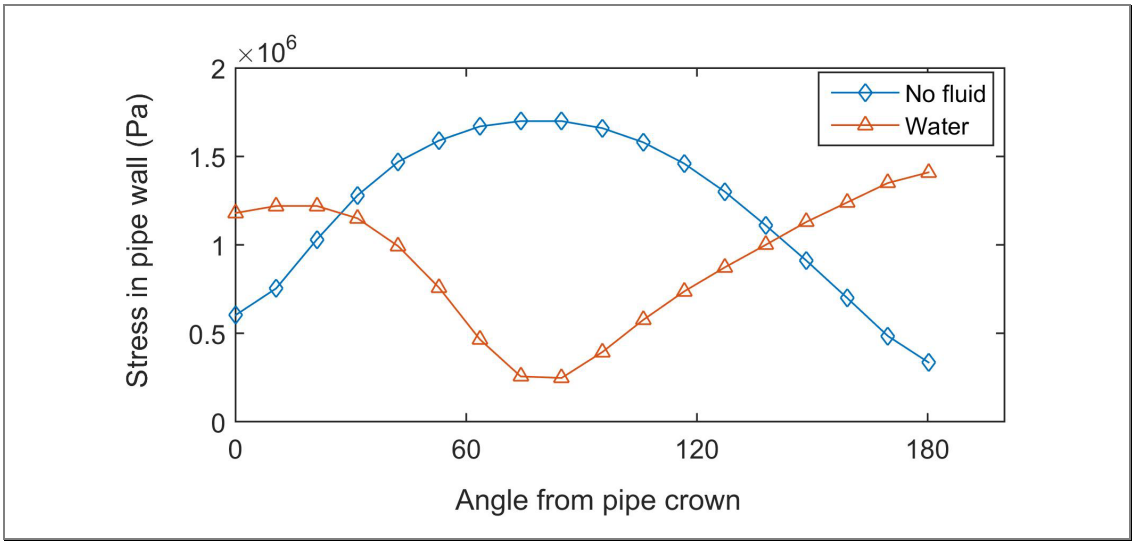

Figure 3-17 Change in stress distribution at the pipe interface due to fluid pressure

3.2.2.5 Effect of friction coefficient

To investigate the impact of interaction coefficient value on model response, the numerical model was executed with different interaction coefficient of 0.1, 0.3, 0.5, 0.9 and full-bonded interaction. Results indicate that friction coefficient variation has minor effect on pipe deflection. As illustrated in Figure 3-18-a pipe deflection is not affected by interface conditions significantly. Pipe deflection drops from 0.055% for friction coefficient of 0.1% to 0.051% for a full-bonded case. Increasing interaction coefficient reduces soil surface settlement although this reduction is negligible. As shown in the graph, soil settlement drops from 7.6 cm for friction coefficient of 0.1 to 7 cm for full-bonded interaction. Stress in pipe also is reduced with increasing interaction coefficient and it drops from 2000 to 1100 kPa with increasing the interaction coefficient from 0.1 to full-bonded interaction. And finally maximum earth pressure on pipe decreases from 350 to 260 kPa with increasing friction coefficient from 0.1 to fully bonded interaction.

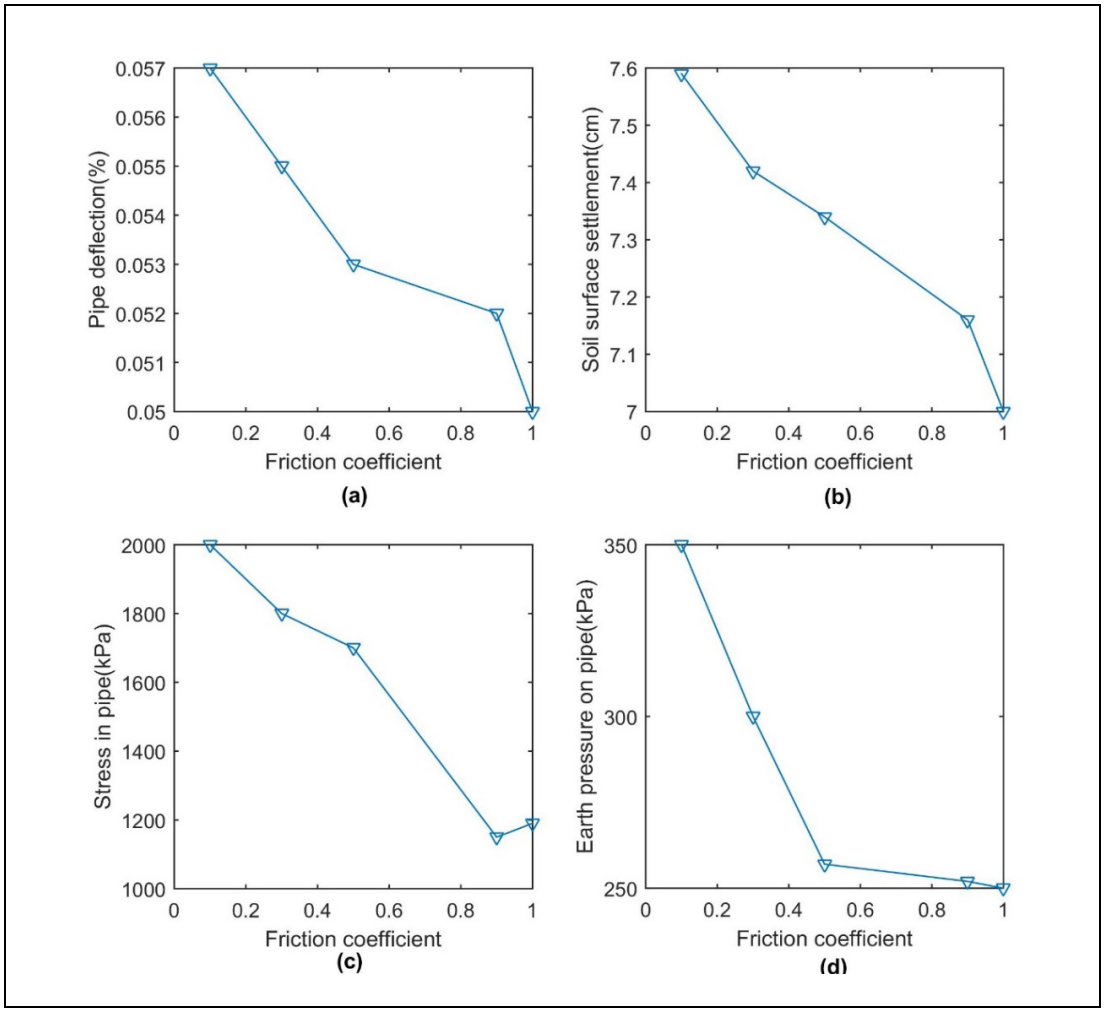

Figure 3-18 Effect of friction coefficient on (a) vertical crown deflection (b) soil surface settlement (c) maximum stress in pipe wall (d) maximum earth pressure on pipe

The results of pipe deflection are consistent with the results from another study in which the effect of interaction on deflection of a concrete pipe was investigated using ABAQUS (Kararam, 2010) . It was shown in that study that increasing friction coefficient from 0.1 to 0.9 leads to decrease in pipe deflection although this decrease was too small. The impact of other parameters was not investigated in their study.

To compare the effect of interface conditions along pipe boundaries, the influence of the friction coefficient of 0.5 is compared with those for full-bonded conditions and results are presented in Figure 3-19. The effect of two interface conditions on pipe displacement is illustrated in Figure 3-19-a. As illustrated, with increasing the angle from 0 to 60 degrees, pipe displacement drops from almost 5.5 cm to 2.5 cm. After this point with increasing angle from 60° to 120° pipe displacement remains steady at 2.5 cm. Then by increasing the angle to 180° pipe displacement reduces to 1.0 cm.

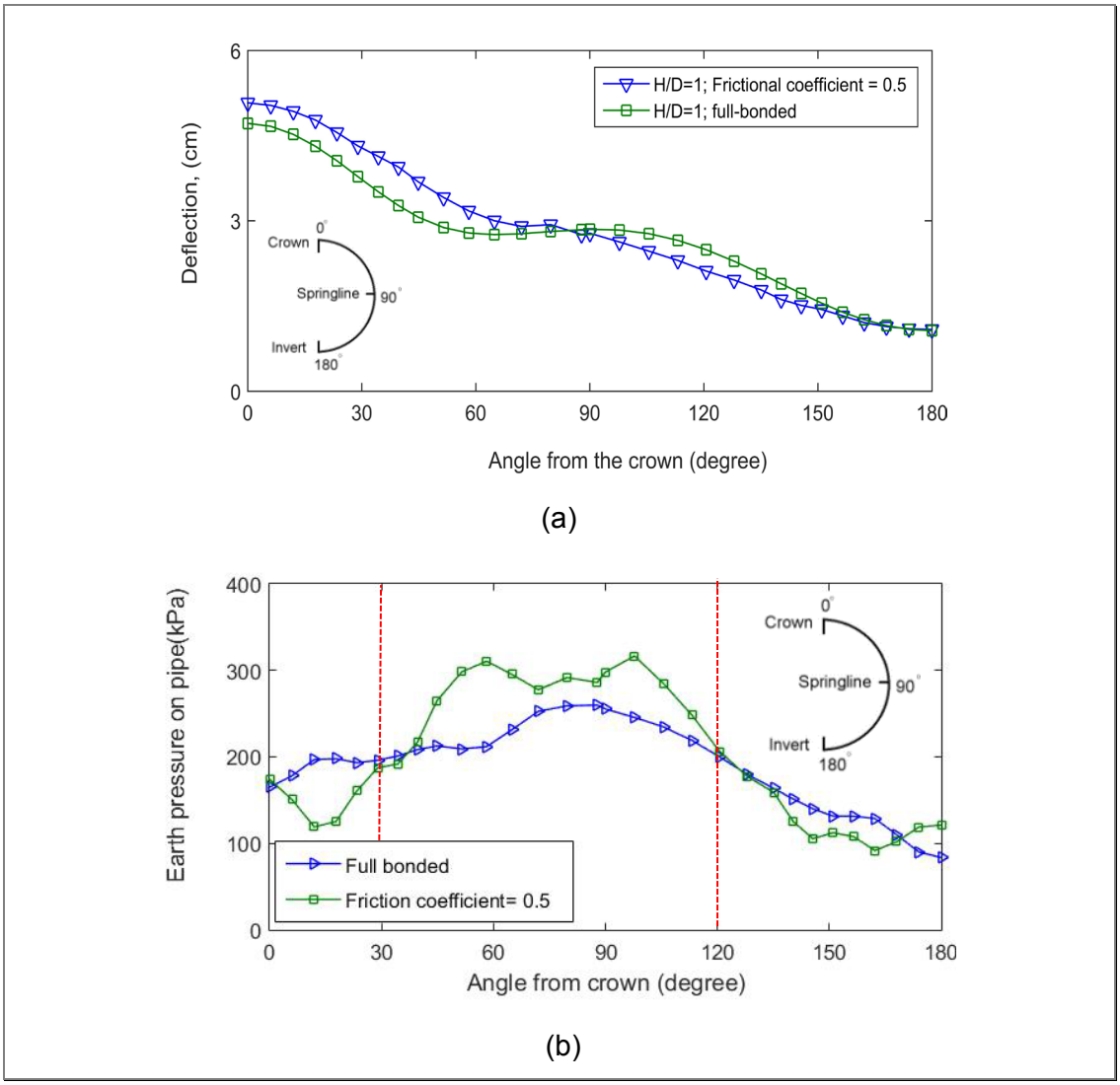

Figure 3-19 Effect of interface conditions along pipe circumference on (a) pipe displacement (b) stress distribution

Overall, the pipe displacement decreases with increasing the angle. However, the effect of friction coefficient value on pipe deflection is higher at pipe crown. Higher values are observed for friction coefficient of 0.5 between 0 to 60 degrees angle from pipe crown. With increasing the angle along pipe circumference the gap between the two graphs decreases.

The effect of interaction properties on earth pressure distribution on pipe as a function of angle from crown is illustrated in Figure 3-19-b. In this figure there are three different sections. Left and right sections demonstrate that earth pressure of full-bonded interaction is higher than those with friction coefficient of 0.5 while in the middle section full-bonded interaction has a lower pressure along the pipe. It should be noted that interaction properties almost has no impact on earth pressure value at crown and invert. Results presented here have a good agreement with those presented by (Yoo & Kang, 2007).

3.2.2.6 Effect of pipe wall thickness

This section investigates the effect of wall thickness on model response by considering three pipe thicknesses of 2, 5 and 10 cm. The effect of pipe thickness variations on pipe deflection, soil surface settlement, stress in pipe wall and pressure on pipe crown is studied. In these cases, the interaction between pipe and surrounding soil is full-bonded and there is no fluid in the pipe and loading area is at maximum or α=2D. Pipe also is buried at H=D under surface pressure of 550 kPa. Surface settlement contours for two cases of 2 and 10 cm pipe thickness are illustrated in Figure 3-20. According to the figures, increasing pipe thickness leads to decrease in soil surface settlement from 7.02 to 6.87 cm. In addition, the pipe deflection decreases with increasing pipe thickness.

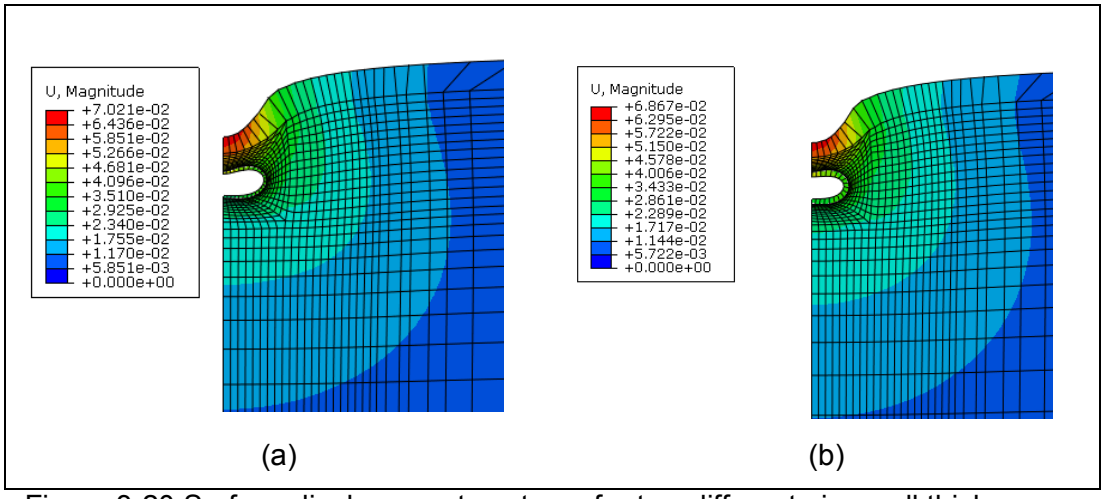

Figure 3-20 Surface displacement contours for two different pipe wall thicknesses (a) 2 cm (b)10 cm

The impact of pipe thickness ratio on different parameters has been analysed and the results for different cases are illustrated in Figure 3-21. It can be seen that increasing pipe thickness from 2 to 5 and 10 cm reduces pipe deflection from 0.6% to 0.052% and 0.045%, respectively. As illustrated earlier in Figure 3-20, increasing pipe thickness reduces soil surface settlement. Similar results are illustrated in Figure 3-21-b. Increasing pipe thickness from 2 to 10 cm reduces soil surface settlement from 7.55 to 6.9 cm, i.e., increasing pipe thickness by 5 times leads to 6.9% reduction in soil surface settlement. As illustrated in Figure 3-21-c, stress in pipe due to change in wall thickness from 2 to 10 cm leads to reduction of stress in pipe dropping from 3000 to 600 kPa. In other words, stress in pipe has 83% reduction in stress around pipe. Increasing pipe thickness from 2 to 10 cm however increases earth pressure in pipe from 230 to 360 kPa showing 44% increase in earth pressure due to wall thickness increase as shown in Figure 3-21-d.

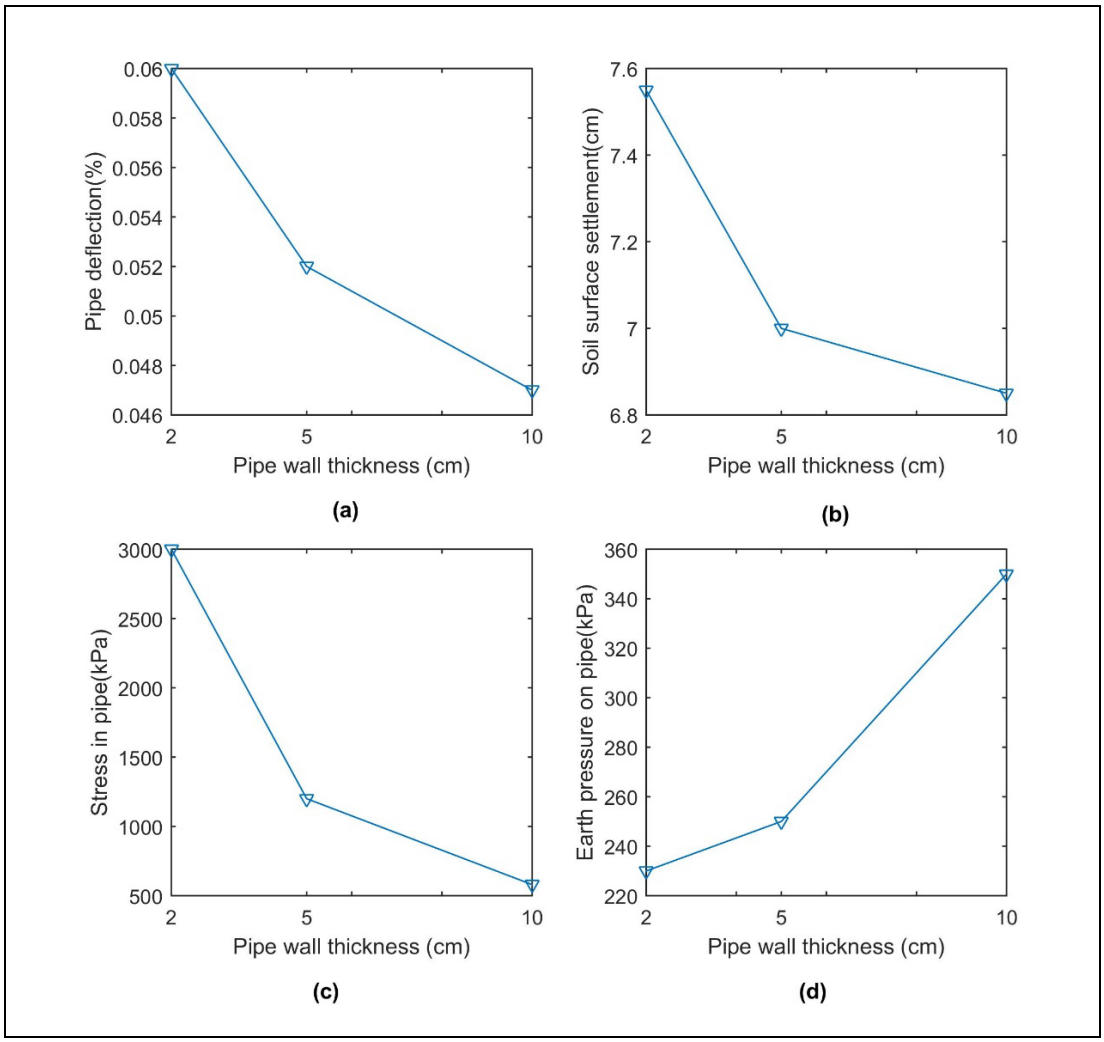

Figure 3-21 Pipe wall thickness impact on (a) vertical crown deflection (b) soil surface settlement (c) maximum stress in pipe (d) the maximum earth pressure on pipe

Pipe stiffness refers to the resistance to deflection. The higher a pipe's wall thickness, the higher is its stiffness and therefore its ability to resist external bending. In addition, the stiffness of the pipe and the stiffness of the soil work in together to resist the load from soil. Future studies however is recommended to investigate the association between wall thickness and earth pressure on pipe.

The same procedure was repeated for 3D model with different element types. or with shell elements of S4R. The results of two pipe wall thicknesses of 5 and 10 cm are shown in Figure 3-22 and Figure 3-23. The results of displacement and stress contours reveal that more displacement and stress on pipe occur when pipe has a smaller thickness as shown in Figure 3-22. For example, Figure 3-22-a shows pipe displacement for pipe thickness of 5 cm is 5.9 cm. However, this value for the thickness of 10 cm is 5.7 cm as illustrated in Figure 3-22-c. Figure 3-23 illustrates shell thickness impact stress and displacement distribution along pipe length at pipe-soil interaction. It can be seen that maximum crown displacement and stress on pipe wall occur in the middle part of the pipe alignment. These values for thinner pipe is higher along pipe pathway and difference between the two graphs are maximum in the middle of pipe when maximum displacement and stress occur.

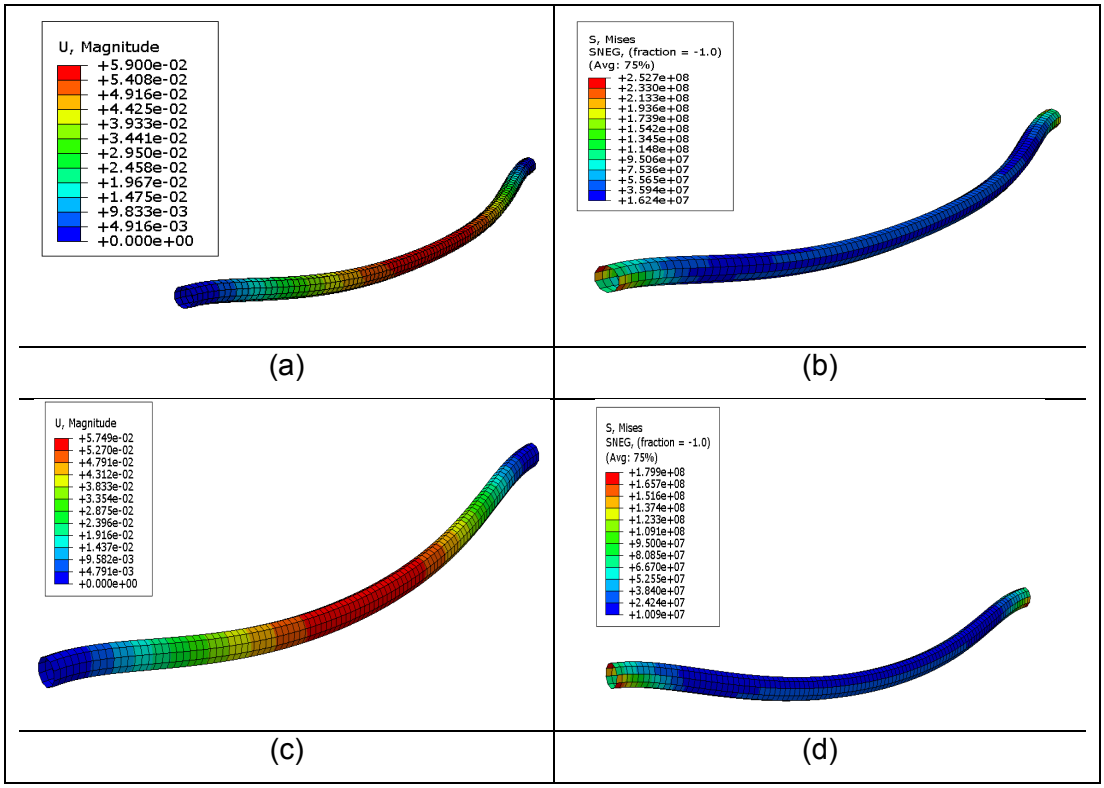

Figure 3-22 (a) Pipe displacement for t=5 cm (b) stress in pipe for t=5 cm (c) pipe displacement for t=10 cm (d) stress in pipe for t=10 cm (Mosadegh. & Nikraz., 2015)

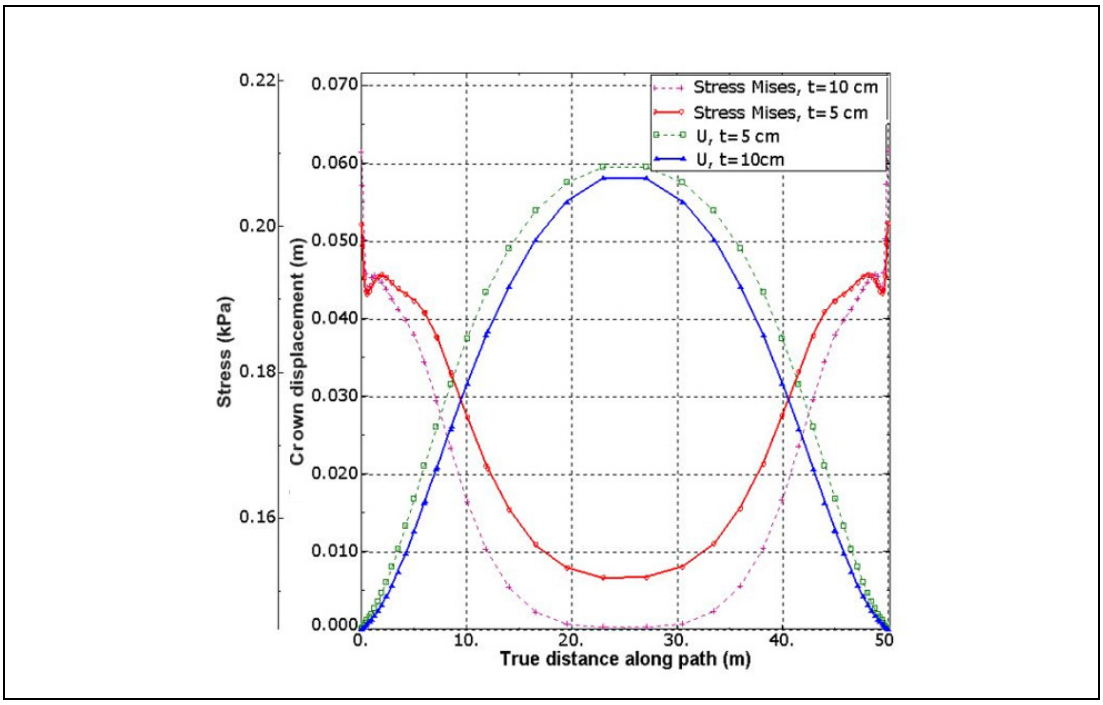

Figure 3-23 Effect of shell thickness on stress and displacement distribution

3.2.2.7 Pipe material properties

To illustrate the impact of pipe material property on model response, three types of pipe, HDPE, PVC and Steel are selected and results are illustrated in Figure 3-24. As shown in Figure 3-24-a, replacing steel with PVC and HDPE pipe increases pipe deflection from 0.05 to 0.052 and 0.06, respectively. It is noted ring deflection is a dimensionless parameter and is a function of stiffness ratio. pipe deflection is only function of E/E' ratio as all parameters except pipe properties remain unchanged. It should be noted that the elasticity modulus of steel is almost 250 times bigger than HDPE pipe. Also, the elasticity modulus of steel is 75 times that of PVC. Thus having lower Young's modulus and weaker pipe leads to increase in pipe deflection as expected. Replacing steel pipe with PVC and HDPE increases the pipe deflection and soil surface settlement as shown in Figures 3-24-a and b. Stress in pipe decreases by replacing steel pipe with PVC and HDPE and pipe can bear less induced stress (Figure 3-24-c). As illustrated in Figure 3-24-d maximum earth pressure on pipe increases in PVC and HDPE pipes comparing to steel pipe. Maximum earth pressure on pipe decreases from 250 to 200 and to 170 kPa by changing material from steel to PVC and from steel to HDPE pipe, respectively.

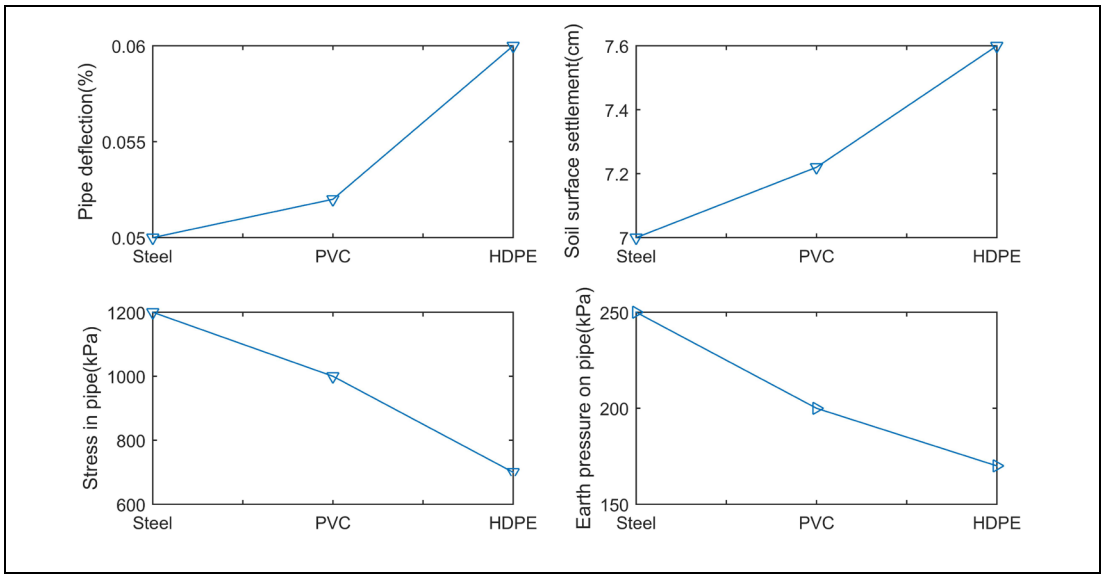

Figure 3-24 Material property impact on (a) vertical crown deflection (b) soil surface settlement (c) maximum stress in pipe (d) maximum earth pressure on pipe

These results are consistent with the results achieved by other researchers in the literature (Cao et al., 2016). They investigated the impact of concrete and high density polyethylene on soil surface settlement and it was shown in their experimental and numerical analysis that pipe type has an impact on soil surface settlement. However, they did not consider the impact of pipe type on stress distribution.

The impact of pipe material on pressure distributions is investigated in this research and results are shown in Figure 3-25. It can be seen that maximum earth pressure occurs in the middle part of pipe or between 60 and 120 degrees from the crown. On the crown however, earth pressure on pipe is maximum for steel and minimum for HDPE. Results also show that the variation of earth pressure along pipe circumference is maximum for HDPE pipe and minimum for steel pipe. For example, the earth pressure on pipe varies between 100 to 350 kPa for HDPE pipe and between 170 to 240 kPa for steel pipe. In a buried situation, the stiffness of the pipe and the stiffness of the soil work in together to resist the load from soil. Thus, a HDPE pipe with a lower stiffness goes under higher pressure and deformation from applied load which is consistent with results of deformations in which HDPE has the highest deformation among all pipes.

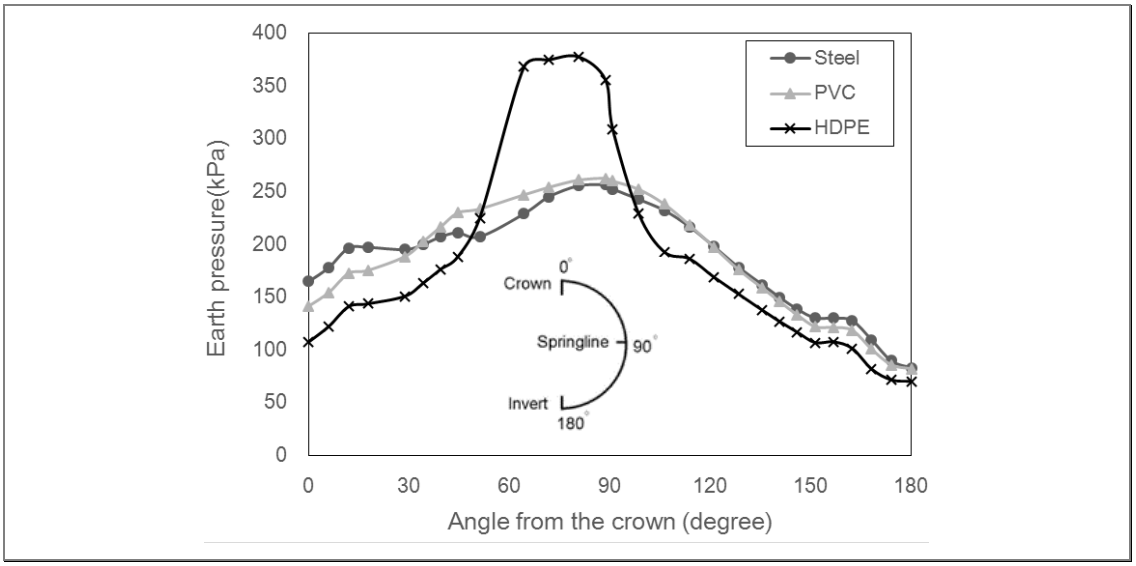

Figure 3-25 Earth pressure distribution along pipe circumference

3.2.2.8 Effect of boundary conditions

So far, all results presented in this chapter were analysed in a 2D plane strain model. Under the plane strain condition, it is assumed that the length of the pipe compared to its width is much higher. However, boundary conditions can be affected by any infrastructure existing on the pipe alignment, as shown in Figure 3-26. In addition, in analysing buried pipe soil behaviour in the laboratory it is important to investigate the best place to install strain gauge and pressure cell where the impact of boundary condition is minimum. To compare the effect of boundary conditions, a 3D model is built to analyse how boundary conditions can affect the stress and displacement distribution along the pipeline. Two types of boundary conditions at the end of pipeline are selected, roller and hinge representing infinite and finite length of the buried pipeline, respectively. For the hinge boundary the left and right hand parts of the model are restricted in movement due to these points while for the roller end there is no restriction in movement. As suggested in many standards, for simulating a pipe in the similar loading conditions, it is better to model pipe elements as a series of shell elements in 3D analysis. Three-dimensional brick elements are used to simulate the surrounding soil (C3D8R) and four-node reduced-integration shell elements (type S4R) are used for the pipe.

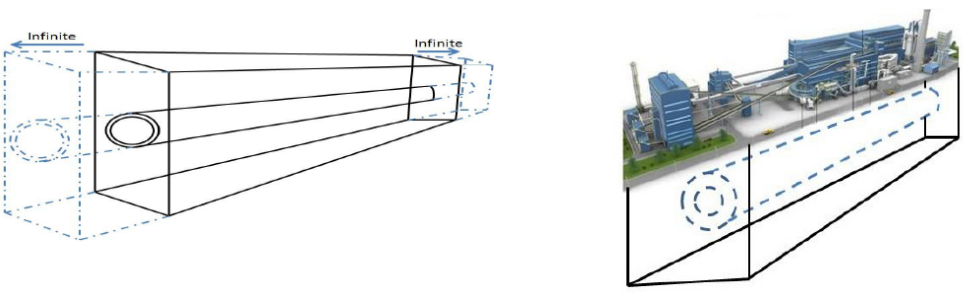

(a) (b)

Figure 3-26 Boundary condition (a) infinite length (b) finite length of buried pipe (Lee., 2010)

In Figure 3-27-a schematic displacement of pipeline for two boundary conditions are illustrated. For a hinge boundary condition, displacement at the pipeline ends is zero. This value increases to maximum by moving towards the middle of pipe. However for the roller boundary the displacement along the pipeline varies just between 5.3 and 5.42 cm. It is concluded that analysing pipe soil behaviour using plane strain conditions should be carried out with care. Existence of any infrastructure over the pipeline alignment can change the boundary conditions from roller to the hinge with restrained ends which cause significant variation of both stress and displacement along the pipeline.

Results in Figure 3-27-b show that at the ends of the pipeline for hinge boundary condition there is no displacement, while maximum stress occurs at these points. In addition, by moving towards the middle of the pipe, there is a downward deformation of 5.4 cm which is maximum in the middle of the pipe. There is a reduction in stress distribution of pipe and stress of the pipe falls from 204 to 160 kPa moving towards the middle of pipe. The results of stress and displacement distribution of pipe with a roller boundary are also shown in in Figure 3-27-b. As illustrated there is no significant change of stress and displacement along the pipeline length.

These results are consistent with those achieved in 2D analysis illustrated in Figure 3-19. For example, maximum crown displacement for pipe under 550 kPa surface pressure and 1 m burial depth is 5.4 cm in both analysis. Results also are consistent with the results achieved in the literature by Lee (Lee., 2010). It was shown in that research that the roller boundary condition at pipeline ends has less impact on both stress and displacement of pipeline.

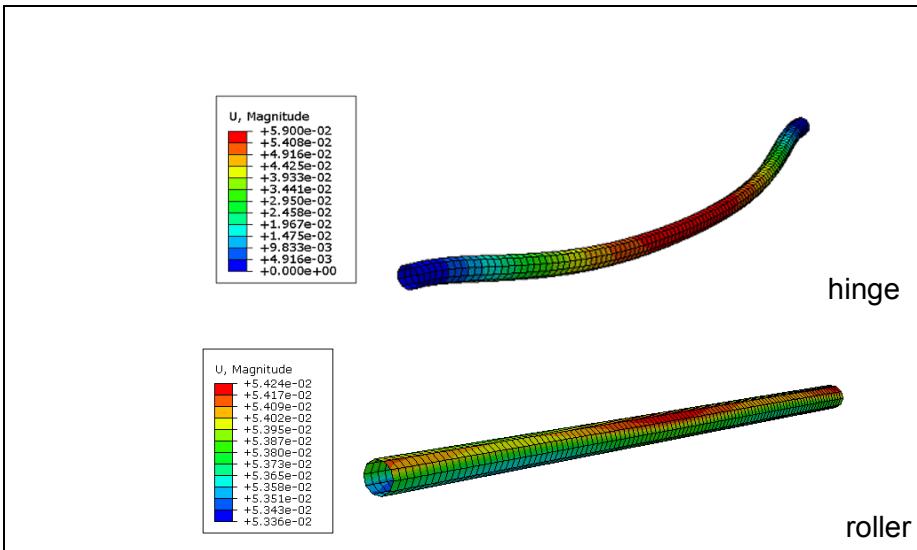

(a)

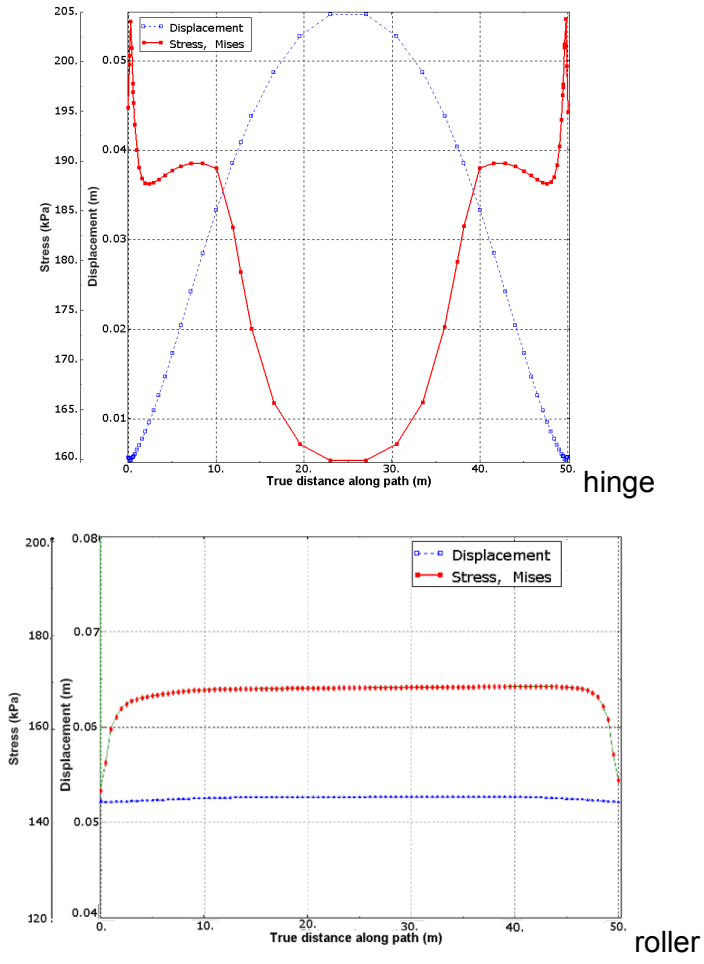

(b)

Figure 3-27 (a) Pipeline deformation according to two boundary conditions at pipeline ends (b) displacement and stress distribution along the length of a pipe with a roller and hinge boundary at the pipeline ends (Mosadegh. & Nikraz., 2015)

3.2.3 Evaluation of Results

The parametric study was conducted to investigate the influence of different factors on buried pipe response due to traffic implementing finite element method. The impact of eight parameters on pipe deflection, soil surface settlement, stress in pipe and earth pressure on pipe were analysed and results were presented in previous section. To provide a quick understanding of each factor impact on model response, all results are presented in the same figure. These graphs compare the impact of each parameter with other factors on model response. The horizontal axis represents the investigating cases and vertical axis represents change in four different examining parameters including pipe vertical deflection, soil surface settlement, stress on pipe wall and vertical earth pressure on pipe crown. Results are shown in Figure 3-28 to Figure 3-31.

Figure 3-28 illustrates the impact of all factors on pipe vertical deflection. It should be noted horizontal axis represents investigating factor. For example, number 1 on the horizontal axis represents case 1 which investigates impact of burial depth variation on model response which is also shown in the table close to Figure 3-28. Overall, case II or surface pressure has the highest impact on pipe vertical deflection variation ranging between 0.02 and 0.08. Case V or change in interaction coefficient value has the minimum impact on pie vertical deflection variation ranging between 0.04 and 0.05 only.

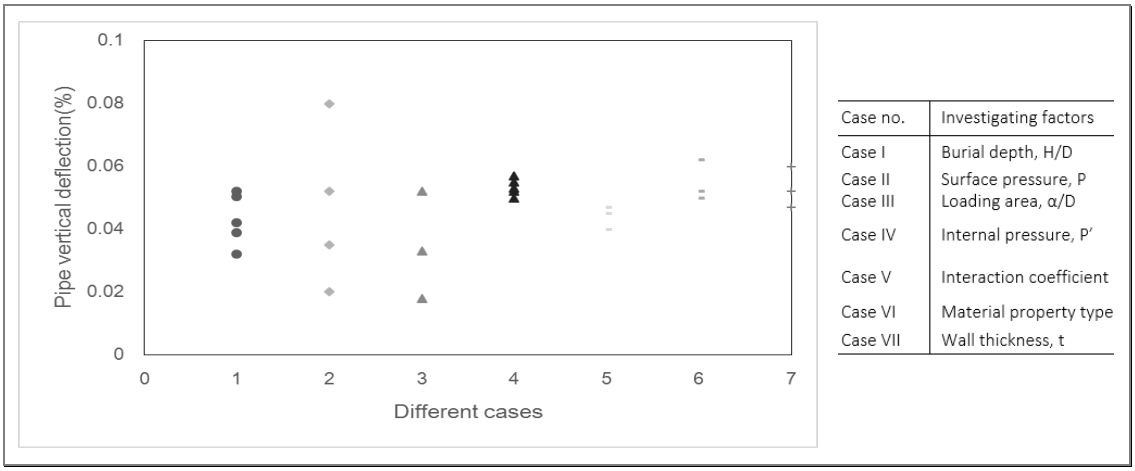

Figure 3-28 Comparing impact of all parameters on pipe deflection

Figure 3-29 illustrates the comparison of all seven cases impact on soil surface settlement. The effect of surface pressure is the most significant and soil surface settlement varies between 2 cm and 10 cm by surface pressure variation. However, friction coefficient has the lowest impact and soil surface settlement is not affected significantly by change of interaction coefficient.

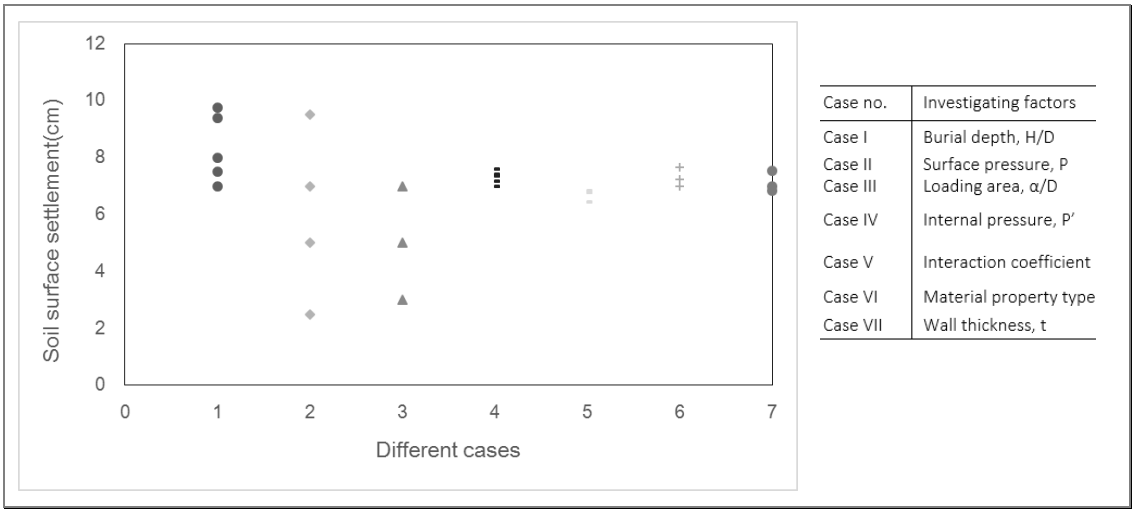

Figure 3-29 Soil surface settlement variation versus all seven cases

The results of parametric study on stress induced in pipe wall are illustrated in Figure 3-30. As can be seen internal pressure has the highest impact on stress in pipe compared to other parameters. Impact of other parameters is not significant comparing to internal pressure impact.

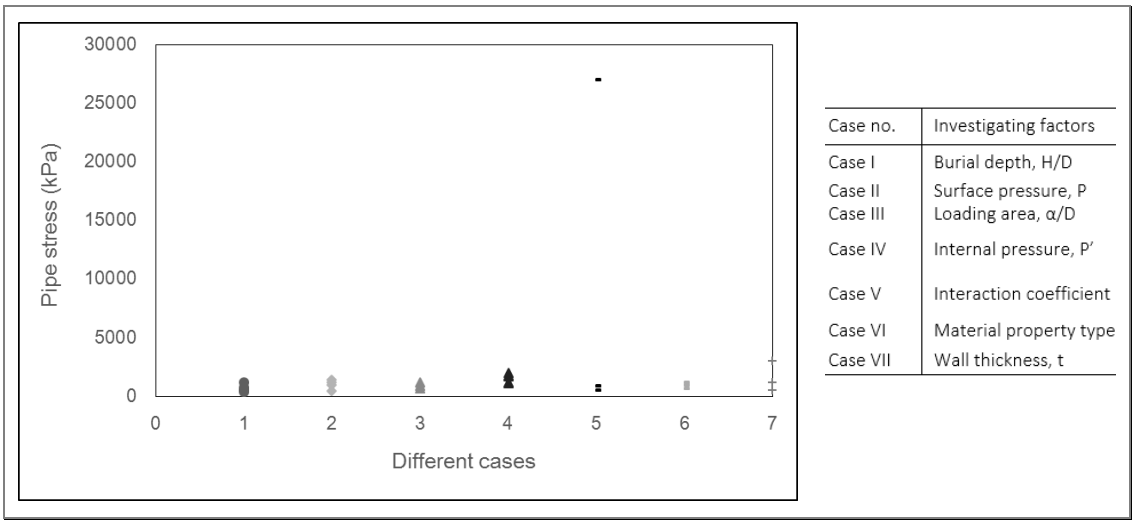

Figure 3-30 Stress in pipe versus all seven cases

The impact of each parameter on earth pressure variation around the pipe is illustrated in Figure 3-31. It is evident that amongst all parameters surface pressure, burial depth and loading area has the highest impact on pressure around the pipe and interaction coefficient has the lowest impact.

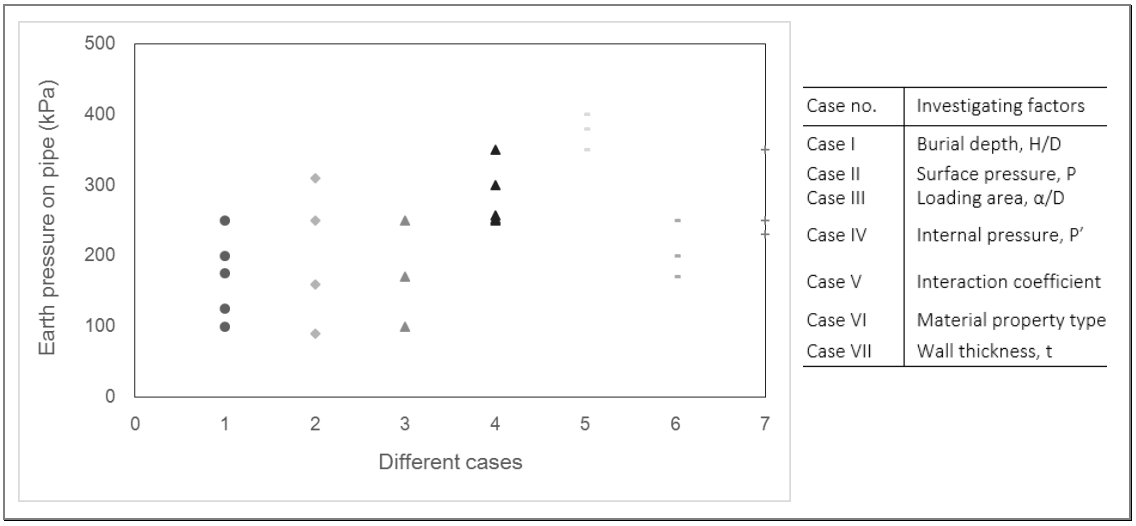

Figure 3-31 Earth pressure on pipe versus all seven cases

It can be concluded from these results that it is not economical, for example, increasing interaction property of pipe only for the purpose of reducing soil surface settlement. Although this parameter reduces soil surface settlement, its impact is not significant. However, based on Figure 3-29 reducing burial depth, surface pressure or loading area can be a solution for this purpose. In the next section, based on results of the parametric study, a sensitivity analysis will be performed to quantify the impact of each parameter on model response by normalising the analysis.

3.3 SENSITIVITY ANALYSIS

As discussed in the previous section, changing the values of different parameters can affect the result of the model in many ways. Results may be changed vastly, poorly or may remain unchanged. Thus a sensitivity analysis is performed to analyse how sensitive the model is to change of each parameter. Performing sensitivity analysis is important showing which parameter requires additional research. For this purpose, all cases presented in the previous section are categorised into standard and nonstandard cases. The standard case consists a steel pipe with thickness of 5 cm, burial depth of H equal to D, surface pressure of 550 kPa and α equal to 2D. A full-bonded interaction without considering internal pressure were also chosen for this case. In addition to the standard case, a total of 29 nonstandard cases, each with only one parameter different from the standard case, are also analysed. For example, case-I which analyses the impact of burial depth is the same property as standard case but has five extra burial depths. In addition, case II which investigates the impact of surface pressure is the same as standard case plus three extra surface pressures. All different cases are illustrated in Table 3-4. The investigating factors are maximum vertical deflection, soil surface settlement, stress in pipe and earth pressure on pipe.

Table 3-4 Different cases considered in sensitivity analysis

Case	Different cases for investigation
Standard case	Steel pipe, burial depth H/D=1, Surface pressure 550 kPa, full- bonded interaction without considering internal pressure
Case I	Impact of burial depth:1, 1.5, 2, 2.5, 3.5, 5
Case II	Impact of surface pressure: 200,400, 550, 700 kPa
Case III	Impact of interaction friction coefficient: 0.1,0.3,0.5, 0.7,0.9, full bonded
Case IV	Impact of loading area: 0.5, 1, 2
Case V	Impact of internal pressure: without fluid,water:414 kPa,Gas: 7500 kPa
Case VI	Impact of material property: HDPE, Steel, PVC
Case VII	Wall thickness: 2, 5, 10 cm

3.3.1 Results

The sensitivity analysis is performed based on results from parametric study and results are presented in the following section. For comparison, results will be presented as the ratio of each case to standard case. Standard case for all cases will

be illustrated on each figure using a red line. As mentioned earlier, for the purpose of comparison the impact of each parameter on model response is normalised. For example, for case-I the soil surface settlement for all six different burial depths are divided to soil surface settlement value for standard case. It should be noted VDS and SSS terms will be used for denoting vertical diametric strain of pipe and soil surface settlement, respectively.

3.3.1.1 Case I: Role of burial depth

Six levels of burial depths are considered in the analysis in which the results are shown in Figure 3-32. A comparison of case-I with the standard case indicates that the effect of burial depth on all investigating parameters is significant.

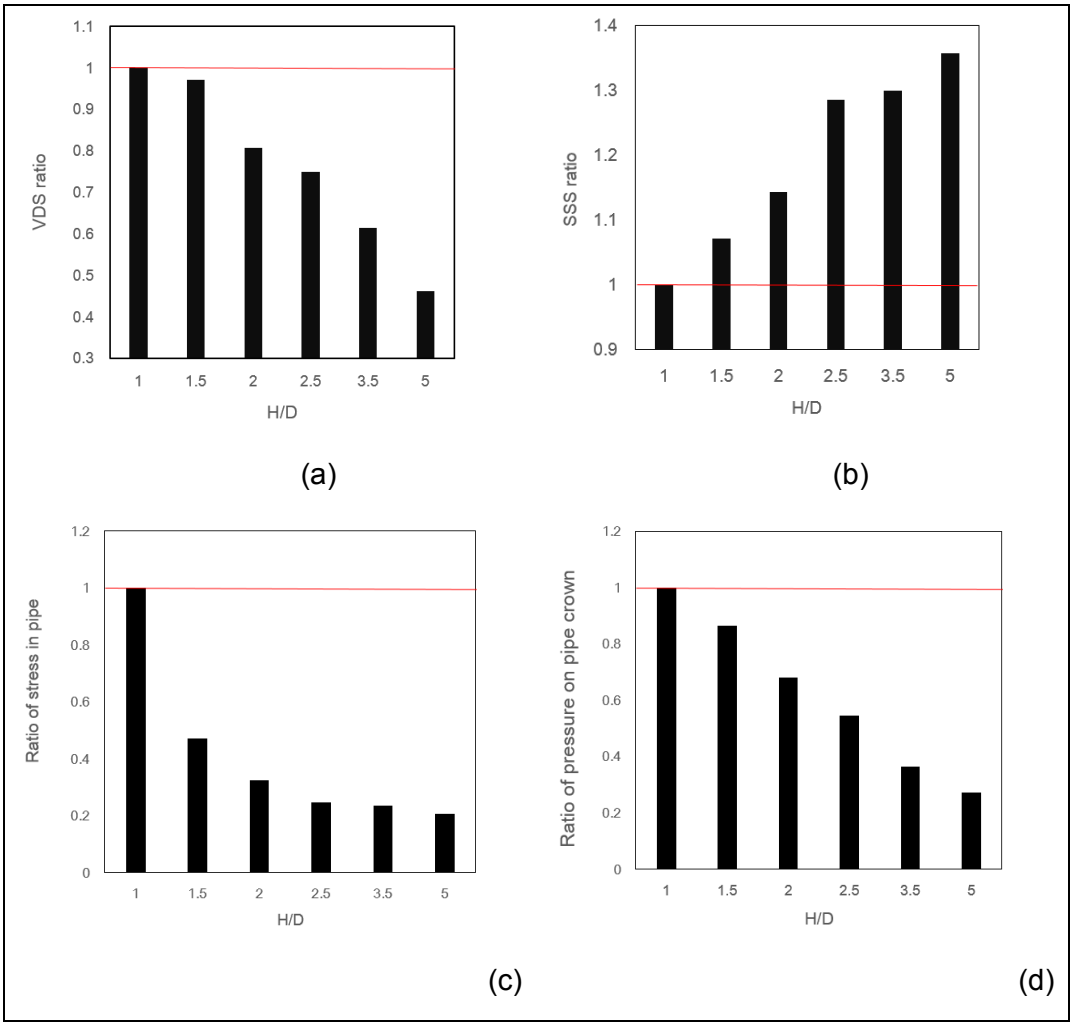

Figure 3-32 Role of burial depth for (a) VDS (b) SSS (c) stress in pipe and (d) maximum pressure on pipe

Overall, increasing burial depth from H=1D to H=5D decreases VDS ratio from 1 to 0.45. Similarly, increasing burial depth from H=1D to 5D results in increase of 1 to 1.35 in SSS ratio, decrease of 1 to 0.25 in stress ratio and decrease of 1 to 0.3 in pressure ratio.

The impact of burial depth on VDS ratio is illustrated in Figure 3-32-a. As illustrated, pipe deflection decreases with increasing H/D and decreases from 1 to 0.4 for deeper burial depths. However, when H/D is minimum, SSS ratio has the lowest value and increasing burial depth increases SSS ratio up to 40%. Sensitivity of pressure on pipe crown is also illustrated in Figure 3-32-c. It can be seen that stress in the pipe is maximum when H/D is minimum. Increasing the H/D leads to a decrease in the stress on the pipe. In addition, increasing burial depth has a significant impact on pressure transmitted to the pipe crown.

3.3.1.2 Case II: Effect of surface pressure

The sensitivity analysis also considered four different surface pressures of 200, 400, 550 and 700 kPa on model response. As expected, increasing surface pressure increases all parameters as illustrated in Figure 3-33. All investigating values are sensitive to change of surface pressure variation. For example, increasing surface pressure value from 200 to 700 kPa increases pipe deflection from 0.4 to 1.6 or 300% increase in VDS. Increasing surface pressure from 200 to 700 increases SSS ratio from 0.3 to 1.4 or 220%. Similarly increase of surface pressure results in, 220% increase in stress in pipe and 200% increase in earth pressure.

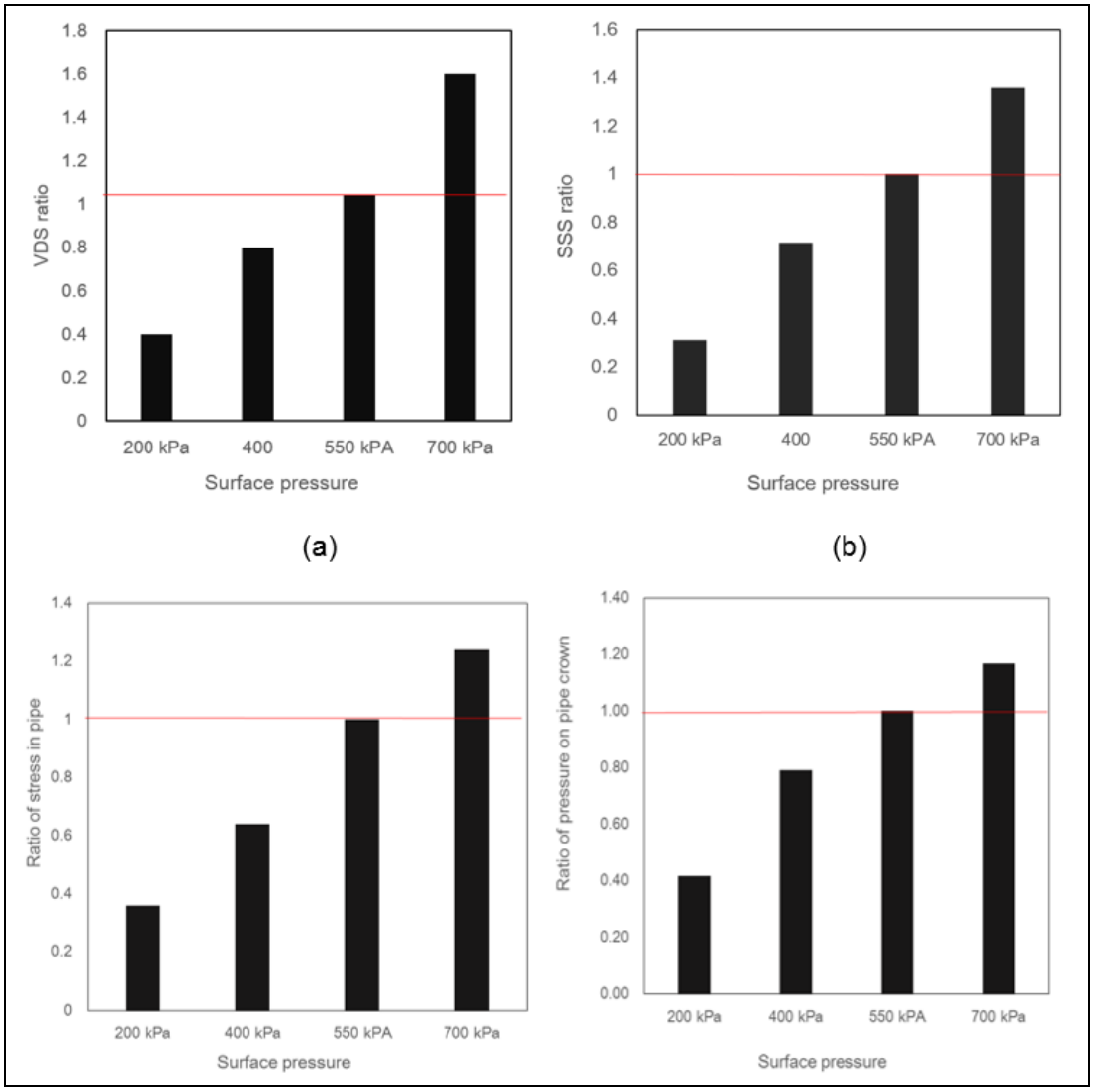

Figure 3-33 Role of surface pressure for (a) VDS (b) SSS (c) stress in pipe and (d) pressure on pipe crown

3.3.1.3 Case III: Interaction coefficient

Five different interaction coefficients of 0.1, 0.3, 0.5, 0.9 and fully-bonded are considered in the sensitivity analysis of system and results are illustrated in Figure 3-34. Overall, three of four investigated parameters are not sensitive to interaction coefficient variation. For example, increasing interaction value from 0.1 to full-bonded reduces pipe deflection from 1.08 to 1 as shown in Figure 3-34-a. Sensitivity of SSS to interaction coefficient is presented in Figure 3-34-b. As illustrated, the largest increase occurs when interaction coefficient is at its minimum of 1 and SSS ratio is 1.1 which means variation in interaction value results in only 10% increase in SSS. Increase of interaction coefficient reduces earth pressure ratio on pipe from 1.08 to 0.98 which is only 10% change. Amongst different investigate parameters, stress in pipe has the highest sensitivity to change of interaction coefficient. As shown in Figure 3-34-c, increase in interaction coefficient reduces ratio of stress in pipe from 1.6 to 1 indicating reduction of 37% in stress on pipe wall.

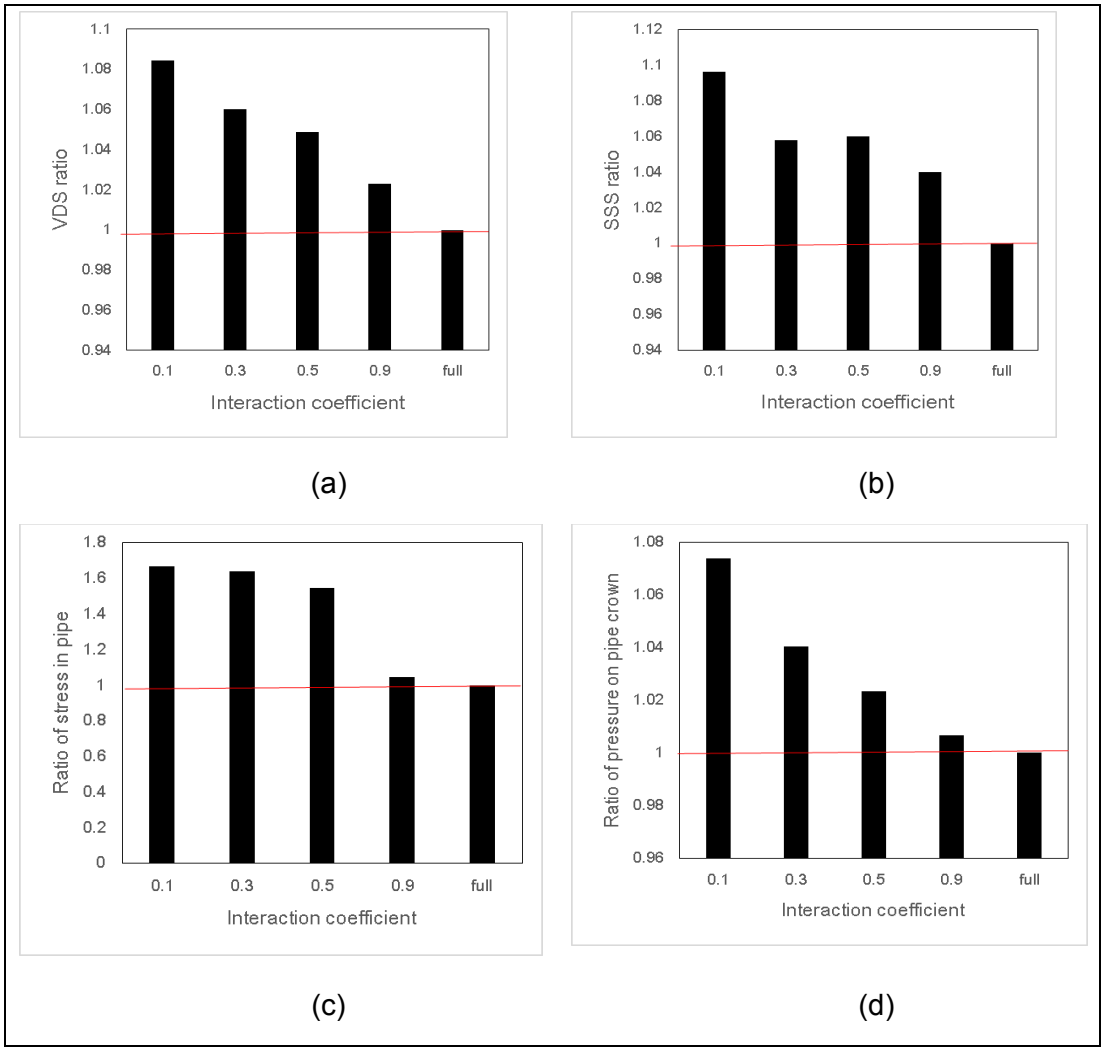

Figure 3-34 Sensitivity of (a) VDS (b) SSS, (c) pressure on pipe wall (d) pressure on pipe crown to interaction coefficient

3.3.1.4 Case IV: Effect of loading area

Three different loading areas of α= 0.5, 1 and 2D are chosen to be analysed and results are illustrated in Figure 3-35. With the same burial depth, surface pressure and interaction coefficient, an increase in tire size causes an increase in all investigating parameters. As shown in Figure 3-35-a increasing loading area from 0.5 to 2D, increases VDS ratio from 0.37 to 1, SSS ratio from 0.4 to 1, stress ratio in pipe from 0.38 to 1 and pressure ratio from 0.4 to 1. The results indicate that minimum increase of 150% occurs on all parameters when loading area increases. This means all parameters are highly sensitive to the size of loading area.

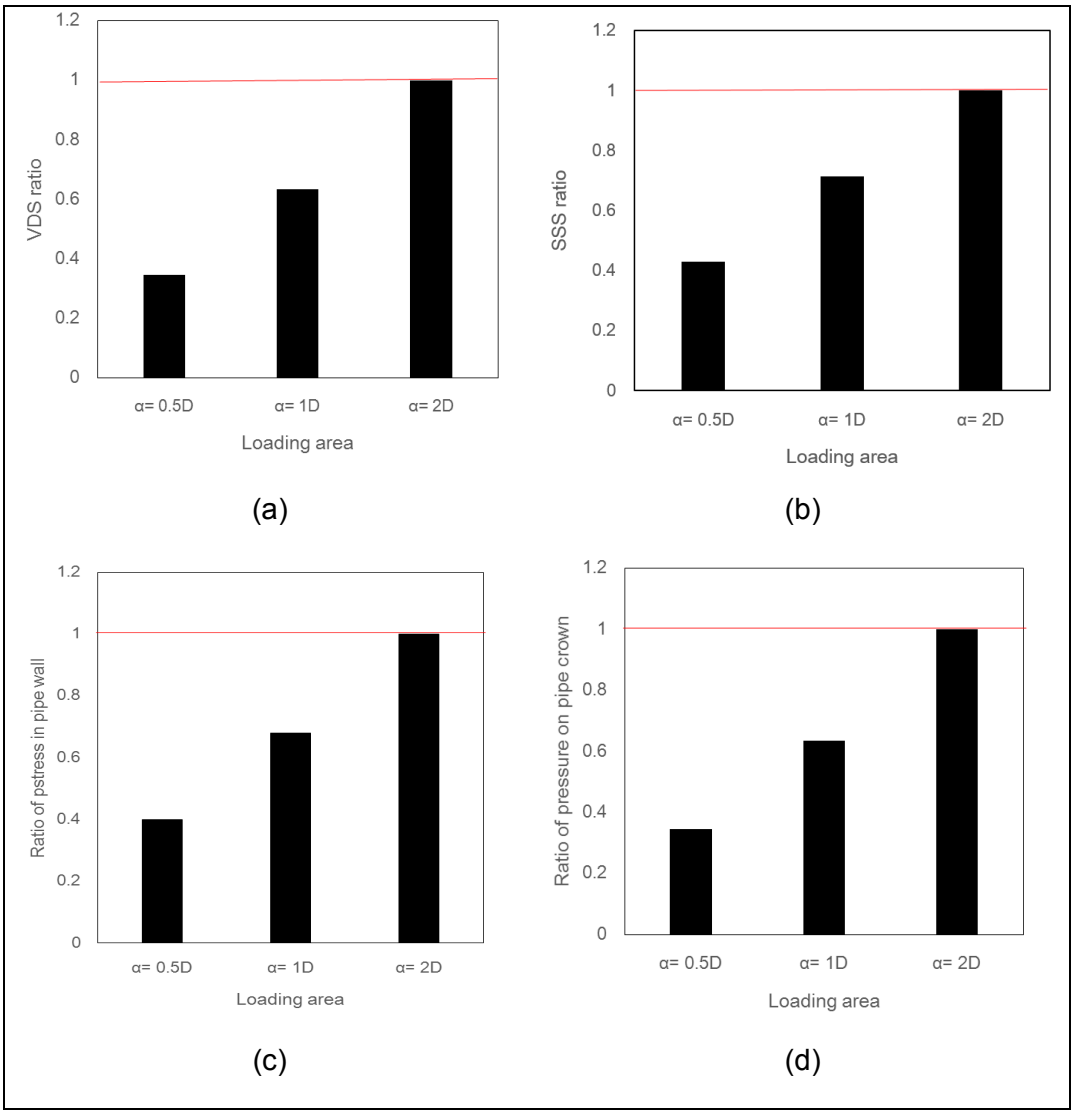

Figure 3-35 Sensitivity to loading area for (a) VDS (b) SSS (c) stress in pipe and (d) maximum pressure on pipe

3.3.1.5 Case V: Internal pressure

The sensitivity analysis also considered the impact of three internal pressures on model response and results are illustrated in Figure 3-36. Overall, amongst all parameters only stress induced in pipe is highly sensitive to internal pressure and other parameters are less sensitive to change in internal pressure of pipeline. Increase in internal pressure results in decrease of VDS ratio from 1 to 0.92, SSS ratio from 1 to 0.85. However, increase in internal pressure results in increase of stress ratio from 1 to 45 and increase in pressure on pipe from 1 to 1.15. In other words, there is a reduction of 17% in VDS ratio and 11% in SSS ratio. An increase of 15% in ratio of earth pressure on pipe occurs with internal pressure increase. However, a significant increase in stress ratio in pipe showing the high sensitivity of stress in pipe to internal pressure.

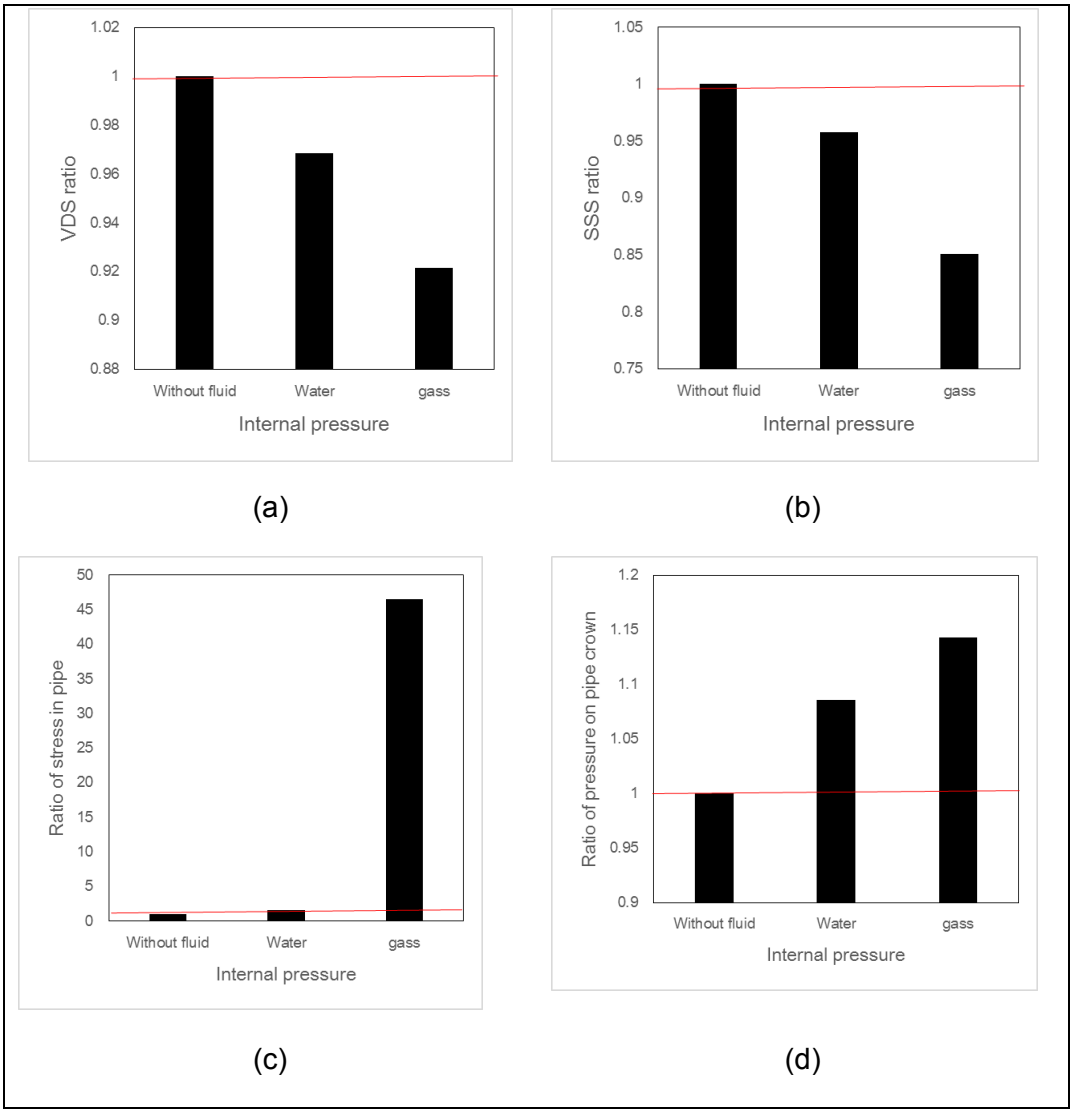

Figure 3-36 Sensitivity to internal pressure for (a) VDS (b) SSS (c) stress in pipe and (d) maximum pressure on pipe

3.3.1.6 Case VI: Material property

The sensitivity analysis also performed on three different pipe materials of steel, PVC and HDPE to identify how sensitive the model is to material property. As shown in Figure 3-37 stronger pipe material causes higher stress in pipe wall and on pipe crown. In addition, it causes lower pipe deflection and soil surface settlement. For example, increasing material strength from steel to HDPE increases VDS ratio from 1.0 to 1.2 and increases SSS ratio from 1 to 1.1. However, it decreases ratio of stress on pipe from 1 to 0.6 and decreases ratio of earth pressure from 1 to 0.75.

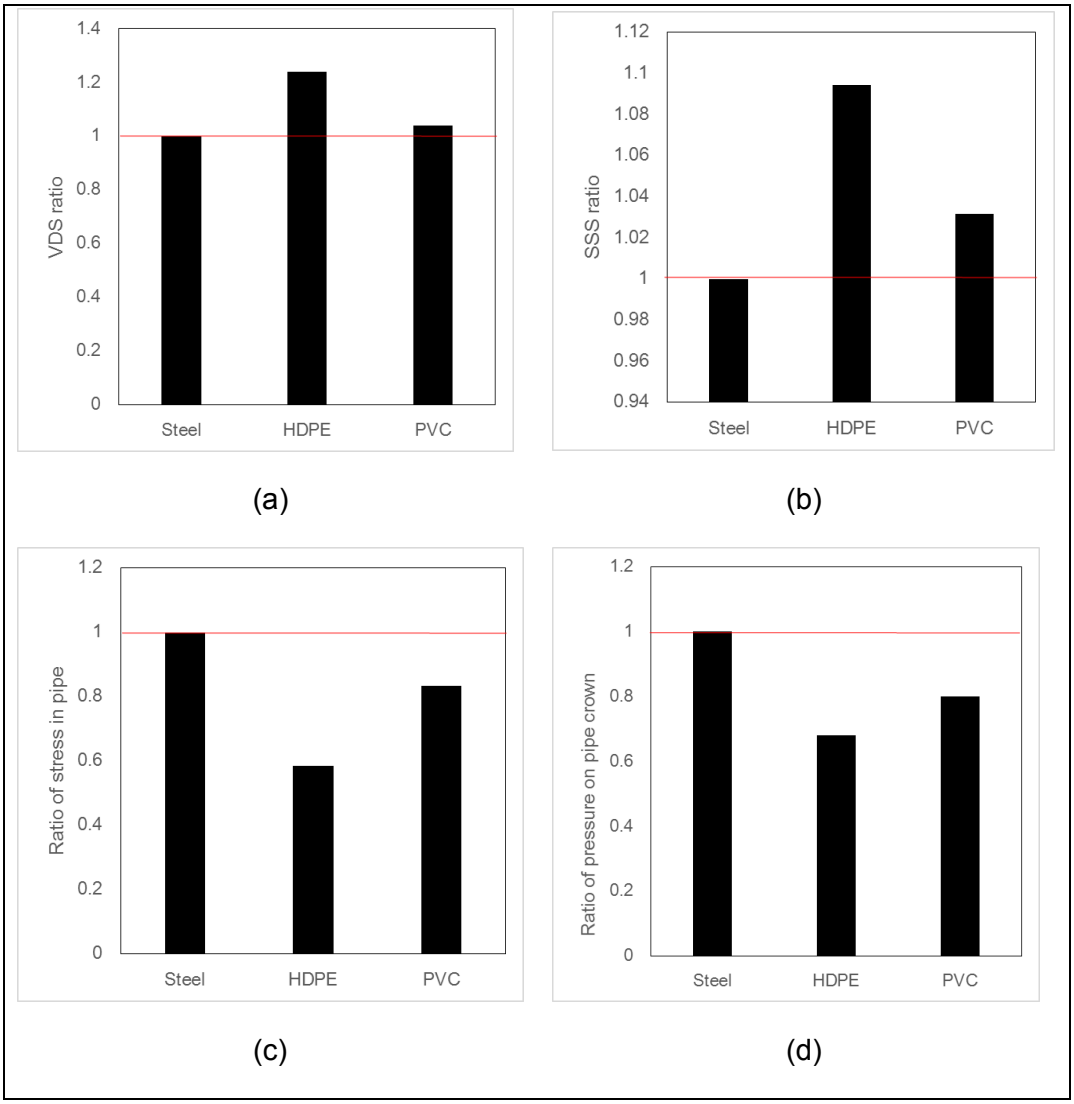

Figure 3-37 Sensitivity to pipe material property for (a) VDS (b) SSS (c) stress in pipe and (d) maximum pressure on pipe

3.3.1.7 Case VII: Wall thickness

To analyse how sensitive the model is to change of pipe wall thickness, the model response is analysed and compared with three different wall thicknesses and results

are illustrated in Figure 3-38. It can be seen that increasing pipe thickness from 2 to 10 cm decreases pipe deflection ratio from 1.2 to 0.95 and soil surface settlement ratio from 1.02 to 0.98. The ratio of stress in pipe significantly drops from 2.5 to 0.4 by increasing pipe thickness. Increasing pipe thickness from 2 to 10 cm however leads to an increase in earth pressure on pipe from 0.9 to 1.4. Overall, it can be seen that amongst different factors, stress in pipe is more sensitive to change in pipe thickness.

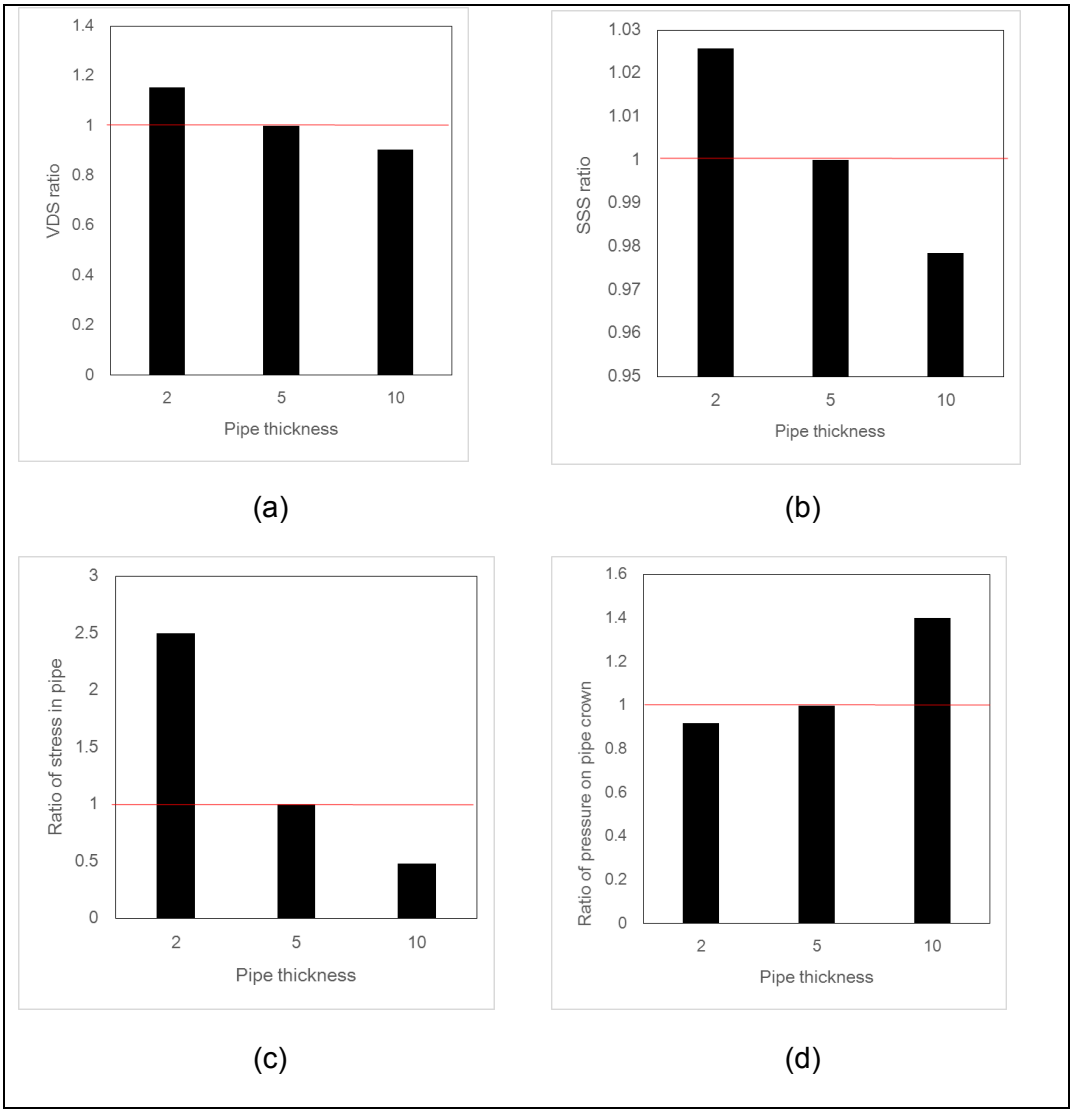

Figure 3-38 Sensitivity to pipe wall thickness for (a) VDS (b) SSS (c) stress in pipe and (d) maximum pressure on pipe

3.3.2 Relative Contribution of Each Parameter

Sensitivity analysis was performed based on the parametric study to determine the effect of various parameters on buried pipe response subjected to traffic load. A comparison of all cases indicates that the model behaviour is more sensitive to some parameters. Thus the relative contribution of each parameter on the sensitivity of model was analysed by calculating the ratio of RC (relative contribution) of each parameter based on the following equation:

$$RC_i = \frac{\Delta Ki}{\sum \Delta Ki} \qquad 3\text{-}2$$

In which ΔKi is the difference between maximum and minimum value of sensitivity ratio for each case. $\sum \Delta Ki$ is sum of all sensitivity coefficients of each parameter calculated in sensitivity analysis. For example, to identify the contribution of burial depth on pipe deflection variation, $\Delta K1$ which is 0.54, is divided by 3.09 which is sum of all sensitivity coefficients of those seven parameters or $\sum \Delta K1$ and result of relative contribution of burial depth and pipe deflection is 17. ΔKi for each parameter is calculated and results are illustrated in Table 3-5. Then, based on these values, RC or relative contribution of each case on variation of deflection, soil surface settlement, stress in pipe and earth pressure on pipe is calculated and results are illustrated in Table 3-6.

Table 3-5 Value of maximum ΔKi for all seven cases

Case1-7	Parameters	Deflection	Settlement ratio	Stress ratio	Pressure ratio
Burial depth	1.00	1.00	1.00	1.00	1.00
	1.50	0.97	1.07	0.63	0.80
	2.00	0.81	1.14	0.48	0.70
	2.50	0.75	1.34	0.46	0.50
	3.50	0.62	1.40	0.33	0.40
	5.00	0.46	1.36	0.29	0.30
	ΔK1	0.54	0.39	0.70	0.70
Surface pressure	200	0.40	0.36	0.42	0.36
	400	0.70	0.71	0.79	0.64
	550	1.04	1.00	1.00	1.00
	700	1.60	1.36	1.17	1.24
	ΔK2	1.20	1.00	0.75	0.88
Loading area	0.50	0.35	0.43	0.55	0.40
	1.00	0.63	0.71	0.75	0.68
	2.00	1.00	1.00	1.00	1.00
	ΔK3	0.70	0.57	0.45	0.60
Interaction	0.10	1.10	1.08	1.67	1.40
	0.30	1.06	1.06	1.64	1.20
	0.50	1.06	1.05	1.55	1.03
	0.90	1.04	1.02	1.05	1.01
	1.00	1.00	1.00	1.00	1.00
	ΔK4	0.05	0.08	0.66	0.40
Internal pressure	no fluid	1.00	1.00	1.00	1.00
	Water	0.96	0.97	1.55	1.09
	Gas	0.85	0.92	46.55	1.14
	ΔK5	0.15	0.10	45.55	0.14
Material properties	Steel	1.00	1.00	1.00	1.00
	HDPE	1.24	1.09	0.58	0.68
	PVC	1.04	1.03	0.83	0.80
	ΔK6	0.20	0.09	0.17	0.32
Thickness	2.00	1.15	1.08	2.50	0.92
	5.00	1.00	1.00	1.00	1.00
	10.00	0.90	0.98	0.48	1.40
	ΔK7	0.25	0.10	2.02	0.48

Table 3-6 Relative contribution of each parameter on model response

Relative Contribution	Cases	Deflection	Settlement	Stress	Pressure
RC1	Burial depth	17.48	16.73	1.48	20.00
RC2	Surface load	38.83	42.89	1.49	25.14
RC3	Loading area	22.65	24.52	0.90	17.14
RC4	Interaction	1.62	3.43	1.33	11.43
RC5	Internal pressure	4.85	4.27	90.46	4.00
RC6	Material type	6.47	3.86	0.33	8.57
RC7	Thickness	8.09	4.29	4.01	13.71
∑ RCi		100	100	100	100

For each output, pie charts are provided to quickly show the weight of all seven different inputs on four analysed parameters visually. The pie charts in Figure 3-39 present the percentage of relative contribution of each parameter on model response. Overall, surface pressure, burial depth and loading area are three parameters which have the highest impact on VDS, SSS and pressure on pipe. As shown in Figure 3-39 contribution of surface pressure is the highest comparing to other parameters. The contribution is 39%, 25% and 43% on variation of VDS, SSS and earth pressure, respectively. As illustrated in Figure 3-39-c, internal pressure has the highest level of contribution on stress in pipe and contribution of other six parameters on stress variations are negligible (less than 7%).

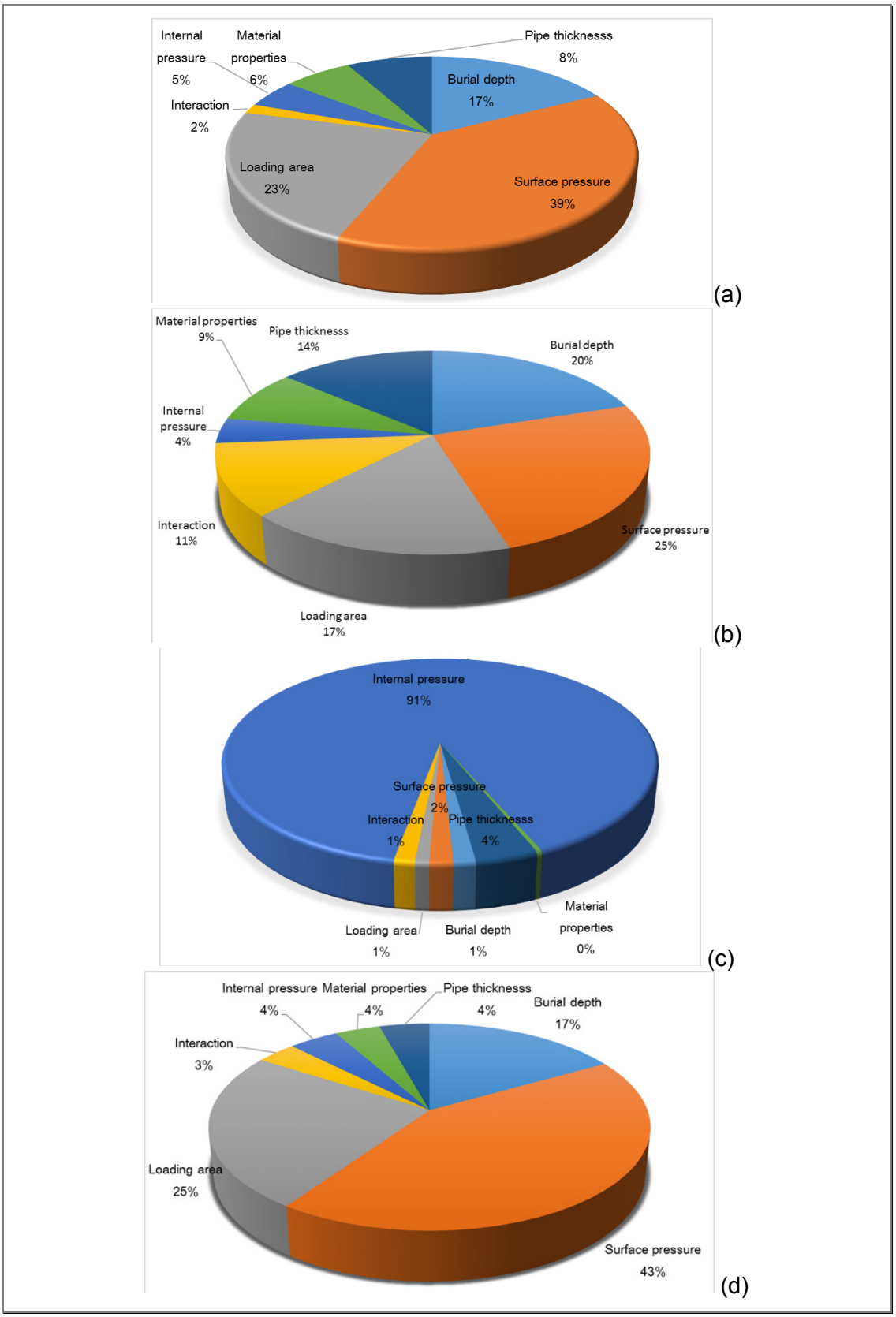

Figure 3-39 The relative contribution of various parameters on the sensitivity of (a) pipe deflection (b) soil surface settlement (c) stress in pipe (d) earth pressure on pipe

3.4 CONCLUSIONS

In this research, a numerical parametric study was carried out to investigate the impacts of different parameters on pipe-soil behaviour under traffic load using the FEM software ABAQUS. The soil model was elasto-plastic and the pipe was elastic linear. The effect of seven different parameters including burial depths of pipe, external pressure, width of loading area, internal pressure, pipe-soil interaction properties, pipe material, wall thickness and boundary conditions at the pipeline ends on pipe deflection, surface settlement, maximum stress in pipe as well as earth pressure on pipe were investigated. The parametric study was followed by sensitivity analysis to investigate how sensitive the model was to change of each above mentioned parameter and to determine the parameters with the highest relative contribution on model response.

The key findings are summarised as below:

- It was demonstrated that increasing burial depth from H/D=1 to H/D=5, reduces pipe deflection significantly. Rate of change is more important for H/D <2.5 which means live load tends to have less effect on pipe deflection for deeper embedment depths. In addition, when H/D is minimum, soil surface settlement is also minimum. Increasing H/D increases displacement at the soil surface, especially for H/D<2.5. Increasing the H/D reduces both stress in the pipe wall and earth pressure on the pipe. These changes are more significant for H/D<2.5.
- The results indicate that increasing surface pressure leads to a significant increase in SSS, VDS, stress in pipe and pressure on pipe crown. Results also show that soil surface settlement is higher above pipe crown. In addition, maximum pressure on pipe occurs in the middle part of the pipe circumference or between 60^o to 100^o from pipe crown.
- The larger the loading area, the higher will be pipe deflection. Increasing loading area also increases soil surface settlement, stress in pipe and earth pressure around the pipe significantly. Internal pressure affects pipe deflection, soil surface settlement and earth pressure around the pipe although these changes are not significant. However, applying internal pressure significantly increases stress in pipe. In addition, applying internal pressure affects the location where maximum stress occurs. Maximum stress happens in the middle part of pipe when there is no fluid while the minimum

stress happens in the middle part of pipe taking into consideration the impact of fluid.

- Results revealed that friction coefficient variation has a small effect on pipe deflection, soil surface settlement and maximum earth pressure variation. However, stress in pipe is more affected by interaction coefficient variation comparing to other parameters. In addition, friction coefficient effects on pipe displacement and pressure distribution along pipe circumference is investigated for only two values of friction coefficient: full-bonded and friction coefficient of 0.5. Results show that the pipe displacement is reduced by moving from crown to pipe invert along pipe circumference. Results also reveal that earth pressure of full-bonded interaction is higher on left and right sides of the pipe and has a lower pressure along its middle part.
- Increasing pipe thickness from 2 to 10 cm reduces pipe deflection, soil surface settlement and stress in pipe. However, increasing wall thickness increases earth pressure on pipe significantly.
- Replacing steel pipe with PVC and HDPE increases pipe deflection, the soil surface settlement and earth pressure on pipe. Stress in pipe, however, decreases by replacing steel pipe with PVC and HDPE.
- Analysing the effect of boundary conditions shows that hinged boundary condition affects stress and displacement distribution along the pipe length, showing that at the ends of the pipeline, when there is no displacement, maximum stress occurs. Maximum displacement also occurs along pipeline path while stress is minimum for hinged boundary condition.
- To provide a quick understanding of each parameter impact on model response, parametric study results were evaluated and impact of all parameters on model response were compared. Impact of all seven parameters on each parameter was investigated and results were presented on the same graph. Overall, surface pressure has the highest impact on VDS, SSS, and earth pressure variation and interaction coefficient value has the lowest impact. Internal pressure has the highest impact on stress in pipe comparing to other parameters.
- A sensitivity analysis was also performed based on the results from parametric study and results were presented as the ratio of each parameter for each case to standard case. It was shown that the model is more sensitive to some parameters than others. The relative contribution of each parameter has been calculated and results indicated that surface pressure contribution is the

highest comparing to other parameters and its contribution is 39%, 25% and 43% on VDS, SSS and earth pressure, respectively. After surface pressure, burial depth and loading area have the highest contribution on above mentioned parameters. Internal pressure has the highest contribution on stress variation in pipe and contribution on other six parameters is negligible.

The impact of surface pressure and burial depth is going to be analysed in phase-II of this research. Another significant parameter is loading area which will not be considered in the next stage of this research due to limitation to the laboratory facilities. Some of the recommendations on parametric study are given below:

- It was found that the model is sensitive to internal pressure affecting stress distribution on pipe wall significantly. It is recommended this factor to be studied further from structural point of view.
- As the pipe installation procedure has not been simulated in the current research and considering pipe installation could affect stress distribution. The author recommends installation procedure to be investigated in the future.
- It was assumed that the pipe did not deform during construction and the relative movement of the pipe and soil was not taken into consideration. It is recommended these parameters to be also investigated in the future.
- In the current study, traffic load has been considered as a static load. Considering traffic load as a cyclic load to assess pipe and soil behaviour and taking into consideration the degradation effect in a real project is recommended.
- Future work on pipeline behaviour should contain physical tests to validate future numerical models.

3.5 SUMMARY OF THE CHAPTER

A numerical parametric study was performed to investigate the impact of different parameters on pipe-soil behaviour under live load using ABAQUS. These parameters were burial depths, surface pressure, loading area, internal pressure, pipe-soil interaction properties, pipe material and boundary conditions. The effect of these parameters was investigated on pipe deflection, soil surface settlement, stress in pipe as well as earth pressure on pipe. This study was followed by the sensitivity analysis to quantify how sensitive the model was to any change of these parameters. Based on the results of parametric study and sensitivity analysis, the burial depth, surface

pressure and loading area had the most significant impact on pipe deflection, soil surface settlement and pressure on pipe crown. The effect of other parameters (e.g. interaction coefficient and internal pressure) was found to be negligible on SSS, VDS and pressure on pipe crown. Therefore, surface pressure and burial depth variation were selected to be analysed in the following phase of this research. The methodology of next phase of this research will be presented and discussed in the next chapter.

4 METHODOLOGY

4.1 INTRODUCTION AND OVERVIEW

In the previous chapter a parametric study was carried out to investigate buried pipe performance under various conditions. Results revealed that surface pressure, burial depth and loading area have the highest impact on the pipe performance. In the following chapters the focus is on buried pipe performance investigation under cyclic load experimentally and numerically. The objective is to conduct experimental tests and numerical simulations to assess pipe deflection, soil surface settlement and pressure on pipe. Experimental tests will be carried out using UTM25 to apply load on surface of a tank in which pipe is buried. The tank was built in Curtin University for the purpose of this project. Then, numerical simulations will be conducted using the Finite Element Method based on laboratory setup to investigate pipe-soil behaviour within numerical context.

This chapter presents the experimental and numerical methodologies employed for current research in three sections. In the first section following the introduction, the test setup and details of the experimental tests will be described. In addition, the specification of the equipment for data acquisition, testing tank and machine for applying load will be presented. This section will be followed by the finite element model analysis suitable for buried pipe simulations. The error associated with this research will be presented briefly at the end of this chapter.

4.2 EXPERIMENTAL SETUP

The experimental studies are conducted at the Curtin University by performing series of cyclic load tests on buried pipe. The objective of experimental study is to measure the changes in pipe deflection, surface settlement and earth pressure on pipe induced at different burial depths, surface pressures and load cycles. Description of different components and procedure of experiments are presented in this section.

4.2.1 Steel Tank

The testing tank was designed and built in Curtin University for the purpose of this research. A Universal Testing Machine, UTM-25, was used to apply both static and dynamic loads which will be described later. The layout of testing tank is shown in Figure 4-1. Some of the key criteria considered in the design and sizing of the tank are as below:

1. Limited size of tank due to size of the UTM 25 ;
2. Minimal effects from end wall and side walls during loading;
3. Promoting plane strain conditions in tests;
4. Front face made of plexiglass for visual observation;

Due to the long length of the buried pipe compared to its diameter, the tank was modelled assuming plane strain conditions. For this condition, it is assumed that in deformation process the strain along the z-axis is zero, i.e., normal planes to the *z* direction do not interfere with each other. In large-scale test, the plane strain condition could be achieved by building the model with the smooth x–y faces in order to prevent any friction that could cause distortion in the longitudinal direction. Another way to achieve plane strain condition is taking the z dimension such that the boundary conditions at the end do not affect the behaviour of the model in the middle. The testing tank used in this research was a rigid steel box using three stiff steel sections of U-230 on the sides and bottom of the tank as shown in Figure 4-1-a. The dimensions of the tank are 700 mm x 600 mm x 230 mm. The testing tank has a smooth back consisting of a steel plate with 10 mm thickness and the front face is made of plexiglass of 20 mm thickness as shown in Figure 4-1-b. Plexiglass is used for visual observations of the sand–pipe system, as well as the photo scanning. On the back face, a layer of smooth material Polytetrafluoroethylene or PTFE was applied to decrease friction between soil and steel. This smooth material on the back face makes the friction similar to front face between plexiglass and soil to impose plane strain condition.

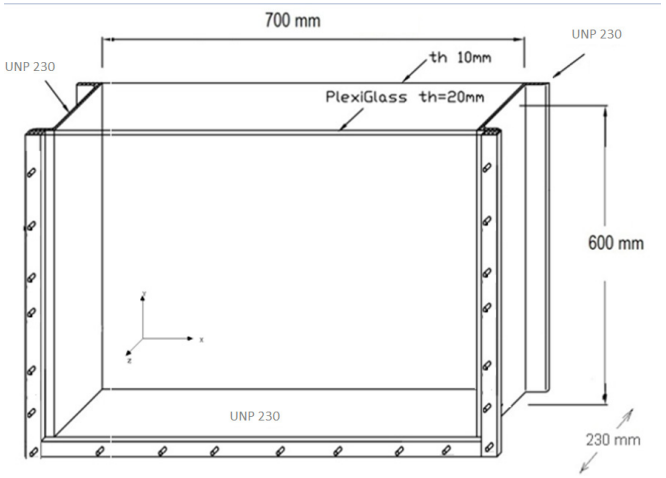

(a)

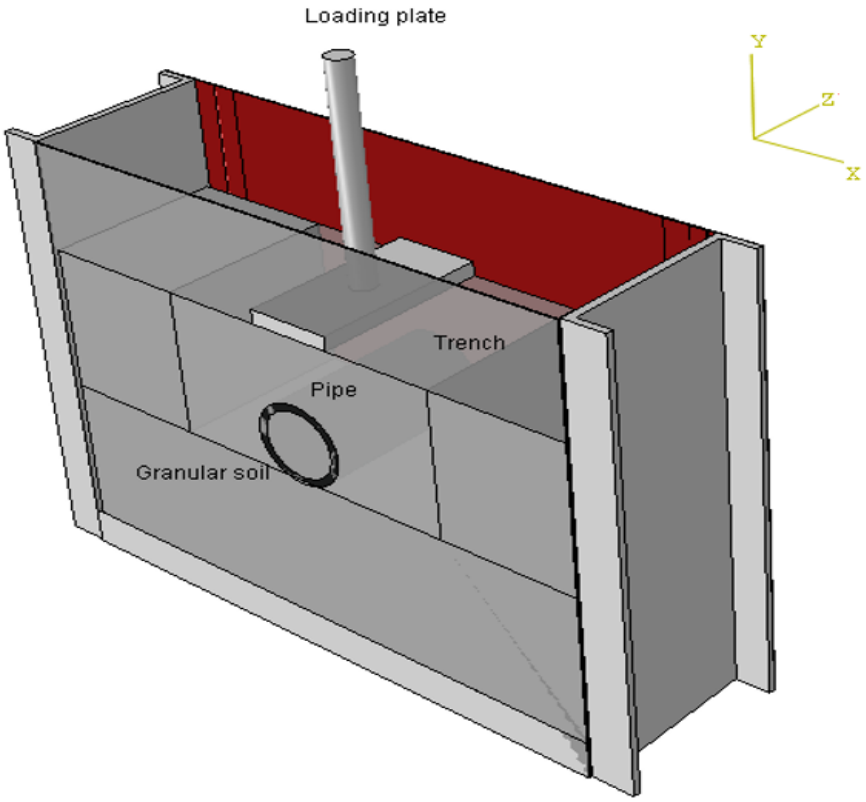

Colour	Parts	Tank material properties
	Back face	Smooth steel plate; 700X600 mm^2; thickness: =10 mm
	sides	Each side consist of stiff steel UNP230; thickness: 10mm
	Bottom	UNP230; thickness: 10 mm
No colour	Front face	Plexiglass, thickness: 20 mm

(b)

Figure 4-1 (a) Schematic diagram of the test box and its dimensions and geometry of the model (b) schematic view of tank and the material properties

4.2.2 Data Acquisition System

All measurements from instrumentations were recorded automatically via different channels to monitor pipe and surface response due to cyclic load. Catman AP version 4.2 was used as data acquisition software (DAQ) allowing for data visualization, analysis and storage during the test. Connection was via socket devices and data were exported to MS Excel for post processing. The details and specifications of these equipment are described in the following sections. The LVDT (Linear Variable Displacement Transducer), strain gauge and pressure cell were also provided to measure displacement, strain and pressure at given points as shown in Figure 4-2. In addition, the value of applied load and soil surface settlement can be read through UTM 25. The UTS002 stress strain test module software developed by IPC Global™ was used to run the test and to capture the data. Based on sensitivity analysis presented in section 3.2.2.8, boundary conditions can affect stress and displacement results of a pipe significantly. Thus, the best place to install strain gauge and pressure cell is where the impact of boundary condition is minimum. Therefore, strain gauges and pressure cells were installed in the middle part of pipe length in *z* direction. It should be noted that the type and location of data each acquisition equipment for experimental tests, were selected based on similar research works in the literature (Ko & Kuwano, 2010; Moghaddas Tafreshi & Khalaj, 2008; Tavakoli Mehrjardi et al., 2013; Yoshimura et al., 2010).

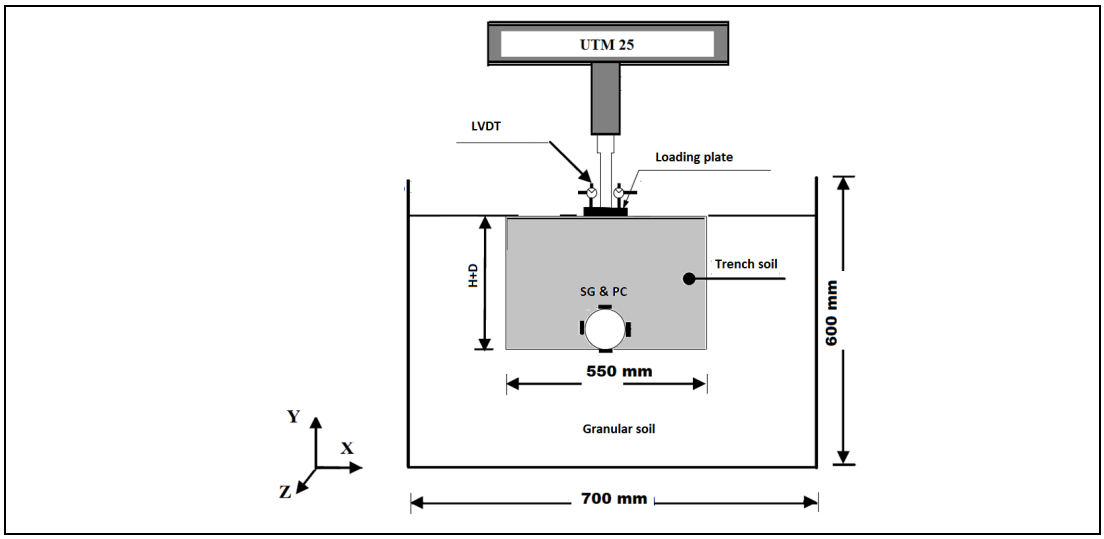

Figure 4-2 Location of pressure cell, strain gauge and LVDT in the model

4.2.2.1 Pressure cell

The pressure cells used in this research were Miniature Pressure Gauge PDA-1 MPA and manufactured by Tokyo Sokki Kenkyujo, Japan. These pressure cells were

installed on pipe surface to capture pressure on pipe-soil interface. The sensing part of the PDA-PA miniature pressure gauges is 6.5 mm in diameter and 1 mm in thickness as shown in Figure 4-3-a and b. These pressure cells are waterproofed with accuracy of 0.1% according to the manufacturer advice. Pressure cell specifications provided by manufacturer are illustrated in Table 4-1. Pressure cells should be connected to the digital convertors and computers using sockets as shown in Figure 4-3-c. The data recorded are exported as mV/V and will be converted to appropriate units based on calibration results. To ensure an accurate reading, all of the devices were calibrated prior to tests.

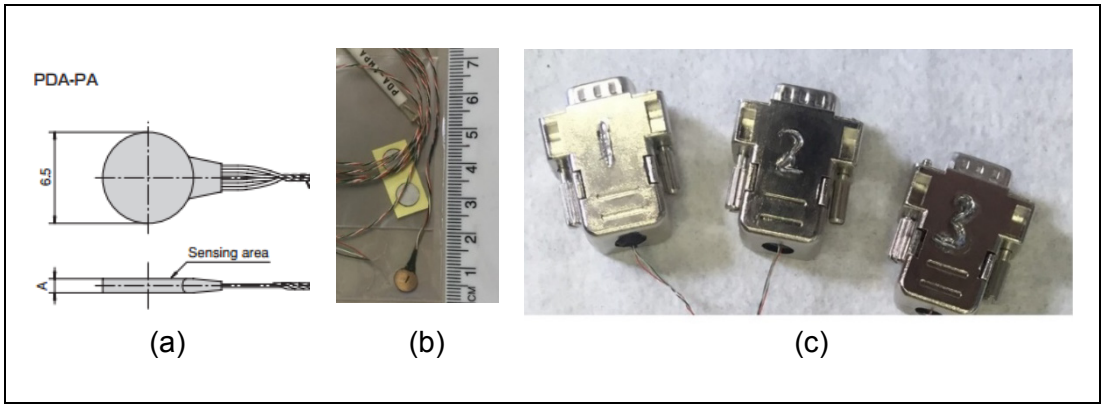

Figure 4-3 Pressure cell

Table 4-1 Pressure cell specifications

Type	PDA-200KPA/PDB-200KPA	PDA-500KPA/PDB-500KPA	PDA-1MPA/PDB-1MPA	PDA-2MPA/PDB-2MPA	PDA-3MPA/PDB-3MPA
Capacity	200kPa	500kPa	1MPa	2MPa	3MPa
Rated output	0.8mV/V (1600×10⁻⁶ strain)	1mV/V (2000×10⁻⁶ strain)			
Non-linearity	1%RO				
Hysteresis	1%RO				
Temperature effect on zero	1%RO/℃				
Temperature effect on span	1%/℃				
Compensated temperature range	−10～+60℃ (no icing)				
Temperature range	−20～+70℃ (no icing)				
Input/output resistance	350Ω				
Recommended exciting voltage	Less than 2V				
Allowable exciting voltage	5V				

Input/output cable : 0.005mm² 4-core Fluoride plastic insulated cable 1m

The calibration of pressure cells PDA-1 MPA was carried out by applying air pressure on each pressure cell using triaxial device as shown in Figure 4-4. First, pressure cells were placed in the cell of triaxial machine. Then the uniform air pressure was applied via triaxial device. Data were recorded based on mV/V via Catman software installed on computer. Then calibration coefficient was calculated for all pressure cells. Calibration coefficients of all three pressure cells are illustrated in Figure 4-5-a to c. For example for the value of -0.5 for PDA 1 in Figure 4-5-a, pressure recorded is equal to 280 kPa. Calibration value is calculated based on equations derived from following figures. Noted that based on calibration results shown in Figure 4-5, the correlation was assessed as good and pressure can be

calculated based on calibration coefficient. Therefore, the final value captured by pressure cells can be calculated as follows:

4-1

Pressure= measured value X calibration coefficient

In which measured value is the reading of the pressure cell and calibration coefficient value is calculated using the calibration graphs shown in Figure 4-5-a to c.

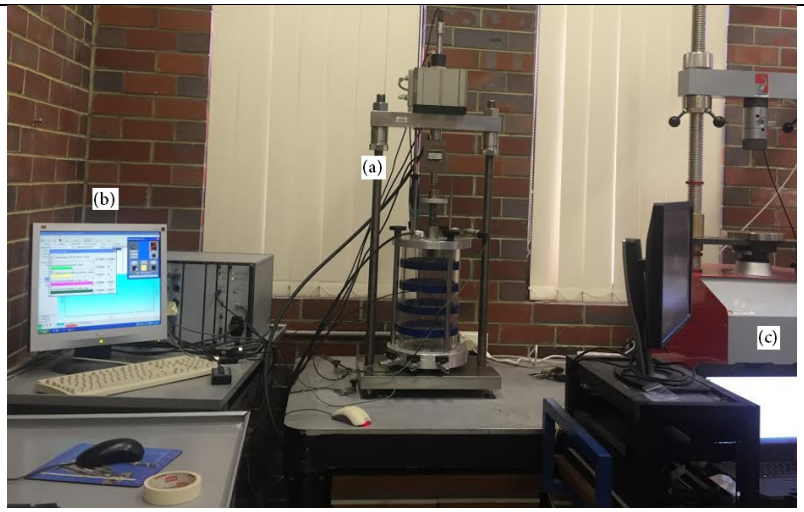

Figure 4-4 Calibration of pressure cells in the laboratory

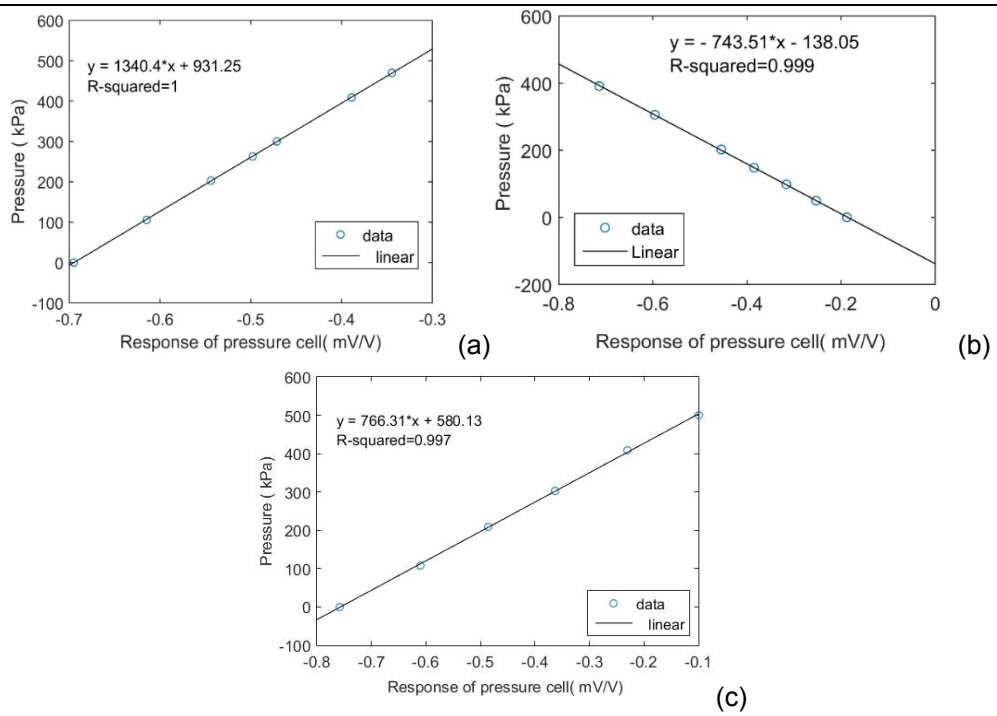

Figure 4-5 Results of three pressure cells calibration

4.2.2.2 Strain gauge

Strain gauge used in this research was an F series Lead wire integrated foil strain gauge type or FLA-2-11 as shown in Figure 4-6, manufactured by Tokyo Sokki Kenkyujo TML. The length and width of strain gauge are 2 and 1.5 mm, respectively.

Figure 4-6 Strain gauge used in the current research

The most important part in using strain gauge is bonding it to the surface. For proper bonding of strain gauges, the testing surface must be chemically clean and totally free of contaminants before applying the adhesive. This condition was applied by using conditioner and neutraliser as shown in Figure 4-7-a. For gluing of strain gauge to the pipe, the pipes were fixed in place using the clippers as shown in Figure 4-7-b. By surface scrubbing with an alkaline solution, as shown in Figure 4-7-c and d, the surface was cleaned at the appropriate pH level. The bonding between strain gauge and pipe was checked by trying to detach strain gauge from pipe for each test. As shown in Figure 4-7-e and f gluing process was quite satisfactory as detaching to the strain gauge was not possible without its destroying.

It is essential to find a relationship between measured circumferential strain on pipe and pipe deflection. For this purpose a test was carried out using a compression testing machine to measure vertical diametrical change of pipe (measured with LVDT) and wall circumferential strain at crown and bottom of pipe (measured with two strain gauges). The details will be explained in Chapter 5.

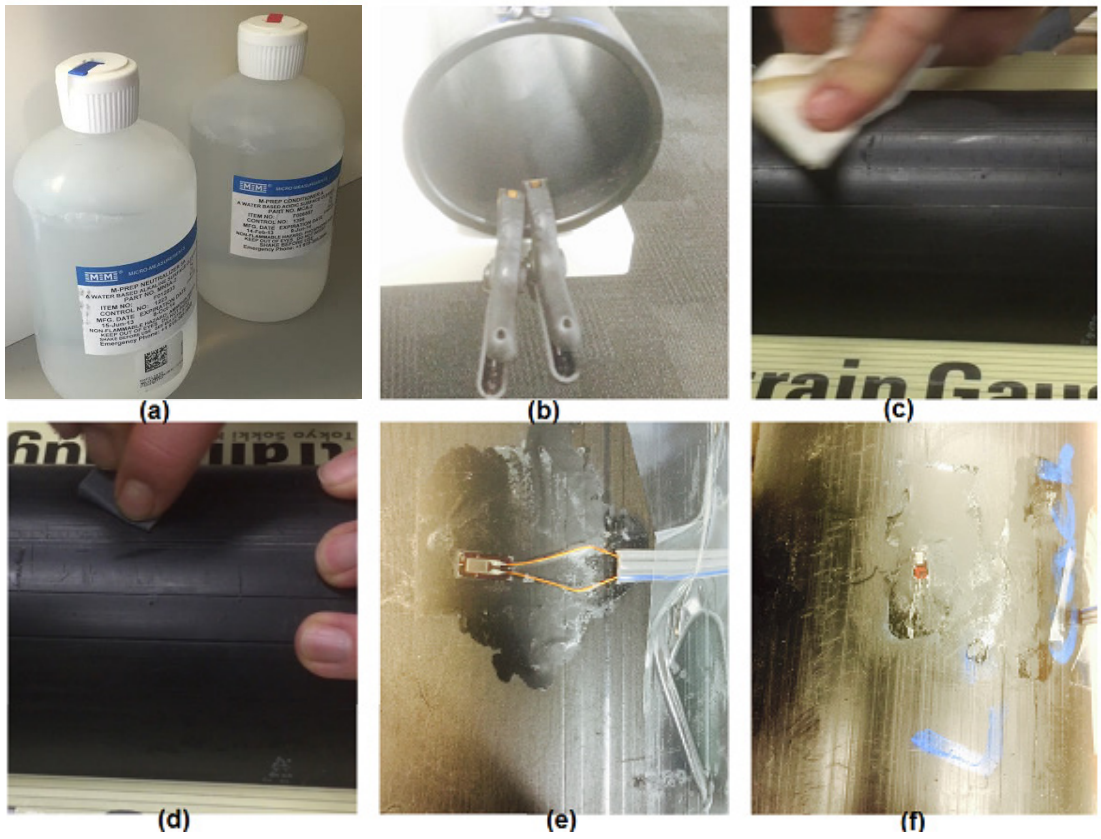

Figure 4-7 Different steps of preparation of strain gauges

4.2.2.3 LVDT

An LVDT with 100 mm travel distance was placed between the loading shaft and soil surface to precisely measure the applied load on the soil surface as shown previously in Figure 4-1-c

4.2.3 Sample Preparation

The soil sample for each test was prepared. First, granular soil was placed at the bottom and lateral sides of the tank in a U shape as shown in Figure 4-8. Before putting the trench material, pipe should be placed while strain gauges and pressure cells were attached to it in appropriate positions as illustrated Figure 4-8-a. After placing pipe, sand material was to be placed and compacted in trench area. The chosen trench width was 55 cm. This width was chosen according to AASHTO recommendation in which trench width should not be less than the greater of 1.5 times of the pipe outside diameter plus 305 mm or the pipe outside diameter plus 406 mm. The trench depth varied in different tests and ranged between 220 and 385 mm which

is sum of the burial depth plus pipe diameter. Soil compaction was performed with an appropriate hammer used to simulate compaction in the field to reach 95% maximum dry density. Height of the trench was divided into equal strips so that the soil in each layer (i.e. 6 cm thickness) was compacted separately, (Figure 4-8-b).The soil weight required in each layer was calculated from considerations of compacted soil unit weight and chamber's volume. At the end, the surface of soil was levelled. In the last step, loading cell and the loading plate were centred in the tank. An extra LVDT was also placed on top of plate to monitor the surface settlement parallel to UTM25 data capturing, (Figure 4-8-c). It should be noted the properties of materials in the current research will be presented in Chapter 5.

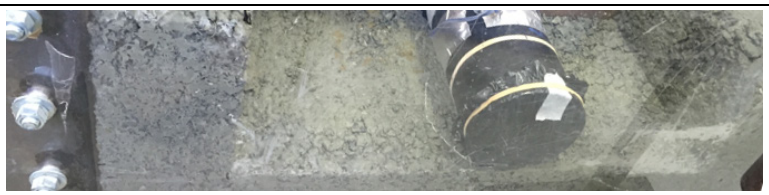

(a)

(b)

(c)

Figure 4-8 (a) Sample preparation and pipe installation (b) sand in the trench (c) installation of loading plate and LVDT in place

For case of cemented material, sand was mixed with 5% of cement using an asphalt mixer. First the thickness of H/5 was chosen for cemented material. However after running two tests and failing of each test at early stage of cyclic load, the higher thickness of cemented layer was selected and thickness of H/3 was then chosen for thickness of cemented layer. It should be noted if the thickness of cemented layer is thin, it constitutes only a small portion of the overall cemented material strength. However, the higher depth of cemented layer causes the higher magnitude of tensile strain at its underside and further increase in cemented layer thickness reduces the flexure of the underlying structure causing crack in cemented material as shown in Figure 4-9-a.

For sample preparation, the Hobart HL-200 mixer was used for homogenization of soil, cement and water. This mixer has three speed settings: 107, 198 and 361 RPM. The mixer has a stainless-steel bowl and a flat-type aluminium grid beater with the base dimensions of 533 x 546 x 1048 cm. The mixer and its tool are illustrated in Figure 4-10-a and b. To achieve a better level of mixing, homogenization was performed manually by operator while mixing. For uniform mixing, first soil was added to the mixer. Then, an appropriate amount of cement was put into the mixer and materials were homogenized and at the end water was added. Five minutes of mixing time was selected for soil. Then the whole material was compacted in the tank and were sealed to avoid moisture loses in the sample. Finally, the sealed tank was kept for seven days of curing time.

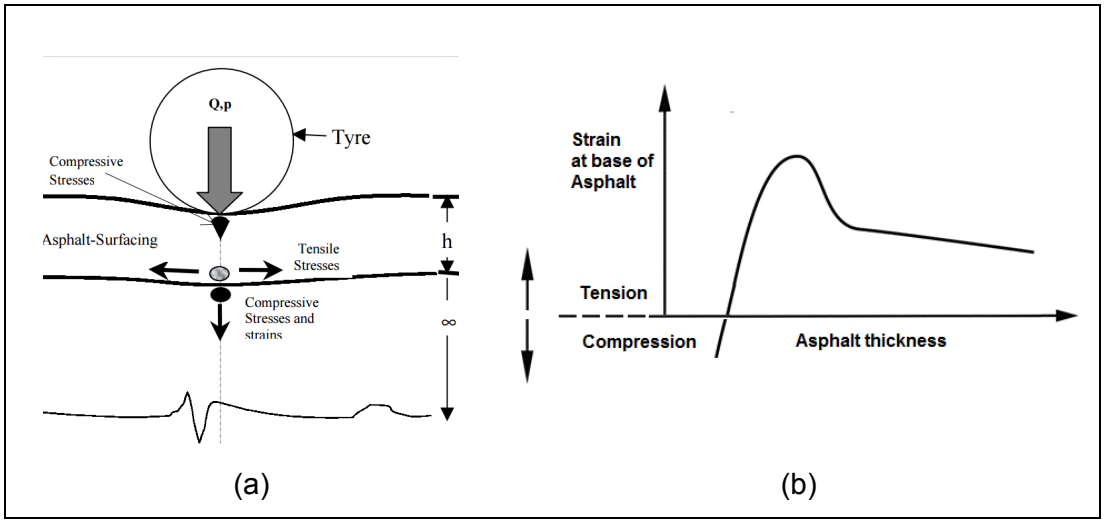

Figure 4-9 Variation of strain at the base of asphalt with asphalt thickness (Austroads, 2012)

(a) (b)

Figure 4-10 (a) Mixer (b) mixing tool

4.2.4 Testing Apparatus

A Universal Testing Machine, UTM-25, was used in this experimental research as shown in Figure 4-11-a. The load frame capacity of the machine is 25 KN in static loading and 20 KN in dynamic loading. The load was applied on soil surface using a rigid steel plate to simulate a distributed surface pressure. This steel plate has the length of 210 mm, width of 100 mm and thickness of 20 mm. The length of footing was almost equal to the width of the tank in order to maintain plane strain condition. In addition, two ends of the footing were smooth to minimize the end friction effects. In order to apply load, the loading plate was centred on the soil surface while the length of footing was parallel to the width of tank. Loading was divided into two stages 250 and 400 kPa to simulate the light and heavy traffic loadings. There was a limitation of 5 cm travel distance in the UTM 25 meaning the maximum soil surface settlement can be 5 cm and test stops automatically at this point. A benefit of the cement stabilization in this study beside soil improvement is the ability of monitoring pipe soil behaviour under more load cycles before reaching its maximum travel distance. The machine also can apply a wide range of frequencies from 0.1 to 20 Hz. To apply traffic load, Harvey sine was chosen without resting time. In Figure 4-11-b the amplitude of applied load in experimental tests is shown. It is noted that in most laboratory studies, fatigue testing is usually carried out through dynamic tests without periods of non-loading which simulates actual field traffic loading. It is worth noting that machine

compliance is a very important issue in fatigue tests. It can be measured easily by comparing the deformation measured from actuator LVDT and on specimen LVDT as shown in Figure 4-12. The results shows actuator movement is transferred well to the specimen.

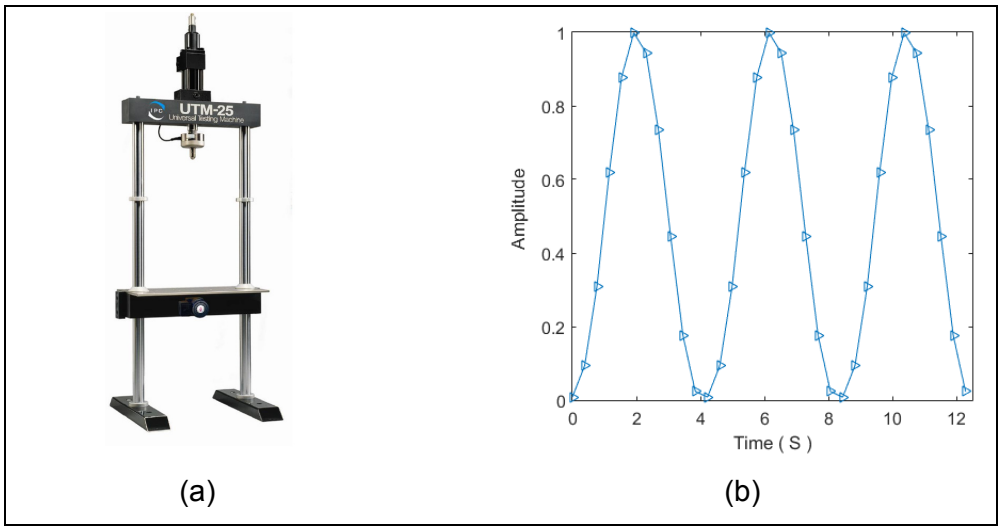

Figure 4-11 (a) UTM25 to apply load (b) the amplitude of applying load

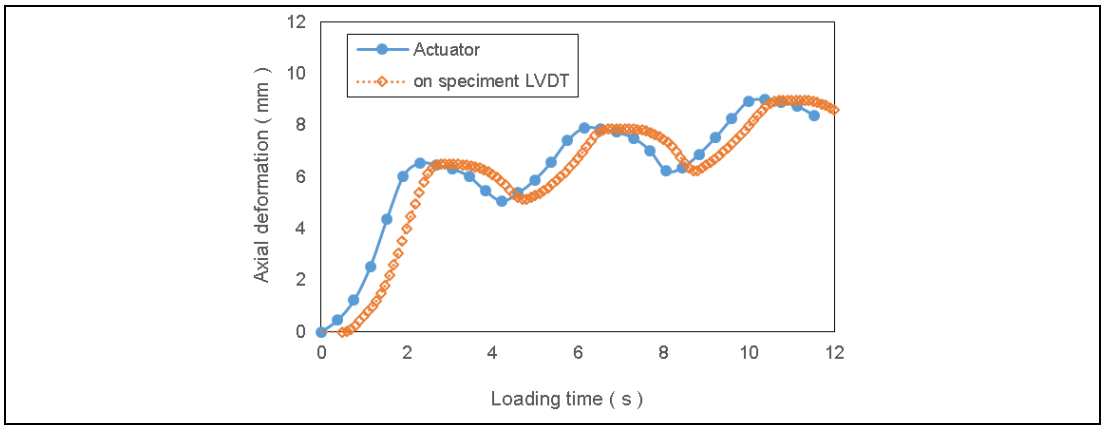

Figure 4-12 Comparison of actuator and LVDT deformations

4.2.5 Testing Program

A total of 27 tests were performed on a buried pipe to investigate the effect of burial depth, pressure magnitude, number of cycles on the soil and pipe response. Two trial tests were performed on static and cyclic load to calibrate the instruments and check the repeatability of results. 15 static and 12 cyclic tests were performed on buried pipe. Static tests includes three bearing capacity tests to investigate ultimate bearing capacity of the model for both pure and cemented sand. Summary of testing program is illustrated in Table 4-2. All tests were carried out on the same scale using same equipment and material.

Table 4-2 Scheme of the monotonic and repeated tests for non-treated and cement-treated sand for buried pipe

Test series	**Type of test**	**Material type**	**Parameters under investigation**			**Purpose of the tests**	**Comparison of cement-treated and non-treated materials**
			Load(kPa)	**H/D**	**Number of tests**		
1	Static	Non-treated	Up to failure	1	2	To determine ultimate bearing capacity of footing	Comparison is made to analyse the impact of cement on increasing bearing capacity
2		Cement-treated	Up to failure	1	1	To determine ultimate bearing capacity of footing on cement treated sand	
3		Non-treated	250,400	1,1.5,2.5	6	To investigate the impact of initial phase	Comparison is made to analyse the impact of cement treatment on model response during static phase
4		Cement-treated	250,400	1,1.5,2.5	6	To investigate the impact of initial phase on cement-treated sand and to determine the effect of various factors	
5	Cyclic	Non-treated	250,400	1,1.5,2.5	6	To quantify the effects of repeated loading and to provide a basis for assessing the benefits of the stabilization	Comparison is made to analyse the impact of cement treatment on pipe performance during cyclic phase
6		Cement-treated	250,400	1,1.5,2.5	6	To study the effect of cyclic load on stabilized sand	

4.3 FINITE ELEMENT MODEL

In this research, the numerical simulation will be conducted to investigate the impact of different factors affecting buried pipe behaviour within numerical context. This section presents the numerical model of the buried pipe under traffic load in plane strain condition. The description of methodology in this section is mainly adopted from ABAQUS user's manual documentation (ABAQUS-6.13, 2013).

4.3.1 Build a FE model Based on Laboratory Setup

In modelling of the pipe soil interaction a number of aspects need to be considered such as the mechanical behaviour of pipe, the behaviour of surrounding soil, the interaction between soil and pipe, the geometry of model and choosing proper elements for pipe and soil and their interaction. In this research the geometry of the model is created which consists of three parts including pipe and two types of soil. Then, the finite element mesh is generated. Later, material properties are assigned to each part, in which pipe is assumed elastic and soil is modelled using an appropriate elasto-plastic constitutive model. The boundary conditions, interactions and stages of analysis will be defined in the following sections.

4.3.1.1 Modelling procedure

For selecting an appropriate element type for the pipe-soil model, several element parameters should be considered such as element family (continuum, shell, beam, rigid elements,…), degrees of freedom (directly related to the element family), number of nodes, formulation and integration .The family of finite elements is a wide category which is used for element classifications. The example of commonly used element families are: continuum, shell, beam, rigid, membrane and etc. as shown in Figure 4-13.

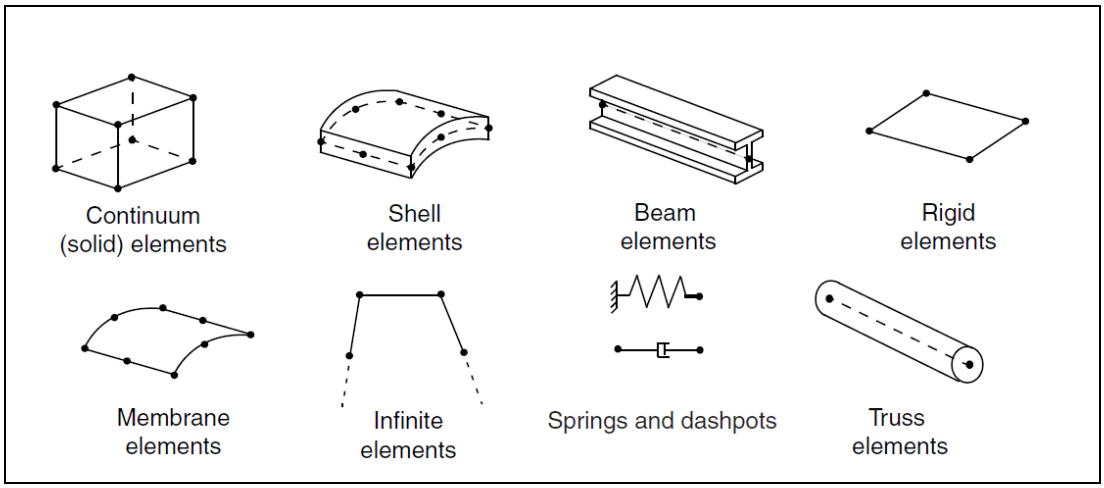

Figure 4-13 Element types in ABAQUS (ABAQUS-6.13, 2013)

Among different element families in ABAQUS, continuum or solid elements models the widest variety of components. They simply model small blocks of material in a component and they can be connected to other elements on any of their faces and can be subjected to any loading. Continuum elements can be used for both linear analysis and also for complex nonlinear analysis, which includes contact, plasticity, and large deformations. In finite element methods for each element, displacement, rotations, pressure and other degrees of freedom are only calculated at the nodes of the element and they are interpolated between nodes for any other point in the element. This interpolation order depends on the number of nodes on that element. Linear or first-order interpolations in each direction is used for the elements with nodes only at their corners, and are often called linear elements or first-order elements. While elements with mid-side nodes, use quadratic interpolation (second-order interpolation). Second-order elements provide a higher accuracy than first-order elements. Since first-order elements are stiff and have a small rate of convergence a very fine mesh is needed. This situation is not beneficial and should be avoided as much as possible in stress analysis problems. Consequently second-order elements, which capture stress concentration more effectively, are better choices for modelling geometric features. The ABAQUS element library includes linear and quadratic interpolation elements in one, two and three dimensions in various shapes. Triangles and quadrilaterals are available in two dimensions while tetrahedral and hexahedral (bricks) are provided in three dimensions which are suitable for large deformation projects. In this project, pipe and soil elements were modelled as CPE4R or 4-node bilinear plane strain quadrilateral, with reduced integration.

4.3.1.2 Pipe and soil modelling

To model material in ABAQUS based on results presented in Chapter 5, the pipe is considered as a solid HDPE pipe with an outer diameter of 110 mm and thickness of 5.5 mm. The pipe has been modelled with a linear elastic material behaviour. For soil, an elasto-plastic material law with Mohr-Coulomb and Dracker Prager failure criterion and a non-associated flow rule were considered to describe the behaviour of dense fine sand. The material property will be described later in Chapter 5. The geometry of tank is based on what described in experimental setup 4.2.

4.3.1.3 **2D**- Boundary conditions

For boundary conditions, as shown in Figure 4-14-a, vertical side of the model is fixed in a horizontal direction with vertical displacement, and the bottom of the model is fixed in both vertical and horizontal directions. Boundaries of the backfill part ranging from 1D to 2.5D, in which D represents pipe diameter.

It should be noted that in this study, the X-Y plane is the area in which the soil is subjected to various loads, e.g. positive direction for Y is opposite direction of the weight. The arrows at the top of the mesh represent the area at which traffic loads applies on soil surface. The impact of boundary condition was not studied here. Loading was simulated by applying a uniform pressure on soil surface on the flexible loading plate with the width of 0.05 m. In all models, the mesh was refined in areas with stress concentration under and near the pipe, which are the main focused area and leads to more accurate results.

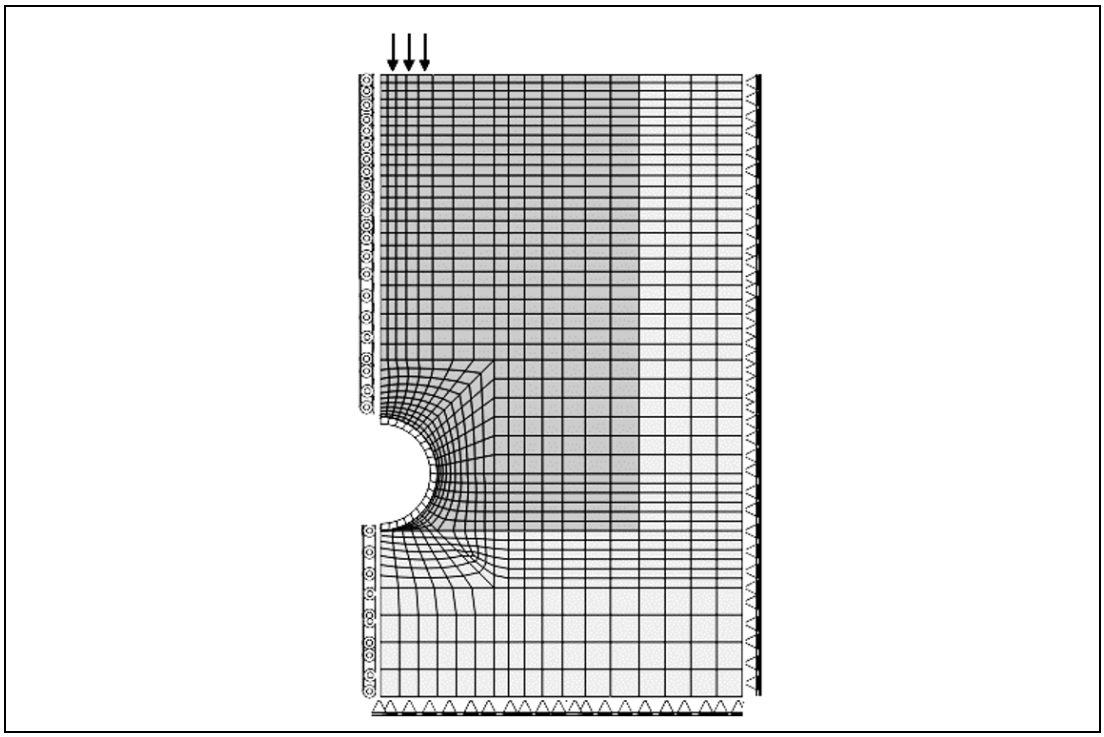

Figure 4-14 Finite element discretization and boundary conditions

4.3.1.4 Interaction

Amongst different contact models available in ABAQUS, surface to surface interaction was chosen to model the interface between pipe and soil. This interface can describe contact between two deformable surfaces or between a deformable surface and a rigid one. As the pipe is stiffer, it is simulated as a master surface and its surrounding soil as a slave surface. To avoid convergence difficulties, an unsymmetrical solver matrix was used to solve the problem as S-to-S discretization has higher tendency to generate unsymmetrical stiffness terms especially when master and slave surfaces are not parallel. The contact pair representing the soil-pipe interface is shown in Figure 4-15. To avoid penetration of the master surface nodes into the slave surface, the slave surface mesh was refined. The benefit of this model is to reduce likelihood of large localized penetrations and to improve accuracy of contact stress. The interaction properties of the model were created by defining both tangential and normal interactions. The tangential behaviour consists of sliding between two surfaces and possibly frictional shear stresses. The normal behaviour is perpendicular to the interaction surface. The pipe-soil interaction was assumed to be an adhesive friction and no sliding occurs before the shear stress reaches to its maximum value. This is numerically achieved by assuming a large friction coefficient in the soil-pipe interface. The tangential friction coefficient between pipe and soil was assumed to be

0.5 and normal contact is considered as hard one which allows separation after contact. To define the interaction in ABAQUS, the pipe element was chosen as the master surface with a stiffer body, and the soil as a slave surface with more refined meshes.

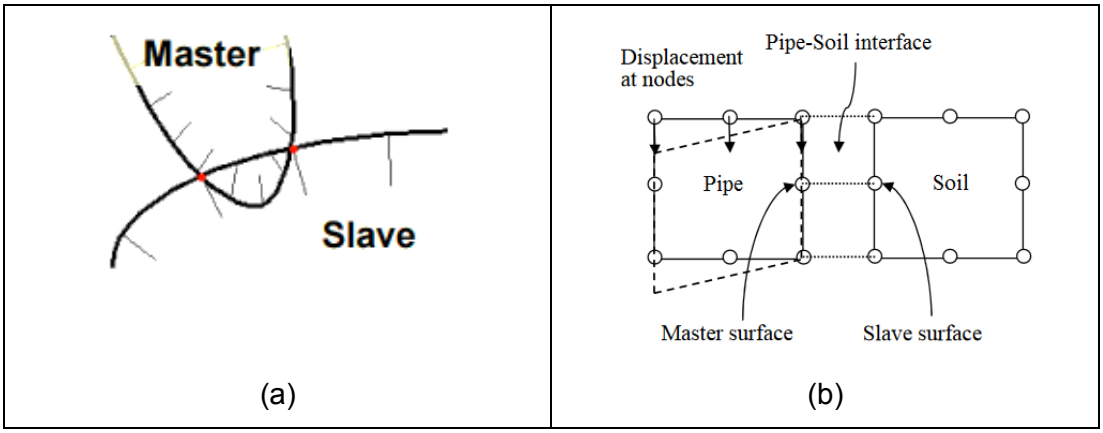

Figure 4-15 Master surface penetrate in slave surface when it is not refined (b) more master nodes per constraint is involved and coupling among slave surface (King & Richards, 2013)

4.3.1.5 Stages of Analysis

The model was created in four steps. In the first step, which was the initial condition, the pipe and soil initial conditions, such as boundary conditions and the interfaces between soil and pipe, are defined. In the next step or in the geostatic step a gravity load was applied to the model and an average initial soil stress was applied throughout the soil mass prior to application of the surface load. It is also decided to apply a uniform vertical stress equivalent to the self-weight of the soil at the level of the pipe spring line. The corresponding horizontal stress was based on earth pressure coefficient of 0.5. It should be noted that ABAQUS checks for equilibrium during this step to establish a stress field which balances the gravity load and satisfies the boundary condition. In the third step, pipe and pipe-soil interaction was activated and the pipe weight was applied to the model. Pipe elements were reactivated during this step allowing movement in a vertical direction. In the last step, traffic load was applied to the soil surface at the trench width, exactly on top of the pipe. It was also assumed that relative movement between the soil and pipe is impossible.

4.4 SOURCES OF ERROR

In this research there are sources of error and uncertainties that can affect the results of the current research, as discussed below:

- Like many experimental works, possible test errors should be taking into consideration in interpretation of data from physical modelling. This can be errors associated with instruments. For example, pressure cells could be source of errors. The difference between the stiffness of pressure cell and soil can cause errors (Biana et al., 2014). Although calibration was performed through applying uniform air pressure still the errors are expected.
- Another possible source of experimental error comes from the strain gauges. Source of error can be voltage drops caused by resistance in the wires connecting the excitation voltage to the bridge. To minimize this error, two strain gauges were installed to read and check the data at pipe springline.
- The method of compacting and homogenising of material is a definite source of error and level of compacting and homogenising of material can vary from test to test. Therefore, a good control of density during compacting was undertaken to minimize such errors.
- For finite element analysis, errors are minimized by appropriate mesh size, boundary conditions and considering error messages during analysis.
- And finally like any other experimental work, random errors and blunders can be the source of errors.

4.5 SUMMARY OF THE CHAPTER

In this chapter the methodology of the research was reviewed starting with presenting the overview of the chapter. In the second section, the experimental setup, the equipment for data acquisition, properties of testing tank and machine for applying load was described. This section was followed by 2D finite element model built in ABAQUS suitable for buried pipe analysis. Then some of possible errors associated to this research was explained. In the next chapter, the properties of material used in the research will be presented.

5 MATERIAL PROPERTIES

5.1 INTRODUCTION

Understanding the buried pipe behaviour is not possible without knowing fundamental mechanical properties of soil and pipe. This section provides information about materials used in this research. Series of tests were performed to define important material strength for sand backfill, cement-treated sand and flexible pipe. For soil, a series of direct shear tests on a compacted sandy soil and cement-treated specimens were performed at different normal stresses. For pipe, a compressive test was carried out to investigate pipe performance under compressive load. The schematic overview of this chapter is shown in Table 5.1. After introduction and chapter overview, different types of materials used in this research and their physical properties are presented. In the next section, the results of laboratory tests to characterize material properties are discussed. This is followed by material behaviour predictions using empirical methods or finite element methods.

Table 5-1 Schematic diagram of chapter review

Introducing types of materials used in the physical model testing	Soil
	Cement
	Pipe
Performing laboratory tests for material characterization	Direct shear tests on non-treated sand
	Direct shear tests on cement-treated sand
	Applying compressive load in axial direction of pipe to find relationship between strain and deflection of pipe

5.2 MATERIALS

In this section the physical properties of two soils, cement and pipe used in this research are presented.

5.2.1 Soils

Two types of soil were used in this research, soil A or backfill soil for soil around pipe and soil B or granular soil used as bedding material.

Soil A used to simulate trench soil or surrounding soil around pipe. This soil was provided from concrete laboratory in Curtin University and known as concrete sand. Grain size distribution test is performed based on Australian standards to determine soil properties. The test for grading of the larger fractions (greater than 75 μm) is carried out by sieving a sample in accordance with the requirements of AS 1141.11.1 (Australian-Standard, 2009). In this process, a sample of aggregate is shaken through a nest of sieves from largest down to smallest. The result is generally reported as the percentage passing each individual sieve size. The test was performed in a dry state and results are illustrated in Figure 5-2. The grain size distribution of this sand is shown in Figure 5-2-a and soil is classified as SP or poorly graded sand. This is a soil with the grain size between 0.07 and 4.75 mm with D_{50}=0.32 mm; C_u=2.11; C_c= 1.14 and ρ_d=1.65 kg/m^3 as shown in Equations 5-1 and 5-2. The results of compaction test is shown in Figure 5-2-b

$$C_C = \frac{(D_{30})^2}{D_{60} * D_{10}} = 1.14 \qquad 5\text{-}1$$

$$C_u = \frac{D_{60}}{D_{10}} = 2.11 \qquad 5\text{-}2$$

Soil B or the granular soil used to simulate the subgrade material. This soil typically is used to simulate road base material under flexible pavements in construction projects. The soil was provided from pavement laboratory in Curtin University and known as base soil. Grain size distribution is performed in accordance with Australian standards. The soil is a gravel soil with the grain size between 0.07 and 26 mm with D_{50}=4.7 mm; C_u=11.33; C_c= 0.078 and ρ_d=2.0 kg/m^3.The grain size distribution of this soil is shown in Figure 5-2-a. This soil is classified as GP or poorly graded gravel. The properties of both soils used in this research are shown in Table 5-2.

(a) (b) (c)

(d)

Figure 5-1 (a) to (c) Tests on physical properties of sand in the laboratory based on AS 1726-1993 (d) granular soil

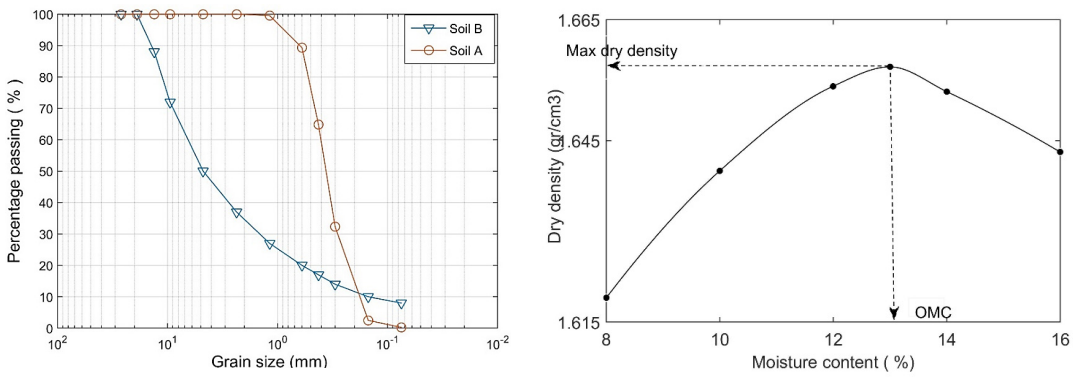

(a) (b)

Figure 5-2 (a) Grain size distribution of soils (b) compaction test results for sand material

Table 5-2 Physical properties of soils

Description	Soil A	Soil B
D_{50} (mm)	0.32	4.7
Coefficient of uniformity (C_u)	2.11	11.33
Coefficient of concavity (Cc)	1.14	0.078
Max. dry unit weight (kN/m^3)	16.6	20
Optimum water content (%)	13.5	5

5.2.2 Cement

A general purpose cement of AS 3972 has been used for sand stabilization. This cement is mainly used in different infrastructure constructions in civil engineering projects in Western Australia. Based on manufacturer catalogue the grey cement has minimum of 92.5% Portland cement and maximum of 7.5 % mineral and other additives. The results of compaction test for 5% cement and sand are illustrated in Figure 5-3. As illustrated cement-treated material has higher density and optimum moisture content compared to non-treated sand. These results are consistent with literature (Kitazume & Terashi, 2013; Sétra-LCPC, 2000).

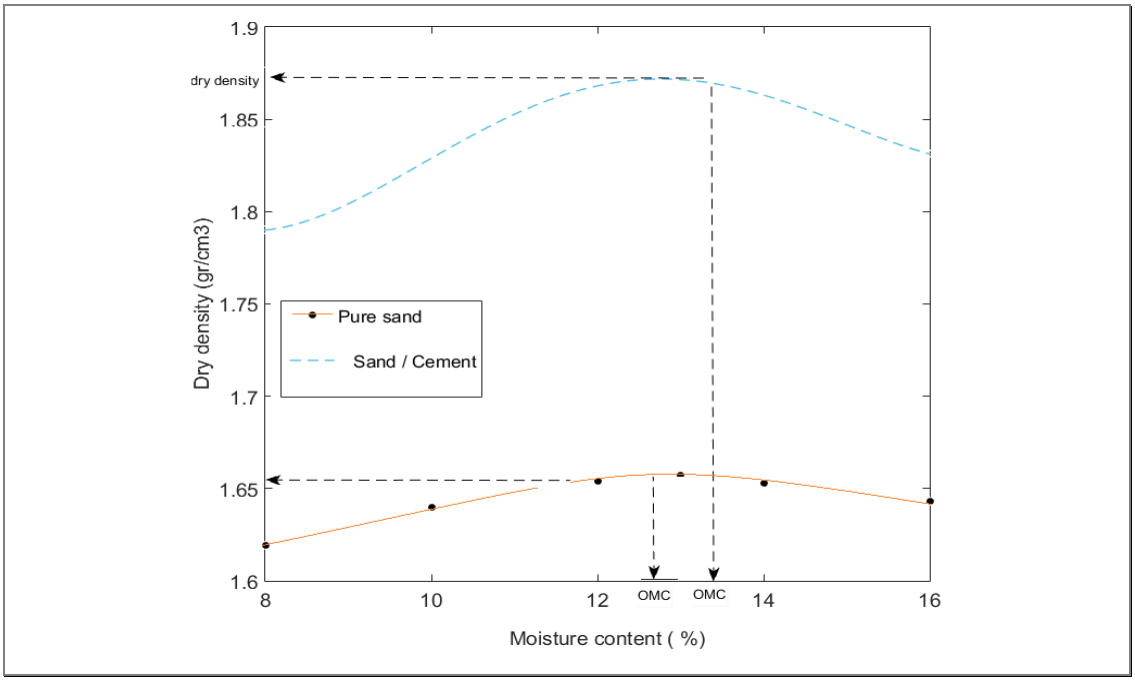

Figure 5-3 Compaction curve of cement-sand material

5.2.3 Pipe

In urban services such as drainage sewer applications, pipe diameters vary widely. For this project a reasonable dimension for pipe representing a common flexible pipe has been chosen. The plastic pipes used in this research has 110 mm external diameter, 5.5 mm thickness and 220 mm length with a Standard Dimension Ratio (SDR)= D/t=20. The pipes were made of polyethylene (HDPE: high-density polyethylene), the manufacturer is Enviropipe (Enviropipes, 2015) and is illustrated in Figure 5-4. The properties of pipe are shown in Table 5-3 based on manufacturer catalogue. To prevent binding against the end walls and boundary condition impacts, the pipe was 10 mm less than the width of the tank. In order to prevent sand particles entering the pipe and to reduce friction between the pipe/tank faces, the two ends of the pipe were covered by plastic before being placed in the tank.

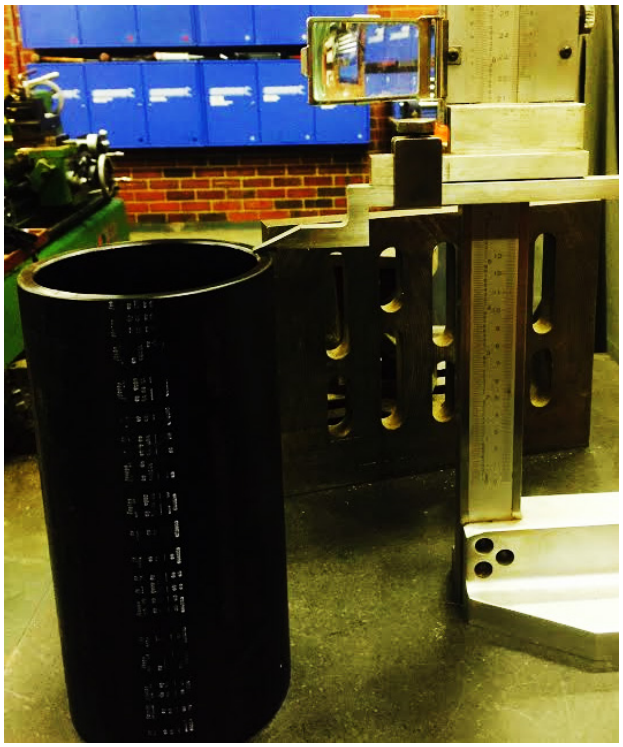

Figure 5-4 HDPE Pipe used in the research

Table 5-3 Pipe properties (Enviropipes, 2015)

Parameter	Test Method	Value for HDPE pipe
Density, ρ (kg/m^3)	ISO 1183D , ISO 1872-ZB	955
Tensile Modulus, Short Term (MPa)	REF. AS/NZS2566	950
Tensile Modulus, Long Term (MPa)	REF. AS/NZS2566	260
Poisson's ratio,		0.4
Yield strength (MPa)	ISO527	23

5.3 CHARACTERIZATION OF MATERIAL

The experimental program summarized in Table 5-4 aims to investigate the characteristics of soil used in this research. Direct shear test was used to evaluate material behaviour. The samples were sheared by applying normal stresses at strain rate of 1 mm/min. To simulate the same condition, a consolidated–drained (CD) test is used to obtain the effective strength parameters of the soil under normal stress of 50, 100 and 150 kPa. Then, in order to obtain reliable and realistic stress-strain characteristics of material a series of triaxial tests were conducted on sand.

Table 5-4 test specifications on soil

Variable	Direct shear test	Triaxial
	Normal stress (kPa)	Confining pressure (kPa)
Sand	50-100-150	50-100-150
Sand-cement		---------
Curing time(days)		
Sand	---------	---------
Sand-cement	1-7-28 days	---------

5.3.1 Direct Shear Test

Since 1700's, geotechnical researchers found out that most soil deformation is irreversible and principles of elasticity is not adequate for predicting soil behaviour. The direct shear test is commonly conducted to obtain the stress-strain relationship, together with the shear strength parameters (i.e. the cohesion *c* and the friction angle *φ*) under different normal stresses. In the following section, the methodology and results of direct shear tests performed on non-treated and cement-treated specimen are discussed.

5.3.1.1 Specimen preparation and testing procedure

The direct shear tests were carried out using a small direct shear apparatus (box size of 63.5 mm × 63.5 mm × 24 mm) according to AS1289.6.2.2 (Australian-Standard, 2001). With reference to the direct shear test theory, the size of the sample is an effective factor for determining strength properties of the soil. In addition, the triaxial test was performed to calibrate the model and predict model response which will be explained later in this chapter. Two types of samples were prepared for direct shear test: pure and cement stabilized sands. Pure sand specimens were compacted at optimum moisture of compaction test and tested after one day. All cement stabilized specimen were treated with 5% cement at optimum moisture content and were compacted properly in direct shear box using a specific hammer as shown in Figure 5-5. After preparation, the treated specimens were stored in three different curing period of one, seven and 28 days in humid condition in which the shear box was covered with sealant to prevent moisture changes. It is noted various factors affect the strength of cement-treated soil and the key factors are cement content, water content, curing time and type of soil (Panda & Rao, 1998). Cement content was chosen to be 5% for backfill material. The soil type does not change in the research and kept as sand. The optimum water content was obtained from compaction test.

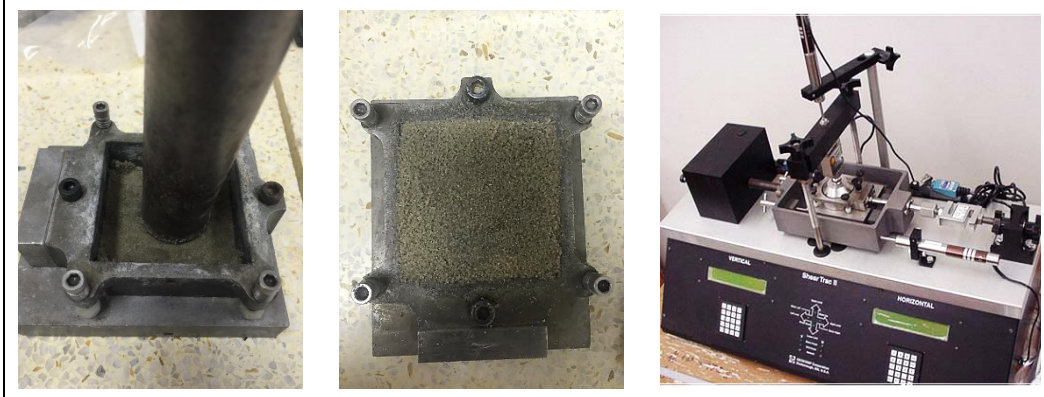

(a) (b) (c)

Figure 5-5 (a) & (b) stages of sample preparation for cement-sand material (c) direct shear test device

5.3.1.2 Test results

To study the impact of cementation on strength of sandy soil, the results of direct shear test based on different times of curing are presented in the following section. All cement treated specimens with cement contents of 5% by weight of dry soil were prepared and cured at room temperature. Figure 5-6 shows the stress strain response for different treated and non-treated specimens conducted at a confining stress of 50, 100 and150 kPa. Horizontal axis represents axial strain and vertical axis represents shear strength of specimens. In the provided plots, pure sand is represented by dashed line in the plot and cement-treated specimens are represented by continuous lines. Overall, the peak deviator stress of cement-treated specimens is higher than those of the non-treated specimens due to the effect of cementation bonds. For example, under normal stress of 50 kPa, pure sand yields at 40 kPa while 1-day cemented sample yield at 55 kPa. Moreover, as the normal stress increases, the peak shear strength of samples increases. Curing time improves soil behaviour and 7-day cemented samples have higher yielding strength. For example, a 7-day cement-treated specimen under normal pressure of 150 kPa has the shear strength of 370 kPa while 1-day cement-treated has 120 kPa shear strength.

In terms of curing time impact on axial strain of samples, same results are concluded. For example, 1-day cemented samples have slightly lower shear strains. For non-treated samples, yielding is observed at an axial strain of 0.5 to 2% while for cement-treated samples yielding is observed at axial strains of 0.5 to 0.8 % for 7-day cured. These specimens have more brittle pattern compared to pure sand as their behaviour is no longer like sand to chemical reactions. In general, a nonlinear stress–

strain behaviour reaching a peak shear strength at an early stage of shearing was observed for pure sand and 1-day cement-treated specimens. However, a linear response in the shear stress-axial strain plot is observed for 7-day cement-treated specimens. After the peak strength is reached, a sharp decrease in strength is observed. This behaviour suggest an elastic response up to the yield point.

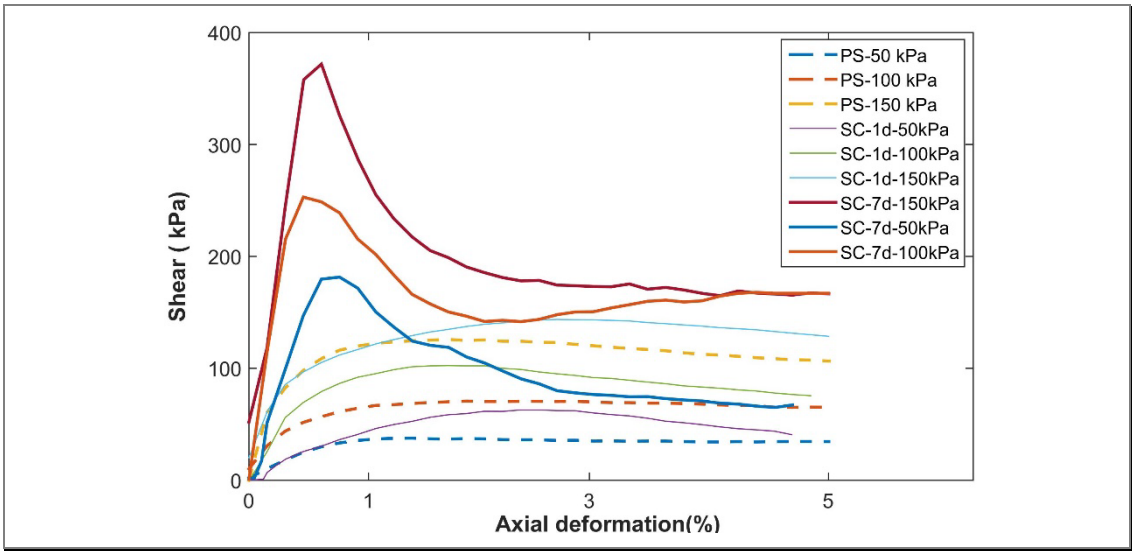

Figure 5-6 Shear test results

Three Mohr's circles corresponding to failure stresses obtained from the direct shear test results for all curing conditions are plotted in Figure 5-7 to Figure 5-10. It can be seen that, for pure sand the line intersects with the vertical axis at zero. The failure envelope for treated sand is steeper than non-treated samples. In other words, the critical state lines become steeper for cement-treated specimens. The shear strength of samples can be assessed using the internal friction angle and the cohesion of the specimens. The Mohr–Coulomb failure criterion is plotted as a straight line which is tangential to all three circles.

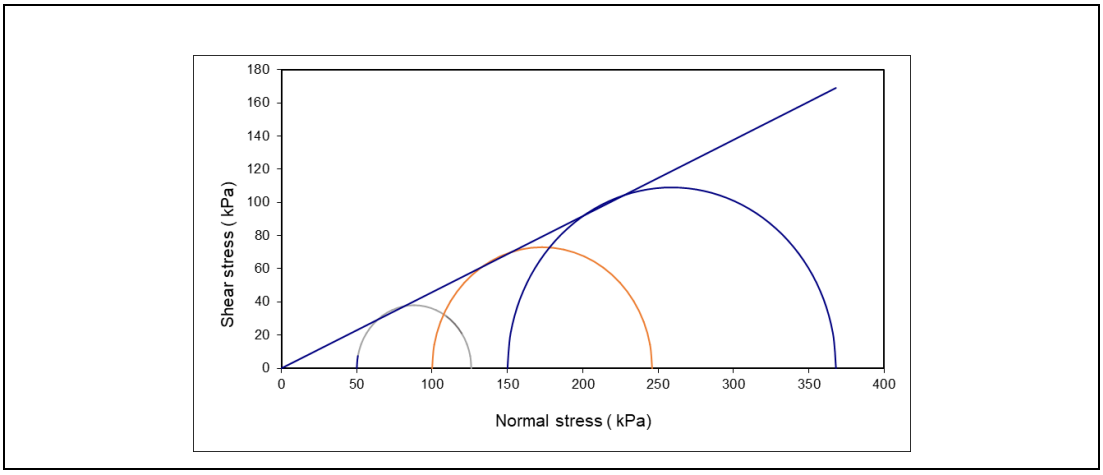

Figure 5-7 Mohr-Coulomb failure criterion for sand

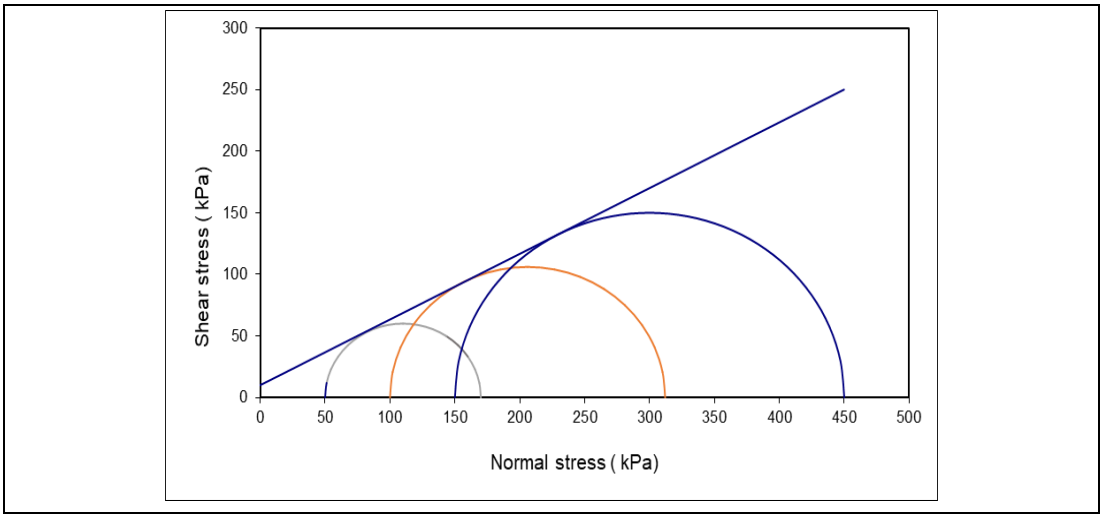

Figure 5-8 Mohr-Coulomb failure criterion for 1-day cement-treated sand

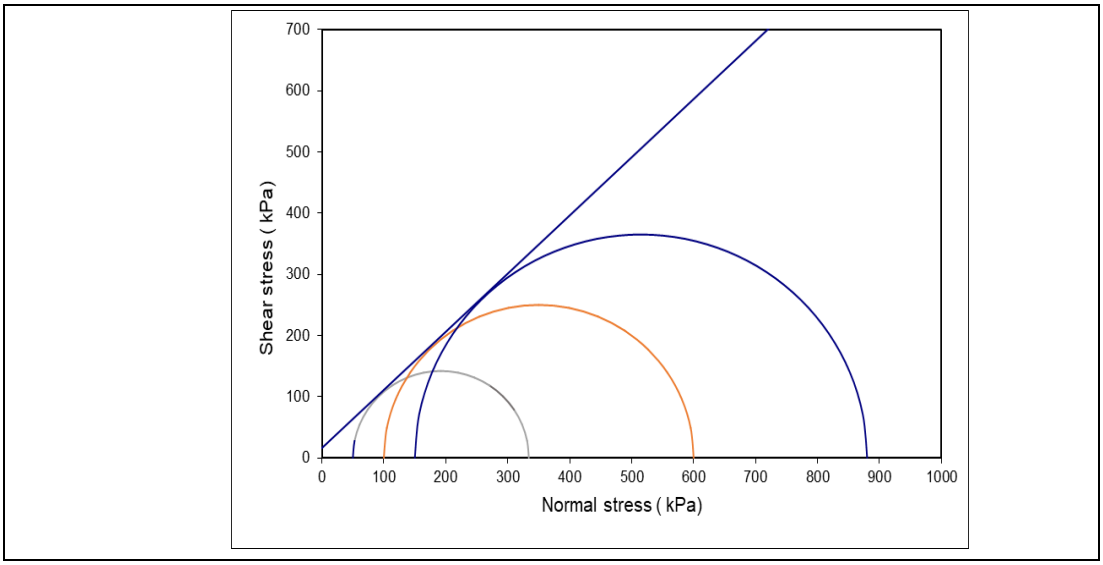

Figure 5-9 Mohr-Coulomb failure criterion for a 7-day cement-treated sand

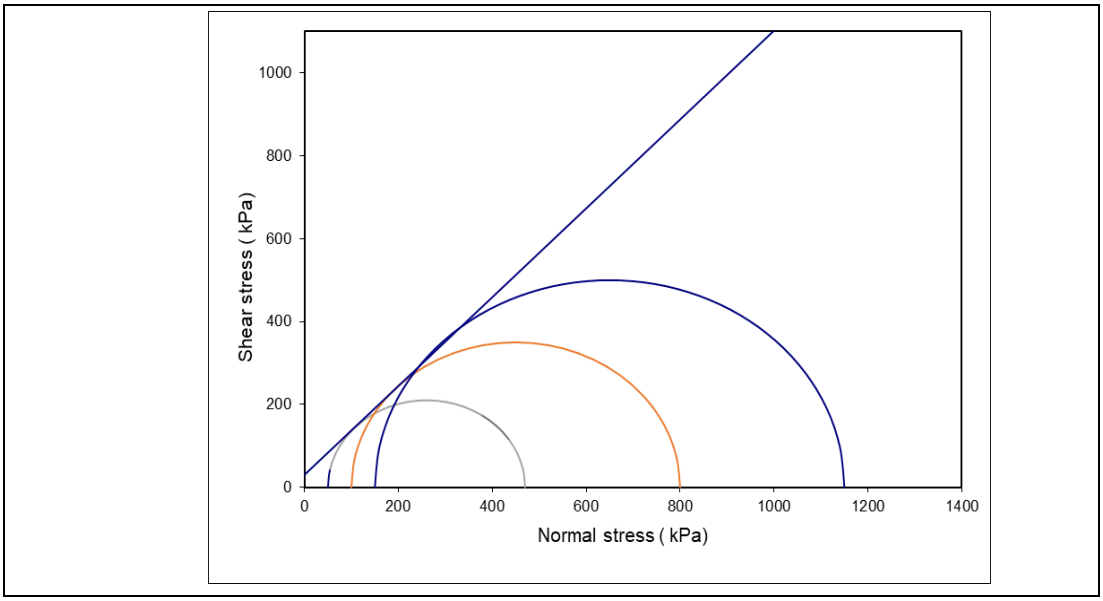

Figure 5-10 Mohr-Coulomb failure criterion for a 28-day cement-treated sand

The soil strength parameters are calculated and results are illustrated in Table 5-5. Although it is suggested in some references that the failure envelope of cemented soil is not linear over a wide range of confining pressure (Lade & Overton, 1989), a straight line strength envelope was used to define friction angle and cohesion intercepts as only three normal stresses were used in this research. It can be seen from the table that soil strength parameters are influenced significantly by time. In addition, cementation improves soil shear strength and angle of friction. For example cohesion of 1-day cemented sample is higher than those related to pure sand.

Table 5-5 Summary of peak shear strength parameters

samples	Peak friction angle	Cohesion (kPa)
Pure sand	29	0
1-day cement-treated	34	8
7-day cement-treated	36	16
28-day cement-treated	39.5	30

To assess the impact of stabilization and curing time, the strength of all samples at different normal stress and curing times of 1, 14 and 28 days are shown in Figure 5-11. Overall, all samples become stronger with increasing normal stress. Cementation increases shear strength of samples and the longer curing time, the higher is shear strength. For example, one day cemented sand under normal stress of 100 kPa, has shear strength of 106 kPa while pure sand yields at 75 kPa. In other words, cementation improves soil property and shear strength increases 40% after only one day curing. Increasing curing time, increases shear strength of the soil significantly. For example, shear strength of samples are 106 to 150 and 350kPa when curing time increases from 1 to 7 and 28 days, respectively. Results presented here are consistent with those presented in the literature in terms of curing time impact of cementation (Kido et al., 2009; Kitazume & Terashi, 2013; Mosadegh. et al., 2017; Yoshizawa H. et al., 1997).

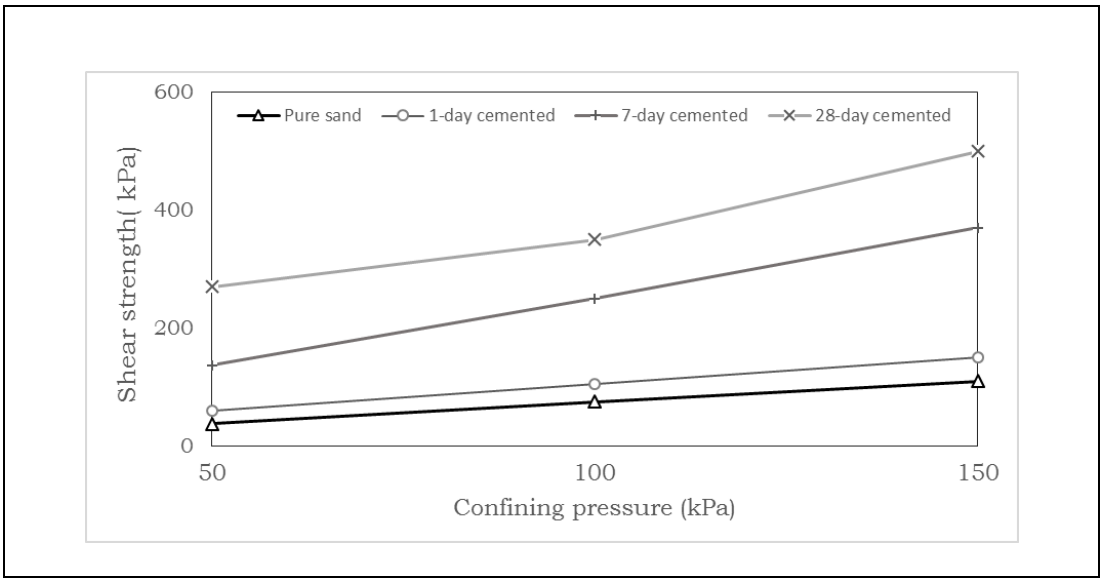

Figure 5-11 Cementation and curing time impact on soil shear test

In order to compare the effects of curing time on mechanical behaviour of the sand, shear strength parameters such as cohesion and angle of friction were selected to be analysed. The soil strength parameters φ and c are obtained from the slope and intercept of the Mohr-Coulomb failure criterion, respectively. A dual axis chart is used for better understanding of the trends of each parameter versus curing time. To assess the impact of curing time on strength properties of sand, two values were determined. These values are represented as change of φ (which is shown on the left Y-axis) and the ratio of C_2/C_1 (which is shown on the right x-axis). Change of φ is the extent to which friction angle gains strength by comparing initial value of friction angle (for pure sand) and final value (for treated sand) at given curing time. Ratio of C_2/C_1 is the ratio of cohesion of treated sample to cohesion of non-treated samples.

The impact of curing time on friction angle and cohesion of cemented samples is investigated and results are shown in Figure 5-12. The impact of early age of curing time can be seen in this figure. The gaining strength rate increases at initial ages of curing but slows down for longer curing time. Overall, both angle of friction and cohesion increase with curing time. For example, there are 40 and 60% increase in friction angle for samples cured for 7 and 28 days. This value for samples at one day of curing time is only 8%. The ratios of cohesion of cement-treated to untreated samples are 20, 44 and 58 for 1-day, 7-day and 28-day samples, respectively. These values show the importance of stabilization and curing time on increasing cohesion of material.

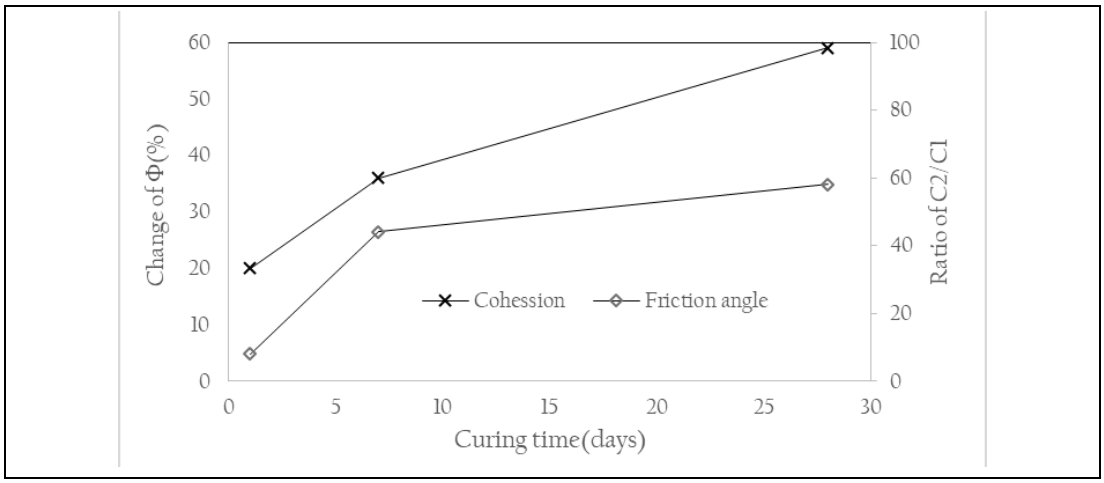

Figure 5-12 Importance of curing time on behaviour of soil

5.3.2 Triaxial Test

In order to obtain the reliable stress-strain characteristics for numerical modelling it was decided to conduct three triaxial tests on pure sand. Triaxial tests were carried out under same conditions as direct shear tests, consolidated drain condition at confining pressures of 50, 100 and 150 kPa. Specimens were prepared by mixing soil and water to produce homogeneous specimens. Specimens were compacted in layers in 65-mm diameter, 130-mm high cylindrical mould, to a dry unit weight of 16.5 kN/m^3, and at an optimum moisture content of 13.5%, corresponding to the average values obtained in standard Proctor compaction tests as illustrated in Figure 5-13 . The static drained triaxial tests were carried out under full saturation, for the confining stresses of 50, 100, and 150 kPa based on ASTM D4767 (ASTM-D4767, 2011). Soil specimen was saturated by circulating water through the specimen, from bottom to top, utilizing the two drainage tubes shown in Figure 5-13-b. In CD test the deviator stress $\sigma_d = \sigma_1 - \sigma_3$ was applied very slowly while the drainage valves were opened, to ensure that no excess pore water pressure was generated. Consequently, the effective stresses are equal to the total stresses during test. Because of its stringent loading requirements, the CD test may take days to carry out, making it an expensive test. The results of triaxial tests are shown in Figure 5-14. Note that ε_a is the axial strain and $\sigma_1 - \sigma_3$ is the deviator stress and sandy soils have smooth nonlinear stress–strain behaviour in these tests.

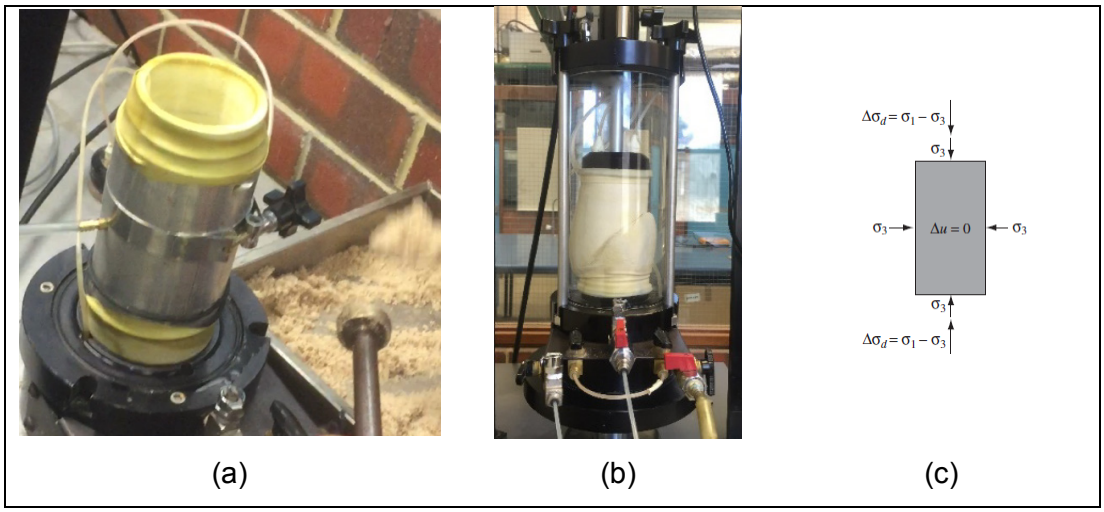

Figure 5-13 (a) sample preparation (b) triaxial test setup

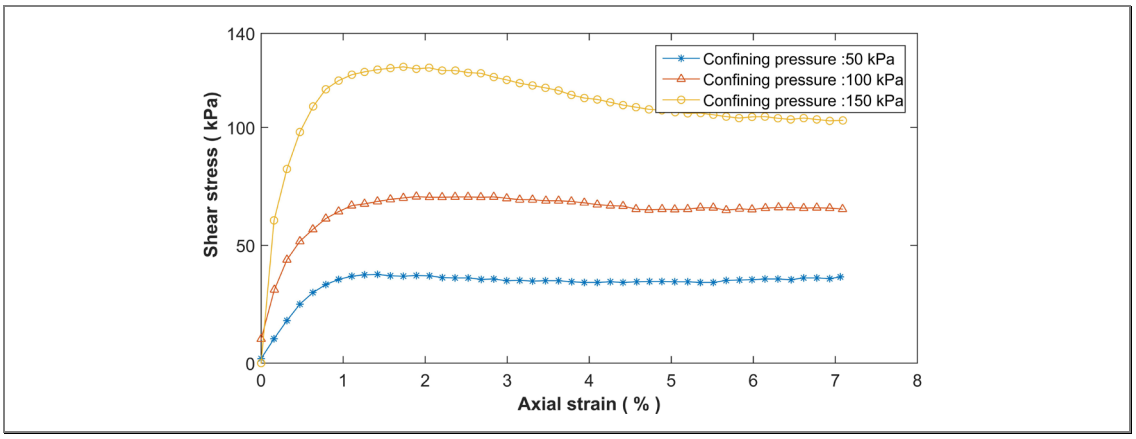

Figure 5-14 Triaxial test results on non-treated sand

Three Mohr's circles corresponding to failure stresses from triaxial test results are plotted in Figure 5-15. It can be seen that, the failure line intersects with the vertical axis at zero with the same friction angle as direct shear test.

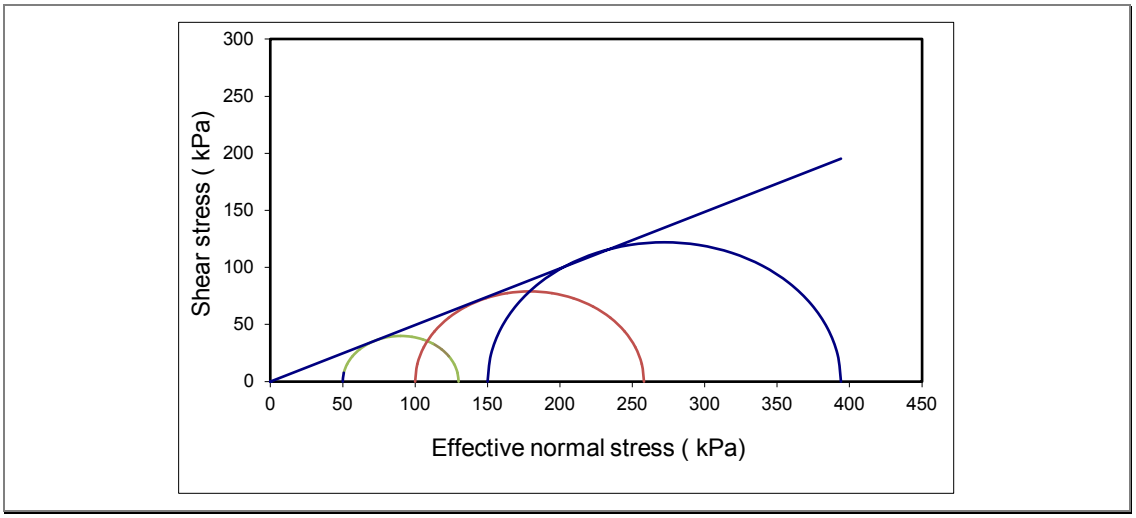

Figure 5-15 Mohr-Coulomb failure criterion for pure sand –triaxial test results

The results of triaxial tests can also be used to estimate initial elastic modulus of soil. As noted by Ducan (1970) after plotting ε1 vs $\varepsilon_1/\sigma_1-\sigma_3$ where ε_1 is axial strain and $\sigma_1-\sigma_3$ is deviatoric stress, the single line through scatter data can be used to calculate initial Young's modulus. The intercept of each line is equal to $1/E_i$. This approach of estimating Young's modulus was repeated for each test and the results for different tests are shown in Figure 5-16-a. Then the calculated Young's modulus for each test is plotted versus confining pressure and results are shown in Figure 5-16-b. The results indicate that the initial modulus of sand is a function of mean stress applied on the soil. It can be seen that Young's modulus varies with confining pressure and for specific confining pressure the Young's modulus can be interpolated. These findings are consistent with findings of other researchers (Cameron, 2005; Karimian, 2006)

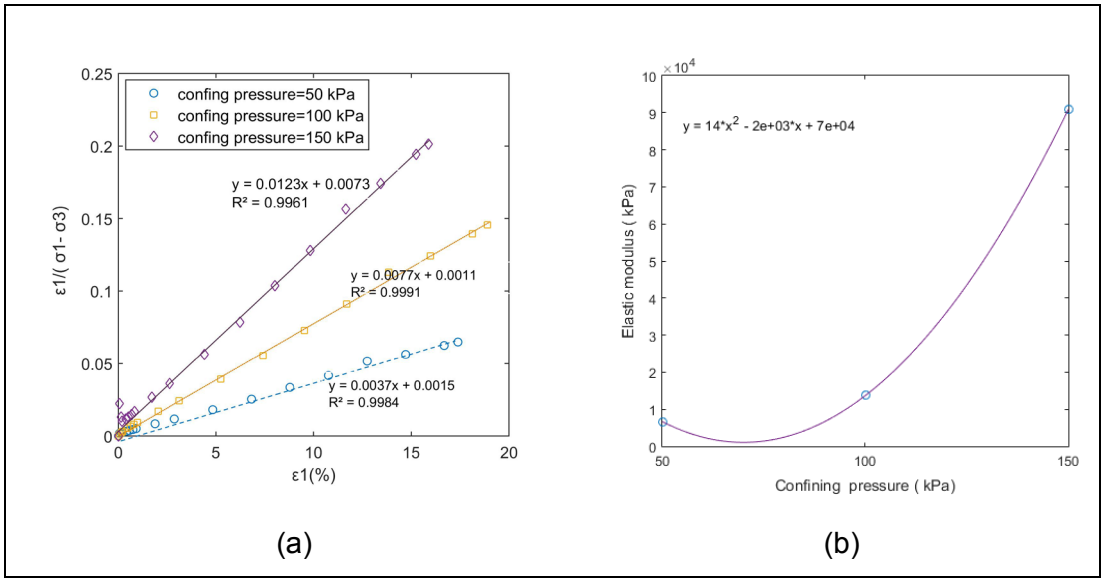

Figure 5-16 (a) Determination of the initial elastic modulus for different confining pressures (b) variation of initial elastic modulus calculated from triaxial tests

5.3.3 Pipe Deflection Measurement in Laboratory

Pipe deflection can be determined from equations or in the laboratory. In order to model pipe behaviour a compressive load in axial direction was applied through a plate on pipe crown. Marshall Stability machine CL40580 was used to apply load with the load cell limit of 50 KN as shown in Figure 5-17. Pipe had a length of 200 mm and the load was controlled and increased by the operator and radial deformations were measured by two LVDTs installed on the pipe. In addition, four strain gauges were installed on crown, invert and cross line of pipe to measure pipe strain under applied load. The reason to have LVDT and strain gauges installed on pipe is to establish a relationship between reading of strain gauges and pipe deflection. It should be noted

that in the current project, the buried pipe is under traffic load parallel to the force. Therefore, the load in the pipe deflection test was only applied in axial direction. The time for stress relaxation was also applied and it was observed that pipe returns to its initial position after few hours of resting.

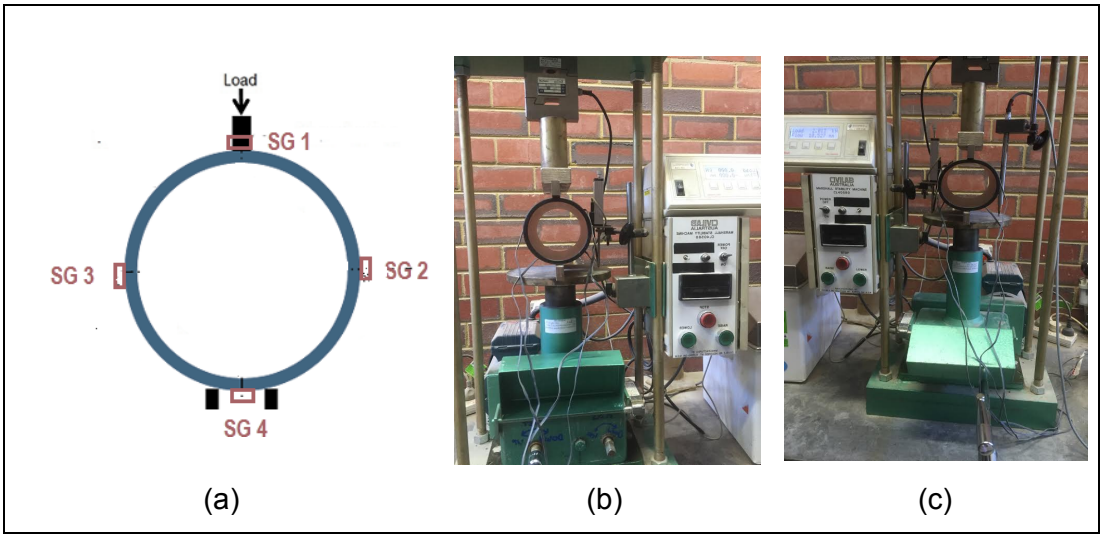

Figure 5-17 Strain gauges positions on the pipe (b) test setup before the test (c) after deformation

The results of strain gauges readings versus time are illustrated in Figure 5-18-a. Positive values are related to strain gauges under tension and negative values are for those under compression. It can be seen that, under a given applied load all strain gauges behave in the same manner and by increasing the applied load, strain gauges read higher values. At 3500 s all strain gauges read their maximum absolute values and after this point there is an unloading. After unloading, all strain gauges merge to almost the same value of zero though it takes almost 1000 seconds of unloading to reach to zero. It is helpful to put multiple data trends onto one graph to be interpreted easily. Figure 5-18-b shows combination of pipe strain and radial displacement versus time. Dashed line and solid lines represent LVDT and strain gauges at pipe crown reading, respectively. These results show that reading from strain gauge reading at pipe crown. Developing relationship between these two variables to predict pipe deflection based on strain gauge reading will be discussed later. Results of pipe deflection under various loads are shown in Figure 5-19. As illustrated there is a linear relationship between these two variables and increasing load from 160 to 850 kPa increases the pipe deflection from 1 to 8%.

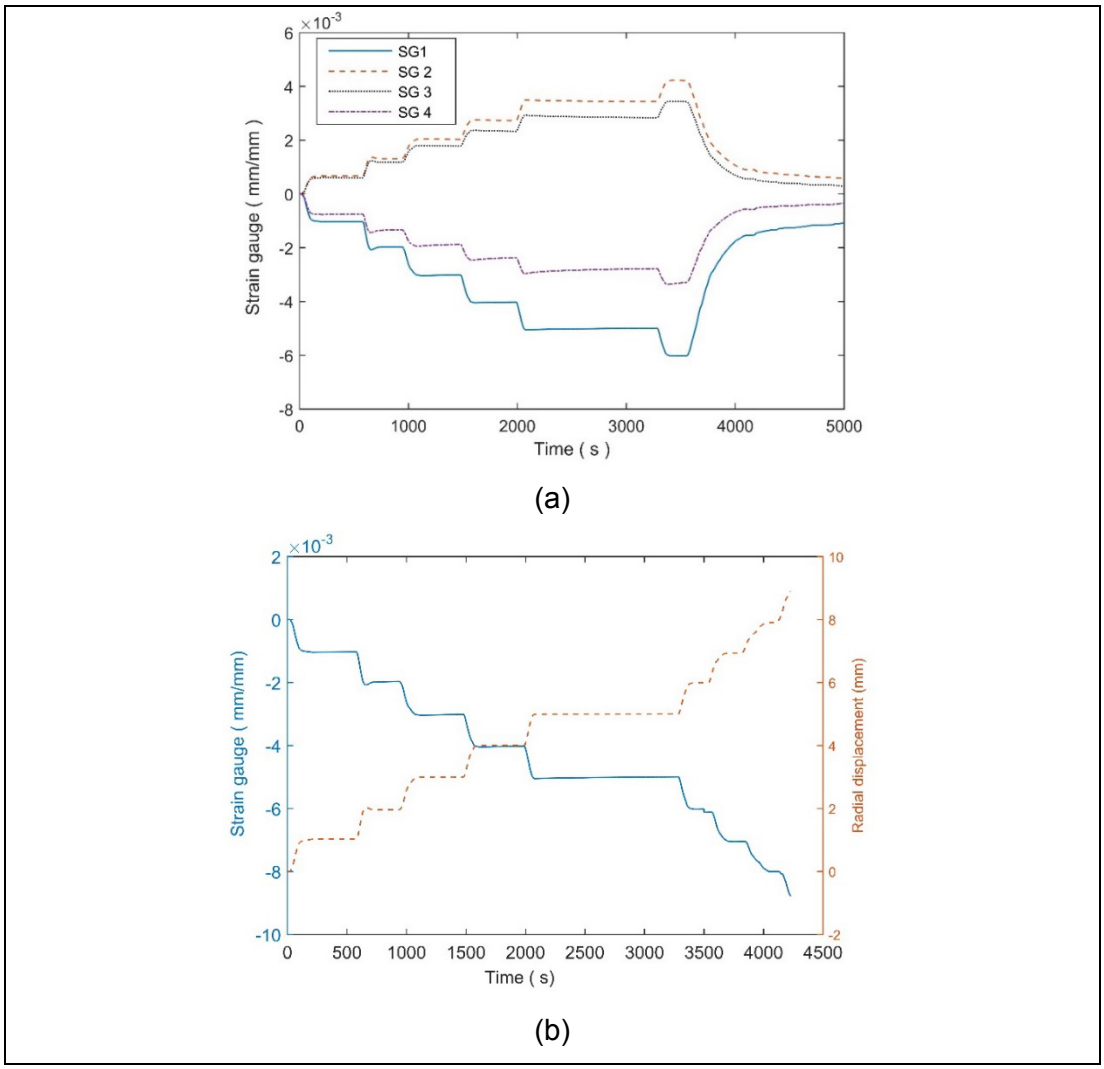

Figure 5-18 Measured strain at 4 points (b) comparison of radial deformation and strain gauge measurements

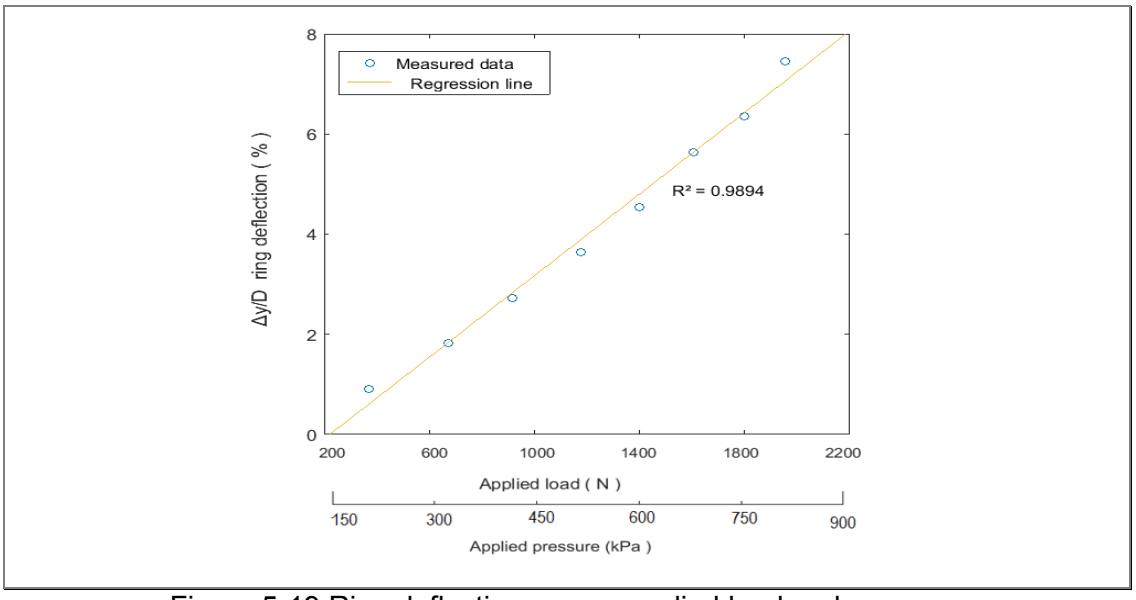

Figure 5-19 Ring deflection versus applied load and pressure

Figure 5-20 illustrates the results of pipe vertical deflection versus strain gauge reading. Horizontal axis represents change of strain gauge and vertical axis represents vertical deflection. As shown, there is a linear relation between and circumferential strain (CS) and vertical diametric strain (VDS) as shown in Equation 5-3:

$$VDS_V = CS \times 0.00045 \qquad 5\text{-}3$$

In which CS is reading of strain gauge (μmm/mm) at pipe crown and VDS is the predicted vertical diametric displacement at top of pipe. For example when strain gauge shows value of 12044, the VDS of pipe is 5% for which LVDT reading for pipe diametric change is 6 mm. It should be noted VDS in vertical direction equals to Δ/D in which Δ is LVDT reading. Another equation from finite element and lab analysis is the relationship between horizontal diametric change of pipe and reading of SG2 and SG3 which will be discussed in section 5.4.

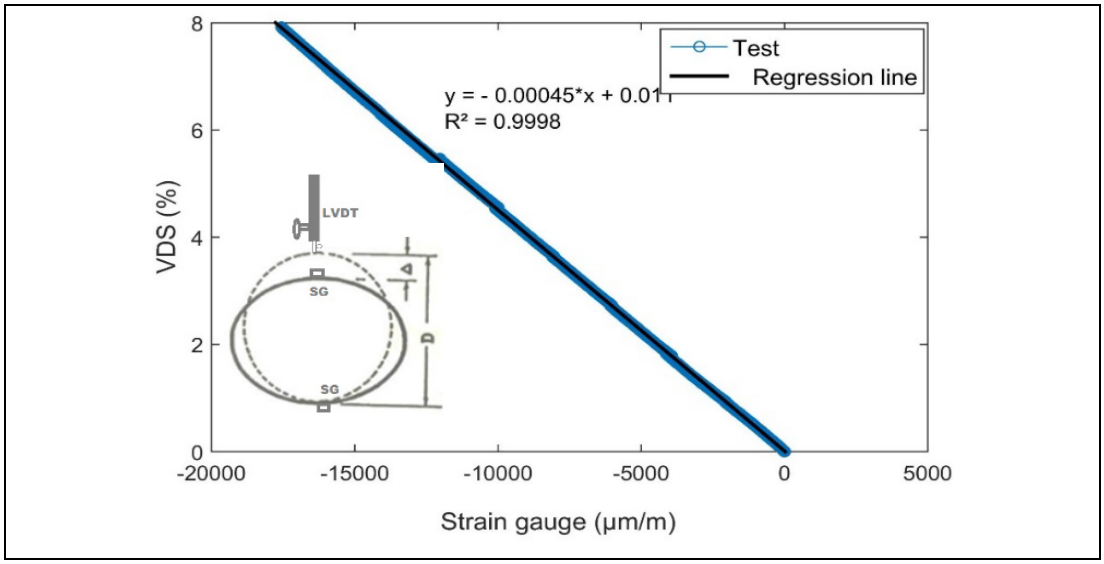

Figure 5-20 Relationship between recorded strain gauge and vertical deflection of pipe

5.4 PREDICTING PIPE RESPONSE

Deflection is a design parameter for flexible pipelines. All flexible pipes should have a design deflection limit as their performance limit considering a safety factor.
Schematic diagram of a flexible pipe deflection is illustrated in Figure 5-21. There are various methods for predicting the behaviour of pipe including strain and pipe

deflection due to loads. In this research, empirical and finite element methods are used to predict pipe behaviour which are discussed in the following sections.

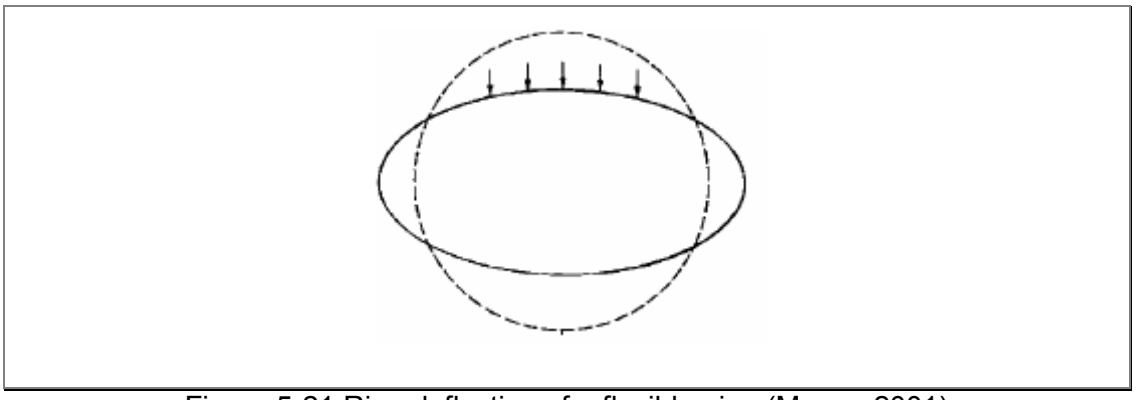

Figure 5-21 Ring deflection of a flexible pipe (Moser, 2001)

5.4.1 Empirical Method

The strain of a plastic flexible pipe can be calculated through the following equation under combined load (Moser, 2001):

$$\varepsilon = \frac{PD}{2Et} + 6\left(\frac{t}{D}\right)X\left(\frac{\Delta y}{y}\right) \qquad 5\text{-}4$$

In which *P* is internal pressure, *D* is pipe diameter, *E* is Young's modulus of pipe, *t* is pipe thickness, and *Δy* is total vertical diametric displacement of pipe. For any given load, calculations were made to predict pipe strain based on different pipe deflection values and results are shown in Figure 5-22. As there is no combined load and the pipe is under compression load only, the first part of Equation 5-4 equals to zero.

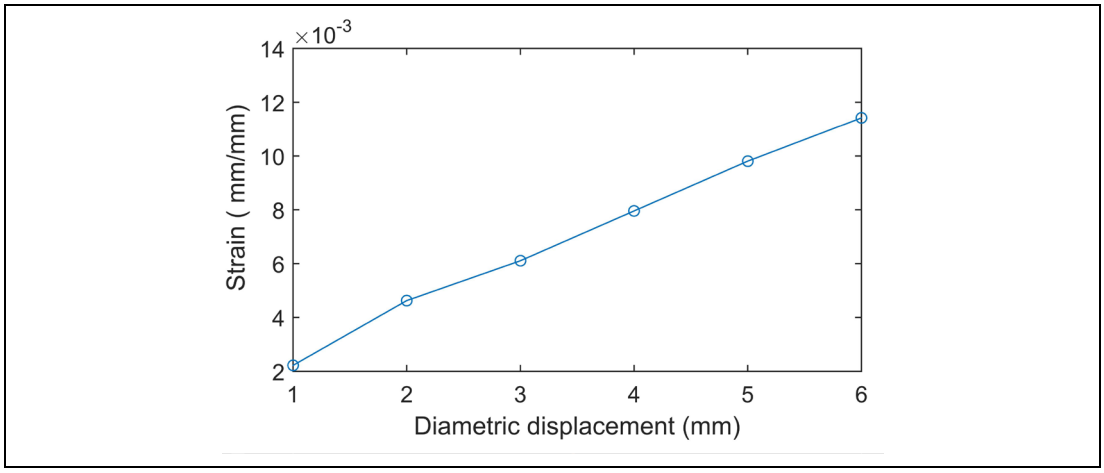

Figure 5-22 Empirical method results

5.4.2 Finite Element Method

The finite element method has shown to be successful in predicting pipe behaviour (Moser, 2001). Recently, in a research performed at Utah State University it was shown that the finite element method is the most successful method in the prediction of the behaviour of large-diameter HDPE pipes (Moser, 2001). In addition, finite element methods are convenient alternatives to overcome the problems associated with different assumptions in empirical and analytical methods (NCHRP, 2009). A finite element model was built to measure pipe deflection and strains. Pipe material is assumed to be isotropic and linear elastic with Young's modulus of 960 MPa and Poisson ratio of 0.40 with tensile yield stress of 23 MPa. As the impact of viscoelasticity or temperature and time are not considered in this research, elasticity and Poisson ratio are not changing. Element type is a three- dimensional elements shell elements (S4R) with linear shape function and reduced integration as shown in Figure 5-23. It should be noted that pipes can achieve their flexibility through a shell-type behaviour, responding to bending loads with significant ovalization of the pipe cross-section. This is in contrast to the beam response of straight pipes, where the cross-section does not deform a significant extent. The model was generated in two stages. In the first step, which is the initial condition, all boundary conditions were defined. In the next step, a downward compressive load was applied as a distributed load on top of a steel plate located at pipe crown. It should be noted the duration of this step was long enough to avoid sudden collapse of numerical modelling and to be consistent with laboratory analysis.

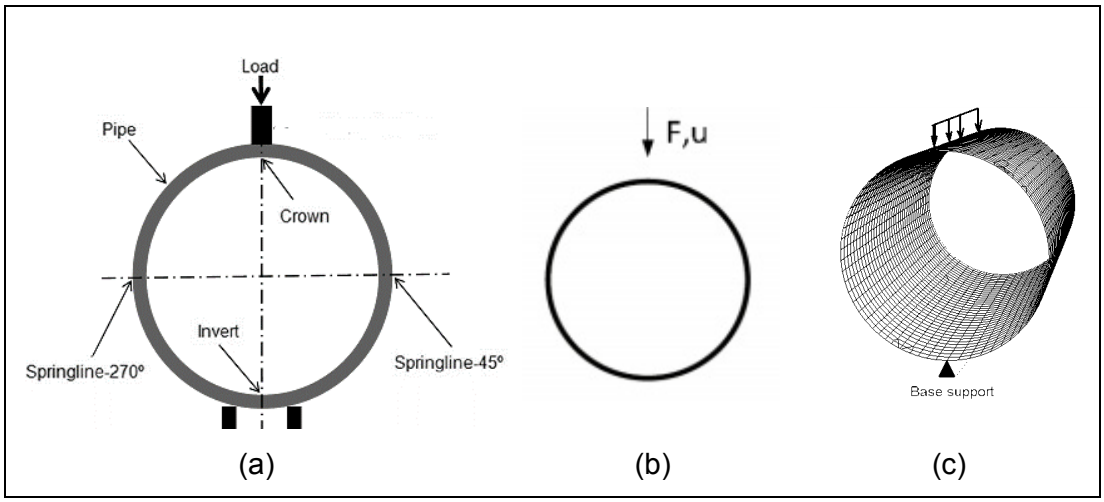

Figure 5-23 (a) Boundary condition of pipe and its support (b) direction of load

(c) FE mesh

The deformed pipe under pressure of 600 kPa or 1400 N is shown in Figure 5-24. It is illustrated that pipe has maximum radial deformation of 5.06 mm at its crown based on ABAQUS results. True measurement of deformation under 1400 N vertical load was 5.30 mm radial deformation in laboratory which shows a good agreement between numerical modelling and experimental results.

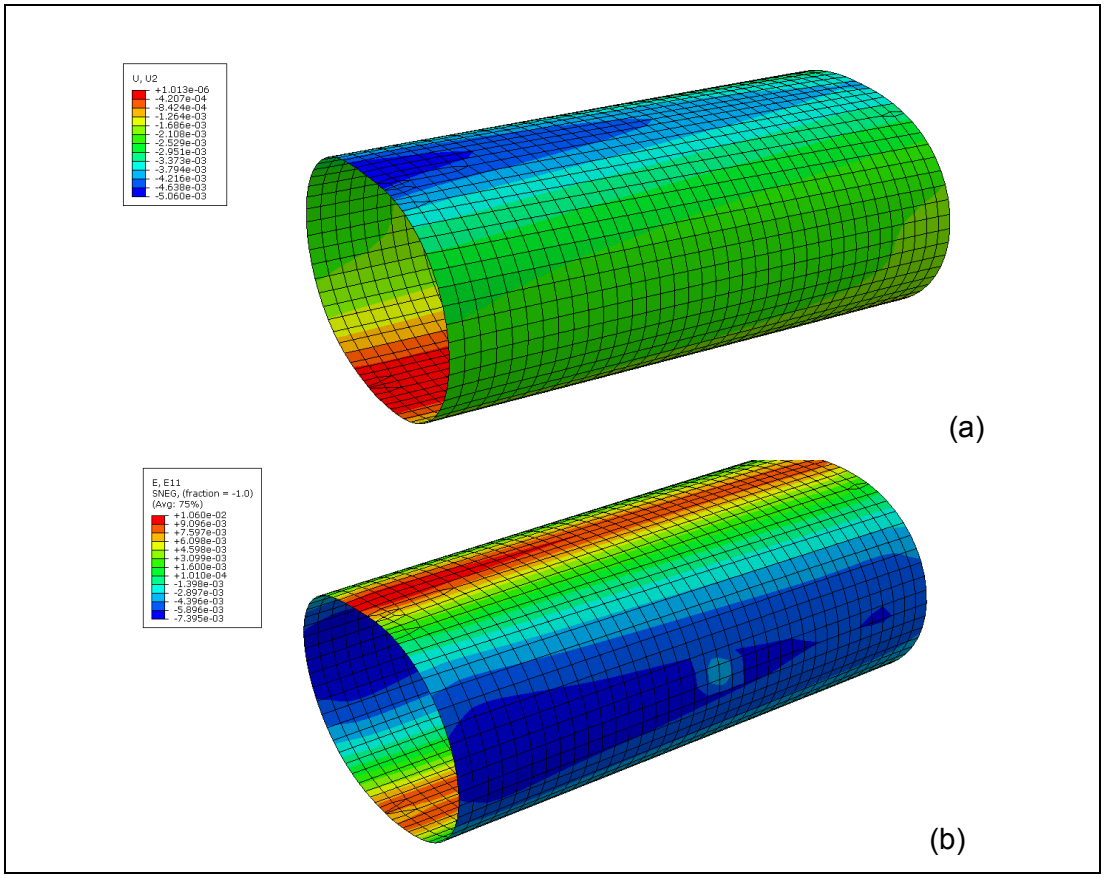

Figure 5-24 Results for FE analysis for compression load of 1400 N # 600 kPa

(a) Pipe radial deformation (b) strain

Figure 5-25 illustrates displacement variations in both vertical and horizontal directions. It can be seen that three main sections exist in the graph. Horizontal displacement, *U1*, is maximum at the middle section (2 mm), while vertical displacement is maximum on the left section (4.8 mm). Both graphs converge on the bottom of pipe to zero which means both horizontal and vertical displacements on the bottom of pipe is minimum almost equals to zero.

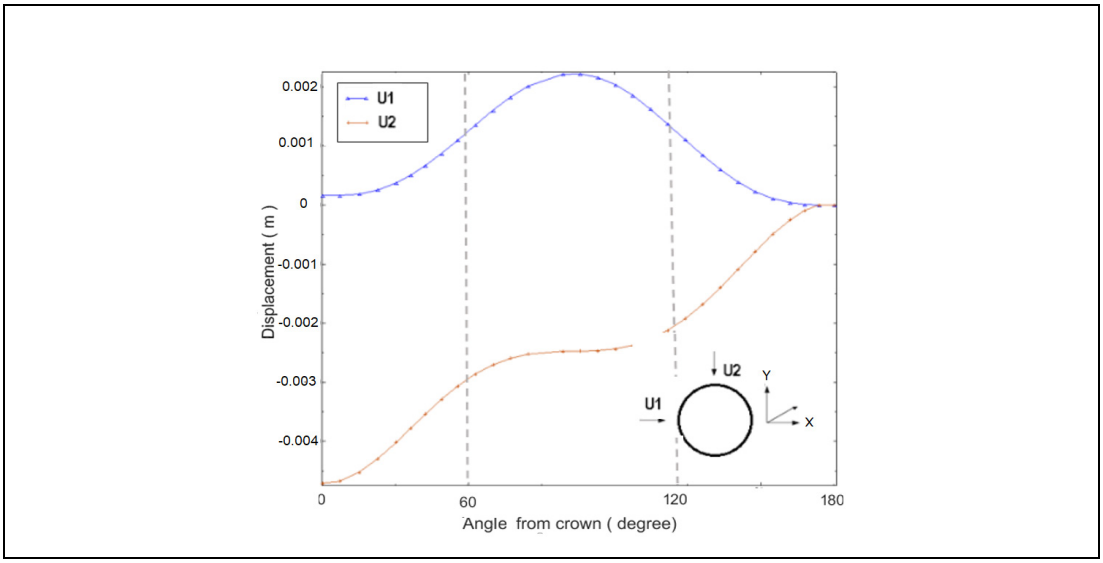

Figure 5-25 Finite element results of displacement along pipe circumference under 1400 N load

Maximum displacements occur at pipe crown and springline for *U2* and *U1*, respectively. It can be seen when a 5 cm vertical diametric displacement occurs on pipe crown, the horizontal displacement at pipe springline is about 2.1 mm. In addition, strain of pipe at these two points are 0.010 and 0.0055 based on numerical results data. For these points, the experimental results of strain gauges 2 and 3 at pipe springline 45^{o} and 270^{o} were 0.006 and 0.0057, respectively showing the consistency between numerical and experimental results. For each applied load, load-displacement and load-strain curves are plotted for both numerical and experimental analysis as shown in Figure 5-26. Figures 5-26 and b are related to strain gauge reading of pipe at pipe crown and springline, respectively. It is clear that results of finite element analysis and experimental results are consistent. These results were used to develop a relationship between strain gauges reading and horizontal deflection of the pipe.

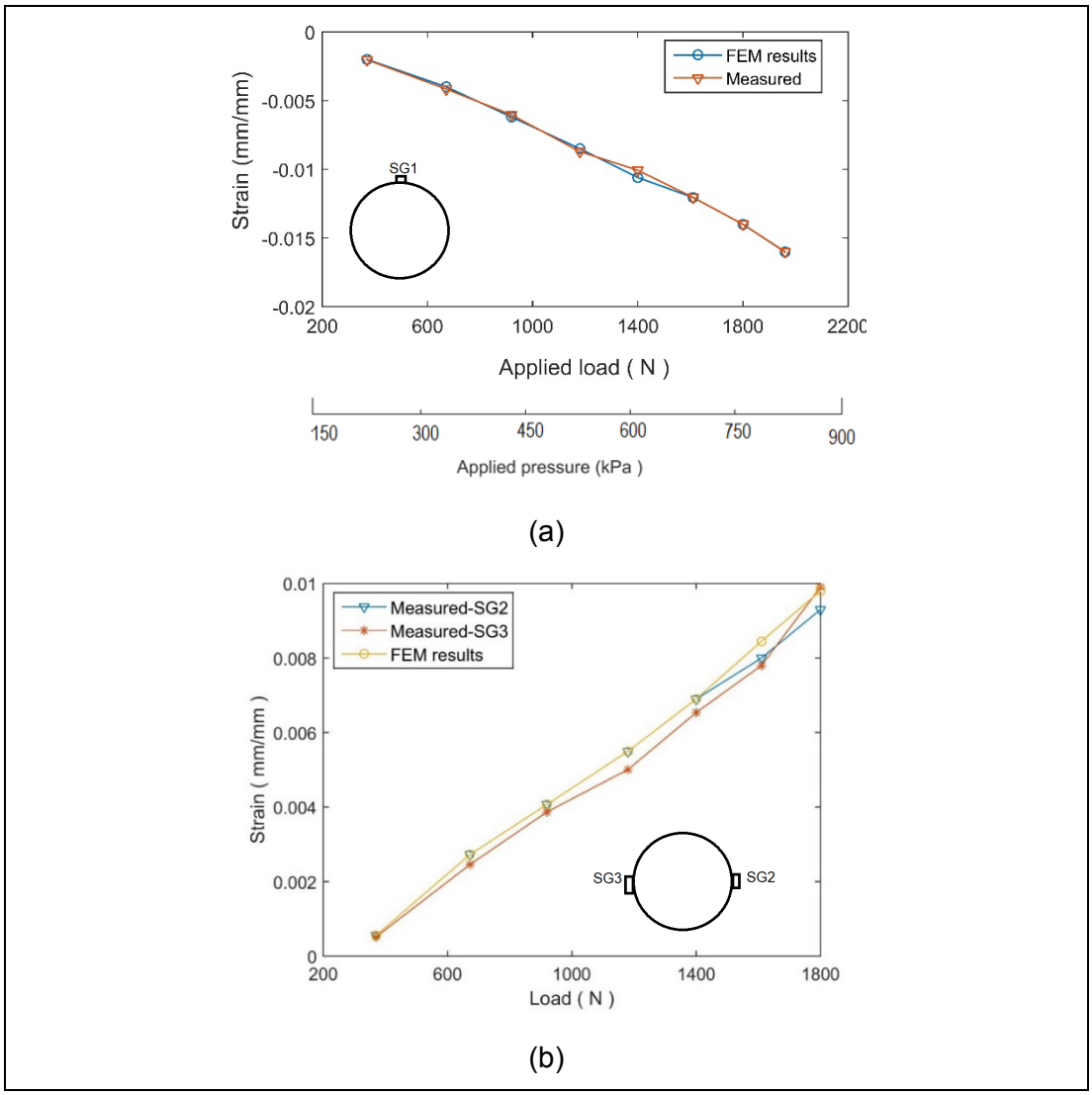

Figure 5-26 Comparison between lab and FEM results (a) SG1 (b) SG2 & 3

For any given load, SG2 reading and displacement in X direction were calculated and results are shown in Figure 5-27. It can be seen that there is a linear relationship between the two variables and Equation 5-5 is developed to relate these variables. The horizontal deflection of pipe is calculated from Equation 5-5:

$$HDS=CS \times 0.000225 \qquad 5\text{-}5$$

In which CS is reading of strain gauge at pipe springline and HDS is predicted horizontal diametric strain at pipe springline. For example, under 1400 N load or 600 KPa, the reading of strain gauge 2 is 5700 μmm/mm or 0.0057 mm/mm which shows the Δ equals 1.7 mm or total horizontal displacement of 3.4 mm. This value equals to vertical deflection of 2.5% based on 5-5.

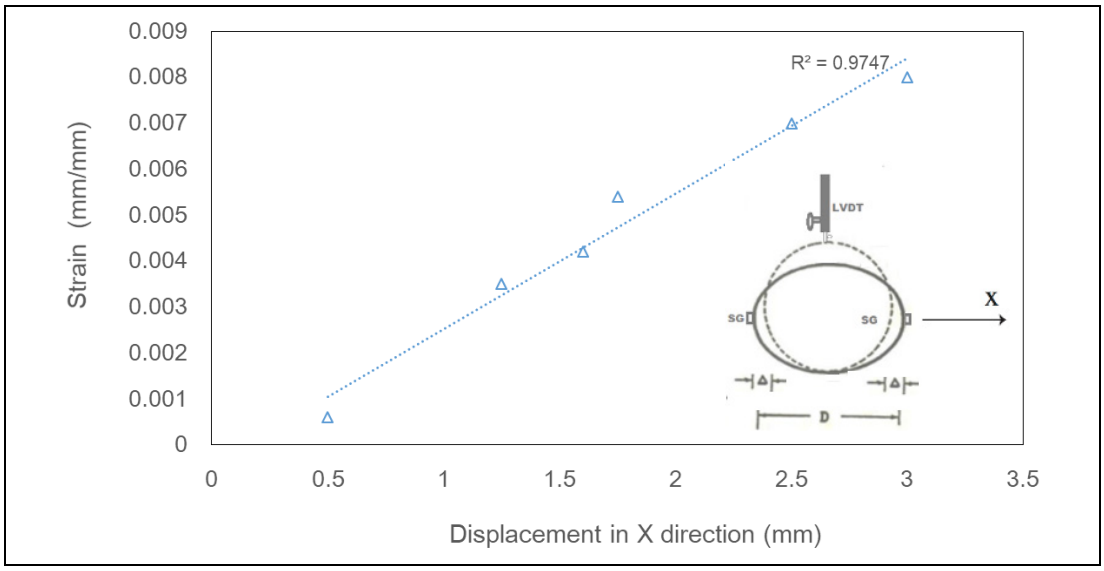

Figure 5-27 Strain gauge reading versus horizontal displacement (SG2)

5.4.3 Comparison of Results Using Different Methods

For six applied load, pipe strain was calculated using different methods and results are shown in the previous sections. For verification, the strain calculated through these methods are compared and results are presented in Figure 5-28. It can be observed that there is a good agreement among the results obtained from different methods.

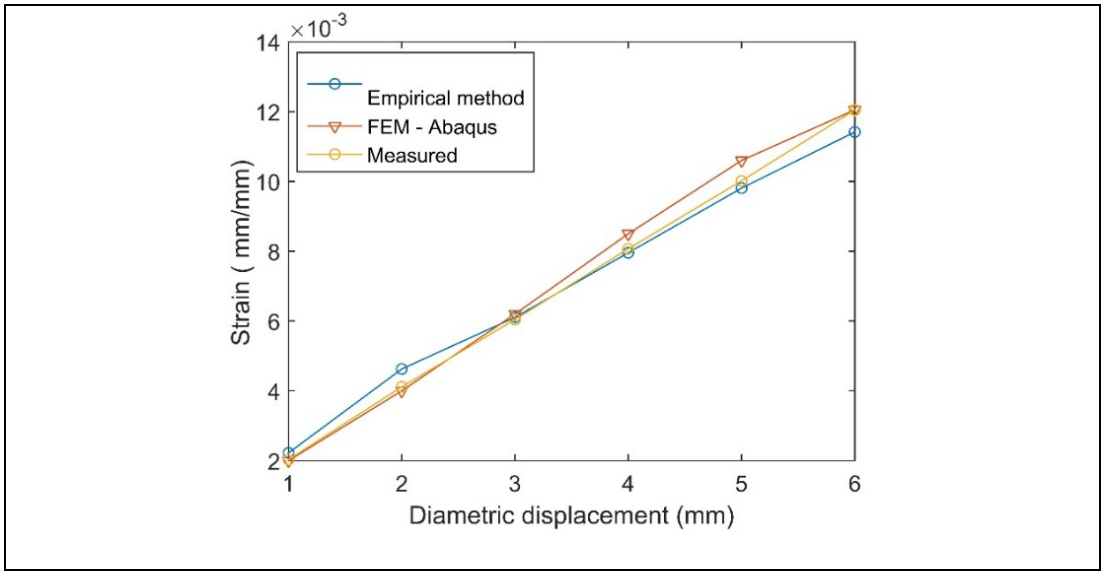

Figure 5-28 Comparison of the results of three methods

5.5 REPRESENTATION OF MATERIAL PROPERTIES

Three types of materials are used in the current project. The model parameters are shown in Table 5-6. The Mohr-Coulomb and Drucker-Prager models are used to represent the backfill material in cement-treated and non-treated conditions. It is worth noting that for plane strain considerations, the Mohr-Coulomb parameters and Drucker-Prager parameters can be converted to each other based on the existing formulations. The method is explained in Appendix C and results of converting material properties are illustrated in Table 5-6. To simulate the granular soil subgrade and pipe, elasto-plastic constitutive models are also used as shown in the following table. It should be noted material properties of granular base materials are provided from existing sources in Curtin Pavement and Geotechnics laboratory as these materials are commonly used for simulating pavement for research works.

Table 5-6 Properties of materials used in the research

Materials	Model and parameters*		Density (Kg/m^3)	E (MPa)	v
Backfill soil*	Mohr Coulomb	φ =29°, c= 0 kPa	1650	10	0.35
Cement-treated	Mohr Coulomb	φ= 36 °, c= 16kPa	1875	60	0.35
Granular base material	Elasto-Plastic	Compressive strength =1.5 MPa	2200	200	0.4
HDPE pipe	Elasto-Plastic	Yield stress =23 MPa	955	816	0.46

* Corresponding Drucker-Prager B=40 °, K=1, d<1 kPa

5.6 SUMMARY OF THE CHAPTER

Understanding the behaviour of soil and pipe is important in analysing the buried pipe response under various loading conditions. Therefore, a series of tests were performed to define important material strength for sand backfill, cement-treated sand and flexible pipe. The results of laboratory tests conducted to characterize material properties and predictions using empirical methods were discussed in this chapter.

Some key findings from this chapter are summarised as below:

- Characterization of backfill material for both pure sand and cement treated specimens was investigated using direct shear tests. Overall, the strength of cement-treated samples is higher than those non-treated.
- To assess the impact of curing time on shear strength of material, all treated specimens were cured at different curing times of 1, 7, and 28 days at room temperature. As it is expected the curing time has a significant effect on the improvement of strength properties of cement-treated material.
- To obtain more reliable data, triaxial tests were conducted on pure sand samples to compare with direct shear test results. Results were consistent with the results obtained from direct shear test for sand. The results of triaxial tests were also used to calculate initial elastic modulus of soil.
- It is essential to find a relationship between measured circumferential strain on pipe and pipe deflection. For this purpose a compressive loading test was carried out using a compression testing machine to measure vertical diametrical change of pipe (measured with LVDT) and wall circumferential strain at crown and bottom of pipe (measured with two strain gauges). The relationship between measured circumferential strain, CS, and pipe deflection, VDS, was derived. Equations were also developed for both vertical and horizontal directions.
- To predict pipe behaviour, a FE model was developed to measure pipe deflection and strains. For validation, results obtained from experimental and numerical analysis were compared with those calculated from empirical method. It was observed there is a good agreement among the results obtained from different methods.

In the next chapter, the results from experimental and numerical analysis for both static and cyclic tests will be presented.

6 RESULTS

EXPERIMENTAL AND NUMERICAL

Some parts of this chapter were published as journal paper as below:

Mosadegh. A; Nikraz.H , BURIED PIPE RESPONSE SUBJECTED TO TRAFFIC LOAD EXPERIMENTAL AND NUMERICAL INVESTIGATIONS, International Journal of GEOMATE, Nov., 2017, Vol.13, Issue 39, pp.01-08, ISSN:2186-2990, Japan, DOI: https://doi.org/10.21660/2017.39.91957

6.1 INTRODUCTION

This chapter presents the results from buried pipe tests due to traffic loading as well as findings from numerical simulations. The laboratory tests and simulations were carried out on the pipe buried in both non-treated and cement-treated sand.

In the first section, research approach will be discussed. Then, laboratory test results will be presented starting with ultimate bearing capacity test results. Then, the impact of traffic load and pipe burial depth on the model response will be experimentally investigated during initial and cyclic phases. Experimental test results will be followed by the results of numerical analysis. The overview of chapter is illustrated in Table 6.1.

Table 6-1 Chapter overview

Investigated factor	Test conditions	Test series no.	Analysis method	Section
Bearing capacity of loading plate	Non-treated	1	Experimental and numerical	6.2.1, 0
	Cement-treated sand	2		6.2.2, 6.3.2
Model response during initial phase	Non-treated	3	Experimental and numerical	6.2.3, 6.3.3
	Cement-treated sand	4		6.2.4
Model response during cyclic phase	Non-treated	5	Experimental only	6.2.6, 6.2.7
	Cement-treated sand	6		6.2.7

6.2 EXPERIMENTAL TESTS

The laboratory test program consists of twenty seven tests using a flexible HDPE pipe to investigate the effects of burial depth, surface pressure and number of cycles on the soil and pipe performance. The tests include twelve static and twelve cyclic as well as bearing capacity investigations. Similar to any research program, the repeatability of test procedure was performed to establish the testing technique.

The results of two repeated load test with same initial conditions and magnitude of 250 kPa at H/D=1 for cement-treated case are illustrated in Figure 6-1. As illustrated, the maximum values of VDS and SSS for two tests are almost the same. For example, maximum VDS at 300th second is 0.82 which is the same for trial 1 and 2. However, the minimum value has minor difference. These figures show that the developed procedure and technique of these tests are reliable.

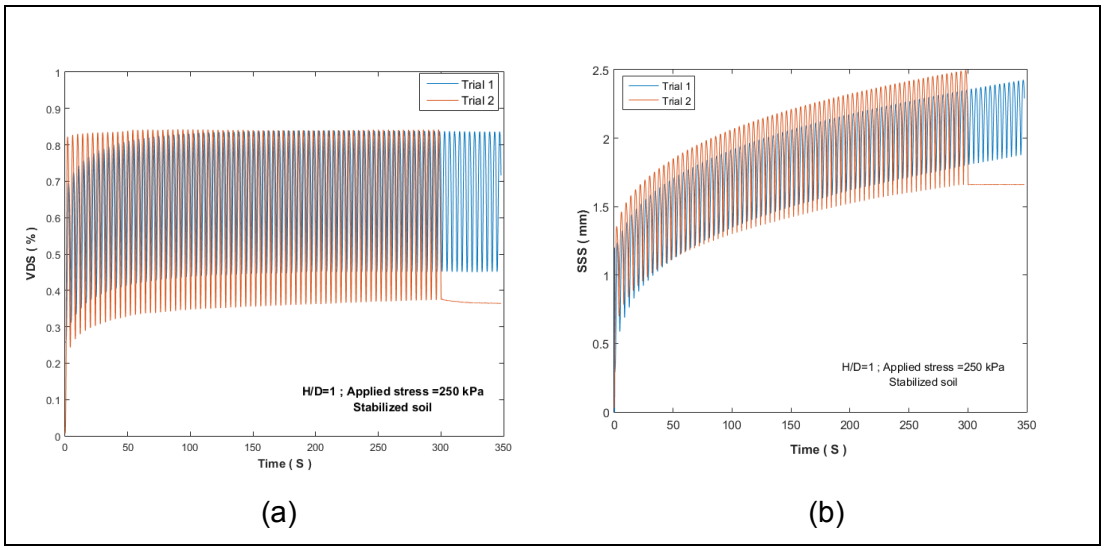

(a) (b)

Figure 6-1 Repeatability of tests (a) VDS (b) SSS diagrams

6.2.1 Test Series Number 1: Bearing Capacity of Non-treated

The bearing capacity of footing on sand was investigated using load control method. The aim of this test is not to analyse failure criteria or failure mode of footing but to identify the maximum load that can be applied on the soil. Thus a downward load was applied on top of the soil under footing to examine collapse load of the footing. It should be noted that the duration for this load was chosen to be 65 seconds to avoid sudden collapse of soil mass. The experimental setup and loading plate was presented in Chapter 4. Data acquisition is through one LVDT located on loading plate and from UTM25 and strain gauges installed at different points on the pipe circumference to capture soil and pipe deformations. Specifications of all these equipment and testing tank are the same as those presented in Chapter 4.

Failure mode of footing laid on pure sand is shown in Figure 6-2-a. As illustrated, the failure planes have developed clearly from the edge of footing to the ground surface and can be identified by the changes in the grid markers. Results of bearing capacity tests are illustrated in Figure 6-2-b. A prominent peak of 550 kPa can be seen and after the peak, the vertical displacement increases although the load decreases. Different modes of failure is shown in Figure 6-2-c. The general shear pattern failure, local shear failure and punching shear failure can be observed (Vesic, 1973). Based on these results, it is concluded that general failure was observed for the loading plate on dense sand.

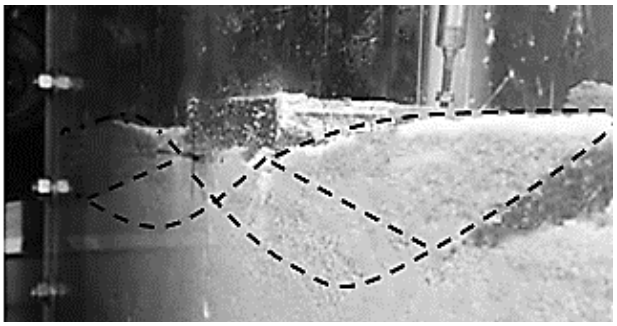

(a)

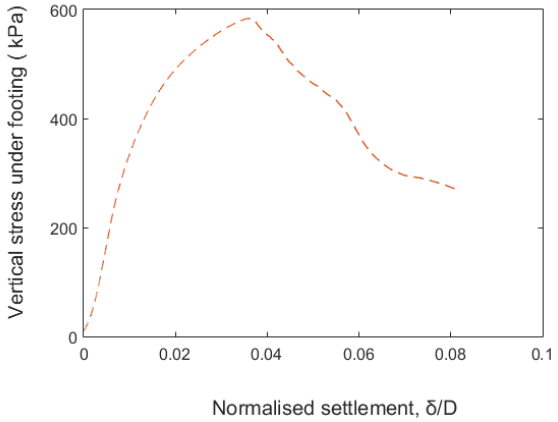

(b)

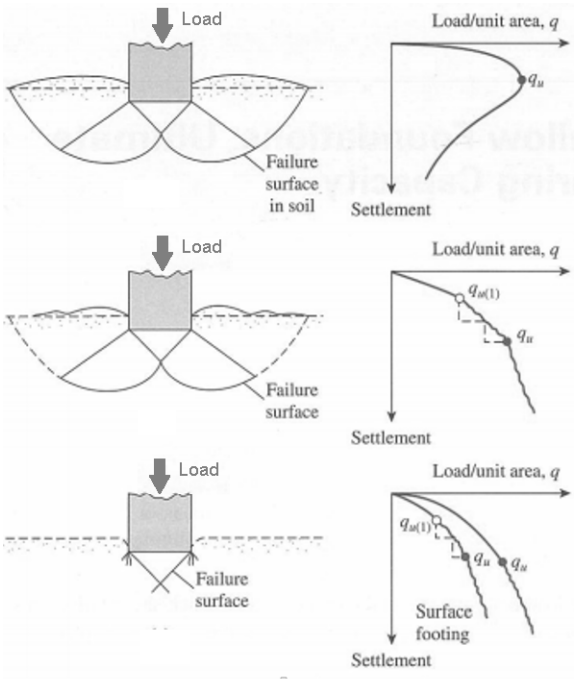

(c)

Figure 6-2 (a) Bearing capacity failure (Mosadegh & Nikraz, 2017)(b) load–displacement curve (c) modes of bearing capacity failure after Vesic : general, local and punching failure (Vesic, 1973)

The impact of compaction and material density on bearing capacity of soil was also investigated. For this purpose, another test was performed on a sandy material with a relative density of 75 percent. Figure 6-3 compares the results of bearing capacity for dense and loose sand. Vertical axis represents bearing capacity and horizontal axis represents normalised displacement. Dashed line illustrates results of loose sand and triangle marker represents result of dense sand. It can be seen that footing ultimate bearing capacity dropped from almost 600 kPa for dense sand to less than 120 kPa for loose material which is less than 250 kPa, the considered applied traffic load for this project. This means the loose with the relative density of 75 percent cannot be used for this study.

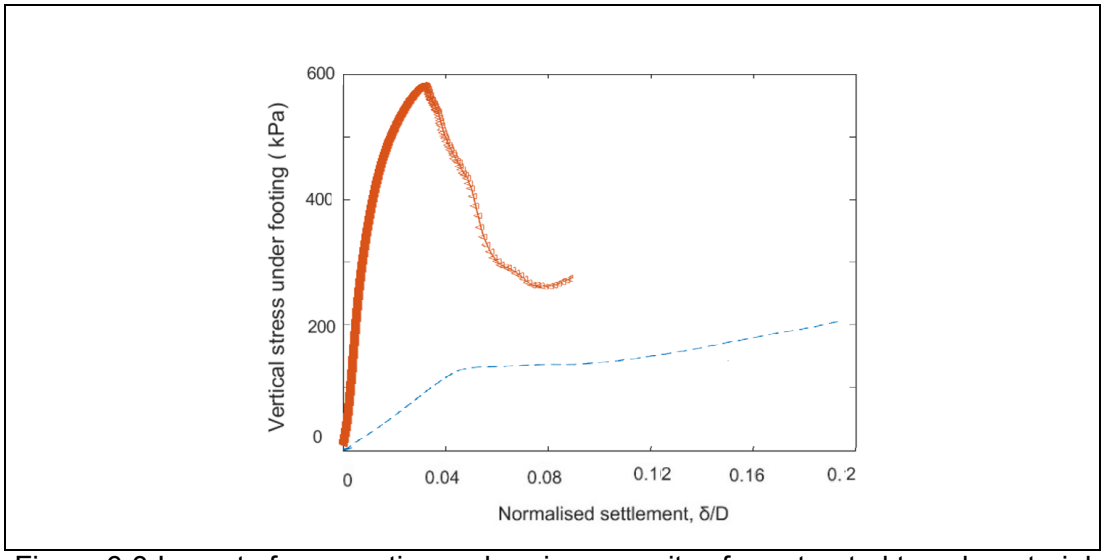

Figure 6-3 Impact of compaction on bearing capacity of non-treated trench material

6.2.2 Test Series Number 2: Bearing Capacity of Cement-treated

In this section, the impact of stabilization on bearing capacity of footing on cement-treated material is investigated. The depth of cement treated layer was chosen as l=H/3 and a downward load of 25 KN or 1400 kPa was applied in 65 seconds. Results are presented in Figure 6-4. Figure 6-4-a compares bearing capacity of non-treated and cement-treated sand. It can be seen that adding cement increases the bearing capacity from 600 kPa to almost 1100 kPa. In addition, by adding cement, the footing normalised displacement decreases to one quarter of its value, dropping from 0.04 to 0.01. It is noted that reducing footing displacement at specific stress level is an important aim of stabilization besides increasing bearing capacity value. Figure 6-4-b compares pipe deflection for non-treated and cement-treated sands. As shown, pipe deflection decreases from 6% to 1% after adding 3 cm of cement-treated material on top of sand. It means there is 83% reduction in pipe deflection after adding cement to the material. Figure 6-5 compares the bearing capacity and pipe vertical deflections

of all three cases. It can be seen that both compaction and stabilization have significant impact on reducing pipe deflection and increasing bearing capacity of the material.

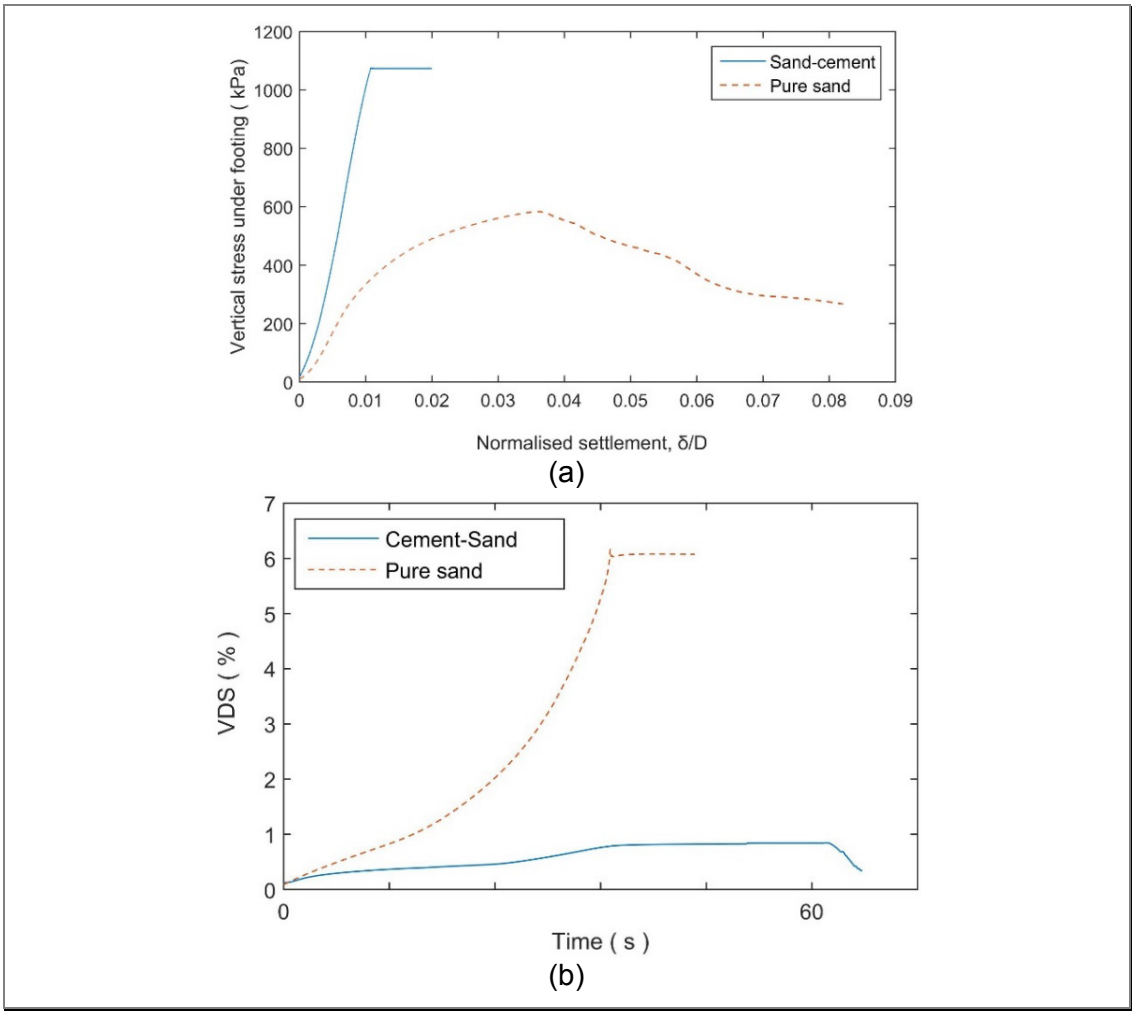

Figure 6-4 (a) Comparing results of (a) maximum bearing capacity (b) maximum deflection of buried pipe for non-treated and cement-treated soil

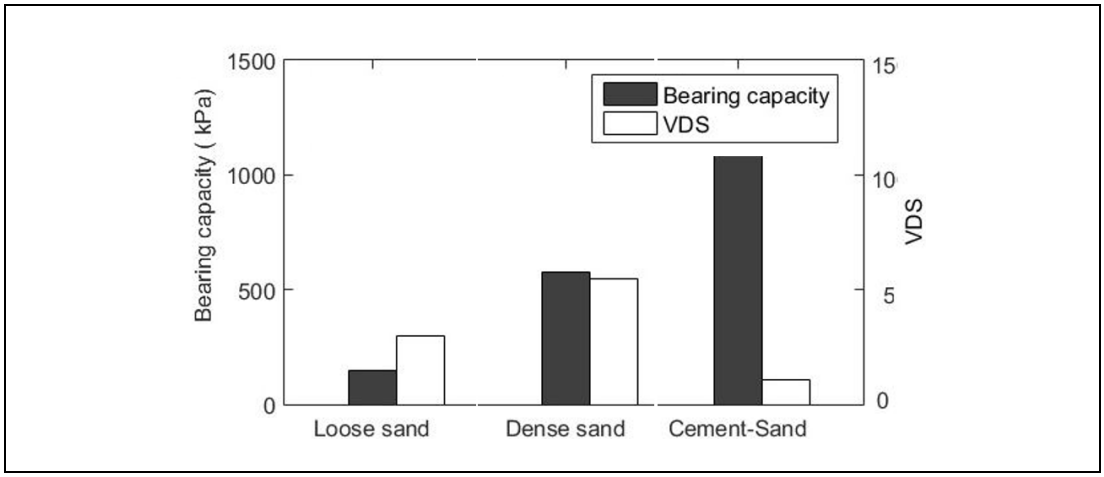

Figure 6-5 Comparison of three cases

6.2.3 Test Series No 3: Initial Phase - Non-treated

Large portion of pipe deformation and soil surface settlement occurs at the end of first cycle. Therefore, static tests were performed to investigate surface settlement and pipe behaviour at the end of first cycle. Static load was applied during 65 seconds to avoid sudden collapse of soil under loading plate. Then, the influences of surface pressure and pipe burial depth on soil surface settlement, pipe deflection and soil pressure at pipe crown were investigated. Results are presented in Figure 6-6 to Figure 6-8. Solid and dashed lines represent pressure of 400 and 250 kPa, respectively. The no marker, triangle and diamond marker illustrate burial depth of 1D, 1.5D and 2.5D, respectively. The information of each test is shown in the legend for each graph. Each symbol consists of two parts representing information on burial depth and surface pressure.

Figure 6-6 illustrates pipe deflection versus time for all non-treated cases during initial phase. It can be seen that pipe deflection varies with change of burial depth and surface pressure. Higher surface pressures and shallower burial depths cause higher pipe deflections. For example, maximum deflection of 2.5 % occurs when burial depth is minimum at H=1D and surface pressure is maximum at 400 kPa.

Figure 6-7 shows soil surface settlement variation versus time. Overall, higher surface pressure causes higher surface settlement as expected. In addition, soil surface settlement increases when burial depth increases. It can be seen that maximum surface settlement occurs while surface pressure and burial depths are maximum. For example, maximum SSS of 5 mm occurs under surface pressure of 400 kPa at H=2.5D.

For each test, increase in vertical stress was measured at pipe crown during initial phase. The results are shown in Figure 6-8. As expected, surface pressure of 400 kPa causes more earth pressure at pipe crown compared to pressure of 250 kPa. Moreover, maximum pressure at pipe crown occurs while burial depths is minimum. As shown in the graph, maximum pressure at pipe crown is 220 kPa happening under surface pressure of 400 kPa at H=1D.

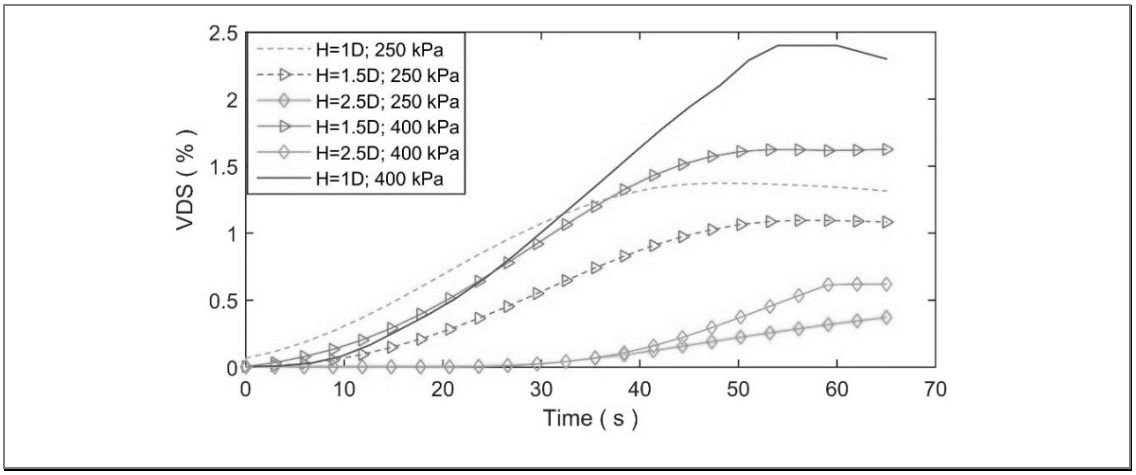

Figure 6-6 Pipe deflection versus time –pure sand

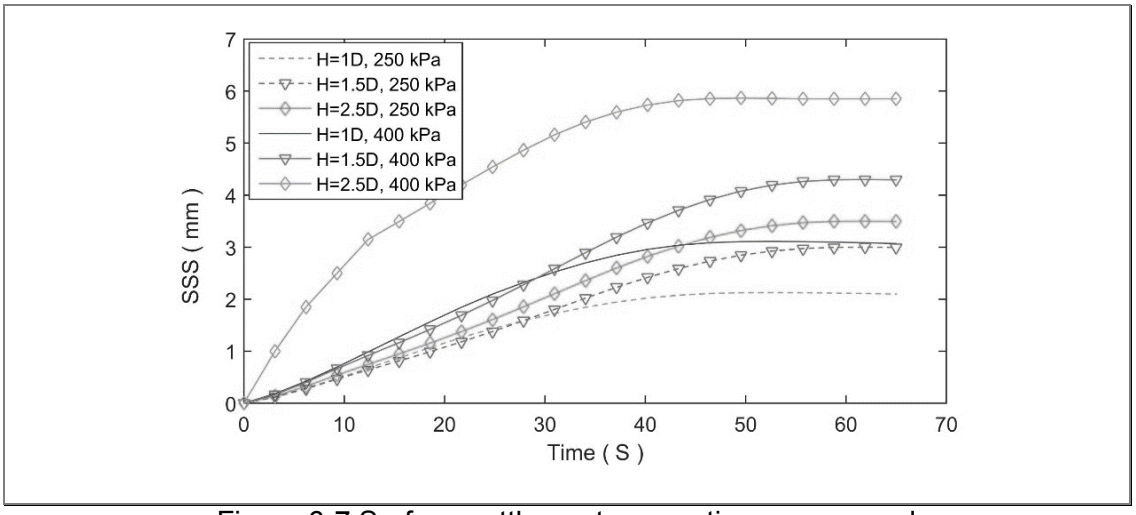

Figure 6-7 Surface settlement versus time –pure sand

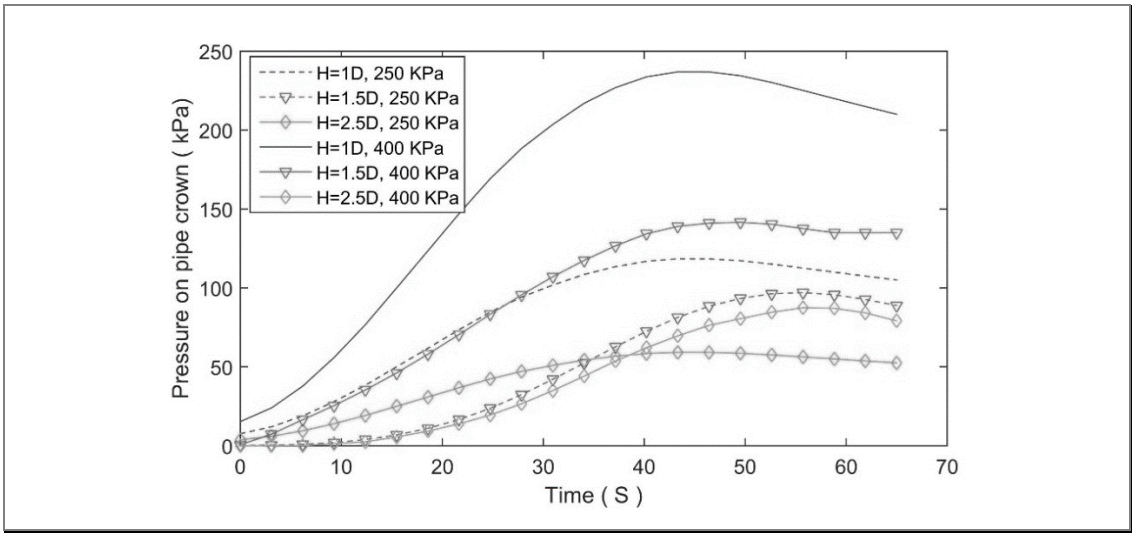

Figure 6-8 Pressure at pipe crown versus time –pure sand

6.2.4 Test Series No 4: Initial Phase - Cement-treated

Static tests were also performed to investigate pipe behaviour during initial phase for cement-treated material and results are presented in this section. Rate of applying static load is the same as previous section. Results are presented in Figure 6-9 to Figure 6-11. In all figures, the horizontal axis represent time and vertical axis represent change of VDS, SSS and earth pressure on pipe, respectively. Moreover, all legend symbols consist of two parts representing burial depth and applied surface pressure. For example, 2.5- 400 is referring to test condition of H=2.5D under surface pressure of 400 kPa.

The results of tests on pipe deflection buried in cement-treated sand during initial phase are presented in Figure 6-9. It can be seen that pipe deflection varies with change of burial depth and surface pressure. Maximum deflection of 1.2 % occurs when burial depth is minimum at H=1D and surface pressure is maximum or 400 kPa. Minimum deflection occurs under surface pressure of 250 kPa and burial depth of H=2.5D.

Figure 6-10 shows the results of soil surface settlement under different surface pressure for different burial depths. It can be seen that maximum surface settlement occurs while surface pressure is maximum and burial depth is minimum. Maximum SSS occurs under surface pressure of 400 kPa at H=1D.

Results of soil pressure at pipe crown under different surface pressure for different burial depths are illustrated in Figure 6-11. It can be seen that under a given surface pressure, the pressure on pipe decreases when burial depth increases. For example, under surface pressure of 400 kPa, when burial depth increase from H=1D to H=1.5 and 2.5D, stress on pipe drops from 176 kPa to 82 and 73 kPa, respectively. Also for a given burial depth, a higher stress on pipe occurs under higher applied surface pressure. For example, for a burial depth of H=1.5D increase of surface pressure from 250 to 400 kPa increase the stress on pipe from 47 to 61 kPa.

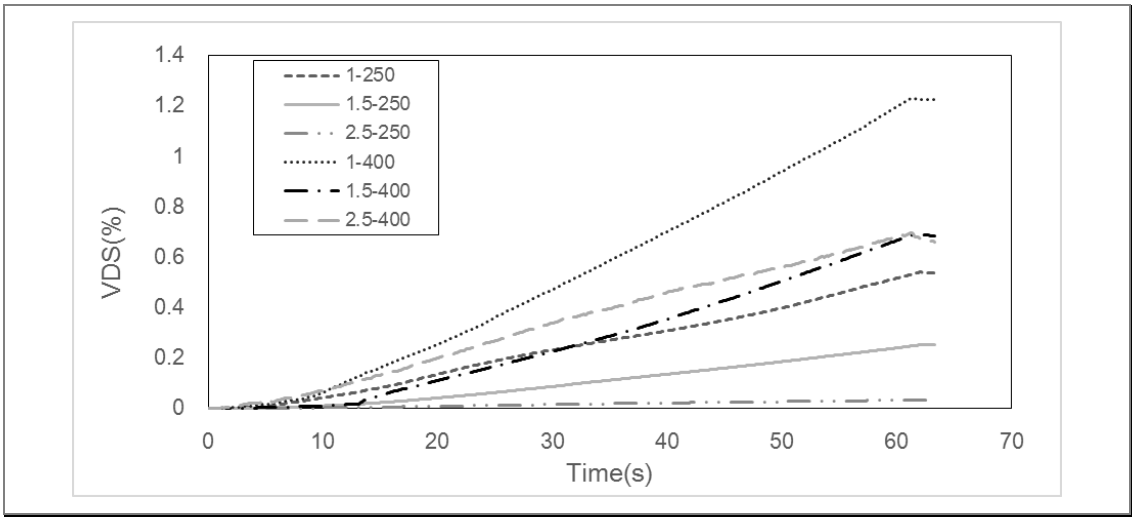

Figure 6-9 Pipe deflection versus time –cement-treated sand

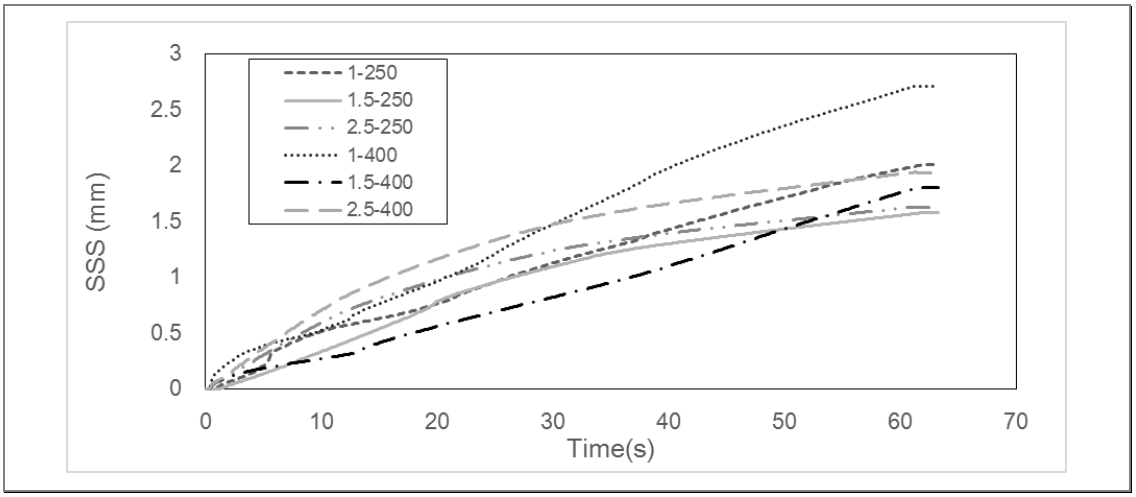

Figure 6-10 Soil surface settlement versus time – cement-treated sand

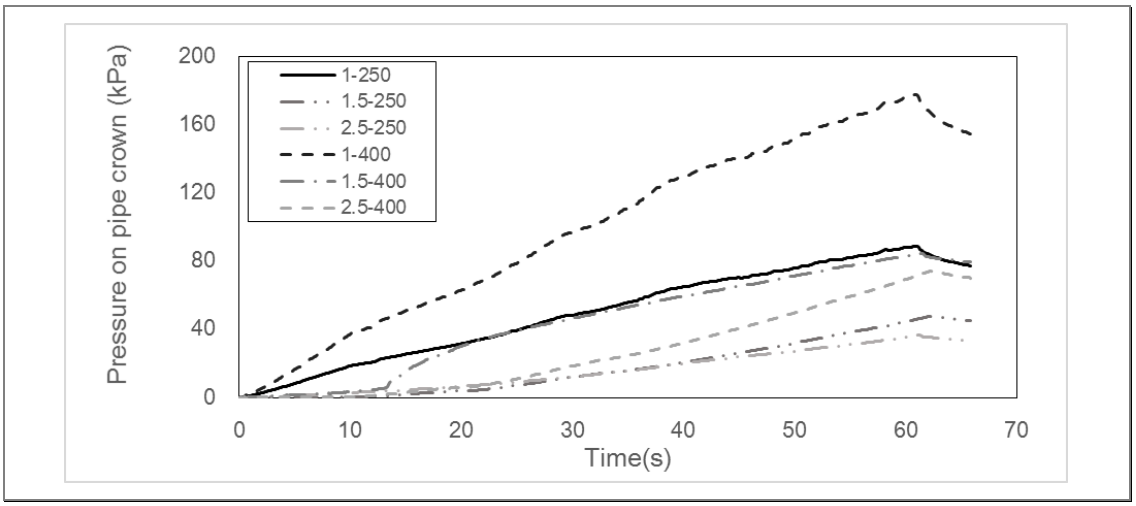

Figure 6-11 Stress on pipe versus time – cement-treated sand

6.2.5 Pipe Deformation Mode

More output can be derived from initial phase test results to investigate the mode of pipe deformation. Figure 6-12 represents the variation of maximum deflection in both vertical and horizontal directions. Horizontal axis represents test number and vertical axis represents calculated deflections. The information of each test is shown on the legend which consists of two parts representing test condition and direction of measuring strain. For example, NC-V is referring to strain measurement during the test on non-cement treated sand in vertical direction. It can be seen that the pipe has higher deflection in vertical direction compared to horizontal for both cases. Results also reveal that both surface pressure and burial depth have impact on horizontal as well as vertical deflections. It can be seen that both horizontal and vertical pipe deflections are maximum under shallower burial depths and higher surface pressures.

Modes of pipe deformation can be illustrated graphically based on the results from all strain gauges attached to the pipe at different positions. Pipe deformation modes are illustrated in the Figure 6-12-b. It should be noted that test conditions are shown in the legend adjacent to each figure. For example, value 1 in the legend represents the test under surface pressure of 250kPa at H=1D. Overall, the deformation of pipe buried in non-treated sand is higher compared to cement-treated one. For example, maximum strain measured at pipe crown for non-treated case is almost 4000 μmm/mm. This value drops to less than 1500 μmm/mm after stabilization. In addition, for both cases pipe at H=1D and under surface pressure of 400 kPa have the highest deformations illustrated as symbol of 4 on the figure. For example, for non-treated trench material, the maximum strain measured for case number 4 is 3500 μmm/mm and pipe tends to deflect to heart shape as shown in the figure. The pipe shape almost remains unchanged in case number 3 in which it is buried at H=2.5D under 250 kPa. In this case very small strains were recorded by all starin gauges.

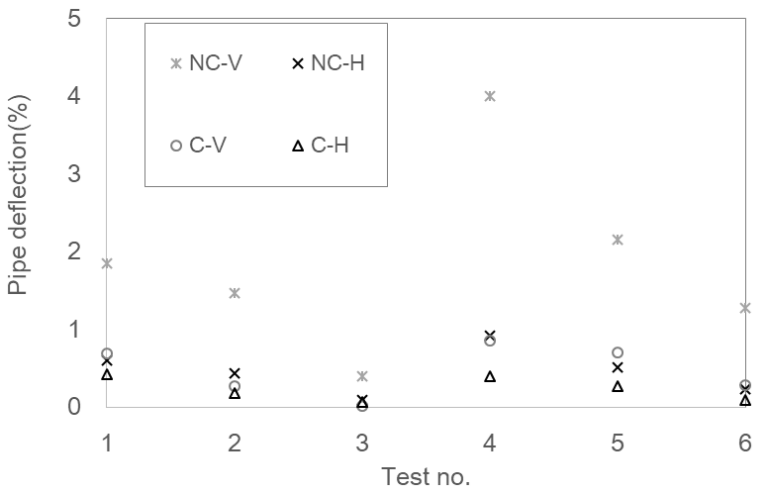

(a)

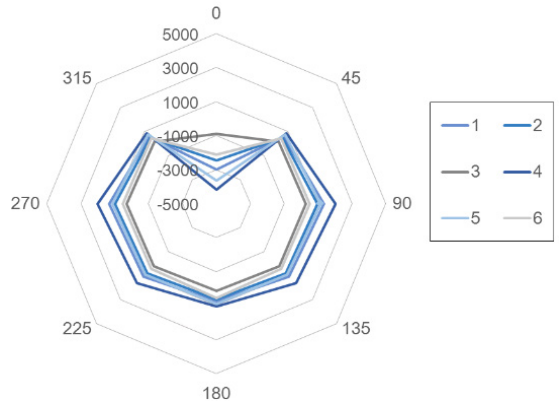

Non-treated sand

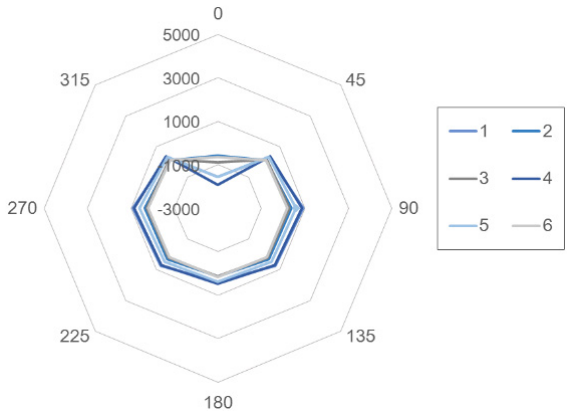

Cement treated sand

1	250 kPa-H=1D
2	250 kPa-H=1.5D
3	250 kPa-H=2.5D
4	400 kPa-H=1D
5	400 kPa-H=1.5D
6	400 kPa-H=2.5D

(b)

Figure 6-12 Comparison of strain in horizontal and vertical directions for (a) non-treated (b) cement-treated sands

6.2.6 Test series No 5: Cyclic Phase – Non-treated

A series of tests were carried out to investigate the buried pipe response under repeated loading conditions. It should be noted that 500th cycle is chosen as a benchmark to compare results of cyclic tests. Some tests were stopped before reaching cycle 500th or at 2000 seconds. This is because there was a limitation of travel distance in UTM 25 machine meaning the maximum settlement happening on soil surface during tests has reached 50 mm. Therefore, if soil surface settlement reaches 50 mm the test would stop automatically. The change in pipe deflection, surface settlement and soil pressure on pipe under various conditions were investigated and results are presented in this section.

6.2.6.1 Vertical Diametric Strain (VDS)

The change in pipe deflection versus number of cycles for pure sand is illustrated in Figure 6-13. Overall, maximum VDS decreases when H/D increases. As shown in Figure 6-13-a at 200th cycle under surface pressure of 250 kPa, maximum VDS is 1.8 % and 0.5% for H/D=1 and H/D=2.5, respectively. The same result is concluded for surface pressure of 400 kPa. VDS decreases from 5% to 1.5% when burial depth increases from H=1D to H=2.5D. It means increasing burial depth from H=1D to H=2.5D decreases pipe deflection by 73%.

In addition, the variation of VDS is more significant for shallower burial depths. For example, the variation or the difference between maximum and minimum value of VDS at each cycle is 1% for burial depth of H=1D. This value drops to 0.1% for burial depth of H=2.5D under surface pressure of 250 kPa. Figure 6-13-b shows a clearer view of the VDS variation at each cycle which is extracted as the zoom layout from Figure 6-13-a. Overall, the range of VDS variation is higher for shallower burial depths and it decreases as burial depth increases. The red dashed bracket in the Figure 6-13-b shows variations of VDS at cycle 100. It can be seen that the difference between maximum and minimum deflection of pipe at 100th cycle are 2% and 0.4% for H=1D and H=2.5D, respectively. These results reveal that under shallower burial depths VDS variations of pipe is an important factor to be considered besides its maximum absolute value. This factor can be used to investigate plastic deformation of pipe in cyclic loading.

Hysteresis loops of load–VDS can be used as an indicator of the mechanical responses of the materials. These graphs of VDS for all cases during the first 20 cycles are calculated and shown in Figure 6-13-c. It can be seen that under a given surface pressure, the deeper the pipe the closer the hysteresis loop. This verifies the

result of previous paragraph indicating that for shallower burial depth, range of VDS variation is larger. Under surface pressure of 400 kPa, VDS varies between 0.75 to 1.1% at burial depth of H=2.5D. This value for shallower depth of H=1D is between 1.7 to 3.7%. This means, during 20 first cycles the variation of VDS for shallower burial depth is 2% and for deeper burial depth of is 0.7%.

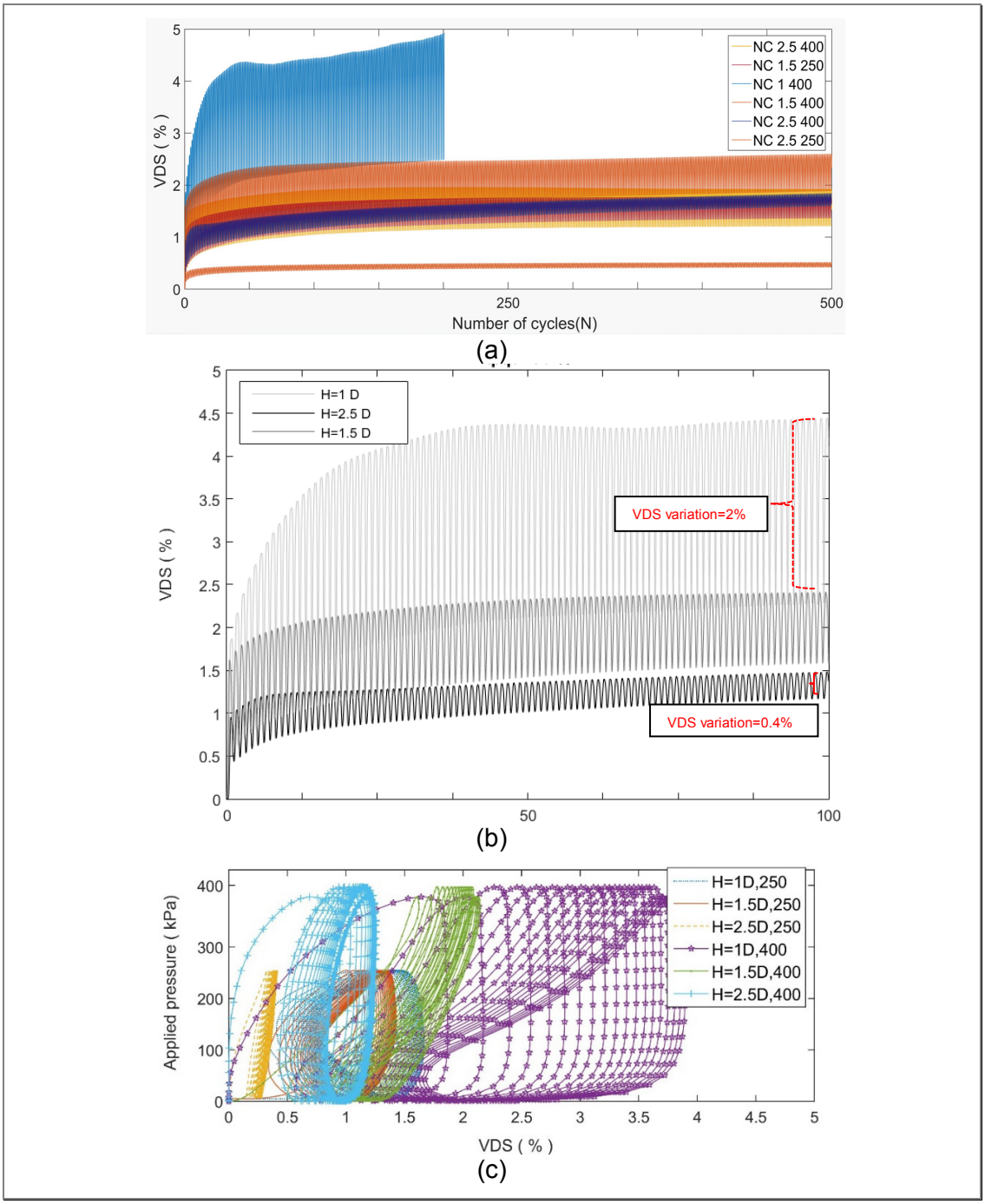

Figure 6-13 (a) VDS versus number of cycles at different burial depths (b) zoom layout of part a (c) hysteresis graphs for 20 cycles

6.2.6.2 Soil Surface Settlement (SSS)

The change in soil surface settlement versus number of cycles under surface load of 250 and 400 KPa at three different burial depths is shown in Figure 6-14. Horizontal axis represents number of cycles and vertical axis represents SSS variations. Overall, SSS increases when H/D increases. For example, under surface pressure of 400 kPa, increasing burial depth from H=1.5D to H=2.5D increases SSS from 25 to 35 mm at cycle 200th. In addition, increase of surface pressure increases SSS significantly. For example, increase of pressure from 250 to 400 kPa at depth of H=1D increases SSS from 15 to 49 mm at cycle 200th. To show how maximum and minimum value of SSS varies at each cycle, Figure 6-14-b is prepared. This is a zoom layout of Figure 6-14-a to better view SSS variation under different conditions. Overall, the range of SSS variation for all cases is almost the same although this value is slightly higher for shallower burial depths and for higher surface pressures. In addition Figure 6-14-a and b can be compared to investigate soil surface variations at cycles 50th and 500th. As mentioned, SSS increases when H/D increases for majority of cases. As illustrated in Figure 6-14-a SSS increases when H=D increases except for H=1D under surface pressure of 400 kPa. For example, at cycle 200th, the value of SSS is higher for H=1D than H=2.5D. However, during the first cycles, the condition is different as shown in Figure 6-14-b. In other words, during first 40 cycles as shown with red dashed line, increase of H/D increases SSS for all cases. After cycle 40^{th,} increase of burial depth increases SSS for all cases except H=1.5D; 400 kPa. Future studies is recommended to investigate the reason for this exception and how number of cycles could change the model behaviour.

Figure 6-15 shows hysteresis behaviour of footing under surface pressure of 250 kPa at H=1D. It can be seen that with increasing number of cycles, hysteresis loops become less open. Results reveal that SSS hysteresis graphs move to the right even after 500 cycles which means soil surface still undergoes deformation or SSS still increases even after large number of cycles.

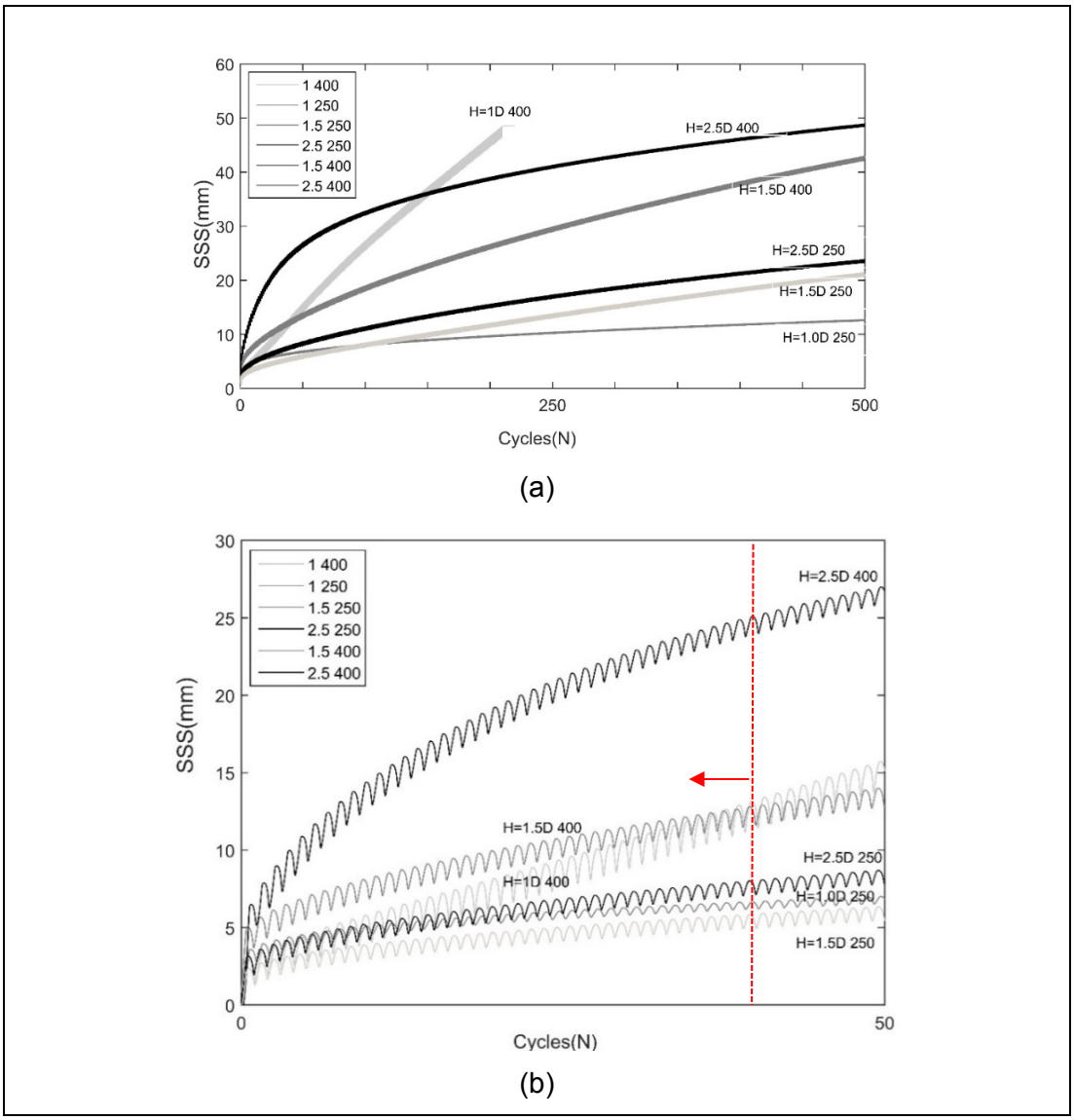

Figure 6-14 soil surface settlement versus number of cycles for all non-cemented cases 500 and 50 cycles (b) zoom lay out of SSS

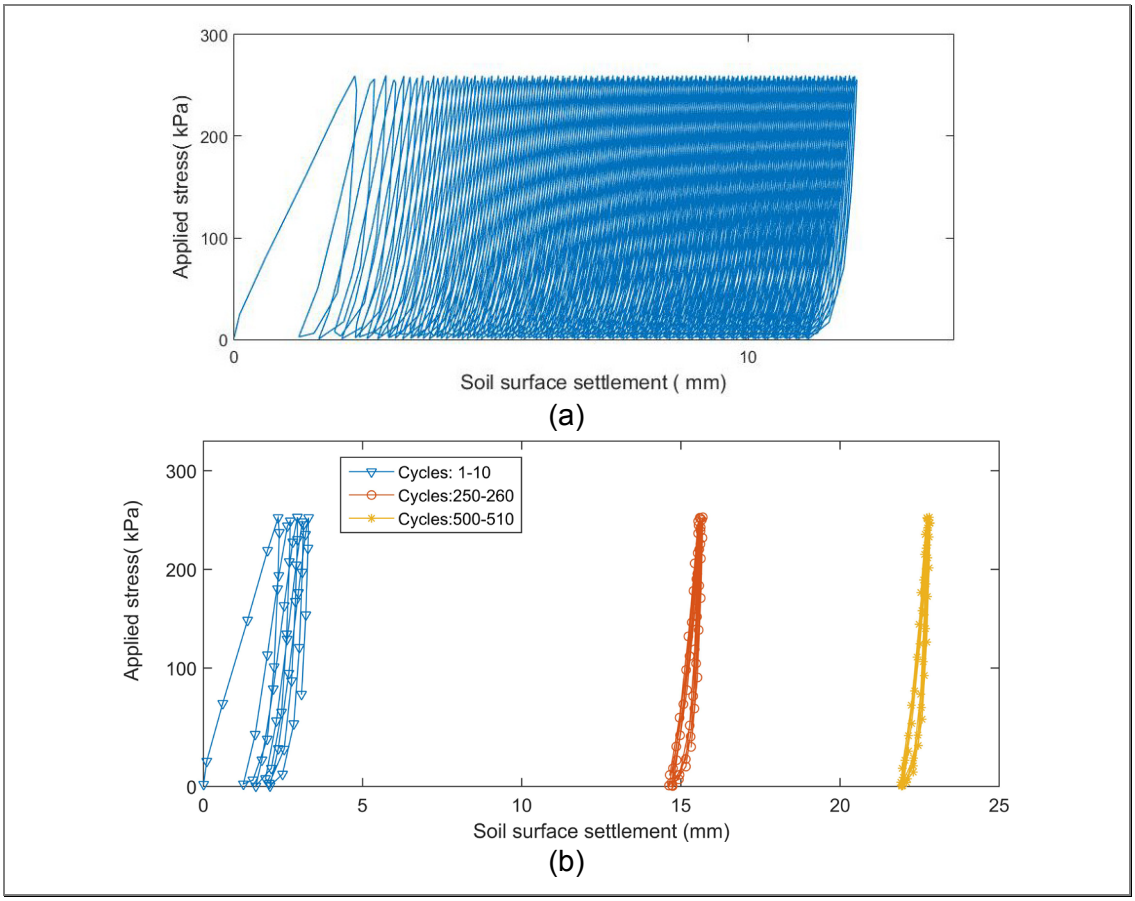

Figure 6-15 Hysteresis curve of SSS (a) during first 200 cycles (b) SSS variations at given cycles

6.2.6.3 Vertical Stress (σ)

For each test, increase in vertical stress was measured at pipe crown during cyclic phase and results are shown in Figure 6-16-a and b. Overall, surface pressure of 400 kPa causes more pressure at pipe crown compared to pressure of 250 kPa as expected. Moreover, maximum pressure at pipe crown occurs while surface pressure is maximum and burial depths is minimum. In other words, impact of live load is more significant under shallower burial depths and higher pressure occurs on pipe crown at lower burial depths. For example, under surface pressure of 250 kPa, maximum pressure on pipe crown is 140 kPa at H=1D as shown in Figure 5-20-a. In addition, variation of stress on pipe crown is negligible and remains almost steady during cycles.

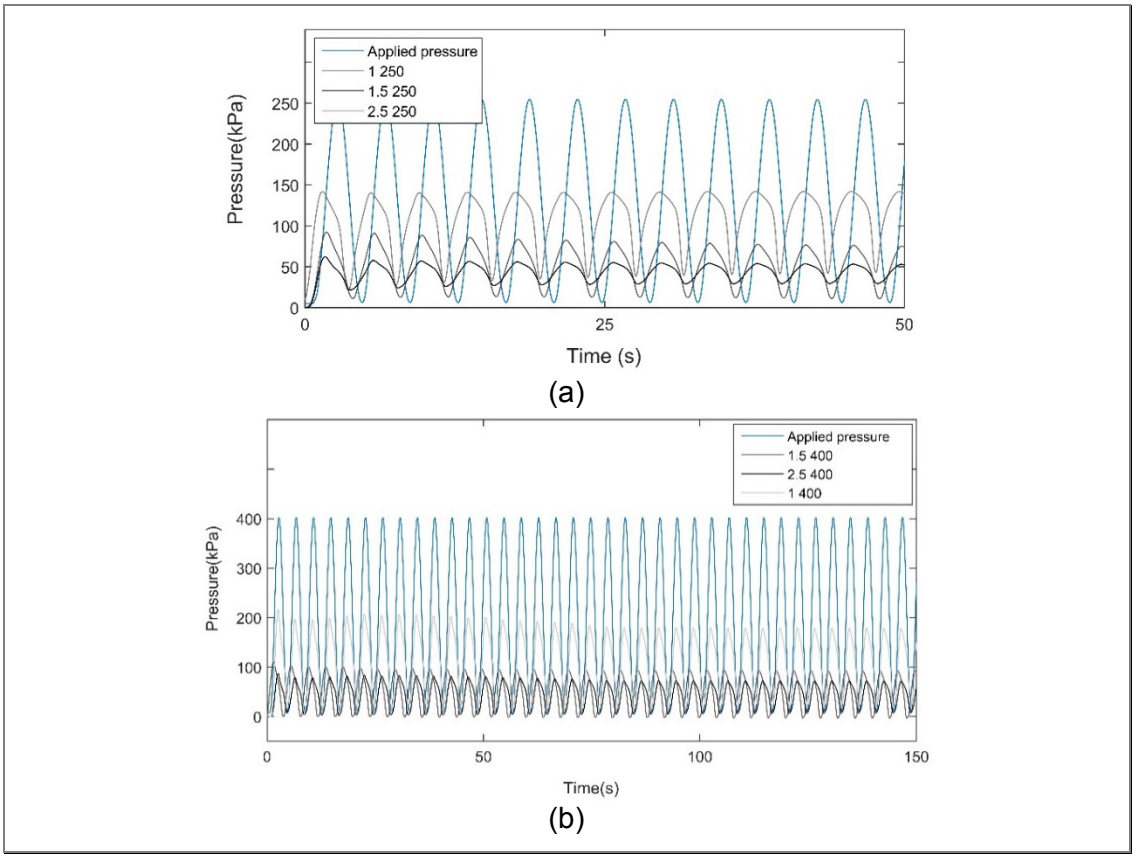

Figure 6-16 Impact of increase in vertical stress on pipe crown stress (a) 250 (b) 400 kPa

6.2.7 Test Series No 6: Cyclic Phase – Cement-treated

In this section the test results of cyclic load impact on buried pipe response in cement-treated trench material is presented. Similar to previous section cycle 500th is chosen as a benchmark to compare the results. The change in pipe deflection, surface settlement and soil pressure on pipe under various conditions are studied and results are presented in this section. The pipe deformation mode will be discussed briefly at the end of this section for both non-treated and cement-treated cases.

6.2.7.1 Vertical Diametric Strain (VDS)

The change in pipe deflection versus number of cycles for pipe buried in cement-treated sand under surface load of 250 and 400 kPa at three different burial depths is illustrated in Figure 6-17-a. Overall, maximum deflection happens under surface pressure of 400 kPa at H=1D. For example at cycle 500 under surface pressure of 400 kPa maximum VDS is 2 % for H=1D and is 0.3% for H/D=2.5. The same result is concluded for surface pressure of 250 kPa and VDS decreases when burial depth increases. The VDS variation at each cycle was also investigated to study plastic deflection of pipe at each cycle. As illustrated by red dashed line bracket on the right side of graph, the variation of VDS is more significant for shallower burial depths. It can be seen that the variation of VDS at each cycle is almost 1% for burial depth of H=1D and this value drops to 0.3% for burial depth of H=2.5D. As concluded from previous section, these results reveal that under shallower burial depth both maximum deflection value of pipe and its plastic deformation are important factors to be considered in the design.

The results of hysteresis curves for VDS are illustrated in Figure 6-17-b. It can be seen that by increasing number of cycles, hysteresis loops get closer. Results also reveal that after few cycles, equilibrium condition is achieved and load – VDS curves form a closed hysteresis loop and VDS does not change significantly anymore.

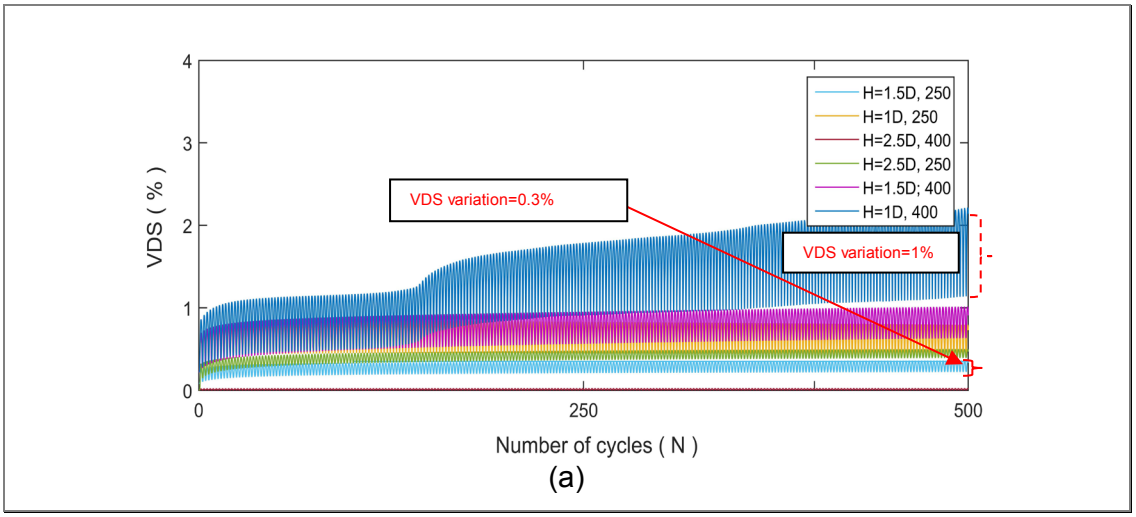

Figure 6-17 (a) VDS versus number of cycles at different burial depths (b) hysteresis graphs for VDS

6.2.7.2 Soil Surface Settlement (SSS)

The change in soil surface settlement under cyclic load for cement-treated material is shown in Figure 6-18-a to c. Figure 6-18-a shows SSS variation versus number of cycles. It can be seen that for the majority of the cases, variation of surface settlement is maximum during the first cycles and remains steady after 50 cycles. Results also reveal that SSS decreases when H/D increases. For example, under surface pressure of 400 kPa, increasing burial depth from H=1.0D to H=2.5D reduces SSS from 17 to 3 mm at 500th cycle. In addition, increase in surface pressure, increases SSS as expected. To illustrate plastic deformation of soil surface at each cycle, Figure 6-18-b is prepared. This is a zoom layout of Figure 6-18-a to see more clearly the SSS variation under different conditions. Overall, the range of SSS variation for all cases is almost the same and around 1mm. The results of hysteresis behaviour of surface

settlement under surface pressure of 250 kPa at H=1.5D are illustrated in Figure 6-18-c. It can be seen that by increasing number of cycles, hysteresis loops become less open.

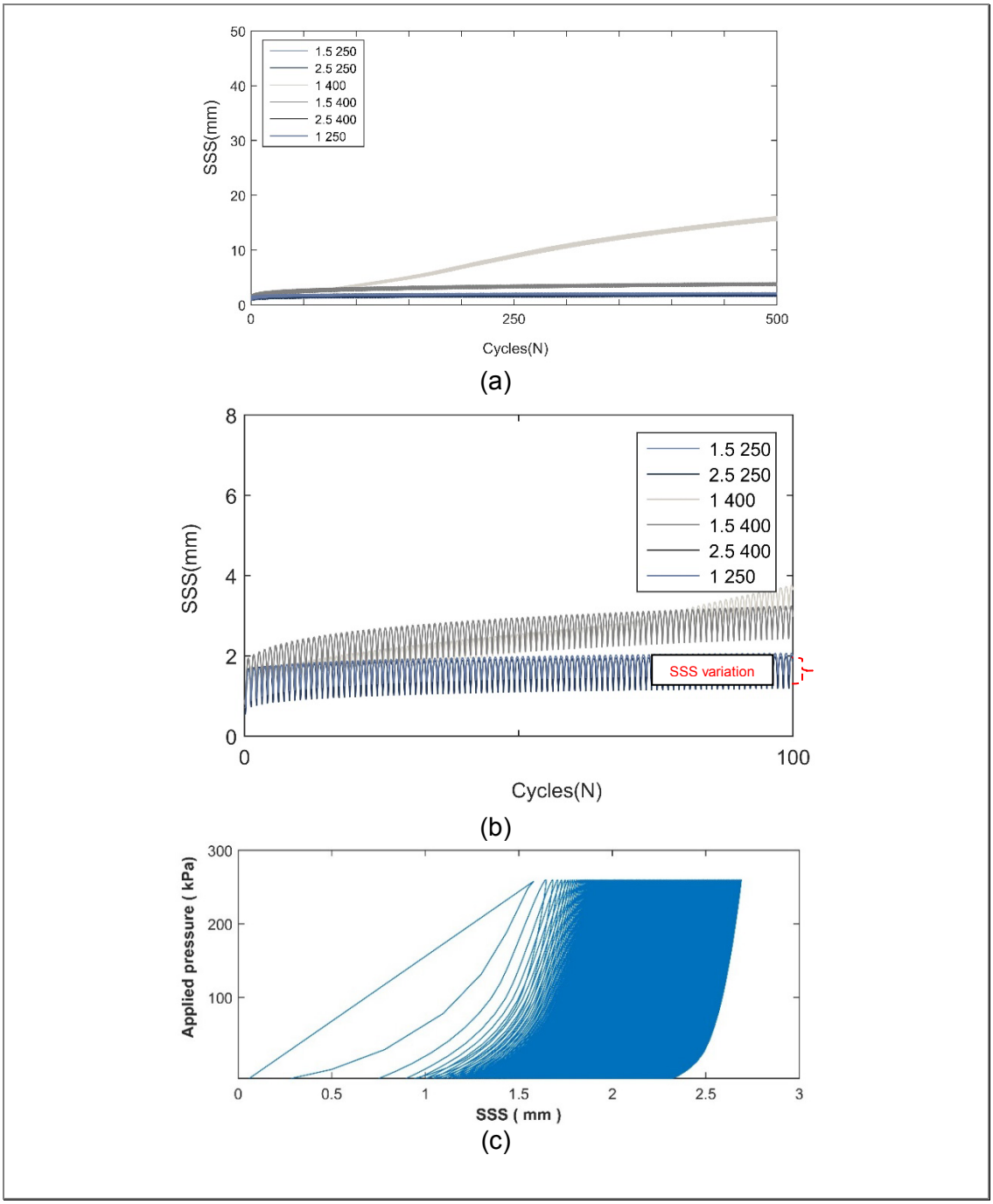

Figure 6-18 SSS variation (b) zoom layout of part: a (c) SSS hysteresis curve during cyclic load

The results of hysteresis curves for SSS and VDS are compared and are shown in Figure 6-19. For repeated load on soil surface an equilibrium condition is achieved where the load path (load-VDS) forms a close hysteresis loop after almost 500 cycles. Variation of VDS becomes more stable and after 500 cycles VDS remains almost the

same and does not increase. This does not happen for SSS as it increases when number of cycle increases. In other words, even after 4000 cycles, SSS still increases although the changes are not significant. This may be due to the early process of re-orientation of sand particles in the backfill around the pipe.

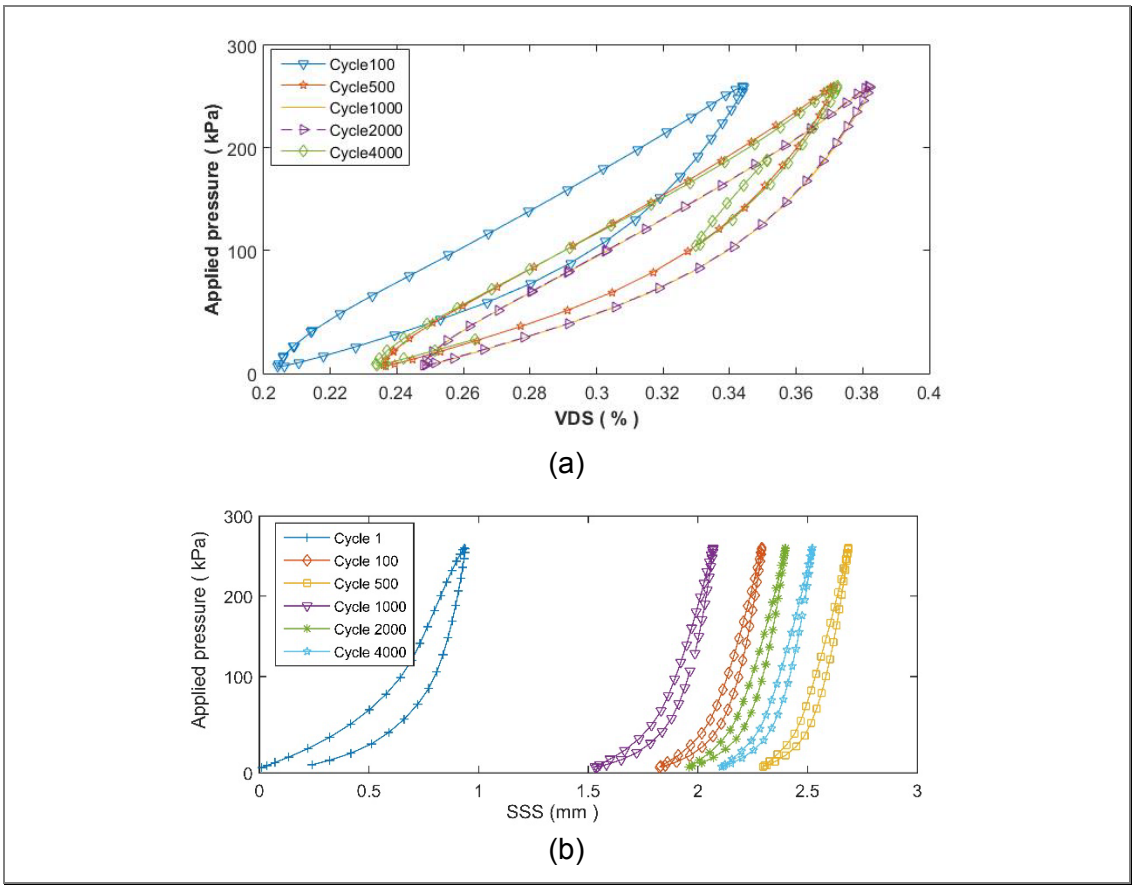

Figure 6-19 Hysteresis curve during repeated load (a) VDS (b) SSS

6.2.7.3 Vertical stress (σ)

For each test, increase in vertical stress was measured at pipe crown during cyclic phase and results are shown in Figure 6-20. Overall, surface pressure of 400 kPa causes higher pressure at pipe crown compared to pressure of 250 kPa as expected. Moreover, maximum pressure at pipe crown occurs while surface pressure is maximum and burial depths is minimum. In other words, in cement-treated materials the impact of live load is more significant under shallower burial depths and higher pressure occurs on pipe crown at lower burial depths. For example, under surface pressure of 400 kPa maximum pressure on pipe crown is 140 kPa occurring at H=1D as shown in Figure 6-20-c. In addition, variation of stress on pipe crown over the time is negligible and stress at pipe crown remains almost steady during cyclic tests.

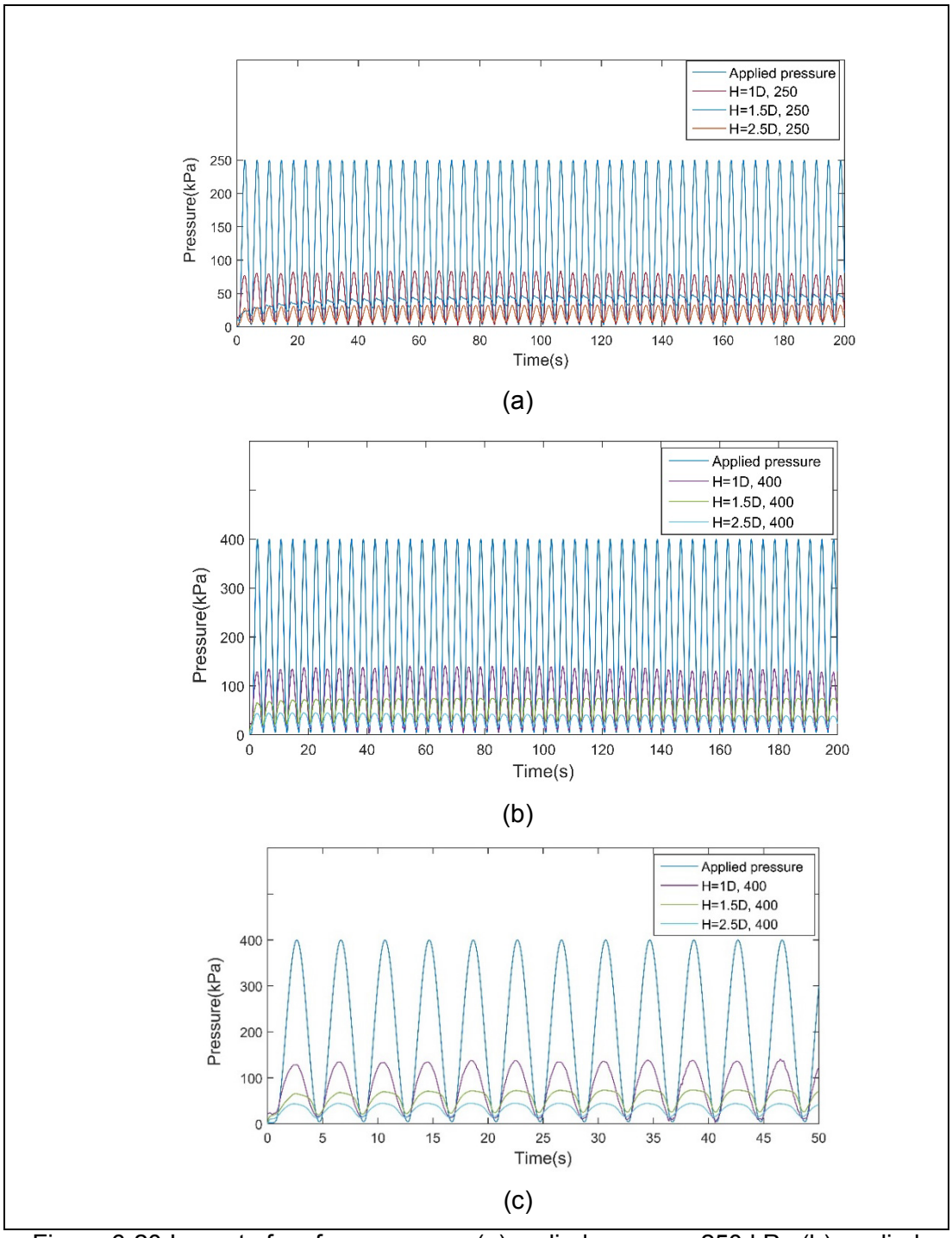

Figure 6-20 Impact of surface pressure (a)applied pressure 250 kPa (b) applied pressure 400 kPa (c) zoom layout of part (b)

6.2.7.4 Pipe deformation mode

Pipe diametric changes were measured using strain gauges installed at different points on the pipe circumference. Figure 6-21 illustrates strain gauges measurements due to cyclic load at different loading conditions. As mentioned in Chapter 4, for each test four different strain gauges at different points were glued directly to the external

face of the wall of the pipe to capture pipe deformation. Those strain gauges located at pipe springline, right and left sides show the same values. The readings of strain gauge 4 were too small. Therefore, the results of strain gauge at top and pipe springline are only illustrated in this section.

Figure 6-21-a compares the variations of strain at pipe crown and pipe springline denoting as SG1 and SG2 for non-cemented trench material. It should be noted that the diametric strain is positive if the pipe diameter is under tension, and negative if the pipe diameter is compressed. Overall, the strain gauge measurements at pipe crown show higher values compared to horizontal data for all cases. Results also reveal that both surface pressure and burial depth have impact on horizontal strain variations at pipe springline. Pipe vertical and horizontal deflections are maximum under shallower burial depth and higher surface pressure. In addition, the variation of horizontal and vertical deflections are higher under shallower burial depths and higher surface pressures. Same results are observed for cement-treated cases as shown in Figure 6-21-b.

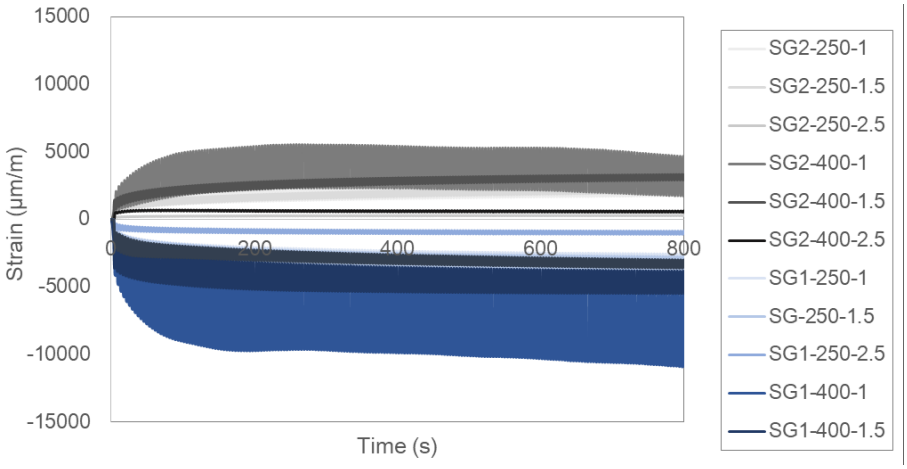

Non-treated sand

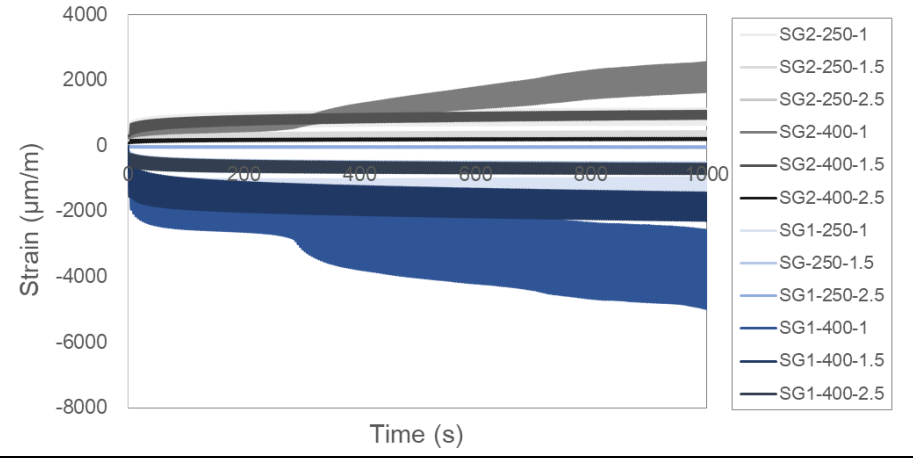

cement-treated sand

Figure 6-21 Pipe horizontal and vertical deflection versus time

Modes of pipe deformation are also illustrated graphically based on the results from all strain gauges measurements. Pipe deformation modes at cycle 100th are illustrated in the Figure 6-22 based on maximum values of strains recorded at different points on pipe circumference. Overall, the deformation of pipe buried in non-treated sand is significantly higher compared to cement-treated case. For example, maximum strain measured at pipe crown for non-treated case is almost 9000 μmm/mm. This value drops to less than 3000 μmm/mm after cement stabilization. In addition, the pipe at H=1D and under surface pressure of 400 kPa has the highest deformations as illustrated with legend symbol of 4 on the figure. For example, for non-treated trench material, the maximum strain measured for case 4 is 8000 μmm/mm and pipe tends to deflect to heart shape. The minimum strain measurements were recorded at H=2.5D under 250 kPa for cement-treated case and pipe almost remains unchanged with very small strains.

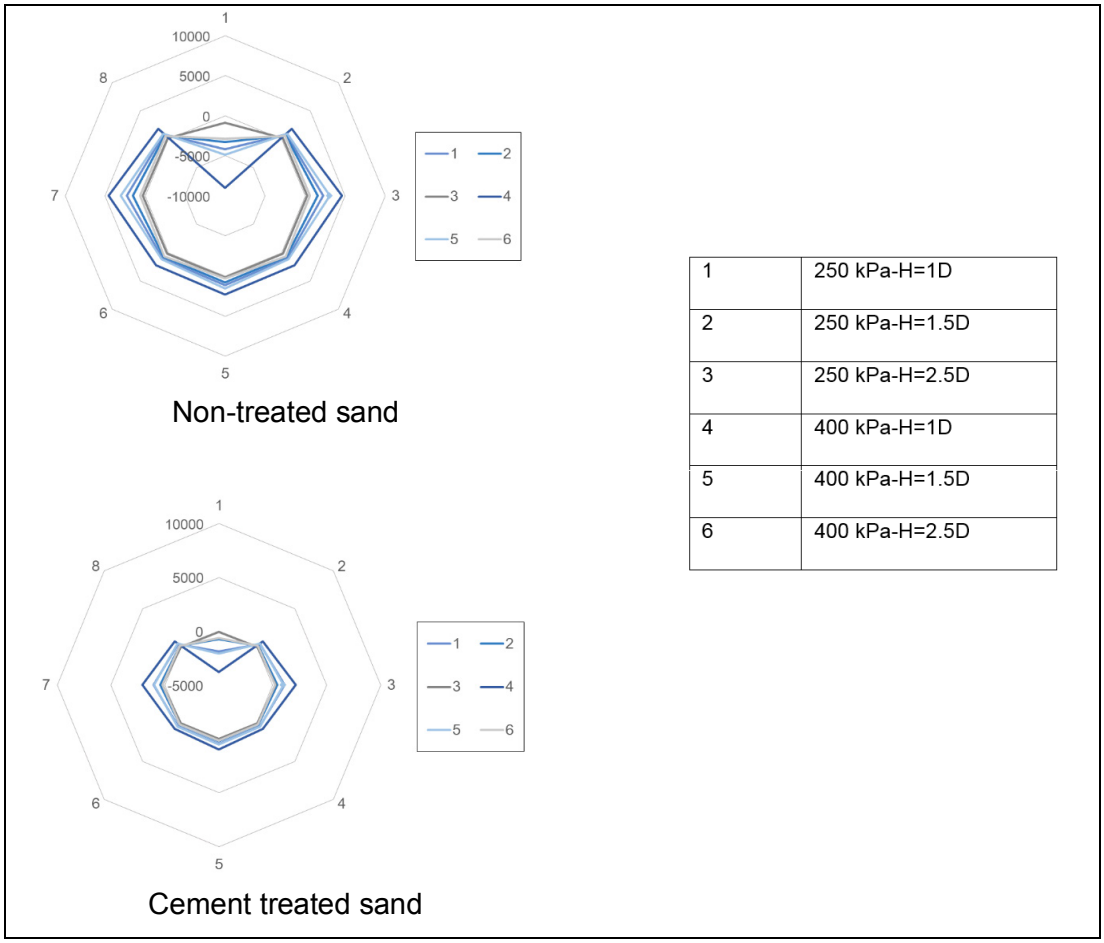

1	250 kPa-H=1D
2	250 kPa-H=1.5D
3	250 kPa-H=2.5D
4	400 kPa-H=1D
5	400 kPa-H=1.5D
6	400 kPa-H=2.5D

Figure 6-22 Impact of surface pressure and stabilization on pipe deformation at cycle 100th

6.3 NUMERICAL MODELING

The results from experimental tests performed on a plastic pipe presented in previous section. These results provide an opportunity to understand the relation between different factors affecting pipe behaviour. Numerical modelling is also carried out using ABAQUS (ABAQUS-6.13, 2013) and results are presented in the following section. It is noted numerical simulation develop a better understanding of pipe behaviour under different condition. It also provides more data to predict pipe behaviour under traffic load. The numerical simulations also provide more data at any given points while in experimental testing only at specific points the data is available. Before presenting the numerical simulation results, the numerical model is validated by simulating the actual experimental model and comparing the results from laboratory with those calculated through finite element model. The validated model then can be used to examine the effects of various parameters on model response.

6.3.1 Model Validation

The validation of finite element model was performed considering two aspects for model behaviour (1) vertical stress on pipe (2) soil surface settlement.

The validation of pressure on pipe crown was performed through comparing numerical results with empirical and experimental results. To measure increase in vertical stress under a rectangular area, a uniformly loaded rectangular area with length *L* and width *B* as shown in Figure 6-23 can be considered. Note that *L* is always greater than *B*. The uniform load *q* is expressed in force per unit area (pressure units). Equation 6-1 is used to calculate the increase of vertical stress under the corner of a rectangular area based on Boussinesq solutions (Boussinesq, 1885; Helwany, 2007). To calculate the stress increase under the centre of a loaded rectangle, whole area can be divided into four rectangles. The increase in the vertical stress under the corner *A* of each small rectangle can be calculated assuming that *L* and *B* are the length and width of the small rectangle as shown in Figure 6-23. The total increase in vertical stress is then calculated by sum of the stress increases of the four identical small rectangles. Note if $m^2 + n^2 + 1 < m^2n^2$, then π must be added to the bracketed quantity in the last term.

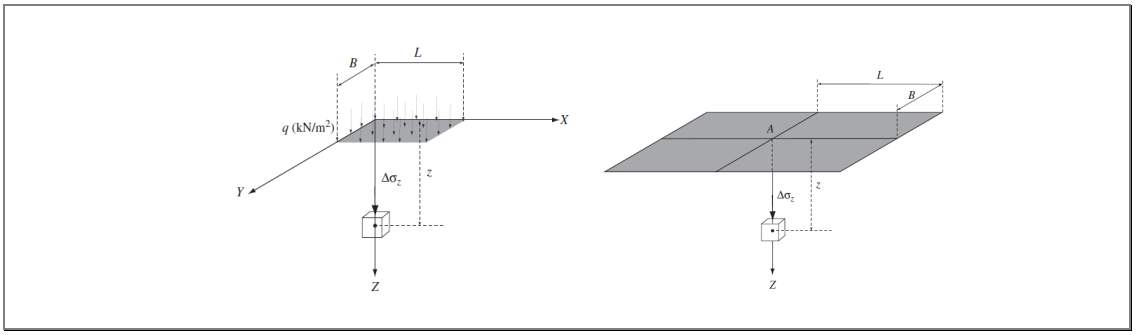

Figure 6-23 Increase of stress over uniformly loaded rectangular area (Helwany, 2007)

$$I(|m|,|n|)=\frac{1}{4\pi}\left[\frac{2mn\sqrt{m^2+n^2+1}}{m^2+n^2+m^2n^2+1}\left(\frac{m^2+n^2+2}{m^2+n^2+1}\right)+\tan^{-1}\left(\frac{2mn\sqrt{m^2+n^2+1}}{m^2+n^2-m^2n^2+1}\right)\right] \quad 6\text{-}1$$

Figure 6-24 compares the results obtained through empirical method and those obtained from laboratory and numerical simulations. The figure illustrates increase in vertical stress under the surface pressure of 250 and 400 kPa and the depth between H=0 and H=2.5D. Horizontal axis represents increase in vertical stress and vertical axis represents depth below the soil surface. It can be seen that for both numerical and Boussinesq solutions increase in vertical stress is a function of depth. Both graphs have almost the same pattern especially for shallower depths (H<1D). However, finite element analysis predicts higher stress in deeper depths especially on pipe crown compared with Boussinesq solution. The value predicted using finite element analysis has a good agreement with those captured in laboratory at pipe crown. For example, at depth of H=2.5 D under surface pressure of 400 kPa pressure cell on pipe crown shows a pressure of 78 kPa and finite element analysis predicts earth pressure of almost 80 kPa. However, the difference between finite element method and Boussinesq solution can be due to different assumptions in two approaches. For example, in Boussinesq method the soil is assumed to be weightless, linear elastic, isotropic while in nature and in this study the soil is assumed to be elasto-plastic and has weight.

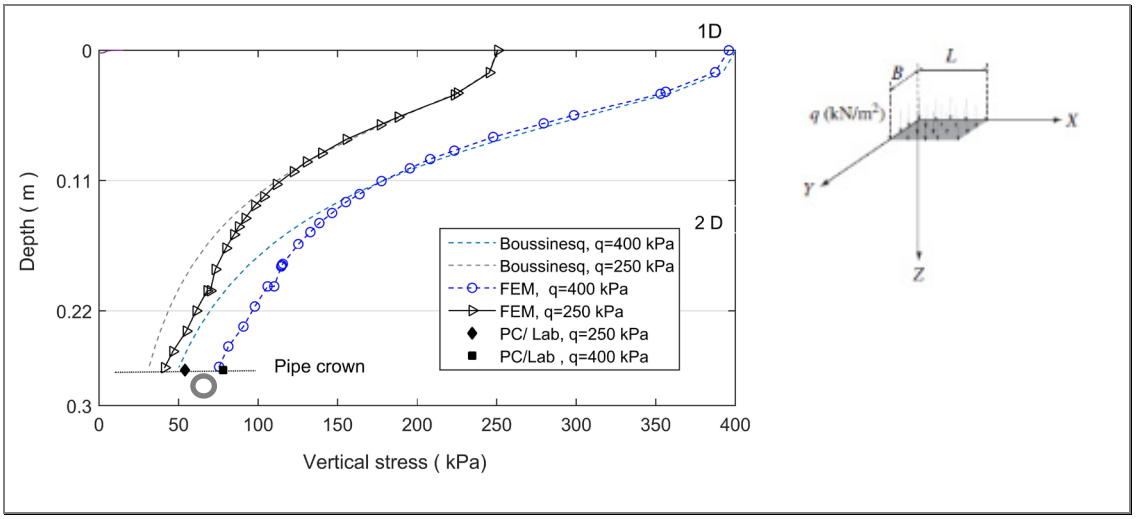

Figure 6-24 Stress caused by the strip footing on soil using finite element versus analytical solution and laboratory results

In the second verification test, the surface deflection of soil under surface pressure is analysed. The maximum surface settlement captured by LVDT was compared with those calculated through numerical simulations and empirical equations. For example, the deflection of soil for a rigid plate on homogenous elastic half space can be calculated through Equation 6-2 (Huang, 2004)

$$w_0 = \frac{\pi(1-\mu^2)qa}{2E} \qquad 6\text{-}2$$

Where, w_0 = the deflection of loading plate; μ = Poisson ratio of material; E = Elastic modulus of material; q = load on the loading plate; a = radius of the loading plate. Figure 6-25 compares the surface deformation calculated by Equation 6-2 with those measured in the laboratory and calculated by numerical analysis. Horizontal axis shows test number while each number represents test conditions as explained in the legend of the figure. For example test number one is a case in which applied load is 250 kPa and burial depth is H=1D. Vertical axis represents surface deflection. It can be seen the computed surface deformation based on the empirical equation matches well with the measured results in the laboratory. In addition, the maximum surface settlements values calculated through numerical analysis are consistent with other results from other methods.

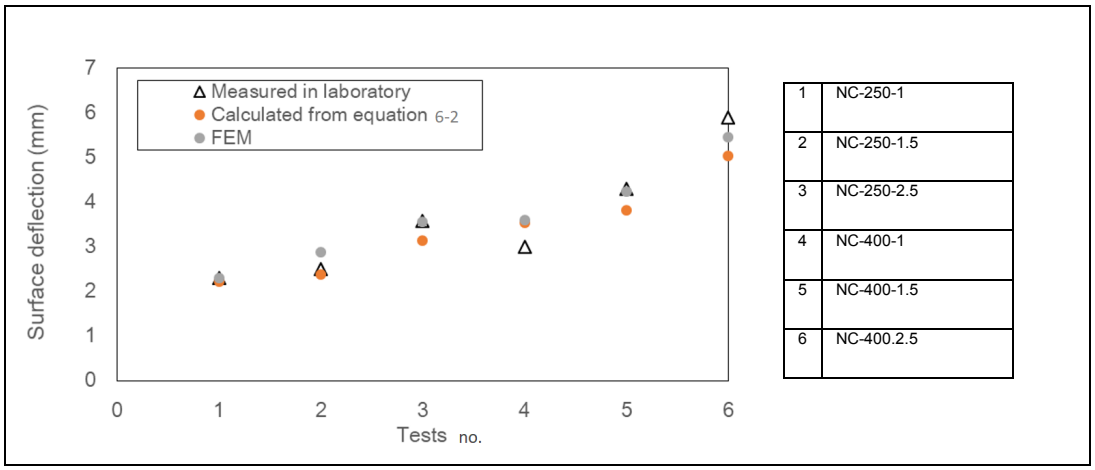

Figure 6-25 Comparing surface deflections from different methods

Figure 6-26 compares the results obtained from numerical simulations with the experimental data measured from the same test configurations for both pure sand and cement-treated material. Horizontal axis represents distance from centreline and vertical axis represents soil surface settlement. In addition, all legend symbols consist of different parts representing the method of calculation, type of soil and applied surface pressure. For example, FEM/NC 400 is referring to surface settlement related to finite element calculation for the pipe in non-treated trench under surface pressure of 400 kPa. Overall, there is a good match between the numerical and experimental results. For example, under surface pressure of 250 kPa maximum surface settlement of 2.2 mm is calculated for a pipe in non-treated soil. This value is very close to 2.15 mm from laboratory observation representing as a yellow circle point on the graph. It is also obvious from the figure that numerical simulations provide an opportunity to understand the behaviour of the model and change of soil surface at any point through surface contours while experimental results provides only one point in a scatter plot.

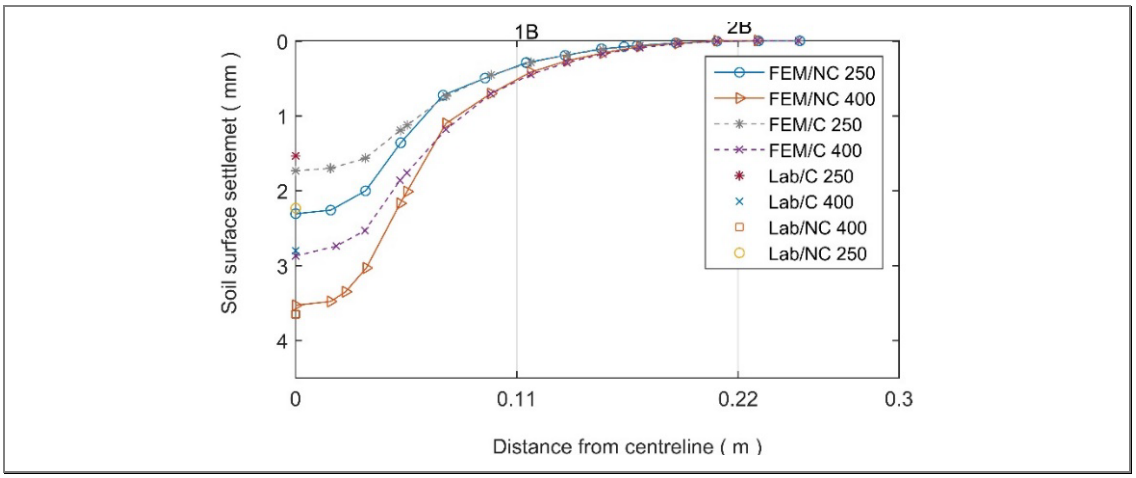

Figure 6-26 Comparing numerical and experimental results of soil surface settlement

Assuming unpaved road as a homogenous elastic half-space with Poisson ratio of 0.3, the secant modulus can be back calculated using total deformation. The secant modulus can be found from following equation:

$$E = \frac{\pi(1-\mu^2)\mathrm{qa}}{2w0} \qquad 6\text{-}3$$

Results for some cases are shown in Table 6-2. Although this equation is based on assuming a homogeneous half-space, it can be used to assume elastic modulus of material. For example, under surface pressure of 250 kPa at H=2.5D the total deformation is 3.59 mm and based on calculation, elastic modulus is 13324.57 kPa. For finite element calculation average elastic modulus of 15000 kPa was assumed. This value gives the ratio of lab/num results as 0.951 which is reasonable. It is noted that the difference between laboratory and numerical values can be due to the fact that these secant modulus values correspond to the deformations which includes plastic deflection component. However, the elastic modulus is the modulus of the slope of the rebounding load-deformation curve. These values and verification method will be used to verify input values for numerical simulations only.

Table 6-2 Measured Young's modulus – Back calculation

	NC-250-1	NC-250-1.5	NC-250-2.5	NC-400-1
Total deformation(mm)	2.3	2.5	3.59	3
E from back calculation (kPa)	20797.91	19134.078	13324.57	15945.06

6.3.2 Numerical Results

The previous section reveals that numerical analysis based on ABAQUS can simulate the performance of buried pipe under traffic loading and different geometric conditions. In the following section the results of numerical analysis is presented. Some parts of this section has been published and can be found in

6.3.2.1 Ultimate bearing capacity

In this section, the result of the finite element method used for investigation of the ultimate bearing capacity of the backfill material is presented. The results of numerical simulations of footing laid on pure and cement-treated sands will be calculated and

then compared with experimental tests data. The methodology of this section is adopted from literature and mainly from the article presented in APPENDIX A (Mosadegh & Nikraz, 2015; Mosadegh & Nikraz, 2017).

Problem definition is illustrated in Figure 6-27. The vertical side of the model is fixed in horizontal direction, and the bottom of the model is fixed in both vertical and horizontal directions. In all cases footing is subjected to a load control simulation. The footing is also assumed as rough rigid with no horizontal movement. In all models, the mesh has been refined in areas with stress concentration under and near the footing. The model is created in three steps. In the first step, which is the initial condition, all boundary conditions are defined. In the next step, the gravity load is applied to the model in the geostatic step. In the third step, a downward load is applied on top of the soil under footing. After applying the load, foundation pressure will be increased up to a failure point which is bearing capacity term. It should be noted that the duration of applied load is 65 seconds to avoid sudden collapse of soil mass and to be consistent with laboratory test. Moreover, it is assumed that relative movement between soil and footing is impossible. From experimental results, when failure takes place, the slip planes under the footing and its sides can be identified as shown earlier.

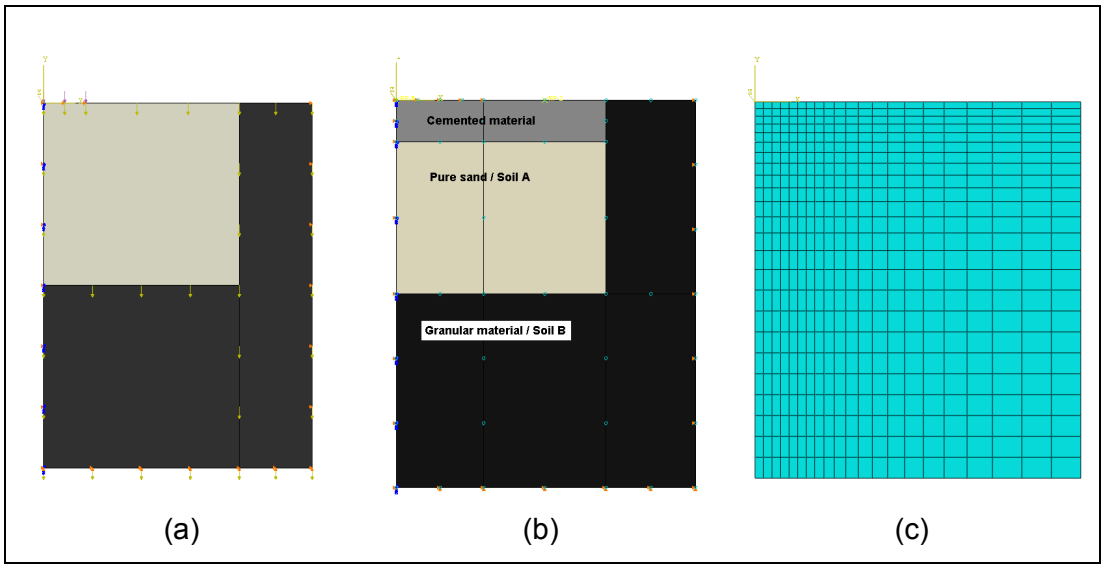

Figure 6-27 Problem definition of footing laid on (a) pure sand (b) cement treated sand(c) finite element mesh model

Results of numerical simulations at failure point are illustrated in Figure 6-28. Figure 6-28-a illustrates soil displacement contours showing that displacements are 4.92 cm and 0.9 cm for non-treated and cement-treated sands, respectively. Figure 6-28-b shows Terzaghi's general shear failure zones. From numerical simulations presented in Figure 6-28-c there are three different distinct zones under the footing at failure point: triangular zone immediately under the footing; two radial

zones, and two Rankine passive zones (Terzaghi & Peck, 1948). Displacements are deeper and wider for non-treated case. Results of plastic shear strains are also plotted at failure point for both non-treated and cement-traded cases in Figure 6-28-c. It can be seen that higher plastic shear strains are observed over a bigger area for non-treated trench.

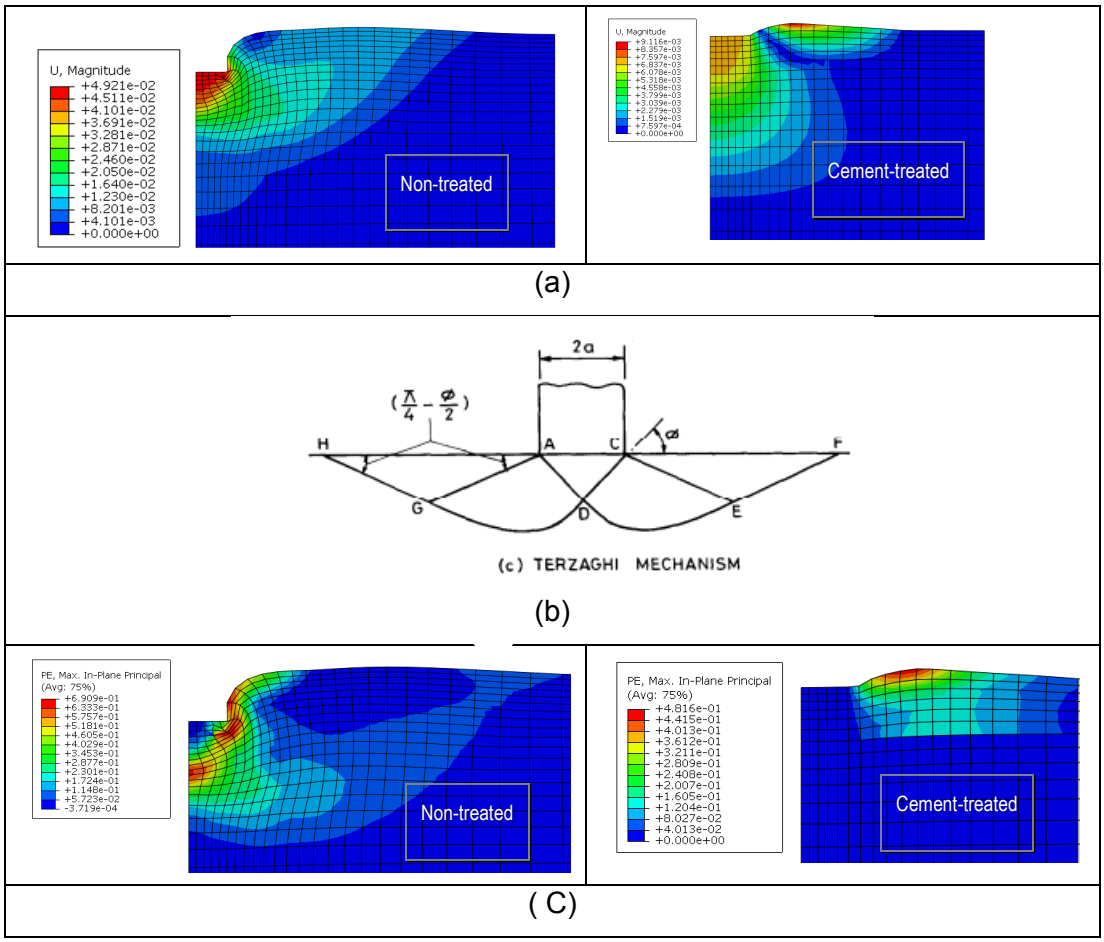

Figure 6-28 (a) Footing settlement, (b) general shear failure of a strip footing: Terzaghi's assumption (Manoharan & Dasgupta, 1995)(c) plastic shear distributions at failure

Figure 6-29 compares pressure–settlement curve for bearing capacity of footing on both dense and cemented sands. Horizontal and vertical axis represent normalised settlement of footing and vertical stress under footing, respectively. This figure also compares the values obtained from numerical simulations and experimental tests. It should be noted that for pure sand in numerical analysis the curves are based on the results using Drucker-Prager model without considering dilation angle and Mohr-Coulomb plasticity for cemented soil. It can be seen that for pure sand the bearing capacity is almost 590 kPa in experimental test and 600 kPa in numerical analysis which is slightly bigger than those obtained by experimental

tests. In addition, bearing capacity of footing after stabilization increases and reaches to almost 1100 kPa. In other words, adding cement shows a significant increase of 80% in bearing capacity. It can be concluded that bearing capacity increases from 600 kPa to 1100 kPa by adding 5 cm of cement treated layer which is minimum depth of cement layer in the current study. It is noted although the numerical results do not fully correspond with the experimental results, but the results are in good agreement. Any discrepancy may be related to the chosen model for soil and foundation parameters, and differences between the boundary conditions in the numerical and experimental models.

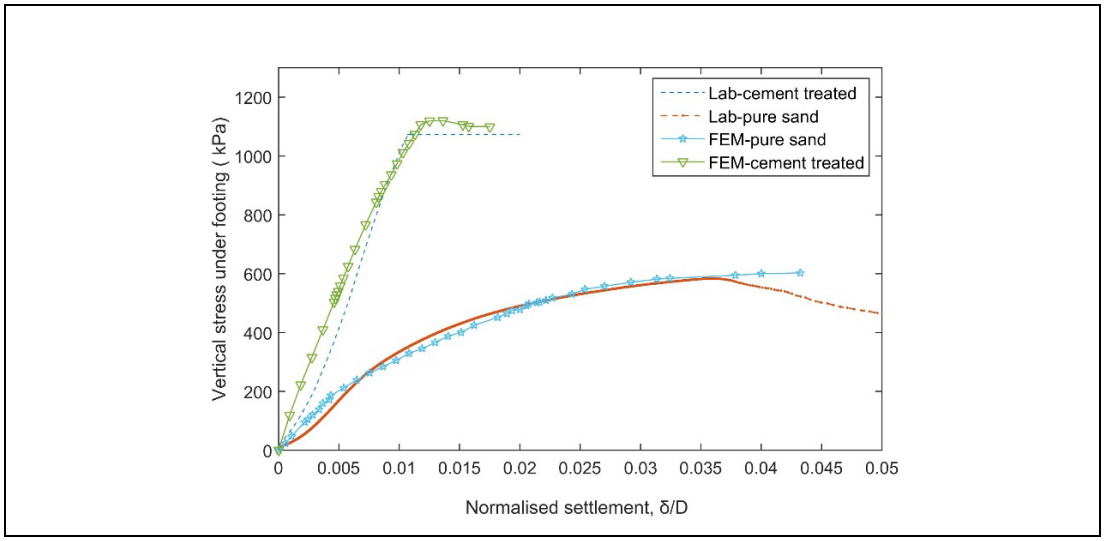

Figure 6-29 Comparison of load–displacement curves from FEM and experimental results

6.3.3 Traffic Load – Static Phase/Non-treated

Traffic load was applied on a buried pipe model to compare pipe behaviour due to change in surface pressure and burial depth during static phase. In order to validate the FE model, the results of numerical simulations are compared with those from experimental results and are investigated later. It should be noted that the reason to apply traffic load as static load is tis the fact that a large portion of the pipe deformation and soil surface settlement occur at the end of first cycle, showing the importance of the first cycle. In addition, applying static load is less time consuming and soil constitutive model is less complicated compared with cyclic simulations. Therefore, it would be a cost-effective way to analyse static phase of similar projects instead of cyclic phases to estimate model response. The results of numerical simulations through finite element analysis will be presented in the following section.

6.3.3.1 Pipe vertical deflection

In this section the impact of burial depth and surface pressure on pipe deflection is presented. Figure 6-30 illustrates displacement contours of the deformed pipe at different burial depths under surface pressures of 250 and 400 kPa. Figure 6-30-b compares results for different surface pressure at the same burial depth of H=1D. Results show that under higher surface pressure, higher displacement occurs at pipe crown. For example, pipe crown displacement at H=1D under surface pressure of 400 kPa is 1.53 mm and this value drops to 0.97 mm under surface pressure of 250 kPa as shown in Figure 6-30-b. In addition, comparing Figure 6-30-a and c shows that maximum vertical displacement occurs at pipe crown (Figure 6-30-a) while maximum horizontal displacement occurs at pipe springline (Figure 6-30-c).

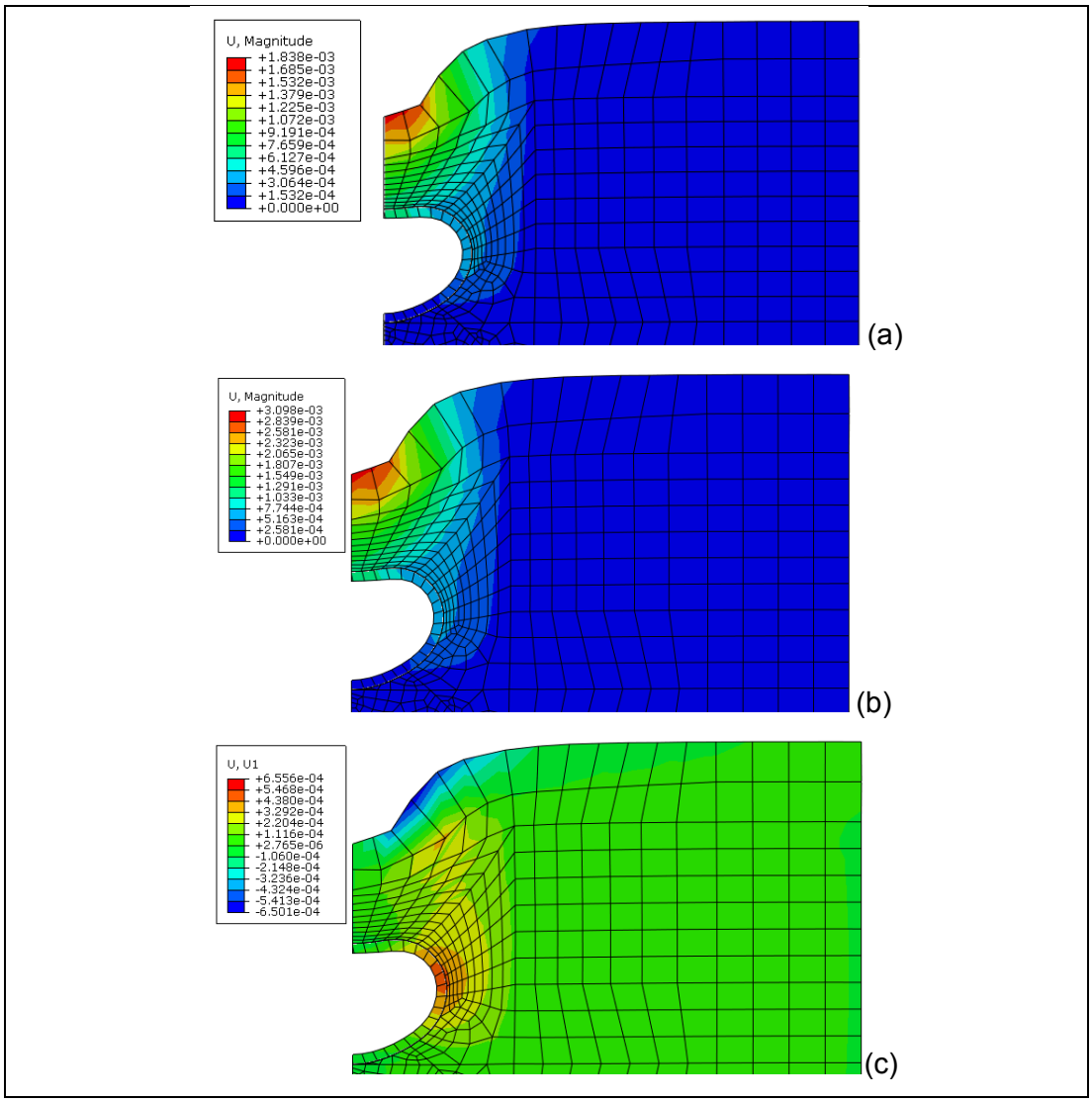

Figure 6-30 Displacement contours: (a) vertical displacement at H=1D, 400 kPa (b) vertical displacement at H=1D, 250 kPa (c) horizontal displacement at H=1D, 400 kPa

The numerical simulation of pipe displacement variation on the pipe crown and along its circumference for all burial depths under surface pressures of 250 and 400 kPa is presented in Figure 6-31. Overall, increasing burial depth decreases pipe vertical displacement while increasing surface pressure, increases pipe vertical displacement. Pipe vertical displacement is maximum when burial depth is minimum (H=1D) and surface pressure is maximum (P=400 kPa). The zero value on horizontal axis indicates the point on the crown at centre of loading. All graphs converge on the bottom of pipe to zero which means under any surface pressure and burial depth, pipe displacement at its bottom is minimum close to zero. In addition, when angle from centreline is between 60 and 120º, settlement decreases significantly and converge to smaller values. For example, at H=1D under surface pressure of 400 kPa, pipe vertical settlement at pipe crown is 1.5 mm. After this point with increasing angle from 60º to 120º pipe displacement remains steady at 0.8 mm. Then, pipe displacement on the bottom plunges to almost zero with increasing angle to 180º. Almost the same pattern is obtained for all other cases. In addition, the effect of burial depth is higher at pipe crown and by increasing the angle along pipe circumference the gap between graphs decreases.

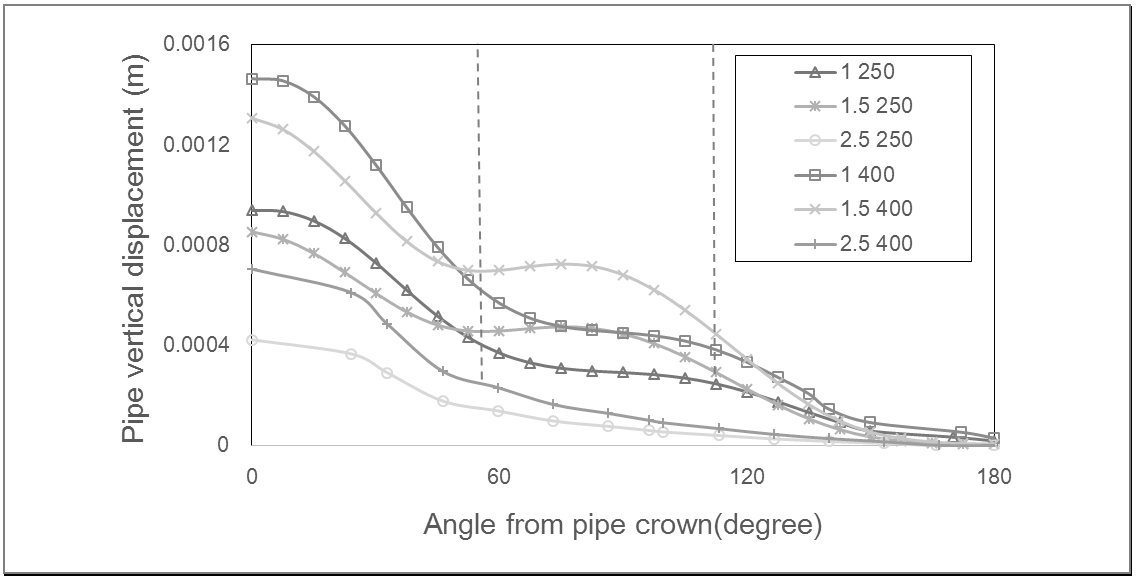

Figure 6-31 FE results for variation of pipe displacement along its circumference

Additional comparisons were made for the case of H=2.5D under surface pressure of 250 kPa to compare displacement on pipe soil interface. In previous figure only the results of vertical displacement along the pipe circumference was presented. Figure 6-32 compares vertical displacement at pipe soil interface along pipe and its surrounding soil. It can be seen that both pipe and soil have the same vertical displacement at pipe crown while pipe has higher displacement along its

circumference although the difference is negligible. Both graphs merge to the same value at pipe invert. This result reveals that for this case either the pipe or soil at the interface can be used to simulate vertical deflection of pipe.

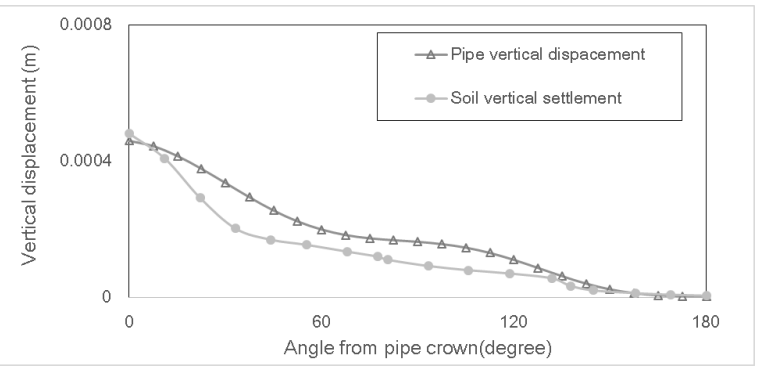

Figure 6-32 Vertical displacement at pipe-soil interface

6.3.3.2 Soil surface settlement variation

The impact of burial depth and surface pressure on soil settlement has experimentally been investigated and the results were discussed briefly in the previous section. The numerical simulation of soil surface settlement for all burial depths under surface pressure of 250 and 400 kPa is illustrated in Figure 6-33. Maximum settlement for all burial depths occurs on soil surface over the area above pipe crown as shown. In addition, regardless of burial depth, the soil surface settlement decreases away from the centre of loading. It is clear also that soil surface settlement for all burial depths converges to a minimum value over 2B distance from centre or two times of loading area. In addition, both burial depth and surface pressure affect soil surface settlement as illustrated. For a given surface pressure, soil settlement increases when burial depth increases. For example under surface pressure of 400 kPa at H/D=1, maximum SSS is 3.5 mm and increasing burial depth from H/D=1 to 1.5 and 2.5, increases maximum SSS from 3.5 to 5.1 and 8.2 mm, respectively. This can be due to presence of compressive layer above the pipe. By increasing burial depth the thickness of compressive layer increases meaning that soil settles more when burial depth increases. These results are consistent with results achieved through laboratory tests and those provided in the literature (Moghaddas Tafreshi & Khalaj, 2008).

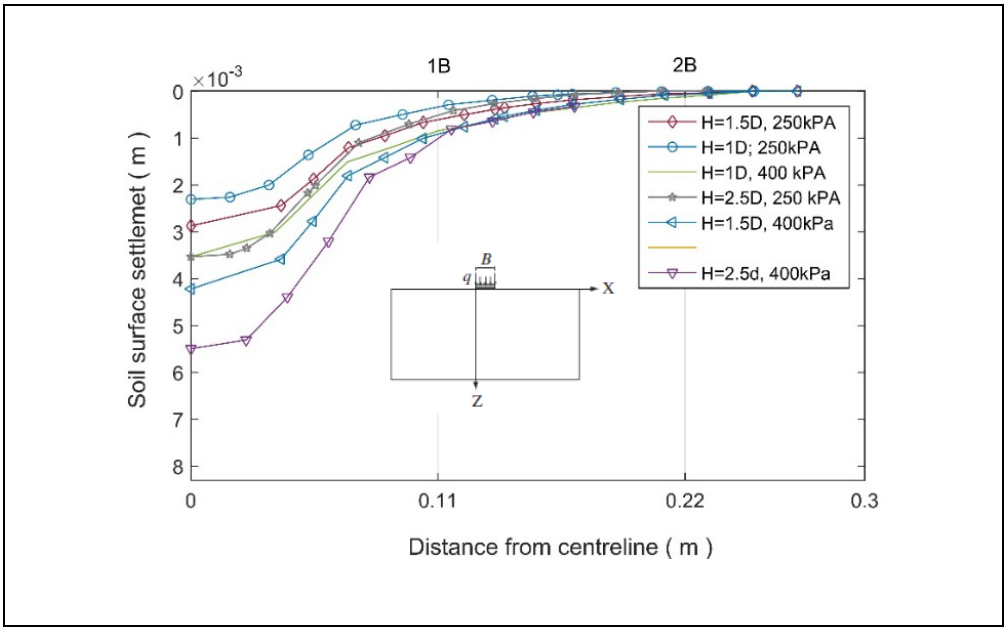

Figure 6-33 Contours of soil surface settelement for all non-terated cases

Vertical displacement on soil surface is shown in Figure 6-34. The results show that the maximum soil surface settlement occurs at the centreline. For all contours, soil surface settelement decreases when soil depth increases. In addition, under a given surface pressure and burial depth, the value for soil surface settlement is equal to those maximum values obtained in Figure 6-33. For example, at H=2.5D under surface pressure of 400 kPa, soil vertical displacement at centreline is 5.5 mm. This is the same value which was observed in Figure 6-33 for the same case.

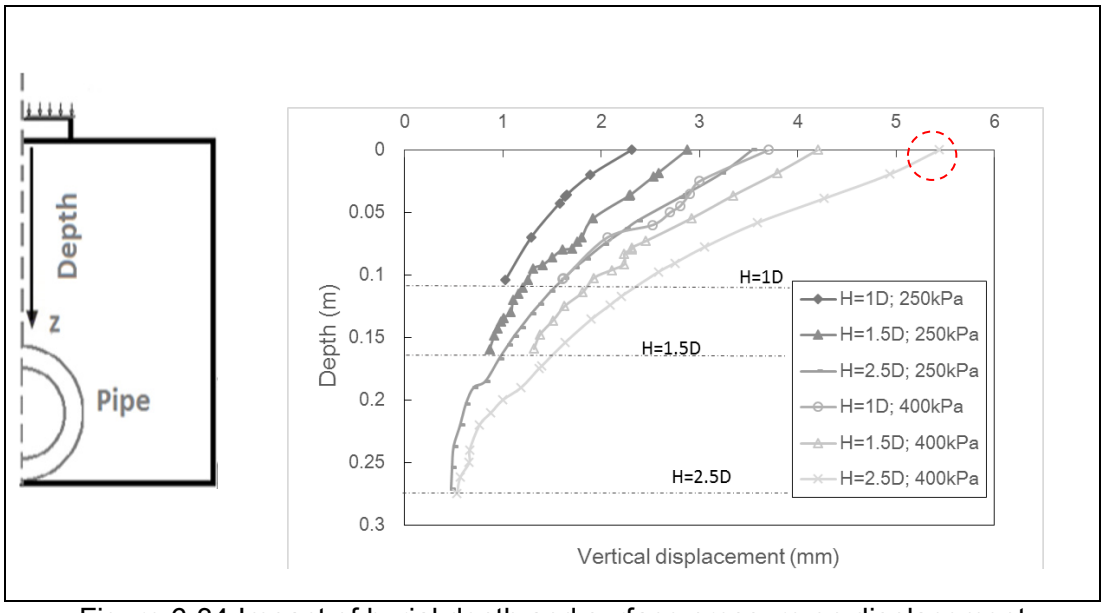

Figure 6-34 Impact of burial depth and surface pressure on displacement underneath the centre of loading area

6.3.3.3 Stress distribution variation

The vertical stress distribution induced by loading plate for z=0 to z=2.5D is calculated and results are illustrated in Figure 6-35. These calculations are repeated for different burial depths and two different surface pressures. Overall, all diagrams have almost the same pattern. Stress decreases in a very similar manner when burial depth increases. In addition, under a given surface pressure, all stress induced in soil profile decrease until they merge to the same value for deeper burial depths. For example, at H=1D under surface pressure of 400 kPa, the stress in soil profile drops from 400 kPa to almost 200 kPa on the pipe crown. The same pattern can be observed for burial depth of H=2.5D where stress on pipe is reduced to almost 100 kPa. It is noted that some cases from this part were presented in verification section and were compared to those predicted by Boussinesq solution.

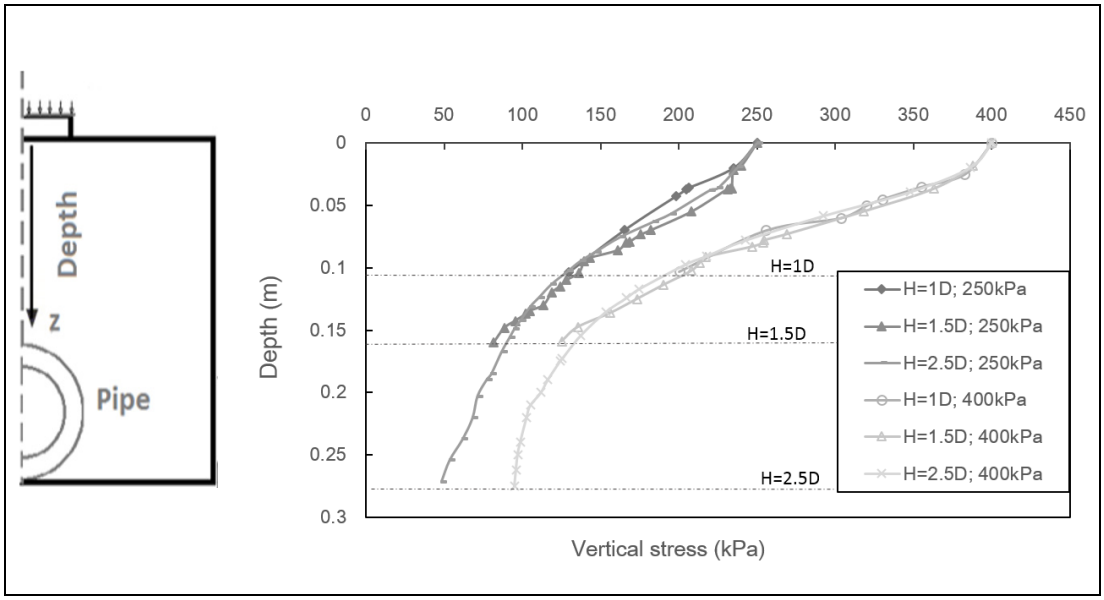

Figure 6-35 Vertical stress distribution on soil profile as a function of depth

For better understanding of burial depth and surface pressure impacts on pressure at pipe crown, pressure distribution along pipe circumference is calculated and results are illustrated in Fig. 6-36. It is evident from the figure that three different sections exist and earth pressure is maximum in the middle part. For example for H=1D and under surface pressure of 400 kPa, earth pressure increases from 85 kPa to 105 kPa when angle increases from 0^o to 60^o. After this point by increasing angle from 60^o to 100^o earth pressure reaches to its maximum value of 115 KPa. Then by increasing angle to 180^o pipe earth pressure reaches to about 46 kPa on pipe invert. Red brackets compare pressure variation at pipe crown and invert. It can be seen that the earth pressure variation is more significant on pipe crown compared to its invert. This value is nearly three times higher at pipe crown as shown in the figure.

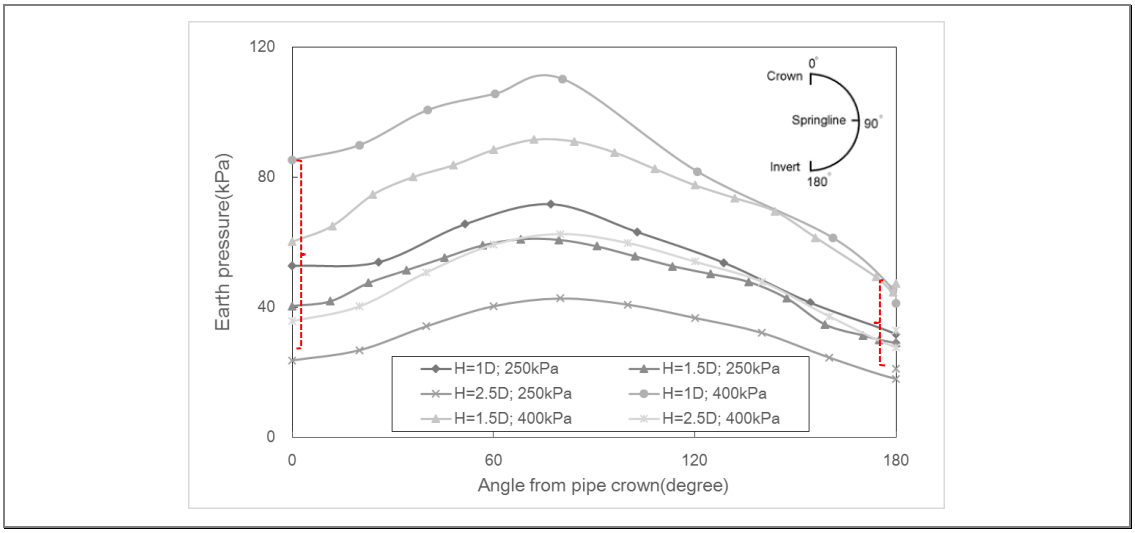

Fig. 6-36 Earth pressure distribution along pipe circumference

It is helpful to put multiple data trends onto one graph which facilitates review of the results. For example, Figure 6-37 shows combinations of vertical displacement and earth pressure along the pipe circumference. This figure reveals that maximum pipe displacement occurs at pipe crown while earth pressure at this point is not maximum. Pipe deflection is maximum at pipe crown while earth pressure is maximum in the middle part of pipe circumference between 60 to 120 degrees. This can be explained using pressure distribution graph close to the graph showing pressure is maximum in the middle part of pipe. This pressure is combination of vertical pressure *(q)* and horizontal pressure or *(kq)* (Spangler, 1941). This result show the importance of two investigating points including pipe crown and middle part of the pipe circumference.

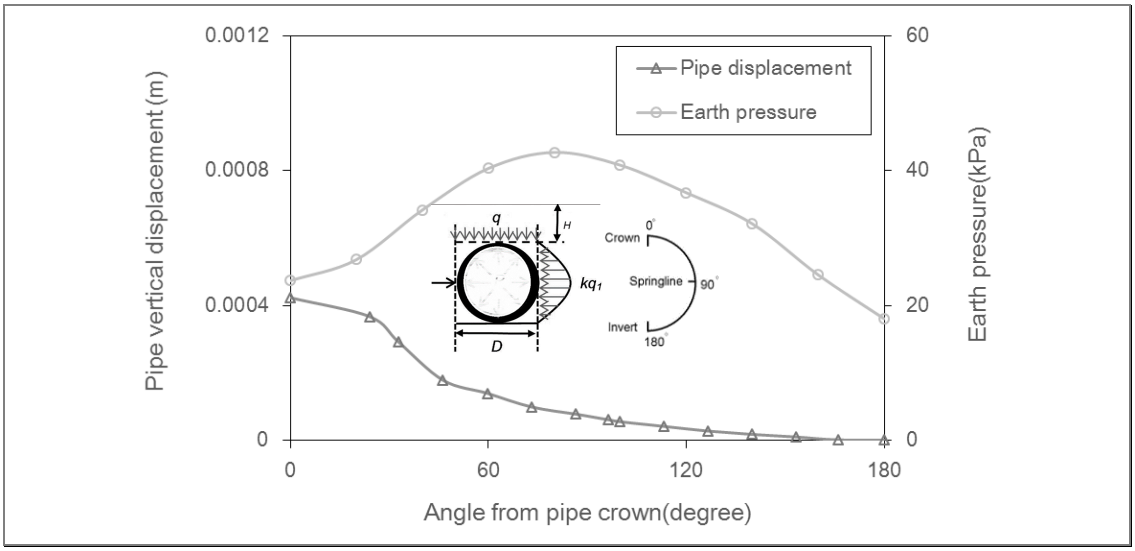

Figure 6-37 Combination of earth pressure and pipe vertical deflection along pipe circumference

6.3.4 Traffic Load – Static Phase / Cement-treated

In this section, the numerical results of stabilization impact on model response are presented. In all graphs dashed lines represent non stabilized samples and solid lines represent cement- treated ones. Legend symbols of NC and C also denote results of non-treated and cement-treated tests, respectively.

6.3.4.1 Pipe vertical deflection variation

Figure 6-38 shows the results of pipe vertical displacement under different conditions along its circumference for both non-treated and cement-treated trench material. Overall, higher pipe deflections are observed for the cases of non-treated soil. It can be seen that the maximum surface settlement of soil for non-treated sample, is in the range of 0.4 to 1.6 mm. This value for cement-treated tests is between 0.05 and 0.8 mm. For example, under surface pressure of 400 kPa, at H=1D for non-treated pipe crown displacement is 1.5 mm. Stabilization of soil decreases pipe deflection and this value drops to 0.9 mm. All graphs converge to the value of zero at the bottom of pipe at 180 degree from the crown. As explained in section 6.3.3.1 there are three different sections and pipe deflection is maximum in the first section between 0 to 60 degrees from pipe crown.

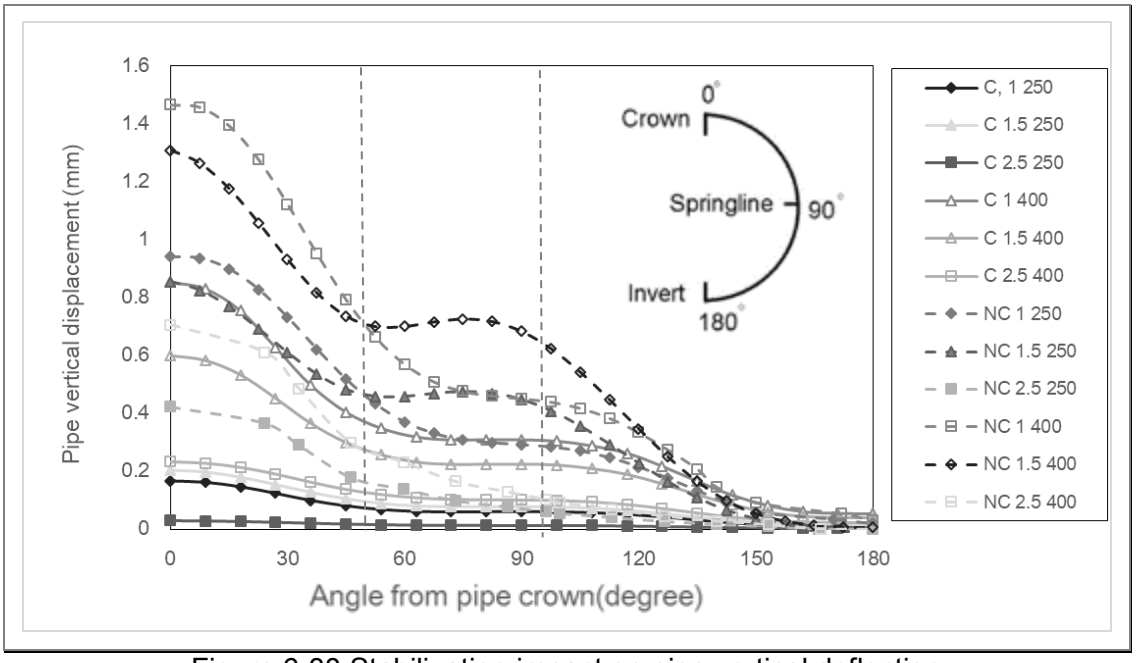

Figure 6-38 Stabilization impact on pipe vertical deflection

6.3.4.2 Soil surface settlement variation

Figure 6-39 shows the effect of stabilization on surface settlement of soil. It can be seen that stabilization decreases surface settlement. For example, surface settlement at H=2.5D under surface pressure of 400 kPa for non-treated case is 5.2 mm. Stabilization reduces surface settlement to 1.8 mm after adding cement. All graphs converge to the value of zero at a distance of 2B as shown in Figure 6-39. In addition, surface settlements are maximum at the loading area and above pipe crown.

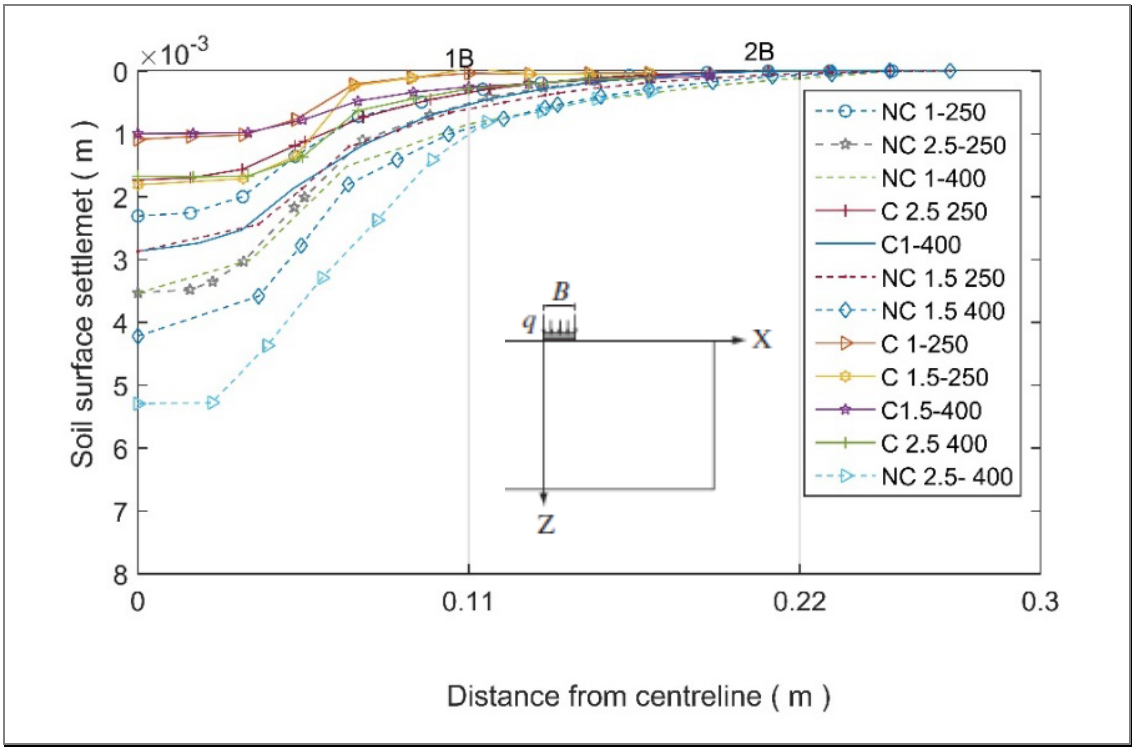

Figure 6-39 Impact of stabilization on soil surface settlement

Figure 6-40 shows stabilization impact on soil vertical displacement under the footing centreline along the soil depth. Horizontal axis represents the vertical displacement and vertical axis represents soil depth. Overall, stabilization reduces soil displacement over the soil depth. For example, comparing the case of NC 2.5 400 and C 2.5-400 reveals that under the surface pressure of 400 kPa at H=2.5D, stabilization reduces pipe deformation significantly. At soil surface when z=0, soil displacements are 5.5 mm and 2 mm for non-cement treated and cement treated samples. At z=1D soil displacements drop to 2.5 and 1.1 mm for non-cement treated and cement-treated samples, respectively. However, displacement of non-treated case for all depths is still higher. These results reveal that stabilization not only improves soil displacement on the soil surface but also reduces soil displacement along its depth.

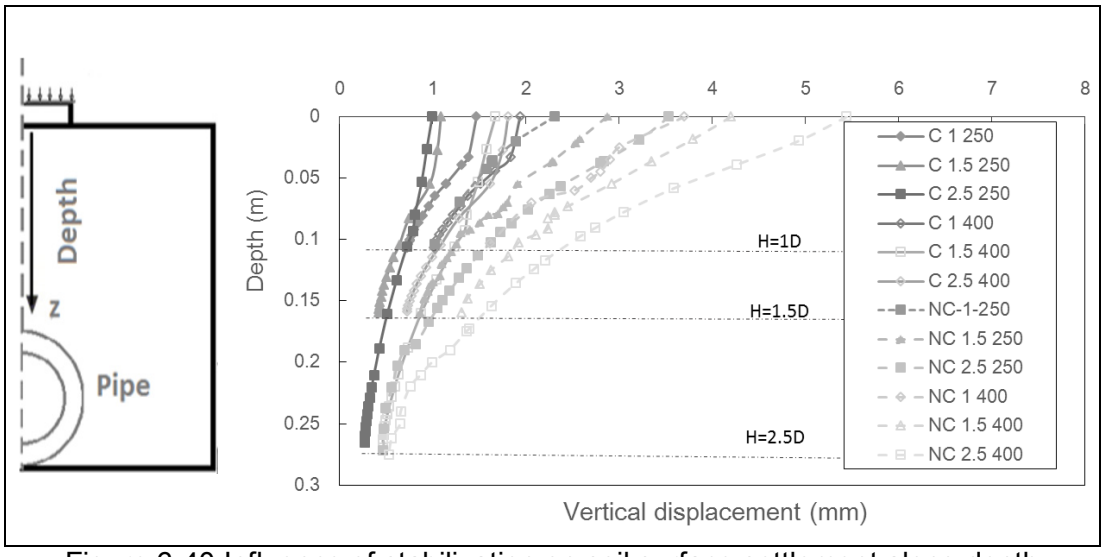

Figure 6-40 Influence of stabilization on soil surface settlement along depth

6.3.4.3 Stress distribution variation

Vertical stress distribution under centre of loaded area is shown in Figure 6-41. Overall, stabilization slightly reduces vertical stress distribution transferred to the pipe. In addition, stabilization provides stiffer layer which makes higher vertical stress in the cemented layer in the stronger layer of cemented material. However, stabilization reduces earth pressure on pipe causing lower earth pressures for pipe in cement-treated trenches.

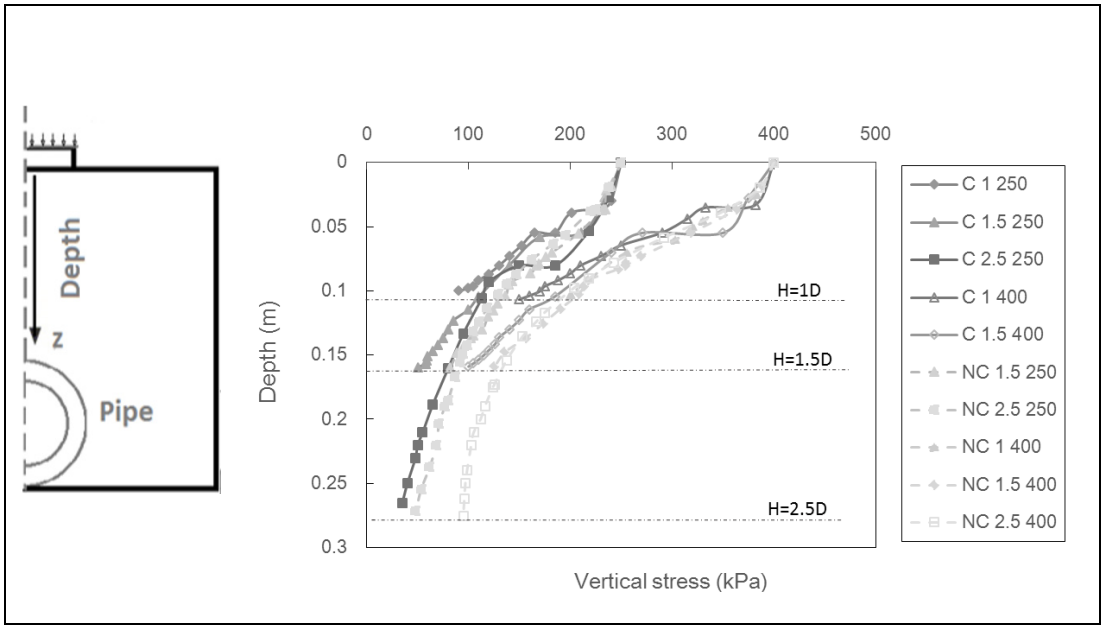

Figure 6-41 Impact of stabilization on stress distribution underneath the loaded area

These results are consistent with the results of earth pressure on pipe circumference illustrated in Figure 6-42, where horizontal axis represents the angle

from pipe crown and vertical axis represents earth pressure. Overall, stabilization reduces earth pressure on pipe circumference for all samples. For example, under surface pressure of 400 kPa at H=1D, maximum earth pressure for non-treated soil is 110 kPa and this value at pipe crown is 85 kPa. After stabilization for the same condition maximum earth pressure drops to 70 kPa starting from 60 kPa at pipe crown showing the impact of stabilization on reducing earth pressure on the pipe circumference. As explained earlier, the earth pressure variation is more significant on pipe crown compared to pipe invert for all cases. In addition, maximum earth pressure is not happening at pipe crown but at an angle between 60 and 90 degree.

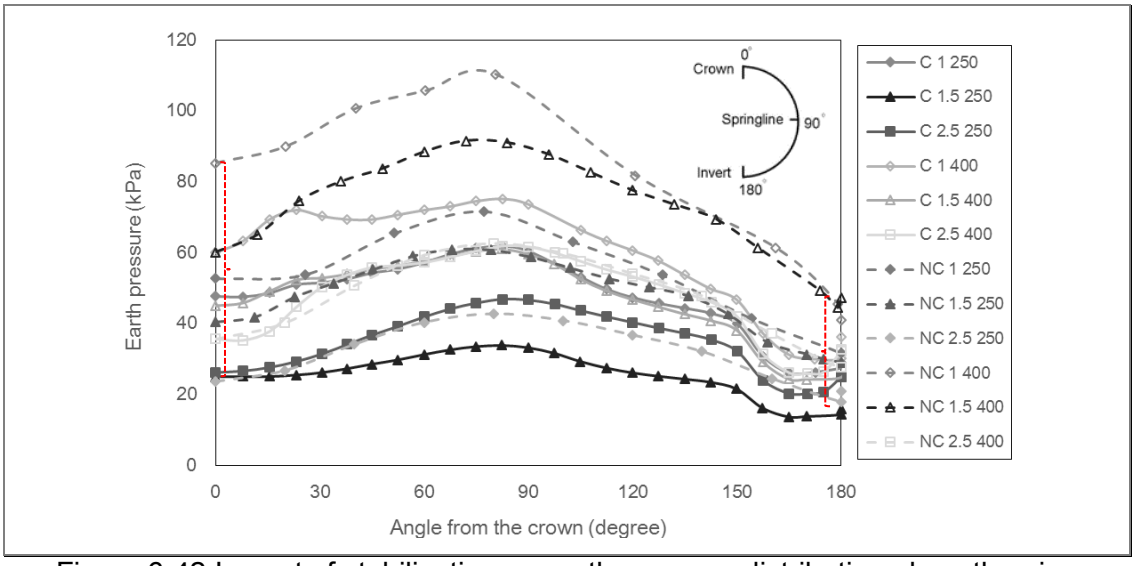

Figure 6-42 Impact of stabilization on earth pressure distribution along the pipe circumference

6.3.4.4 Pipe deformation mode

The results of finite element simulations for pipe deformations in both vertical and horizontal directions are shown in Figure 6-43-a and b. Results are for the case of H=1D under surface pressure of 400 kPa for non-treated trench material only. It can be seen that the pipe vertical displacement is maximum at pipe crown and pipe horizontal displacement is maximum at pipe springline. Higher displacement occurs in vertical direction compared to horizontal and pipe tends to deform to the elitipical shape as shown in the figure. For example, the maximum displacements at pipe crown are 1.2 mm and 0.46 mm in vertical and horizontal directions, respectively. To investigate the mode of pipe deformation, the ratio of vertical to horiozntal displacement for all samples are calculated and results are illustrated in Figure 6-43-c. Horizontal axis represents test number and vertical axis represents the ratio of maximum vertical to maximum horizontal displacements. It can be seen that measured displacement at pipe crown is always higher compared to horizontal displacement as the ratio is bigger than 1. In addition, non-treated samples have higher ratio of vertical to horiozntal displacement which indicates elliptical deformation is more likely to occur in non-treated samples.

The bending strains may also be considered as a performance criterion in pipeline design. Bending strain considerations are based on the pipe deformation into an elliptical shape due to ring deflection. Bending strain variations were calculated for non-cement treated case and results are shown in Figure 6-44. The pipe-strain plots transitioned from positive value at the crown to negative at the side, and back to the positive value at the invert. It shows very similar peaks of large strain at the 60° position and low strains from 120^{o} to pipe invert. It can be seen that maximum strain happens for minimum burial depth of H=1D and under maximum surface pressure of 400 kPa showing both surface pressure and burial depth have impact on strain variations. These results also reveal that another important section on pipe circumference rather than pipe crown is the area around a point 60^{o} from pipe crown.

Distribution of strains induced due to live load in the pipe wall can be illustrated on pipe section as shown in Figure 6-44. It can be seen that, at a given burial depth, higher deformations occur on both vertical and horizontal direction under higher surface pressures. This causes horizontal stretching and the pipe tends to deform to the ‘heart shape under higher surface pressure. However, after stabilization, lower strain occurs in the pipe and its deformation is flatter as shown in the figure.

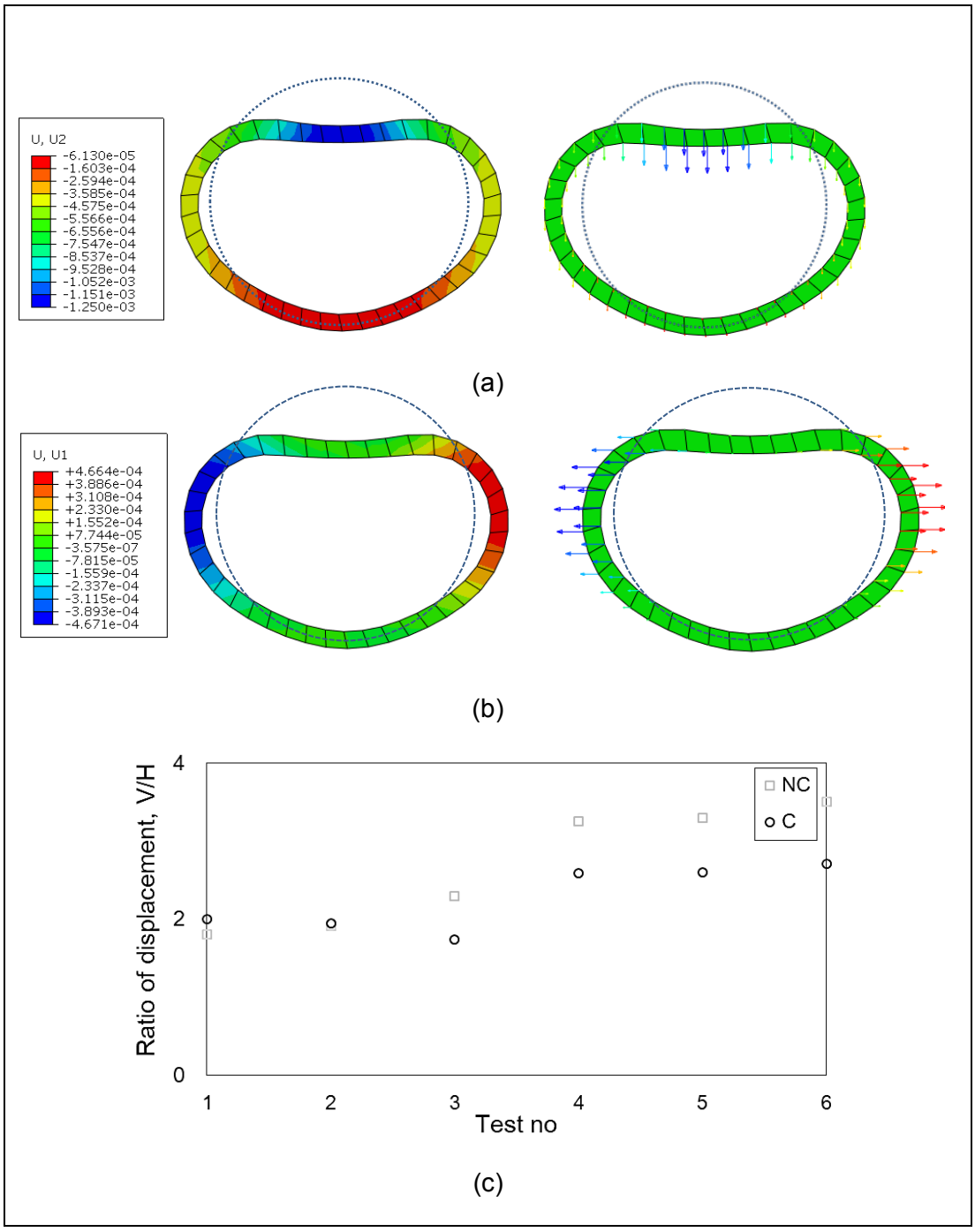

Figure 6-43 Pipe deformation mode in (a) vertical direction(b) horizontal direction (c)ratio of vertical to horizontal displacements for all tests

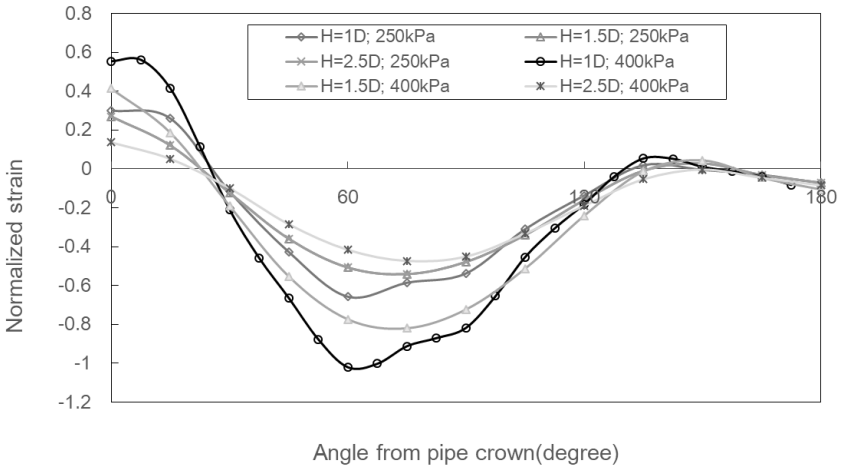

Bending strain as function of circumferential position- non-treated case

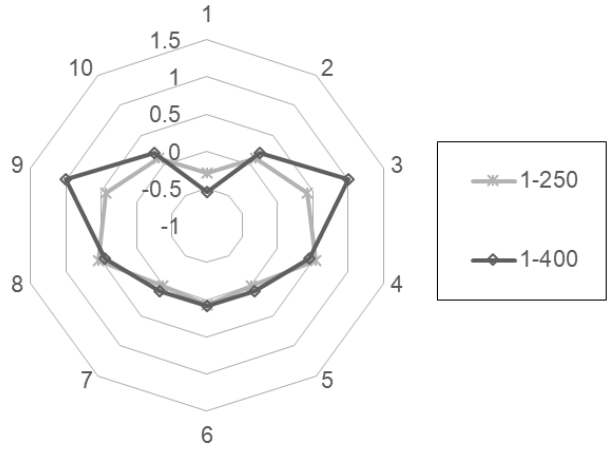

Impact of surface pressure on pipe deformation; non-treated case

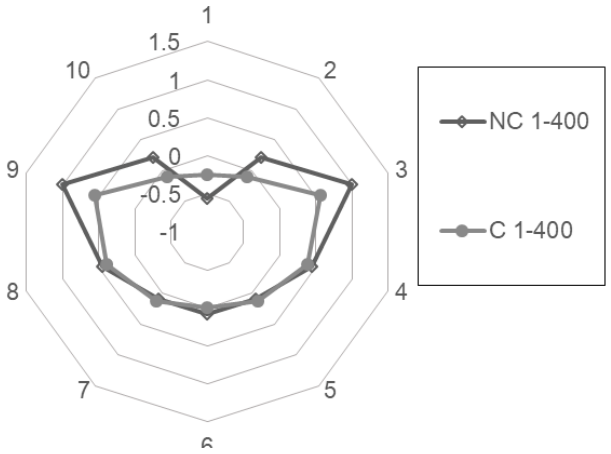

Impact of stabilization on pipe deformation; cement treated and non-treated cases

Figure 6-44 Pipe deformation different conditions

6.4 SUMMARY OF CHAPTER

The performance of a buried pipe due to traffic load was investigated through laboratory tests conducted at Curtin University. Numerical model was also developed as part of this research to study the impact of different factors on model response. Impact of stabilization for both experimental and numerical simulations were investigated and results were presented in this chapter. This chapter was presented in three subsections starting with introduction. In the second section, experimental test results were presented. These results were categorised in accordance with types of applying load and test results were presented for both static and cyclic phases. Ultimate bearing capacity of soil under loading plate was also investigated. Then, in the third section numerical simulation results were presented. Before presenting numerical simulations results, finite element model was validated by considering two aspects including vertical stress on pipe and soil surface settlement.

Some of the key findings from experimental data are as below:

- The results from experimental investigation indicated that the ultimate loading capacity of footing was almost 570 kPa for both analyses. Footing ultimate loading capacity dropped from 570 kPa for dense sand to less than 120 kPa for loose material. This means that it is not possible to apply the load of 250 and 400 kPa on the footing on loose material as it fails at 120 kPa before reaching 250 kPa. Therefore, in this research only traffic load was applied on dense sand not loose sand.
- Cement stabilization increased bearing capacity of soil. Ultimate bearing capacity of footing increased from 600 kPa to almost 1100 kPa while its displacement decreases significantly. Reducing footing displacement at specific stress level is an important aim of stabilization besides increasing its bearing capacity.
- The results from initial phase revealed that pipe burial depth and surface pressure have significant impact on the performance of model. In addition, results revealed that stabilization not only reduces pipe deflection but also reduces soil surface settlement and pressure on pipe.
- Cyclic tests was also performed to investigate the impact of cyclic load on the performance of pipe and soil. Results for non-treated trench material revealed that pipe deflection, soil surface settlement and pressure on pipe were affected by change in burial depth, surface pressure and number of cycles. Results showed that for all cases, maximum VDS and pressure on pipe decreases when H/D

increases while SSS increases when H/D increases. Both pipe vertical deflection and surface settlement were significantly affected by number of cycles while no significant difference was observed in on changes of stress on pipe crown with regard to number of cycles was observed.

- It was also observed that variation of VDS is more significant for shallower burial depths while SSS variation for all cases is almost the same. It means pipe plastic deformation is more significant under shallower burial depths and higher surface pressure while plastic deformation of soil surface is almost the same for different tests.
- Hysteresis graphs show that with increasing number of cycles, hysteresis loops for Load-VDS graphs get closer while Load-SSS graphs move to the right which means soil surface settlement still increases even after large number of cycles while VDS does not.
- Modes of pipe deformation were also investigated based on the results from strain gauges attached to different points of pipe circumference. Results revealed that pipe has higher deformation when it is buried in non-treated trench material and the deformation is maximum under higher surface pressure and minimum burial depths. Pipe tends to deform to a heart shape under shallower burial depths while it almost remains unchanged at deeper burial depths.

Some of key findings from numerical simulations are as below:

- The validation of finite element model was performed considering two aspects including vertical pressure on pipe and surface settlement. Results showed that the computed results based on finite element simulations matched well with the measured results in the laboratory and those achieved based on the empirical equation.
- Numerical simulations results revealed that stabilizing the trench material has an important effect on improving soil bearing capacity and reducing footing displacement. Results of plastic shear strains measurements also revealed that at failure point higher plastic shear strains are observed over a bigger area for non-treated trench material. Good agreement between numerical and experimental test results was observed for both test series.
- The numerical simulation of pipe displacement was carried out for both non-treated and cement-treated cases. Results revealed that vertical and horizontal displacements are maximum at pipe crown and springline, respectively. In

addition, vertical displacement variations along pipe circumference showed that all graphs have almost the same pattern with maximum value at pipe crown and are converging to zero on the bottom of the pipe. Both burial depth and surface pressure affect pipe deflection. Pipe deformation decreases when burial depth increases.

- The numerical simulation of soil surface settlement for both non-treated and cement-treated cases was carried out. Results revealed that maximum settlement for all cases occurs on soil surface above the pipe crown. In addition, regardless of burial depth, the soil surface settlement decreases by moving away from the centre of loading. Soil settlement converges to the minimum value over 2B distance from centre or two times the width of the loading area. Both burial depth and surface pressure affect soil surface settlement. Soil settlement increases when burial depth increases. Results of vertical displacement along the soil depth also revealed that soil displacement decreases significantly when soil depth increases.
- The increase in vertical stress under the centre of loading area as a function of depth for all cases was investigated. Results showed that all diagrams have almost the same pattern and stress decreases in a very similar manner when burial depth increases.
- Results of pressure distribution on pipe circumference also showed that three different sections exist and earth pressure is maximum in the middle part around 60 degree from the crown.
- Results revealed that cement stabilization of soil reduces pipe deflection, soil surface settlement and pressure on pipe significantly.
- Bending strain variations at pipe wall were also investigated showing pipe-strain plots transitioned from positive value at the crown to negative at the side, and back to the positive at the invert. Distribution of strains reveals that at a given burial depth higher deformations occur on both vertical and horizontal directions under higher surface pressures causing horizontal stretching where the pipe tends to deform to a ‘heart shape under higher surface pressure. However, after stabilization, lower deformations occur in the pipe.
- As illustrated numerical simulation has the capability to better explain the model performance under traffic load at different conditions. The soil surface settlement, pipe deflection and pressure measurement on the pipe also provide an independent a set of data which would assist in validation of numerical models and to understand model behaviour.

- The numerical simulation results agreed well with the experimental data within an acceptable accuracy. Although the numerical results did not fit fully with the experimental results, the results are in good agreement. Any discrepancy may be related to the chosen model for soil and foundation parameters, and differences between the boundary conditions in the numerical and experimental models.

In the next chapter, the results from experimental and numerical analysis for both static and cyclic tests will be presented. Equations will also be developed to investigate the relationship between burial depth, surface pressure on pipe and soil performance.

7 ANALYSIS AND DISCUSSION

Some parts of this chapter were published as journal paper as below:

Mosadegh. A; Nikraz.H , BURIED PIPE RESPONSE SUBJECTED TO TRAFFIC LOAD EXPERIMENTAL AND NUMERICAL INVESTIGATIONS, International Journal of GEOMATE, Nov., 2017, Vol.13, Issue 39, pp.01-08, ISSN:2186-2990, Japan, DOI: https://doi.org/10.21660/2017.39.91957

7.1 INTRODUCTION

In the previous chapter the results of experimental and numerical analysis of buried pipe were presented. This chapter reviews test results from previous chapter with focus on analysing the impact of different factors, i.e.: stabilization and initial phase impact on model performance. The summary of chapter is presented in Table 7-1 listing objectives, methods and the relevant section in the chapter.

After introduction, the impact of various factors on model response during initial phase and cyclic phase is investigated. Then, the influence of stabilization on bearing capacity and model response is discussed. In order to assess the impact of adding cement on model behaviour, stabilization ratio is calculated and presented in the form of non-treated to cement-treated ratio. This section will be followed by investigating on the impact of first cycle on model response. At the end of the chapter equations will be developed using regression analysis and neural network to predict model response.

Table 7-1 Chapter overview

Objective	Phase	Methods and considerations	Section
Analysing impact of various factors	Initial phase	SSS_0,VDS_0 and σ_0	7.2
		SSS_N,VDS_N and σ_N	
	Cyclic phase		
Analysing impact of stabilization	Bearing capacity	Quantifying impact of stabilization	7.3
	Initial phase		
	Cyclic phase		
Considering impact of first cycle	Calculating the ratio of I_0/I_N	Both non-treated and cement-treated soils	7.4
Predicting the model response	Initial phase	Regression method	7.5
	Cyclic phase	Regression method	
		Neural Network method	

7.2 IMPACT OF BURIAL DEPTH AND SURFACE PRESSURE ON MODEL RESPONSE

In this section, the impact of various factors on model response during initial and cyclic phase is investigated. The impact of burial depth, surface pressure and number of cycles on VDS, SSS and σ is discussed. Initial and cyclic phase will be presented in two separate sections.

7.2.1 Initial Phase

In the initial phase analysis, the results obtained from experimental tests and numerical simulations are compared and the impacts of burial depth and surface pressure on VDS, SSS and σ v are discussed. For each case the maximum values extracted from test results and numerical simulations presented in Chapter 6 are provided in Table 7-2. This table compares results of experimental tests and numerical simulations for non-treated tests only. Columns two and three from left represent different conditions of laboratory tests or numerical simulations. Maximum VDS, SSS and σ at the end of first cycle are compared with those calculated using numerical simulations and presented in columns four to nine. It can be seen that there is a good agreement between numerical and experimental test results. Results also reveal that accuracy of the two methods showing the reliability of data which will be used in the next sections to predict model response.

Table 7-2 Initial phase numerical and experimental results

Test No	Surface pressure	H/D	VDS (%)		SSS(mm)		σ (kPa)	
			Exp.	Num.	Exp.	Num.	Exp.	Num.
1	250	1	1.4	1.38	2.32	2.3	128	120
2	250	1.5	1.09	1.11	2.99	2.89	90	85
3	250	2.5	0.32	0.36	3.59	3.56	55	55
4	400	1	1.86	1.8	3.65	3.6	225	225
5	400	1.5	1.62	1.7	4.3	4.24	128	130
6	400	2.5	0.95	1.04	5.9	5.45	78	80

Figures 7-1 a to c are prepared in order to visualize the impact of the factors discussed earlier during initial phase. Overall, there is a good agreement between

findings from experimental tests and numerical simulations.

The impact of surface pressure and burial depth on pipe deflection is illustrated in Figure 7-1-a. It can be seen that for all graphs increasing burial depth reduces VDS and maximum VDS occurs when burial depth is minimum. Variation of load pressure has a significant impact on change of VDS and increasing surface pressure increases VDS significantly. For example, increasing pressure from 250 to 400 kPa increases VDS from 1.2% to 2.5% at H/D=1. These results confirm previous findings in the literature (Moghaddas Tafreshi & Khalaj, 2008).

The influence of burial depth and surface pressure on soil surface settlement of the model is illustrated in Figure 7-1-b. As shown, for a given surface pressure SSS increases when burial depth increases. For example under surface pressure of 400 kPa at H/D=1, SSS is 3.05 mm and increasing burial depth from H/D=1 to 1.5 and 2.5, increases SSS from 3.05 to 5.1 and 6.8 mm, respectively. This is due to thicker soil layer above the pipe causing soil to settle more when burial depth increases. In addition, the gap between two graphs for different surface pressures is higher for deeper burial depths meaning the impact of burial depth is more significant for deeper pipes. These results are consistent with the results presented in the literature (Moghaddas Tafreshi & Khalaj, 2008).

Figure 7-1-c shows the impact of change in burial depth and surface pressure on stress transmitted to the pipe crown obtained through experimental and numerical analysis. As illustrated, results from two methods follow the same pattern and increasing burial depth leads to decrease in pressure on pipe crown. In addition, increasing surface pressure increases stress on the pipe as expected. The gap between two graphs for different surface pressures is smaller for deeper burial depths meaning the impact of surface pressure is more significant for shallower pipes compared to deeper ones. These results are consistent with results presented in the literature

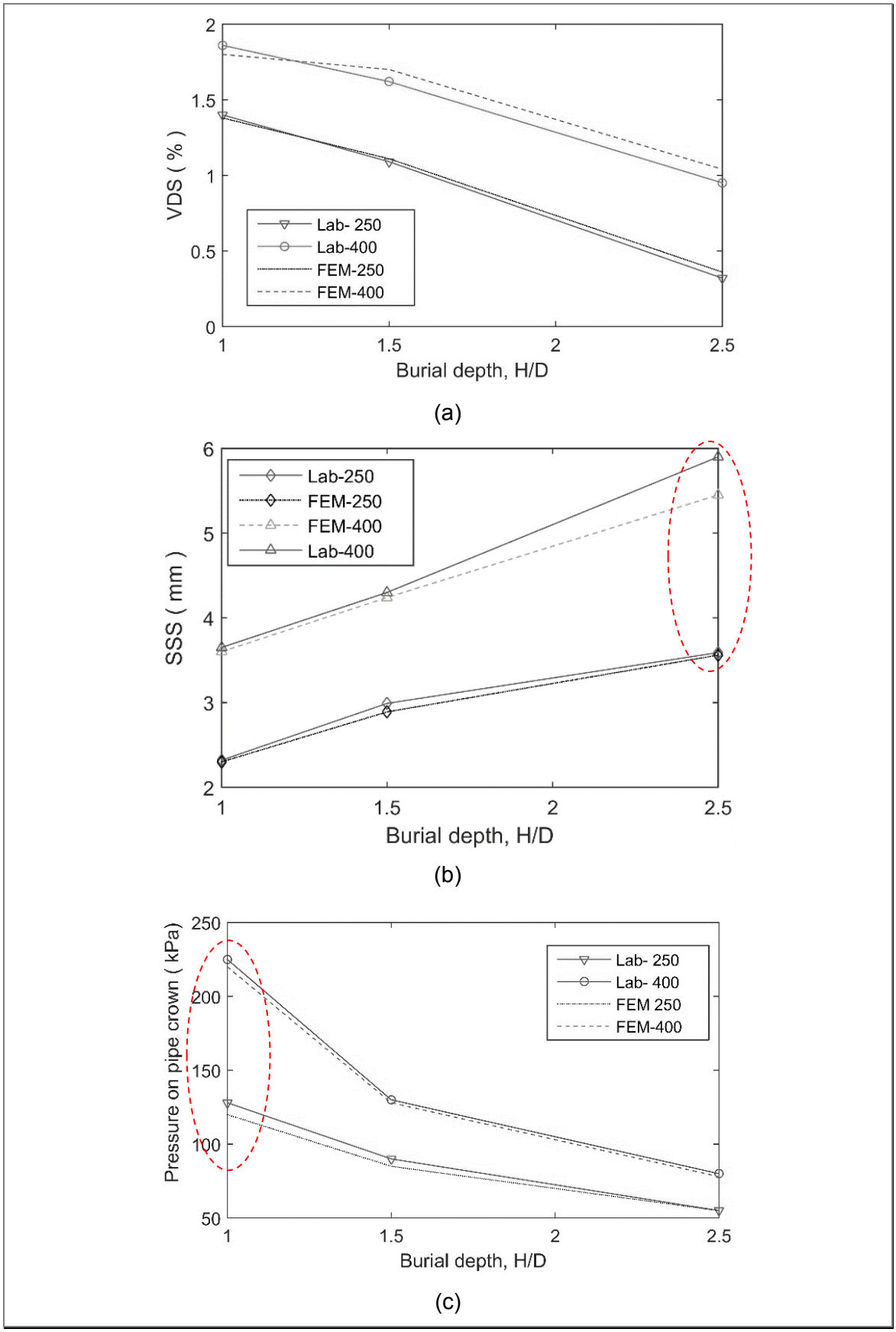

Figure 7-1 (a) Variation of the maximum VDS of pipe (b) Soil surface settlement (c) earth pressure on pipe crown

7.2.2 Cyclic Phase

The results of experimental tests for different surface pressures and burial depths were presented in the previous chapter. The relation between VDS and burial depth, surface pressure and number of cycles is discussed in this section.

Figure 7-2 illustrates the variation of VDS during first 500 cycles for all non-treated and cement-treated samples. Horizontal axis represents number of cycles and vertical axis represents VDS variations. In addition, abbreviations cited in figure legend are presenting stabilization condition, burial depth and applied surface pressure. Each symbol consists of three parts. For example, NC 2.5 400 denotes pipe in non-treated trench material with burial depth of H=2.5D under surface pressure of 400 kPa.

Overall, higher deflection is observed for non-treated samples which will be discussed in more details later in this chapter. In addition, increase in burial depth decreases pipe deflection and increase of surface pressure increases pipe deflection for all cases. Pipe deflection variation is also influenced by surface pressure and burial depth and higher values are observed under higher surface pressures and shallower burial depths.

For better understanding of the impact of various factors on pipe deflection, another graph is prepared and illustrated in Figure 7-3. This figure illustrates the impact of burial depth and surface pressure at three different cycles of 1, 100 and 500 on maximum pipe deflection. The figure only shows non-treated cases. Overall, with increasing burial depth, VDS decreases while increasing surface pressure increases VDS for all cases. For example, at 100^{th} cycle for non-treated soil, VDS decreases from 4.3% to 2.8% with increase of burial depth from H=1D to H=2.5D under surface pressure of 400 kPa. It means increase of burial depth leads to 37% reduction in VDS. Moreover, reduction of surface pressure from 400 to 250 kPa for cycle 100 at H=D, decreases VDS from 4.3% to 1.9% meaning 55% reduction in VDS of the pipe buried in sand. In addition, increase of number of cycles significantly affects VDS. For example, at H=1D increase of number of cycles from 1 to 100 increases VDS from 1.8% to 4.2% meaning 130% increase.

The results are in in good agreement with results presented in the literature (Moghaddas Tafreshi & Khalaj, 2008). In their research the impact of various parameters on a buried HDPE pipe with the D/t=27 has been investigated. They found that pipe vertical deflection was highly affected by both surface pressure and burial depth with higher values of deflection. It is also noted that the burial depth of H=1D was not considered in their research. The difference between findings of the two researches

could be due to different methods of compaction and different pipe geometry (Moghaddas Tafreshi & Khalaj, 2008).

As shown earlier, surface pressure and number of loading cycles lead to increase in VDS. In addition, burial depth has a significant impact on VDS. Thus equations can be developed to find a relationship between VDS and surface pressure, burial depth and number of cycles which will be discussed later in this chapter.

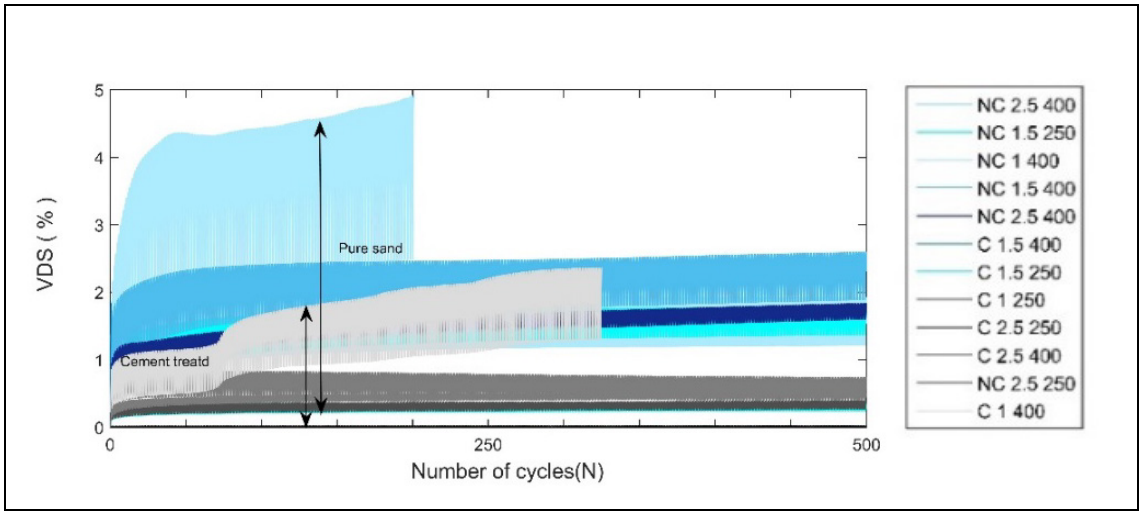

Figure 7-2 VDS versus number of cycles

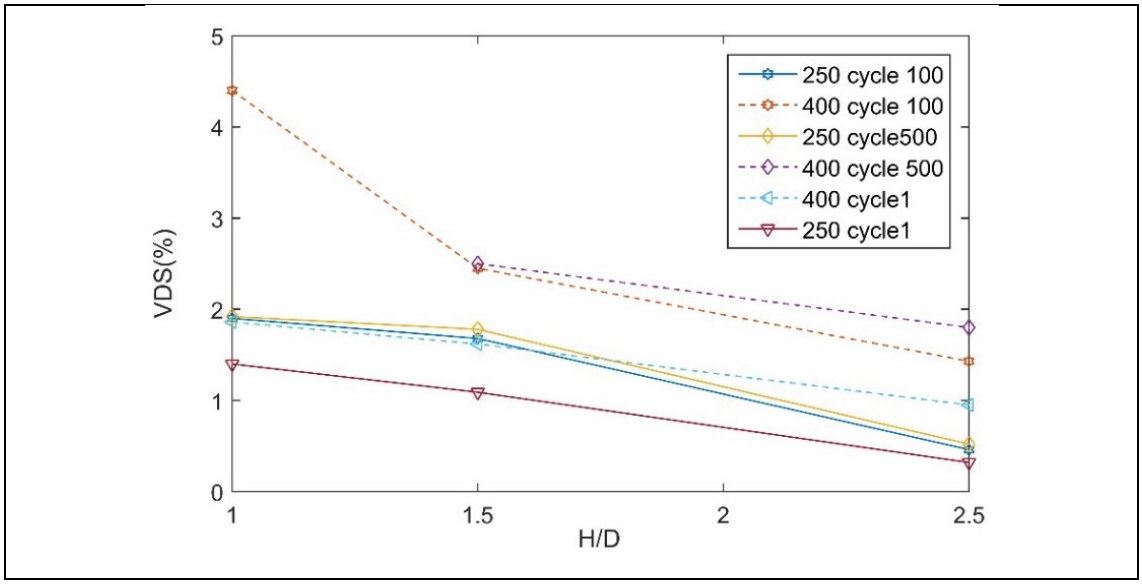

Figure 7-3 Maximum VDS versus burial depth at different surface pressures and loading cycles

The change of SSS for all cases during first 500 cycles are shown in Figure 7-4. Horizontal axis represents number of cycles and vertical axis represents SSS variations. Each test condition is illustrated in the figure. For example, NC 1 400 denotes pipe in non-treated trench material with burial depth of H=1D under surface pressure of 400 kPa.

Overall, higher surface settlement is observed for non-treated samples. The impact of soil stabilization will be discussed in more details later in this chapter. In addition, increase in burial depth and surface pressure, increases surface settlement. Another graph is prepared to assess the impact of burial depth and surface pressure which is illustrated in Figure 7-5. The impact of burial depth under three different number of cycles of 1, 100 and 500 on maximum soil surface settlement is investigated for non-treated cases only. Overall, with increasing burial depth soil surface settlement increases for majority of cases while increasing surface pressure increases SSS for all cases. As discussed in the previous chapter, this is due to compressibility of soil layer above pipe. The higher burial depth has the higher void ratio leading to higher surface settlement of soil. For example, at 100^{th} cycle soil settlement increases from 8.5 mm to 11.5 mm with increase of burial depth from H=1D to H=2.5D under surface pressure of 250 kPa. It means increase of burial depth leads to an increase of 30% in SSS. Moreover, increase of surface pressure from 250 to 400 kPa for the same burial depth increases SSS from 10 to 17 mm meaning 70% increase. Increase of number of cycles also significantly affects SSS. For example, at H=1D increasing of number of cycles from cycle 1 to cycle 100 increases the surface settlement from 3 mm to 22 mm or 600% increase in SSS. This means number of cycles has a significant impact on SSS.

Results are in in good agreement with the results presented in the literature (Moghaddas Tafreshi & Khalaj, 2008). In their research the impact of various parameters on a buried HDPE pipe with the D/t=27 was investigated. It was found that soil surface settlement was highly affected by both surface pressure and burial depth. The difference between findings of the two researches could be due to different methods and levels of compaction. It is noted the impact of cement stabilization was not taken into consideration in their research (Moghaddas Tafreshi & Khalaj, 2008).

It can be seen that increasing burial depth and surface pressure lead to increase in SSS. As shown previously the number of cycles has a significant impact on SSS. An equation can be developed to find a relationship between SSS and surface pressure, burial depth and number of cycles which will be discussed later in this chapter.

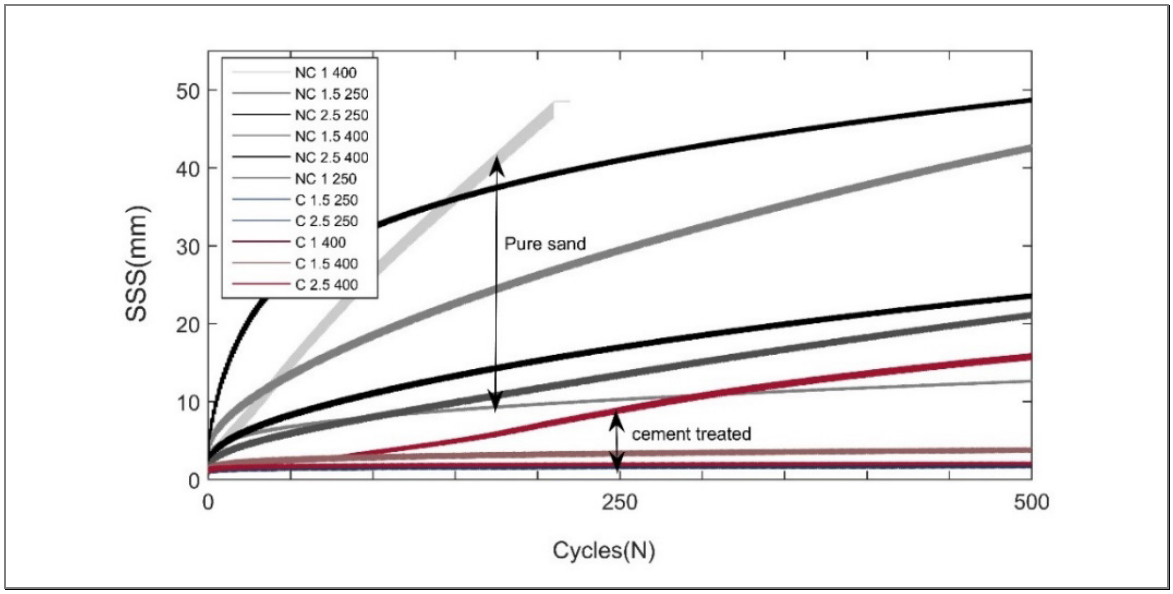

Figure 7-4 SSS variations versus number of loading cycles

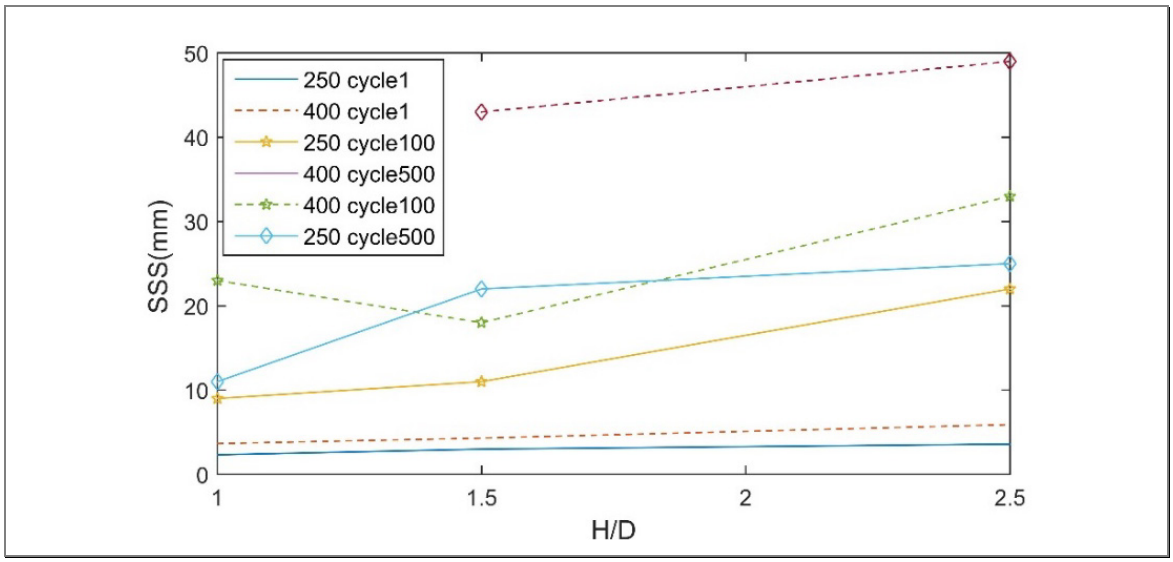

Figure 7-5 Maximum SSS versus burial depth at different surface pressure and cycles

Figure 7-6 compares the variation of pressure on pipe crown under various applied pressure and burial depths at cycle 1st and 100th. It can be seen that the transferred pressure on pipe decreases when burial depth increases. In addition, increasing surface pressure increases transferred pressure on pipe crown. It is also obvious that increasing number of cycles has a minor impact on change of pressure on pipe. The depth soil layer above the pipe is not significantly affected by number of cycles, therefore, pressure on the pipe is not significant affected by number of cycles. The results of this research showed that number of cycles have lower impact on stress on pipe compared to other two variables of burial depth and surface pressure. These results are consistent with the results obtained by Ko in 2010 (Ko & Kuwano, 2010). They have found in their research that stress on a buried pipe is affected by level of compaction for a given surface pressure and burial depth. For example, after few cycles of loading the average stress on a buried pipe remained unchanged in a medium compacted sand. The stress on pipe slightly increased for dense sand and slightly decreased for very loose sand.

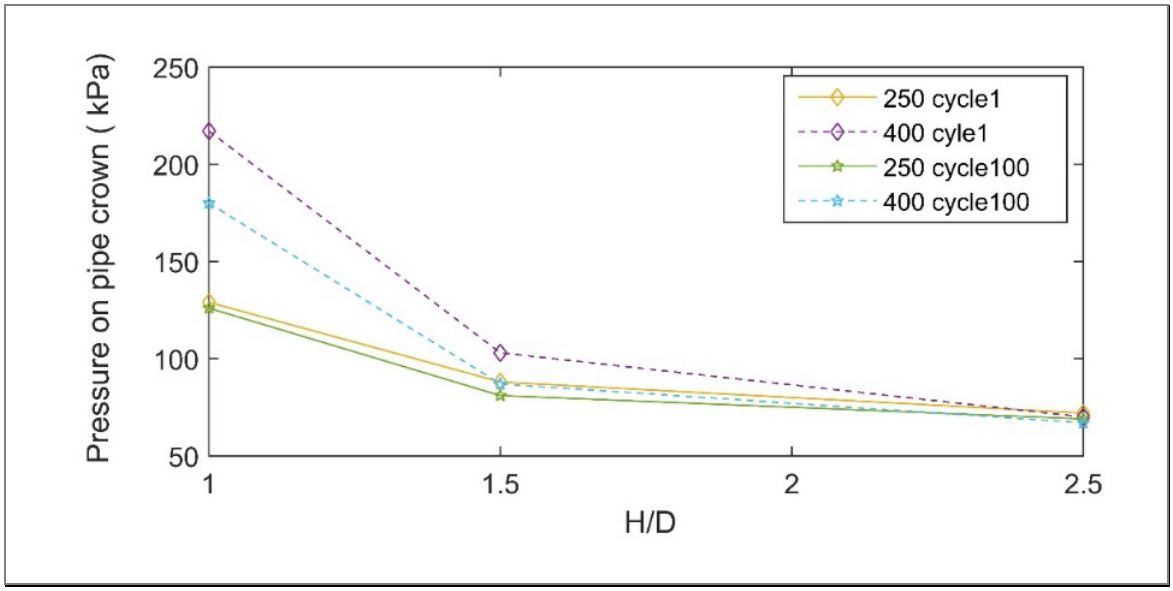

Figure 7-6 Maximum σ versus burial depth at different surface pressure and laoding cycles

The pipe deformation in horizontal direction is also investigated and results are discussed briefly in this section. Figure 7-7-a compares the variation of vertical to horizontal strain for cycle 1st and 100th for different test series. Overall, the ratio of SG1/SG2 is higher for non-treated sand as illustrated in Figure 7-7-a. The results also reveal that the ratio for non-treated soil varies between 1 and 6 which is higher compared to cement-treated tests. The results also show that variation of these ratios is higher during early cycles and then it remains steady, especially for cement-treated samples. Figure 7-7-b also illustrates the impact of burial depth on horizontal strain of pipe under different surface pressures at two cycles of 1 and 100. In general, pipe horizontal strain decreases when burial depth increases. Both surface pressure and number of loading cycles have significant impact on strain variations.

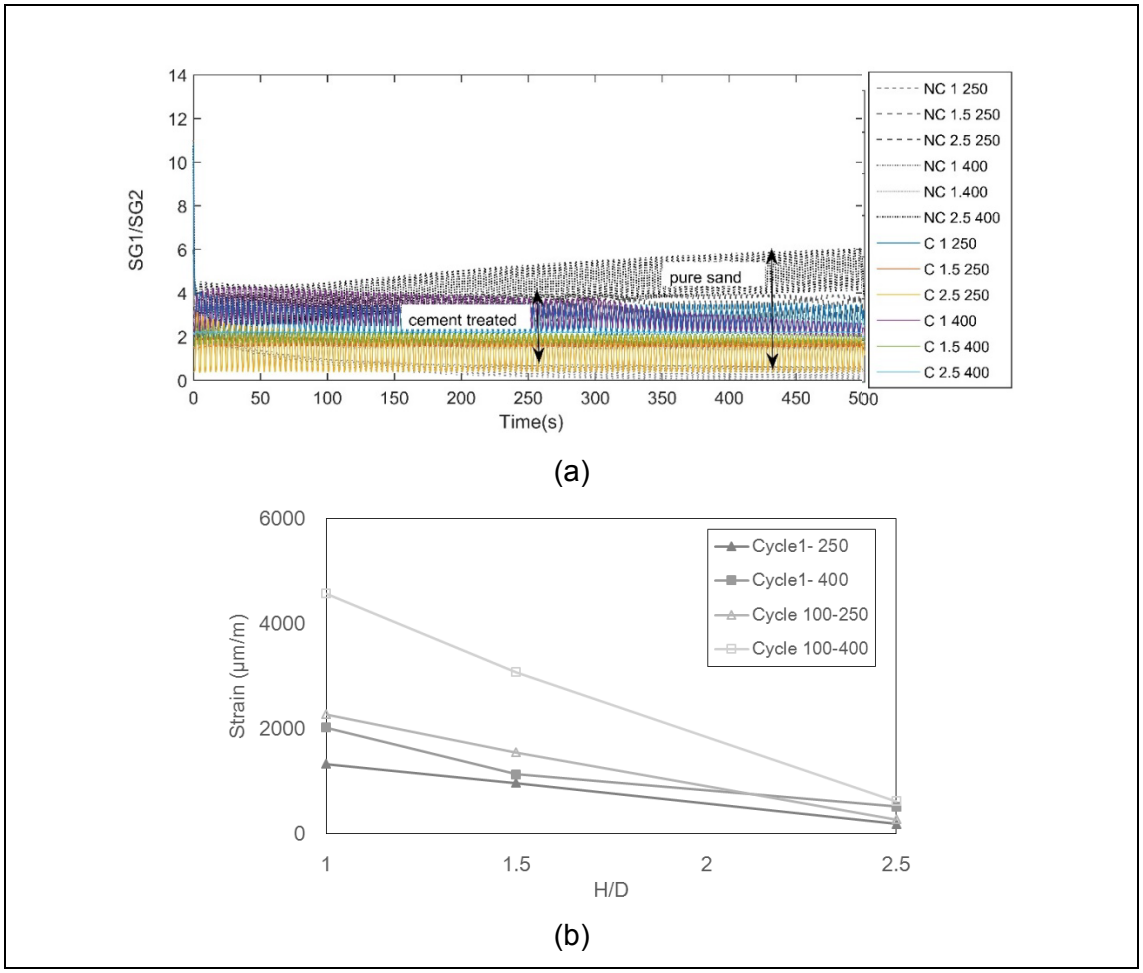

Figure 7-7 (a) Vertical to horizontal strain variation due to cyclic load (b) maximum horizontal strain versus burial depth at different surface pressure and loading cycles

7.3 IMPORTANCE OF SOIL STABILIZATION

To improve the strength properties of trench material and to increase the safety of embedded pipe, trench material was stabilized with cement and results were presented in the previous chapter. Results revealed that cement stabilization improves sand properties and reduces pipe deflection, surface settlement and pressure on the pipe. In the following section, the efficiency of adding cement to the soil on model response is investigated. The impact of stabilization on improvement of bearing capacity of trench material and model performance during initial and cyclic phases are discussed separately in this section.

7.3.1 Bearing capacity

The impact of stabilization on bearing capacity of loading plate is investigated and results are shown in Figure 7-8. The results show that adding cement can significantly improve the ultimate bearing capacity of soil and pipe deflection. Pipe deflection decreases from almost 6% to less than 1% after stabilization. In addition, bearing capacity of loading plate increases from 600 kPa to almost 1100 kPa.

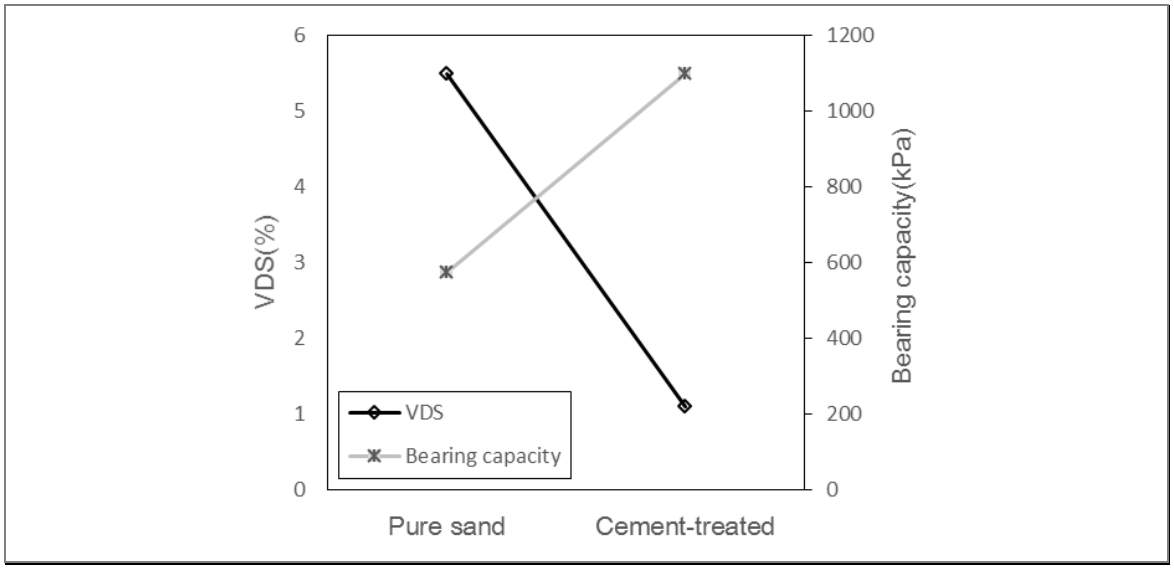

Figure 7-8 Impact of cement stabilization of sand

7.3.2 Initial Phase

The impact of stabilization during initial phase on model response is assessed and results are presented in this section. Table 7-3 compares the results of pipe deflection, surface settlement and pressure on pipe for non-treated and cement-treated material. Comparison of these results shows that stabilization improves model response for all cases. For example, at H=1D under surface pressure of 250 kPa, stabilization reduces

pipe deflection from 1.4% to 0.22%. In other words, the ratio of pipe deflection for cement-treated to pure sand is 0.19. It means stabilization reduces pipe deformation by 81% reduction in pipe deflection. For the same burial depth of H=1D under surface pressure of 250 kPa, soil surface settlement is 1.33 mm. This value for non-treated sand was 2.32 mm. It means stabilization improves soil surface settlement by 42%. Pressure on pipe crown is recorded as 110 kPa for case number one. This value is 128 kPa for pure sand meaning that due to stabilization lower pressure is transmitted to pipe crown by 15% reduction. Impact of stabilization on each parameter is shown visually in Figure 7-9. The results of all burial depths under surface pressures of 250 and 400 kPa are illustrated in Figure 7-9. Triangle and square marker represent non-treated and cross and circle represent cement-treated samples. Overall, stabilization improves model response for all cases with remarkable reduction in pipe deflection, soil settlement and stress on pipe.

Table 7-3 Comparison of model response for non-treated and cement-treated sands at different burial depth and surface pressure

Test No	Surface pressure (kPa)	H/D	VDS (%)		SSS(mm)		σ (kPa)	
			Pure sand	Cement-treated	Pure sand	Cement-treated	Pure sand	Cement-treated
1	250	1	1.4	0.22	2.32	1.33	128	90
2	250	1.5	1.09	0.24	2.99	1.2	90	50
3	250	2.5	0.32	0.03	3.59	1.62	55	30
4	400	1	1.86	1.125	3.65	1.45	225	180
5	400	1.5	1.62	0.8	4.3	1.8	128	75
6	400	2.5	0.95	0.27	5.9	1.75	78	60

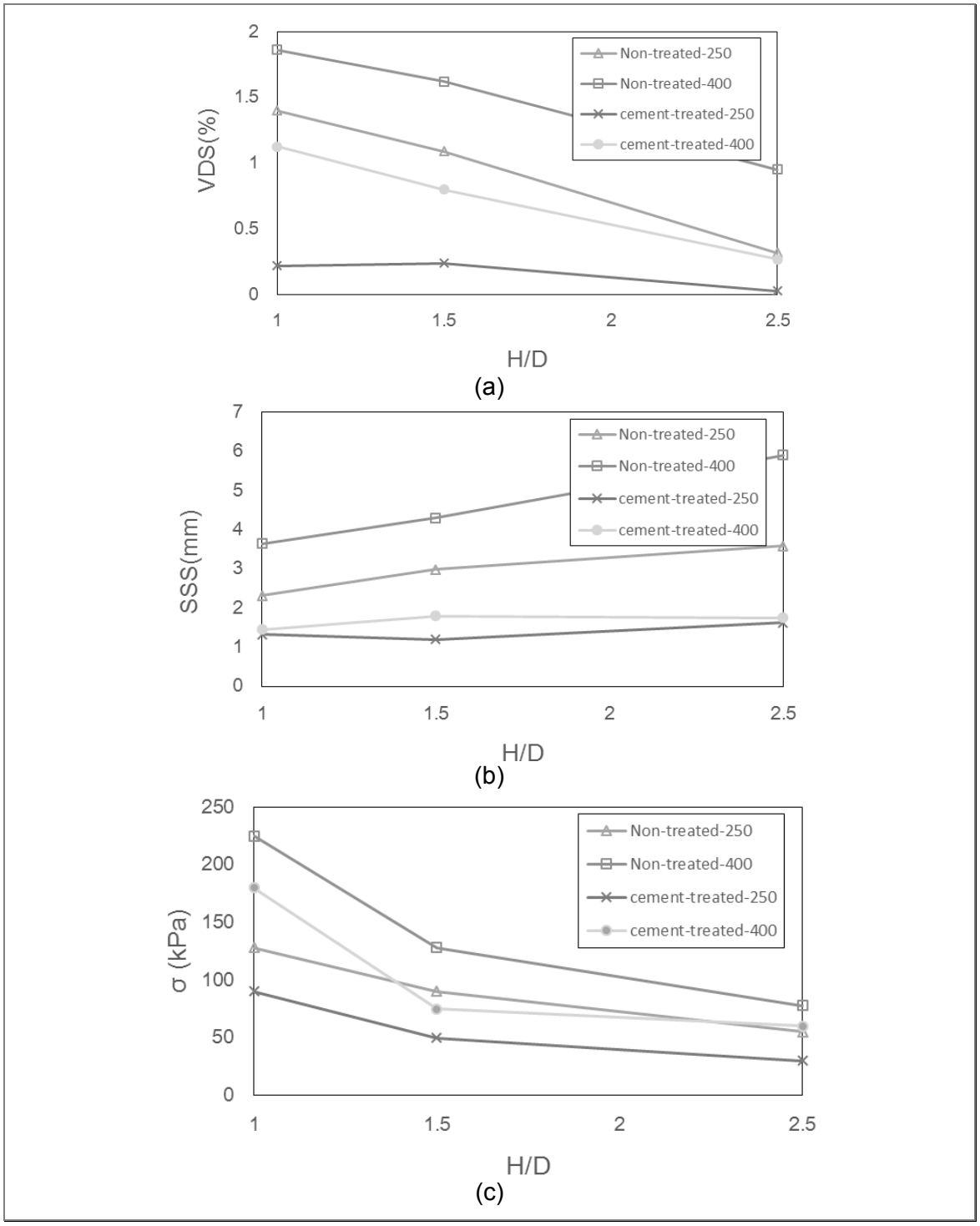

Figure 7-9 Impact of stabilization on model performance during initial phase (a) pipe deflection (b) surface settlement (c) pressure on pipe

7.3.3 Cyclic Phase

The impact of stabilization during cyclic phase on model response is also assessed and results are presented in this section. The solid line in the graphs represent pipe in pure sand and dashed lines represent pipe in cement-treated material.

Figure 7-10-a compares the maximum pipe vertical deflection under cyclic load for pipe buried in sand and cement-treated backfill material. Vertical axis represents maximum pipe deflection and horizontal axis represents number of examined data. It can be seen that for 3000 data and for all 12 cases, stabilization reduces pipe deflection. For example, for the first case burial depth of H=1D and 250 kPa, maximum VDS of pipe for non-treated and cement-treated cases are 2 and 0.3%, respectively. It means adding cement improves pipe performance and its maximum deflection drops to 80% of its original value. Stabilization affects VDS of pipe as illustrated earlier in Figure 7-2. The pipe deflection is also higher for pure sand than cement treated one. For example, the difference between maximum and minimum value of VDS at cycle 100^{th} for NC 1 400 and C 1 400 are 2.2% and 1%, respectively. This difference is more significant for deeper burial depth as shown in Figure 7-2. Moreover, for both cases of stabilized and pure sand, the pipe deflection variation for shallower burial depths is higher than those buried in deeper depths. Impact of stabilization on VDS v is illustrated in Figure 7-10-b. Horizontal axis represents VDS variations and vertical axis represents applied pressure. The figure compares vertical deflection of pipe for non-treated and cement-treated material under surface pressure of 400 kPa during the first 20 cycles. The hystersis graph shows after 20 cycles, the maximum pipe deflection for non-treated trench material and cement-treated are 0.45 and 0.31, repectively. Results also confirm VDS is higher for non-cemented material as illustrated in Figure 7-10-b and loops for cement treated materials get closer.

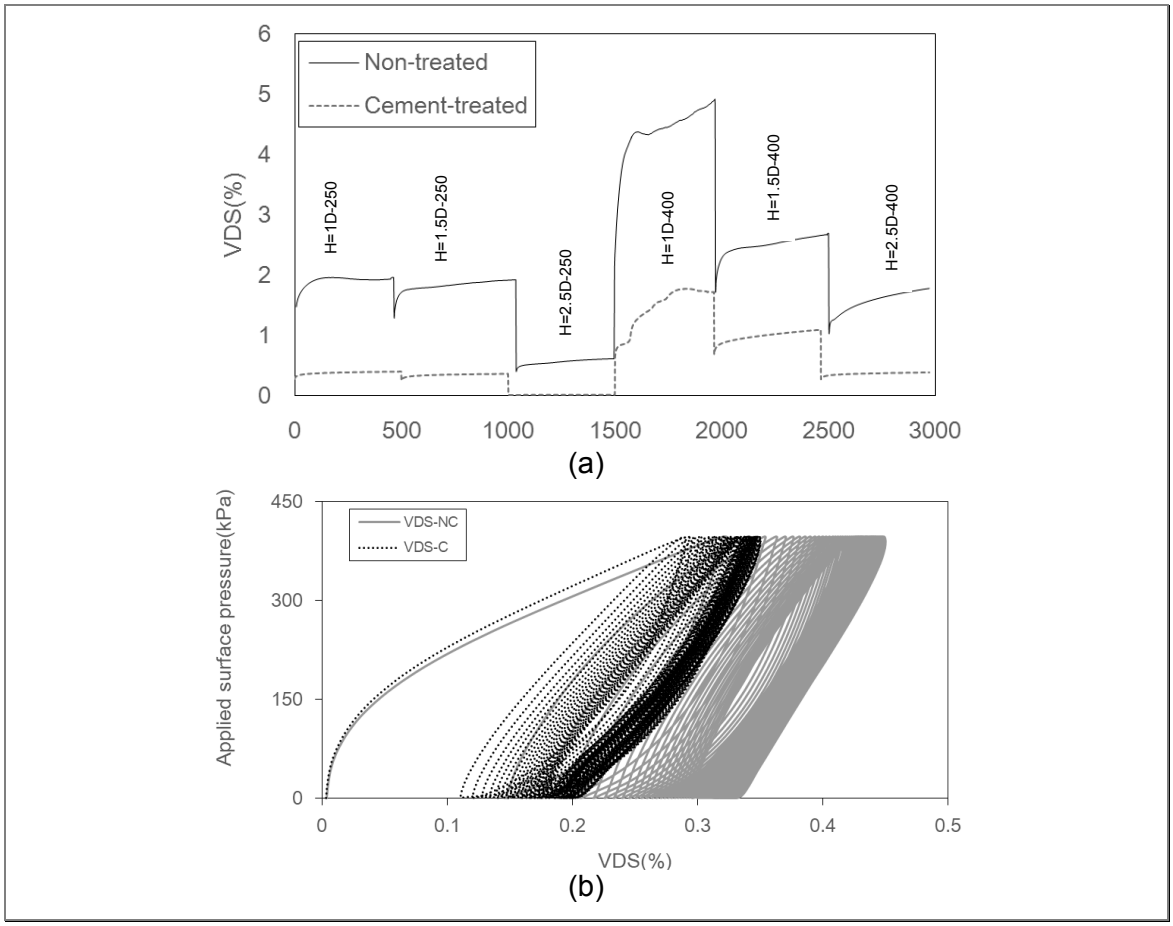

Figure 7-10 Pipe deflection comparison between cement-treated and non-treated material

Figure 7-11-a compares the maximum values of SSS under cyclic load for pipe buried in non-treated and cement-treated materials. Vertical axis represents maximum normalized surface settlement or SSS/H and horizontal axis represents number of examined data. It can be seen that stabilization reduces soil surface settlement significantly for all cases. For example, for the first case, burial depth of H=1D and 250 kPa, SSS/H of pure sand reaches to 0.22. After stabilization this value hardly reaches to 0.01 and it remains steady. It means adding cement reduces soil permanent deformation with 95% reduction in surface settlement. The impact of stabilization on SSS is illustrated in a hystersis graph for one case only, Figure 7-11-b. After 20 cycles, the surface settlement for non-treated trench material and cement-treated are 7.2 mm and 2.1 mm, repectively. Results also confirms that the impact of stabilization on SSS variation is more significant compared to VDS. The results of load-SSS paths are also reveal that SSS is higher for non-cemented material and loops get closer for cement-treated sand. Comparison of Figure 7-10-a and Figure 7-11-b shows that the rate of increasing surface settlement is higher compared to VDS.

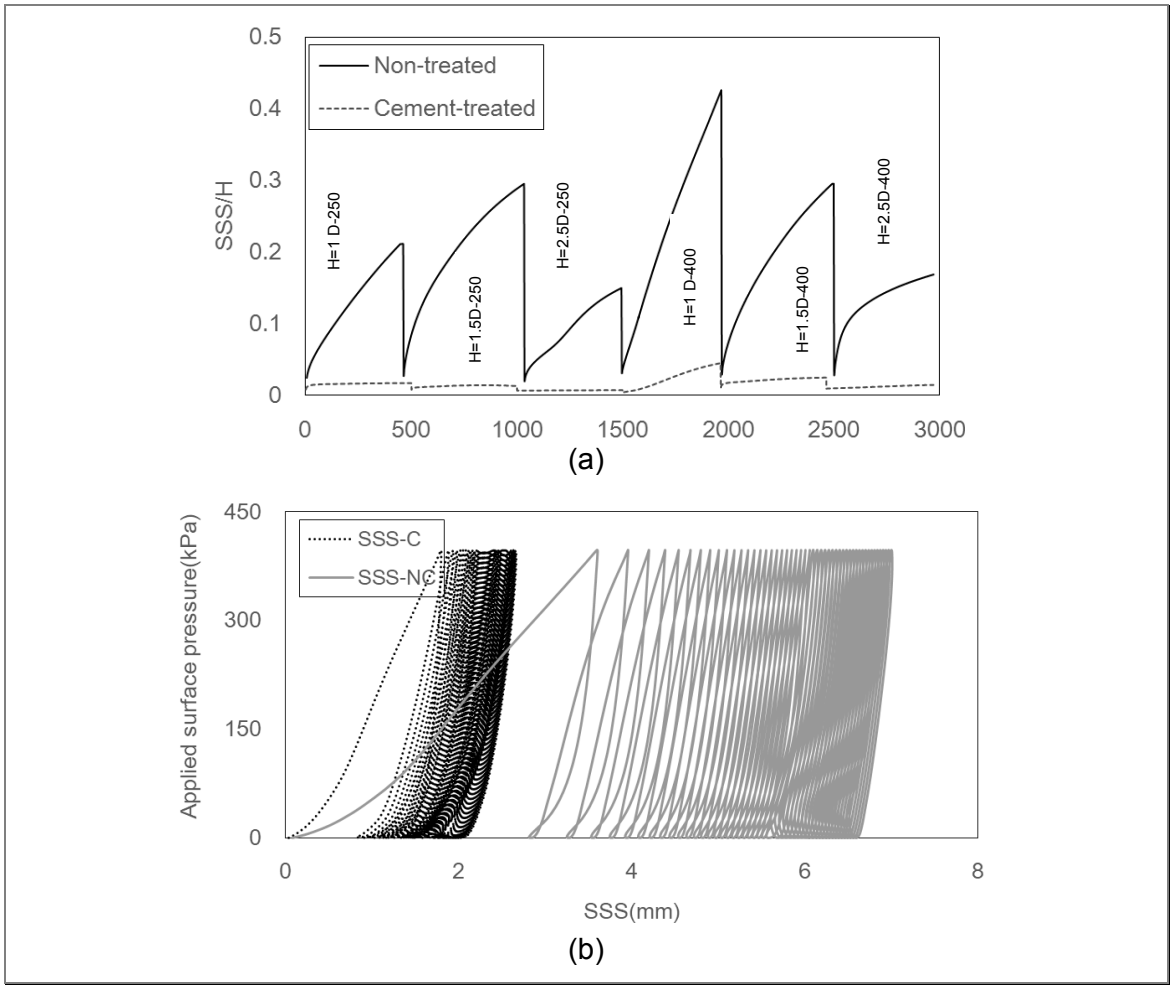

Figure 7-11 Comparison of soil surface settlement in stabilized and non-stabilized trench material

Figure 7-12-a compares the impact of stabilization on stress on pipe crown buried in pure sand and cement-treated backfill material. Vertical axis represents the ratio of maximum normalized stress at pipe crown to applied stress and horizontal axis represents number of examined data. It can be seen that stabilization reduces stress on pipe. For example, for burial depth of H=1D and surface pressure of 250 kPa, the ratio of transferred stress to applied stress for pure sand is more than 0.5. After stabilization this value is 0.32 and it remains steady. It means adding cement to soil reduces earth pressure on pipe and by 40%. Figure 7-12-b compares the stress variation under cyclic load for pipe buried in sand and cement-treated backfill material for only one case. Graphs in solid line represent pipe in pure sand, dashed line graphs represent pipe in cement-treated material and blue dashed line represents applied stress. Vertical axis represents stress and horizontal axis represents time. Stress on pipe for non-treated sand under 250 kPa applied stress is around 60 kPa. After stabilization this value drops to less than 35 kPa although these values fluctuate over time.

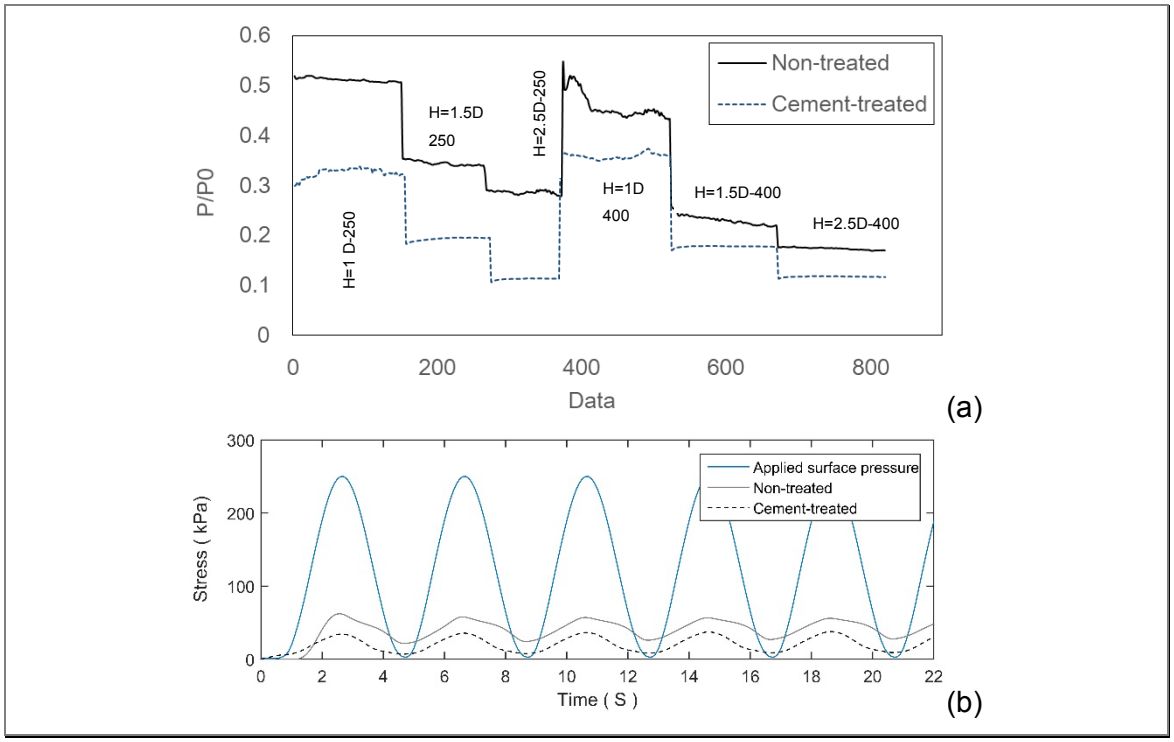

Figure 7-12 (a) Impact of stabilisation on stress on pipe (b) zoom lay out for case of H/D=2.5-250 kPa

Figure 7-13 compares horizontal strain of pipe under cyclic load for non-treated and cement-treated trench material. Vertical axis represents strain gauge readings at pipe springline and horizontal axis represents number of data. Overall, stabilization reduces strain at pipe springlie for all cases. For example, for burial depth of H=1D and 250 kPa surface pressure, horizontal strain gauge reading for pure sand reaches to 2500. After stabilization this value is 1000 and it remains almost steady. It means adding cement reduces horizontal strain of pipe by 60%.

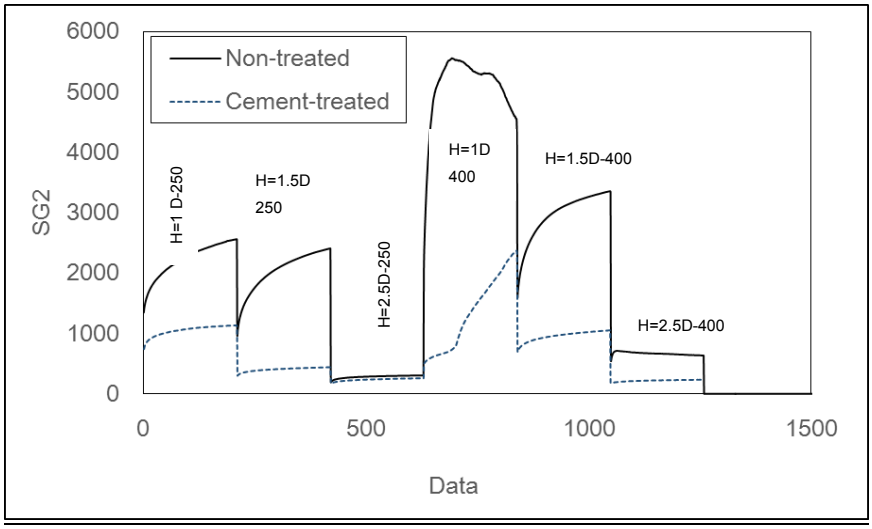

Figure 7-13 Impact of stabilisation on horizontal strain gauge

7.3.4 Quantifying the Impact of Stabilization

Results presented in the previous chapter and this chapter reveal that adding cement to the soil improves model performance. In order to assess the impact of adding cement on model behaviour, E_i value is determined as below:

$$E_i = X_c / X_p \qquad 7\text{-}1$$

In which X_c and X_p are related to the properties of cement-treated and untreated soil, respectively. E_i is calculated based on Equation 7-1 and results are presented in terms of $E_1 = VDS_C/VDS_{PS}$, $E_2 = SSS_c / SSS_{Ps}$, $E_3 = \sigma_C / \sigma_{PS}$ and $E_4 = SG2_c / SG2_{PS}$. The smaller the E_i value is, the more efficient is stabilization. For better understanding of the impact of stabilization, E_i is calculated separately during initial and cyclic phase. The results of initial phase are illustrated in Table 7-4. It can be seen that the ratio is less than 1 for all cases showing the efficiency of adding cement in model performance improvement. Considering E_1 or impact of adding cement on pipe deflection shows that stabilization reduces pipe deflection significantly and the ratio of pipe deflection for cement-treated over pure sand fluctuates between 0.09 and 0.65 meaning that stabilization can reduce pipe deflection up to 90%.

Table 7-4 Stabilization impact ratio during initial phase

Test No	Surface pressure	H/D	E_1	E_2	E_3	E_4
1	250	1	0.16	0.57	0.70	0.69
2	250	2	0.22	0.40	0.56	0.40
3	250	3	0.09	0.45	0.55	0.60
4	400	1	0.60	0.40	0.80	0.43
5	400	2	0.49	0.42	0.59	0.53
6	400	3	0.28	0.30	0.77	0.69

In order to assess the impact of adding cement on model behaviour during cyclic phase, E_i value is determined based on Equation 7-1 and results are presented in Figure 7-14. These values are calculated for cycle 1, 100^{th} and 500^{th}. It can be seen that the ratio is less than 1 for all cases showing the efficiency of adding cement in model performance. For example, VDS_C/VDS_{PS} fluctuates between 0.02 and 0.6 and SSS_C/SSS_{PS} varies between 0.05 and 0.6. It means stabilization reduces pipe deflection and soil permanent deformation for all cases.

However, comparison of E_i for cycle 1, 100 and 500 shows that it is lower at cycle 500. It means stabilization is more efficient in cyclic load than static load. For example, the ratio of SSS_C/SSS_{PS} for case 4 drops from 0.5 at cycle 1 to less than 0.1 at cycle 500th. It has been shown previously that SSS_C for cement treated cases remain steady and does not change under higher number of cycles. However, for non-treated sand SSS_{PS} increases when number of cycles increases. It means the rate of increasing SSS_c is less than SSS_{SP} and in Equation 7-1 the ratio becomes smaller as the numerator stays steady while the denominator becomes bigger. These ratios are calculated for pipe deflection, stress on pipe crown and readings of strain gauges at pipe springline as well. The results are illustrated in Figure 7-14-c and Figure 7-14-d. All ratios are less than 1 showing the efficiency of stabilization.

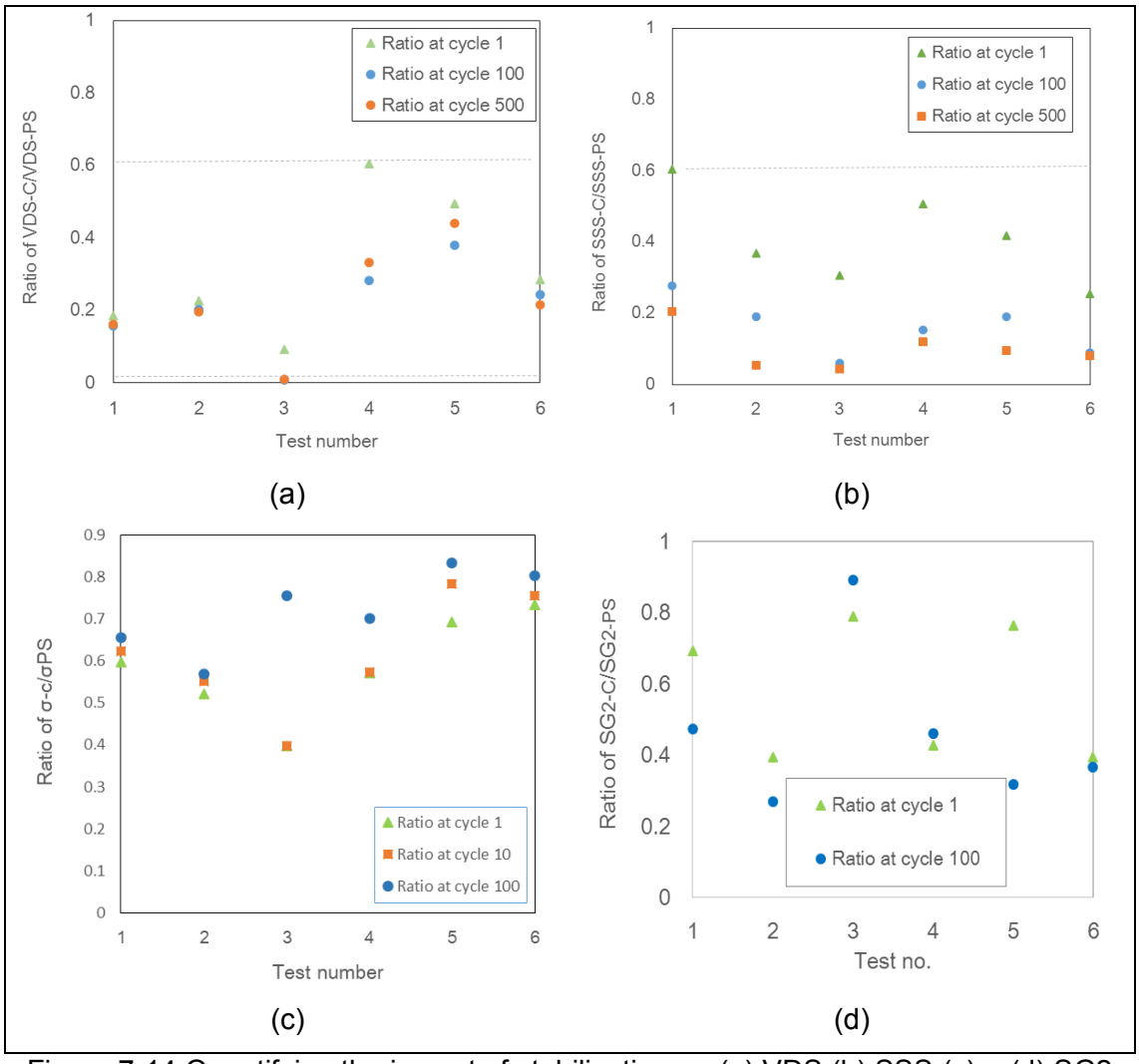

Figure 7-14 Quantifying the impact of stabilization on (a) VDS (b) SSS (c) σ (d) SG2

7.4 Importance of Initial Phase

As shown in previous sections, large portion of pipe deformation and soil surface settlement occurs at the end of first loading cycle. These values are significant compared to the total values after large number of cycles. Therefore, the impact of initial phase for both non-treated and cement-treated is calculated and results are presented in Figure 7-15-a-c. The horizontal axis represents test series number and vertical axis represents the ratio of I_0/I_N in which I represents VDS, SSS and SG. For example VDS_0/VDS_N represents the ratio of VDS_0 or pipe deflection at the end of first cycle to VDS_N which represents pipe deflection at cycle N. N is chosen to be 100^{th} and 500^{th}.

Overall, for both VDS and SSS, the ratio for cement treated materials is higher than those related to non-treated samples. For example, the ratio of soil surface settlement in first cycle to cycle N, varies between 0.05 and 0.35 for non-treated material. This value is higher for cement-treated material and varies between 0.25 and 0.75. It means for some cases only 5% of surface settlement occurs during first cycle for non-treated material. However, for cement treated cases minimum 25% of surface settlement occurs in the first cycle. This means the impact of cyclic load is more significant for non-stabilized sand compared to stabilized sand. In other words, rate of increasing surface settlement for pure sand is higher than those for non-stabilized sand. The ratio of I_0/I_N is smaller for non-treated sand as the numerator of I_N is bigger in the equation for non- due to higher soil surface settlement.

The same conclusions can be made for pipe deflection in both vertical and horizontal directions. The ratio of pipe vertical deflection in the first cycle to cycle N is higher for cement-treated material. High portion of model deformation occurs during first cycle for both cement-treated and non-treated cases. However, the impact of first cycle is more significant for cement-treated material.

The results achieved here are consistent with those achieved in the literature (Moghaddas Tafreshi & Khalaj, 2008). They also found that large portion of the pipe deformation and soil settlement occurs at the end of the first cycle. The ratio they found varied between 0.60 and 0.85. As mentioned earlier the level of compactions of their samples were lower than current research. In addition, the cyclic load impact was investigated at 100 cycles only. It should be noted that the impact of cement-stabilization was not considered in mentioned research.

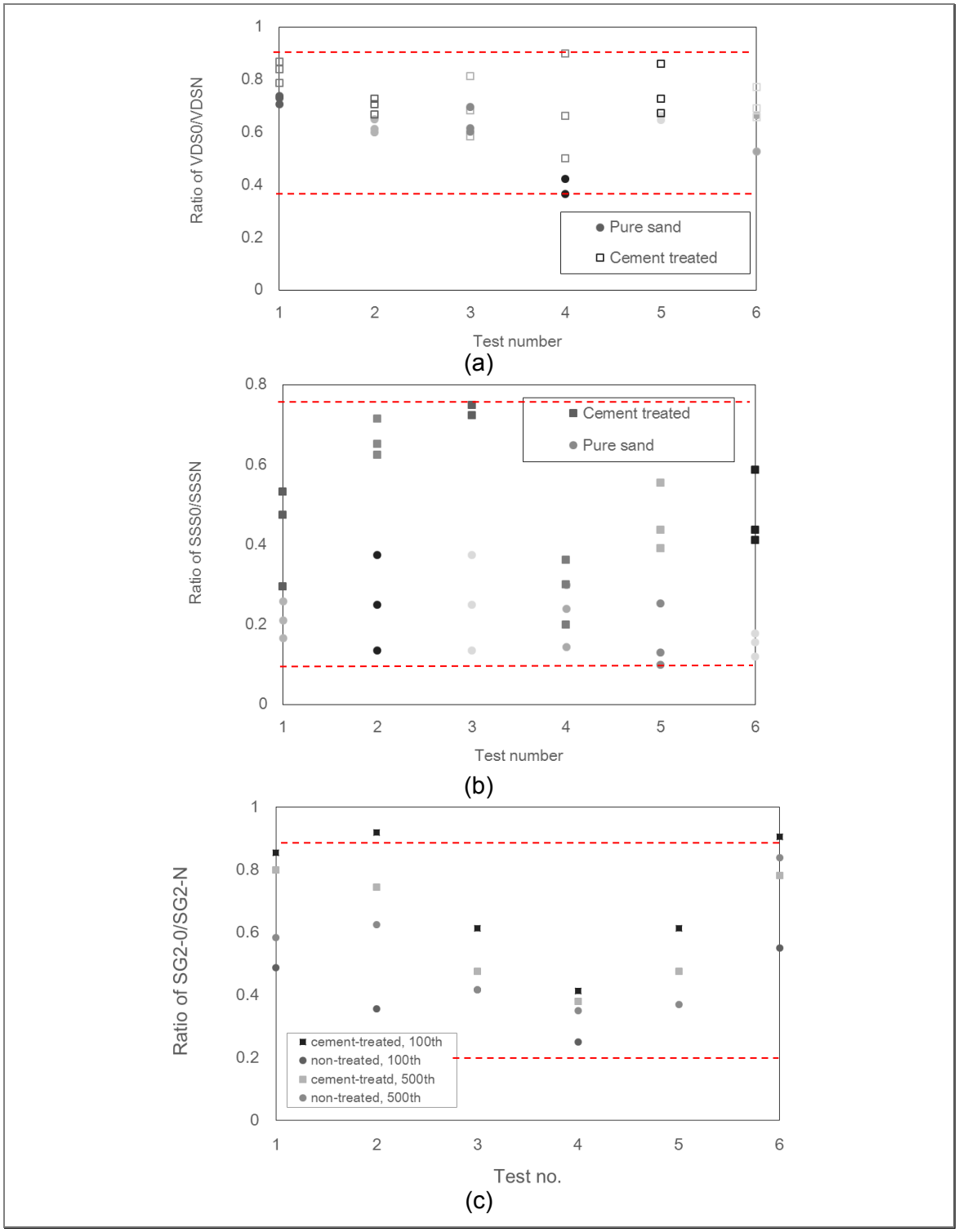

Figure 7-15 impact of first cycle loading on (a) VDS (b) SSS (c) SG2

7.5 Predicting Model Response

The main objective of many engineering projects is predicting the model response. As shown in this research the deflection of pipe, soil surface settlement and pressure on

pipe were found to be function of burial depth, surface pressure and number of loading cycles. Therefore, equations can be developed to estimate pipe deflection, soil surface settlement and pressure on pipe. To have dimensionless equations, relationships were developed as normalized. Dependent variables of SSS, soil surface settlement, vertical diametric strain, VDS and vertical earth pressure on pipe, σ are influenced by independent variables of burial depth, surface pressure and number of loading cycles. Thus, for initial phase there are only two variables for each analysis and polynomial regression will be appropriate to predict model response and the results will be displayed in three dimensional plots. However, for cyclic phase, three independent variables of number of cycles, burial depth and surface pressure have impact on SSS, VDS and σ. Therefore, for cyclic phase, Regression method and Artificial Neural Network approach were chosen to predict model response due to traffic load. It should be noted that all equations are normalised using dimensionless values for both predictors and variables. For example, variable x represents burial depth (H/D) and y represents loading conditions (P/P_0) which is magnitude of surface pressure to minimum applied pressure. For predictors normalised equations were used. Pipe deflection is dimensionless predictor while SSS and σ were normalised by dividing to depth of pipe (SSS/H) and applied load (σ/P), respectively. In the following sections, the methodology for predicting model response for each phase will be addressed. Then, developed equations are presented for untreated and cement-treated cases separately. Following this, comparison will be made between observed and predicted values. Finally, cumulative error histograms will be calculated to show precision of each method. Table 7-5 summarises different methods for predicting equations in the current research.

Table 7-5 Different methods for predicting equations in the current research

Phase	**Predicting methods**	**Objectives**
Initial phase • Non-treated • Cement-treated	Regression model Section 7.5.1	Developing equation to predict model response Comparison between predicted results and experimental and numerical data
Cyclic phase • Non-treated • Cement-treated	Regression model 7.5.2.1 Neural network 7.5.2.2	Developing equations to predict model response using two methods Comparison between predicted results of regression model, neural network and those obtained from experimental data

7.5.1 Prediction Model Response in Initial Phase

A regression model has been developed to predict VDS, SSS and σ in initial phase using Curve Fitting Toolbox in Matlab (MATLAB, 2015a). This toolbox provides an app and functions for fitting curves and surfaces to data. After few trial and errors a linear polynomial model found to be best to predict model response. The function used was a polynomial surface with f= fit ([x, y], z, 'poly23') or a degree 2 in x and degree 3 in y. The general equation is as follows:

$$f(x\,y) = p00 + p10 * x + p01 * y + p20 * x\text{^}2 + p11 * x * y \quad (7\text{-}2)$$

where x and y are variables representing burial depth and surface pressure, respectively. More details about this method can be found in (Matlab, 2005).

7.5.1.1 Non- treated

From all tests and finite element analysis the partial regression coefficients (p00, p10, p01, p20 and p11) are calculated and presented in Table 7-6. Some parts of this section can be found in other published references (Mosadegh & Nikraz, 2017).

Table 7-6 Coefficients and goodness to fit

Prediction	P00	P10	P01	P20	P11	R-square	SSE
VDS_{Pr}	1.115	-0.3348	0.5405	-0.1683	0.2274	0.9959	0.04097
SSS_{Pr}/H	0.1546	-0.1579	+0.2216	0.04111	-0.04243	0.9899	0.001035
$\sigma_{Pr/P}$	0.9808	-0.7082	0.1485	0.1723	-0.08357	0.9842	0.003398

$$VDS_{pr} = 1.115 - 0.3348 * \frac{H}{D} + 0.5405 * \frac{P}{P0} - 0.1683 * (\frac{H}{D})^2 + 0.2274 * (\frac{H}{D}) * \frac{P}{P0} \quad (7\text{-}3)$$

$$\frac{SSS_{Pr}}{H} = 0.1546 - 0.1579\ \frac{H}{D} + 0.2216 * \frac{P}{P0} + 0.04111 * \left(\frac{H}{D}\right)^2 - 0.04243 \left(\frac{H}{D}\right) * \frac{P}{P0} \quad (7\text{-}4)$$

$$\sigma_{Pr/P} = 0.9808 - 0.7082 * (\frac{H}{D}) + 0.145 * \frac{P}{P0} + 0.1723 * (\frac{H}{D})^2 - 0.08357 * (\frac{H}{D}) * \frac{P}{P0} \quad (7\text{-}5)$$

In order to show the change of three predictors with burial depth and surface pressure variations, results are presented in a three-dimensional plot in Figure 7-16. *X* axis represents change of burial depth and *Y* axis represents change of surface

pressure. *Z* axis shows change of investigated factors (for example in Figure 7-16-a *Z* axis represents VDS variations). It can be seen that increasing burial depth leads to a decrease in VDS and increasing surface pressure leads to an increase in VDS.

Predicted values for VDS, SSS and σ are calculated using Equations 7-3 to 7-5 and results are presented in Table 7-7 to Table 7-9. In addition, for each value a further assessing of accuracy of the model as percentage of error is calculated based on following equations:

$$Epexp = (\frac{A_{exp} - A_{pr}}{A_{exp}})\text{X}100 \qquad 7\text{-}6$$

$$Ep_{Num} = (\frac{A_{Num} - A_{pr}}{A_{Num}})\text{X}100 \qquad 7\text{-}7$$

In which Ep_{exp} and Ep_{Num} are error percentages for experimental and finite element analyses, respectively. $A_{exp,}$ A_{Num} *and* A_{pr} are observed experimental, observed numerical and predicted value at each test series, respectively. All predicted values and errors are calculated and results are in the last two columns in Table 7-7 to Table 7-9.

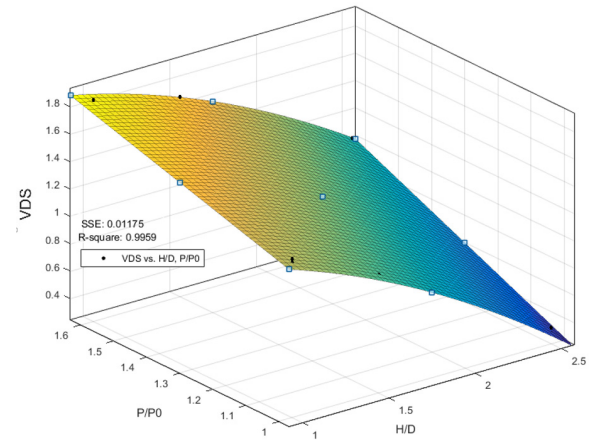

(a)

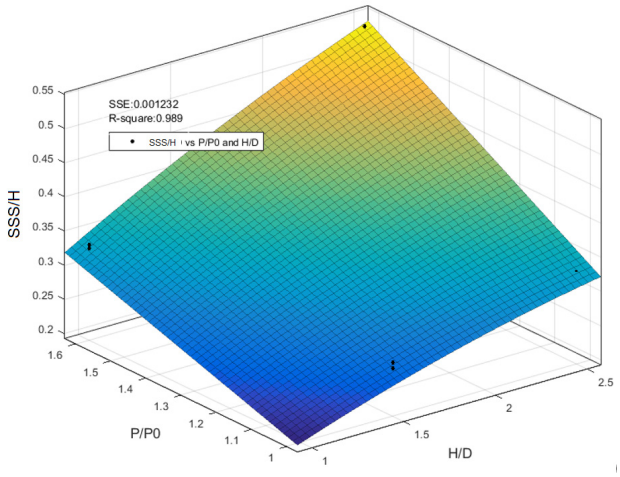

(b)

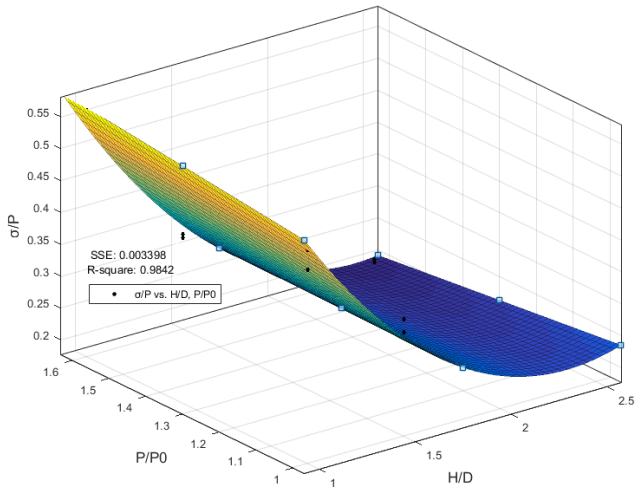

(c)

Figure 7-16 Response surface model (a) VDS (b) SSS (c) σ

Table 7-7 Comparison of maximum pipe deflection with predicted value

H/D	Applied pressure	VDS_{exp}	VDS_{FEM}	VDS_{Pr}	Ep_{exp} (%)	Ep_{Num} (%)
1	250	1.4000	1.3800	1.3797	1.45	0.0163
1.5	250	1.0900	1.1100	1.1156	-2.35	-0.51
2.5	250	0.3200	0.3600	0.33505	-4.70	6.927
1	400	1.8600	1.8000	1.8405	1.04	-2.25
1.5	400	1.6200	1.7000	1.6446	-1.52	3.25
2.5	400	0.9500	1.0400	1.0004	-5.30	3.805

Table 7-8 Comparison of maximum surface settlement with predicted value

H/D	Applied pressure	$SSS_{exp/H}$	$SSS_{FEM/H}$	$SSS_{Pr/H}$	Ep_{exp} (%)	Ep_{Num} (%)
1	250	0.2109	0.2091	0.2170	-2.87	-3.77
1.5	250	0.181	0.1752	0.1682	7.17	3.967
2.5	250	0.1305	0.1295	0.1323	-1.35	-2.20
1	400	0.3318	0.3273	0.3245	2.21	0.85
1.5	400	0.2606	0.2570	0.2630	-0.90	-2.33
2.5	400	0.2145	0.1982	0.2016	6.02	-1.738

Table 7-9 Comparison of maximum stress on pipe with predicted value

H/D	Applied pressure	σ_{exp}/P	σ_{FEM}/P	σ_{Pr}/P	Ep_{exp} (%)	Ep_{Num} (%)
1	250	0.512	0.48	0.5063	1.10	-5.485
1.5	250	0.36	0.34	0.3258	9.49	4.1705
2.5	250	0.22	0.22	0.2232	-1.47	-1.477
1	400	0.5625	0.5625	0.5431	3.43	3.4332
1.5	400	0.32	0.325	0.3376	-5.50	-3.879
2.5	400	0.195	0.2	0.1848	5.182	7.552

Figure 7-17 compares observed versus predicted data for VDS, SSS/H and σ/P. Plotting predicted and observed values graphically illustrates different R-squared values for regression models. Diagonal line is where observed and predicted values are exactly equal. It is shown that data are well distributed around the diagonal line and high values of R-squared in each graph indicate the model fits the data in a convenient way.

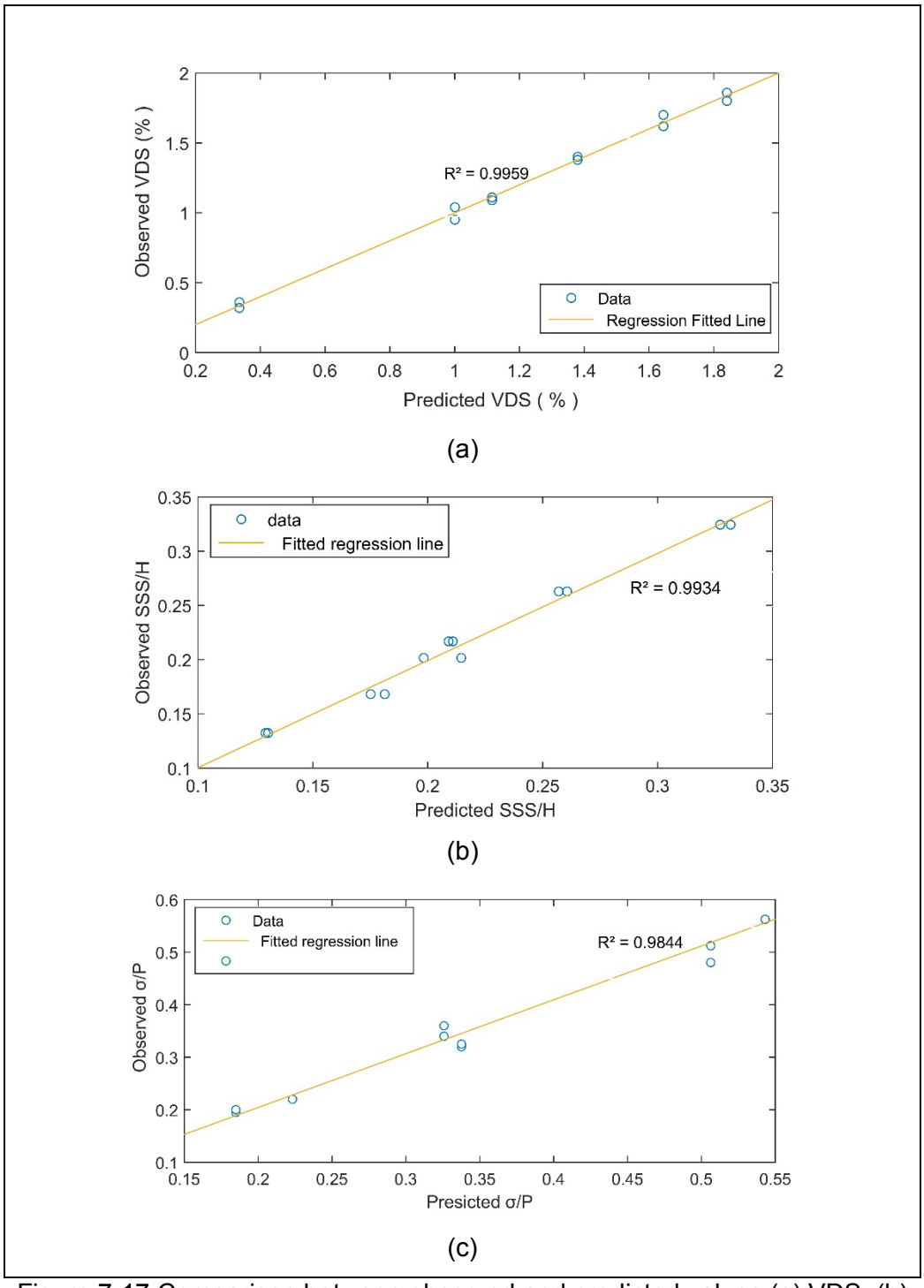

Figure 7-17 Comparison between observed and predicted values (a) VDS, (b) SSS/D (c) σ/P

Cumulative error can provide an easy way to compare different sets of data and is calculated by dividing the cumulative frequency by the total number of observations (n), multiplied by 100. In order to show the precision of predicted results, the cumulative histogram percentage of errors for all prediction of VDS, SSS/H and σ/P are calculated and results are shown in Figure 7-18. Results reveal that the maximum error is 10% for pressure on pipe. For all data maximum errors are approximately 4%, 7% and 10% for SSS/H, VDS and σ/P, respectively.

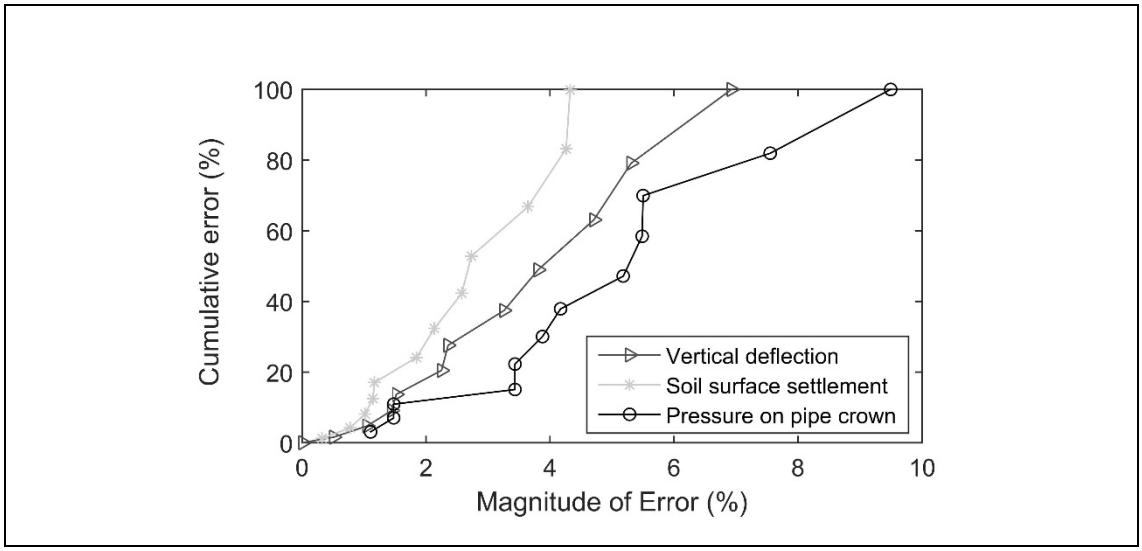

Figure 7-18 Cumulative histogram percentage of error for the prediction of SSS, VDS and σ

7.5.1.2 Cement-treated soil

A regression model was also developed to predict the VDS, SSS/H and σ /P in initial phase for cemented sand. The function is a polynomial equation and methodology is the same as those explained in the previous section. Linear functions to predict model response are developed and illustrated in Equations 7-8, 7-9 and 7-10.The coefficient for each equation is calculated and results are shown in Table 7-10.

Table 7-10 Coefficients and goodness to fit

	p00	p10	p01	p20	p11	RMSE	R-square
VDS_{Pr}	-2.254	1.211	2.21	-0.1758	-0.7399	0.0802	0.9645
SSS_{Pr}/H	0.02002	-.01917	0.0099	0.0049	-0.0030	0.0015	0.9162
σ_{Pr}/P	1.015	-0.9129	0.0601	0.2188	-0.0098	0.0271	0.962

$$VDS_{pr} = -2.54+1.211*(H/D) + 2.21*P/P_0 -0.175*(H/D)^2 -0.7399 *(H/D)* P/P_0 \quad (7\text{-}8)$$

$$SSS_{pr}/H =0.02002-0.01917*(H/D)+ 0.009923* P/P0+0.004965*(H/D)^2-0.003084*(H/D)* P/P_0 \quad (7\text{-}9)$$

$$\sigma_{pr}/P= 1.015-0.9129*(H/D) 0.06012*(P/P_0)+ 0.2188*(H/D)^2 -0.009821*(H/D)* P/P_0 \quad (7\text{-}10)$$

Similar to previous section, results are presented in a three-dimensional plot in Figure 7-19. *X* axis represents burial depth and *Y* axis represents surface pressure. *Z* axis shows the investigated factors. For example, change of VDS versus burial depth and surface pressure is illustrated in Figure 7-19-a. It can be seen that increasing burial depth leads to a decrease in VDS and increasing surface pressure increases VDS. Predicted values for VDS, SSS/H and σ/P are calculated and results are presented in Table 7-11 to Table 7-13. In addition, similar to previous section for each predictor, the percentage of error is calculated and results are illustrated in the relevant table.

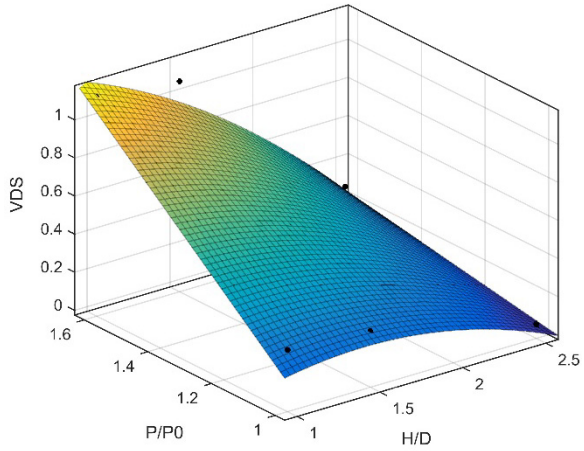

(a)

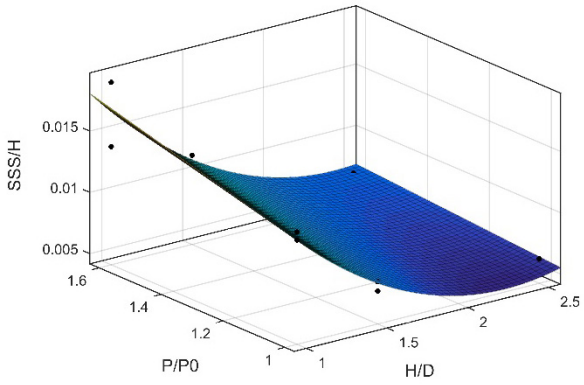

(b)

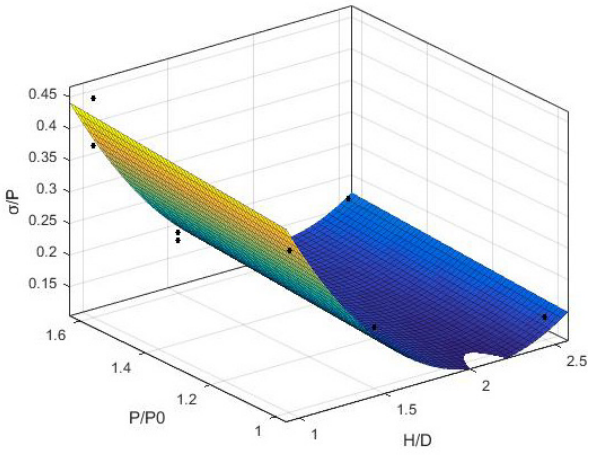

(c)

Figure 7-19 Response surface model (a) VDS (b) SSS/H (c) σ/P

Table 7-11 Comparison of maximum pipe deflection with predicted value

H/D	Applied pressure	VDS_{exp}	VDS_{Num}	VDS_{pr}	Ep_{exp} (%)	Ep_{Num} (%)
1	250	0.2200	0.3000	0.2513	-14.23	16.23
1.5	250	0.2400	0.2700	0.2671	-11.29	1.07
2.5	250	0.0300	0.0400	0.0350	-16.67	12.50
1	400	1.1250	1.1250	1.1334	-0.74	-0.74
1.5	400	0.8000	1.0800	0.9272	-15.90	14.15
2.5	400	0.2700	0.2250	0.2512	6.98	-11.62

Table 7-12 Comparison of maximum surface settlement with predicted value

H/D	Applied pressure	SSS_{exp} /H	SSS_{Num} /H	SSS-pr/H	Ep_{exp} (%)	Ep_{Num} (%)
1	250	0.0127	0.01333	0.01265	0.100	5.095
1.5	250	0.0076	0.00686	0.00773	-1.499	-12.777
2.5	250	0.00617	0.00488	0.00534	13.484	-9.496
1	400	0.01668	0.01905	0.01676	-9.970	12.024
1.5	400	0.0114	0.01143	0.01091	4.525	4.525
2.5	400	0.0067	0.00636	0.00667	-0.006	-4.796

Table 7-13 Comparison of maximum stress on pipe with predicted value

H/D	Applied pressure	σ_{exp} /P	σ_{Num}/P	σ_{pr}/P	Ep_{exp} (%)	Ep_{Num} (%)
1	250	0.3600	0.3712	0.371	-3.111	-3.111
1.5	250	0.2000	0.1833	0.183	8.331	8.331
2.5	250	0.1200	0.1358	0.136	-13.181	2.988
1	400	0.4500	0.4014	0.401	10.805	-7.034
1.5	400	0.1875	0.2106	0.211	-12.305	-5.286
2.5	400	0.1500	0.1572	0.157	-4.772	10.195

To understand the accuracy of model, observed values are plotted versus predicted and results are shown in Figure 7-20. The R^2 of regression for the predicted versus observed values is shown in each graph. Overall, a good agreement exists between predicted and observed values and R^2 ranges between 0.9 and 0.97 showing acceptable accuracy of predicted results.

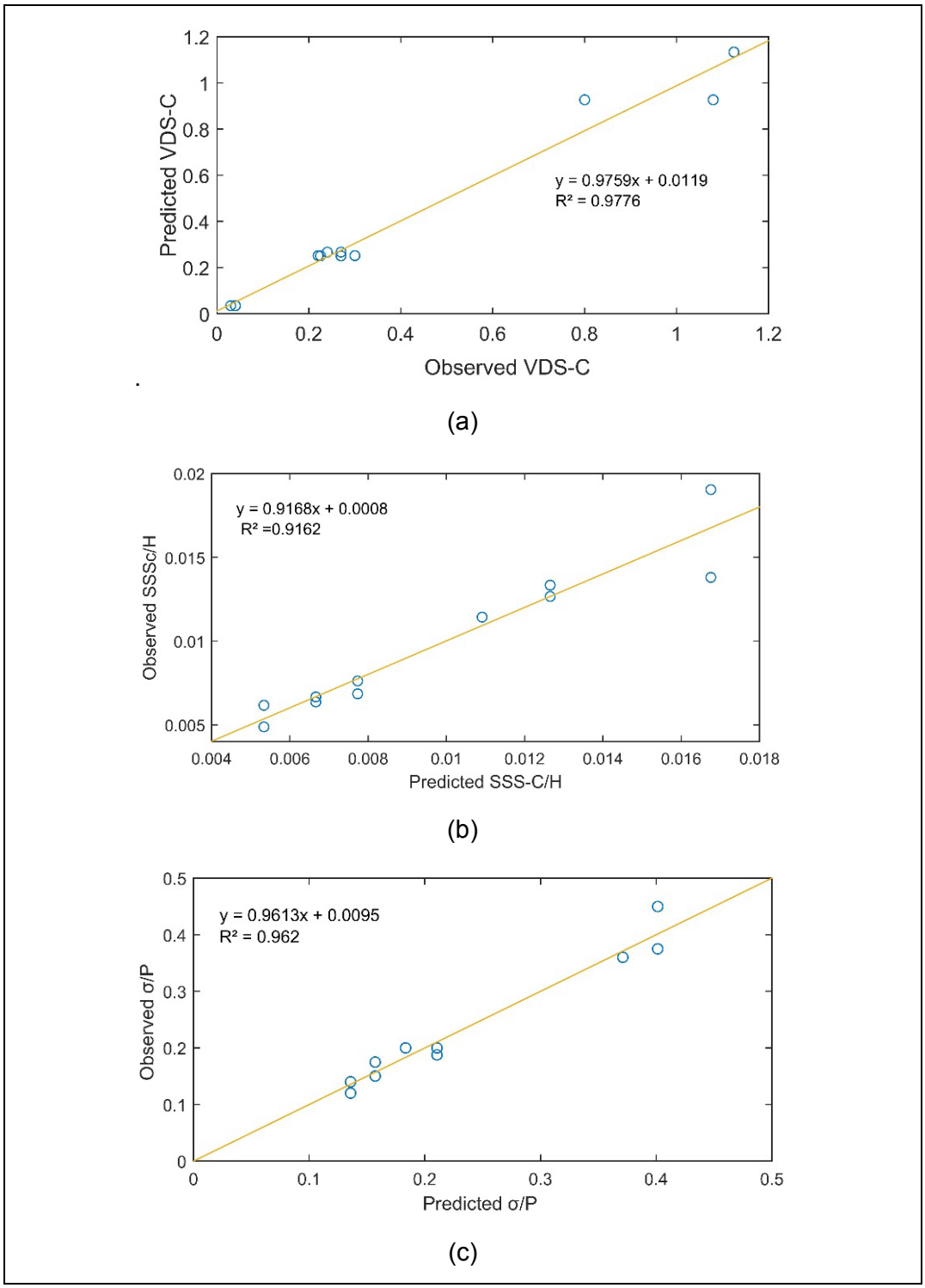

Figure 7-20 Comparison between observed and predicted values for cemented sand during initial phase (a) VDS, (b) SSS/H (c) σ/P

To show precision of the predicted results, a cumulative histogram of the proposed model is developed and illustrated in Figure 7-21. Overall, around 80% of all data have less than 12%, 13% and 16% error for pressure on pipe, soil surface settlement and pipe vertical deflection, respectively. However, for all data maximum errors are approximately 14%, 14% and 17% for σ, SSS, VDS, respectively.

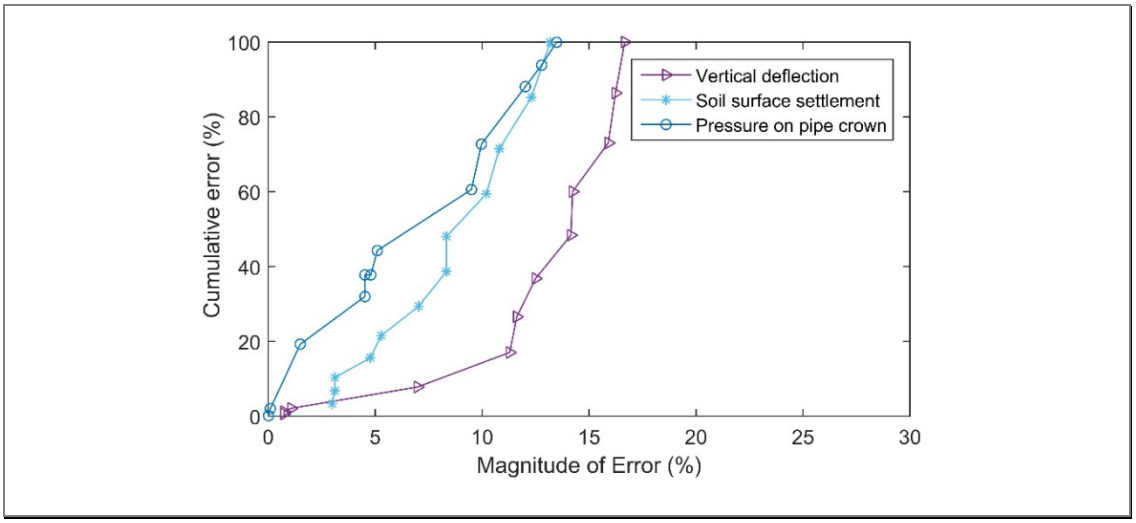

Figure 7-21 Cumulative histogram percentage of error for the prediction of SSS, VDS and σ

7.5.2 Predicting Model Response in Cyclic Phase

As mentioned earlier for cyclic phase, three independent variables including number of cycles, burial depth and surface pressure have impact on model performance. In this section, both multiple linear regression method and artificial neural network models are chosen to predict model response due to cyclic load (MATLAB, 2015a). Regression model utilizes the relation between two or more quantities variables to predict the response model. Neural network is basically a model structure using different algorithms for fitting the model with architecture inspired by the humane brain. Unlike regression model, neural network models are not limited by simplifying mathematical assumptions.

In the following sections, two different methods for predicting model response for cyclic phase are discussed. First, methodology and definitions of each model is briefly discussed. Then, equations are developed for each method for both non-treated and cement-treated cases. This will be followed by comparison between observed and predicted values and calculating cumulative error histograms to show accuracy of each method.

7.5.2.1 Multiple Linear Regression

Linear Regression Model Regression analysis is a mathematical approach for prediction and forecasting the model response. In this section, multiple linear regression models are introduced to find a relationship between dependent variable *y* and the independent variable *x*. The equation can be described as follows in which the relationship between dependent variable *y* and *n* independent variables X_i is presented.

$$y=\beta_0+\beta_1X_1+\beta_2X_2+\beta_3X_3+\ldots. B_nX_n. \quad 7\text{-}11$$

Where β_i are the *n+1* regression coefficient of the linear model. The regression coefficients are estimated by minimizing the mean-squared difference between predicted and observed values. More details can be found in (Trauth, 2015)

In this section, the relationship between independent variables of *H/D* or burial depth ratio, *P* or stress ratio, *N* (and *LogN*) or number of cycles, and dependent variables of *VDS*, *SSS/H* and *σ/P* are determined. First, all variables are defined in a table as input values for data processing. Input parameters stored in the table shown as *tbl* in the Equation 7-11. Then all beta coefficients of 7-11are calculated using *fitlm* in Matlab as shown in Equation 7-12. The calculations are repeated for each factor to find fitted output in the *modelspace*. After running *fitlm,* the equations will be displayed along with a table with the regression coefficient estimated for each predictor variable in the first column. The standard error, the F-statistic, and the p-values of the estimated coefficient are displayed in other columns. The quality of the model is very good if the p-value of the model constant is zero. Tables illustrating estimated coefficients along with estimated errors and P-Values are presented in Appendix D.

```
mdl= fitlm(tbl, modelspec);
```
7-12

The following section, discusses the results of predicted versus observed data for each test as shown in Figure 7-22 and Figure 7-23 for non-treated and cement-treated cases. As mentioned in the previous section, the higher the R^2 value, the more accurate the results are. It can be seen that R^2 varies between 0.95 and 0.99 showing the model has accurate predictions.

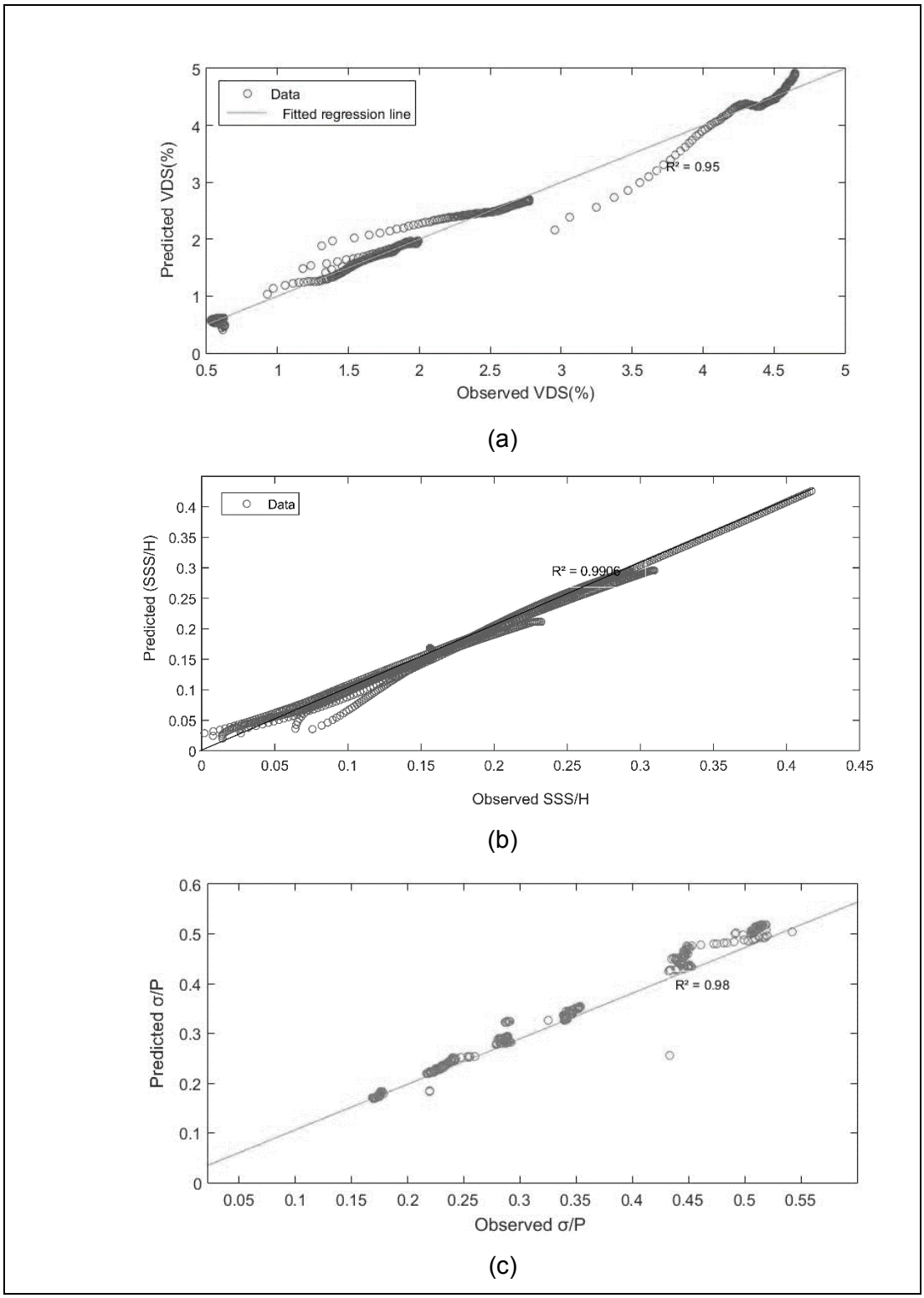

Figure 7-22 Comparison between observed and predicted values for non-treated case during cyclic phase (a) VDS, (b) SSS/H (c) σ/P

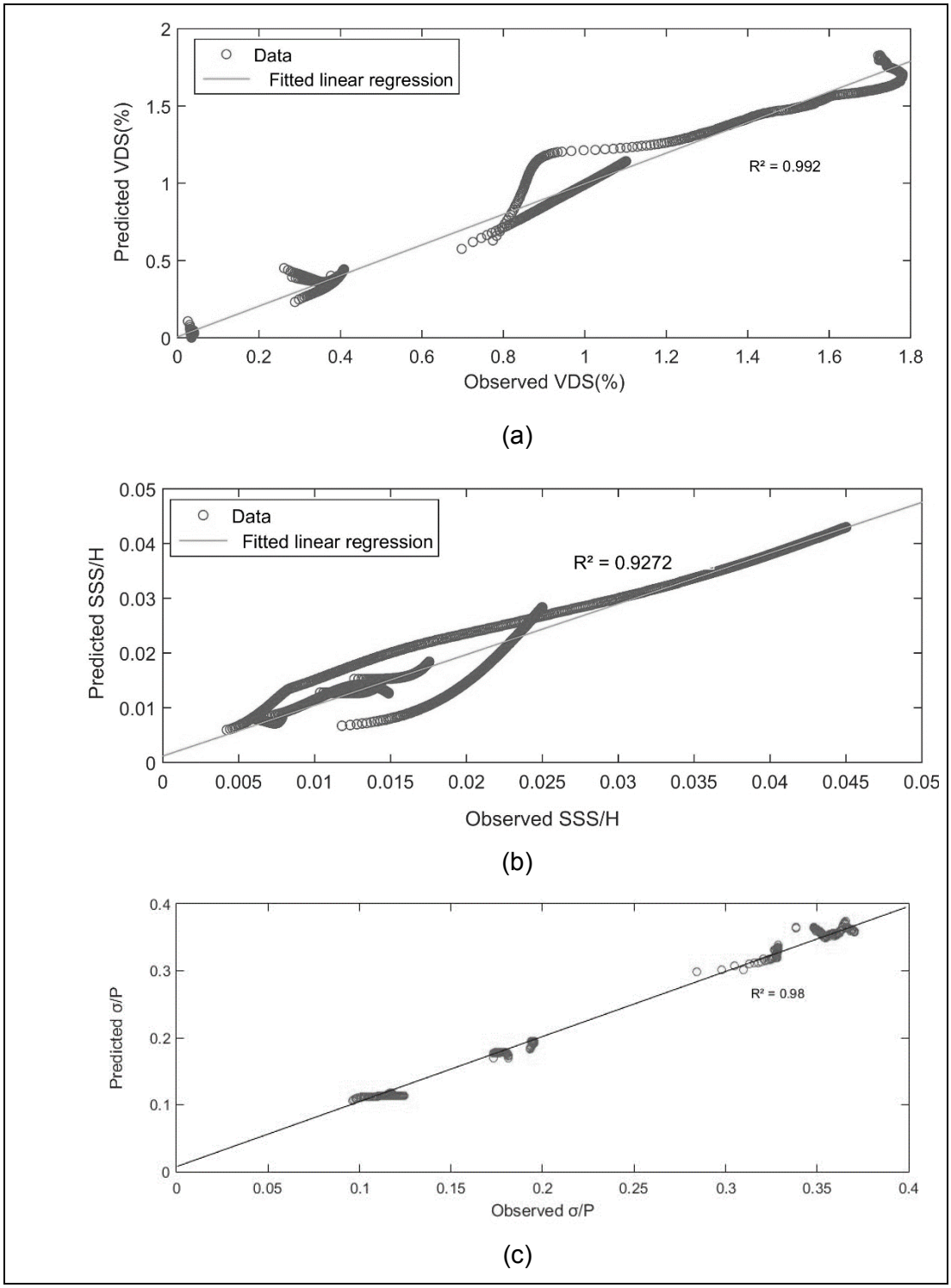

Figure 7-23 Comparison between observed and predicted values for cement-treated case during cyclic phase (a) VDS, (b) SSS/H (c) σ/P

7.5.2.2 Second method: Neural network

The Neural Fitting application will help to select data, create and train a network, and evaluate its performance using mean square error and regression analysis. In fitting problems, neural network will map between a data set of numeric inputs and a set of numeric targets. The default performance function for feedforward networks is mean square error mse which is defined as following equation:

$$F = mse = \frac{1}{N}\sum_{i=1}^{N}(ei)^2 = \frac{1}{N}\sum_{i=1}^{N}(t - a_i)^2 \quad 7\text{-}13$$

ANNs can be grouped into two major categories: feed-forward and feedback networks. In the feed-forward network, no loops are formed by the network connections, while one or more loops may exist in the feedback. The most commonly used family of feed-forward networks is a layered network in which neurons are organized into layers with connections strictly in one direction from one layer to another (Jain et al., 1996). If the neurons in a hidden layer are too few, the neural network will not be able to model the data accurately. If the number of neurons in a hidden layer is too large it may lead to over-training. This research used 10 hidden nodes as shown in Figure 7-24 and Equations 7-13 to 15. Where 3-NH-1 label denotes that there are 3 inputs and 1 output and NH indicates the number of hidden nodes.

$$\{SSS|H\}=\text{ANN}_{3\text{-NH-}1}\left\{\frac{H}{D}, P, LOGN\right\} \quad 7\text{-}14$$

$$\{VDS\}=\text{ANN}_{3\text{-NH-}1}\left\{\frac{H}{D}, P, LOGN\right\} \quad 7\text{-}15$$

$$\{\sigma/P\}=\text{ANN}_{3\text{-NH-}1}\left\{\frac{H}{D}, P,\ LOGN\right\} \quad 7\text{-}16$$

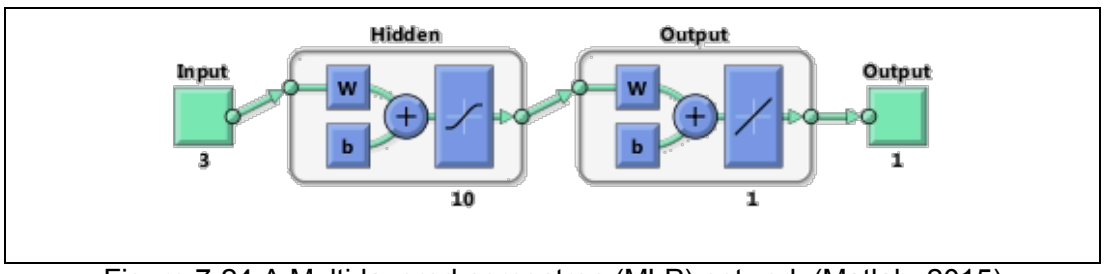

Figure 7-24 A Multi-layered perceptron (MLP) network (Matlab, 2015)

In particular, three data sets are commonly used in different stages of the creation of the model. Three types of data and stages are as follows:

(1) Training: which is presented to the network during training and the network is adjusted according to its error.
(2) Validation which is used to measure network generalization
(3) Testing which have no effect on training and thus provide an independent measure of network performance during and after training.

In the current research a Levenberg algorithm was used which typically takes more memory but less time. Training automatically stops when generalization stops improving, as indicated by an increase in the mean square error of the validation samples. Overall, in this research the modelling process for neural network is adapted through the following steps:

1. Creating a database from laboratory cyclic test, and separated randomly into three distinct groups: training, testing and validation;
2. Creating the basic architecture of the neural network model using inputs, outputs and the number of hidden layers;
3. Training and testing the neural network model to create the optimal structure, which includes determining the optimal number of hidden nodes and iterations;
4. Comparing the statistical accuracy of the calculations from the training, testing and validation phases; is the statistical accuracy from training, testing, and validation sets comparable?
5. If no, go back to step 3; if yes, go to step 6;
6. The neural network model with an acceptable structure for the desired model is created.

The next step is creating a regression plot, which shows the relationship between the outputs of the network and the targets. The regression results for VDS, SSS/H and σ/P are illustrated in Figure 7-25 and Figure 7-26. If the training is perfect, the network outputs and the targets would be exactly equal, but the relationship is rarely perfect in practice. In each regression analysis, there are four regression charts including the training, validation, testing and all dataset. The dashed line in each plot represents the perfect result and the solid line represents the best fit linear regression line between outputs and targets.

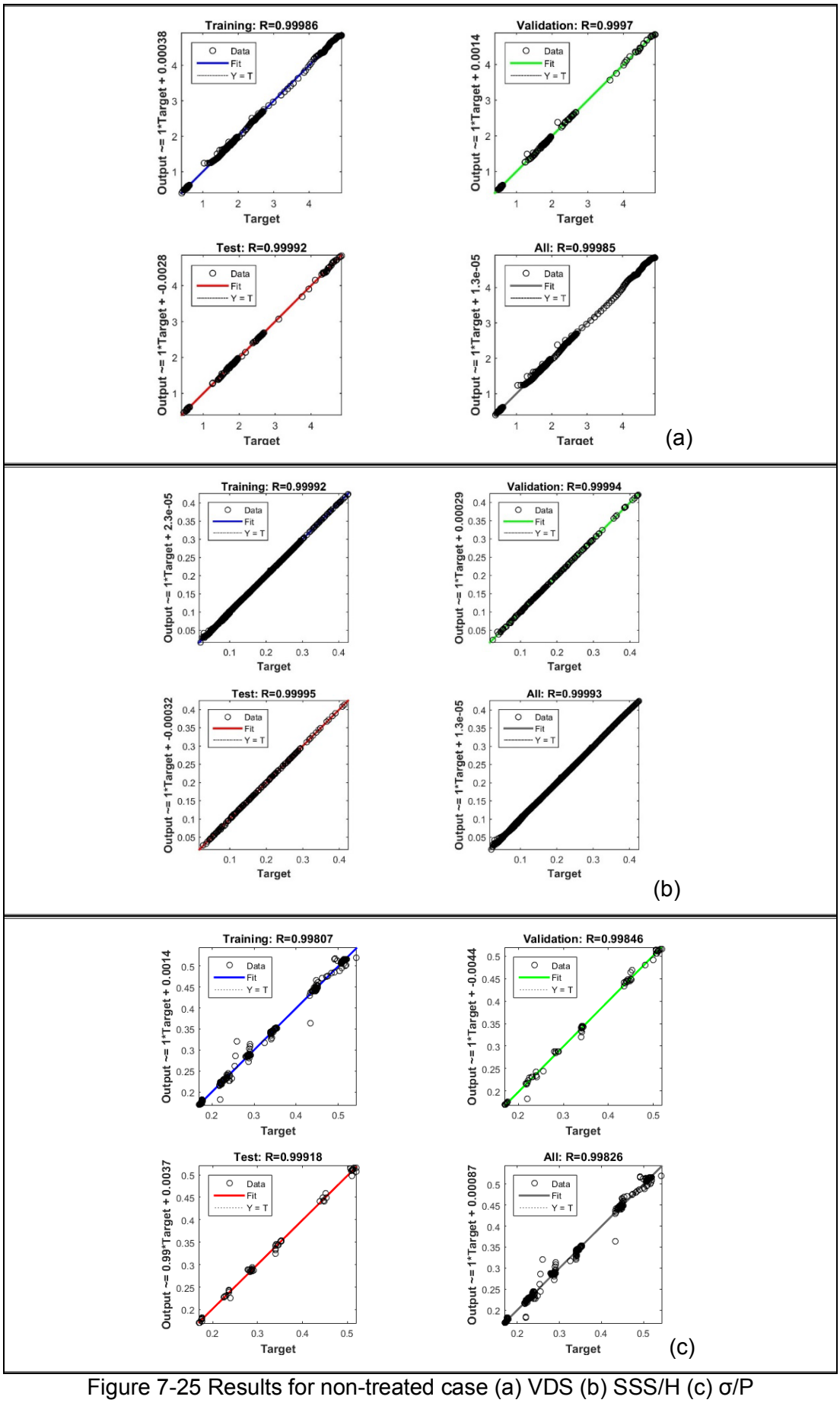

Figure 7-25 Results for non-treated case (a) VDS (b) SSS/H (c) σ/P

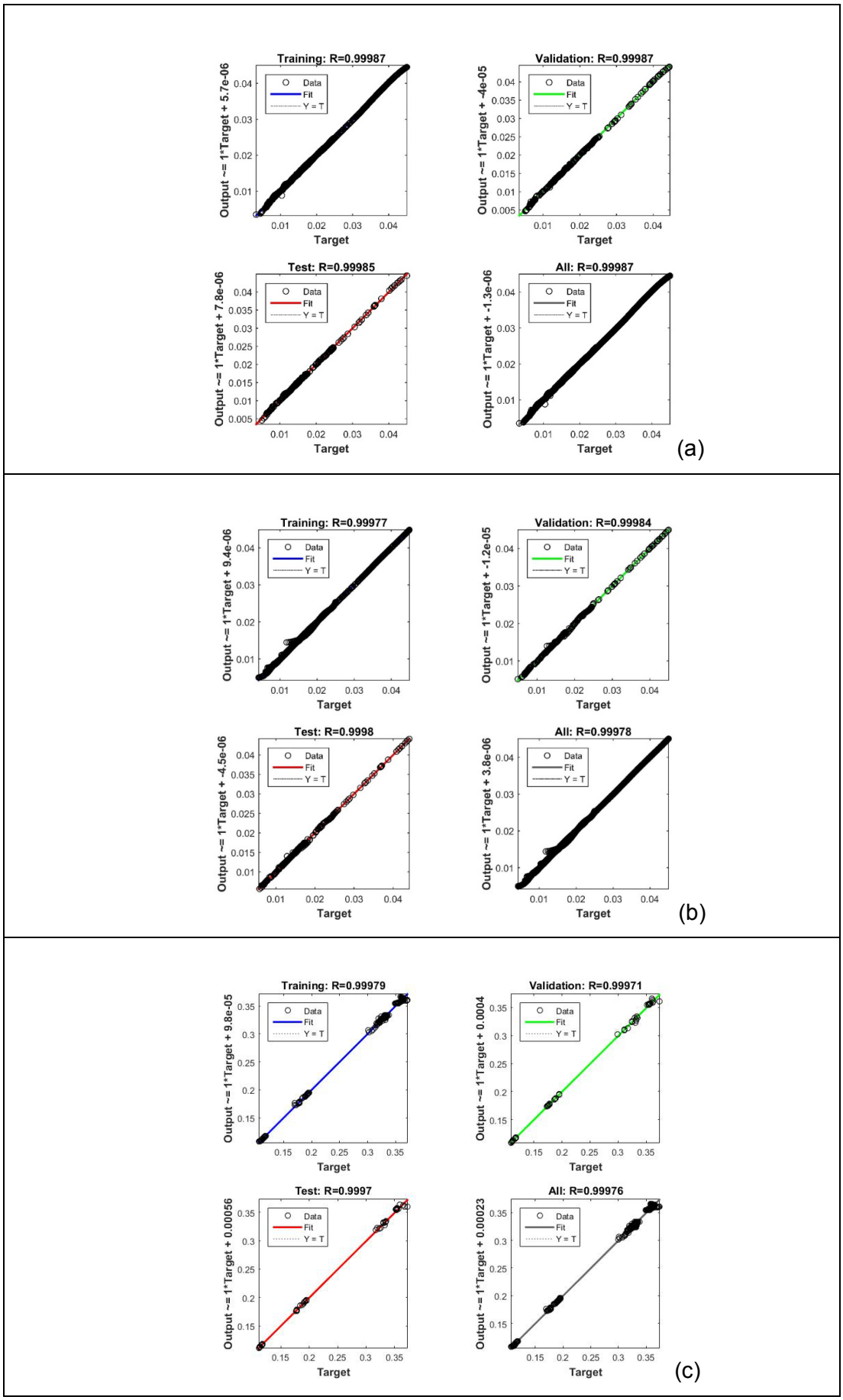

Figure 7-26 Results for cement-treated case (a) VDS (b) SSS/H (c) σ/P

To investigate the performance of neural network model, the value of *R* and MSE are calculated and summarised Table 7-14. It can be seen for all cases values of *R* are very close to 1 and MSE values are very small showing the reliability of the results. It is worth noting that *R* Values measure the correlation between outputs and targets. A value of 1 means a close relationship and 0 is a random relationship. In addition, Mean Squared Error or *MSE* is the average squared difference between outputs and targets and lower values are better.

Table 7-14 Statistical parameters for non-treatd and cement-treated cases

	Non-treated			**Cement-treated**		
VDS	Training	Validation	Testing	Training	Validation	Testing
Number of samples	875	185	185	2081	446	446
R	0.99992	0.9996	0.9994	0.9997	0.9997	0.9997
MSE	7.00E-05	4.00E-05	6.00E-05	1.20E-05	1.50E-05	1.75E-05
SSSH	Training	Validation	Testing	Training	Validation	Testing
Number of samples	875	185	185	2081	446	446
R	0.998	0.9992	0.9997	1.00E-08	9.00E-09	1.00E-08
MSE	1.00E-06	1.20E-06	2.50E-06	0.9908	0.9992	0.9998
σ/P	Training	Validation	Testing	Training	Validation	Testing
Number of samples	288	62	62	288	62	62
R	0.9	0.99	0.99	0.999	0.998	0.998
MSE	5.00E-05	4.10E-05	1.90E-04	1.00E-05	1.10E-05	2.00E-05

7.5.3 Comparison of Two Methods

Two methods of regression model and neural network were developed based on experimental data to predict model response during cyclic phase. It should be noted that the neural network methodology is based on the attempt to model the way a biological brain processes data. It is thus quite different from standard regression analysis for prediction. Numerous studies have shown neural network models represent a promising modelling technique especially for data sets having non-linear relationships which are frequently encountered in engineering processes. Unlike the regression model, neural network models are not constrained by simplifying mathematical assumptions (e.g. linear system, normal distribution, etc.). The results of predicting model response based on two methods were presented in this chapter. In this section, results achieved using the two methods are compared. First, the predicted values based on each method will be compared with experimental data. Then, in order to show the accuracy of the predicted results in cyclic phase, the magnitude of error and cumulative histogram percentage of errors will be calculated.

7.5.3.1 Verification of models

In order to verify the proposed models, the predicted values of VDS, SSS/H and σ/P through two methods were plotted versus raw experimental data. Results for non-treated and cement-treated cases are illustrated in Figure 7-27 and Figure 7-28, respectively. The horizontal axis represents data from all six series of tests. Vertical axis represents change of *VDS*, *SSS/H* and *σ/P* in which *H* is burial depth of the pipe in each test and *P* is applied surface pressure. It should be noted that all data were chosen based on maximum values of each parameter at each cycle. Overall, for both figures neural network results are more accurate compared to those calculated using regression method especially at the beginning of each test.

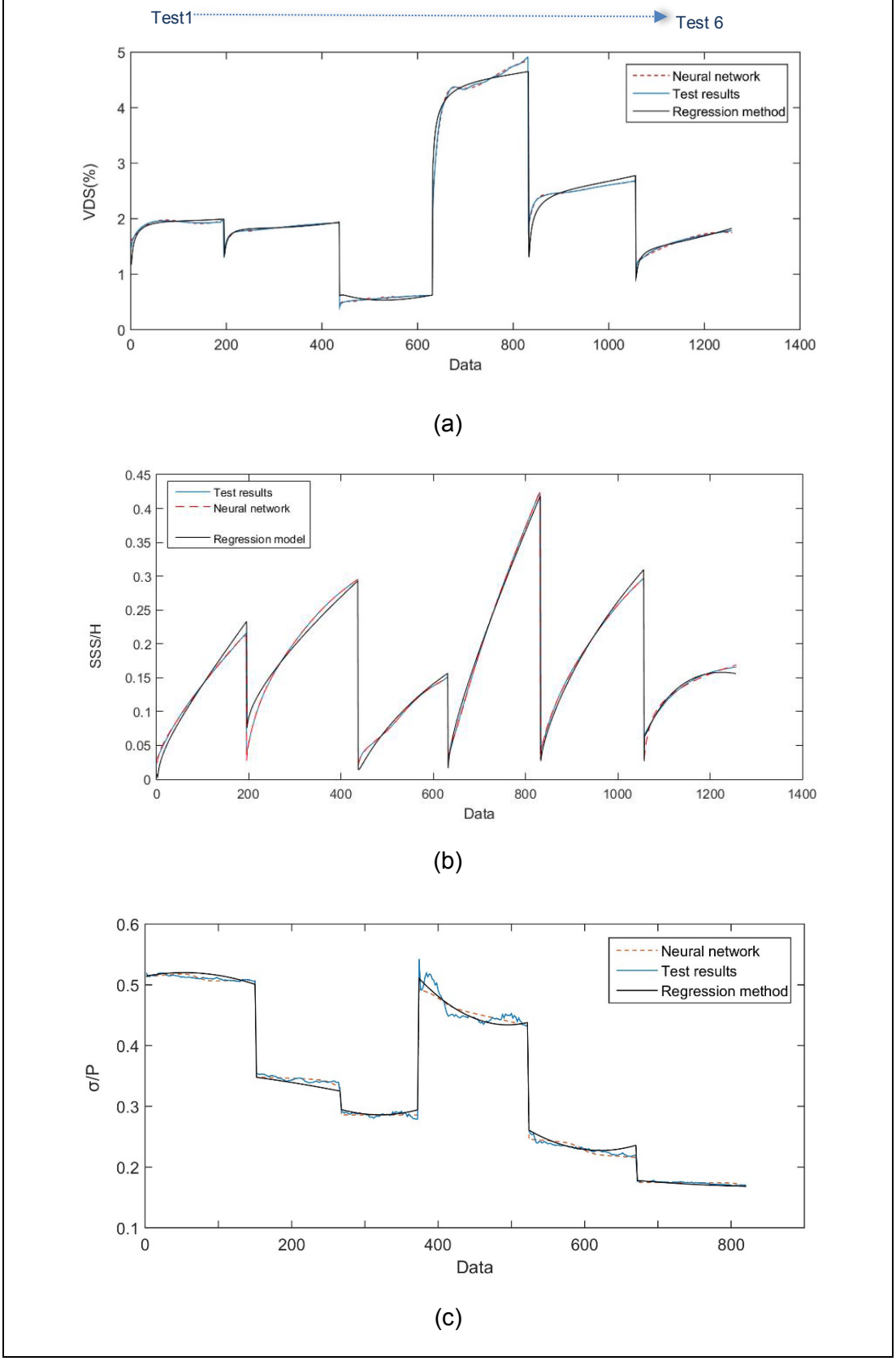

Figure 7-27 Comparison of neural network predicted values with test results of non-stabilized specimens (a) VDS (b) SSS/H (c) σ/P

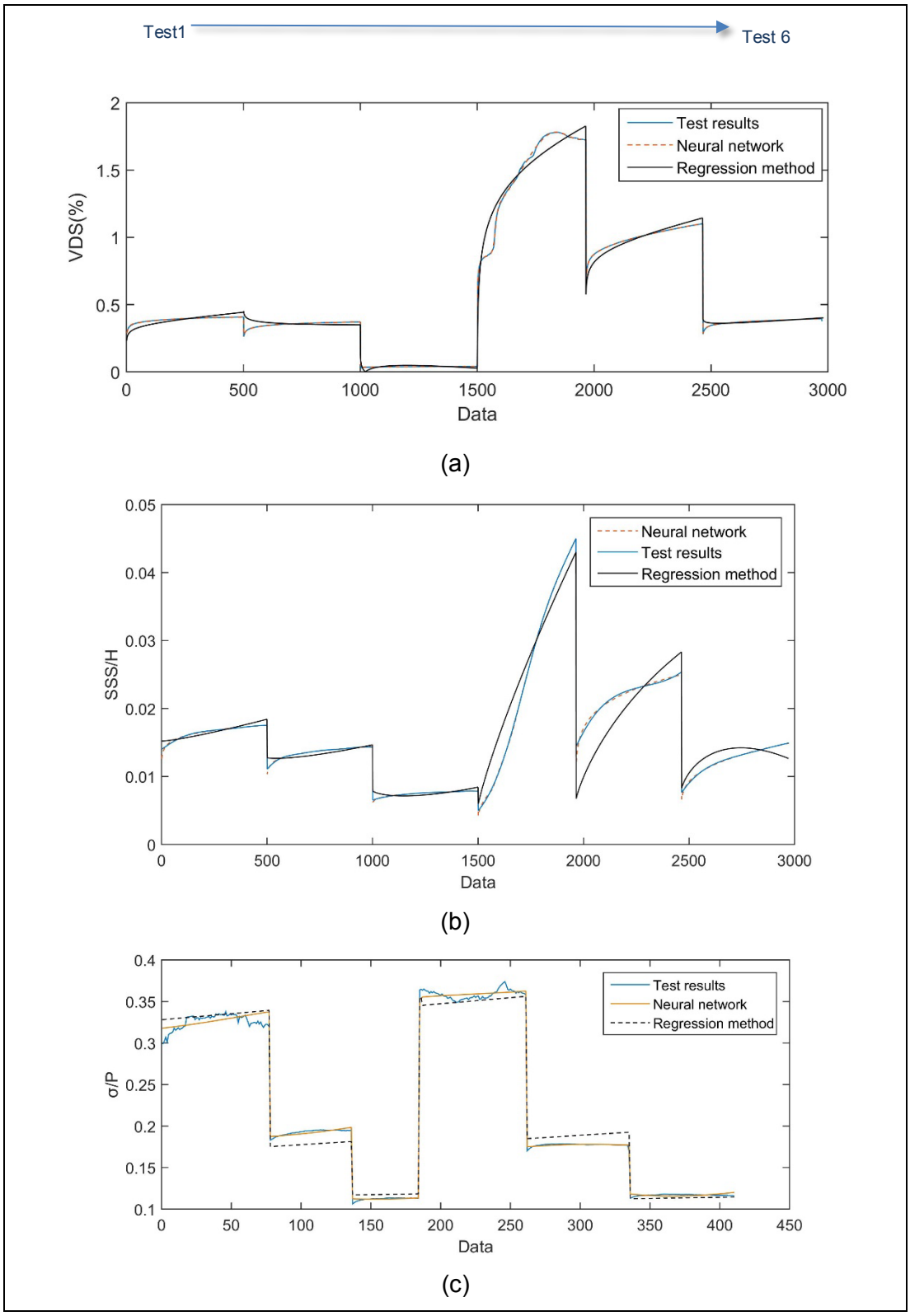

Figure 7-28 Comparison of neural network predicted values with test results of cement-treated specimens (a) VDS (b) SSS/H (c) σ/P

In order to show the accuracy of the predicted results, the magnitude of error and cumulative histogram percentage of errors are calculated and results are shown in Figure 7-29 and Figure 7-30 for non-treated and cement-treated materials, respectively. The information of each graph is shown on the legend consisting of three parts representing method of prediction, investigating value and test condition. For example, RM-VDS-NC is referring to deflection measurement using regression method for non-cement treated soil. Overall, for all data the cumulative percentage error for neural network method is less than those calculated through regression method. In all figures, all data have less than 15% error for non-treated and 20% error for cement-treated materials. These values for regression models are 40% and 42%. The comparison of two methods reveals that the predicted values of VDS, SSS/H and σ/P using neural network is more convenient than regression method.

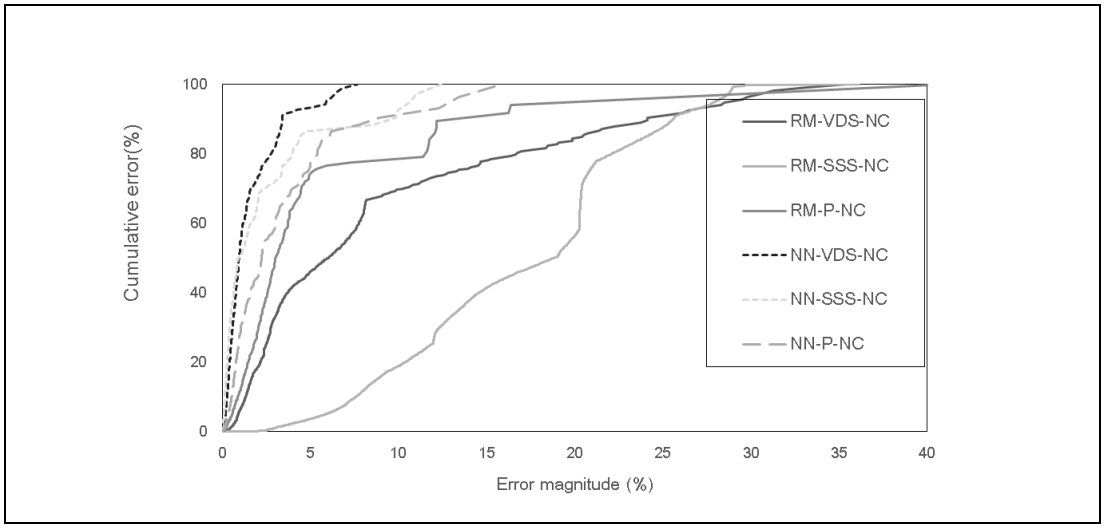

Figure 7-29 Cumulative histogram percentage of errors for the prediction of VDS, SSS/H and σ/P

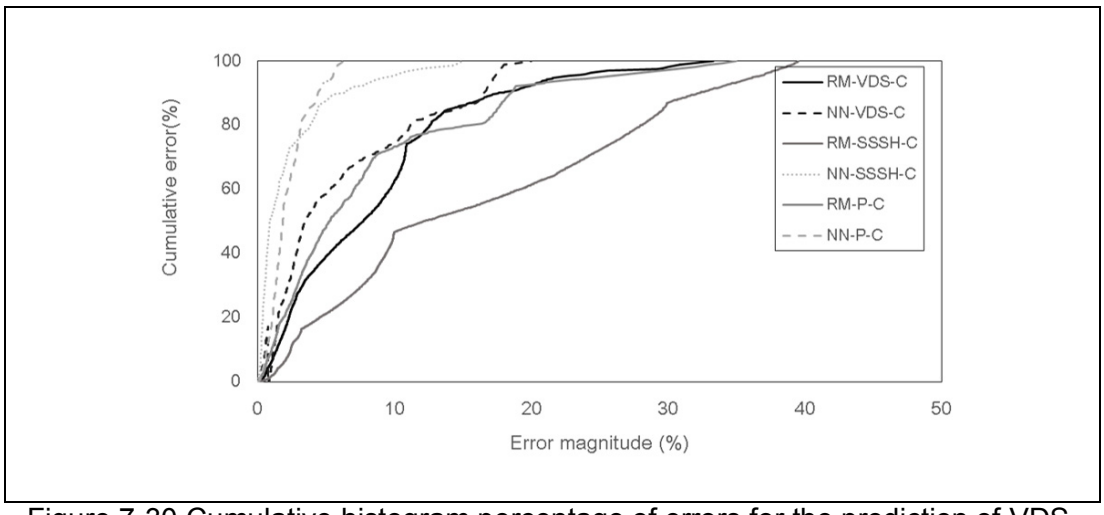

Figure 7-30 Cumulative histogram percentage of errors for the prediction of VDS, SSS/H and σ/P

Table 7-15 and Table 7-16 summarise statistical parameters to quantify the accuracy of each method. It should be noted that e_{max} is the maximum percentage error, *R-square* is the coefficient of determination and *MSE* is mean squared error. Overall, lower errors are observed in neural network methods. For example, the maximum error for predicted VDS for non-treated materials are 38% and 10% for regression method and neural network model, respectively. For the same case, higher R squared and lower MSE values are observed for neural network prediction. Comparison of the two methods in this section show that the predictions obtained from the neural network are more accurate compared to those obtained using regression method.

Table 7-15 Comparing statistical parameters of two methods for non-treated material

Parameter	Method	e_{max} (%)	R-square	MSE
VDS	Regression	38	0.95	0.0083
	Neural network	10	0.999	7e-5
SSS/H	Regression	36	0.99	6e-4
	Neural network	12	0.999	1e-6
σ/P	Regression	40	0.98	2.9e-5
	Neural network	15.9	0.998	6e-5

Table 7-16 Comparing statistical parameters of two methods for cement-treated material

Parameter	Method	e_{max} (%)	R-square	MSE
VDS	Regression	32	0.9911	0.0022
	Neural network	19	0.99	1.1e-4
SSS/H	Regression	40	0.92	4.4e-6
	Neural network	16	0.99	1e-8
σ/P	Regression	40	0.98	1e-4
	Neural network	5.8	0.9997	3e-5

It is noted regression and neural network models can be used to predict soil and pipe behaviour for more cases. In other words, these methods can be used to

predict values of VDS, SSS and σ on pipe for any combination of input variables as long as these values are within the coverage range of database. However, the number of data for number of cycles or *N* are much higher than number of other variables such as burial depths *H/D* and surface pressure, *P*. This means further investigations are needed for a broader range of variables to have a balance matrix of variables in predicting equations by implementing neural network.

7.6 SUMMARY AND CONCLUSSION

This chapter reviewed test results with focus on analysing the impact of different factors and stabilization on model performance. The main conclusions through this chapter are summarised as follows:

- Impact of various factors on model response during initial phase and cyclic phase was investigated. Results revealed that pipe burial depth has a significant impact on all variables. Soil surface settlement increases as pipe burial depth increases. Increasing burial depth reduces pressure on pipe crown as well as pipe deflection. In addition, increasing surface pressure has a significant impact on increasing pipe deflection, soil surface settlement and pressure on pipe as expected.
- The impact of stabilization on bearing capacity and model response was also discussed. The results indicated that material stabilization improves load bearing capacity. Adding cement significantly increases ultimate bearing capacity of loading plate and decreases pipe deflection and surface settlement. Bearing capacity of the material increases from 600 kPa to almost 1100 kPa. Pipe deflection decreases from almost 6% to less than 1% after stabilization. Surface settlement also drops to one fourth of its original value after stabilization.
- Impact of stabilization on pipe vertical deflection, soil surface settlement, pressure on pipe and pipe horizontal deflection was investigated during initial and cyclic phases. Results revealed that stabilization improves model response for all cases with remarkable reduction in pipe deflection in both directions, soil settlement and stress on pipe.
- In order to assess the impact of adding cement on model behaviour, the ratio of non-treated to cement-treated for VDS, SSS and pressure on pipe was calculated. Results showed this ratio is less than 1 for all cases showing the

efficiency of adding cement in model performance. In addition, stabilization is more efficient in cyclic load than static load. It is noted the impact of cement stabilization is more remarkable with increasing the number of cycles.

- The impact of first cycle on model response was also investigated. Results showed high portion of model deformation occurs during the first cycle. However, impact of first cycle is more important in cement-treated material. Rate of model deformation for non-treated material is higher than those for cement-treated ones which results in higher values in both pipe deflection and surface settlement.
- Equations were developed using Regression model to estimate pipe vertical deflection, soil surface settlement and pressure on pipe crown based on all numerical and experimental tests data during initial phase. Equations were developed for both non-treated and cement-treaded cases. Results showed that there is a good agreement between predicted and observed values. In order to show the accuracy of results cumulative error was also calculated showing that all predicted values have less than 10% error.
- Two different methods for predicting model response for cyclic phase were employed including multiple regression method and neural network model. It was shown that while linear regression modelling approach was deficient to predict desired parameters, more accurate results were obtained using neural network model. In addition, verification of the two models and calculating errors revealed that higher errors are observed at the beginning of each cyclic phase. Cumulative error analysis showed that all predicted parameters in neural network have less than 20% error. This value for regression method is 42%.

8 CONCLUSIONS AND FUTURE RESEARCH

8.1 INTRODUTION

The main objective of this study was to investigate the performance of buried pipe subjected to traffic load. The work included physical modelling and numerical analysis. First, 31 parametric study was conducted considering some design factors affecting buried pipe response. The results were presented in terms of impact on pipe deflection, soil surface settlement, maximum earth pressure and stress in pipe wall. Then, a sensitivity analysis was performed and relative contribution of each factor was investigated to identify the most sensitive factors. The results indicated that surface pressure contribution is the most comparing to other parameters followed by burial depth and loading area. Then in the following phase of this research, the impact of burial depth and surface pressure on a buried pipe was investigated by performing a series of loading tests in laboratory and by implementing numerical modelling. The effects of various factors on the performance of pipe were also investigated.

The contribution of the current research to the state of art are summarised as follows:

- Evaluation of the effect of eight design factors on buried pipe response by implementing numerical parametric study and sensitivity analysis;
- Development of laboratory model capable of testing pipe subjected to cyclic load;

- Evaluating the effectiveness of cement stabilization on improving model performance;
- Development of numerical model to assess the response of buried pipe subjected to surface load;
- Development of equations to predict soil surface settlement, pipe vertical diametric strain and pressure on pipe using the Neural Network and Linear Regression models in Matlab;

8.2 ACHIVEMENT OF OBJECTIVES

To clarify conclusions of this research work, the results will be presented separately based on achievement objectives of this research. It is noted only significant findings will be highlighted in each section.

8.2.1 Findings from Parametric Study / In situ condition

A numerical parametric study was carried out to investigate the impact of different factors on pipe-soil behaviour subjected to surface load using ABAQUS. The effects of eight different factors such as burial depth, pressure magnitude, width of loading area, internal pressure, pipe-soil interaction properties, pipe material, wall thickness and boundary condition at the pipeline ends were investigated with in situ condition. Results were presented in terms of pipe deflection, surface settlement, and maximum stress in pipe wall as well as earth pressure on pipe crown. The parametric study was followed by a sensitivity analysis. Based on the results of 29 built in models in parametric study, following important conclusions are drawn:

- Results indicated that surface pressure has the highest contribution on model response following by burial depth and loading area. Internal pressure has the highest contribution on stress variation in pipe wall but its contributions on other factors including pipe deflection, surface settlement and earth pressure on pipe is not remarkable. Contribution of other investigating factors on model performance is not remarkable. Based on findings from parametric study burial depth impact is more considerable in the depths of H <2.5D.
- As a result, the impact of surface pressure and burial depth was selected to be investigated in the second phase of this research. The selected pipe is HDPE and burial depth varies between 1D<H <2.5D.

- The findings from this study reveal that maximum pressure on pipe occurs in the middle part of the pipe circumference or between 60^{o} to 100^{o} from crown. Applying internal pressure affects the location where maximum stress occurs.
- Replacing steel pipe with PVC and HDPE increases pipe deflection, the soil surface settlement and earth pressure on pipe. The highest pipe deflection, soil surface settlement and earth pressure was observed for HDPE pipe.

8.2.2 Findings from Experimental Analysis

Twenty six tests were conducted on a buried pipe to investigate model response during initial and cyclic phase for both non-treated and cement-treated trench materials. For this purpose, a new laboratory modeling was developed to investigate buried pipe performance comprising a large soil box to apply cyclic load on top of trench soil. To find a relationship between measured circumferential strain on pipe and pipe deflection, a compressive loading test was carried out and pipe deflection and strain were investigated using LVDT and strain gauges. Results were presented in terms of pipe deflection, soil surface settlement and earth pressure on pipe and the impact of burial depth, surface pressure and cycles were investigated.

- The impact of various factors on model response during initial phase and cyclic phase was investigated. Results revealed that pipe burial depth has a significant impact on all variables. Soil surface settlement increases as pipe burial depth increases. Increasing burial depth reduces pressure on pipe crown as well as pipe deflection. Increasing surface pressure has a significant impact on increasing pipe deflection, soil surface settlement and pressure on pipe as expected.
- The influence of stabilization on bearing capacity and model response was also discussed during initial and cyclic phases. Results revealed that stabilization improves soil bearing capacity. In addition, cement stabilization improves model performance for all cases with remarkable reduction in pipe deflection in both directions, soil settlement and stress on pipe. It was also found that stabilization is more efficient in cyclic load than static load. In addition, for cement-treated cases impact of cement stabilization is more remarkable with increasing the number of cycles meaning stabilization is more efficient under higher number of cycles.
- The impact of first cycle on model response was also investigated. Results showed that high portion of model deformation occurs during the first loading

cycle. However, the impact for cement treated materials is higher than those for non-treated ones.

8.2.3 Findings from Numerical Analysis

A series of nonlinear finite element analyses were developed to investigate model performance during initial phase. To get the input material properties, a series of direct shear tests were performed to define material strength taking into consideration the impact of curing time. All direct shear samples were cured at different curing times of 1, 7, and 28 days at room temperature. Results illustrated that adding 5% of cement at 7-day of curing time increased sand strength significantly. Drucker-Prager model and Mohr-Coulomb constitutive models were selected for numerical modelling using finite element method. Before performing simulations, validation of finite element model was performed with respect to experimental results. Results showed that the computed results based on finite element simulations matched well with the measured results in the laboratory and those achieved based on the empirical equation.

- The same conclusions were obtained in both numerical simulations and experimental investigations. The numerical simulations results agreed well with the experimental results within acceptable accuracy.
- Results of numerical simulation of soil surface settlement revealed that maximum settlement for all cases occurs on soil surface above pipe crown and the minimum value occurs over 2B distance from centre or two times of width of loading area. Both burial depth and surface pressure affect soil surface settlement. The increase in vertical stress under the centre of loading as a function of depth for all cases was investigated. Results showed that all diagrams have almost the same pattern and stress reduces in a very similar manner when burial depth increases. Results of pressure distribution on pipe circumference also showed that three different sections exist and earth pressure is maximum in the middle part around 60 degree from the crown. Bending strain variations at pipe wall were also investigated showing pipe-strain plots transitioned from positive at the invert to negative at the sides, and back to the positive at the invert. The peaks of large strain occur at the 60° position and low strains at 120° from pipe invert.
- Numerical simulations results revealed that stabilizing the trench material has an important effect on improving model performance. Stabilization increases soil bearing capacity and reduces footing displacement with lower plastic shear strains over a smaller area for cement-treated material. Stabilization

decreases pipe deflection, soil surface settlement and pressure on pipe significantly. The improvement in stress distribution due to stabilization was also observed by a decrease in the maximum stress on pipe soil interface. After stabilization lower strain occurred in the pipe and pipe deformation is more flat and restricted while in non-treated sand pipe deformation is heart-shape.

- Higher deformations occur on both vertical and horizontal sides of pipe under higher surface pressures at shallower burial depths. This causes horizontal stretching and pipe tends to deform to a 'heart shape under higher surface pressure. However, after stabilization lower strain occurs in the pipe and pipe deformation is more restricted and flatter.

8.2.4 Predicting Model Response

- During initial phase, equations were developed using Regression model to estimate pipe vertical deflection, soil surface settlement and pressure on pipe crown based on all numerical and experimental tests results for both non-treated and cement-treaded cases. Cumulative error histogram showed that all predicted values using regression model have less than 10 % error during initial phase.
- For cyclic phase, two different methods for predicting model response were employed including multiple regression and neural network model. Comparison of multiple linear regression model and neural network for predicting model response during cyclic phase revealed that while linear regression modelling approach was deficient to predict desired parameters, more accurate results were obtained using neural network model. In addition, cumulative error analysis showed that all predicted parameters in neural network have less than 20% error. This value for regression method is 42%.

8.3 SUGGESTED FUTURE RESEARCH

The research reported in this thesis could be extended in the following ways:

- In the parametric study, traffic load was considered as static load. Considering traffic load as cyclic load and investigating degradation effect on model response is recommended. It is also recommended that future work contain physical tests to validate numerical models. It was found that the model is

sensitive to internal pressure affecting stress distribution on pipe wall significantly. It is recommended this factor to be studied further in structural point of view.

- It is important to investigate the impact of other factors from parametric study such as loading area and internal pressure on model response talking into consideration the cyclic behaviour of pipe and soil by implementing appropriate constitutive models. Therefore, it is recommended to develop appropriate constitutive models under cyclic load for different materials used in this research.
- The current study in experimental section was performed in the laboratory only. Thus, a full-scale field verification is still needed.
- Pipe failure could be avoided by using more accurate factors in pipeline design to consider impact of degradation. Further research is required to develop the necessary algorithms of pipelines performance under cyclic traffic load.
- The neural networks can be used to predict pipe deflection, soil surface settlement and pressure on pipe for any combinations of input variables. It is noted that these values should be within the coverage of training in the current research. However, in the current research the number of data for number of cycles were much higher than number of other variables such as burial depths and surface pressure. The author recommends such research to be further carried out concentrating on broader range of variables in order to achieve more accurate results.

9 REFERENCES

AASHTO. (1996). Standard Specifications for Highway Bridges. Washington: American Association of State Highway and Transportation Officials, Inc.

AASHTO. (1998). American Association of State Highway and Transportation Officials (AASHTO). Washington DC USA.

ABAQUS-6.13. (2013). ABAQUS/CAE User's Manual. USA: Dassault Systèmes.

ABAQUS. (2013). Dassault Systèmes.

ABC-NEWS. (2014). Natural gas reserves and contingent resources. Retrieved from http://www.abc.net.au/news/2014-09-03/natural-gas-reserves-and-contingent-resources,-august-2014/5715466

Abo-Elnor, M., Hamilton, R., & Boyle, J. T. (2004). Simulation of soil–blade interaction for sandy soil using advanced 3D finite element analysis. *Soil and Tillage Research, 75*(1), 61-73. doi:http://dx.doi.org/10.1016/S0167-1987(03)00156-9

Abolmaali, A., & Kararam, A. (2010). Nonlinear Finite-Element-Based Investigation of the Effect of Bedding Thickness on Buried Concrete Pipe. *Journal of Transportation Engineering, 136*(9), 793-799. doi:doi:10.1061/(ASCE)TE.1943-5436.0000135

Åhnberg, H., & G, H. (2009). *Influence of laboratory procedures on properties of stabilised soil specimens*. Paper presented at the The International Symposium on Deep Mixing and Admixture Stabilization.

ASCE. (2001). Guidelines for the Design of Buried Steel Pipe: americanlifelinesalliance.

ASCE. (2009). *Buried flexible steel pipe : design and structural analysis / prepared by the Task Committee on Buried Flexible (Steel) Pipe Load Stability Criteria & Design of the Pipeline Division of the American Society of Civil Engineers*

edited by William R. Whidden. Reston, VA: Reston, VA : American Society of Civil Engineers.

ASTM-D4767. (2011). Standard Test Method for Consolidated Undrained Triaxial Compression Test for Cohesive Soils. USA.

Australian-Standard. (2001). Methods of testing soils for engineering purposes in soil strength and consolidation tests-determination of the shear strength of a soil-direct shear test using a shear box *1289.6.2.2*. Australia.

Australian-Standard. (2009). Australian Standard *Methods for sampling and testing aggregates; Particle size distribution—Sieving method*. Australia: SAI Global.

Austroads. (2012). Part 2: Pavement Structural Design. Sydney

Biana, X., Jianga, J., Chengb, C., Chena, Y., Chena, R., & Jiangb , J. (2014). Full-scale model testing on a ballastless high-speed railway under simulated train moving loads. *Soil Dynamics and Earthquake Engineering, 66*, 368-384. Retrieved from http://refhub.elsevier.com/S0266-1144(15)00092-8/sref6

Boussinesq, J. (1885). *Application des potentiels à l'étude de l'équilibre et du mouvement des solides élastiques.* . USA: University of Michigan.

Bowles, J. E. (1988). *Foundation Analysis and Design*: McGraw-Hill.

Bryden, P., El Naggar, N., & Valsangkar, A. (2015). Soil-Structure Interaction of Very Flexible Pipes: Centrifuge and Numerical Investigations. *ASCE, Int. J. Geomech., 6*(15), 1-11

Burns, J. Q., & Richard, R. M. (1964). Attenuation of Stresses for Buried Cylinders. *Symposium on Soil Structure Interaction*, 378-392.

Calvetti, F., di Prisco, C., & Nova, R. (2004). Experimental and Numerical Analysis of Soil–Pipe Interaction. *Journal of Geotechnical and Geoenvironmental Engineering, 130*(12), 1292-1299. doi:10.1061/(ASCE)1090-0241(2004)130:12(1292)

Cameron, D. A. (2005). *Analysis of Buried Flexible Pipes in Granular Backfill Subjected to Construction Traffic*: Graduate School of Engineering, University of Sydney.

Cao, Z., Han, J., Xu, C., Khatri, D. K., Corey, R., & Cai, Y. (2016). Road surface permanent deformations with a shallowly buried steel-reinforced high-density polyethylene pipe under cyclic loading. *Geotextiles and Geomembranes, 44*(1), 28-38. doi:http://dx.doi.org/10.1016/j.geotexmem.2015.06.009

Chatterjee, S., White, D. J., & Randolph, M. F. (2013). Coupled consolidation analysis of pipe–soil interactions. *Canadian Geotechnical Journal, 50*(6), 609-619. doi:10.1139/cgj-2012-0307

Cubrinovski, M., Hughes, M., Bradley, B., McCahon, I., McDonald, Y., Simpson, H., . . . O'Rourke, T. (2011). Liquefaction Impacts on Pipe Networks-Civil & Natural Resources Engineering. University of Canterbury

Dean , E. T. R. (2010). *Offshore Geotechnical Engineering*. UK: Thomas Telford

Department of Resources, E. a. T. (2012). Australian Gas Resource Assessment Geoscience Australia

ureau of Resources and Energy Economics. Australia.

EIA. (2016). Energy Information Administration Retrieved from https://www.eia.gov/analysis/studies/worldshalegas/

Enviromental Justice Atlas. (1994). Oil spills in Komi Republic, Russia. Retrieved from https://ejatlas.org/conflict/oil-spills-around-usinsk-komi-republic

Enviropipes. (2015). Product Catalogue (Second edition ed.). Australia.

Farhadi Hikooei, B. (2013). *Numerical Modeling of Pipe-Soil Interaction under Transverse Direction.* (MEng Thesis), University of Calgary, Canada.

Gonzales, S. (2016). Texas fertilizer plant blast that killed 15 was criminal act: ATF. *Reuters.*

Grace, R. (2014). Flood creates sinkhole that engulfs cars in Port Melbourne. *The Age Victoria*.

Hadi Meilani, M., Elhoud, A., Sadou, M., Bouledroua, O., & Pluvinage, G. (2015). *Degradation of sewage pipe caused Sinkhole : A real case study in a main Road*. Paper presented at the 22 ème Congrès Français de Mécanique

Heger, F. J., Liepins, A. A., & Selig, E. T. (1985). SPIDA: An analysis and design system for buried concrete pipe. *ASCE-Advances in Underground Pipeline Engineering*, 143-154.

Helwany, S. (2007). *Applied Soil Mechanics with ABAQUS*: John Wiley & Sons, INC.

Huang, Y. H. (2004). *Customers who viewed Pavement Analysis and Design* USA: University of Kentucky.

Idriss, I. M., Dobry, R., & Singh, R. D. (1978). Nonlinear Behaviour of Soft Clays During Cyclic Loading. *Geotechnical Engineering Division*(104), 1427-1447.

Järvenkylä, J. J. (1989). Thin-walled thermoplastic pipes. *Construction and Building Materials, 3*(4), 191-200. doi:https://doi.org/10.1016/0950-0618(89)90013-5

Joseph, G. (2016). 30 Years of Oil and Gas Pipeline Accidents, Mapped. Retrieved from http://www.citylab.com/weather/2016/11/30-years-of-pipeline-accidents-mapped/509066/

Jung, J., Koo, D. H., & Zhang, K. (2012). Verification of the Pipe Depth Dependent Model using a finite element analysis. *Tunnelling and Underground Space Technology*(0). doi:http://dx.doi.org/10.1016/j.tust.2012.02.024

Kamal, S. (2012). *EXPERIMENTAL AND NUMERICAL INVESTIGATIONS OF THE IMPACT OF EROSION VOIDS ON RIGID PIPES.* McGill University, Montreal, Quebec, Canada.

Kang, J., Jung, Y., & Ahn, Y. (2013). Cover requirements of thermoplastic pipes used under highways. *Composites Part B: Engineering, 55*, 184-192. doi:https://doi.org/10.1016/j.compositesb.2013.06.025

Kang, J., Parker, F., & Yoo, C. H. (2008). Soil–structure interaction for deeply buried corrugated steel pipes Part I: Embankment installation. *Engineering Structures, 30*(2), 384-392. doi:http://dx.doi.org/10.1016/j.engstruct.2007.04.014

Kararam, A. (2010). Nonlinear Finite-Element-Based Investigation of the Effect of Bedding Thickness on Buried Concrete Pipe. *Journal of Transportation Engineering, 136*(9), 793-799. doi:doi:10.1061/(ASCE)TE.1943-5436.0000135

Karimian, A. (2006). *Response of buried steel pipelines subjected to longitudinal and transverse ground movement.* (PhD), Thesis British Columbia.

Katona, M. G. (1978). CANDE: a versatile soil—structure design and analysis computer program. *Advances in Engineering Software (1978), 1*(1), 3-9. doi:https://doi.org/10.1016/0141-1195(78)90016-5

Kestler, M. A. (2009). *Stabilization Selection Guide for Aggregateand Native-Surfaced Low-Volume Roads*. Retrieved from USA:

Kido, Y., Nishimoto, S., Hayashi, H., & Hashimoto, H. (2009). *Effects of curing temperatures on the strength of cement-treated peat.* Proceedings of International Symposium on Deep Mixing and Admixture Stabilization.

King, S., & Richards, T. (2013). Solving Contact Problems with Abaqus: SIMULIA.

Kitazume, & Terashi. (2013). *The Deep Mixing Method*: Taylor & Francis.

Ko, D. H., & Kuwano, R. (2010). Model tests on behaviour of buried pipe in a large soil chamber. *Taylor and Francis group (Physical Modeling in Geotechnics)*, 625-631.

Kunert, H. G., Otegui, J. L., & Marquez, A. (2012). Nonlinear FEM strategies for modeling pipe–soil interaction. *Engineering Failure Analysis, 24*(0), 46-56. doi:http://dx.doi.org/10.1016/j.engfailanal.2012.03.008

Kvalstad, T. J., Nadim, F., & Harbitz, C. B. (2001). *Deepwater Geohazards: Geotechnical Concerns and Solutions*, Texas, USA.

Kyriakides, S., & Corona, M. (2007). *Mechanics of Offshore Pipelines* (Vol. Volume 1 Buckling and Collapse): Elsevier Science.

Lade, P., & Overton, D. (1989). Cementation effects in frictional

materials. *Journal of Geotechnical Engineering, 115*(10), 1373-1387.

Laffer, S. (2015). Burst water main at Lyons Rd, Windsor Gardens, causes flooding. In G. P. Residents watch the burst water main at the intersection of Aberdeen Ave and Lyons Rd (Ed.): Advertiser

Lee, & Sheu, S. (2007). The stiffness degradation and damping ratio evolution of Taipei Silty Clay under cyclic straining. *Soil Dynamics and Earthquake Engineering, 27*(8), 730-740. doi:https://doi.org/10.1016/j.soildyn.2006.12.008

Lee, J., Salgado, R., & Carraro, A. (2004). Stiffness degradation and shear strength of silty sands. *Canadian geotechnique, 41*, 831-843.

Lee., H. (2010). *Finite element analysis of a buried pipeline.* (Master of Science by Research), The University of Manchester , Faculty of Engineering and Physical Science.

Leng, J. (2003). *Characteristics and Behavior of Geogrid-Reinforced Aggregate under Cyclic Load.* (PhD), North Carolina State University, Raleigh

Liu, P. F., Zheng, J. Y., Zhang, B. J., & Shi, P. (2010). Failure analysis of natural gas buried X65 steel pipeline under deflection load using finite element method. *Materials & Design, 31*(3), 1384-1391. doi:http://dx.doi.org/10.1016/j.matdes.2009.08.045

Makusa, G. P. (2012). *SOIL STABILIZATION METHODS AND MATERIALS*. Retrieved from Luleå, Sweden:

Manoharan, N., & Dasgupta, S. P. (1995). Bearing capacity of surface footings by finite elements. *Computers & Structures, 54*(4), 563-586. doi:https://doi.org/10.1016/0045-7949(94)00381-C

Marston, A., & Anderson, A. O. (1913). *The theory of loads on pipes in ditches : and tests of cement and clay drain tile and sewer pipe*. Ames, Iowa: Iowa State College of Agriculture and Mechanic Arts.

MATLAB. (2015a). Natick, Massachusetts The MathWorks Inc.

McGowan, G., & Prangnell, J. (2015). A method for calculating soil pressure overlying human burials. *Journal of Archaeological Science, 53*, 12-18. doi:https://doi.org/10.1016/j.jas.2014.09.016

Moayed, Z., R, R., & E., I. (2012). Evaluation on Bearing Capacity of Ring Foundations on two-Layered Soil. *World Academy of Science, Engineering & Technology*(61), 1108.

Moghaddas Tafreshi, S. N., & Khalaj, O. (2008). Laboratory tests of small-diameter HDPE pipes buried in reinforced sand under repeated-load. *Geotextiles and*

Geomembranes, 26(2), 145-163. doi:http://dx.doi.org/10.1016/j.geotexmem.2007.06.002

Moghaddas Tafreshi, S. N., & Khalaj, O. (2011). Analysis of repeated-load laboratory tests on buried plastic pipes in sand. *Soil Dynamics and Earthquake Engineering, 31*(1), 1-15. doi:http://dx.doi.org/10.1016/j.soildyn.2010.06.016

MoncefL, N., Nedal, M., & Ahmed M, S. (2016). Investigation of buried full-scale SFRC pipes under live loads. *Construction and Building Materials, 102*, 733-742. doi:https://doi.org/10.1016/j.conbuildmat.2015.10.203

Mosadegh, A., & Nikraz, H. (2015). Bearing Capacity Evaluation of Footing on a Layered-Soil using ABAQUS. *Earth Sci Clim Change., 6*(264). doi:0.4172/2157-7617.1000264

Mosadegh, A., & Nikraz, H. (2017). BURIED PIPE RESPONSE SUBJECTED TO TRAFFIC LOAD EXPERIMENTAL AND NUMERICAL INVESTIGATIONS. *International Journal of GEOMATE, Japan, 13*(39), 1-8. doi:https://doi.org/10.21660/2017.39.91957

Mosadegh., A., & Nikraz., H. (2015). *Finite Element Analyses of Buried Pipeline Subjected to Live Load Using ABAQUS.* Geoquebec conference., Quebec City, Canada

Mosadegh., A., Szymkiewicz., F., & Nikraz., H. (2017). An Experimental Investigation of the Impact of Specimen Preparation and Curing Conditions on Cement-Treated Material Strength (Deep Mixing Method). *Taylor and Francis*.

Moser, A. P. (1990). *Buried Pipe Design*: McGraw-Hill.

Moser, A. P. (2001). *Buried Pipe Design, 2nd Edition*: Mcgraw-hill.

NCHRP. (2009). Test and Design Methods for Thermoplastic Drainage Pipe *Report 631*. Washigton DC: Transportation Research Board.

NTSB. (2016). Pipeline Accident Reports Retrieved from https://www.ntsb.gov/investigations/AccidentReports/Pages/pipeline.aspx. from National Transportation Safety Board https://www.ntsb.gov/investigations/AccidentReports/Pages/pipeline.aspx

Panda, A. P., & Rao, S. N. (1998). Undrained strength characteristics of an artificially cemented marine clay, . *Marine georesources & geotechnology, 16*, 335-353.

Parker, E. J. (2008). *Evaluation of Landslide Impact on Deepwater Submarine Pipelines.* OTC 19459, Houston, Texas.

PHMSA. (2017). Pipeline Failure Investigation Reports Retrieved from https://www.phmsa.dot.gov/

Qiao, W. (2011). Water pipeline failures: Field verification and risk-based corrosion-fracture models

Rajeev, P., & Kodikara, J. (2011). Numerical analysis of an experimental pipe buried in swelling soil. *Computers and Geotechnics, 38*(7), 897-904. doi:http://dx.doi.org/10.1016/j.compgeo.2011.06.005

Rajeev, P., Kodikara, J., Robert, D. J., Zeman, P., & Rajani, B. (2013). *FACTORS CONTRIBUTING TO LARGE DIAMETER WATER PIPE FAILURE AS EVIDENT FROM FAILURE INSPECTION*.

Randolph, M., Gaudin, C., Gourvenec, S., White, D., Boylan, N., & Cassidy, M. (2011). Recent advances in offshore geotechnics for deep water oil and gas developments. *Ocean Engineering, 38*(7), 818-834. doi:http://dx.doi.org/10.1016/j.oceaneng.2010.10.021

Randolph, M., & Gourvenec, S. (2011). *Offshore Geotechnical Engineering* UK: CRC Press.

Rathnayaka, R. M. S. U. P. (2016). *A STUDY OF WATER PRESSURE INFLUENCE ON FAILURE OF LARGE DIAMETER WATER PIPELINES.* (Doctor of Philosophy), Monash, Australia.

Roberge, P. R., & Revie, R. W. (2007). *Corrosion Inspection and Monitoring*: Wiley.

Robins, R. (2013). Australia's shale reserves among world's biggest.

Rogers, C., Fleming, PR, Loeppky, MWJ, Faragher,. (1995). The structural performance of profile-wall drainage pipe-stiffness requirements contrasted with the results of laboratory and field tests. . *Portation Research Board, Washington*, 83-92.

Rojhani, M., Moradi, M., Galandarzadeh, A., & Takada, S. (2012). Centrifuge modeling of buried continuous pipelines subjected to reverse faulting. *Canadian Geotechnical Journal, 49*(6), 659-670. doi:10.1139/t2012-022

Sétra-LCPC. (2000). Le traitement des sols à la chaux et/ou aux liants hydrauliques-Application à la réalisation des remblais et des couches de forme, guide technique. France.

Shaalan, H. H. (2014).*]parametric study of oil and gas internal pressures in buried pipes.* (Master of Science), ATILIM University, Graduate School Of Natural And Applied Sciences.

Sherwood, P. T., & Transport Research, L. (1993). *Soil stabilization with cement and lime*. London: HMSO.

Spangler, M. G. (1941). The structural design of flexible pipe culverts. Ames, Ia.: Iowa State College of Agriculture and Mechanic Arts.

Suzuki, Y., & Minai, R. (1988). Application of stochastic differential equations to seismic reliability analysis of hysteretic structures. *Probabilistic Engineering Mechanics, 3*(1), 43-52. doi:https://doi.org/10.1016/0266-8920(88)90007-0

Takacs, S. A., & Cline, E. H. (2015). *The Ancient World*: Taylor & Francis.

Tavakoli Mehrjardi, G., Moghaddas Tafreshi, S. N., & Dawson, A. (2016). Numerical analysis on Buried pipes protected by combination of geocell reinforcement and rubber-soil *International Journal of Civil Engineering, 13 (2). , 13*(2), 90-104.

Tavakoli Mehrjardi, G., Moghaddas Tafreshi, S. N., & Dawson, A. R. (2012). Combined use of geocell reinforcement and rubber–soil mixtures to improve performance of buried pipes. *Geotextiles and Geomembranes, 34*, 116-130. doi:http://dx.doi.org/10.1016/j.geotexmem.2012.05.004

Tavakoli Mehrjardi, G., Moghaddas Tafreshi, S. N., & Dawson, A. R. (2013). Pipe response in a geocell-reinforced trench and compaction considerations. *Geosynthetics International, 20*(2), 105-118. doi:10.1680/gein.13.00005

Terzaghi, K., & Peck, R. B. (1948). Soil Mechanics in Engineering Practice.

The Advertiser. (2015). *Burst water main at Lyons Rd, Windsor Gardens, causes flooding*. Retrieved from Australia:

The New York Times. (2011). Panel Seeking Answers in Fatal Pipeline Blast. Retrieved from https://www.nytimes.com/2011/03/01/us/01sanbruno.html

Trauth, M. H. (2015). *Matlab recipes for earth sciences*. New York: Springer.

Trautmann, C., & O'Rourke, T. (1985). Lateral Force-Displacement Response of Buried Pipe. *Journal of Geotechnical Engineering 111*(9), 1077-1092.

Tudorica, D. (2014). A Comparative Analysis of Various Methods of Gas, Crude Oil and Oil Derivatives Transportation. *International Journal of Sustainable Economies Management (IJSEM), 3*(1). doi:10.4018/ijsem.2014010102

Uni-Bell, P. V. C. P. A. (2012). *Handbook of PVC pipe design and construction / Uni-Bell PVC Pipe Association* (5th ed.. ed.). New York, NY: New York, NY : Industrial Press.

Vazouras, P., Karamanos, S., & Dakoulas, P. (2010). Finite elementanalysisofburiedsteelpipelinesunder strike-slip faultdisplacements. *Soil DynamicsandEarthquakeEngineering (Elsevier), 30*, 1361–1376.

Vesic, A. (1973). Analysis of Ultimate Loads of Shallow Foundations. *Soil Mechanics and Foundation, 99*(SM1), 45-73.

Yoo, C. H., & Kang, J. (2007). *Soil-structure Interaction for Deeply Buried Corrugated PVC and Steel Pipes*. IR-07-01. Highway Research Center , Aubrun University.

Yoshimura, H., Tohda, J., Shimazu, T., Nishida, H., Inoue, Y., Ko, H., & Wallen, R. B. (2010). Dynamic response of sewer pipes buried in sloping-sided ditches. *Taylor & Francis*, 663-669.

Yoshizawa H., Okumura R., Hosoya Y., Sumi M., & Yamada T. (1997). Factor affecting the quality of treated soil during execution of DMM. *Ground Improvement Geosystems, 2*, 931-937.

Zaman, M., Desa, C., & Drumm, E. (1984). Interface Model for Dynamic Soil-Structure Interaction. *Journal of Geotechnical Engineering, 110*, 1257-1273.

Zheng, J. Y., Zhang, B. J., Liu, P. F., & Wu, L. L. (2012). Failure analysis and safety evaluation of buried pipeline due to deflection of landslide process. *Engineering Failure Analysis, 25*(Supplement C), 156-168. doi:https://doi.org/10.1016/j.engfailanal.2012.05.011

Appendices

Table of Contents Page

APPENDIX A

Part 1- PUBLISHED PAPERS

Australian Journal of Civil Engineering

ISSN: 1448-8353 (Print) 2204-2245 (Online) Journal homepage: http://www.tandfonline.com/loi/tcen20

An experimental investigation of the impact of specimen preparation and curing conditions on cement-treated material strength (deep mixing method)

Ahdyeh Mosadegh, Fabien Szymkiewicz & Hamid Nikraz

To cite this article: Ahdyeh Mosadegh, Fabien Szymkiewicz & Hamid Nikraz (2017) An experimental investigation of the impact of specimen preparation and curing conditions on cement-treated material strength (deep mixing method), Australian Journal of Civil Engineering, 15:1, 49-60, DOI: 10.1080/14488353.2017.1372685

To link to this article: https://doi.org/10.1080/14488353.2017.1372685

AUSTRALIAN JOURNAL OF CIVIL ENGINEERING, 2017
VOL. 15, NO. 1, 49–60
https://doi.org/10.1080/14488353.2017.1372685

Taylor & Francis
Taylor & Francis Group

An experimental investigation of the impact of specimen preparation and curing conditions on cement-treated material strength (deep mixing method)

Ahdyeh Mosadegh[a§], Fabien Szymkiewicz[b] and Hamid Nikraz[a]

[a]Department of Civil Engineering, School of Civil and Mechanical Engineering, Curtin University, Perth, Australia; [b]Université Paris Est-IFSTTAR, Paris, France

ABSTRACT

In recent decades, the use of Deep Mixing Method (DMM) has developed considerably and its applications are increasing continuously. Although during the past few decades various DMM techniques and methods have been introduced in different projects, there are many changing parameters which make it necessary to evaluate the impact of each condition in any specific project. The present laboratory study has been carried out to determine the impact of mixer type and curing time and conditions on soil stabilised with cement as used in soil mixing methods. Three different types of soil have been used in this research. Unconfined Compression Strength (UCS) and Secant Modulus (E_{50}) were chosen to assess the impact of various parameters on soil improvement in terms of strength. Results after a 28-day curing period indicate that the type of mixing method has a slight impact on the strength of all types of cement-treated soil. It is also concluded that different curing conditions and suction using various salt solutions have a significant impact on the strength of stabilised soil.

ARTICLE HISTORY
Received 12 April 2016
Accepted 19 August 2017

KEYWORDS
Soil mixing; sand; cement; strength; curing; deep mixing

1. Introduction

Over the past 40 years, Deep Mixing Method (DMM) has seen a continuous growth and has been an economical and ecological alternative to improve soil properties for engineering infrastructures constructions. Soil mixing methods can be subdivided into four general types including deep, shallow, wet and dry mixing. Deep Soil Mixing is the mechanical mixing of *in situ* soil with cement and/or lime as a stabilising agent which creates soil-treated columns or walls and improves the engineering properties of the ground. In this method, soil treatment is performed to a minimum depth of 3 m. Shallow mixing is another method to improve soft and compressible soil properties. The treatment depth is limited to a few meters and traditionally involves the shallow subgrade stabilisation in road constructions. For both deep and shallow mixing methods, there are two different mixing methods: the existing soil which has to be improved can be mixed mechanically either with a cement-based slurry (wet method) or dry additives such as cement and lime (dry method) are added (Massarsch and Topolnicki 2005).

In deep mixing which is the method used for this study, shear strength increases by reducing the compressibility of the soil structure which produces a low permeability ground type. This method has usually been applied for the improvement of soil in embankments, foundations elements (temporary or permanent), bridge and wind turbine foundations, excavation stabilisation, secant walls and barriers, slope stabilisation, encapsulation and immobilisation of pollutants (Indraratna 1996; Porbaha, Tanaka, and Kobayashi 1998). The general expectation of using DMM is a significant change to the properties of the soil such as increasing soil strength, change in water content, density, permeability, elastic modulus and limitation of settlement (Bouazza et al. 2006). Many researches were performed to investigate the impact of different parameters on soil-cemented strength in deep mixing. The main parameters affecting soil strength investigated by researchers are soil and binder physical and organic properties (Kitazume and Terashi 2013), curing condition (Babasaki et al. 1996; Hirabayashi et al. 2009; Kitazume and Terashi 2013), mixing method including mixing time and speed (Kitazume and Terashi 2013), mellowing time (Åhnberg 2009; Marzano, Al-Tabbaa, and Grisolia 2009), soil compaction (Åhnberg 2009; Hirabayashi et al. 2009; Kitazume and Nishimura 2009), mixing procedure (Kitazume and Terashi 2013; Szymkiewicz et al. 2012; Yoshizawa et al. 1997) and mixing tools (Åhnberg 2009; Larsson 2003; Szymkiewicz 2011).

This paper focuses on the impact of some laboratory factors including mixing methods, curing time, curing condition and relative humidity on the strength of cement-treated material in deep mixing. In order to analyse the reason for mixer impact on soil-cement strength, density variation of all mixtures and the relation between

CONTACT Ahdyeh Mosadegh ahdyeh.mosadegh@postgrad.curtin.edu.au
[§]École des ponts ParisTech & IFSTTAR, Paris, France

secant modulus of all material and unconfined compressive strength were discussed and analysed.

2. Materials and methods

This laboratory study has been carried out in order to determine the impact of mixer type, curing conditions on the stabilised soil strength. The unconfined compression strength test on cylindrical samples has been chosen to analyse soil–cement strength. In the following section, materials used in this research are presented. Then, the methods and different curing conditions investigated in this study will be discussed and finally the results of several laboratory tests will be presented followed by discussion and analysis.

2.1. Soil and binder

In this section, characteristics of different materials used in this study will be presented. These materials are Fontainebleau sand, kaolinite and cement. It is noted this article is part of a research programme that took place in a research centre called IFSTAR in Paris; therefore, the materials were selected from local resources and Fontainebleau sand is a French reference sand commonly used for geotechnical researches.

Fontainebleau sand is a uniform sand consisting of fine and rounded particles with an average mean particle size of D_{50}#0.2 and Dmax#0.4 mm. This sand is a reference sand in France, commonly used by many French universities and for many geotechnical researches. The other soil is kaolinite, which was chosen for its extremely high fines content (more than 80% of the particles are smaller than 2 mm), as well as its low plasticity.

The grain size distribution curves were determined by tests carried out according to French standards NF P 94-056 (AFNOR 1996) and NF P 94-057 (AFNOR 1992), grain size distribution curves are presented in Figures 1 and 2. Chemical proprieties of the kaolinite are presented in Table 1. The soil has a neutral pH of (7.5 ± 0.5). In addition to basic characterisation tests, Methylene Blue Adsorption (MBA) test was performed in order to better analyse the mineralogical composition of kaolinite and the amount of methylene blue adsorbed by a given mass of clay was MBA = 1.25. For stabilisation purposes, cement was chosen as the stabiliser and it is classified as CEM III/C 32.5 NCE PM-ES NF which is the cement commonly used in France for foundation works.

2.2. Sample preparation

In this study, three types of cement-treated mixtures including 'Fontainebleau sand-cement', 'kaolinite–cement' and Fontainebleau sand-kaolinite-cement' were used. For the last mixture or sand-kaolinite-cement, the percentage of each soil was 50%. Other mixture properties including cement and water content of each mixture are presented in Table 2. It should be noted that DMM is a method that is implemented without compaction. It means that the material should be self-compacting or they should be fluid enough to flow under its own weight. In general, water is an essential material in deep mixing and in case of cementitious material, *C/W* or ratio of cement to water is important. It is also noted that the material's workability limit varies greatly with cement content. The lower the cement to water ratio, the higher

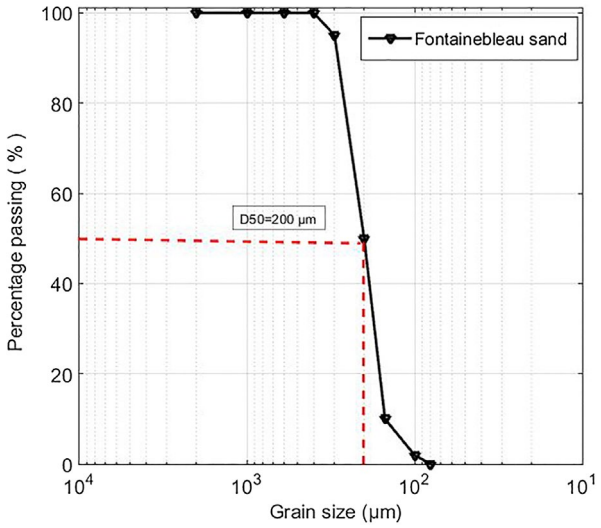

Figure 1. Particle distribution of Fontainebleau sand.

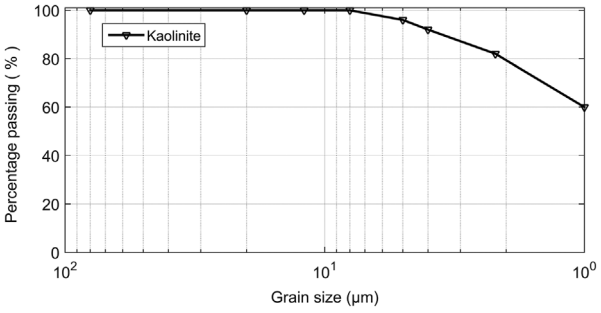

Figure 2. Particle distribution of kaolinite.

Table 1. Chemical composition of kaolinite.

Chemical component	Percentage of component
Al_2O_3	38.6
SiO_2	46.1
Fe_2O_3	0.5
TiO_2	0.7
K_2O	0.01
Na_2O	0.2
CaO	0.01

Table 2. Mixtures Properties.

Soil type	Cement (kg/m3)	W (%)	C/W
Fontainebleau sand	265	19	0.73
kaolinite (Clay)	400	120	0.21
Fontainebleau – kaolinite (50–50)	210	65	0.2

the void ratio and the lower the strength; thus, W must be at least equal to liquid limit of the mix. Therefore, it is possible, knowing only the plasticity index of the soil to be treated, to estimate the optimum amount of water to add to the mix, after having previously determined the dosage of cement to be used. To determine the workability evolution of the material, the result of a laboratory research programme carried out by Szymkiewicz et al. was adopted for this study. More details can be found in (Szymkiewicz 2011; Szymkiewicz et al. 2013).

2.3. Mixing process

A mixer should be capable of mixing soil and binder uniformly. Two types of mixers, small and grand, were chosen to mix the soil and binder as shown in Figure 3. The small mixer is a variable speed 5-L mixer which is used for preparation of mixtures of not very high viscosity according to EN 196-1 ('NF EN 196-1,' 1988). The rotation speed is 230 rpm and machine power is 300 W.

The grand mixer is a variable speed 12-L mixer. This mixer is recommended in French standard NF P 94-093 to be used for mixing stabilised soil (AFNOR 1999, 2003). It has two options of slow and fast mixing while both movements of tank and shaft cutter ensuring perfect homogenisation. The slow speed was selected and to achieve a better level of mixing, homogenisation was also performed manually by operator while mixing. This grand mixer has a power of 2800 W.

For uniform mixing, soil was first inserted in the mixer. Then, an appropriate amount of cement was put into the mixer and materials were homogenised in a dry state and at the end water was added. Mixing time varies based on type of soil and was selected 5 minutes for granular soils and 15 min for cohesive ones. These times were defined based on various trial tests carried out during the first stage of the research (see Szymkiewicz 2011). Also, the literature available on the subject was a big help to define these times. The main goal was to achieve, for both mixer, the highest strength possible. And it is well known that extending the mixing time does not automatically equal to increasing the strength. After some time, a plateau is reached. These mixing times remain unchanged during this study.

2.4. Moulding

In the following step, the homogenised material was poured in an appropriate mould by filling the mould in three layers through tapping against the surface of a table to remove air bubbles. The lightweight plastic mould of 52-mm diameter and 110-mm height was chosen considering the height of specimen was set to be 2.0–2.5 times of the diameter, as shown in Figure 4.

Figure 3. Electric mixers (a) small mixer with flat-type binder (b) grand mixer and sharp binder.

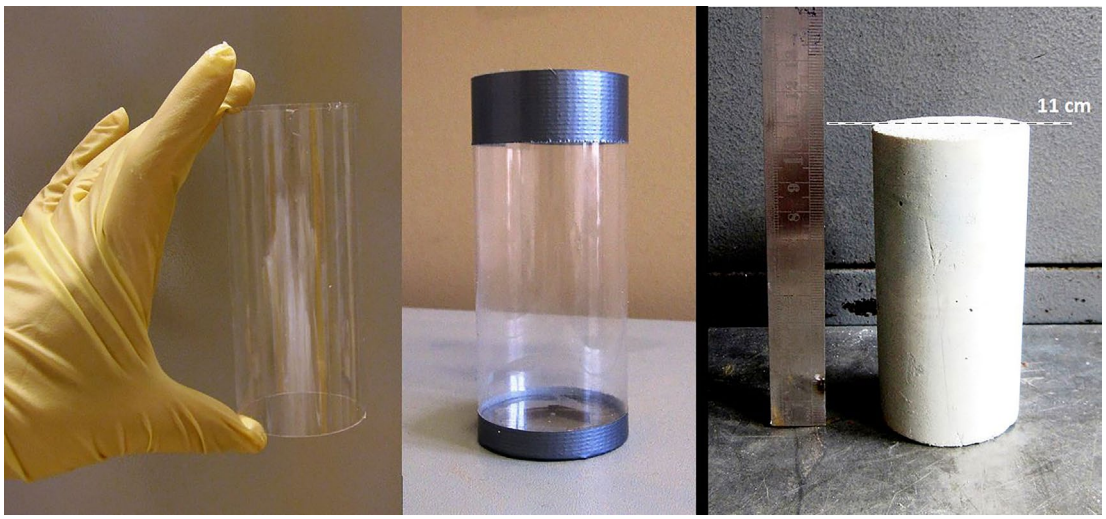

Figure 4. Different stages of specimen preparation.

2.5. Curing conditions

All cement-treated samples were stored in three different curing conditions of humid, submerged and under suction conditions. In humid condition, the specimens in the mould were covered by sealant to prevent the change of water content and cured at ~20 °C over a prescribed curing period (Figure 5(a)). In submerged condition, the specimens were submerged in a container of tap water after removal from their moulds (Figure 5(b)). In suction-controlled condition, the removed specimen was put in sealed containers with different salt solutions in order to create different relative humidity (RH) conditions (Figure 5(c)). The desired relative humidity selected in this research was 0, 29, 55 and 76% and salts selected to produce this humidity are listed in Table 3. The suction values that can be achieved in the specimen range from 37 to 250 MPa. The glass desiccators were then placed in a room temperature for 14 and 28 days at 20°. Abbreviations cited in Table 4 present type of soils, mixing process and curing conditions. Each symbol consists of three parts separated by dash line. First part presents material type in which *FS*, *K* and *SK* symbolise Fontainebleau sand, kaolinite and sand–kaolinite materials, respectively. Second part presents type of mixing method in which *GM* and *SM* are represent preparation by grand or small mixer. Third part indicates curing condition in which *H*, *S* and *C* are symbols of humid, submerged and crystallised conditions. For example, FS-GM-H denotes Fontainebleau sand material prepared by grand mixer and kept under humid condition.

2.6. Unconfined compressive testing

The stabilised soil specimens are mostly used for the Unconfined Compression (UCS) test to measure some factors affecting strength increase of cement-treated materials. In order to conduct the UCS test, all samples were removed from the mould and the dimensions and weight were measured to calculate the density of each sample. The vertical load was applied on specimen with the speed of 0.3 mm/min and test was performed based on *NF EN 13286-41* standard which is a French guideline applicable to determine the compressive strength of mixtures treated with hydraulic binders (AFNOR 2003).

3. Experimental results

To study the influence of different parameters, the results of UCS test based on different types of preparation and curing conditions are presented in the following section. The average of unconfined compressive strength (UCS) values of triplicate samples is presented as the final result. It is worth noting that to assess the impact of each parameter on sample strength, only one parameter changed while the others remained constant. For example, to consider the impact of mixing process, two mixing methods were used while curing condition for all mixtures remained unchanged. However, for considering the impact of humidity, five different salts were used on samples prepared by same mixer but under different curing conditions and humidity. All samples were treated with cement and UCS test were carried out at room temperature.

3.1. Influence of mixing processes

To assess the impact of mixing conditions, UCS tests were carried out on samples cured under humid conditions at different curing times. Results are presented in Figure 6. The charts compare the average of UCS values on three mixtures of soil-treated samples prepared by small and grand mixers and are tested after 7, 14, 21 and 28 days curing time. In all three charts (Figure 6(a)–(c)), black and white bars present the UCS average of grand and small mixers, respectively. Results show that the strength of all samples prepared by grand mixer is higher than those prepared by small one at any curing time except for kaolinite-treated at 14 days. Moreover, this result is consistent with the results of other researches showing the importance of mixing procedures (Babasaki et al. 1996; Coull 1997; Kitazume and Terashi 2013; Larsson 2003; Szymkiewicz et al. 2011).

Figure 5. Different curing conditions (a) humid (b) submerged and (c) crystallised.

Table 3. Salts and relative humidity.

Chemical	Relative humidity
Silica gel	0
$CaCl_2$, 2 H_2O	29
$Mg(NO_3)$,$6H_2O$	55
NaCl	76

3.2. Impact of curing time

To assess the impact of curing time, the UCS of all samples (excluding those cured under suction) prepared by two mixers at different curing times of 7, 14, 21 and 28 days are measured and results are shown in Figure 7. For sand (Figure 7(a)), the compressive strength increases from 2000 to 2500 kPa at 7 days to 4000–5000 kPa at 28 days for all four different curing conditions. For kaolinite- and Fontainebleau sand-kaolinite (Figure 7(b) and (c))-treated materials, there is a significant increase in strength from 600 to 2100 kPa and from 700 to 2100 kPa, respectively. These results show that curing time has a major impact on strength increase of cement-treated material, with a continuous increase of strength with time. Results presented here are in good agreement with those presented by other researchers, in terms of strength gain ratio between 7, 14 and 28 days (Åhnberg 2009; Kido et al. 2009; Kitazume and Terashi 2013; Yoshizawa et al. 1997)

3.3. Impact of relative humidity

It is recommended to cure samples at 95–100% relative humidity to have the most appropriate results (Kitazume and Terashi 2013). However, it is not always possible to keep relative humidity at 95–100% for stabilisation purposes. In addition, the difference between strength of samples under different curing conditions which will be illustrated in Figure 10 could be due to humidity level of samples. Therefore, it is important to consider the impact of relative humidity on strength variation of soil-treated materials. Because of time constrains, the impact of relative humidity in the curing conditions was only investigated on sand–cement samples: results are presented in Figure 8. As mentioned previously, samples were kept under suction control condition and were put in sealed containers with different salt solutions to create various relative humidity. It can be seen that for both groups, 14 and 28 days, the higher the relative humidity, the higher the strength, except for samples kept under 0% relative humidity. For all other samples, reducing relative humidity leads to a decrease in material strength. To assess the efficiency of salts in inducing suction, the density of sand-treated mixture was calculated and results of 28 days sand-treated samples are plotted in Figure 9. The graph shows that density increases with increasing relative humidity confirming all salts had reasonable impact on reducing humidity and creating suction in samples. This result is also consistent with UCS results presented in Figure 8. The impact of humidity on other mixtures was not investigated here. However, considering the impact of material could affect the results. Thus, it is recommended that impact of humidity on other mixtures be considered in the future.

3.4. Impact of immersion

To consider the impact of immersion on soil-treated strength, the results of UCS test after submerging specimens are presented in Figure 10. Darker bar charts present soil strength after immersion for both mixer groups. It can be seen that immersion causes a decrease in UCS compared to humid condition apart from sand-treated material at 21 and 28 days prepared by grand mixer. For all other samples prepared by small mixer, the strength of submerged soil is lower than those kept in humid conditions. Similar results were obtained by other researchers (Yoshizawa et al. 1997).

4. Analysis and discussion

In the previous section, it was concluded that the strength of samples changes with type of mixer. To assess the exact effect of mixers on soil strength, the N value was determined and defined as below:

$$N = R_{c-GM}/R_{c-SM} \quad (1)$$

in which $R_{C\text{-}GM}$ is the UCS strength of mixtures achieved by grand mixer and $R_{c\text{-}SM}$ is the UCS strength of samples prepared by small mixer and N is calculated based on Equation (1) and results are presented in the Table 5. It should be noted that in Table 5, N is average of all 3 samples prepared at 7, 14, 21 and 28 days. It is clear that N is always bigger than 1, meaning the grand mixer is more efficient than the small one. In addition, grand

Table 4. Scheme of tests and symbols.

Soil type	Mixing conditions	Curing conditions	Symbol	Soil type	Curing conditions	Symbol	Soil type	Curing conditions	Symbol
Fontainebleau sand	Grand mixer	Humid	FS-GM-H	kaolinite	Humid	K-GM-H	Fontainebleau sand- kaolinite	Humid	SK-GM-H
		Submerged	FS-GM-S		Submerged	K-GM-S		–	–
		Crystallised	FS-GM-C		–	–		–	–
	Small Mixer	Humid	FS-SM-H		Humid	K-SM-H		Humid	SK-SM-H
		Submerged	FS-SM-S		Submerged	K-SM-S		Submerged	SK-SM-S
		Crystallised	FS-SM-C		–	–		–	–

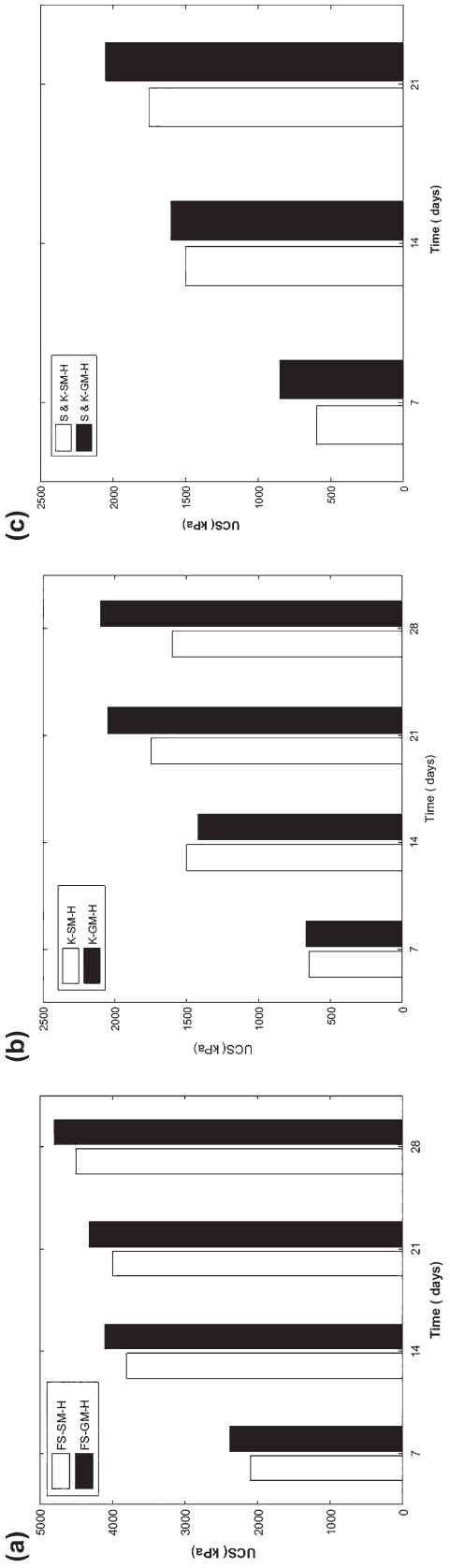

Figure 6. Impact of mixing method on cement-treated material (a) Fontainebleau sand (b) Kaolinite (c) Fontainebleau sand-kaolinite under humid conditions.

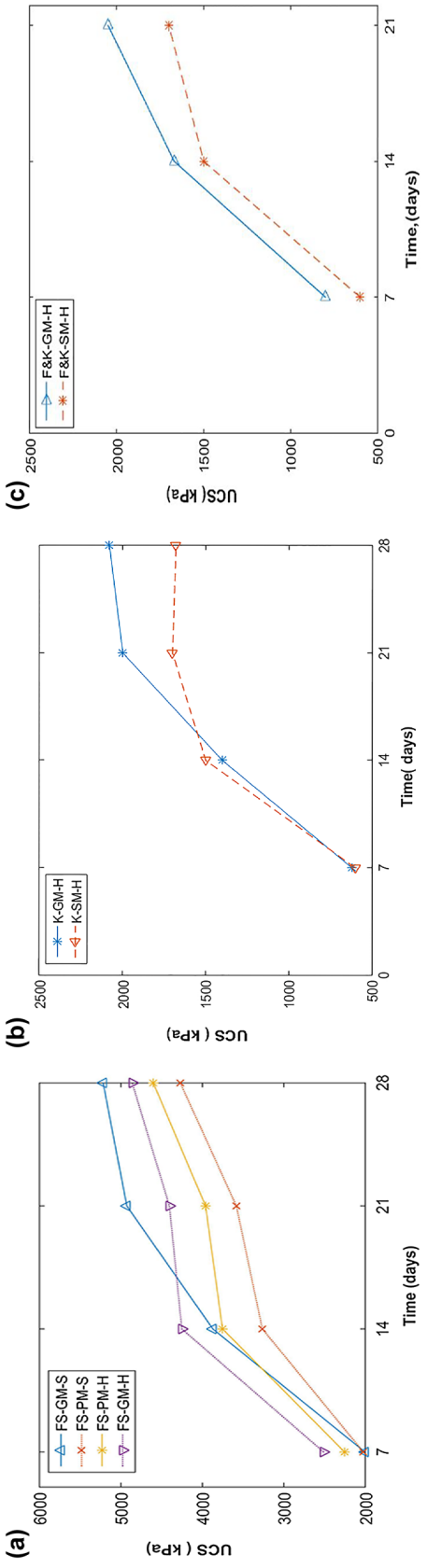

Figure 7. Strength versus curing period (a) Fontainebleau sand (b) Kaolinite-cement (c) Fontainebleau-Kaolinite-cement treated.

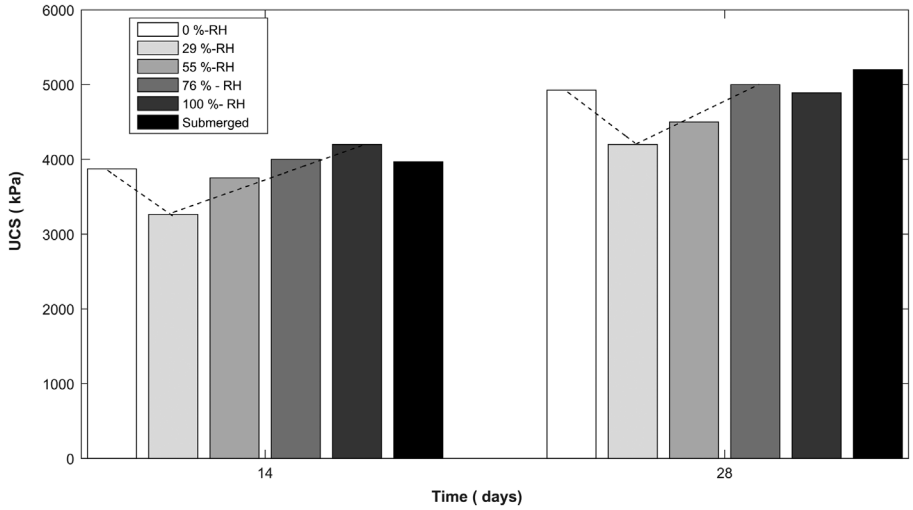

Figure 8. Influence of relative humidity on sand–cement-treated material strength at room temperature.

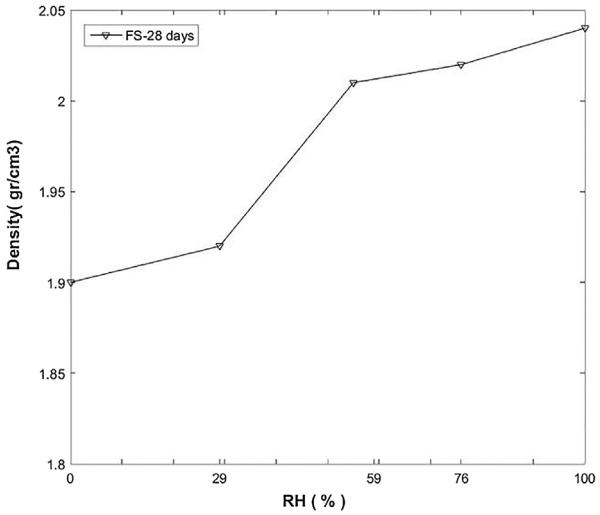

Figure 9. Density versus relative humidity – Sand.

Table 5. Mixer type effect.

Soil	Curing condition	*N*
Fontainebleau sand	FS-GM-H FS-SM-H $N=R_{c\text{-}GM}/R_{c\text{-}SM}$	1.11
Kaolinite	K-GM-H K-SM-H $N=R_{c\text{-}GM}/R_{c\text{-}SM}$	1.15
Fontainebleau sand- kaolinite	S-K-GM-H S-K -SM-H $N=R_{c\text{-}GM}/R_{c\text{-}SM}$	1.21

mixer is more efficient for clayey material as *N* has bigger value when kaolinite quantities increase in the mixture.

To consider the reason why the strength of samples prepared by bigger mixer is higher than those prepared by smaller one, the following section will focus on density variation and determining E_{50} which could be a tool to understand the reason of mixer impact.

As said before, *N* for clayey soils is bigger than *N* for sand soil. For example, for sand- and clay-treated material, *N* is 1.11 and 1.21, respectively, which means the strength of clayey material prepared by bigger mixer is higher. This can be explained by the fact that the mixers, for a same mixing time, do not deliver the same amount of mixing energy. Therefore, the GM is more appropriate for the clayey soils.

4.1. Density

The density of material prepared at different curing and preparing conditions is investigated and results are illustrated in Figure 11. The Figure 11(a) shows that neither time nor submerged or humid curing conditions has an impact on density change. However, soil density changes with the type of soil (Figure 11(b)) and by relative humidity (as shown in Figure 9). It can be seen that the average density value for Fontainebleau-, kaolinite- and sand-kaolinite-treated material was 2.05, 1.45 and 1.62 gr/m^3, respectively. Average density changes with relative humidity as well. For the specimen prepared at 0%, RH density is 1.9 gr/cm^3 and with increasing relative humidity to 100%, density increases to 2.04 gr/cm^3. Therefore, it is difficult to conclude how the mixer type affects the results. It is also important to investigate other factors' impact on soil strength such as energy of mixing and geometry of mixer tool which could affect the soil strength results. The combination of all these factors could be the reason and the study of these factors would be interesting to be assessed in future studies.

4.2. Secant modulus E_{50}

The secant modulus (E_{50}) values are obtained from the stress–strain curves and defined as the ratio between the half of maximum deviator stress and the strain corresponding to each stress (Eurosoilstab 2002). The impact of mixer type on material elasticity change is investigated and results are shown in Figure 12. Vertical axis represents E_{50} and horizontal axis represents the UCS of

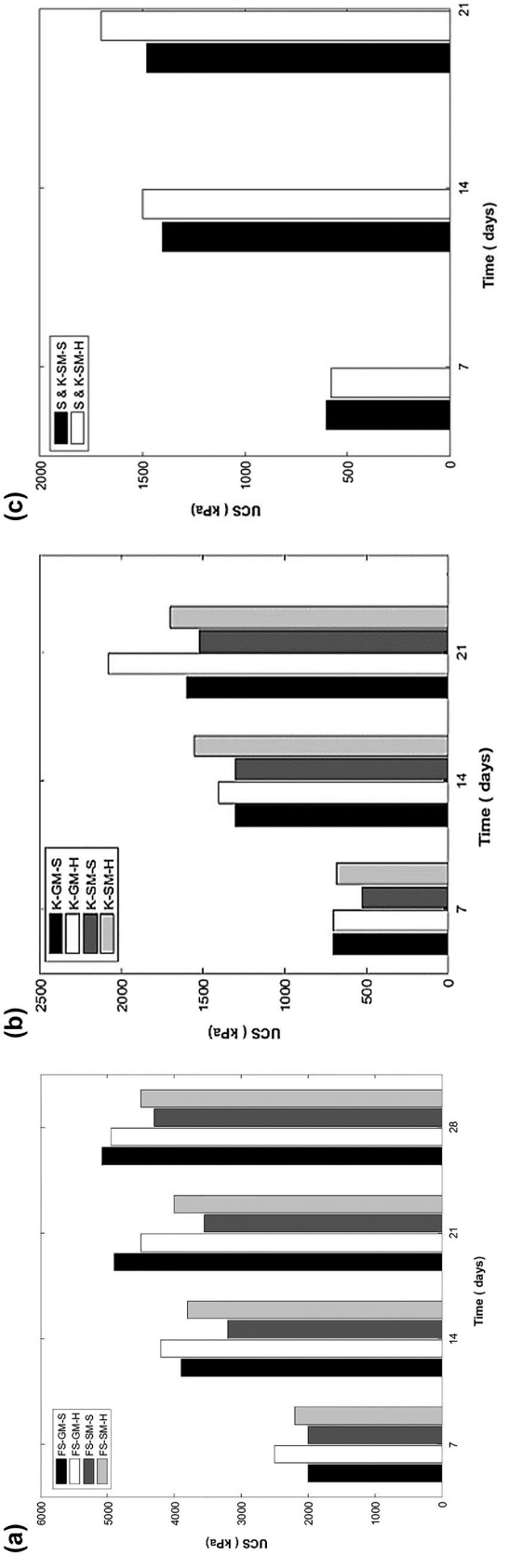

Figure 10. Immersion impact on the strength of (a) Fontainebleau sand-cement (b) Kaolinite-cement (c) Sand and kaolinite-cement material.

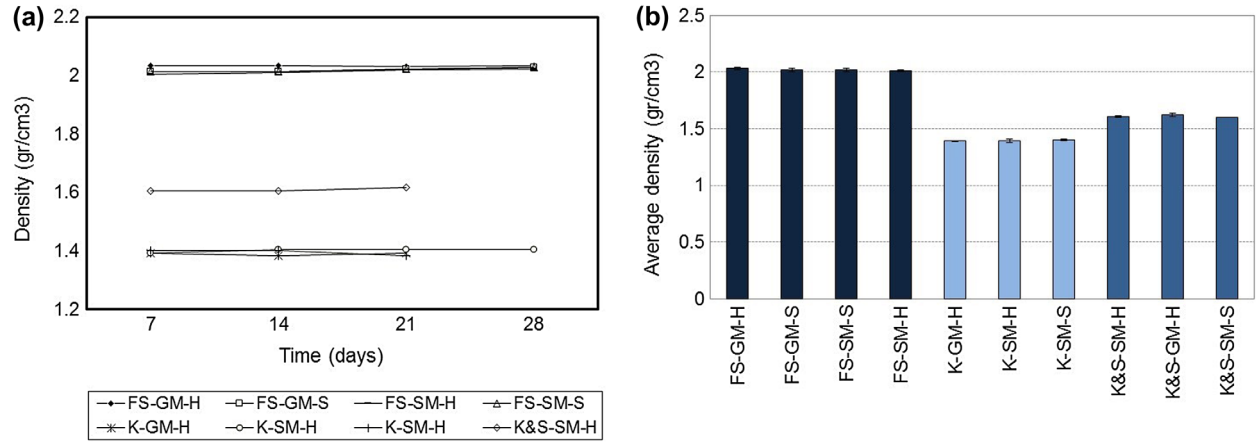

Figure 11. Change of density with (a) time (b) type of soil and curing conditions.

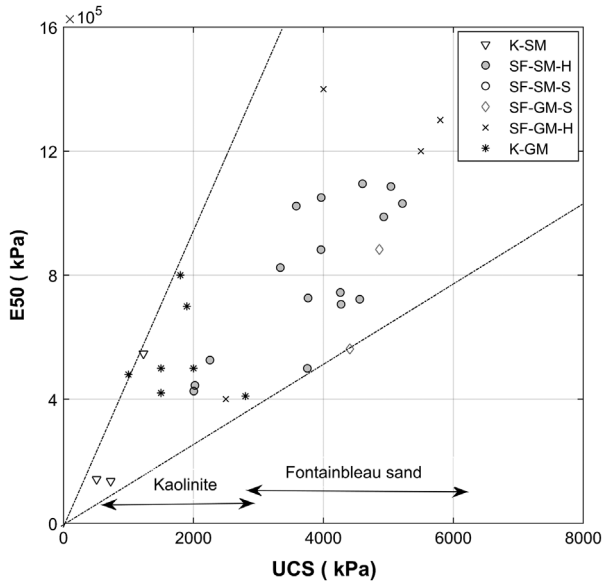

Figure 12. E_{50} versus UCS based on type of soil.

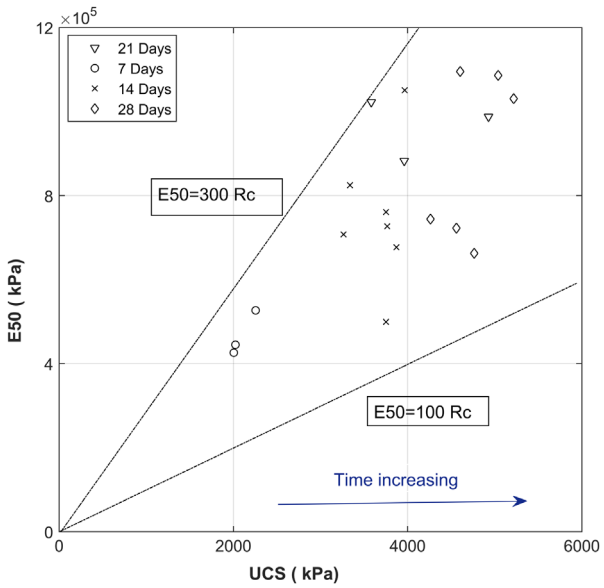

Figure 13. E_{50} versus UCS changes based on curing time – Fontainebleau sand-treated.

samples. It is noted that circle and triangle markers illustrate small mixer and diamond, asterisk and cross-markers denote grand mixers' deformation modulus. It can be seen that the mixer type has no significant impact on the sample modulus variations. As shown in Figure 12, the data points of the plot are spread out across the graph regardless of mixer type. However, type of soil has a significant impact on treated soil deformability and higher material strength and deformation modulus are observed for sand material as shown in Figure 12. The impact of curing time on material modulus is investigated and results are shown in Figure 13. It can be seen that both UCS and E_{50} increase by time and at 28 days curing, the values of E_{50} are at least two times higher than those cured at 7 days which shows the impact of curing time on increasing $E_{50.}$ It is noted that a linear relationship between E_{50} and the UCS exists which is shown as dashed lines on both graphs. It can be concluded in this study that the magnitude of E_{50} increases with UCS and is 125–500 UCS depending on type of soil and curing time. These intervals values are consistent with those proposed by other researchers in the literature. (Porbaha, Shibuya, and Kishida 2000; Terashi 1977).

5. Conclusions

Laboratory study for three types of soil stabilised with cement was conducted to investigate the improvement in compressive strength based on mixing method and curing conditions for application in Deep Soil Mixing Method. Two types of mixer and different curing conditions were studied and results were compared. Based on the test results, specific conclusions can be drawn as follows:

- The strength of all samples prepared with grand mixer is higher than those prepared by small mixer at any curing time. The density of specimens does not change with mixer type which makes it difficult to conclude the main reason for strengths

variation by two mixers. This difference might be related to the energy of mixing or the geometry of tools which would be of interest to be furthered.
- For all samples the strength decreases by submerging samples except for sandy samples which were prepared by grand mixer at 21 and 28 days of curing.
- As it is expected, the curing time has a significant effect on the improvement of compressive strength of all cement-treated material.
- The results of UCS test for the specimens kept under different relative humidity show that the higher the humidity, the higher the strength except for sample which was kept under 0% humidity.
- Results obtained from unconfined compressive strength test are consistent with the results obtained from E_{50} values and E_{50} has a similar trend with UCS results. As mentioned previously, mixer type has no impact on the samples modulus variations, while type of soil does.
- With increasing $E_{50,}$ UCS increases and an approximate relationship of 100–500 UCS was found between E_{50} and UCS. In addition, the ratio of $E_{50}/_{UCS}$ is higher for clayey material than sandy ones. Those results are in accordance with past studies from other researchers.
- It would be interesting to study further the importance of different factors such as viscosity of liquids, distribution of suspensions and external forces which might affect soil strength in different mixing methods.

Disclosure statement

No potential conflict of interest was reported by the authors.

Notes on contributors

Ahdyeh Mosadegh is a PhD candidate at Curtin University working on soil behaviour, numerical and experimental aspects. Cyclic behaviour of pipe–soil interaction is the main part of her research. She graduated with a master's degree in Geotechnical Engineering from Ecole National des Ponts et Chaussées in France 2010. Previously, she finished her first master's in Road & Transportation from University of Tehran, 2007. She has worked over eight years in civil engi-neering such as design and supervision of different infra-structures, performing research projects in Iran and France. Currently, she is doing a doctoral research under the supervi-sion of Hamid Nikraz in Civil Engineering School of Curtin University. Her research interests are soil stabilisation, finite element analysis focusing on buried pipe and soil deep mix-ing stabilisations.

Fabien Szymkiewicz is a researcher at French institute of science and technology for transport, development and networks (IFFSTAR) in Paris, France. He obtained his PhD at University of Paris-Est in France in 2011. His interests in particular are related to the topics of foundations and soil improvement. He has work experience in running educational activities and developing protocols. He also teaches Geotechnics and Soil Mechanics at the Ecole Spéciale des Travaux Publics (ESTP), and has supervised many students during their internships. His research has led to numerous publications and presentations at conferences in France and abroad.

Hamid Nikraz is a professor at the Department of Civil Engineering, School of Engineering, Curtin University, Australia. Prior to his academic career, he had many years of experience working in industry in the Middle East, Europe and Australia. He has provided numerous consultancy services in his field to over 200 organisations nationally and internationally. He obtained his PhD at Curtin University of Technology in 1989. Nikraz is a fellow member of the Institution of Engineers Australia with over 400 publications in various journals, books and conference proceedings. Nikraz has initiated research works in the area of Geopolymers, Concrete, Soil Stabilisation and Pavement Engineering. Nikraz is also the reviewer of many national and international journals.

References

AFNOR. 1992. *NF P 94-057. Sols: reconnaissance et essais – Analyse granulométrique des sols – Méthode par sédimentation*, Paris, France.

AFNOR. 1996. *NF P 94-056. Sols : reconnaissance et essais – Analyse granulométrique – Méthode par tamisage à sec après lavage*, Paris, France.

AFNOR. 1999. *Détermination des références de compactage d'un matériau*, Paris, France.

AFNOR. 2003. *Mélanges traités et mélanges non traités aux liants hydrauliques -Partie 41: méthode d'essai pour la détermination de la résistance à la compression des mélanges traités aux liants hydrauliques*, Paris, France.

Åhnberg, H. H. G. 2009. "Influence of Laboratory Procedures on Properties of Stabilised Soil Specimens." Paper presented at the The International Symposium on Deep Mixing and Admixture Stabilization.

Babasaki, R., M. Terashi, T. Suzuki, A. Maekawa, M. Kawamura, and E. Fukazawa. 1996. "Factors Influencing the Strength of Improved Soil." *Japanese Geotechnical Society Technical Committee Reports* 2: 913–918.

Bouazza, A., A. Haque, P. Kwan, and G. Chapman. 2006. "Strength Improvement of Coode Island Sand by the Soil Mixing Method." *Australian Geomechanics, 41*(3): 101–106.

Coull, M. 1997. *The Use of Deep Mixing Methods to Improve Foundations for Port Structures and Their Application to the Dalian Grain Terminal Project*. Canterbury: University of Canterbury.

Eurosoilstab. 2002. *The Deep Mixing Method: Principle, Design and Construction*. Swedish Ministry of Transport: Taylor & Francis.

Hirabayashi, H., H. Taguchi, S. Tokunaga, N. Shinkawa, T. Fujita, H. Inagawa, and N. Yasuoka. 2009. *Laboratory Mixing Tests on Cement Slurry Preparation, Specimen Preparation and Curing Temperature*.

Indraratna, B. 1996. "Utilization of Lime, Slag and Fly Ash for Improvement of a Colluvial Soil in New South Wales."

Australia. Geotechnical & Geological Engineering 14 (3): 169–191. doi:10.1007/BF00452946.

Kido, Y., S. Nishimoto, H. Hayashi, and H. Hashimoto 2009. "Effects of Curing Temperatures on the Strength of Cement-treated Peat." In *Proceedings of International Symposium on Deep Mixing and Admixture Stabilization*.

Kitazume, Masaki, and S. Nishimura. 2009. "Influence of Specimen Preparation and Curing Conditions on Unconfined Compression Behaviour of Cement-treated Clay." In *Proceedings of International Symposium on Deep Mixing and Admixture Stabilization*.

Kitazume, M., and M. Terashi. 2013. *The Deep Mixing Method*. Swedish Ministry of Transport: Taylor & Francis.

Larsson, A. 2003. *Mixing Processes for Ground Improvement by Deep Mixing*.

Marzano, I., Al-Tabbaa, A., and Grisolia, M. 2009. "Influence of Sample Preparation on the Strength of Cement-stabilised Clays." In *Proceedings of Deep Mixing '09, Okinawa*.

Massarsch, K. R., and M. Topolnicki. 2005. "Regional Report: European Practice of Soil Mixing Technology." In *Proceedings of International Conference on Deep Mixing*, Vol. 1, R1 – R28. Stockholm, Accessed May 23 – 25 2005.

NF EN 196-1. 1988. *Méthodes d'essais des ciments- - Partie 1: détermination des résistances mécaniques*. France.

Porbaha, A., H. Tanaka, and M. Kobayashi. 1998. "State of the Art in Deep Mixing Technology: Part II. Applications." *Proceedings of the ICE-Ground Improvement* 2 (3): 125–139.

Porbaha, A., Shibuya, S., and Kishida, T. 2000. "State of the Art in Deep Mixing Technology. Part III: Geomaterial Characterization." *Proceedings of the ICE-Ground Improvement* 4 (3): 91–110.

Szymkiewicz, F. 2011. "Évaluation des propriétés mécaniques d'un sol traité au ciment." PhD thesis, Université Paris-Est, Paris, France.

Szymkiewicz, F., A. Guimond-Barrett, A. Pantet, F. Reiffsteck, F. Szymkiewicz, J. Mosser, and A. Lekouby. 2011. *Influence des conditions de mélange et de cure sur les caractéristiques de sols traités au ciment par soil mixing*.

Szymkiewicz, F., A. Guimond-Barrett, A. Le Kouby, and P. Reiffsteck. 2012. "Influence of Grain Size Distribution and Cement Content on the Strength and Aging of Treated Sandy Soils." *European Journal of Environmental and Civil Engineering* 16: 882–902.

Szymkiewicz, F., A. Guimond-Barrett, A. Le Kouby, and P. Reiffsteck. 2013. "Optimization of Strength and Homogeneity of Deep Mixing Material by the Determination of Workability Limit and Optimum Water Content." *Canadian Geotechnical Journal* 50 (10): 1034–1043.

Terashi, M. 1977. "Deep Mixing Method-brief State-of-the-art." 14th International Conference on Soil Mechanicsand Foundation Engineering.

Yoshizawa, H., R. Okumura, Y. Hosoya, M. Sumi, and Yamada, T. 1997. "Factor Affecting the Quality of Treated Soil During Execution of DMM." *Ground Improvement Geosystems* 2: 931–937.

Earth Science & Climatic Change

Mosadegh and Nikraz, J Earth Sci Clim Change 2015, 6:3
http://dx.doi.org/10.4172/2157-7617.1000264

Research Article Open Access

Bearing Capacity Evaluation of Footing on a Layered - Soil using ABAQUS

Mosadegh A* and Nikraz H

Department of Civil Engineering, Curtin University, Australia

Abstract

In this paper, finite element method (FEM) is applied to calculate bearing capacity of a strip footing on one-layer and two-layer soil.To investigate the effect of various parameters on soil failure mechanism under the footing a commercial finite element software, ABAQUS, has been used. Soil profile contains two soil types including sand and clay. Soil behaviour is represented by the elasto-plastic Drucker-Prager model and footing material is assumed isotropic and linear elastic. For a homogenous soil profile, the effect of soil properties such as dilation angel, initial condition and footing roughness on soil failure mechanism under the footingare assessed. For a one-layer case, the bearing capacity also is calculated which has a good agreement with Terzaghi's equation. For a layered soil, soft-over-strong soil, the effect of layer thickness, soil shear strength and material property on bearing capacity value and failure mechanism of footing is investigated. It is concluded that the bearing capacity of footing decreases as the height of clayey soil increases whilst the displacement under footing increases. There is a critical depth where the stronger bottom layer does not affect ultimate bearing capacity and failure mechanism of footing.

Keywords: Bearing capacity; FEM; strip footing; one-layer soil; two-layer soil

Introduction

Geotechnical engineers often should solve problems in layered soil while the majority of existing studies have mostly focused on homogeneous continuum [1,2]. Predicting ultimate bearing capacity of footings on layered soil is very important as it is a requirement for any design and the failure mechanism of soil under footing and the bearing capacity value mainly depend on soil properties of each layer and the layer thickness. Terzaghi and Peck for the first time in 1948 [1] analysed strip footing behaviour on sand overlaying clay which followed by many researchers. Methods of solving bearing capacity of footing are classified in four major approaches: limit equilibrium, limit analysis approach, semi empirical approach and finite element method. In recent years, Finite Element Method (FEM) have been widely using in geotechnical studies to investigate soil behaviour[3-6]. In practice, for bearing capacity analysis engineers are seeking less complicated solutions to simplify computations as experimental analysis is time consuming and commonly used solutions such as limit equilibrium are no longer applicable. Therefore, computer programs developed based on the finite element method have been receiving much attention over recent decades as the powerful tool for solving complex cases. Hence, the application of FEM to evaluate bearing capacity evaluation of a footing on a layered soil is the objective of this study.

In the current study after describing problem definition, the bearing capacity analysis of a strip footing on one-layer soil will be presented. In addition, the effect of different parameters on soil failure mechanism and on bearing capacity value will be discussed. Then, in the following section the bearing capacity analysis of a two-layer-soil will be presented and the results will be compared with the results from the literature. Computations will be carried out using a commercial finite element software ABAQUS, version 6.13[7]. Finally, the conclusions and final remarks will be discussed in the last section of this study.

Materials and Methods

Following section presentes problem definition and the methodology used for modelling of footing. Due to the long length of the foundation compared to its width, the problem can be analysed assuming plane strain conditions and because of symmetry only half of the system can be modelled.

Two different main cases will be investigated in this paper. In the first case, it is assumed that foundation is resting on one-layer soil and in the second one there is a two-layer system. For the first case, it is assumed that the one- layer system is sandy soil and footing overlays on Soil (2). For this case, to validate FE results, bearing capacity value of soil will be compared with Terzaghi calculation [1]. In addition, the effect of three different parameters on soil behaviour under the footing will be considered for one-layer system. The parameters those effects will be taken into considerations are footing type, dilation angel and initial condition. For analysing the effect of footing, once the footing will be modelled as a rigid rough footing with no horizontal movement of soil immediately under footing and once as a rigid smooth one which implies horizontal soil movements at soil-footing interface. Then, for invesigating the effect of dilation angel the effect of three dilation angel of 0º, 10 º and 25º will be taken into considerations.

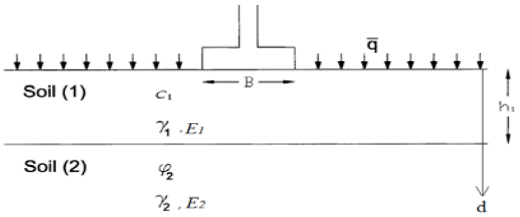

Figure 1: Problem definition

***Corresponding author:** Mosadegh A, Department of Civil Engineering, Curtin University, Australia, Tel: (+618) 9266 2631; E-mail: ahdyeh.mosadegh@postgrad.curtin.edu.au

Received February 22, 2015; **Accepted** February 26, 2015; **Published** March 06, 2015

Citation: Mosadegh A, Nikraz H (2015) Bearing Capacity Evaluation of Footing on a Layered-Soil using ABAQUS. J Earth Sci Clim Change 6: 264. doi:10.4172/2157-7617.1000264

And in the third case the effect of K_0 or initial conditions on bearing capacity of soil will be studied considering K_0 values of 0.4, 1 and 10.

For analysing two-layer soil as a second case it is assumed that the clayey soil is resting on top of the sandy soil and the footing is sitting on top of clayey soil. Based on Figure 1, Soil (1) is clayey and Soil (2) is sandy. It should be pointed out that for this case the effect of clay depth on bearing capacity value will be investigated considering clay depth, h_1, has different thicknesses and h_1/B has the value of 0.15, 0.5, 1 and 1.5 in which B is total width of footing. For one–layer case soil is modelled as an isotropic ealsto-plastic material satisfying Drucker-Prager failure criterionadapted from Helwany which presented in Table.1[8]. For comparing with Terzaghi's equation for a one-layer sand, it is assumed that soil layer is replaced with the overburden of q= ϒ.D=9.60 kPa due to a 0.5-m-thick foundation. For the top clayey layer soil parameters are adapted from Ziaei et al. [9].

It is worth noting that for plane strain considerations, the Mohr-Coulomb parameters and Drucker-Prager parameters are converted to each other based on existing formulations as follows [8]:

$$\tan\beta' = \frac{3\sqrt{3}\tan\phi'}{\sqrt{9+12\tan^2\phi'}} \text{ and } d' = \frac{3\sqrt{3}C'}{\sqrt{9+12\tan^2\phi'}}.$$

β' and d' are representing friction and cohession in Drucker-Prager model. As is illustrates in Figure 2, only half of the system is modelled due to symmetry. The length and height of the model are large enough to keep the boundary conditions away from affecting soil behaviour incorrectly. It should be noted that in this study, the X-Y plane is the area in which the soil is subjected to various loads, e.g. positive direction for Y is opposite direction of the weight. For boundary conditions, as shown in Figure 2, vertical side of the model is fixed in a horizontal direction with vertical displacement, and the bottom of the model is fixed in both vertical and horizontal directions. In all models, the mesh has been refined in areas with stress concentration under and near the footing, which leads to more accurate answers. However, the smaller the elements are, the larger the computational time is needed. For this purpose and to achieve the reasonable number of meshes, mesh convergence study was carried out. It was found from the results that a model of 510 elements is accurate enough for this problem. The element adjacent to the footing, as shown in Figure 2, has the width of w=0.13m which is small enough for analysis according to Day and Potts [10].

Table 1: Material Properties of Sandy soil-Drucker-Prager

Type of soil	Term	Value
Soil (2)	Density, ϒ (kg/m³)	1920
	Young's Modulus, E' (MPa)	182
	Poisson's Ratio, ϑ	0.3
	Cohesive strength, d' (kPa)	<1
	Friction angle, β' (plane strain), (deg)	46°
	Dilation angle, ψ (deg)	4°
	Flow stress ratio, K	1

Table 2: Material Properties of clayey soil Mohr-Coulomb

Type of soil	Term	Value
Soil (1)	Density, ϒ (kg/m³)	1600
	Young's Modulus, E' (MPa)	5
	Poisson's Ratio, ϑ	0.3
	Cohesive strength, C' (kPa)	20
	Dilation angle, ψ' (deg)	5°
	Dilation angle, ψ,(deg)	1°

The model is created in three steps. In the first step which is the initial condition, all boundary conditions are defined as described previously and surcharge load is applied on top of the model. In the next step, a geostatic step is applied in which the gravity load is applied to the model. In the third step, a downward movement of δ/B=0.1 is applied on top of the soil under footing where δ is vertical displacement and B is the width of footing. It should be noted that the duration for this lstep is 100 seconds to avoid sudden collapse of soil body. Moreover, it is assumed that relative movement between soil and footing is impossible.

During the generation of initial condition and stress prior to loading of footing, a lateral pressure coefficient of K_o is calculated based on following formulation for sand and clay. According to Jaky's formula $K_0=1-sin\Phi$ for the sand and $K_0=0.95-sin\Phi$ for the clay [11]. So for this study K_0 is 0.4 for the sand and 0.86 for the clay due to 37.5° and 5° friction angel of sand and clay, respectively. A short–term stability of footing in particular is considered, so the sand is assumed to be fully drained and the clay is considered to be undrained.

Results

In the following sections the effect of different parameters summarised in Table 3 are investigated on the failure mechanism and bearing capacity of footing. Firstly, the bearing capacity assessment of one-layer soil will be presented and the effect of parameters variation on one-layer soil behaviour will be discussed and then in the following section for a two-layer soil, the effect of soil parameters and depth of top layer on bearing capacity value and on failure mechanism will be argued.

Table3. Variables of the study

Different footing configurations	Constant parameter	Variable parameter
Case I One-Layer: sand	Geometry of model, Width of footing Soil properties-Table1	Footing roughness and properties Dilation angel ψ=0°; 10°; 25° Initial condition; K_o=0.4; 1;10
Case II Two-Layer: Clay-over-Sand	Width of footing Soil properties-Tables 1 and 2	$\frac{h1}{B}$ = 0.15; 0.5; 1; 1.5; 2 C_u

$\frac{h1}{B}$ =The ratio of clay depth to footing width

Bearing capacity ealuation of of footing on one-layer soil

As discussed earlier, the footing undergoes a downward movement of δ/B=0.1 during 100 seconds while in the beginning of the analysis there is only gravity load and surcharge applying to the soil body. This downward movement leads to an increase in pressure under the footing up to failure point. In Figure 3-a general shear failure of soil under footing based on Terzaghi model is illustrated. It can be easily noticed from Figure 3-a that there are three different distinct area zones under the footing at failure point: triangular zone immediately under the footing; two radial zones, and two Rankine passive zones[1]. The result of plastic shear at failure point of footing in the present study is illustrated in Figure 3.b. Immediately the existence of different areas in failure zone can be noticed under the footing which is in a good agreement with the failure mechanism suggested by Terzaghi. Terzaghi also derived the bearing capacity equation for a shallow strip footing on a thick layer of homogeneous soil based on general shear failure:

$$q_u = C'N_c + qN_q + 0.5\gamma BN_\gamma$$
$$Nq = e^{\pi \tan\Phi'} tan^2(45 + \frac{\Phi'}{2})$$
$$Nc = (Nq - 1)Cot\ \Phi'$$
$$N\gamma = (Nq - 1)tan\ 1.4\ \varphi'$$

C' is cohesion, q is overburden pressure, Nc, Nq and N are non-dimensionl bearing capacity of footing as a function of ϕ .

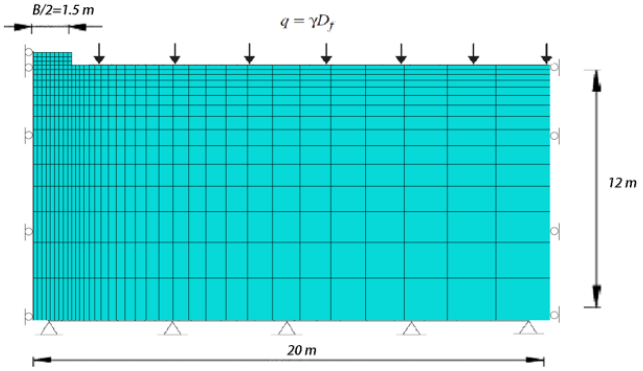

Figure 2: Finite element discretization and boundary condition selection of the model

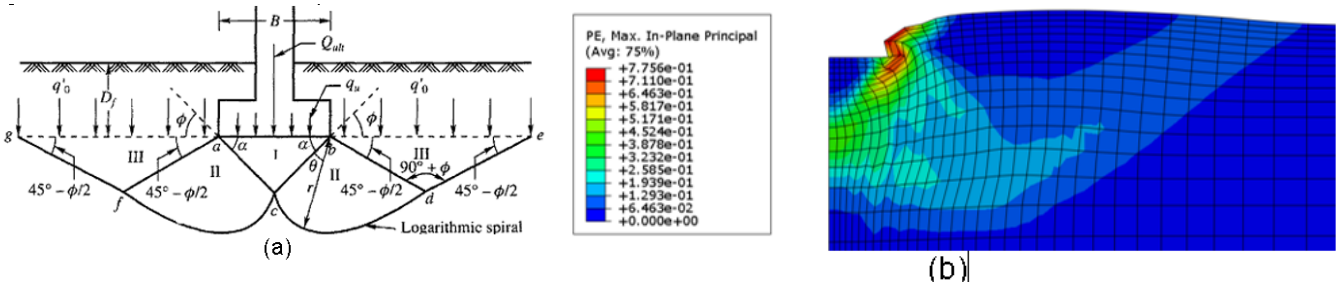

Figure. 3- (a) General Shear failure of a strip footing: Terzaghi's assumption (**b)** Plastic shear distribution of stip footing at failure

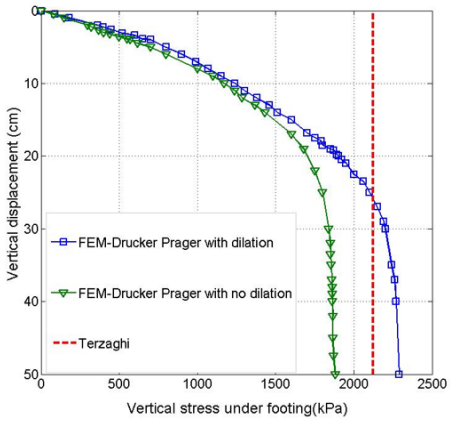

Figure 4: Load-displacement curve under centre of footing: comparison of FEM results with Terzaghi calculation

Figure 4 illustrates pressure–settlement curve results through FEM analysis and the results are compared with bearing capacity calculated based on Terzaghi method. It should be noted that for FEM analysis the curves are based on the results using Drucker-Prager model, once dilation angel is taken into consideration and once without considering that. It can be seen that in FEM analysis with considering dilation angel the bearing capacity value is 2200 kPa while in the case of no dilation angel the predicted bearing capacity is 1900 kPa. In other words, the bearing capacity in FEM analysis with dilation angel is 13% higher than those with no dilation angel. The bearing capacity calculated through Terzaghi equation is 2124 kPa which is slightly smaller than those obtained by FEM analysis with dilation angel and is higher than those calculated by FEM analysis without dilation angel. The main reason of this difference can be due to different assumptions in the methods used, e.g. in Terzaghi's equation soil is assumed to be perfectly plastic while in current finite element analysis soil is an elasto-plastic material. The results found in the current study are in good agreement with the results achieved by other researchers in the past[12] [13]. It should be noted in this section the dilation angel is assumed to be 4° which is equal to ϕ-34° [14].

Effect of footing roughness on failure mechanism and soil settlement

To evaluate the effect of soil interface on soil failure mechanism, three analyses are carried out for the case of non-dilatants one-layer soil. The results for smooth and rough interface of a rigid and flexible footing are presented in Figure 5. In all cases footing is subjected to a load control situation (ΔFy) and ΔU and Δv are representing horizontal and vertical movement of footing. As can be seen in Figure 5 horizontal movement occur at the soil interface immediately under the smooth footing, Figures 5-a and 5-c, while for the rough footing there is no horizontal movements due to boundary conditions, Figure 5-b. In addition, for the flexible footing maximum settlement occurs at the edge of footing, 5-c, while for rigid footing it happens under footing considering longer arrows show maximum displacement. It is clear that soil failure mechanism in rigid case for rough footing, Figure 5-b, is deeper and wider than those for smooth ones. These results are in a good agreement with the results presented by other researchers in the past[15]. It should be noted that the effect of interaction between two parts was not taken into consideration.

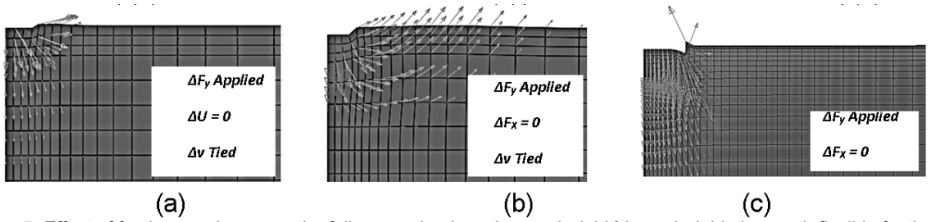

Figure 5: Effect of footing roughness on the failure mechanism **a)** smooth rigid **b)** rough rigid **c**) smooth flexible footing

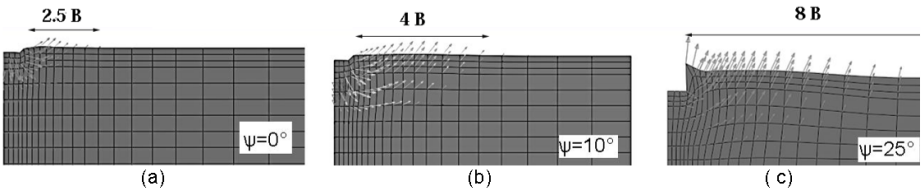

Figure 6: Effect of dilation on failure mechanism of a strip footing on cohesion-less soil

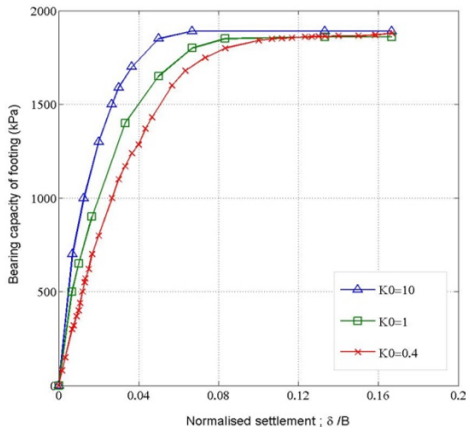

Figure 7: Effect of K_0 on load displacement behavior

Effect of dilation angel on failure mechanism

The vectors of incremental displacement for the last increment of a smooth footing are shown in the Figure 6. As can be seen with increasing dilation angel from 0º to 25º the failure mechanism width increases from 2.5 B to 8B. In other words, for all cases the failure mechanism is deeper and wider when dilation angel is higher. In addition, the higher the dilation angel is, the more the tangential angel appears besides footing edge. As was illustrated in Figure 4 dilation angel has an important effect on the bearing capacity value showing a satisfactory agreement with results from the literature [16].

Effect of initial condition on failure mechanism

To investigate the effect of K_0 or initial condition, the analysis with rigid footing is repeated with K_0 value of 1.0, and 10 for smooth footing with no dilation angel. The results of load- displacement curves are shown in Figure 7. It is evident that the value of K_0 has an impact on load displacement curve prior to failure but not on ultimate bearing capacity value.

Evaluation of bearing capacity in a two-Layer soil

In the following section, ultimate bearing capacity prediction of a strip footing on two-layer soil is presented. Footing material is assumed to be linear-elastic, rigid, rough resting on a two-layer system in which top layer is clayey soil with soil parameters matches to Mohr-Coulomb plasticity presented in Table 2. It should be noted that the parameters of a Drucker-Prager and Mohr-Coulomb can be converted to each other based on existing formulation presented earlier. Soil parameters for the bottom layer or sand are based on Table 1. However, those parameters were converted to Mohr Coloumb and parameters for sand are chossien of zero and friction of 37.5º. Other elastic parameters are based on Tables 1 and 2.

Effect of clay depth on bearing capacity and displacement

This section investigates the effect of clay thickness at five different clay depth of h_1/B varying between 0.15, 0.5, 1, 1.5 and 2 times footing width on bearing capacity value and on vertical settlement of footing and results are shown in Figure 8.

Figure 8.a illustrates the effect of adding clay on bearing capacity reduction of the footing. As is shown bearing capacity drops from 1900 kPa to 530 kPa by adding 45 cm of clay layer, h_1/B =0.15, showing a dramatic fall of %70 in bearing capacity reduction. Figure 8.b shows the effect of change in clay depth on bearing capacity by considering h_1/B =0.15, 0.5, 1, 1.5 and 2. It can be seen that the bearing capacity drops from 530 kPa to 250 kPa when h_1/B increases from 0.15 to 0.5. Increasing h_1/B from 0.5 to 1.5 leads a reduction of 100 kPa in bearing capacity and bearing capacity goes down to 150 kPa at h_1/B=1.5. After this point increasing h_1/B has no effect on bearing capacity. In other words, the depth for which the bottom layer strength does not affect the bearing capacity value of the entire model is when h_1 reaches 4.5 m or h_1/B=1.5. Figure 8.c presents the effect of clay thickness on soil displacement under the footing. For this purpose, 140 kPa of pressure has been applied on top of footing to analyse soil displacement behaviour under the same load pressure at different clay depths. This pressure has been selected due to weight of footing plus weight of any machinery on top of it. With increasing depth of clay from h_1/B=0.15 to 1.5, the vertical settlement under footing increases from 8 to 20 cm and increasing h_1/B from 1.5 to 2 causes a reduction in displacement from 20 to 18 cm showing displacement does not increse after h_1/B=1.5. The displacement reaches its peak at depth of 4.5 m or when h_1/B=1.5. These results have a good agreement with results published by other researchers [1], [14], [9]. So far the effect of various parameters on bearing capacity of footing on a layered soil has been investigated. The effect of both initial condition and depth of clayey soil on bearing capacity of

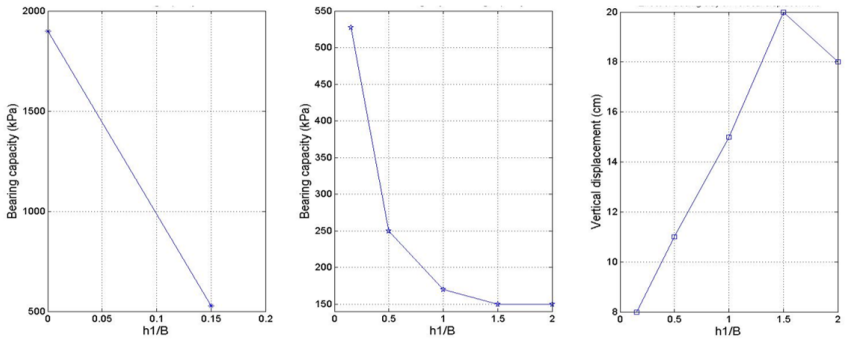

Figure 8: The effect of increasing h_1/B **a)** and **b)** changes in bearing capacity and **c)** changes in displacement

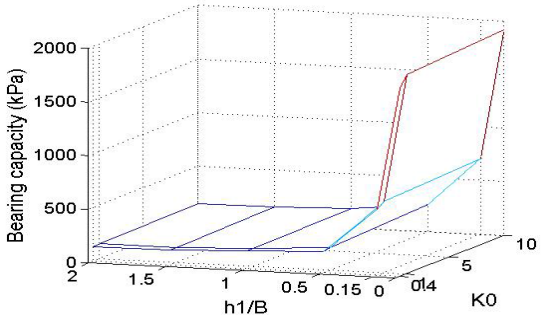

Figure 9: Comparison of depth effect and initial condition on total bearing capacity of footing in layered soil

layered soil has been compared and results are shown in Figure 9. It can be seen that when h_1/B= 0.15 or is constant, bearing capacity varies between 1800 to 1920 kPa considering K_0 varies between 0.4 to 10. When K0 is constant at 0.4, the bearing capacity decreases dramatically from 1900 kPa to 150 kPa when h_1/B increases from 0 to 2. It means that depth of clay layer has much more effective influence on bearing capacity of footing compared with initial condition.

Effect of soil layer parameters on vertical stress distribution

Figure 10 provides increase in vertical stress as a function of depth directly under the footing from z=0 to 8m which z is representing the depth. Increase in vertical stress distribution calculation is carried out for two cases based on FEM. For FEM analysis, the first case is a homogenous case considering E_2/E_1=1 and the results will be compared with those calculated from Boussinesq solutions [18]. And the second one is a two-layer soil when top layer is clayey soil with E_2/E_1=30, considering h_1=0.45. To validate the results with Boussinesq solution in FEM analysis it is assumed soil is weightless. At top of the soil profile the load of q=12 KN/m^2 or 12 kPa is applied which is due to weight of a 3-m-wide concrete footing. The increase in vertical stress under centre of footing is plotted and results are shown in Figure 9. It can be seen that for a one-layer soil both diagrams; Boussinesq and FEM; have almost the same pattern especially for deeper depths (Z>2m) although FEM solution has higher values than Boussinesq solution. These differences can be because of different assumptions in two approaches here, e.g. in Boussinesq formulation the soil is assumed to be linear elastic isotropic while in nature and in this study soil is assumed to be elasto-plastic. For a layered system, E_2/E_1 =30, when the surface layer is weaker then vertical stresses in upper layer exceeds the Boussinesq values.

At the interface, the vertical stress goes down to less that 4kPa from almost 13kPa or dropped to less than 70% of its origin value. This means first layer transfers less vertical stress to the second layer. In other words, the effect of the strength of bottom layer has less contribution to stress distribution when the upper soil becomes weaker compared to the bottom layer. In addition, for deeper values and near to depth of 8 m all graphs tend to have the same value of 4 kPa.

Figure 11 shows the effect of clay depth on stress distribution at four different values of h_1/B =0.15, 0.5, 1 and 1.5. It can be seen that for smaller value of h_1/B, e.g., for the value of 0.15 stress is higher near earth surface: almost 550 kPa, and moving from soil surface toward soil depth leads to a decrease in stress: to 200 kPa at the depth of 8m. It should be noted for the depth of more than 6 metres h_1/B variation has small effect on vertical stress distribution and all graphs tend to have same values.

Shear strength effect of clay on failure mechanism development

In Figure 12 the results of plastic shear strain are plotted at failure point for smooth rigid footing for the case of clay-over-sand. The interface of two layers is shown with a dark line in each figure. As a quick review, it is obvious that failure mechanism is deeper when h_1/B is higher. It should be noted that in the present method it is assumed that soil with elasto-plastic behaviour deforms under load while footing as a rigid body does not. In addition, soil element yields progressively in soil body from any element to the next element and a shear surface can be obtained as shown in Figure 12. It can be seen from Figure 12a when h_1 is smaller, the failure mechanism does not only shrink into the top layer.

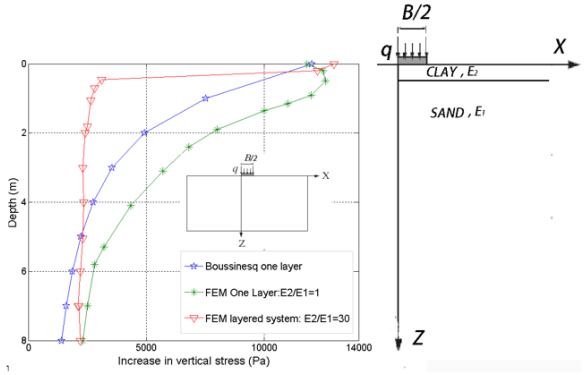

Figure 10: Increase in vertical stress distribution on soil profile of one layer and layered system

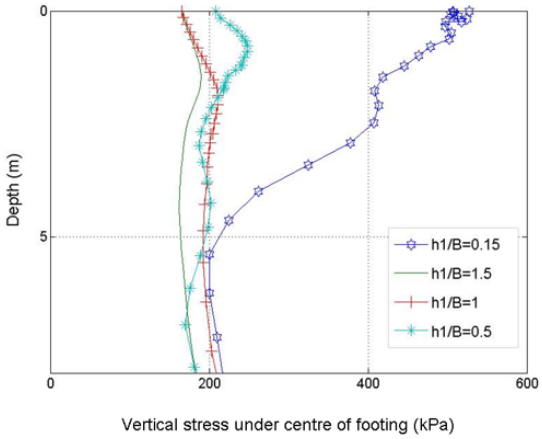

Figure 11: Vertical stress distribution on soil profile of one layer and layered system

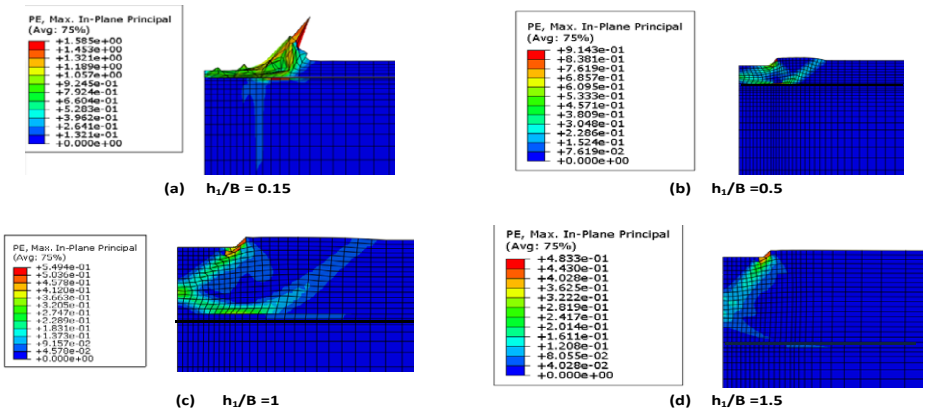

Figure 12: Plastic strain distribution at failure point

In other words, for the smaller value of h_1/B plastic zone goes to bottom layer and does not stay only in top layer. With increasing h_1, the plastic zone only stays in top layer and bottom layer's strength has no effect on bearing capacity value after specific depth. The plastic zone tends to stay in top layer as the height of weak soil increases and does not go to the stronger layer which aggresses well with results obtained by Potts et al. [16] and Zhu [2].

The summary of clay depth effect on plastic shear strain value, PE, is shown in Figure 13. It can be seen that the smallest thikckness of clay layer, h_1/B=0.1 has the maximum plastic shear strain of 1.5 % and increasing clay depth to 0.5, 1 and 1.5 leads to a decrease in plastic shear strain going down to 0.9, 0.54 and 0.48 % .

Effect of material properties on magnitude and direction of displacement

Figure.14 illustrates displacement vectors at failure for clay-over-sand and sandy soil in the case of smooth rigid footing under same magnitude downward displacement applying on both footings.

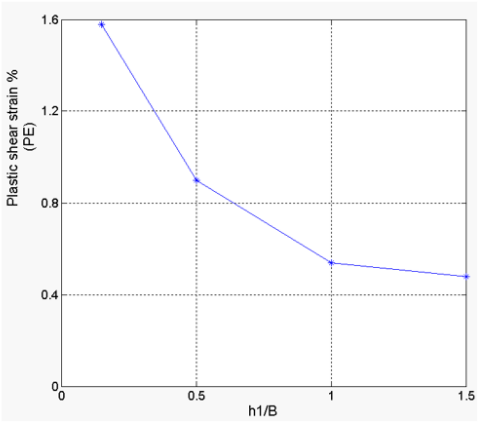

Figure 13: Effect of clay depth on shear strain distribution value

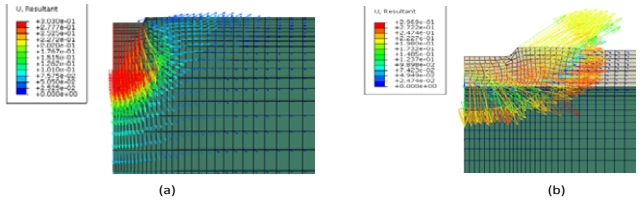

Figure 14: Vectors of displacement at failure (a) sand-on-top and (b) clay–on-top profiles

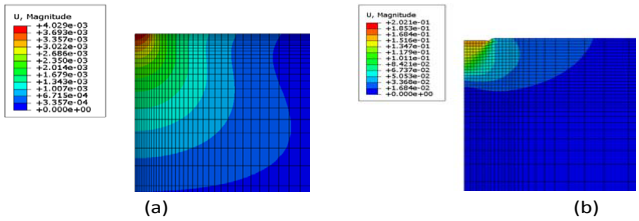

Figure 15: Displacement value under same pressure (a) sandy soil and (b) clay–on-top of sand

It can be seen that the displacement at top of the surface near the footing has a downward direction in sandy soil, Figure 14a, while in clayey soil displacement vectors are about 45° to the horizontal axis, Figure 14b. These results have a good agreement with those obtained by Ziaei et al. [9] and Potts [6]. It should be noted that in both cases same displacement value has been applied on top of soil.

In addition, after applying the same pressure on top of soil, 140 kPa, displacement under both footings is observed and the results are illustrated in Figure 15. It can be seen that under same pressure, maximum displacement in clayey soil is almost 50 times higher than those happen in sandy soil. In other words, in the case of $h_1/B=0.5$ the displacement under footing has a value of 0.2 m for clayey soil, Figure 15b, while under same pressure only 0.004 m displacement occurs in sandy soil, Figure 15a.

Conclusions

In this paper, a numerical analysis was carried out to investigate the influence of different parameters on ultimate bearing capacity of layered soil and on soil failure mechanism. The soil was modelled as an elasto- plastic material and computation were carried out using FEM software, ABAQUS.

For homogenous soil profile, the effect of soil parameters such as dilation angel, footing roughness and initial condition was studied on soil behaviour. It is found that with increasing dilation angel the wider and the deeper failure mechanism is accrued under the footing. In addition the failure mechanism for rough interaction is deeper and wider than those for smooth ones. The initial condition, K_0, has an effect on soil behaviour before failure but has no effect on bearing capacity value.

The bearing capacity value of one-layer sandy soil obtained through ABAQUS was compared with those predicted by Terzaghi's equation. It is concluded that for FEM analysis, the values for bearing capacity with considering dilation angel is 13% higher than those with no dilation and bearing capacity obtained by Terzaghi has the value between those two FEM values.

In two-layer-soil comparing to one-layer-soil, bearing capacity decreases dramatically to less than 70% of its value by adding the clay thickness of $h_1/B=0.15$ on top of sand. Increasing depth of clay leads to smaller values for bearing capacity showing that top layer mainly controls bearing capacity value.

According to Michalowski [18], a so-called critical depth in which strength of bottom layer has no influence on bearing capacity of whole model exists and this depth in this study is $h_1/B=1.5$ or $h_1=4.5$.

For smaller values of h_1, the failure mechanism goes further to the bottom layer while with increasing thickness of clay, the plastic zone only shrinks into top layer.

Direction and magnitude of displacement vectors are much smaller and more downward when the top layer is sandy soil.

In the presented study the approach applied is straightforward for a two-layer soil and is applicable for multi-layer soil profiles as well. However, in this study only a short–term stability of footing was considered, the study on long-term behaviour of material would be of interest. In addition, the effect of footing-soil interaction can be taken into consideration in the future analysis.

References

1. Terzaghi K (1996) Soil Mechanics in Engineering Practice. John Wiley and Sons, New York, United States.
2. Zhu M (2004) Bearing Capacity of Strip Footings on Two-layer Clay Soil by Finite Element Method. ABAQUS Users' Conference, Boston.
3. Burd H, Frydman S (1997) Bearing capacity of plane-strain footings on layered soils. Canadian Geotechnical Journal 34: 241-253.
4. Griffiths DV (1989) Computation of collapse loads in geomechanics by finite elements. Ingenieur-Archiv 59: 237-244.
5. Potts DM, Zdravkovic L (1999) Finite Element Analysis in Geotechnical Engineering: Volume One-Theory. Thomas Telford, UK.
6. Ghazavi ME, Amir (20008) A Simple Limit Equilibrium Approach for Calculation of Ultimate Bearing Capacity of Shallow Foundations on Two-Layered Granular Soils. Geotechnical and Geological Engineering 26: 535-542.
7. ABAQUS 6.13 (2013) ABAQUS/CAE User's Manual, Dassault Systems, USA.
8. Helwany S (2007) Applied Soil Mechanics with ABAQUS Applications. John Wiley and Sons, New York, United States.
9. Ziaie Moayed R, Rashidian V, Izadi E (2012) Evaluation on Bearing Capacity of Ring Foundations on two-Layered Soil. World Academy of Science, Engineering and Technology 61: 1108-1112.
10. Day RA, Potts DM (2000) Discussion on 'Observations on the computation of

the Bearing Capacity Factor Nγ by Finite Elements' by Woodward & Griffiths. Geotechnique 50: 301-303.

11. Jaky J (1944) The coefficient of earth pressure at rest. J Soc Hungarian Architects Eng 1944: 355-358.
12. Borst RD, Vermeer PA (1984) Possibilites and Limitations of Finite Elements for Limit Analysis. Géotechnique 34: 199-210.
13. Zienkiewicz OC, Humpheson C, Lewis RW (1975) Associated And Non-Associated Visco-Plasticity And Plasticity In Soil Mechanics Source. Géotechnique 25: 671-689.
14. Shiau JS, Lyamin AV, Sloan SW (2011) Bearing capacity of a sand layer on clay by finite element limit analysis. Canadian Geotechnical Journal 40: 900-915.
15. Houlsby GT (1991) How the dilatancy of soils affects their behaviour. University of Oxford, Oxford, UK.
16. Potts DM, Zdravkovic L, Zdravković L (2001) Finite Element Analysis in Geotechnical Engineering: Application. Thomas Telford.
17. Boussinesq J (1885) Application des potentiels à l'étude de l'équilibre et du mouvement des solides élastiques. Gauthier-Villars, Paris.
18. Michalowski RL (2002) Collapse Loads over Two-layer Clay Foundation Soils. Soils and Foundations 42: 1-7.

Citation: Mosadegh A, Nikraz H (2015) Bearing Capacity Evaluation of Footing on a Layered-Soil using ABAQUS. J Earth Sci Clim Change 6: 264. doi:10.4172/2157-7617.1000264

Finite Element Analyses of Buried Pipeline Subjected to Live Load Using ABAQUS

Mosadegh A.*, Nikraz H.**
E-mail: ahdyeh.mosadegh@postgrad.curtin.edu.au; H.Nikraz@curtin.edu.au)
Department of Civil Engineering, Curtin University, Perth, Western Australia, Australia

ABSTRACT
This paper shows the methodology used for modelling the behaviour of a buried pipeline subjected to traffic load using the finite element method (FEM). Soil behaviour is represented by the elasto-plastic Drucker-Prager model and the pipe material is assumed to be isotropic and linear elastic using FEM software ABAQUS 6.13. For the whole system, the effect of surface pressure amplitude (magnitude of 200 and 550 kPa) on pipe-soil displacement and stress distribution is investigated at different pipe burial depths of 1–5 times the pipe diameter. In addition, the influence of pipe-soil interaction properties, boundary conditions at pipeline ends, pipe material properties and internal pressure are taken into consideration. For all cases, the results are compared with predictions obtained through numerical and experimental research, which shows satisfactory agreement with results from the literature.

RÉSUMÉ
Cet article présent la méthodologie adoptée pour modéliser du fonctionnement d'un tuyau enfouis soumis à la charge trafic par la Méthode des Éléments Finis (MÉF). La loi de comportement du sol est représentée par la modèle élastoplastique avec un critère de Drucker-Prager et le tuyau matériau est décrit par un comportement isotrope et élasticité linéaire réalise par le logiciel d'éléments finis, ABAQUS 6.13. Pour l'ensemble du système, l'influence de la charge trafic (200 et 550 kPa) aux différentes profondeurs d'enfouissement de 1 jousqu'ai1 5 fois de diamètre du tuyau sur les déplacements et les pressions de sol- tuyaux a été réalisé. En plus, l'effet sol-tuyaux interaction, l'influence de conditions aux limites, l'effet de matériaux de tuyau ainsi que l'effet de la pression du fluide dans tuyaux ont été pris en considération. Pour tous les cas, les résultats obtenus ont été comparés avec ceux existent dans la littérature et ont été vérifiées avec des prédictions recherches numériques et expérimentaux qui montrent un accord satisfaisant.

1. INTRODUCTION

Pipelines are essential infrastructure for providing water and gas to urban areas. They are typically buried in onshore and offshore applications for protection. In many cases, pipelines are buried in shallow foundations under highways or railways. Any damage due to traffic load, ground movement or any other reason can cause failure in the pipeline or malfunctioning of the system.

In recent decades, many numerical and experimental studies have investigated the response of buried pipes subjected to different conditions focusing on pipe-soil interaction. In the 1970s, pipe-soil interaction analysis received attention from many researchers. For numerical studies, the American Concrete Pipe Association made a serious study of buried concrete pipe behaviour using a finite element method (FEM) computer programme. The use of FEM to simulate problems was introduced by Culvert in 1976, and in 1984 ASCE introduced the Winkler model, an elasto-plastic soil spring model based on the model developed by Audibert (Audibert & Nyman 1977). Since then, many numerical and experimental analyses have been performed to investigate buried pipe response under various conditions such as moisture change, cyclic load, installation procedure effects and so on (Trautmann 1985; Zaman M M, Desa Ch. & Drumm E.C. 1984; Abo-Elnor, Hamilton & Boyle 2004; Kang, Parker & Yoo 2008; Chatterjee, White & Randolph 2013; Farhadi Hikooei 2013; Rajeev & Kodikara 2011; Calvetti, di Prisco & Nova 2004; Liu et al. 2010).

In a numerical study carried out on buried pipe behaviour, the effect of interaction properties, backfill geometry and material properties on pipe-soil interaction was investigated using the FEM software ABAQUS (Kararam 2006). It was found that increasing the friction coefficient leads to a reduction in pipe deflection and the effect of bedding material is more significant than the effect of bedding thickness on induced stress. In another study, the behaviour of an HDPE pipe buried in a sandy soil under cyclic load was analysed through an experimental approach (Tafreshi & Khalaj 2011). A formulation was developed to calculate soil surface settlement and pipe crown displacement based on soil density, burial depth variation and stress. It was found that burial depth, amplitude of surface pressure and soil density dramatically affects pipe behaviour. The results from this research showed that increasing the burial depth leads to an increase in soil settlement and a decrease in pipe displacement. Also increasing the burial depth leads to a considerable reduction in the rate of pipe displacement conducted another investigation in which a steel pipe was subjected to a repeated load up to 100 kPa(Mir Mohammad Hosseini & Moghaddas Tafreshi 2002). It was found that pipe embedment depth and soil density were the most significant parameters, amongst others. Another study considered the effect of various conditions on pipe-soil interaction subjected to a

surface surcharge load. Soil and pipe were modelled as a continuous area with two different nodes and their interaction modelled as a surface to node. The researchers found that the impact of bedding stiffness and compaction levels on the induced stresses were more important than the effect of bedding thickness (Abolmaali & Kararam 2010). In another research carried out using Plaxis, the effect of different parameters including pipe burial depth, surface pressure, internal pressure, pipe diameter and thickness were taken into consideration (Shaalan 2014).

The objective of this paper is to determine the performance of a buried pipeline subjected to traffic load, taking into consideration the effect of internal pressure. The computations are done using the commercial finite element software ABAQUS, version 6.13 (ABAQUS-6.13 2013). For the whole system, the study investigates the effect of a surface pressure amplitude of 200 and 550 kPa at different pipe burial depths, varying between 1, 1.5, 2, 2.5, 3.5 and 5 times the pipe diameter, on pipe-soil interaction, on soil surface settlement and on stress distribution. In addition to this, the effect of pipe-soil interaction properties, pipe material, boundary conditions at the pipeline ends and the internal pressure of different fluids are investigated. All results obtained through this research will be presented in the following sections and verified against predictions published in the existing literature.

2. MODEL DESCRIPTION

The following section presents the definition of the problem, as shown in Figure 1. Due to the long length of the pipe compared to its width, the problem can be modelled assuming plane strain conditions. The size of the model should be sufficient to keep the boundary conditions from affecting the soil movements due to traffic loading. It should be noted that in this study, the X-Y plane is the area in which the soil is subjected to various loads, e.g. positive direction for Y is opposite direction of the weight. For boundary conditions, as shown in Figure 1, both vertical sides of the model are fixed in a horizontal direction with vertical displacement, and the bottom of the model is fixed in both vertical and horizontal directions. In all models, the mesh has been refined in areas with stress concentration around the pipe. Pipe and soil elements were modelled as CPE4R or 4-node bilinear plane strain quadrilateral, with reduced integration. To calculate thickness of pipe, based on the hoop stress formula for a pipe with an internal pressure of σ_p, with a tensile pressure of P and an outside diameter of D_0, a minimum thickness of $t_0 = \frac{PD0}{2\sigma p}$ is required (ASCE 2009). This means that a thickness of 5 cm is satisfactory for a pipe of 1 m, with an internal pressure of 414 kPa, yield stress of 490 MPa and tensile strength of 690-840 MPa. The width of the trench should not be less than the greater of 1.5 times of the pipe outside diameter (1 m) plus 305 mm or the pipe outside diameter plus 406 mm (AASHTO 1998). The chosen trench width is therefore 2 m with material properties being a well-graded or gravelly sand with a 90% compaction (SW90) used based on ASTM recommendations (ASCE 2001).

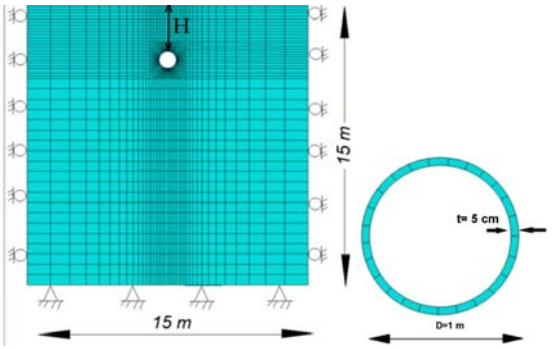

Figure 1. Finite element discretization and boundary condition selection of the model

To predict live load effects on pipe-soil behaviour, the best constitutive soil model is elasto-plastic. In this study, the soil is modelled as an isotropic elasto-plastic material satisfying the Drucker-Prager failure criterion. Since the pipe is stiffer than its surrounding soil, the plastic behaviour of the pipe is not investigated here and the pipe is classified as linear elastic. Two types of pipe are selected due to investigate the impact of pipe properties on pipe-soil behaviour: steel pipe and high density polyethylene, referred to hereafter as HDPE. Soil and pipe properties are illustrated in Table 1. The properties of the soil, steel pipe and HDPE pipe are adapted from (NCHRP 2009; Tafreshi & Khalaj 2011).

Table 1 Material property of sandy soils and pipes

Type of soil	Term	Value
Trench soil	Density, ϒ (kg/m^3)	2144
	Young's Modulus, E' (MPa)	18
	Poisson's Ratio, ϑ	0.3
	Cohesive strength, d' (kPa)	<1
	Friction angle, β' (plane strain), (deg)	48.5°
	Dilation angle, ψ (deg)	12°
	Flow stress ratio, K	1

Parameters	Steel pipe	HDPE pipe
Density, ϒ (kg/m^3)	7850	9550
Young's Modulus, E' (GPa)	200	816
Poisson's Ratio, ϑ	0.3	0.46

From the different contact models in ABAQUS, surface-to-surface interaction is chosen to model the interaction of soil and pipe as two deformable parts. It is worth noting that the interaction between pipe and soil has two components, of which one is perpendicular to the surface and the other is tangential to the surface. The friction coefficient between the pipe and soil is assumed to vary from 0.1 to 1. It should be noted that for this case or for

tangential contact, separation is allowed after contact and slipping is allowed during analysis. Hard contact is chosen for the normal direction, means there is pressure just only when there is contact. To define the interaction in ABAQUS, the pipe element is chosen as the master surface with a stiffer body, and the soil as a slave surface with more refined meshes (King & Richards 2013). The model is created in four steps. In the first step, which is the initial condition, all boundary conditions are defined as described previously. In the next step, a geostatic step a gravity load is applied to the model. In the third step, pipe and pipe-soil interaction are activated and the pipe weight is applied to the model. Pipe elements are reactivated during this step allowing movement in a vertical direction. In the last step, traffic load is applied to the soil surface at the trench width, exactly on top of the pipe. In addition, when considering the effect of internal pressure, fluid pressure is applied to the pipe's internal walls. It should be noted it is assumed that relative movement between the soil and pipe is impossible.

3. RESULTS AND DISCUSSION

The following sections present the results of numerical analysis along with discussions highlighting the effect of different factors on buried pipeline behaviour. Pipe behaviour and deformation depend on the geometry and properties of the surrounding soil, pipe properties, pipe-soil interaction and pressure values (Whidden 2009). In this study, the effect of some of parameters summarised in Table 2 on pipe-soil behaviour will be investigated while pipe diameter, trench width and properties remain unchanged.

Table 2 Scheme of different cases for buried pipe behaviour investigation

$\frac{H}{D}$	Surface load (kPa)	Pipe type	Internal Pressure (kPa)			Interaction (friction coefficient)	Boundary condition
			Without fluid	Water	Gas		
1						0.1	
1.5	200	Steel				0.3	Hinged &
2			---	414	7500	0.5	
2.5	550	HDPE				0.7	Roller ends
3.5						0.9	
5						1	

$\frac{H}{D}$ = embedded depth of pipe (the ratio of soil cover height; H to pipe diameter; D)

3.1 Effect of Burial Depth and Surface Pressure on Displacement at Soil Surface and Pipe Crown

Figures 2(a) and 2(b) show the displacement on the soil surface and at the pipe crown versus the burial depth of a pipeline subjected to live load with amplitude of 200 and 550 kPa. The recommended axle load of the truck is 18000 kg over two twin pairs of wheels, which creates a stress of 8.5 kg/cm^3. It is assumed that the stress in this case is applied to the soil and there is no flexible pavement overlaying the soil surface, which would considerably reduce the stress. If a 5 cm layer of asphalt was taken into account, the maximum applied stress on the soil surface would be reduced to 5.5 kg/cm^3 or 550 kPa. Amplitudes of 200 and 550 kPa were chosen to apply on soil surface to simulate a variety of vehicles(Hunang 1993).

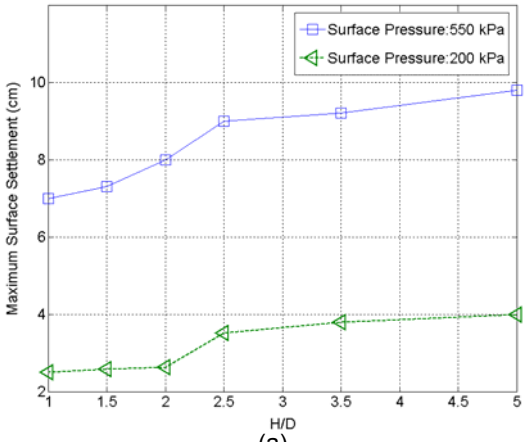

(a)

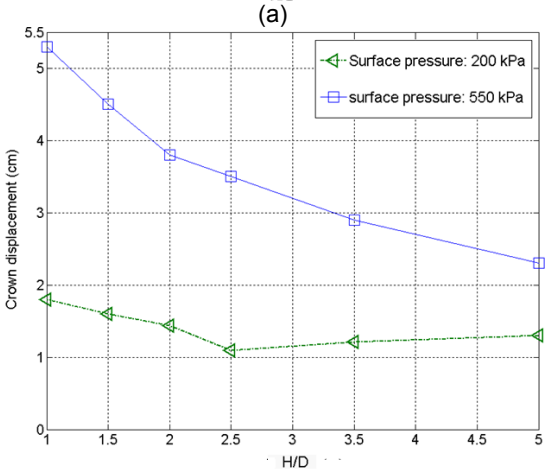

(b)

Figure 2. Vertical displacement as a function of depth and surface pressure (a) on soil surface (b) on pipe crown

Figure 2(a) describes the vertical displacement at the soil surface for six different burial depths $1 \leq \frac{H}{D} \leq 5$ under a surface pressure of 200 and 550 kPa. It can be seen that under a surface pressure of 200 kPa, at H/D=1, the soil surface displacement is about 2 cm and with an increase in H/D from 1 to 5, the soil surface displacement increases to 4 cm. For a surface pressure of 550 kPa, with increasing depth of embedment from 1 to 5, the surface settlement increases from 7 to 10 cm. It should be noted that both graphs display the same pattern and the gap between these graphs is almost consistent. Displacement rate varies significantly on the soil surface for shallower burial depths compared to deeper burial depths. Overall, for a burial depth of H/D=1, surface displacement is at its minimum, and increasing the H/D leads to greater displacement at the soil surface.

Figure 2(b) illustrates the crown displacement of the pipe at six different burial depths under surface pressures of 200 and 550 kPa. It can be seen that

the crown displacement of a steel pipe is a function of burial depth and surface pressure, and it is more sensitive to surface pressure variation rather than burial depth changes. Under a surface pressure of 200 kPa with a burial depth increasing from H/D=1 to H/D=5, the pipe crown displacement decreases from 2 cm to 1 cm. For a surface pressure of 550 kPa, crown displacement is 5.5 cm at H/D=1 and with a burial depth increasing to H/D=5, crown displacement goes down to 2.5. In addition, the gap between the two graphs is more significant at shallower depths and this gap tends to become narrower with an increasing H/D. In other words, surface pressure value tends to have less effect on pipe displacement at deeper embedment depths.

Another study analysed the behaviour of a buried pipe under cyclic load through an experimental approach(Tafreshi & Khalaj 2011). The result of this research shows that increasing burial depth leads to increased settlement on the soil surface and decreased crown displacement. It was found as well that increasing the surface pressure leads to more displacement in both the soil surface and pipe crown. The results found in the abovementioned research were in good agreement with the results of the current research.

3.2 Effect of Burial Depth and Surface Pressure on Stress Transmitted to Pipe

This section analyses the stress distribution transmitted to a shallow buried pipe. Vertical pressure transmitted to the pipe is the sum of the dead load due to the weight of the soil cover on top of the pipe (Moser 1990) and the live loading caused by traffic or wheel load. As the basics of numerical calculation of the total stress on a pipe is not the purpose of this research, the stress on pipe is calculated based using Eq. 1.in (ASCE 2009).

$$P_{total} = P_d + P_l = \gamma H + \frac{W}{C_d H^2} \qquad [1]$$

In Eq. 1, P_{total} is the sum of the dead load and live load. Dead load, P_d , is a function of γ or the density of the soil and a function of H or soil depth. Live load or P_l is a function of W and H, representing dual wheel load and soil depth cover respectively. C_d is a coefficient based on the Boussinesq solution which has been developed by Hall and Newmark (Moser 2001). Hall and Newmark integrated the Boussinesq solution to obtain the load on the pipe under a live load, and in their formulation, the fraction of the wheel transmitted to the pipe is a function of burial depth called the Boussinesq curve in which for H>1 m the factor is 1.0 (Moser 2001) and the Eq.1 is applicable. A comparison of two methods, the numerical and FEM solution is presented in Figure 3. In both methods, the stress on the crown is calculated for different burial depths under a surface pressure of 550 kPa.

It can be seen in Figure 3 that the stress values on pipeline obtained by FEM and through the numerical method show almost the same pattern. In the numerical method, increasing the H/D from 1 to 2.5 causes the stresses on the pipe to drop dramatically from 300 kPa to less than 100 kPa. When the H/D increases from 2.5 to 3.5 the graph remains almost steady at 100 kPa, and increasing the H/D to 5 causes a slight increase in the stress value. In the FEM method, increasing the embedment depth from 1 to 3.5 causes the stress on the pipe to fall from 260 kPa to less than 80 kPa. After this point the graph begins to rise, and as for the numerical method, there is a slight increase in stress reaching 100 kPa at H/D=5. Overall, the stress on the pipe is higher using the FEM method for shallower depths except at H/D=1, compared to the numerical solution. This difference can be due to the different assumptions made in the two methods. For example, in the Boussinesq solution soil is supposed to be elastic while in the FEM method, soil shows elasto-plastic behaviour. In addition, the effect of lateral earth pressure is not considered in the numerical method, while in nature and in the FEM solution, soil is not classified as an isotropic and homogenous material. It is worth noting that the stress on the pipe is at its maximum when the burial depth is at its minimum. Increasing the burial depth from 1 to 2.5, causes the stress on the pipe to down from 300 kPa to 100 kPa, and increasing the burial depth after this point does not significantly affect the stress on the pipe.

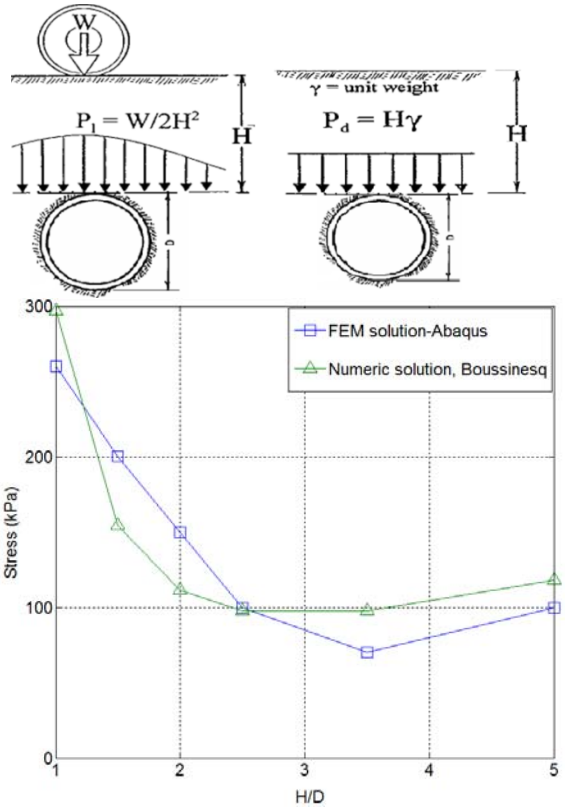

Figure 3. Stress distribution on the pipe at various burial depths under a pressure of 550 kPa on the soil surface (ASCE 2009)

3.3 Effect of Internal Pressure

This section investigates the performance of buried pipelines subjected to a surface load with regard to the internal pressure effect. The influence of internal fluid pressure was investigated under a surface

pressure of 550 kPa at two different burial depths of H/D=1, 2.5. It is assumed that the fluids in the pipe are water and gas, which induce internal pressures of 414 and 7500 kPa, respectively.

Figure 4 illustrates the effect of liquid pressure on pipe displacement for two burial depths of 1 and 2.5. For H/D=1 and a thickness of 5 cm, when there is no fluid pipe crown displacement is 5.3, and with the application of water pressure, the crown displacement drops to 5 cm It can be seen in Figure 4 that the pipe tends to deflect more when there is no liquid. However, applying higher pressure causes the calculations to stop due to failure in the pipeline. To solve this issue, the thickness of the pipe was increased to 10 cm for those cases dealing with gas pressure.

Figure 5 illustrates the effect of internal pressure on the maximum stress on a pipe wall for two burial depths of H/D=1 and 2.5. It can be seen that applying internal pressure causes an increase in the maximum stress value. The higher the pressure is, the greater the stress on the pipe. It should be noted that stress on a pipe for high pressure liquids or gas is highly affected by the burial depth of the pipe.

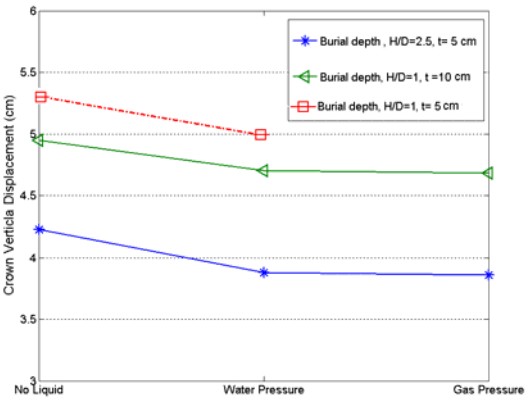

Figure 4. Effect of internal pressure on vertical crown displacement for a steel pipe

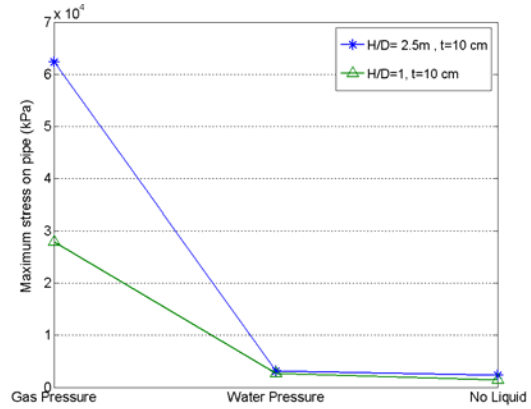

Figure 5. Effect of internal pressure on the maximum stress in a steel pipe

In another study, the effect of three fluid pressures on steel pipeline was investigated using PLAXIS 2D program software (Shaalan 2014). It was concluded that increasing the internal pressure leads to a decrease in pipe crown displacement for shallower burial depths $\frac{H}{D} \leq 3$ although this decrease is not remarkable. This shows a good agreement between the two studies.

3.4 Effect of Pipe Material Properties

This section investigates the effect of pipe material on crown deflection by considering two types of pipe, HDPE and steel, whose properties are based on those listed in Table 1. The effect of interaction is not taken into consideration for this analysis and it is supposed that the contact pairs are a tied surface to surface. In addition, the results presented are for the case in which surface pressure is 550 KPa and H/D=2.5. Figure 6 shows the ring deflection of the pipe represented as a function of E. Ring deflection is a function of different parameters including pipe stiffness, geometry and soil parameters (ASCE 2009). In this case, as the properties and geometry of the pipe and the soil properties remain unchanging, deflection is only a function of the ratio of E/E' in which the E of steel is almost 250 times greater than the E' of HDPE pipe.

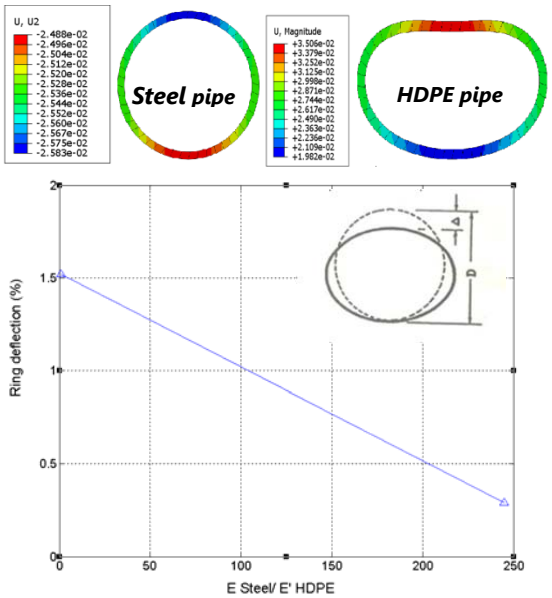

Figure 6. Ring deflections of HDPE and steel pipe as a function of E

It is clear that the ring deflection plunged from 1.5% for steel to 0.2% for HDPE. Looking closely at the figure reveals that for the steel pipe, the crown and bottom have almost the same value of displacement, while for the HDPE pipe these values are different. For example, the bottom of the HDPE pipe has a displacement of 2 cm while its crown has a displacement of 3.56 cm; this difference leads to a higher value of ring deflection for the HDPE pipe. The parameter of *d* or ring deflection values are 1.52% and 0.2% for the HDPE and steel pipes respectively.

3.5. Effect of Friction Coefficient on Pipe-Soil Interaction

In ABAQUS, the interface can be used to simulate the interaction between a pipe and its surrounding

soil using surface-to-surface contact. As the pipe is a stiffer material, it is simulated as a master surface and its surrounding soil as a slave surface, based on the FEM recommendation. To avoid convergence difficulties, an unsymmetric solver matrix was used to solve the problem, and to avoid the penetration of the master surface nodes into the slave surface, the master surface mesh was refined. The interaction properties of the model were created by defining both tangential and normal behaviour at a depth of $\frac{H}{D} = 1$ and under a surface pressure of 550 kPa. To assess the effect of the friction coefficient on pipe behaviour, different friction coefficient values for the pipe and surrounding soil surfaces were selected, varying from 0.1 to 0.9 and value of 1 is presenting full-bonded situation.The effects of the friction coefficient on the deflection of both HDPE and steel pipes are shown in Figure 7.

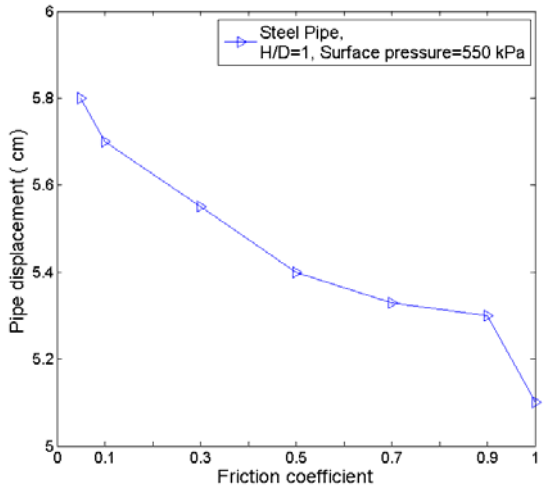

Figure 7 Effect of friction coefficient on pipe-soil deflection

It can be seen that friction coefficient variation has a small effect on pipe displacement. Pipe displacement under a surface pressure of 550 kPa drops from 5.8 cm for friction coefiicient of 0.1 to 5.1cm for a full-bondad case. In another study the effect of interaction on deflection of a concrete pipe was investigated using ABAQUS(Kararam 2010). It is shown in that study that increasing friction coefficient from 0.1 to 0.9 leads to decrease in pipe deflection although this decrease is too small changing which is in a good agreement with results of current study.

To compare the effect of interface conditions along pipe boundaris, the influence of the friction coefficient of 0.5 are compared with those for full-bonded conditions and results are presented in Figures 8 and 9. In Figure 8 the effect of two interface conditions on pipe displacement under a surface pressure of 550 kPa and H/D=1 and 3.5 are illustrated. As is illustrated by the graph, for H/D=1 and friction coefficient of 0.5 pipe displacements drops from 5.5 cm to 3.0 cm while angel from crwon is increasing. Similarly for a full-bonded case, pipe displacement drops from 5.1 cm to 4 cm when angel increases from 0^o to 60^o. After this point with inceasing angel from 60^o to 120^o. pipe displacement remains steady at 4 cm. Then with increasing angel to 180^o pipe displacement decline to 3.0 cm. Overall, the pipe displacement decrease with increasing angel and for friction coeficient of 0.5 and the same pattern is obtained for deeper burial depth or for H/D=3.5.

The effect of interaction properties on stress distribution of pipe as a funtion of angel from crown is illustrated in Figure 9. As can be seen from the graph three different sections exist in the graph. Left and right parts for which stress of full-bonded interaction is bigger than those with friction coefficient of 0.5. While in the middle area where full-bonded interaction has a lower stress along pipe. It should be noted at crown and invert interaction propertis almost has no impact on stress. Results presented here had a good agreement with those presented by (Kang 2007)

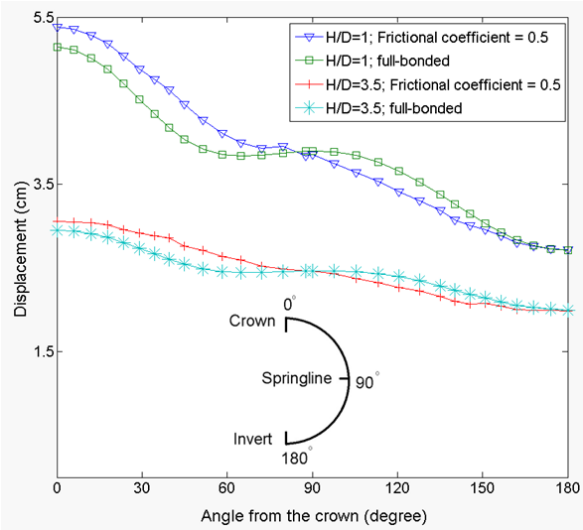

Figure 8 Effect of interface conditions on pipe displacement along pipe circumference

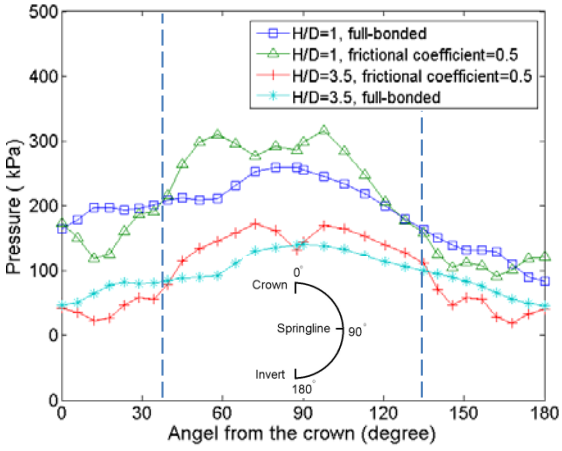

Figure 9 Effect of interface conditions on stress distribution along pipe circumference

3.6 Effect of Boundary Condition

So far, all of the results presented here have been for a 2D plane strain model. Under the plane strain condition, it is assumed that the length of the pipe

compared to its width is sufficient. However, boundary conditions can be changed for any infrastructure through the pipe length. To compare the effect of boundary conditions, a 3D model was built to analyse how boundary conditions can affect the stress and displacement along the pipe path. Two types of boundary conditions at the end of pipeline were selected, roller and hinge. As suggested in many standards for three-dimensional analysis, it is better to model pipe elements as a series of shell elements (ASCE 2009; Kunert, Otegui & Marquez 2012). Three-dimensional brick elements are used to simulate the surrounding soil (C3D8R) and four-node reduced-integration shell elements (type S4R) are used for the pipe, as shown in Figure 10.

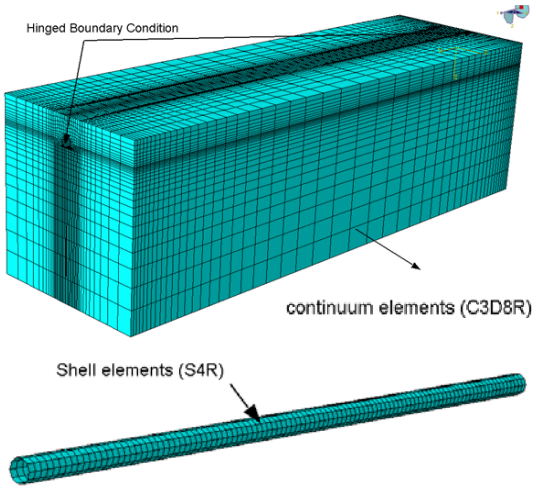

Figure 10. Finite element discretization and boundary condition selection of the model (a); and pipe mesh elements (b)

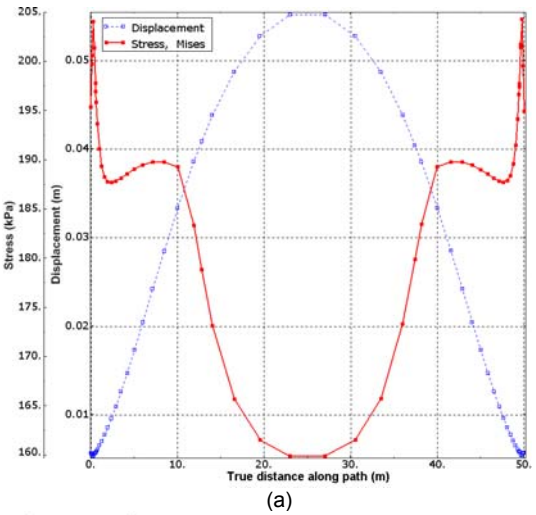

(a)

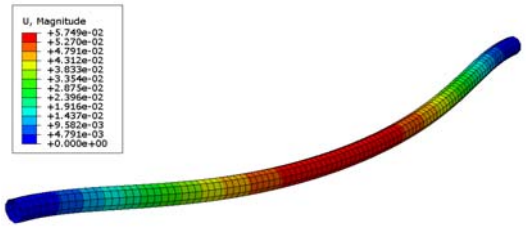

(b)

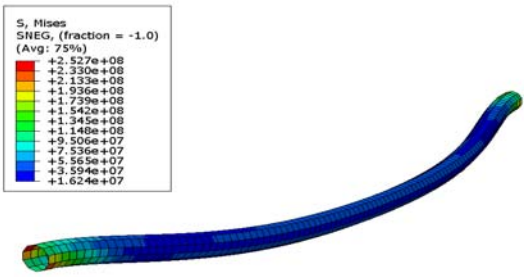

(c)

Figure 11. Displacement and stress on the pipe-soil interaction along the whole length of a pipe with a hinge boundary at the pipeline ends

As can be seen from the results in Figure 11(a), the left and right hand parts of the graph are restricted in movement due to these points. Moving towards the middle of the pipe, there is a downward deformation of 5 cm which is the maximum. At the ends of the pipeline and at the hinge boundary condition there is no displacement, while maximum stress occurs at these points. In addition, from the sides of the pipe to the middle, there is a decrease in the stress of the pipe from 204 to 160 kPa, while displacement increases from 0 to 5 cm in the middle. Figures 11(b) and 11(c) illustrate the displacement and stress distribution along the pipeline. It is concluded that analysing pipe soil behaviour using plane strain conditions should be done with caution, as any infrastructure along the pipeline path can change the boundary conditions and both stress and displacement can vary dramatically along the pipeline length.

4. SUMMARY AND CONCLUSIONS

In this research, a numerical analysis was carried out to investigate the influence of different parameters on pipe-soil behaviour under live load using the FEM software ABAQUS. The soil model was elasto-plastic and the pipe was elastic linear. The effect of surface pressure amplitudes of 200 and 550 kPa at different pipe burial depths, H/D= 1, 1.5, 2, 2.5, 3.5 and 5 on settlement and stress distribution at the pipe-soil interaction and soil surface were investigated. In addition, the influence of pipe-soil interaction properties, pipe material, boundary conditions at pipeline ends and internal pressure from different fluids were taken into consideration. All results obtained through this research were verified with predictions published in the existing literature.

The effect of burial depth and surface pressure for six different burial depths, $1 \leq \frac{H}{D} \leq 5$, under a surface pressure of 200 and 550 kPa on soil settlement at the soil surface and on the pipe crown was investigated. It was demonstrated that when H/D is at a minimum, surface displacement is also at a minimum, and an increasing H/D leads to more displacement at the soil surface, especially for H/D<2.5. However, displacement at the crown decreases with increasing H/D. This rate of change for H/D <2.5 is more significant. In other words, surface pressure tends to have less of an effect on

pipe displacement for deeper embedment depths. In addition, stress on the pipe is at a maximum when H/D is at a minimum. Increasing the H/D leads to a decreased in the stress on the pipe, and for H/D>2.5, increasing the depth does not significantly affect the stress on the pipe. Variations in internal pressure and interaction properties affect pipe displacement, although these changes are not remarkable. Increasing the friction coefficient leads to a decrease in pipe deflection, although this decrease is not significant. A hinged boundary condition affects stress and displacement distribution along the pipe length, showing that at the ends of the pipeline, when there is no displacement, maximum stress occurs at these points. It is worth noting that one of the limitations in this research was that the pipe installation procedure was not simulated. In addition, it was assumed that the pipe did not deform during construction, and the relative movement of the pipe and soil was not taken into consideration which are recommended to be investigated. Considering traffic load as a cyclic load to assess pipe-soil interaction behaviour and degradation effect is another area of interest.

5. REFERENCES

AASHTO 1998, *American Association of State Highway and Transportation Officials (AASHTO)*, Washington DC USA.

ABAQUS-6.13 2013, *ABAQUS/CAE User's Manual*, Dassault Systèmes, USA.

Abo-Elnor, M, Hamilton, R & Boyle, JT 2004, 'Simulation of soil–blade interaction for sandy soil using advanced 3D finite element analysis', *Soil and Tillage Research*, vol. 75, no. 1, pp. 61-73.

Abolmaali, A & Kararam, A 2010, 'Nonlinear Finite-Element-Based Investigation of the Effect of Bedding Thickness on Buried Concrete Pipe', *Journal of Transportation Engineering*, vol. 136, no. 9, pp. 793-799.

.ASCE 2009, *Buried flexible steel pipe : design and structural analysis / prepared by the Task Committee on Buried Flexible (Steel) Pipe Load Stability Criteria & Design of the Pipeline Division of the American Society of Civil Engineers*

edited by William R. Whidden, Reston, VA : American Society of Civil Engineers, Reston, VA.

Audibert, JME & Nyman, KJ 1977, 'Soil Restraint against Horizontal Motion of Pipe, 1142', *ASCE, Journal of Geotechnical Engineering Division*, vol. 103, no. GT10, pp. 1119-1142.

Calvetti, F, di Prisco, C & Nova, R 2004, 'Experimental and Numerical Analysis of Soil–Pipe Interaction', *Journal of Geotechnical and Geoenvironmental Engineering*, vol. 130, no. 12, pp. 1292-1299. [2013/03/27].

Chatterjee, S, White, DJ & Randolph, MF 2013, 'Coupled consolidation analysis of pipe–soil interactions', *Canadian Geotechnical Journal*, vol. 50, no. 6, pp. 609-619.

Hunang, YH 1993, *Pavement Analysis and Design*, Prentice Hall Inc., Englrwood Cliffs, NJ.

Kang, CHYJ 2007, *Soil-structure Interaction for Deeply Buried Corrugated PVC and Steel Pipes* in IR-07-01, Highway Research Center , Aubrun University, p. 110.

Kang, J, Parker, F & Yoo, CH 2008, 'Soil–structure interaction for deeply buried corrugated steel pipes Part I: Embankment installation', *Engineering Structures*, vol. 30, no. 2, pp. 384-392.

Kararam, A 2006, Nonlinear Finite Element-based Investigation Of The Effect Of Bedding Thickness On Underground Pipe, thesis, The University of Texas.

Kararam, A 2010, 'Nonlinear Finite-Element-Based Investigation of the Effect of Bedding Thickness on Buried Concrete Pipe', *Journal of Transportation Engineering*, vol. 136, no. 9, pp. 793-799.

King, S & Richards, T 2013, *Solving Contact Problems with Abaqus*, SIMULIA.

Liu, PF, Zheng, JY, Zhang, BJ & Shi, P 2010, 'Failure analysis of natural gas buried X65 steel pipeline under deflection load using finite element method', *Materials & Design*, vol. 31, no. 3, pp. 1384-1391.

Mir Mohammad Hosseini, SM & Moghaddas Tafreshi, SN 2002, ' Soil-Structure Interaction of Embedded Pipes Under Cyclic Loading Conditions', *International Journal of Engineering*, vol. 15, no. 2, pp. 117-124.

Moser, AP 1990, *Buried Pipe Design*, McGraw-Hill.

Moser, AP 2001, *Buried Pipe Design, 2nd Edition*, Mcgraw-hill.

NCHRP 2009, *Investigation of Suitable Soil Constitutive Models for 3-D Finite Element Studies of Live Load Distribution Through Fills Onto Culverts*.

Rajeev, P & Kodikara, J 2011, 'Numerical analysis of an experimental pipe buried in swelling soil', *Computers and Geotechnics*, vol. 38, no. 7, pp. 897-904.

Shaalan, HH 2014]parametric study of oil and gas internal pressures in buried pipes, thesis, ATILIM University.

Tafreshi, SNM & Khalaj, O 2011, 'Analysis of repeated-load laboratory tests on buried plastic pipes in sand', *Soil Dynamics and Earthquake Engineering*, vol. 31, no. 1, pp. 1–15.

Trautmann, CaTOR 1985, 'Lateral Force-Displacement Response of Buried Pipe', *Journal of Geotechnical Engineering* vol. 111, no. 9, pp. 1077-1092.

Whidden, WR 2009, *Buried flexible steel pipe : design and structural analysis / prepared by the Task Committee on Buried Flexible (Steel) Pipe Load Stability Criteria & Design of the Pipeline Division of the American Society of Civil Engineers*

Zaman M M, Desa Ch. & Drumm E.C. 1984, 'Interface Model for Dynamic Soil-Structure Interaction', *Journal of Geotechnical Engineering*, vol. 110, pp. 1257-1273.

International Journal of GEOMATE, Nov., 2017, Vol.13, Issue 39, pp.01-08
Geotec., Const. Mat. & Env., ISSN:2186-2990, Japan, DOI: https://doi.org/10.21660/2017.39.91957

BURIED PIPE RESPONSE SUBJECTED TO TRAFFIC LOAD EXPERIMENTAL AND NUMERICAL INVESTIGATIONS

*Ahdyeh Mosadegh[1] and Hamid Nikraz[2]

[1,2] Department of Civil Engineering, Faculty of Science and Engineering, Curtin University, Australia

*Corresponding Author, Received: 13 April 2017, Revised: 06 May 2017, Accepted: 10 June 2017

ABSTRACT: In this paper, a flexible buried pipe response subjected to traffic load is investigated through laboratory experiments and numerical analysis. A series of laboratory tests and numerical simulations were carried out to investigate the impact of surface pressure and burial depth on the model response. Experimental tests were carried out using UTM25 to apply load on surface of a tank in which pipe was buried. Numerical simulations were conducted using the Finite Element Method, ABAQUS software to develop a better understanding of the pipe behavior. Results indicate that a good agreement between numerical and experimental test results was observed. In addition, experimental and numerical analysis reveal that increasing burial depth decreases pipe deflection, increases soil surface settlement and decreases pressure on pipe while increasing surface pressure increases all mentioned parameters. From all numerical and experimental results and using the Curve Fitting analysis in Matlab, equations were developed to predict soil surface settlement, pipe vertical diametric strain and pressure on pipe. Cumulative error analysis shows that all predicted parameters have less than 10% error.

Keywords: HDPE pipe, Traffic load, Laboratory tests, Numerical analysis, Finite element

1. INTRODUCTION

Since the dawn of civilization underground pipelines have been serving humans life to improve their standard of living. Pipelines are a common and reliable mode of transportation and in general they represent a small risk to human life and to the environment. However, they can be a big threat and can represent large capital cost when they fail. Based on available data from the U. S. Pipeline and Hazardous Materials Safety Administration (PMHSA 2011), the average damage cost arising from significant pipeline damage incidents over the past 10 years was more than $400M/year[1]. In many cases of failures those buried pipelines are subjected to traffic load. Therefore, a comprehensive research on pipe-soil interaction subjected to traffic loads to minimize costs of coming failures is needed.

Over past decades numerous experimental and numerical researches have been carried out to investigate the pipe-soil response due to either moisture change or geometrical condition, soil types and burial depth impact, ground condition and failure effects. However, the research effort on pipeline behavior due to traffic loads is limited and still is a challenging task. In recent years, some researches have been investigated the behavior of buried flexible pipe under traffic load through experimental approaches. In a recent research the behavior of pipe in a large scale soil chamber under surface load was investigated by KO and Kuwano in 2010[2]. They investigated the performance of surrounding soil and distribution of acting stress on the pipe by using load cells installed on PVC pipe. It was found that in loose sand pipe deformation was much greater than those in dense backfill. Tafreshi and Khalaj analyzed the behavior of a buried plastic pipe and soil surface changes under traffic load [3]. It was found that burial depth, amplitude of surface pressure and soil density dramatically affects pipe behavior. The results from this research showed that increasing burial depth increases soil settlement and decreases pipe deflection[4].

The use of finite element method to simulate problems in pipe soil interaction analysis was introduced by Culvert in 1976 and Heger in 1985. Since then, many numerical investigations have been carried out to investigate pipe-soil interaction using finite element methods. In recent years, Tavakoli and Moghaddas Tefreshi carried out a research on buried pipe response protected by combination of geocell and rubber mixers subjected to traffic load. They used a finite element package, FLAC to model cyclic behavior of pipe and surrounding soil [5, 6]. A good agreement between numerical and experimental results was observed and results showed that the use of geocell and rubber mixture significantly reduces pipe deflection and soil surface settlement. Mosadegh and Nikraz in 2015 performed a parametric study with the use of ABAQUS on both 2D and 3D models to illustrate the impact of surface pressure, loading area, boundary conditions, pipe material properties, internal pressure and pipe-soil interaction properties on buried pipe response and soil surface settlement. Amongst all parameters, surface pressure, burial depth and loading area had the most significant

impact on model response. In their research the impact of cycles was not considered and traffic load was applied on soil surface as the static load[7]. From the literature review, previous studies are limited to either experimental or numerical analysis. An experimental and numerical study both together investigating the impact of traffic load on buried pipe response is needed see also [4]

The specific aims of this study are to examine the response of buried pipeline subjected to traffic load considering changes in pipe deflection, soil surface settlement, and increase on earth pressure on pipe through experimental and numerical investigations. A series of tests were conducted to analyze the impact of traffic load and burial depth on model response through full scale tests. A numerical simulation of laboratory model was developed to analyze those parameters impact on model response parallel to experimental tests. Finally, a relationship between parameters to predict pipe behavior, and surface changes and pressure on pipe due to traffic load was developed.

2. EXPERIMENTAL SETUP

A testing tank was designed and built as a rigid steel box with the dimensions of the 700 mm x 600 mm x 230 mm (700 mm in width in X direction, 600 in length in Z direction and 230mm in depth in Y direction) and its detail is shown in Fig.1. The tank was built in Curtin University for the purpose of this project. The selected sizes are due to limitation from load applying machine. UTM 25 was used to apply load on soil through a footing as load plate. The footing was modelled as a steel plate with the length of 220 mm, width of 100 mm and thickness of 20mm.

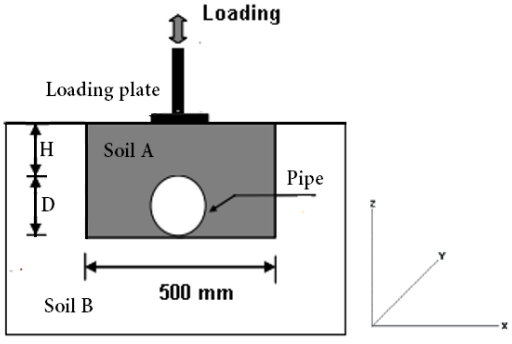

Fig.1. Schematic representation of test setup

The length of footing is almost equal to the width of the tank in order to maintain plain strain condition. For applying the load the footing is centred in the tank while the length of footing is parallel to the width of tank and buried pipe. It is noted that on the back face of tank a layer of smooth material was applied to decrease friction between soil and steel and make the friction similar to front face. Two types of soil used in this study, trench soil or soil A and granular soil or Soil B as shown in Fig.2. Error! Reference source not found.Trench soil is a sandy soil with the grain size between 0.07 and 4.75 mm and its grain size distribution is shown in Fig. 2. Soil B or granular soil typically is used for flexible road bases with the grain size between 0.07 and 26. Soil A is classified as SP or poorly graded sand and soil B is classified as GP or poorly graded gravel based on the Unified Soil Classification System (USCS). The properties of both soil used in this research are shown in Table 1.

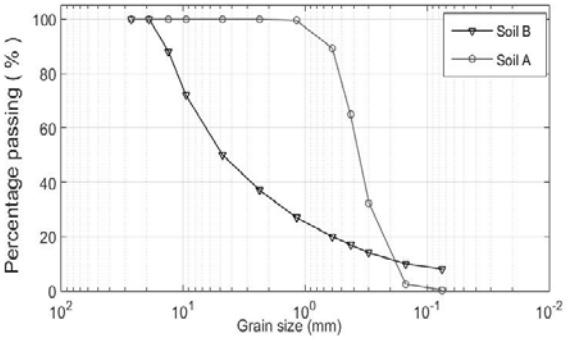

Fig. 2. Particle size distribution

Table 1 Physical properties of soils

Description	SoilA	SoilB
D_{50} (mm)	0.32	4.7
Coefficient of uniformity (C_u)	2.11	11.33
Coefficient of concavity (C_c)	1.14	0.078
Max. dry unit weight (kN/m^3)	16.5	20
Optimum moisture (%)	13	5

The pipe was a 110mm diameter HDPE or high-density polyethylene pipe. It is noted in urban services such as drainage sewer applications, pipe diameters vary widely however, a reasonable dimension representing a common small pipe diameter has been chosen. The pipe has 6.8 mm thickness and 220mm length with the Standard Dimension Ratio (SDR) or D/t of 16. Based on properties provided by manufacturer, envoiropipe, the pipe density is 955 (kg/m^3), its yield strength is 23 MPA and has a Young modulus of 950 MPA. The length of the pipe is 1 cm less than the width of tank to prevent binding against the end walls and boundary condition impacts. In addition, in order to prevent sand particles enter the pipe, the two ends of the pipe were covered by plastic as shown in Fig.3.

Tank sample for each test was prepared separately by placing granular soil or soil B at the bottom and lateral sides of tank in a U shape. Before putting the trench material, pipe should be in place while strain gauges and pressure cells were attached to the pipe in appropriate positions. Then, after placing pipe, soil A

or sand material was to be placed and be compacted in trench area. The chosen trench width is 50 cm and this width was chosen according to AASHTO recommendation in which trench width should not be less than the greater of 1.5 times of the pipe outside diameter (1 m) plus 305 mm or the pipe outside diameter plus 406 mm [8]. Trench depth varied in different tests and changes between 220 to 385 mm which is sum of burial depth plus pipe diameter. Soil compaction was performed with an appropriate hammer to simulate compaction in the field to reach 95% maximum dry density based on ASTM recommendations [9]. Height of the trench was divided into equal strips so that the soil in each layer (i.e. 6 cm thickness) was compacted separately. The soil weight required in each layer was calculated from considerations of soil unit weight and chamber's volume. At the end, the surface of soil was levelled. In the last step, loading cell and the loading plate were centred in the tank as shown in Fig. 3. An extra LVDT was placed on top of plate to monitor the surface settlement parallel to UTM25 data capturing. In the current experiment program, desired monitored data includes pipe deflection VDS, surface deformation SSS, increased vertical pressure distribution σ on pipe soil interaction. Strain gauges used to capture pipe deflection were an F series Lead wire integrated foil strain gauge type: FLA-2-11 and manufactured by Tokyo Sokki Kenkyujo TML. They have the length and width of 2 and 1.5 mm, respectively. Four of them were installed on pipe circumference. Later, it will be explained how strain gauges reading will be converted to pipe deflection. Soil surface settlement was monitored through two LVDTs, one built in UTM25 and the other provided on soil surface. To capture pressure on pipe, the pressure cells were Miniature Pressure Gauge type: PDA-1 MPA manufactured by Tokyo Sokki Kenkyujo with 6.5 mm diameter and 1 mm in thickness. Two pressure cells were placed on pipe crown for each test. It is noted the repeatability of tests to achieve reliable results were assessed prior to test program.

3. NUMERICAL MODEL

A numerical simulation was conducted and a FE model was built based on laboratory setup to investigate pipe-soil behaviour subjected to traffic load within numerical context.

The geometry of the model consists of three parts including pipe and two types of soil. As shown in m.at either ends of the mesh (y = 0 and y = 0.23 m), all nodes are free in the y-direction and due to symmetry, only half of model is considered. The boundary conditions at the sidewalls are fixed in one direction and can move in z direction. Boundaries of the backfill part are changing from 1D to 2.5D, in which D represents pipe diameter.

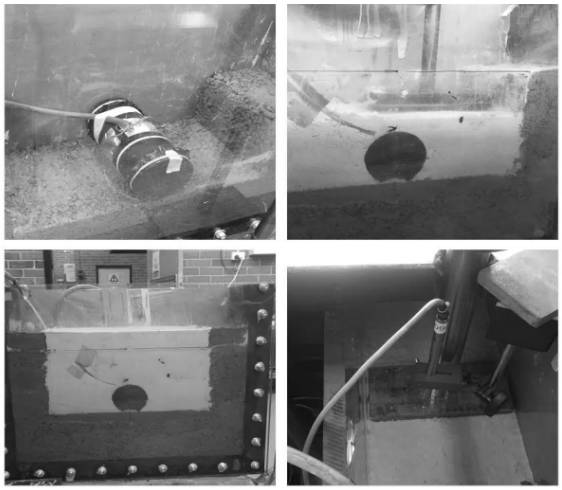

Fig. 3. Sample preparation from left to right and up to dawn: placing pipe; compacting trench; tank is ready, placing load plate and LVDT in place

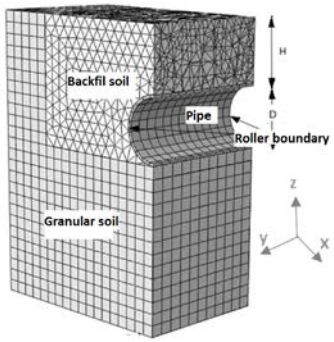

Fig. 4. Finite element discretization

The initial horizontal stresses are based on an arbitrary earth pressure coefficient of 0.4. Three-dimensional brick elements are used to simulate the surrounding soil (C3D8R) and four-node reduced-integration shell elements (type S4R) are used for the pipe. In all models, the mesh has been refined in areas with stress concentration around the pipe. Amongst different contact models available in ABAQUS, surface to surface interaction is chosen to model the interface between pipe and soil[10]. This interface can describe contact between two deformable surfaces or between a deformable surface and a rigid one. As the pipe is stiffer, it is simulated as a master surface and its surrounding soil as a slave surface. To avoid convergence difficulties, an unsymmetrical solver matrix is used to solve the problem as S-to-S discretization. Pipe is assumed to behave linear elastic and the properties of the HDPE pipe are adapted from provider as described earlier in section 2. To model soil material series of triaxial and direct shear tests were performed on trench soil and an elasto-plastic material law with Drucker-Prager failure criterion and a non-associated flow rule were considered to describe the behavior of dense sand.

This soil has a friction angel of 38.5° and cohesion of 5 kPa, Young's Modulus, E' of 9.8 MPa and Poisson's Ratio, ϑ of 0.3. As granular soil has less influence on test results its plasticity was not considered and it models a linear elastic with Young's Modulus, E' of 300 MPa and Poisson's Ratio, ϑ of 0.4. The model is created in four steps. In the first step, which is the initial condition, the pipe and soil initial conditions such as the boundary conditions and the interfaces between soil and pipe, have been defined. In the next step, geostatic step, a gravity load is applied to the model and an average initial soil stress state is applied throughout the soil mass prior to application of the surface load. In the third step, pipe and pipe-soil interaction are activated and the pipe weight is applied to the model. Pipe elements are reactivated during this step allowing movement in a vertical direction. In the last step, traffic load is applied to the soil surface at the trench width, exactly on top of the pipe acting over a rectangular of 0.2 length and 0.1 width immediately over the centreline of pipe.

It is essential to find a relationship between measured circumferential strain on pipe and pipe deflection. For that purpose a parallel plate test was carried out, as shown in Fig. 5, using a compression testing machine to measure vertical diametrical change of pipe (measured by LVDT) and wall circumferential strain at crown and bottom of pipe (measured by two strain gauges). Once the bedding is formed, pipe deflections can be calculated through measuring strain at SG s. To predict pipe behavior a FEM model was built to measure pipe deflection and strains. Pipe element type was a three- dimensional element shell elements (S4R) with reduced integration and fixed boundary condition on the bottom as shown in Fig. 5 . For validation, results obtained from experimental and numerical analysis were compared with those calculated from empirical method in Eq(1) [11]:

$$\boldsymbol{\varepsilon} = \frac{\boldsymbol{PD}}{\boldsymbol{2Et}} + \boldsymbol{6}\left(\frac{\boldsymbol{t}}{\boldsymbol{D}}\right)\boldsymbol{X}\left(\frac{\boldsymbol{\Delta y}}{\boldsymbol{y}}\right) \quad (1)$$

where $\boldsymbol{\varepsilon}$ is pipe strain, P is internal pressure, D pipe diameter, E Young Modulus of pipe, t pipe thickness, and Δy is total vertical diametric displacement of pipe. As there is no combined load and the pipe is under a compression load only, the first part of Eq(1) equals zero. Results of comparison between three methods are shown in Fig. 6 in which for six applied loads, the strain of pipe was calculated. It can be observed there is a good agreement among results obtained from different methods. In addition, a relationship between measured circumferential strain, CS, and pipe deflection, VDS, can be derived as Eq(2),

$$\text{VDS}=\text{CS X } 0.00045 \quad (2)$$

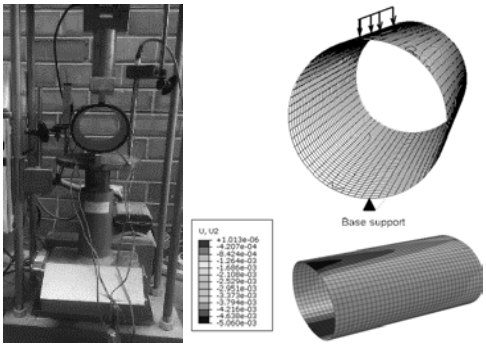

Fig. 5. (a) Applying pressure on pipe crown in vertical direction of pipe diameter in laboratory (left image) schematic view of FE results for pipe vertical displacement under load of 1400 N(600 kPa) (right image)

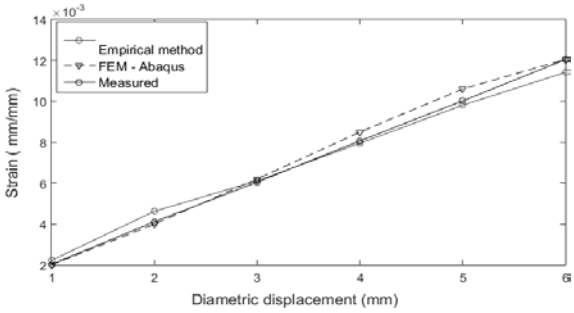

Fig. 6. Comparison of three methods

4. RESULTS AND DISCUSSION

In this section the results of numerical and experimental analysis of buried pipe are presented. First, the ultimate bearing capacity of loading plate on sand will be presented calculated through experimental and numerical investigations. Then, the impact of traffic load and influences of pressure magnitude and pipe burial depth on model response will be investigated, experimental test results followed by numerical investigations. Due to paper length limitation just a brief overview of experimental results and numerical modelling will be presented.

4.1. Ultimate bearing Capacity

In this section, the result of laboratory tests and finite element method to investigate the ultimate bearing capacity of loading plate is presented. The methodology of this section is adopted from literature review which is not explained here because of page length limitation[12, 13]. For bearing capacity analysis a downward load has been applied on top of the soil during 65 seconds to avoid sudden collapse of soil under footing. After applying pressure, foundation pressure will be increased up to failure point which will be bearing capacity term. Then after performing the test and simulation, experimental

results will be compared with numerical analysis. From experimental results, when failure takes place, the slip surfaces under the footing and its sides can be identified as shown in Fig. 7-a and they have developed clearly from the edge of footing to the ground surface. The result of plastic shear at failure point of is illustrated in Fig. 7-b. Results show that there are three different distinct area zones under the footing at failure point: triangular zone immediately under the footing; two radial zones, and two Rankin passive zones [14]. The pressure–settlement curve of both analysis are shown in Fig. 7-c. It can be seen that there is a prominent peak of 550 kPa for both graphs. Based on experimental results after a certain load, the vertical displacement increases even for a lower load. In general, although the numerical results do not fit completely with the experimental results, the results are in good agreement. Any discrepancy may be related to the chosen model for soil and foundation parameters, and differences between the boundary conditions in the numerical and experimental models.

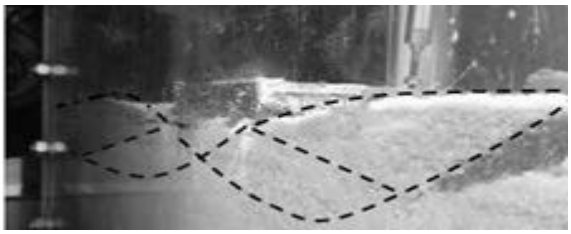

(a)

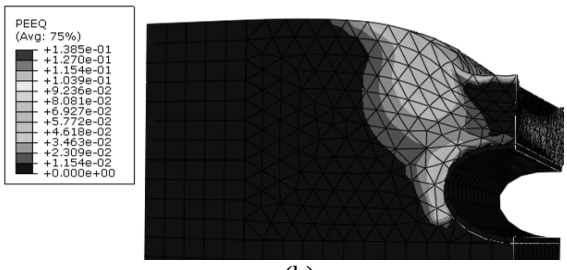

(b)

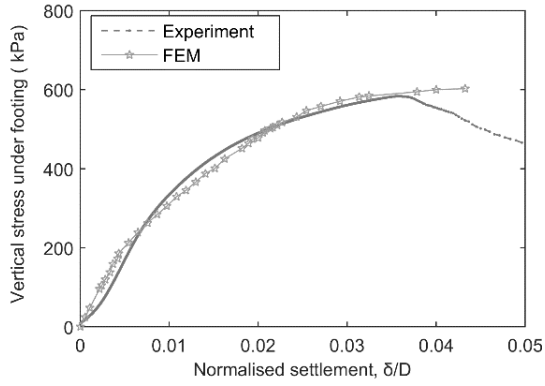

(c)

Fig. 7. (a) Bearing capacity failure (b) Plastic shear strain distribution at failure (c) Load–displacement curve comparison of FEM and experimental results

4.2. Traffic Load

Traffic load tests were performed to compare pipe behaviour due to change in surface pressure and burial depth during a static phase. In order to validate the FE model the results of numerical simulations will be compared with those from experimental results. It is noted the reason to apply traffic load as static load and not cyclic load is that the large portion of the pipe deformation and soil surface settlement occurs at the end of first cycle showing the importance of first cycle. In addition, performing static load is less time consuming compared with cyclic tests and simulations. Results of experimental tests for different surface pressure and burial depths are presented in Table **2**. All tests are simulated through finite element analysis and some of the calculated results will be presented in the following section.

Table 2 Values of VDS, SSS and σ for different surface pressures and burial depths; experimental results

Test No	Surface pressure	H/D	VDS (%)	SSS (mm)	σ (kPa)
1	250	1	1.4	2.32	128
2	250	1.5	1.09	2.99	90
3	250	2.5	0.32	3.59	55
4	400	1	1.86	3.65	225
5	400	1.5	1.62	4.3	128
6	400	2.5	0.95	5.9	78

Fig. **8**-a presents the numerical simulation of pipe displacement variation on its crown and along its circumference at two burial depths of H=1D and H=2.5D under surface pressure of 400kPa. The value of zero on horizontal axis indicates the point on the crown at centre of loading. For example, for H=1D deflection at pipe crown is 1.8 mm and it decreases away from its centre and its value is minimum on the bottom of pipe plunged to almost zero. Both graphs converge on the bottom of pipe to zero which means under any surface pressure and burial depth pipe displacement on its bottom is minimum and is almost zero.

In Fig. **8**-b the variation of surface settlement under loading area calculated through finite element method is illustrated. As it is shown maximum settlement for all burial depths occurs at pipe crown as expected. In addition, regardless of burial depth, the soil surface settlement decreases away from the centre of loading. It is clear that soil surface settlement for all burial depths converges to the minimum value over 2B distance from centre or two

times of loading area.

Fig. **8**-c compares results obtained through experimental and numerical methods at H/D=2.5 for two surface pressures of 250 and 400 kPa. It can be seen that the value predicted with FEM analysis have a good agreement with those captured in laboratory at pipe crown. For example, at depth of H=2.5 D under surface pressure of 400 kPa PC on pipe crown shows pressure of 78 kPa and FEM analysis predicts stress of almost 80 kPa. Maximum values of pipe deflection, soil surface settlement and pressure on pipe crown at any surface pressures and burial depths calculated through FE will be compared with experimental results summarised in Table **2** and will be discussed in the following section.

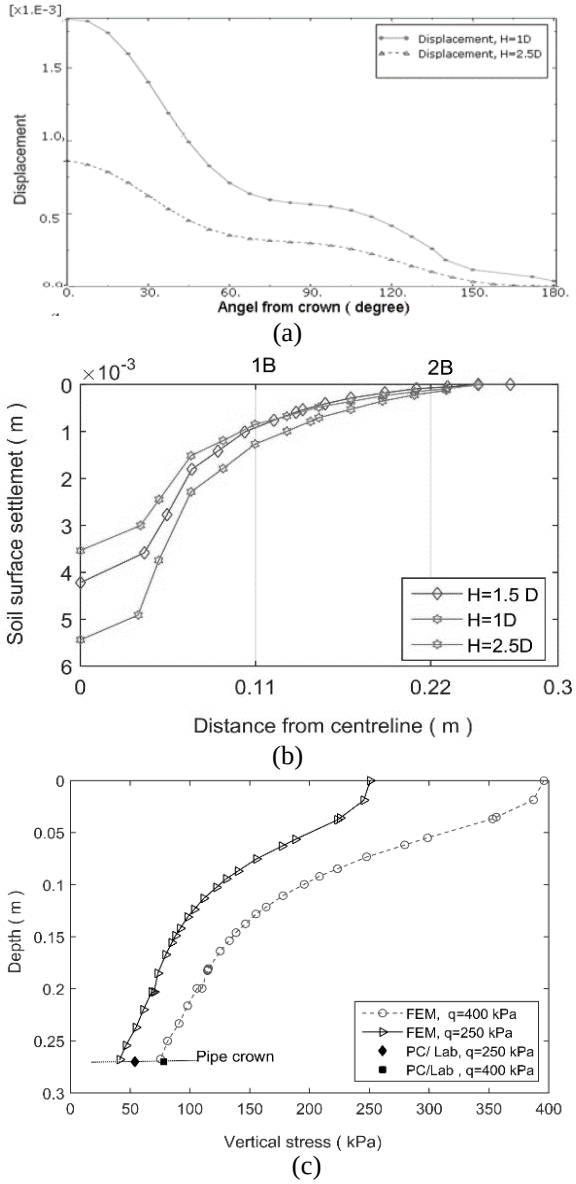

Fig. 8. FE results (a) pipe deflection (b) surface contours under surface pressure of 400 kPa (c) vertical stress caused by the strip footing

4.3. Comparison and Discussion of Results

In this section, the results obtained from experimental tests and numerical simulations will be compared and the impact of burial depth and surface pressure on VDS, SSS and σ variation will be discussed.

VDS: The impact of surface pressures of 250 and 400 kPa and burial depths of H=1, 1.5 and 2.5D on pipe deflection is illustrated in Fig. **9**. It can be seen that for both graphs increasing burial depth reduces VDS and maximum VDS occurs when burial depth is minimum. Increase in load pressure has a significant impact on change of VDS and increasing surface pressure increases VDS significantly. As illustrated, there is a good agreement between numerical and experimental results.

SSS: The influence of burial depth and surface pressure on soil surface settlement of model is illustrated in Fig. **9**-b. As shown, for the specified surface pressure, SSS increases when burial depth increases. For example under surface pressure of 400 kPa at H/D=1, SSS is 3.05 mm and increasing burial depth from H/D=1 to 1.5 and 2.5, increases SSS from 3.05 to 5.1 and 6.8 mm, respectively. This can be due to compressive layer above the pipe and with increasing burial depth the thickness of compressive layer increases. Means soil settles more when burial depth increases.

σ: Fig. **9**-c shows the impact of change in burial depth and surface pressure on stress transmit to the pipe crown obtained through experimental and numerical analysis. As illustrated results from two methods follow the same pattern and increasing burial depth leads to decrease in pressure on pipe crown. In addition, increasing surface pressure increases stress on the pipe as expected. The gap between two graphs for different surface pressures is lower for deeper burial depths means the impact of surface pressure is more significant for shallower pipes compared to deeper pipes.

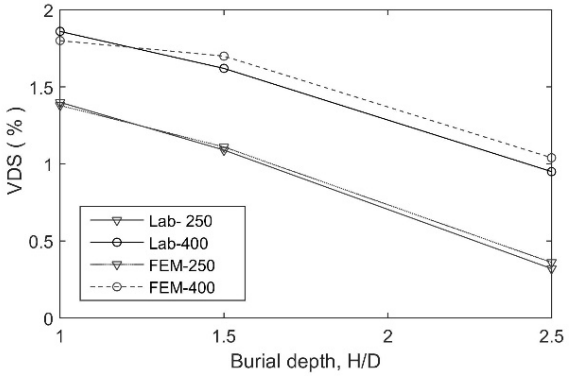

(a)

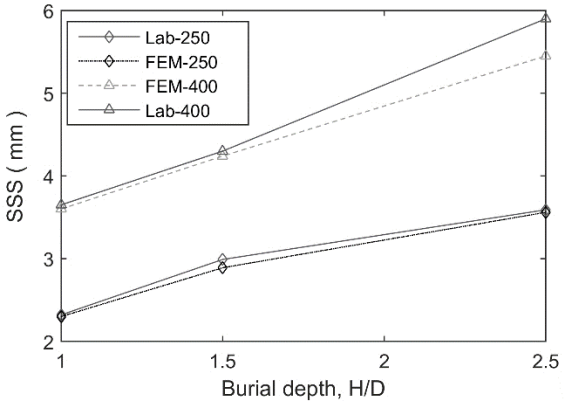

(b)

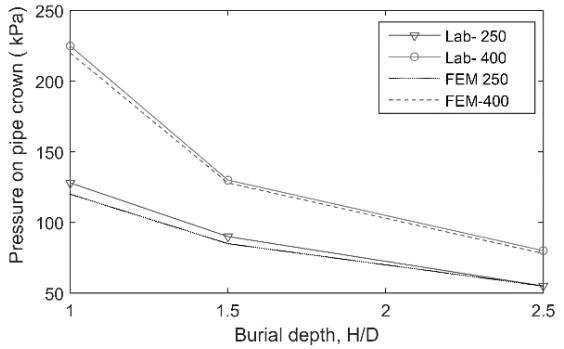

(c)

Fig. 9. (a) Variation of the maximum VDS of pipe (b) Soil surface settlement (c) earth pressure on pipe crown

4.4. Regression model

Based on experimental and numerical data, ration of soil surface settlement to pipe diameter, SSS/H, pipe vertical diametric strain, VDS, and stress on pipe crown to applied pressure, σ/P can be predicted as a function of pipe burial depth, H/D and magnitude of applied stress on soil surface, P. For this purpose, a regression model has been developed using Curve Fitting Toolbox in Matlab. This toolbox provides functions for fitting curves and surfaces to data and performs exploratory data analysis, pre-process and post-process data, compares candidate models, and removes outliers. After few trial and errors a linear polynomial model found to be best to predict model response. The function to fit a polynomial surface is f= fit ([x, y], z, 'poly23') or a degree 2 in x and degree 3 in y. So, the general equation to find a function between parameters will be:

$$f(x\,y) = p00 + p10 * x + p01 * y + p20 * x\hat{}2 + p11 * x * y \quad (3)$$

Where x and y are predictors variables while x is burial depth, H/D, and y is magnitude of surface pressure to minimum pressure, P/P_0. It is noted the equation is normalised using dimensionless values for pressure and surface settlement diving them by initial pressure and depth of pipe, respectively. From all tests and finite element analysis the partial regression coefficients (p00, p10, p01, p20 and p11) are calculated and are illustrated in Table **3**. It is noted R-square of VDS, SSS/H and σ/P are 0.9959, 0.9899 and 0.9842, respectively.

Table 3 Coefficients of regression model

Prediction	P00	P10	P01	P20	P11
VDS	1.11	-0.33	0.54	-0.16	0.22
SSS/H	0.15	-0.15	+0.22	0.04	-0.04
σ/P	0.98	-0.70	0.14	0.17	-0.08

The predicted values for VDS, SSS and σ were calculated based on developed equations and for each value the accuracy of parameter was assessed based on percentage of error calculating through Eq(4)

$$\boldsymbol{Ep} = \left(\frac{A_i - A_p}{A_i}\right)\text{X}100 \quad (4)$$

In which Ep is error percentage for both experimental and numerical analysis. A_i, is observed value of experimental test or numerical analysis and A_p is predicted value at each test series. In order to show the precision of predicted results, the cumulative histogram percentage of errors of the model for the prediction of SSS/H, VDS and σ/P for data are shown in Fig.10. It shows that for predicted parameters, for example, 80% of data have less than 6% error for SSS while this error for VDS is 6% and for σ is 10%.

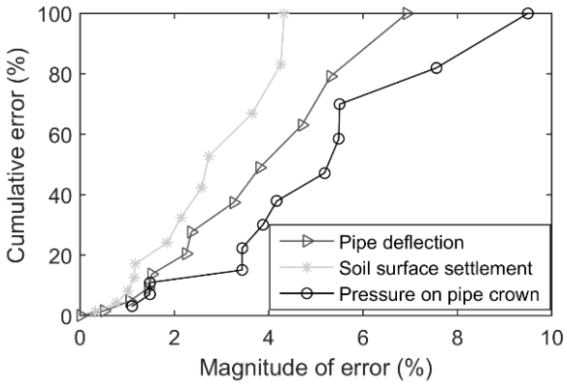

Fig. 10. Cumulative histogram percentage of error for the prediction of SSS, VDS and σ

5. CONCLUSION

In this research, an experimental and numerical analysis were carried out to investigate the impact of

pipe embedment depth and surface pressure on buried pipe response under traffic load. Two test series were performed (1) the ultimate bearing capacity of soil (2) traffic load tests to simulate traffic load on buried pipe. Numerical simulations were performed to better understand model behaviour under different conditions. The main conclusions through this study can be summarised as follows:

- Good agreement between numerical and experimental test results was observed for both test series.
- The results from experimental investigation and numerical simulations indicates that the ultimate bearing capacity of footing was almost 570 kPa for both analysis.
- Traffic test results reveal that pipe burial depth has a significant effect on surface settlement. Soil surface settlement increases as pipe burial depth increases. Increasing burial depth reduces pressure on pipe crown as well as pipe deflection.
- In addition, increasing surface pressure had a significant impact on increasing pipe deflection, soil surface settlement and pressure on pipe as expected.
- Regression model to estimate vertical diametric strain VDS and settlement of soil surface SSS and pressure on pipe crown σ was developed based on all numerical and experimental tests data.
- Cumulative error show that all predicted values have less than 10 % error.
- To provide further understanding of the behavior of buried pipes in response to external cyclic loading, this research could be extended in cyclic phase.
- In addition, the current study in experimental section was in the laboratory only and a full scale field verification is still needed.

6. ACKNOWLEDGMENT

The first author is the recipient of APPA-CUPS Scholarship of Curtin University. This support is highly acknowledged. The authors acknowledge help of Mark, Arne, Darren and Mirzet to run equipment and prepare samples at geotechnical laboratory of Curtin.

7. REFERENCES

1. Pipeline incident,. Pipeline Failure Causes. 2003.
2. Ko , D.H. and R. Kuwano, Model tests on behaviour of buried pipe in a large soil chamber , 2010 , London Taylor and Francis group, 2010: p. 625-631.
3. Moghaddas Tafreshi, S.N. and O. Khalaj, Analysis of repeated-load laboratory tests on buried plastic pipes in sand. Soil Dynamics and Earthquake Engineering, 2011. 31(1): p. 1-15.
4. Cao, Z., et al., Road surface permanent deformations with a shallowly buried steel-reinforced high-density polyethylene pipe under cyclic loading. Geotextiles and Geomembranes, 2016. 44(1): p. 28-38.
5. Tavakoli Mehrjardi, G., S.N. Moghaddas Tafreshi, and A.R. Dawson, Combined use of geocell reinforcement and rubber–soil mixtures to improve performance of buried pipes. Geotextiles and Geomembranes, 2012. 34: p. 116-130.
6. Tavakoli Mehrjardi, G., S.N. Moghaddas Tafreshi, and A.R. Dawson, Numerical analysis on Buried pipes protected by combination of geocell reinforcement and rubber-soil International Journal of Civil Engineering, 13 (2). , 2016. 13(2): p. 90-104.
7. Mosadegh. A and Nikraz. H. Finite Element Analyses of Buried Pipeline Subjected to Live Load Using ABAQUS. in Geoquebec conference. Sep 2015. Quebec City, Canada
8. AASHTO, American Association of State Highway and Transportation Officials (AASHTO). 1998: Washington DC USA.
9. ASCE, Guidelines for the Design of Buried Steel Pipe. 2001, americanlifelinesalliance.
10. ABAQUS-6.13, ABAQUS/CAE User's Manual. 2013, Dassault Systèmes: USA.
11. Moser, A.P., Buried Pipe Design, 2nd Edition. 2001: Mcgraw-hill.
12. Moayed, Z., R. R, and I. E., Evaluation on Bearing Capacity of Ring Foundations on two-Layered Soil. World Academy of Science, Engineering & Technology, 2012(61): p. 1108.
13. Mosadegh, A. and H. Nikraz, Bearing Capacity Evaluation of Footing on a Layered ‐ Soil using ABAQUS. Earth Sci Clim Change 2015 6(3): p. 1-8.
14. Terzaghi. K. and P. R.B., Soil Mechanics in Engineering Practice. 1948.

Advanced Engineering Forum
ISSN: 2234-991X, Vol. 16, pp 69-81
doi:10.4028/www.scientific.net/AEF.16.69

Submitted: 2015-12-01
Accepted: 2016-02-08

Evaluation of Permanent Deformation of BRA Modified Asphalt Paving Mixtures Based on Dynamic Creep Test Analysis

Muhammad Karami[1,2,a *], Ainalem Nega[2,b], Ahdyeh Mosadegh[3,c], and Hamid Nikraz[4,d]

[1] Department of Civil Engineering, Curtin University, GPO Box U1987, Perth, WA 6845, Australia
[2] Department of Civil Engineering, Lampung University, Bandar Lampung 35415, Indonesia
[3] Department of Civil Engineering, Curtin University, GPO Box U1987, Perth, WA 6845, Australia
[4] Department of Civil Engineering, Curtin University, GPO Box U1987, Perth, WA 6845, Australia
[5] Professor, Department of Civil Engineering, Curtin University, GPO Box U1987, Perth, WA 6845, Australia

[a] muhammadkarami@postgrad.curtin.edu.au, [b]Ainalem.Nega@curtin.edu.au, ,
[c]ahdyeh.mosadegh@postgrad.curtin.edu.au, [d]H.Nikraz@curtin.edu.au

Keywords: Permanent deformation; buton rock asphalt (BRA); unmodified asphalt binder; modified asphalt binder; dynamic creep test; flow number (FN); rutting

Abstract. The main objective this study is to evaluate the permanent deformation of buton rock asphalt (BRA) modified asphalt paving mixtures using dynamic creep test so that long term deformation behavior of asphalt mixtures can be characterized. The dynamic creep test was conducted on unmodified and BRA modified asphalt mixture using UTM25 machine. Asphalt cement of C170 from a regional supplier in Western Australia was used as the base asphalt binder for unmodified asphalt mixture; and BRA modified asphalt mixtures were made by substituting the base asphalt with 10, 20, and 30% (by weight of total asphalt binder) natural binder continuing granular BRA modified binder. The granular (pellets) BRA modified binder with a diameter of 7-10 mm was produced and extracted according the Australia Standard. Crushed granite was taken from a local quarry of the region; and dense graded for both unmodified and BRA modified asphalt mixture with the nominal size of 10 mm was used. The results of this analysis showed that BRA modified had a good performance as compared with unmodified asphalt mixtures, and increase in the content modified binder to 10%, 20%, and 30% resulted in decrease of the total permanent strain.

Part 2- UNPUBLISHED PAPERS

ONLY ABSTRACTS ARE PROVIDED

Numerical Analysis of a Small Flexible Pipe Subjected to Surface Load / Buried in Non-Treated and Cement Treated Trench

Ahdyeh MOSADEGH[a], Hamid NIKRAZ[b],

Department of Civil Engineering, Faculty of Science and Engineering, Curtin University, Australia

Abstract

The performance of a buried pipe subjected to traffic load was investigated using. Finite Element analysis, ABAQUS software. Impact of earth pressure, pipe burial depth and stabilization was investigated on model performance. Results were presented in terms of pipe deflection, soil surface settlement and pressure on pipe. For validation, numerical results obtained were compared with those from experimental investigations.

The results showed that a good agreement between numerical and experimental test was observed. Results also revealed that increasing burial depth decreases pipe deflection, increases soil surface settlement and decreases pressure on pipe while increasing surface pressure increases all mentioned parameters. Results also indicated that cement stabilization improved pipe behavior and reduced surface settlement of trench and pipe deflection. After stabilization lower strain occurred in the pipe and pipe deformation was more flat compared to pipe deformation mode in non-treated sand. From all results, equations were also developed for both non-treated and cement-treaded cases using Regression model in MATLAB. Cumulative error histogram showed that all predicted values have less than 10 % error.

Keywords: buried flexible pipe, surface load, numerical simulations, Abaqus, cement-stabilization

This paper is submitted to Geo-Edmonton 2018

Evaluating the Impact of Stabilization on Performance of Buried Pipe / Experimental Investigations

Ahdyeh MOSADEGH[a], Hamid NIKRAZ[b], Omid Khalaj[c]

[A and b] *Department of Civil Engineering, Faculty of Science and Engineering, Curtin University, Australia*
[C] *Department of Civil Engineering, University of West Bohemia, Czech Republic*

Abstract

In this paper, the impact of stabilization on a performance of buried pipe was investigated using experimental investigations. For this purpose, a series of static and cyclic load plate tests were conducted on a buried pipe to investigate model response during initial and cyclic phase. Results were presented in terms of pipe deflection, soil surface settlement and earth pressure on pipe.

Results revealed that stabilization improves model bearing capacity. In addition, cement stabilization improves model performance for all cases with remarkable reduction in pipe deflection, soil settlement and stress on pipe. It was also found that stabilization is more efficient in cyclic load than static load. A comparison of static and cyclic results signified the importance of first cycle showing up to 0.85 of model deformation occurs during the initial cycle. It is noted only one type of pipe, sand and cement are used in this laboratory study.

Keywords buried flexible pipe, cyclic load, experimental investigations, cement stabilization

A Numerical Parametric Study on Buried Pipe Performance Subjected to Various Loading Conditions

Ahdyeh MOSADEGH[a], Hamid NIKRAZ[b],

[a] *PhD Candidate of Civil Engineering, Curtin University, Perth, Australia*

[b] *Professor of Civil Engineering, Curtin University, Perth, Australia*

Abstract

A numerical parametric study was carried out to investigate the influence of different factors on pipe-soil behaviour under live load using ABAQUS. The effect of seven different factors including burial depth of pipe, pressure magnitude, width of loading area, internal pressure, pipe-soil interaction properties, pipe material and wall thickness on pipe deflection, surface settlement, maximum stress in pipe wall as well as earth pressure on pipe were investigated. Results indicated that surface pressure has the highest contribution on model response following by burial depth and loading area. Internal pressure has the highest contribution on stress variation in pipe wall but its contributions on other factors including pipe deflection, surface settlement and earth pressure on pipe is not remarkable. The contribution of other investigating factors on model performance was not remarkable.

KEY WORDS: Parametric study, finite element analysis, Abaqus, buried pipe

Experimental Investigations of Buried Pipe Performance under Cyclic Load

Ahdyeh MOSADEGH[a], Hamid NIKRAZ[b], Omid Khalaj[c]

[A and b] *Department of Civil Engineering, Faculty of Science and Engineering, Curtin University, Australia*

[C] *Department of Civil Engineering, University of West Bohemia, Czech Republic*

Abstract

In this paper, a flexible buried pipe response under cyclic load is investigated using experimental investigations. A series of laboratory tests were carried out to investigate the impact of surface pressure and burial depth and number of cycles on the model response. Experimental tests were carried out using UTM25 to apply cyclic load on surface of a tank in which pipe was buried.

Results revealed that pipe burial depth has a significant impact on all variables. Soil surface settlement increases as pipe burial depth increases. Increasing burial depth reduces pressure on pipe crown as well as pipe deflection. Increasing surface pressure has a significant impact on increasing pipe deflection, soil surface settlement and pressure on pipe as expected. Results also showed that high portion of model deformation occurs during first cycle. This ratio of soil surface settlement in first cycle to cycle N, varies between 0.05 and 0.35 while N is chosen to be 100^{th} and 500^{th}. In addition, between 0.35 and 0.75 of pipe deformation occurs during first cycle.

KEY WORDS: buried flexible pipe, cyclic load, experimental investigations

Comparison of Neural network and Regression Model in Developing Equations to Predict Pipe Performance under Traffic Load

Ahdyeh MOSADEGH[a], Hamid NIKRAZ[b]

A and b Department of Civil Engineering, Faculty of Science and Engineering, Curtin University, Australia

Abstract

In this paper, two different methods of Linear Regression Model (LRM) and Artificial Neural Network (ANN) were implemented including for predicting model response. Equations were developed using Matlab software to estimate pipe vertical deflection, soil surface settlement and pressure on pipe crown based on experimental tests data during initial and cyclic phase for both non-treated and cement-treaded cases. Then, the predicted values based on each method were compared with experimental data. Finally, in order to show the precision of predicted results the magnitude of error and cumulative histogram percentage of errors were calculated.

It was shown that while linear regression modelling approach was deficient to predict desired parameters, more accurate results were obtained using neural network model. In addition, verification of two models and calculating errors revealed that higher errors are observed in the beginning of each cyclic phase. Cumulative error analysis showed that all predicted parameters in neural network have less than 20% error. This value for regression method is 42%.

KEY WORDS: Neural network, linear regression model, experimental data, predicting equations, Matlab, buried pipe response

APPENDIX B

VALIDATION OF ABAQUS MODEL WITH PLAXIS

B.1. INTRODUCTION

The validation of ABAQUS model for evaluating behaviour of buried pipe subjected to surface live load was carried out using PLAXIS 2D (Brinkgreve et al., 2011; Plaxis, 2011). A set of soil-structure interaction analysis was conducted to investigate the suitability of the ABAQUS to examine whether both software can produce the same results.

B.2. METHODOLOGY AND MATERIAL PROPERTIES

In this section, the methodology and material properties for modelling with PLAXIS is presented (Brinkgreve et al., 2011). It is noted that the methodology and material properties for simulation with ABAQUS is similar to those presented in Chapter 3 and is not presented here.

Due to the long length of the pipe compared to its width, the problem was modelled assuming plane strain conditions. The geometry of model is shown in Figure-B-1. For boundary conditions, both vertical sides of the model are fixed in a horizontal direction with vertical displacement, and the bottom of the model is fixed in both vertical and horizontal directions. The same material properties for soils and pipe were used in Chapter 3 were used in PLAXIS as well. For trench soil, sand material was chosen based on the appropriate constitutive model in PLAXIS library. The hyperbolic hardening soil model was used which is a refinement of Duncan and Chang model (M. Duncan & Chang, 1970). Therefore, Hardening-Soil mode was chosen to model trench soil and input parameters were selected from literature and adopted from Simpson et al (Simpson, 2009). SW90 represents sand material with cohesion of 0.001 KPa, friction angel of 45.5 degrees and dilation angel of 15.5 degrees. (Likitlersuang et al., 2013). Granular soil properties were the same as those used in parametric study in Chapter 3. Steel pipe was modelled using plate elements assuming elastic behaviour and flexural rigidities based on gross pipe dimensions. $EI = 1.4 \times 10^3\ KN.m^2$, axial rigidity $EA = 1.2 \times 10^6\ KN/m$ and Poisson ratio v=0.3. In all models, the mesh has been refined in areas with stress concentration around the pipe. The 15-node triangular elements for interaction interface elements were used at pipe-soil interaction area consisting five pairs of nodes with zero thickness. Interface elements were used to simulate the interaction between the pipe and the soil. Two types of interaction properties were considered in the analysis, one rigid interaction and the other one elastic-perfectly plastic springs with strength reduction factor of 0.5. The applying load in PLAXIS was chosen to be staged construction. Traffic load was applied at the final stage of modelling.

Traffic load was simulated as a uniform distributed load of 200, 400 and 550kPa acting on 2 m length as shown in Figure B-1.

Table B-1 Soil properties

Soil			
γ_{sat}	*22*	v	*0.3*
γ_{unsat}	*20*	M (power)	*0.75*
e_{int}	*0.5*	d KN/m^2	*0.01*
E_{oed} *KN/m^2*	*32e3*	ϕ	*45*
E_{50} *KN/m^2*	*32e3*	ψ	*15*
E_{ur} *KN/m^2*	*97e3*	R	*0.5*

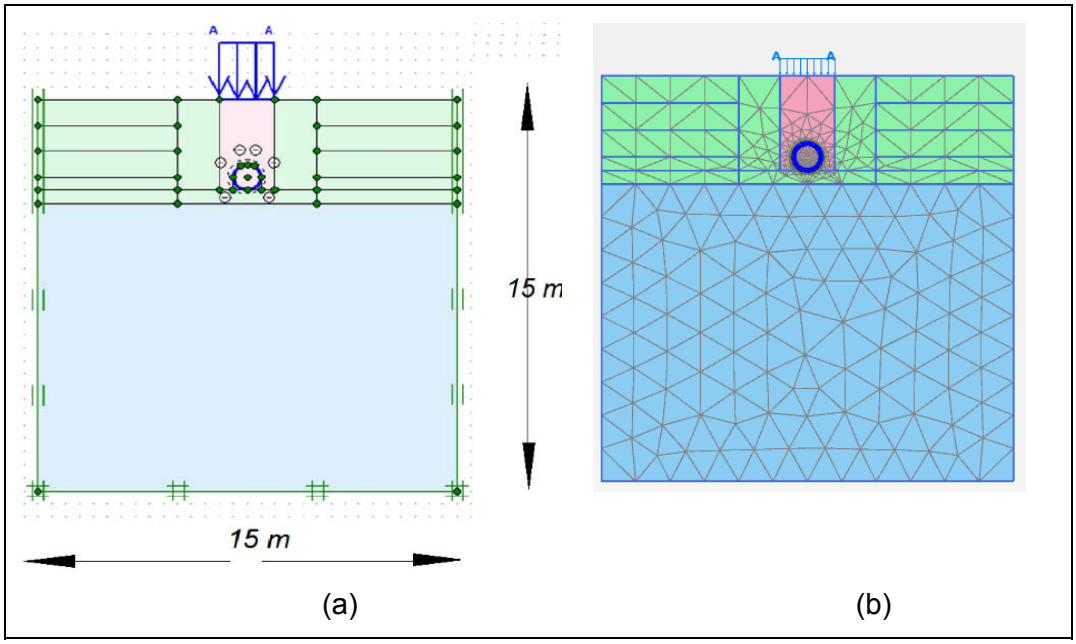

Figure B-1 (a) Boundary condition of the model (b) finite element discretization

B.3. RESULTS

The results of PLAXIS simulations to investigate buried steel pipe response due to surface pressure are briefly presented in this section. Two criteria were selected to be assessed (1) impact of surface load magnitude and (2) interface properties impact. The impact of change in surface pressure and interface properties on model response are investigated and results are discussed in the following section. Figure B-2 shows deformations of whole model due to live load for the case of H=2.5D under surface pressure of 550 kPa. It can be seen that the deflection on soil surface and pipe crown

are about 8 cm and 5 cm, respectively. These values are consistent with those achieved with ABAQUS presented in Chapter 3.

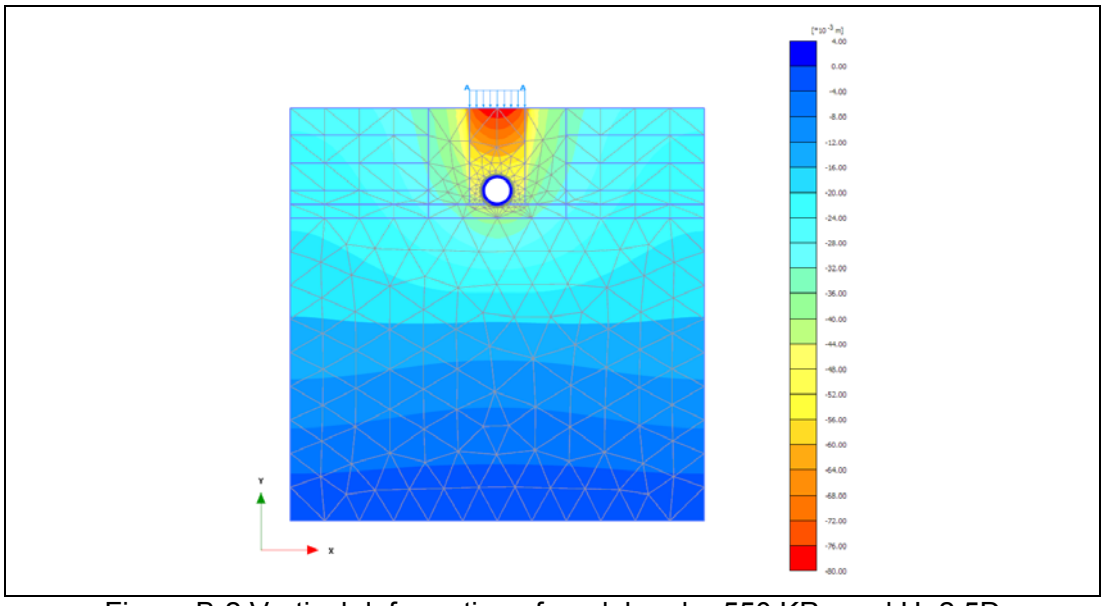

Figure B-2 Vertical deformation of model under 550 KPa and H=2.5D

Impact of surface pressure magnitude on model deformation is analysed and results are illustrated in Figure B-3-a. The vertical axis represents vertical deformation and horizontal axis represents depth from soil surface. For example, zero on horizontal axis represents soil surface and 2.5 represents pipe crown as illustrated on the figure. It can be seen that higher surface pressure induces higher vertical deformation in the model. For example, under surface pressure of 550 kPa, soil surface deformation is 7.8 cm while this value for surface pressure of 400 and 200 kPa are 6 cm and 2.3 cm, respectively. The gap between graphs or impact of surface pressure is maximum on soil surface. This impact is minimum at pipe invert and the gap between three graphs is minimum.

Impact of interface properties is also studied. The impact of two different types of friction coefficient under surface load of 550 and 200 KPa is investigated and results are illustrated in Figure B-3-b. It can be seen that strength reduction interface transmits lower vertical deformation within the soil body although this difference is negligible. For example, under surface pressure of 550 kPa, soil surface settlement is 8 cm for rigid body interface. This value for the interface with interaction ratio of 0.5 is 7.8 cm.

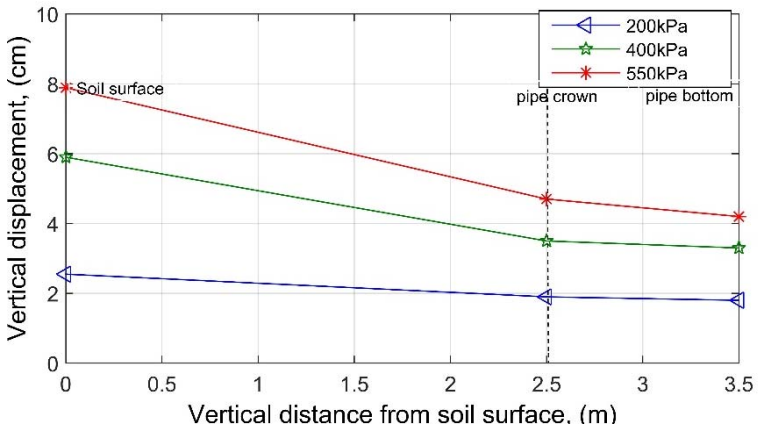

(a)

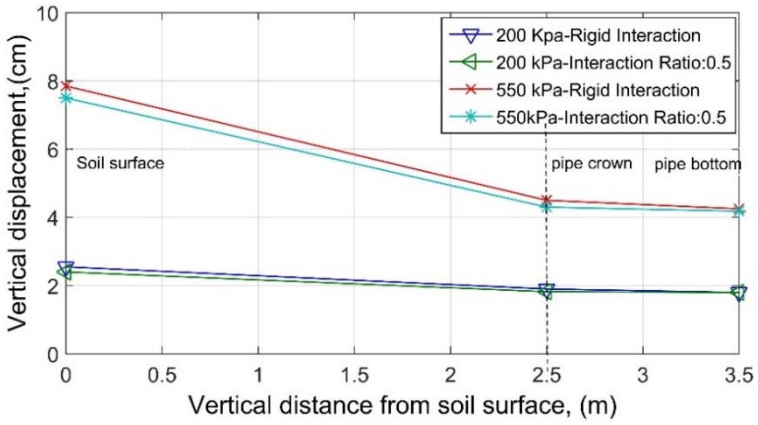

(b)

Figure B-3 Impact of surface (a) pressure (b) interface properties on model vertical displacement

B.4. VALIDATION

The results from ABAQUS and PLAXIS simulations are compared and illustrated in Figure B-4. The figure compares results from ABAQUS and PLAXIS for two different surface pressure and two different types of interaction properties. It can be seen that results from PLAXIS simulations and ABAQUS calculations are in good agreement.

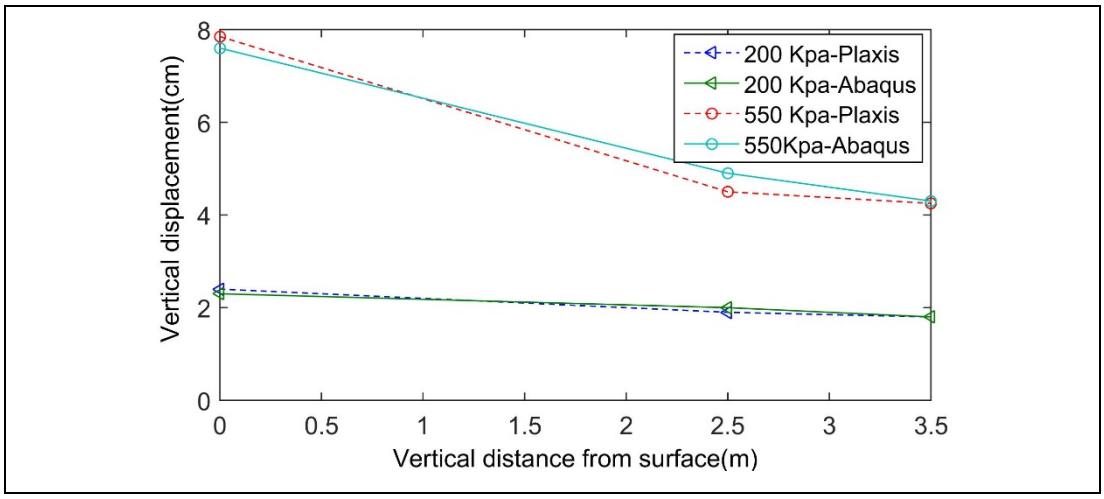

Figure B-4 Comparison of results from PLAXIS with ABAQUS

B.6. REFERENCES

Brinkgreve, R. B. J., Swolfs, W. M., & Engin, E. (2011). *Plaxis Introductory: Student Pack and Tutorial Manual 2010*: CRC Press, Inc.

Likitlersuang, S., Surarak, C., Balasubramaniam, A., Oh, E., Ryull K, S., & Wanatowski, D. (2013). *Duncan-Chang -Parameters for Hyperbolic Stress Strain Behaviour of Soft Bangkok Clay*.

M. Duncan, J., & Chang, C. Y. (1970). *Nonlinear analysis of stress and strain in soils* (Vol. 96).

Plaxis. (2011). Plaxis Validation & Verification *Essential for geotechnical professionals*.

Simpson, G. H. (2009). *Investigation of Suitable Soil Constitutive Models for 3-D Finite Element Studies of Live Load Distribution Through Fills Onto Culverts*. Retrieved from

APPENDIX C

CONSTITUTIVE MODELS FOR SOIL

C.1 INTRODUCTION

Two constitutive modelling of soil plays an important key role in obtaining accurate numerical results. As mentioned in Chapter 4, two types of sandy soil and cement-treated soils were used in this research. These soils were modelled using Drucker-Prager and Mohr-Coulomb constitutive models for numerical simulations. In the following section, first a brief review of Mohr-Coulomb plasticity model is described. Then, Drucker-Prager plasticity model is explained and some advantages and limitations of each model are addressed in each section.

C.2. MOHR-COULOMB PLASTICITY MODEL

A common and simple yield criterion for soil is Mohr Coulomb. In this model elastic properties are required as well as parameters describing soil failure. For elastic properties Poisson ratio and elastic modulus describe soil behaviour. For plastic properties friction angle and dilation angle as well as cohesion are required to describe material properties. Although Byrne et al in 1987 showed that Poisson ratio (ϑ) can change between 0.1 to 0.5 for different value of strain, a constant value of 0.3 to 0.35 is selected in practice. Other elastic properties can be obtained through triaxial results. The Mohr-Coulomb plasticity model is a perfect plasticity model proposed by Coulomb in 1773 for cohesive frictional materials. In the model shear strength τ, is a function of the applied normal stress σ. The Mohr-Coulomb model provides the relationship between the two:

$$\tau = c + \sigma tan\varphi \qquad \text{C-1}$$

Where *C* is the cohesion intercept and φ is the internal friction angle. The model is based on plotting Mohr's circle for states of stress at failure in the plane of the maximum and minimum principal stresses. The failure envelope is a curved line obtaining from a plot of the shear strength of a material versus the applied normal stress. Mohr's circles as shown in Figure C-1.

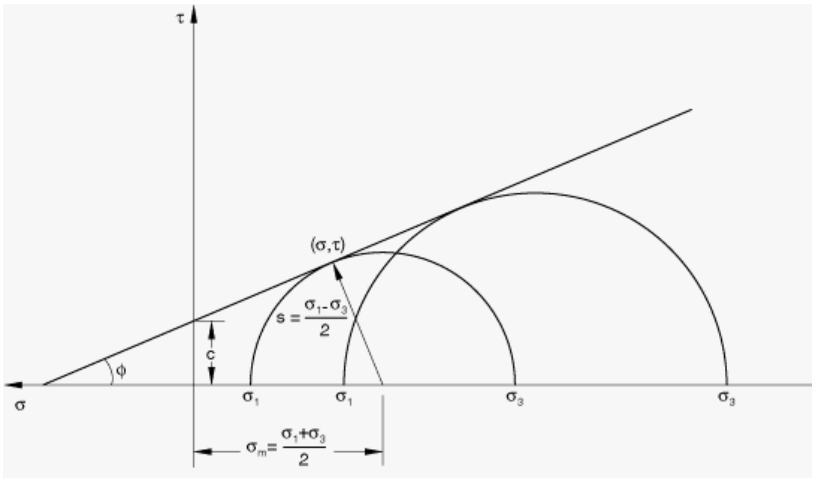

Figure C-1. Mohr Coulomb failure envelope (ABAQUS, 2013)

The yield criterion of Mohr-Coulomb model can be also expressed in terms of principal stress as well as follow.as below

$$f = (\sigma_1 - \sigma_3) - (\sigma_1 + \sigma_3)sin\varphi - 2ccos\varphi = 0 \qquad \text{C-2}$$

In which σ_1 and σ_3 are maximum and minimum principal stresses.

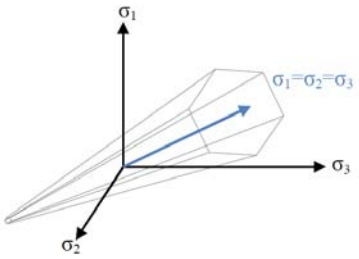

Figure C-2. The Mohr –Coulomb yield criterion on a deviatoric plane

The yield function of built-in Mohr-Coulomb model of ABAQUS is based on classic model and equation is shown in equation C-3 and Figure C-3.

$$f=R_{mc}q - ptan\varphi - c=0 \qquad \text{C-3}$$

Where R_{mc} is a measure of the shape of yield surface in the deviatoric plane. Φ is slope of the Mohr-Coulomb yield surface. However, the flow potential is a hyperbolic function in p-R_{mc}q plane with no corners instead of hexagon. More details can be found in (ABAQUS, 2013, Helwany, 2007).

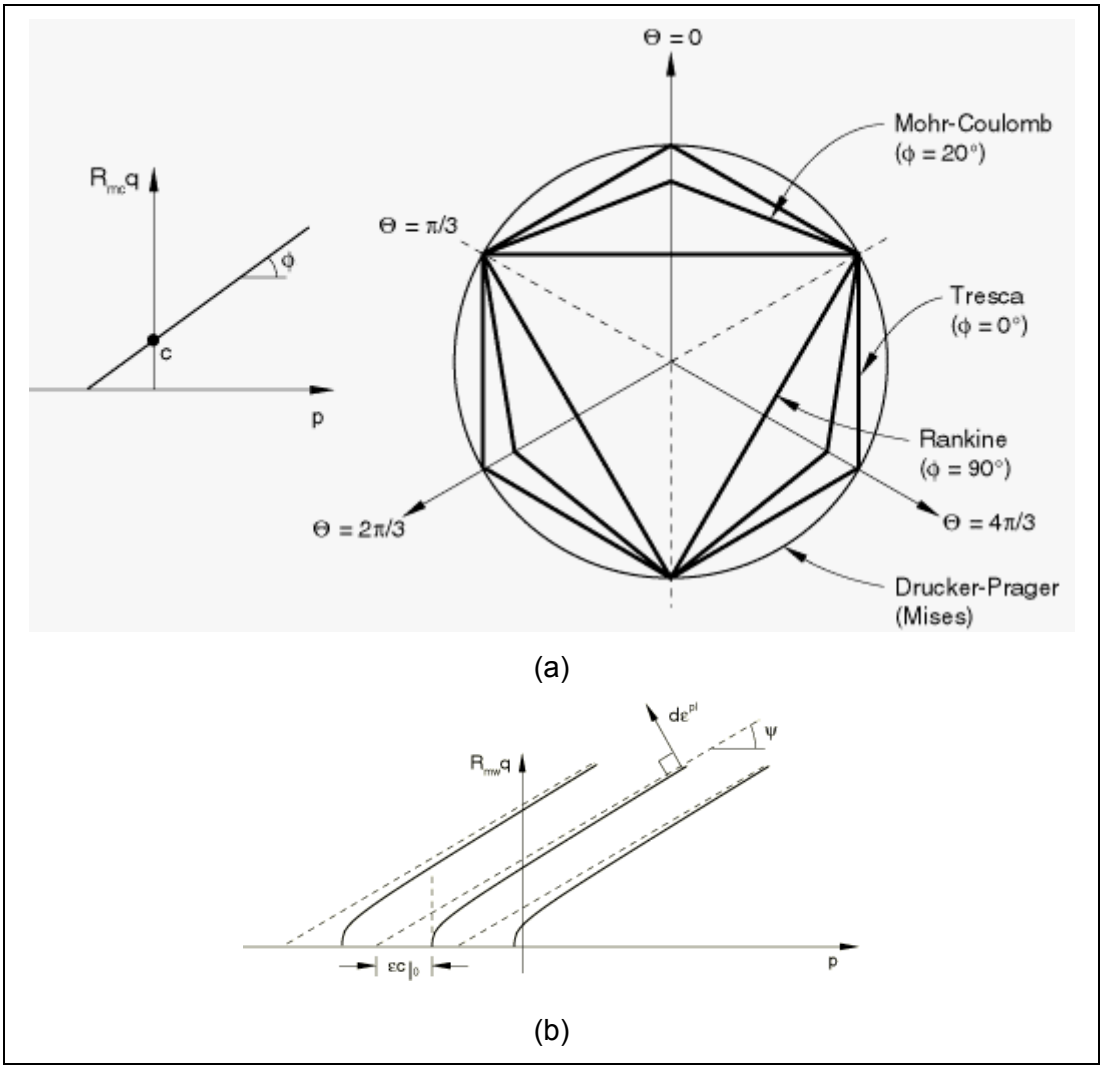

Figure C-3. Yield surface in the meridional plane (b) Mohr Coulomb flow potential in the meridional plane

Some advantages of using Mohr-Coulomb model are:

- It is simple.
- The model is identified for granular material like soils under monotonic loads.
- Yield surface has corners.
- It is valid for many soils.
- Model parameters can be easily obtained from soil experiments.

One major limitation of Mohr Coulomb model is that yield surface has corners while in built-in model in ABAQUS this problem has been solved.

C.3. DRUCKER-PRAGER PLASTICITY MODEL

The Drucker-Prager plasticity first introduced by Drucker and Prager in 1952 for frictional soil. The yield criterion uses the mean pressure, to create a smoothed version of above condition which results in a semi-infinite cone, defined by equation C-4 and equation C-5 for linear and hyperbolic behaviour, respectively:

$$F = t - d - ptan\beta = 0 \quad \text{C-4}$$

$$F = \sqrt{(d_0' - P_1\tan)^2 + q^2} - ptan\beta - d' = 0 \quad \text{C-5}$$

The variable *t* is a measure of deviator stress and more details as shown in Figure C-4 (ABAQUS, 2013). It is worth noting that for plane strain considerations, the Mohr-Coulomb parameters and Drucker-Prager parameters can be converted to each other based on existing formulations as follows in plain strain condition

$$\tan\beta' = \frac{3\sqrt{3}\,tan\phi\prime}{\sqrt{9+12tan^2\phi\prime}},\ d' = \frac{3\sqrt{3}\,C\prime}{\sqrt{9+12tan^2\phi\prime}} \quad \text{C-6}$$

In three dimensional problems:

$$\tan\beta' = \frac{6\,sin\phi\prime}{3\pm sin\phi\prime},\ d' = \frac{6c\cos\phi\prime}{3\pm sin\phi\prime} \quad \text{C-7}$$

It is noted more details about this model can be found in section 23.3 in ABAQUS documents (ABAQUS, 2013).

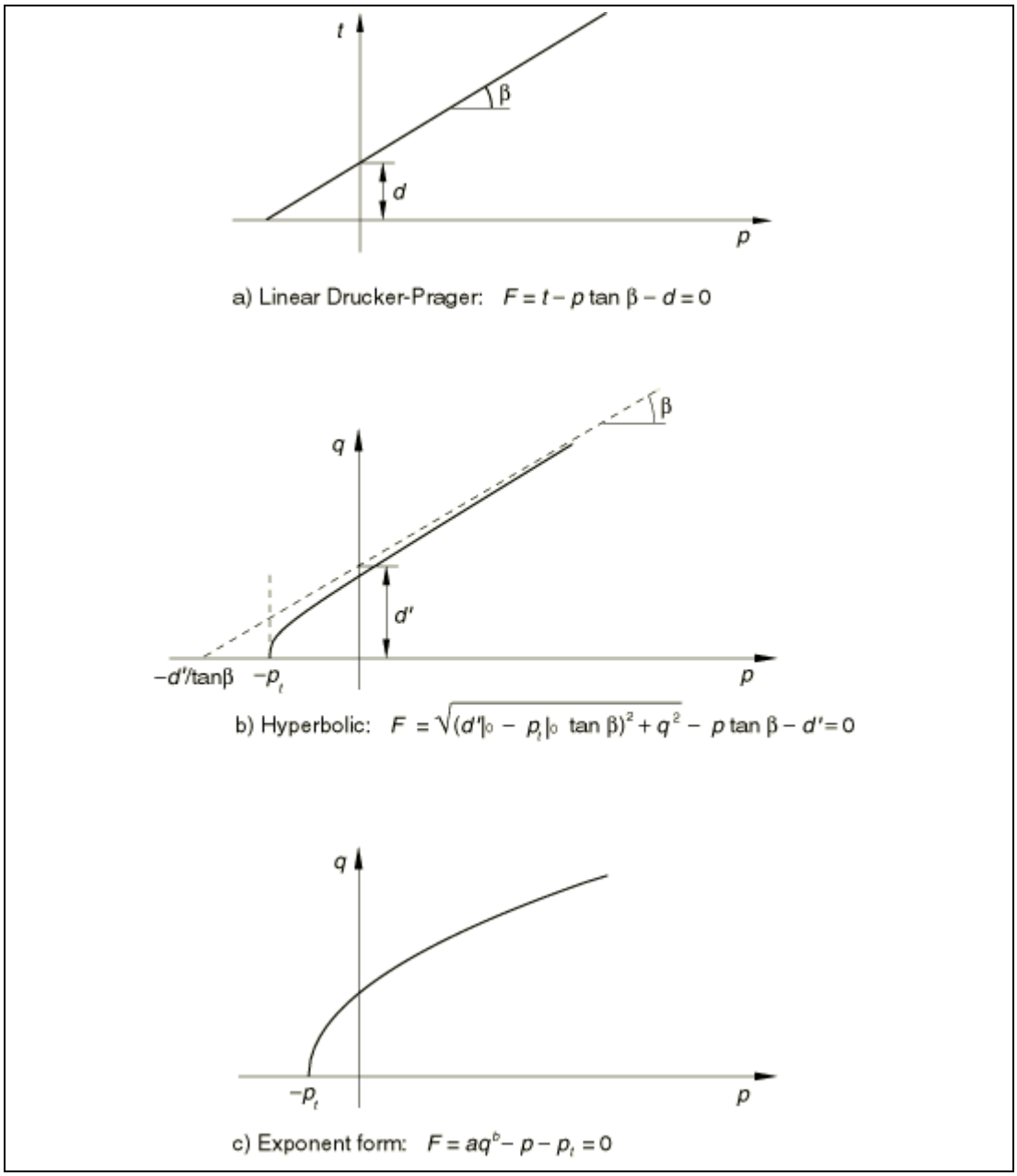

Figure C-4 Yield criteria of Drucker Prager (ABAQUS, 2013)

Some advantages of using Drucker-Prager are:

- It is simple to use.
- It can be easily matched with Mohr-Coulomb model.
- It satisfies the associate flow rules.

One major limitation of Drucker-Prager model is that it cannot reproduce the hysteretic behaviour within failure surface.

C.4. DESCRIPTIONS OF MATERIAL PROPERTIES IN ABAQUS

In the model in ABAQUS.CAE following descriptions are used in defining material properties of current project based on Drucker-Prager and Mohr-Coulomb models.

For backfill material an extended Drucker-Prager model was used as follows:

- The shear criterion parameter was set to linear and hyperbolic.
- Unsymmetrical solver was defined as *STEP,UNSYMM=YES for plastic flow rule as non-associated
- The Drucker-Prager plasticity options were used to define β, ε and K, the flow potential eccentricity parameter was used as ε =0.1 and other properties are illustrated in Figure C-5. D=35 and K=1.
- The Drucker-Prager hardening option was also defined as *Drucker Prager Hardening 100000, 0 in which 100000 is yield stress and 0 is plastic strain at failure.

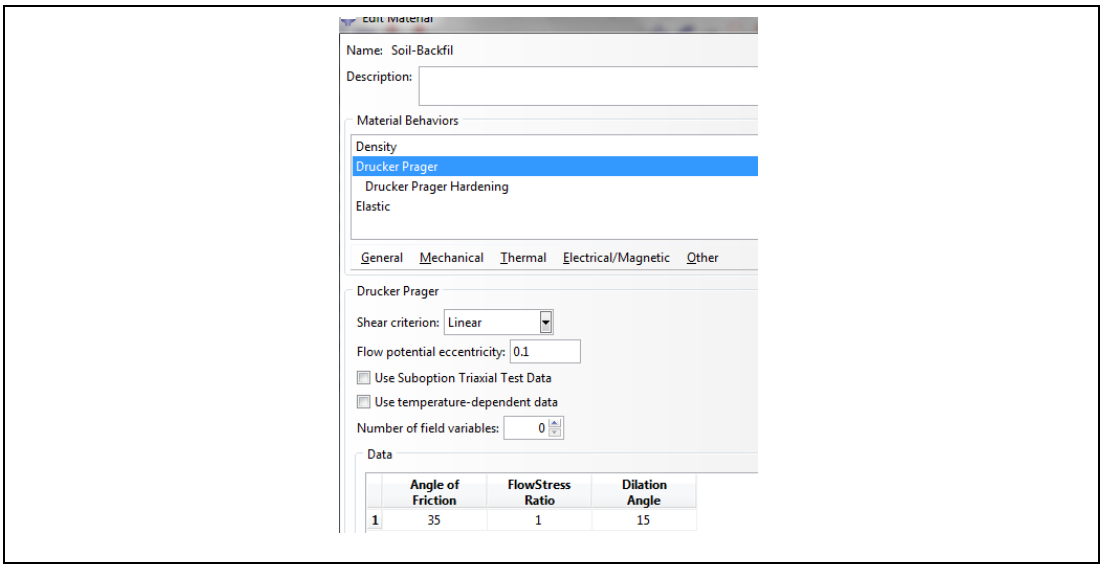

Figure C-5 Drucker-Prager plasticity data input in ABAQUS for sand in the current project

For cohesive / cemented material the Mohr Coulomb model was used as follows:

- Linear, isotropic elasticity was used.
- Non-associate flow rule was considered to define material property and unsymmetrical solver was needed to be applied as *STEP,UNSYMM=YES
- The Mohr-Coulomb option was used to define φ, ψ and ε

- The eccentricity parameter was used as 0.1.
- And dilation angle and friction of soil was chosen not to be functions of temperature.

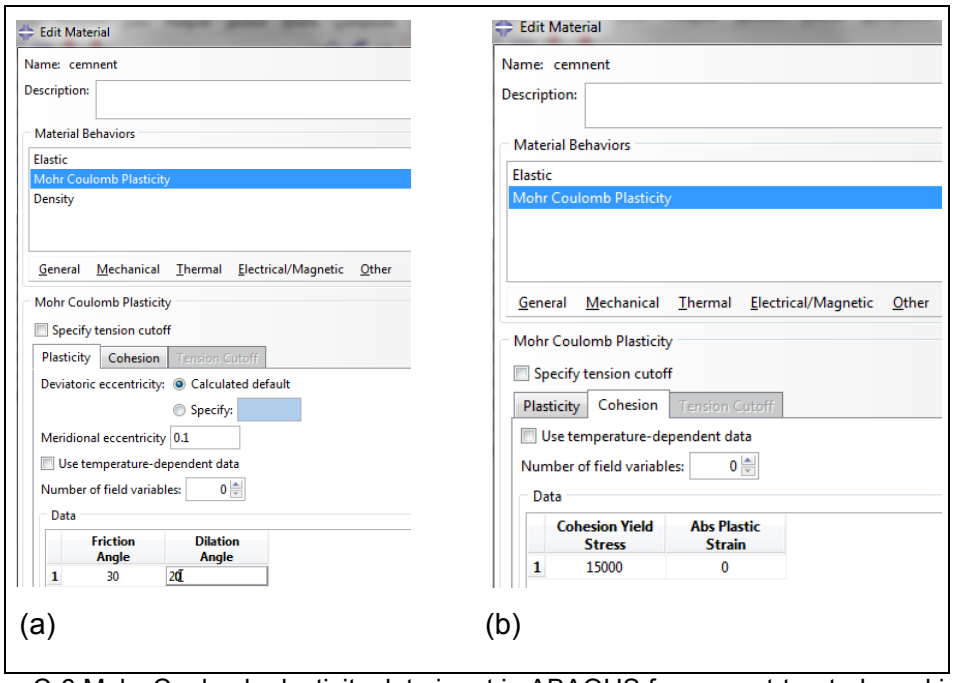

Figure C-6 Mohr-Coulomb plasticity data input in ABAQUS for cement-treated sand in the current project

C.4. SUMMARY

The general plasticity and two soil constitutive models available in ABAQUS have been discussed in this section. The theory of each model were briefly discussed. At the end constitutive models used in the current project to define material properties in ABAQUS input file were discussed.

C.5. REFERENCES

ABAQUS-6.13 2013, *ABAQUS/CAE User's Manual*, Dassault Systèmes, USA.

Helwany S (2007) Applied Soil Mechanics with ABAQUS Applications. John Wiley and Sons, New York, United States.

APPENDIX D

PREDICTING MODEL RESPONSE

D.1. MATLAB CODE FOR MULTIPLE REGRESSION MODEL

In this section the results of multiple linear regression equations for predicting model response are presented. The output, predicted values and method were addressed in Chapter7.

The predicted equations are represented in terms of H/D, P and N and denoting burial depth, surface pressure and number of cycles. It is noted for some cases, predicted equations include LG N which is natural logarithmic function of number of cycles.

D.1. M-FILE IN MATLAB

To implement the regress command, the m-file was used. One example of m-file used in the research to predict VDS is illustrated as below.

```
%% Regression models
%
%
clear;
clc;
warning('off','MATLAB:xlswrite:AddSheet');

%% Import Data from xlsx file
%
path_input='put directory';
file_input=fullfile(path_input,'name of file.xlsx');
% By default it reads the first sheet page of the xls file
VDS_tbl = readtable(file_input,'ReadRowNames',true);

%% Create fitted models
%
% GENERAL Model
modelspec = 'VDS ~HD^2:LG2^2+P+N';
mdl = fitlm(VDS_tbl,modelspec);

%
coefnames = mdl.CoefficientNames;
coefvals = mdl.Coefficients(:,1); % table
coefvals = table2array(coefvals);
mdl;
mdl.Formula

%% SIMPLIFIED MODEL
mdl1= step(mdl,'NSteps',10);

coefnames1 = mdl1.CoefficientNames;
% mdl1.Formula can be used to show the formula of the model
% table new model
coefvals1 = mdl1.Coefficients(:,1); % table
coefvals1 = table2array(coefvals1);
mdl1;
mdl1.Formula
```

MULTIPLE LINEAR REGRESSION EQUATIONS

After running the m-file, equations are displayed along with tables showing estimated coefficients. Equations are shown in equations D-1 to D-6 and estimated coefficients are presented in Tables D-1 to D-6. The regression coefficient estimated for each case including predictor variables, coefficient estimates, the standard error, T-statistic, and P-values are displayed in the first column to the fifth column. It can be seen that predicted equations using linear regression model are quite long equations. However, the quality of all models are excellent as p-value are very small and R-squared are close to 1 as were discussed earlier in Chapter 7. Predicted equations and estimated coefficients are presented as follows.

NON-TREATED CASE

VDS-NC ~ 1 + HD*P + HD*N + HD*LG + P*LG + N*LG + HD^2 D-1

SSSH ~ 1 + HD:P:LG + HD:P:N:LG + (HD^2):P:LG D-2

P/P ~ 1 + HD*LG + P*N + P*LG + (HD^2):LG + HD*P*N*LG D-3

Table D-1 Estimated coefficients for VDS-Non-treated sand

	Est	SE	Tsat	Pvalue
'(Intercept)'	-15.925	0.156	-101.831	0
'HD'	19.266	0.178	108.173	0
'P'	15.512	0.110	140.681	0
'N'	-0.018	0.002	-9.528	8.04E-21
'LG'	0.429	0.058	7.395	2.60E-13
'HD:P'	-17.100	0.131	-130.157	0
'HD:N'	0.002	0.000	9.924	2.17E-22
'HD:LG'	-0.407	0.023	-17.811	2.19E-63
'P:LG'	0.691	0.021	32.999	4.61E-172
'N:LG'	0.006	0.001	8.102	1.28E-15
'HD^2'	-5.124	0.049	-105.101	0
'HD^2:P'	4.421	0.037	121.101	0

Table D-2 Estimated coefficients for SSS-Pure sand

	Est	SE	Tsat	Pvalue
'(Intercept)'	-15.925	0.156	-101.831	0
'HD'	19.266	0.178	108.173	0
'P'	15.512	0.110	140.681	0
'N'	-0.018	0.002	-9.528	8.04E-21
'LG'	0.429	0.058	7.395	2.60E-13
'HD:P'	-17.100	0.131	-130.157	0
'HD:N'	0.002	0.000	9.924	2.17E-22
'HD:LG'	-0.407	z	-17.811	2.19E-63
'P:LG'	0.691	0.021	32.999	4.61E-172
'N:LG'	0.006	0.001	8.102	1.28E-15
'HD^2'	-5.124	0.049	-105.101	0
'HD^2:P'	4.421	0.037	121.101	0

Table D-3 Estimated coefficients for pressure sand

	Est	SE	Tsat	Pvalue
'(Intercept)'	-3.983	0.483	-8.240	2.48E-15
'HD'	-0.262	0.062	-4.254	2.62E-05
'P'	4.754	0.508	9.359	5.88E-19
'N'	-0.004	0.001	-7.291	1.66E-12
'LG'	2.509	0.246	10.211	6.58E-22
'HD:LG'	-0.226	0.034	-6.561	1.66E-10
'P:N'	0.004	0.001	6.992	1.14E-11
'P:LG'	-2.355	0.260	-9.059	5.90E-18
'HD^2:LG'	0.085	0.002	43.166	1.28E-152
'HD:P:N:LG'	0.000	0.000	-3.860	0.000132

CEMENT-TREATED CASE

VDS ~ 1 + P*HD + P*N + P:LG + HD*N + HD^2+ P:HD:LG + (P^2):LG + (P^2):HD2:LG+ P:(HD^2):LG2 + (P^2):(HD^2):LG D-4

SSS/H ~ 1 + P*HD + P*N + HD*N + HD:LG:N + P:HD:LG:N2 + (HD^2):LG:N+ P:(HD^2):LG:N D-5

$\sigma/P \sim 1 + (H/D)*N + (H/D)^2 + (P)^2$ D-6

Table D-4 Estimated coefficients for VDS-cement-treated sand

'(Intercept)'	-0.46585	0.085864	-5.42548	6.25E-08
'P'	-0.73827	0.047696	-15.4785	5.03E-52
'HD'	1.470729	0.079688	18.45605	4.45E-72
'N'	-0.00018	6.37E-05	-2.84938	0.004411
'P:HD'	0.629536	0.025032	25.14947	1.18E-126
'P:N'	0.00053	4.18E-05	12.67763	6.64E-36
'P:LG'	-0.53919	0.053423	-10.0928	1.43E-23
'HD:N'	-0.00021	2.01E-05	-10.5495	1.44E-25
'HD^2'	-0.6647	0.020235	-32.8499	4.68E-202
'P:HD:LG'	-0.01956	0.05728	-0.34148	0.73277
'P^2:LG'	1.104077	0.027876	39.60666	1.22E-275
'P^2:HD:LG'	-0.70529	0.026778	-26.3388	1.56E-137
'P:HD^2:LG'	0.133576	0.015411	8.667653	7.14E-18
'P^2:HD^2:LG'	0.079361	0.006976	11.37606	2.22E-29

Table D-5 Estimated coefficients for SSS-cement-treated sand

	Est	SE	Tsat	Pvalue
'(Intercept)'	0.046643	0.00099	47.09102	0
'P'	-0.02653	0.000746	-35.5657	5.06E-231
'HD'	-0.01567	0.000511	-30.6541	1.78E-179
'N'	-0.00027	8.05E-06	-34.0683	6.05E-215
'P:HD'	0.010781	0.000378	28.51144	3.30E-158
'P:N'	0.000288	6.09E-06	47.36563	0
'HD:N'	-1.77E-05	3.08E-06	-5.74672	1.00E-08
'HD:N:LG'	7.91E-05	3.57E-06	22.12777	1.55E-100
'P:HD:N:LG'	-7.61E-05	2.60E-06	-29.2385	2.49E-165
'HD^2:N:LG'	-1.35E-05	9.54E-07	-14.1318	6.27E-44
'P:HD^2:N:LG'	1.41E-05	7.17E-07	19.71897	1.99E-81

Table D 6 Estimated coefficients for stress on pipe in cement-treated trench

	Est	SE	Tsat	Pvalue
'(Intercept)'	0.925264	0.008885	104.14	5.91E-294
'HD'	-0.76989	0.009787	-78.67	4.49E-247
'N'	0.000225	2.76E-05	8.17	3.86E-15
'HD:N'	-7.93E-05	8.16E-06	-9.71	3.57E-20
'HD^2'	0.179065	0.002641	67.80	7.78E-223

APPENDIX E

PERMISSION EMAILS FROM COPYRIGHT OWNERS

PERMISSION TO USE COPYRIGHT MATERIAL AS SPECIFIED BELOW:

Mosadegh. A; Nikraz.H , BURIED PIPE RESPONSE SUBJECTED TO TRAFFIC LOAD EXPERIMENTAL AND NUMERICAL INVESTIGATIONS, International Journal of GEOMATE, Nov., 2017, Vol.13, Issue 39, pp.01-08, ISSN:2186-2990, Japan,
DOI: https://doi.org/10.21660/2017.39.91957

I hereby give permission for **Ahdyeh Mosadegh** to include the abovementioned material(s) in his/her higher degree thesis for Curtin University, and to communicate this material via the espace institutional repository. This permission is granted on a non-exclusive basis and for an indefinite period.

I confirm that I am the copyright owner of the specified material.

Signed: 

Name: Prof. Dr. Zakaria Hossain

Position: Editor-in-Chief, International Journal of GEOMATE

Date: 28 Nov. 2017

Please return signed form to **ahdyeh.mosadegh@postgrad.curtin.edu.au**

ELSEVIER LICENSE
TERMS AND CONDITIONS

Jul 22, 2018

This Agreement between Curtin University ("You") and Elsevier ("Elsevier") consists of your license details and the terms and conditions provided by Elsevier and Copyright Clearance Center.

License Number	4394260253498
License date	Jul 22, 2018
Licensed Content Publisher	Elsevier
Licensed Content Publication	Probabilistic Engineering Mechanics
Licensed Content Title	Application of stochastic differential equations to seismic reliability analysis of hysteretic structures
Licensed Content Author	Yoshiyuki Suzuki,Ryoichiro Minai
Licensed Content Date	Mar 1, 1988
Licensed Content Volume	3
Licensed Content Issue	1
Licensed Content Pages	10
Start Page	43
End Page	52
Type of Use	reuse in a thesis/dissertation
Intended publisher of new work	other
Portion	figures/tables/illustrations
Number of figures/tables/illustrations	4
Format	both print and electronic
Are you the author of this Elsevier article?	No
Will you be translating?	No
Original figure numbers	Figure 1 Figure 4 Figure 5 Figure 6
Title of your thesis/dissertation	Experimental and Numerical Investigations to Assess the Performance of a Buried Pipe Subjected to Traffic Load / Non-Treated and Cement-Treated Trench
Expected completion date	Aug 2018
Estimated size (number of pages)	300
Requestor Location	Curtin University 24 Everingham Street Clarkson, Western Australia 6030 Australia Attn: Curtin University
Publisher Tax ID	GB 494 6272 12
Total	0.00 AUD
Terms and Conditions	

INTRODUCTION

1. The publisher for this copyrighted material is Elsevier. By clicking "accept" in connection with completing this licensing transaction, you agree that the following terms and conditions apply to this transaction (along with the Billing and Payment terms and conditions established by Copyright Clearance Center, Inc. ("CCC"), at the time that you opened your Rightslink account and that are available at any time at http://myaccount.copyright.com).

GENERAL TERMS

2. Elsevier hereby grants you permission to reproduce the aforementioned material subject to the terms and conditions indicated.

3. Acknowledgement: If any part of the material to be used (for example, figures) has appeared in our publication with credit or acknowledgement to another source, permission must also be sought from that source. If such permission is not obtained then that material may not be included in your publication/copies. Suitable acknowledgement to the source must be made, either as a footnote or in a reference list at the end of your publication, as follows:

"Reprinted from Publication title, Vol /edition number, Author(s), Title of article / title of chapter, Pages No., Copyright (Year), with permission from Elsevier [OR APPLICABLE SOCIETY COPYRIGHT OWNER]." Also Lancet special credit - "Reprinted from The Lancet, Vol. number, Author(s), Title of article, Pages No., Copyright (Year), with permission from Elsevier."

4. Reproduction of this material is confined to the purpose and/or media for which permission is hereby given.

5. Altering/Modifying Material: Not Permitted. However figures and illustrations may be altered/adapted minimally to serve your work. Any other abbreviations, additions, deletions and/or any other alterations shall be made only with prior written authorization of Elsevier Ltd. (Please contact Elsevier at permissions@elsevier.com). No modifications can be made to any Lancet figures/tables and they must be reproduced in full.

6. If the permission fee for the requested use of our material is waived in this instance, please be advised that your future requests for Elsevier materials may attract a fee.

7. Reservation of Rights: Publisher reserves all rights not specifically granted in the combination of (i) the license details provided by you and accepted in the course of this licensing transaction, (ii) these terms and conditions and (iii) CCC's Billing and Payment terms and conditions.

8. License Contingent Upon Payment: While you may exercise the rights licensed immediately upon issuance of the license at the end of the licensing process for the transaction, provided that you have disclosed complete and accurate details of your proposed use, no license is finally effective unless and until full payment is received from you (either by publisher or by CCC) as provided in CCC's Billing and Payment terms and conditions. If full payment is not received on a timely basis, then any license preliminarily granted shall be deemed automatically revoked and shall be void as if never granted. Further, in the event that you breach any of these terms and conditions or any of CCC's Billing and Payment terms and conditions, the license is automatically revoked and shall be void as if never granted. Use of materials as described in a revoked license, as well as any use of the materials beyond the scope of an unrevoked license, may constitute copyright infringement and publisher reserves the right to take any and all action to protect its copyright in the materials.

9. Warranties: Publisher makes no representations or warranties with respect to the licensed material.

10. Indemnity: You hereby indemnify and agree to hold harmless publisher and CCC, and their respective officers, directors, employees and agents, from and against any and all claims arising out of your use of the licensed material other than as specifically authorized pursuant to this license.

11. No Transfer of License: This license is personal to you and may not be sublicensed, assigned, or transferred by you to any other person without publisher's written permission.

12. No Amendment Except in Writing: This license may not be amended except in a writing signed by both parties (or, in the case of publisher, by CCC on publisher's behalf).

13. Objection to Contrary Terms: Publisher hereby objects to any terms contained in any purchase order, acknowledgment, check endorsement or other writing prepared by you, which terms are inconsistent with these terms and conditions or CCC's Billing and Payment

terms and conditions. These terms and conditions, together with CCC's Billing and Payment terms and conditions (which are incorporated herein), comprise the entire agreement between you and publisher (and CCC) concerning this licensing transaction. In the event of any conflict between your obligations established by these terms and conditions and those established by CCC's Billing and Payment terms and conditions, these terms and conditions shall control.

14. Revocation: Elsevier or Copyright Clearance Center may deny the permissions described in this License at their sole discretion, for any reason or no reason, with a full refund payable to you. Notice of such denial will be made using the contact information provided by you. Failure to receive such notice will not alter or invalidate the denial. In no event will Elsevier or Copyright Clearance Center be responsible or liable for any costs, expenses or damage incurred by you as a result of a denial of your permission request, other than a refund of the amount(s) paid by you to Elsevier and/or Copyright Clearance Center for denied permissions.

LIMITED LICENSE

The following terms and conditions apply only to specific license types:

15. **Translation**: This permission is granted for non-exclusive world **English** rights only unless your license was granted for translation rights. If you licensed translation rights you may only translate this content into the languages you requested. A professional translator must perform all translations and reproduce the content word for word preserving the integrity of the article.

16. **Posting licensed content on any Website**: The following terms and conditions apply as follows: Licensing material from an Elsevier journal: All content posted to the web site must maintain the copyright information line on the bottom of each image; A hyper-text must be included to the Homepage of the journal from which you are licensing at http://www.sciencedirect.com/science/journal/xxxxx or the Elsevier homepage for books at http://www.elsevier.com; Central Storage: This license does not include permission for a scanned version of the material to be stored in a central repository such as that provided by Heron/XanEdu.

Licensing material from an Elsevier book: A hyper-text link must be included to the Elsevier homepage at http://www.elsevier.com . All content posted to the web site must maintain the copyright information line on the bottom of each image.

Posting licensed content on Electronic reserve: In addition to the above the following clauses are applicable: The web site must be password-protected and made available only to bona fide students registered on a relevant course. This permission is granted for 1 year only. You may obtain a new license for future website posting.

17. **For journal authors:** the following clauses are applicable in addition to the above:

Preprints:

A preprint is an author's own write-up of research results and analysis, it has not been peer-reviewed, nor has it had any other value added to it by a publisher (such as formatting, copyright, technical enhancement etc.).

Authors can share their preprints anywhere at any time. Preprints should not be added to or enhanced in any way in order to appear more like, or to substitute for, the final versions of articles however authors can update their preprints on arXiv or RePEc with their Accepted Author Manuscript (see below).

If accepted for publication, we encourage authors to link from the preprint to their formal publication via its DOI. Millions of researchers have access to the formal publications on ScienceDirect, and so links will help users to find, access, cite and use the best available version. Please note that Cell Press, The Lancet and some society-owned have different preprint policies. Information on these policies is available on the journal homepage.

Accepted Author Manuscripts: An accepted author manuscript is the manuscript of an article that has been accepted for publication and which typically includes author-incorporated changes suggested during submission, peer review and editor-author communications.

Authors can share their accepted author manuscript:

- immediately

- via their non-commercial person homepage or blog
- by updating a preprint in arXiv or RePEc with the accepted manuscript
- via their research institute or institutional repository for internal institutional uses or as part of an invitation-only research collaboration work-group
- directly by providing copies to their students or to research collaborators for their personal use
- for private scholarly sharing as part of an invitation-only work group on commercial sites with which Elsevier has an agreement

- After the embargo period
  - via non-commercial hosting platforms such as their institutional repository
  - via commercial sites with which Elsevier has an agreement

In all cases accepted manuscripts should:

- link to the formal publication via its DOI
- bear a CC-BY-NC-ND license - this is easy to do
- if aggregated with other manuscripts, for example in a repository or other site, be shared in alignment with our hosting policy not be added to or enhanced in any way to appear more like, or to substitute for, the published journal article.

Published journal article (JPA): A published journal article (PJA) is the definitive final record of published research that appears or will appear in the journal and embodies all value-adding publishing activities including peer review co-ordination, copy-editing, formatting, (if relevant) pagination and online enrichment.
Policies for sharing publishing journal articles differ for subscription and gold open access articles:
Subscription Articles: If you are an author, please share a link to your article rather than the full-text. Millions of researchers have access to the formal publications on ScienceDirect, and so links will help your users to find, access, cite, and use the best available version.
Theses and dissertations which contain embedded PJAs as part of the formal submission can be posted publicly by the awarding institution with DOI links back to the formal publications on ScienceDirect.
If you are affiliated with a library that subscribes to ScienceDirect you have additional private sharing rights for others' research accessed under that agreement. This includes use for classroom teaching and internal training at the institution (including use in course packs and courseware programs), and inclusion of the article for grant funding purposes.
Gold Open Access Articles: May be shared according to the author-selected end-user license and should contain a CrossMark logo, the end user license, and a DOI link to the formal publication on ScienceDirect.
Please refer to Elsevier's posting policy for further information.
18. **For book authors** the following clauses are applicable in addition to the above: Authors are permitted to place a brief summary of their work online only. You are not allowed to download and post the published electronic version of your chapter, nor may you scan the printed edition to create an electronic version. **Posting to a repository:** Authors are permitted to post a summary of their chapter only in their institution's repository.
19. **Thesis/Dissertation**: If your license is for use in a thesis/dissertation your thesis may be submitted to your institution in either print or electronic form. Should your thesis be published commercially, please reapply for permission. These requirements include permission for the Library and Archives of Canada to supply single copies, on demand, of the complete thesis and include permission for Proquest/UMI to supply single copies, on demand, of the complete thesis. Should your thesis be published commercially, please reapply for permission. Theses and dissertations which contain embedded PJAs as part of the formal submission can be posted publicly by the awarding institution with DOI links back to the formal publications on ScienceDirect.

Elsevier Open Access Terms and Conditions
You can publish open access with Elsevier in hundreds of open access journals or in nearly 2000 established subscription journals that support open access publishing. Permitted third

party re-use of these open access articles is defined by the author's choice of Creative Commons user license. See our open access license policy for more information.

Terms & Conditions applicable to all Open Access articles published with Elsevier:

Any reuse of the article must not represent the author as endorsing the adaptation of the article nor should the article be modified in such a way as to damage the author's honour or reputation. If any changes have been made, such changes must be clearly indicated.

The author(s) must be appropriately credited and we ask that you include the end user license and a DOI link to the formal publication on ScienceDirect.

If any part of the material to be used (for example, figures) has appeared in our publication with credit or acknowledgement to another source it is the responsibility of the user to ensure their reuse complies with the terms and conditions determined by the rights holder.

Additional Terms & Conditions applicable to each Creative Commons user license:

CC BY: The CC-BY license allows users to copy, to create extracts, abstracts and new works from the Article, to alter and revise the Article and to make commercial use of the Article (including reuse and/or resale of the Article by commercial entities), provided the user gives appropriate credit (with a link to the formal publication through the relevant DOI), provides a link to the license, indicates if changes were made and the licensor is not represented as endorsing the use made of the work. The full details of the license are available at http://creativecommons.org/licenses/by/4.0.

CC BY NC SA: The CC BY-NC-SA license allows users to copy, to create extracts, abstracts and new works from the Article, to alter and revise the Article, provided this is not done for commercial purposes, and that the user gives appropriate credit (with a link to the formal publication through the relevant DOI), provides a link to the license, indicates if changes were made and the licensor is not represented as endorsing the use made of the work. Further, any new works must be made available on the same conditions. The full details of the license are available at http://creativecommons.org/licenses/by-nc-sa/4.0.

CC BY NC ND: The CC BY-NC-ND license allows users to copy and distribute the Article, provided this is not done for commercial purposes and further does not permit distribution of the Article if it is changed or edited in any way, and provided the user gives appropriate credit (with a link to the formal publication through the relevant DOI), provides a link to the license, and that the licensor is not represented as endorsing the use made of the work. The full details of the license are available at http://creativecommons.org/licenses/by-nc-nd/4.0.

Any commercial reuse of Open Access articles published with a CC BY NC SA or CC BY NC ND license requires permission from Elsevier and will be subject to a fee.

Commercial reuse includes:

- Associating advertising with the full text of the Article
- Charging fees for document delivery or access
- Article aggregation
- Systematic distribution via e-mail lists or share buttons

Posting or linking by commercial companies for use by customers of those companies.

20. **Other Conditions**:

v1.9

Questions? customercare@copyright.com or +1-855-239-3415 (toll free in the US) or +1-978-646-2777.

PERMISSION TO USE COPYRIGHT MATERIAL AS SPECIFIED BELOW:

Mosadegh. A; Nikraz.H , BURIED PIPE RESPONSE SUBJECTED TO TRAFFIC LOAD EXPERIMENTAL AND NUMERICAL INVESTIGATIONS, International Journal of GEOMATE, Nov., 2017, Vol.13, Issue 39, pp.01-08, ISSN:2186-2990, Japan,
DOI: https://doi.org/10.21660/2017.39.91957

I hereby give permission for **Ahdyeh Mosadegh** to include the abovementioned material(s) in his/her higher degree thesis for Curtin University, and to communicate this material via the espace institutional repository. This permission is granted on a non-exclusive basis and for an indefinite period.

I confirm that I am the copyright owner of the specified material.

Signed: 

Name: Prof. Dr. Zakaria Hossain

Position: Editor-in-Chief, International Journal of GEOMATE

Date: 28 Nov. 2017

Please return signed form to **ahdyeh.mosadegh@postgrad.curtin.edu.au**

L

Lisa McJunkin, CGS Administration <admin@cgs.ca>

Wed 29/11/2017, 04:42

Noosha Mosadegh; info@geoedmonton2018.ca

Reply all

Inbox

Hi Noosha,

The copyright is retained by the authors. Please contact them directly to obtain this permission.

Thanks and best regards,

Lisa

Lisa McJunkin

Director, Communications and Member Services |

Directrice, Communications et services aux membres

THE CANADIAN GEOTECHNICAL SOCIETY

LA SOCIÉTÉ CANADIENNE DE GÉOTECHNIQUE

8828 Pigott Road

Richmond, BC, Canada V7A 2C4

604-277-7527 | 1-800-710-9867

admin@cgs.ca | www.cgs.ca

71st Annual CGS Conference – GeoEdmonton 2018

September 23 - 26, 2018

7th Canadian Geohazards Conference – Geohazards 7

June 3 - 6, 2018

T

'Taylor & Francis Customer Services <subscriptions@tandf.co.uk>

Today, 20:54

Noosha Mosadegh

Download

Action Items

Dear Noosha,

Thank you for your e.mail.

We are pleased to hear that you are able to reuse your article.

If you do have any further questions regarding permissions then please contact our permissions department on PermissionRequest@tandf.co.uk

If you have any queries, or if I can be of any further assistance, please do not hesitate to contact me.

Kind Regards,

Lisa Olley
Customer Operations Executive | T&F Subscriptions | UK Shared Services
informa
Sheepen Place | Colchester | Essex | CO3 3LP | United Kingdom
Tel: +44 (0)20 7017 5544

ELSEVIER LICENSE
TERMS AND CONDITIONS

Jul 22, 2018

This Agreement between Curtin University ("You") and Elsevier ("Elsevier") consists of your license details and the terms and conditions provided by Elsevier and Copyright Clearance Center.

License Number	4394270866228
License date	Jul 22, 2018
Licensed Content Publisher	Elsevier
Licensed Content Publication	Soil Dynamics and Earthquake Engineering
Licensed Content Title	The stiffness degradation and damping ratio evolution of Taipei Silty Clay under cyclic straining
Licensed Content Author	Chung-Jung Lee,Sheau-Feng Sheu
Licensed Content Date	Aug 1, 2007
Licensed Content Volume	27
Licensed Content Issue	8
Licensed Content Pages	11
Start Page	730
End Page	740
Type of Use	reuse in a thesis/dissertation
Portion	figures/tables/illustrations
Number of figures/tables/illustrations	1
Format	both print and electronic
Are you the author of this Elsevier article?	No
Will you be translating?	No
Original figure numbers	Figure 1
Title of your thesis/dissertation	Experimental and Numerical Investigations to Assess the Performance of a Buried Pipe Subjected to Traffic Load / Non-Treated and Cement-Treated Trench
Expected completion date	Aug 2018
Estimated size (number of pages)	300
Requestor Location	Curtin University 24 Everingham Street Clarkson, Western Australia 6030 Australia Attn: Curtin University
Publisher Tax ID	GB 494 6272 12
Total	0.00 AUD
Terms and Conditions	

INTRODUCTION

1. The publisher for this copyrighted material is Elsevier. By clicking "accept" in connection with completing this licensing transaction, you agree that the following terms and conditions

apply to this transaction (along with the Billing and Payment terms and conditions established by Copyright Clearance Center, Inc. ("CCC"), at the time that you opened your Rightslink account and that are available at any time at http://myaccount.copyright.com).

GENERAL TERMS

2. Elsevier hereby grants you permission to reproduce the aforementioned material subject to the terms and conditions indicated.

3. Acknowledgement: If any part of the material to be used (for example, figures) has appeared in our publication with credit or acknowledgement to another source, permission must also be sought from that source. If such permission is not obtained then that material may not be included in your publication/copies. Suitable acknowledgement to the source must be made, either as a footnote or in a reference list at the end of your publication, as follows:

"Reprinted from Publication title, Vol /edition number, Author(s), Title of article / title of chapter, Pages No., Copyright (Year), with permission from Elsevier [OR APPLICABLE SOCIETY COPYRIGHT OWNER]." Also Lancet special credit - "Reprinted from The Lancet, Vol. number, Author(s), Title of article, Pages No., Copyright (Year), with permission from Elsevier."

4. Reproduction of this material is confined to the purpose and/or media for which permission is hereby given.

5. Altering/Modifying Material: Not Permitted. However figures and illustrations may be altered/adapted minimally to serve your work. Any other abbreviations, additions, deletions and/or any other alterations shall be made only with prior written authorization of Elsevier Ltd. (Please contact Elsevier at permissions@elsevier.com). No modifications can be made to any Lancet figures/tables and they must be reproduced in full.

6. If the permission fee for the requested use of our material is waived in this instance, please be advised that your future requests for Elsevier materials may attract a fee.

7. Reservation of Rights: Publisher reserves all rights not specifically granted in the combination of (i) the license details provided by you and accepted in the course of this licensing transaction, (ii) these terms and conditions and (iii) CCC's Billing and Payment terms and conditions.

8. License Contingent Upon Payment: While you may exercise the rights licensed immediately upon issuance of the license at the end of the licensing process for the transaction, provided that you have disclosed complete and accurate details of your proposed use, no license is finally effective unless and until full payment is received from you (either by publisher or by CCC) as provided in CCC's Billing and Payment terms and conditions. If full payment is not received on a timely basis, then any license preliminarily granted shall be deemed automatically revoked and shall be void as if never granted. Further, in the event that you breach any of these terms and conditions or any of CCC's Billing and Payment terms and conditions, the license is automatically revoked and shall be void as if never granted. Use of materials as described in a revoked license, as well as any use of the materials beyond the scope of an unrevoked license, may constitute copyright infringement and publisher reserves the right to take any and all action to protect its copyright in the materials.

9. Warranties: Publisher makes no representations or warranties with respect to the licensed material.

10. Indemnity: You hereby indemnify and agree to hold harmless publisher and CCC, and their respective officers, directors, employees and agents, from and against any and all claims arising out of your use of the licensed material other than as specifically authorized pursuant to this license.

11. No Transfer of License: This license is personal to you and may not be sublicensed, assigned, or transferred by you to any other person without publisher's written permission.

12. No Amendment Except in Writing: This license may not be amended except in a writing signed by both parties (or, in the case of publisher, by CCC on publisher's behalf).

13. Objection to Contrary Terms: Publisher hereby objects to any terms contained in any purchase order, acknowledgment, check endorsement or other writing prepared by you, which terms are inconsistent with these terms and conditions or CCC's Billing and Payment terms and conditions. These terms and conditions, together with CCC's Billing and Payment terms and conditions (which are incorporated herein), comprise the entire agreement

between you and publisher (and CCC) concerning this licensing transaction. In the event of any conflict between your obligations established by these terms and conditions and those established by CCC's Billing and Payment terms and conditions, these terms and conditions shall control.

14. Revocation: Elsevier or Copyright Clearance Center may deny the permissions described in this License at their sole discretion, for any reason or no reason, with a full refund payable to you. Notice of such denial will be made using the contact information provided by you. Failure to receive such notice will not alter or invalidate the denial. In no event will Elsevier or Copyright Clearance Center be responsible or liable for any costs, expenses or damage incurred by you as a result of a denial of your permission request, other than a refund of the amount(s) paid by you to Elsevier and/or Copyright Clearance Center for denied permissions.

LIMITED LICENSE

The following terms and conditions apply only to specific license types:

15. **Translation**: This permission is granted for non-exclusive world **English** rights only unless your license was granted for translation rights. If you licensed translation rights you may only translate this content into the languages you requested. A professional translator must perform all translations and reproduce the content word for word preserving the integrity of the article.

16. **Posting licensed content on any Website**: The following terms and conditions apply as follows: Licensing material from an Elsevier journal: All content posted to the web site must maintain the copyright information line on the bottom of each image; A hyper-text must be included to the Homepage of the journal from which you are licensing at http://www.sciencedirect.com/science/journal/xxxxx or the Elsevier homepage for books at http://www.elsevier.com; Central Storage: This license does not include permission for a scanned version of the material to be stored in a central repository such as that provided by Heron/XanEdu.

Licensing material from an Elsevier book: A hyper-text link must be included to the Elsevier homepage at http://www.elsevier.com . All content posted to the web site must maintain the copyright information line on the bottom of each image.

Posting licensed content on Electronic reserve: In addition to the above the following clauses are applicable: The web site must be password-protected and made available only to bona fide students registered on a relevant course. This permission is granted for 1 year only. You may obtain a new license for future website posting.

17. **For journal authors:** the following clauses are applicable in addition to the above:

Preprints:

A preprint is an author's own write-up of research results and analysis, it has not been peer-reviewed, nor has it had any other value added to it by a publisher (such as formatting, copyright, technical enhancement etc.).

Authors can share their preprints anywhere at any time. Preprints should not be added to or enhanced in any way in order to appear more like, or to substitute for, the final versions of articles however authors can update their preprints on arXiv or RePEc with their Accepted Author Manuscript (see below).

If accepted for publication, we encourage authors to link from the preprint to their formal publication via its DOI. Millions of researchers have access to the formal publications on ScienceDirect, and so links will help users to find, access, cite and use the best available version. Please note that Cell Press, The Lancet and some society-owned have different preprint policies. Information on these policies is available on the journal homepage.

Accepted Author Manuscripts: An accepted author manuscript is the manuscript of an article that has been accepted for publication and which typically includes author-incorporated changes suggested during submission, peer review and editor-author communications.

Authors can share their accepted author manuscript:

- immediately
  - via their non-commercial person homepage or blog
  - by updating a preprint in arXiv or RePEc with the accepted manuscript

- via their research institute or institutional repository for internal institutional uses or as part of an invitation-only research collaboration work-group
- directly by providing copies to their students or to research collaborators for their personal use
- for private scholarly sharing as part of an invitation-only work group on commercial sites with which Elsevier has an agreement

- After the embargo period
  - via non-commercial hosting platforms such as their institutional repository
  - via commercial sites with which Elsevier has an agreement

In all cases accepted manuscripts should:

- link to the formal publication via its DOI
- bear a CC-BY-NC-ND license - this is easy to do
- if aggregated with other manuscripts, for example in a repository or other site, be shared in alignment with our hosting policy not be added to or enhanced in any way to appear more like, or to substitute for, the published journal article.

Published journal article (JPA): A published journal article (PJA) is the definitive final record of published research that appears or will appear in the journal and embodies all value-adding publishing activities including peer review co-ordination, copy-editing, formatting, (if relevant) pagination and online enrichment.
Policies for sharing publishing journal articles differ for subscription and gold open access articles:
Subscription Articles: If you are an author, please share a link to your article rather than the full-text. Millions of researchers have access to the formal publications on ScienceDirect, and so links will help your users to find, access, cite, and use the best available version.
Theses and dissertations which contain embedded PJAs as part of the formal submission can be posted publicly by the awarding institution with DOI links back to the formal publications on ScienceDirect.
If you are affiliated with a library that subscribes to ScienceDirect you have additional private sharing rights for others' research accessed under that agreement. This includes use for classroom teaching and internal training at the institution (including use in course packs and courseware programs), and inclusion of the article for grant funding purposes.
Gold Open Access Articles: May be shared according to the author-selected end-user license and should contain a CrossMark logo, the end user license, and a DOI link to the formal publication on ScienceDirect.
Please refer to Elsevier's posting policy for further information.
18. **For book authors** the following clauses are applicable in addition to the above:
Authors are permitted to place a brief summary of their work online only. You are not allowed to download and post the published electronic version of your chapter, nor may you scan the printed edition to create an electronic version. **Posting to a repository:** Authors are permitted to post a summary of their chapter only in their institution's repository.
19. **Thesis/Dissertation**: If your license is for use in a thesis/dissertation your thesis may be submitted to your institution in either print or electronic form. Should your thesis be published commercially, please reapply for permission. These requirements include permission for the Library and Archives of Canada to supply single copies, on demand, of the complete thesis and include permission for Proquest/UMI to supply single copies, on demand, of the complete thesis. Should your thesis be published commercially, please reapply for permission. Theses and dissertations which contain embedded PJAs as part of the formal submission can be posted publicly by the awarding institution with DOI links back to the formal publications on ScienceDirect.

Elsevier Open Access Terms and Conditions
You can publish open access with Elsevier in hundreds of open access journals or in nearly 2000 established subscription journals that support open access publishing. Permitted third party re-use of these open access articles is defined by the author's choice of Creative Commons user license. See our open access license policy for more information.

Terms & Conditions applicable to all Open Access articles published with Elsevier:
Any reuse of the article must not represent the author as endorsing the adaptation of the article nor should the article be modified in such a way as to damage the author's honour or reputation. If any changes have been made, such changes must be clearly indicated.
The author(s) must be appropriately credited and we ask that you include the end user license and a DOI link to the formal publication on ScienceDirect.
If any part of the material to be used (for example, figures) has appeared in our publication with credit or acknowledgement to another source it is the responsibility of the user to ensure their reuse complies with the terms and conditions determined by the rights holder.
Additional Terms & Conditions applicable to each Creative Commons user license:
CC BY: The CC-BY license allows users to copy, to create extracts, abstracts and new works from the Article, to alter and revise the Article and to make commercial use of the Article (including reuse and/or resale of the Article by commercial entities), provided the user gives appropriate credit (with a link to the formal publication through the relevant DOI), provides a link to the license, indicates if changes were made and the licensor is not represented as endorsing the use made of the work. The full details of the license are available at http://creativecommons.org/licenses/by/4.0.
CC BY NC SA: The CC BY-NC-SA license allows users to copy, to create extracts, abstracts and new works from the Article, to alter and revise the Article, provided this is not done for commercial purposes, and that the user gives appropriate credit (with a link to the formal publication through the relevant DOI), provides a link to the license, indicates if changes were made and the licensor is not represented as endorsing the use made of the work. Further, any new works must be made available on the same conditions. The full details of the license are available at http://creativecommons.org/licenses/by-nc-sa/4.0.
CC BY NC ND: The CC BY-NC-ND license allows users to copy and distribute the Article, provided this is not done for commercial purposes and further does not permit distribution of the Article if it is changed or edited in any way, and provided the user gives appropriate credit (with a link to the formal publication through the relevant DOI), provides a link to the license, and that the licensor is not represented as endorsing the use made of the work. The full details of the license are available at http://creativecommons.org/licenses/by-nc-nd/4.0.
Any commercial reuse of Open Access articles published with a CC BY NC SA or CC BY NC ND license requires permission from Elsevier and will be subject to a fee.
Commercial reuse includes:

- Associating advertising with the full text of the Article
- Charging fees for document delivery or access
- Article aggregation
- Systematic distribution via e-mail lists or share buttons

Posting or linking by commercial companies for use by customers of those companies.

20. **Other Conditions**:

v1.9

Questions? customercare@copyright.com or +1-855-239-3415 (toll free in the US) or +1-978-646-2777.

ELSEVIER LICENSE
TERMS AND CONDITIONS

Jul 22, 2018

This Agreement between Curtin University ("You") and Elsevier ("Elsevier") consists of your license details and the terms and conditions provided by Elsevier and Copyright Clearance Center.

License Number	4394300299864
License date	Jul 22, 2018
Licensed Content Publisher	Elsevier
Licensed Content Publication	Composites Part B: Engineering
Licensed Content Title	Cover requirements of thermoplastic pipes used under highways
Licensed Content Author	Junsuk Kang,Younghan Jung,Yonghan Ahn
Licensed Content Date	Dec 1, 2013
Licensed Content Volume	55
Licensed Content Issue	n/a
Licensed Content Pages	9
Start Page	184
End Page	192
Type of Use	reuse in a thesis/dissertation
Intended publisher of new work	other
Portion	figures/tables/illustrations
Number of figures/tables/illustrations	1
Format	both print and electronic
Are you the author of this Elsevier article?	No
Will you be translating?	No
Original figure numbers	Figure 4
Title of your thesis/dissertation	Experimental and Numerical Investigations to Assess the Performance of a Buried Pipe Subjected to Traffic Load / Non-Treated and Cement-Treated Trench
Expected completion date	Aug 2018
Estimated size (number of pages)	300
Requestor Location	Curtin University 24 Everingham Street Clarkson, Western Australia 6030 Australia Attn: Curtin University
Publisher Tax ID	GB 494 6272 12
Total	0.00 AUD
Terms and Conditions	

INTRODUCTION

1. The publisher for this copyrighted material is Elsevier. By clicking "accept" in connection with completing this licensing transaction, you agree that the following terms and conditions apply to this transaction (along with the Billing and Payment terms and conditions established by Copyright Clearance Center, Inc. ("CCC"), at the time that you opened your Rightslink account and that are available at any time at http://myaccount.copyright.com).

GENERAL TERMS

2. Elsevier hereby grants you permission to reproduce the aforementioned material subject to the terms and conditions indicated.

3. Acknowledgement: If any part of the material to be used (for example, figures) has appeared in our publication with credit or acknowledgement to another source, permission must also be sought from that source. If such permission is not obtained then that material may not be included in your publication/copies. Suitable acknowledgement to the source must be made, either as a footnote or in a reference list at the end of your publication, as follows:

"Reprinted from Publication title, Vol /edition number, Author(s), Title of article / title of chapter, Pages No., Copyright (Year), with permission from Elsevier [OR APPLICABLE SOCIETY COPYRIGHT OWNER]." Also Lancet special credit - "Reprinted from The Lancet, Vol. number, Author(s), Title of article, Pages No., Copyright (Year), with permission from Elsevier."

4. Reproduction of this material is confined to the purpose and/or media for which permission is hereby given.

5. Altering/Modifying Material: Not Permitted. However figures and illustrations may be altered/adapted minimally to serve your work. Any other abbreviations, additions, deletions and/or any other alterations shall be made only with prior written authorization of Elsevier Ltd. (Please contact Elsevier at permissions@elsevier.com). No modifications can be made to any Lancet figures/tables and they must be reproduced in full.

6. If the permission fee for the requested use of our material is waived in this instance, please be advised that your future requests for Elsevier materials may attract a fee.

7. Reservation of Rights: Publisher reserves all rights not specifically granted in the combination of (i) the license details provided by you and accepted in the course of this licensing transaction, (ii) these terms and conditions and (iii) CCC's Billing and Payment terms and conditions.

8. License Contingent Upon Payment: While you may exercise the rights licensed immediately upon issuance of the license at the end of the licensing process for the transaction, provided that you have disclosed complete and accurate details of your proposed use, no license is finally effective unless and until full payment is received from you (either by publisher or by CCC) as provided in CCC's Billing and Payment terms and conditions. If full payment is not received on a timely basis, then any license preliminarily granted shall be deemed automatically revoked and shall be void as if never granted. Further, in the event that you breach any of these terms and conditions or any of CCC's Billing and Payment terms and conditions, the license is automatically revoked and shall be void as if never granted. Use of materials as described in a revoked license, as well as any use of the materials beyond the scope of an unrevoked license, may constitute copyright infringement and publisher reserves the right to take any and all action to protect its copyright in the materials.

9. Warranties: Publisher makes no representations or warranties with respect to the licensed material.

10. Indemnity: You hereby indemnify and agree to hold harmless publisher and CCC, and their respective officers, directors, employees and agents, from and against any and all claims arising out of your use of the licensed material other than as specifically authorized pursuant to this license.

11. No Transfer of License: This license is personal to you and may not be sublicensed, assigned, or transferred by you to any other person without publisher's written permission.

12. No Amendment Except in Writing: This license may not be amended except in a writing signed by both parties (or, in the case of publisher, by CCC on publisher's behalf).

13. Objection to Contrary Terms: Publisher hereby objects to any terms contained in any purchase order, acknowledgment, check endorsement or other writing prepared by you, which terms are inconsistent with these terms and conditions or CCC's Billing and Payment

terms and conditions. These terms and conditions, together with CCC's Billing and Payment terms and conditions (which are incorporated herein), comprise the entire agreement between you and publisher (and CCC) concerning this licensing transaction. In the event of any conflict between your obligations established by these terms and conditions and those established by CCC's Billing and Payment terms and conditions, these terms and conditions shall control.

14. Revocation: Elsevier or Copyright Clearance Center may deny the permissions described in this License at their sole discretion, for any reason or no reason, with a full refund payable to you. Notice of such denial will be made using the contact information provided by you. Failure to receive such notice will not alter or invalidate the denial. In no event will Elsevier or Copyright Clearance Center be responsible or liable for any costs, expenses or damage incurred by you as a result of a denial of your permission request, other than a refund of the amount(s) paid by you to Elsevier and/or Copyright Clearance Center for denied permissions.

LIMITED LICENSE

The following terms and conditions apply only to specific license types:

15. **Translation**: This permission is granted for non-exclusive world **English** rights only unless your license was granted for translation rights. If you licensed translation rights you may only translate this content into the languages you requested. A professional translator must perform all translations and reproduce the content word for word preserving the integrity of the article.

16. **Posting licensed content on any Website**: The following terms and conditions apply as follows: Licensing material from an Elsevier journal: All content posted to the web site must maintain the copyright information line on the bottom of each image; A hyper-text must be included to the Homepage of the journal from which you are licensing at http://www.sciencedirect.com/science/journal/xxxxx or the Elsevier homepage for books at http://www.elsevier.com; Central Storage: This license does not include permission for a scanned version of the material to be stored in a central repository such as that provided by Heron/XanEdu.

Licensing material from an Elsevier book: A hyper-text link must be included to the Elsevier homepage at http://www.elsevier.com . All content posted to the web site must maintain the copyright information line on the bottom of each image.

Posting licensed content on Electronic reserve: In addition to the above the following clauses are applicable: The web site must be password-protected and made available only to bona fide students registered on a relevant course. This permission is granted for 1 year only. You may obtain a new license for future website posting.

17. **For journal authors:** the following clauses are applicable in addition to the above:

Preprints:

A preprint is an author's own write-up of research results and analysis, it has not been peer-reviewed, nor has it had any other value added to it by a publisher (such as formatting, copyright, technical enhancement etc.).

Authors can share their preprints anywhere at any time. Preprints should not be added to or enhanced in any way in order to appear more like, or to substitute for, the final versions of articles however authors can update their preprints on arXiv or RePEc with their Accepted Author Manuscript (see below).

If accepted for publication, we encourage authors to link from the preprint to their formal publication via its DOI. Millions of researchers have access to the formal publications on ScienceDirect, and so links will help users to find, access, cite and use the best available version. Please note that Cell Press, The Lancet and some society-owned have different preprint policies. Information on these policies is available on the journal homepage.

Accepted Author Manuscripts: An accepted author manuscript is the manuscript of an article that has been accepted for publication and which typically includes author-incorporated changes suggested during submission, peer review and editor-author communications.

Authors can share their accepted author manuscript:

- immediately

  - via their non-commercial person homepage or blog
  - by updating a preprint in arXiv or RePEc with the accepted manuscript
  - via their research institute or institutional repository for internal institutional uses or as part of an invitation-only research collaboration work-group
  - directly by providing copies to their students or to research collaborators for their personal use
  - for private scholarly sharing as part of an invitation-only work group on commercial sites with which Elsevier has an agreement
- After the embargo period
  - via non-commercial hosting platforms such as their institutional repository
  - via commercial sites with which Elsevier has an agreement

In all cases accepted manuscripts should:

- link to the formal publication via its DOI
- bear a CC-BY-NC-ND license - this is easy to do
- if aggregated with other manuscripts, for example in a repository or other site, be shared in alignment with our hosting policy not be added to or enhanced in any way to appear more like, or to substitute for, the published journal article.

Published journal article (JPA): A published journal article (PJA) is the definitive final record of published research that appears or will appear in the journal and embodies all value-adding publishing activities including peer review co-ordination, copy-editing, formatting, (if relevant) pagination and online enrichment.
Policies for sharing publishing journal articles differ for subscription and gold open access articles:
Subscription Articles: If you are an author, please share a link to your article rather than the full-text. Millions of researchers have access to the formal publications on ScienceDirect, and so links will help your users to find, access, cite, and use the best available version.
Theses and dissertations which contain embedded PJAs as part of the formal submission can be posted publicly by the awarding institution with DOI links back to the formal publications on ScienceDirect.
If you are affiliated with a library that subscribes to ScienceDirect you have additional private sharing rights for others' research accessed under that agreement. This includes use for classroom teaching and internal training at the institution (including use in course packs and courseware programs), and inclusion of the article for grant funding purposes.
Gold Open Access Articles: May be shared according to the author-selected end-user license and should contain a CrossMark logo, the end user license, and a DOI link to the formal publication on ScienceDirect.
Please refer to Elsevier's posting policy for further information.
18. **For book authors** the following clauses are applicable in addition to the above: Authors are permitted to place a brief summary of their work online only. You are not allowed to download and post the published electronic version of your chapter, nor may you scan the printed edition to create an electronic version. **Posting to a repository:** Authors are permitted to post a summary of their chapter only in their institution's repository.
19. **Thesis/Dissertation**: If your license is for use in a thesis/dissertation your thesis may be submitted to your institution in either print or electronic form. Should your thesis be published commercially, please reapply for permission. These requirements include permission for the Library and Archives of Canada to supply single copies, on demand, of the complete thesis and include permission for Proquest/UMI to supply single copies, on demand, of the complete thesis. Should your thesis be published commercially, please reapply for permission. Theses and dissertations which contain embedded PJAs as part of the formal submission can be posted publicly by the awarding institution with DOI links back to the formal publications on ScienceDirect.

Elsevier Open Access Terms and Conditions
You can publish open access with Elsevier in hundreds of open access journals or in nearly 2000 established subscription journals that support open access publishing. Permitted third

party re-use of these open access articles is defined by the author's choice of Creative Commons user license. See our open access license policy for more information.

Terms & Conditions applicable to all Open Access articles published with Elsevier:

Any reuse of the article must not represent the author as endorsing the adaptation of the article nor should the article be modified in such a way as to damage the author's honour or reputation. If any changes have been made, such changes must be clearly indicated.

The author(s) must be appropriately credited and we ask that you include the end user license and a DOI link to the formal publication on ScienceDirect.

If any part of the material to be used (for example, figures) has appeared in our publication with credit or acknowledgement to another source it is the responsibility of the user to ensure their reuse complies with the terms and conditions determined by the rights holder.

Additional Terms & Conditions applicable to each Creative Commons user license:

CC BY: The CC-BY license allows users to copy, to create extracts, abstracts and new works from the Article, to alter and revise the Article and to make commercial use of the Article (including reuse and/or resale of the Article by commercial entities), provided the user gives appropriate credit (with a link to the formal publication through the relevant DOI), provides a link to the license, indicates if changes were made and the licensor is not represented as endorsing the use made of the work. The full details of the license are available at http://creativecommons.org/licenses/by/4.0.

CC BY NC SA: The CC BY-NC-SA license allows users to copy, to create extracts, abstracts and new works from the Article, to alter and revise the Article, provided this is not done for commercial purposes, and that the user gives appropriate credit (with a link to the formal publication through the relevant DOI), provides a link to the license, indicates if changes were made and the licensor is not represented as endorsing the use made of the work. Further, any new works must be made available on the same conditions. The full details of the license are available at http://creativecommons.org/licenses/by-nc-sa/4.0.

CC BY NC ND: The CC BY-NC-ND license allows users to copy and distribute the Article, provided this is not done for commercial purposes and further does not permit distribution of the Article if it is changed or edited in any way, and provided the user gives appropriate credit (with a link to the formal publication through the relevant DOI), provides a link to the license, and that the licensor is not represented as endorsing the use made of the work. The full details of the license are available at http://creativecommons.org/licenses/by-nc-nd/4.0.

Any commercial reuse of Open Access articles published with a CC BY NC SA or CC BY NC ND license requires permission from Elsevier and will be subject to a fee.

Commercial reuse includes:

- Associating advertising with the full text of the Article
- Charging fees for document delivery or access
- Article aggregation
- Systematic distribution via e-mail lists or share buttons

Posting or linking by commercial companies for use by customers of those companies.

20. **Other Conditions**:

v1.9

Questions? customercare@copyright.com or +1-855-239-3415 (toll free in the US) or +1-978-646-2777.

ELSEVIER LICENSE
TERMS AND CONDITIONS

Jul 22, 2018

This Agreement between Curtin University ("You") and Elsevier ("Elsevier") consists of your license details and the terms and conditions provided by Elsevier and Copyright Clearance Center.

License Number	4394561188088
License date	Jul 22, 2018
Licensed Content Publisher	Elsevier
Licensed Content Publication	Geotextiles and Geomembranes
Licensed Content Title	Combined use of geocell reinforcement and rubber–soil mixtures to improve performance of buried pipes
Licensed Content Author	Gh. Tavakoli Mehrjardi,S.N. Moghaddas Tafreshi,A.R. Dawson
Licensed Content Date	Oct 1, 2012
Licensed Content Volume	34
Licensed Content Issue	n/a
Licensed Content Pages	15
Start Page	116
End Page	130
Type of Use	reuse in a thesis/dissertation
Intended publisher of new work	other
Portion	figures/tables/illustrations
Number of figures/tables/illustrations	3
Format	both print and electronic
Are you the author of this Elsevier article?	No
Will you be translating?	No
Original figure numbers	Figure 2 Figure 4 Figure 5
Title of your thesis/dissertation	Experimental and Numerical Investigations to Assess the Performance of a Buried Pipe Subjected to Traffic Load / Non-Treated and Cement-Treated Trench
Expected completion date	Aug 2018
Estimated size (number of pages)	300
Requestor Location	Curtin University 24 Everingham Street Clarkson, Western Australia 6030 Australia Attn: Curtin University
Publisher Tax ID	GB 494 6272 12
Total	0.00 AUD
Terms and Conditions	

INTRODUCTION

1. The publisher for this copyrighted material is Elsevier. By clicking "accept" in connection with completing this licensing transaction, you agree that the following terms and conditions apply to this transaction (along with the Billing and Payment terms and conditions established by Copyright Clearance Center, Inc. ("CCC"), at the time that you opened your Rightslink account and that are available at any time at http://myaccount.copyright.com).

GENERAL TERMS

2. Elsevier hereby grants you permission to reproduce the aforementioned material subject to the terms and conditions indicated.

3. Acknowledgement: If any part of the material to be used (for example, figures) has appeared in our publication with credit or acknowledgement to another source, permission must also be sought from that source. If such permission is not obtained then that material may not be included in your publication/copies. Suitable acknowledgement to the source must be made, either as a footnote or in a reference list at the end of your publication, as follows:

"Reprinted from Publication title, Vol /edition number, Author(s), Title of article / title of chapter, Pages No., Copyright (Year), with permission from Elsevier [OR APPLICABLE SOCIETY COPYRIGHT OWNER]." Also Lancet special credit - "Reprinted from The Lancet, Vol. number, Author(s), Title of article, Pages No., Copyright (Year), with permission from Elsevier."

4. Reproduction of this material is confined to the purpose and/or media for which permission is hereby given.

5. Altering/Modifying Material: Not Permitted. However figures and illustrations may be altered/adapted minimally to serve your work. Any other abbreviations, additions, deletions and/or any other alterations shall be made only with prior written authorization of Elsevier Ltd. (Please contact Elsevier at permissions@elsevier.com). No modifications can be made to any Lancet figures/tables and they must be reproduced in full.

6. If the permission fee for the requested use of our material is waived in this instance, please be advised that your future requests for Elsevier materials may attract a fee.

7. Reservation of Rights: Publisher reserves all rights not specifically granted in the combination of (i) the license details provided by you and accepted in the course of this licensing transaction, (ii) these terms and conditions and (iii) CCC's Billing and Payment terms and conditions.

8. License Contingent Upon Payment: While you may exercise the rights licensed immediately upon issuance of the license at the end of the licensing process for the transaction, provided that you have disclosed complete and accurate details of your proposed use, no license is finally effective unless and until full payment is received from you (either by publisher or by CCC) as provided in CCC's Billing and Payment terms and conditions. If full payment is not received on a timely basis, then any license preliminarily granted shall be deemed automatically revoked and shall be void as if never granted. Further, in the event that you breach any of these terms and conditions or any of CCC's Billing and Payment terms and conditions, the license is automatically revoked and shall be void as if never granted. Use of materials as described in a revoked license, as well as any use of the materials beyond the scope of an unrevoked license, may constitute copyright infringement and publisher reserves the right to take any and all action to protect its copyright in the materials.

9. Warranties: Publisher makes no representations or warranties with respect to the licensed material.

10. Indemnity: You hereby indemnify and agree to hold harmless publisher and CCC, and their respective officers, directors, employees and agents, from and against any and all claims arising out of your use of the licensed material other than as specifically authorized pursuant to this license.

11. No Transfer of License: This license is personal to you and may not be sublicensed, assigned, or transferred by you to any other person without publisher's written permission.

12. No Amendment Except in Writing: This license may not be amended except in a writing signed by both parties (or, in the case of publisher, by CCC on publisher's behalf).

13. Objection to Contrary Terms: Publisher hereby objects to any terms contained in any purchase order, acknowledgment, check endorsement or other writing prepared by you, which terms are inconsistent with these terms and conditions or CCC's Billing and Payment

terms and conditions. These terms and conditions, together with CCC's Billing and Payment terms and conditions (which are incorporated herein), comprise the entire agreement between you and publisher (and CCC) concerning this licensing transaction. In the event of any conflict between your obligations established by these terms and conditions and those established by CCC's Billing and Payment terms and conditions, these terms and conditions shall control.

14. Revocation: Elsevier or Copyright Clearance Center may deny the permissions described in this License at their sole discretion, for any reason or no reason, with a full refund payable to you. Notice of such denial will be made using the contact information provided by you. Failure to receive such notice will not alter or invalidate the denial. In no event will Elsevier or Copyright Clearance Center be responsible or liable for any costs, expenses or damage incurred by you as a result of a denial of your permission request, other than a refund of the amount(s) paid by you to Elsevier and/or Copyright Clearance Center for denied permissions.

LIMITED LICENSE

The following terms and conditions apply only to specific license types:

15. **Translation**: This permission is granted for non-exclusive world **English** rights only unless your license was granted for translation rights. If you licensed translation rights you may only translate this content into the languages you requested. A professional translator must perform all translations and reproduce the content word for word preserving the integrity of the article.

16. **Posting licensed content on any Website**: The following terms and conditions apply as follows: Licensing material from an Elsevier journal: All content posted to the web site must maintain the copyright information line on the bottom of each image; A hyper-text must be included to the Homepage of the journal from which you are licensing at http://www.sciencedirect.com/science/journal/xxxxx or the Elsevier homepage for books at http://www.elsevier.com; Central Storage: This license does not include permission for a scanned version of the material to be stored in a central repository such as that provided by Heron/XanEdu.

Licensing material from an Elsevier book: A hyper-text link must be included to the Elsevier homepage at http://www.elsevier.com . All content posted to the web site must maintain the copyright information line on the bottom of each image.

Posting licensed content on Electronic reserve: In addition to the above the following clauses are applicable: The web site must be password-protected and made available only to bona fide students registered on a relevant course. This permission is granted for 1 year only. You may obtain a new license for future website posting.

17. **For journal authors:** the following clauses are applicable in addition to the above:

Preprints:

A preprint is an author's own write-up of research results and analysis, it has not been peer-reviewed, nor has it had any other value added to it by a publisher (such as formatting, copyright, technical enhancement etc.).

Authors can share their preprints anywhere at any time. Preprints should not be added to or enhanced in any way in order to appear more like, or to substitute for, the final versions of articles however authors can update their preprints on arXiv or RePEc with their Accepted Author Manuscript (see below).

If accepted for publication, we encourage authors to link from the preprint to their formal publication via its DOI. Millions of researchers have access to the formal publications on ScienceDirect, and so links will help users to find, access, cite and use the best available version. Please note that Cell Press, The Lancet and some society-owned have different preprint policies. Information on these policies is available on the journal homepage.

Accepted Author Manuscripts: An accepted author manuscript is the manuscript of an article that has been accepted for publication and which typically includes author-incorporated changes suggested during submission, peer review and editor-author communications.

Authors can share their accepted author manuscript:

- immediately

  - via their non-commercial person homepage or blog
  - by updating a preprint in arXiv or RePEc with the accepted manuscript
  - via their research institute or institutional repository for internal institutional uses or as part of an invitation-only research collaboration work-group
  - directly by providing copies to their students or to research collaborators for their personal use
  - for private scholarly sharing as part of an invitation-only work group on commercial sites with which Elsevier has an agreement
- After the embargo period
  - via non-commercial hosting platforms such as their institutional repository
  - via commercial sites with which Elsevier has an agreement

In all cases accepted manuscripts should:

- link to the formal publication via its DOI
- bear a CC-BY-NC-ND license - this is easy to do
- if aggregated with other manuscripts, for example in a repository or other site, be shared in alignment with our hosting policy not be added to or enhanced in any way to appear more like, or to substitute for, the published journal article.

Published journal article (JPA): A published journal article (PJA) is the definitive final record of published research that appears or will appear in the journal and embodies all value-adding publishing activities including peer review co-ordination, copy-editing, formatting, (if relevant) pagination and online enrichment.
Policies for sharing publishing journal articles differ for subscription and gold open access articles:
Subscription Articles: If you are an author, please share a link to your article rather than the full-text. Millions of researchers have access to the formal publications on ScienceDirect, and so links will help your users to find, access, cite, and use the best available version.
Theses and dissertations which contain embedded PJAs as part of the formal submission can be posted publicly by the awarding institution with DOI links back to the formal publications on ScienceDirect.
If you are affiliated with a library that subscribes to ScienceDirect you have additional private sharing rights for others' research accessed under that agreement. This includes use for classroom teaching and internal training at the institution (including use in course packs and courseware programs), and inclusion of the article for grant funding purposes.
Gold Open Access Articles: May be shared according to the author-selected end-user license and should contain a CrossMark logo, the end user license, and a DOI link to the formal publication on ScienceDirect.
Please refer to Elsevier's posting policy for further information.
18. **For book authors** the following clauses are applicable in addition to the above: Authors are permitted to place a brief summary of their work online only. You are not allowed to download and post the published electronic version of your chapter, nor may you scan the printed edition to create an electronic version. **Posting to a repository:** Authors are permitted to post a summary of their chapter only in their institution's repository.
19. **Thesis/Dissertation**: If your license is for use in a thesis/dissertation your thesis may be submitted to your institution in either print or electronic form. Should your thesis be published commercially, please reapply for permission. These requirements include permission for the Library and Archives of Canada to supply single copies, on demand, of the complete thesis and include permission for Proquest/UMI to supply single copies, on demand, of the complete thesis. Should your thesis be published commercially, please reapply for permission. Theses and dissertations which contain embedded PJAs as part of the formal submission can be posted publicly by the awarding institution with DOI links back to the formal publications on ScienceDirect.

Elsevier Open Access Terms and Conditions
You can publish open access with Elsevier in hundreds of open access journals or in nearly 2000 established subscription journals that support open access publishing. Permitted third

party re-use of these open access articles is defined by the author's choice of Creative Commons user license. See our open access license policy for more information.

Terms & Conditions applicable to all Open Access articles published with Elsevier:

Any reuse of the article must not represent the author as endorsing the adaptation of the article nor should the article be modified in such a way as to damage the author's honour or reputation. If any changes have been made, such changes must be clearly indicated.

The author(s) must be appropriately credited and we ask that you include the end user license and a DOI link to the formal publication on ScienceDirect.

If any part of the material to be used (for example, figures) has appeared in our publication with credit or acknowledgement to another source it is the responsibility of the user to ensure their reuse complies with the terms and conditions determined by the rights holder.

Additional Terms & Conditions applicable to each Creative Commons user license:

CC BY: The CC-BY license allows users to copy, to create extracts, abstracts and new works from the Article, to alter and revise the Article and to make commercial use of the Article (including reuse and/or resale of the Article by commercial entities), provided the user gives appropriate credit (with a link to the formal publication through the relevant DOI), provides a link to the license, indicates if changes were made and the licensor is not represented as endorsing the use made of the work. The full details of the license are available at http://creativecommons.org/licenses/by/4.0.

CC BY NC SA: The CC BY-NC-SA license allows users to copy, to create extracts, abstracts and new works from the Article, to alter and revise the Article, provided this is not done for commercial purposes, and that the user gives appropriate credit (with a link to the formal publication through the relevant DOI), provides a link to the license, indicates if changes were made and the licensor is not represented as endorsing the use made of the work. Further, any new works must be made available on the same conditions. The full details of the license are available at http://creativecommons.org/licenses/by-nc-sa/4.0.

CC BY NC ND: The CC BY-NC-ND license allows users to copy and distribute the Article, provided this is not done for commercial purposes and further does not permit distribution of the Article if it is changed or edited in any way, and provided the user gives appropriate credit (with a link to the formal publication through the relevant DOI), provides a link to the license, and that the licensor is not represented as endorsing the use made of the work. The full details of the license are available at http://creativecommons.org/licenses/by-nc-nd/4.0.

Any commercial reuse of Open Access articles published with a CC BY NC SA or CC BY NC ND license requires permission from Elsevier and will be subject to a fee.

Commercial reuse includes:

- Associating advertising with the full text of the Article
- Charging fees for document delivery or access
- Article aggregation
- Systematic distribution via e-mail lists or share buttons

Posting or linking by commercial companies for use by customers of those companies.

20. **Other Conditions**:

v1.9

Questions? customercare@copyright.com or +1-855-239-3415 (toll free in the US) or +1-978-646-2777.

ELSEVIER LICENSE
TERMS AND CONDITIONS

Jul 22, 2018

This Agreement between Curtin University ("You") and Elsevier ("Elsevier") consists of your license details and the terms and conditions provided by Elsevier and Copyright Clearance Center.

License Number	4394300299864
License date	Jul 22, 2018
Licensed Content Publisher	Elsevier
Licensed Content Publication	Composites Part B: Engineering
Licensed Content Title	Cover requirements of thermoplastic pipes used under highways
Licensed Content Author	Junsuk Kang,Younghan Jung,Yonghan Ahn
Licensed Content Date	Dec 1, 2013
Licensed Content Volume	55
Licensed Content Issue	n/a
Licensed Content Pages	9
Start Page	184
End Page	192
Type of Use	reuse in a thesis/dissertation
Intended publisher of new work	other
Portion	figures/tables/illustrations
Number of figures/tables/illustrations	1
Format	both print and electronic
Are you the author of this Elsevier article?	No
Will you be translating?	No
Original figure numbers	Figure 4
Title of your thesis/dissertation	Experimental and Numerical Investigations to Assess the Performance of a Buried Pipe Subjected to Traffic Load / Non-Treated and Cement-Treated Trench
Expected completion date	Aug 2018
Estimated size (number of pages)	300
Requestor Location	Curtin University 24 Everingham Street Clarkson, Western Australia 6030 Australia Attn: Curtin University
Publisher Tax ID	GB 494 6272 12
Total	0.00 AUD
Terms and Conditions	

INTRODUCTION

1. The publisher for this copyrighted material is Elsevier. By clicking "accept" in connection with completing this licensing transaction, you agree that the following terms and conditions apply to this transaction (along with the Billing and Payment terms and conditions established by Copyright Clearance Center, Inc. ("CCC"), at the time that you opened your Rightslink account and that are available at any time at http://myaccount.copyright.com).

GENERAL TERMS

2. Elsevier hereby grants you permission to reproduce the aforementioned material subject to the terms and conditions indicated.
3. Acknowledgement: If any part of the material to be used (for example, figures) has appeared in our publication with credit or acknowledgement to another source, permission must also be sought from that source. If such permission is not obtained then that material may not be included in your publication/copies. Suitable acknowledgement to the source must be made, either as a footnote or in a reference list at the end of your publication, as follows:
"Reprinted from Publication title, Vol /edition number, Author(s), Title of article / title of chapter, Pages No., Copyright (Year), with permission from Elsevier [OR APPLICABLE SOCIETY COPYRIGHT OWNER]." Also Lancet special credit - "Reprinted from The Lancet, Vol. number, Author(s), Title of article, Pages No., Copyright (Year), with permission from Elsevier."
4. Reproduction of this material is confined to the purpose and/or media for which permission is hereby given.
5. Altering/Modifying Material: Not Permitted. However figures and illustrations may be altered/adapted minimally to serve your work. Any other abbreviations, additions, deletions and/or any other alterations shall be made only with prior written authorization of Elsevier Ltd. (Please contact Elsevier at permissions@elsevier.com). No modifications can be made to any Lancet figures/tables and they must be reproduced in full.
6. If the permission fee for the requested use of our material is waived in this instance, please be advised that your future requests for Elsevier materials may attract a fee.
7. Reservation of Rights: Publisher reserves all rights not specifically granted in the combination of (i) the license details provided by you and accepted in the course of this licensing transaction, (ii) these terms and conditions and (iii) CCC's Billing and Payment terms and conditions.
8. License Contingent Upon Payment: While you may exercise the rights licensed immediately upon issuance of the license at the end of the licensing process for the transaction, provided that you have disclosed complete and accurate details of your proposed use, no license is finally effective unless and until full payment is received from you (either by publisher or by CCC) as provided in CCC's Billing and Payment terms and conditions. If full payment is not received on a timely basis, then any license preliminarily granted shall be deemed automatically revoked and shall be void as if never granted. Further, in the event that you breach any of these terms and conditions or any of CCC's Billing and Payment terms and conditions, the license is automatically revoked and shall be void as if never granted. Use of materials as described in a revoked license, as well as any use of the materials beyond the scope of an unrevoked license, may constitute copyright infringement and publisher reserves the right to take any and all action to protect its copyright in the materials.
9. Warranties: Publisher makes no representations or warranties with respect to the licensed material.
10. Indemnity: You hereby indemnify and agree to hold harmless publisher and CCC, and their respective officers, directors, employees and agents, from and against any and all claims arising out of your use of the licensed material other than as specifically authorized pursuant to this license.
11. No Transfer of License: This license is personal to you and may not be sublicensed, assigned, or transferred by you to any other person without publisher's written permission.
12. No Amendment Except in Writing: This license may not be amended except in a writing signed by both parties (or, in the case of publisher, by CCC on publisher's behalf).
13. Objection to Contrary Terms: Publisher hereby objects to any terms contained in any purchase order, acknowledgment, check endorsement or other writing prepared by you, which terms are inconsistent with these terms and conditions or CCC's Billing and Payment

terms and conditions. These terms and conditions, together with CCC's Billing and Payment terms and conditions (which are incorporated herein), comprise the entire agreement between you and publisher (and CCC) concerning this licensing transaction. In the event of any conflict between your obligations established by these terms and conditions and those established by CCC's Billing and Payment terms and conditions, these terms and conditions shall control.

14. Revocation: Elsevier or Copyright Clearance Center may deny the permissions described in this License at their sole discretion, for any reason or no reason, with a full refund payable to you. Notice of such denial will be made using the contact information provided by you. Failure to receive such notice will not alter or invalidate the denial. In no event will Elsevier or Copyright Clearance Center be responsible or liable for any costs, expenses or damage incurred by you as a result of a denial of your permission request, other than a refund of the amount(s) paid by you to Elsevier and/or Copyright Clearance Center for denied permissions.

LIMITED LICENSE

The following terms and conditions apply only to specific license types:

15. **Translation**: This permission is granted for non-exclusive world **English** rights only unless your license was granted for translation rights. If you licensed translation rights you may only translate this content into the languages you requested. A professional translator must perform all translations and reproduce the content word for word preserving the integrity of the article.

16. **Posting licensed content on any Website**: The following terms and conditions apply as follows: Licensing material from an Elsevier journal: All content posted to the web site must maintain the copyright information line on the bottom of each image; A hyper-text must be included to the Homepage of the journal from which you are licensing at http://www.sciencedirect.com/science/journal/xxxxx or the Elsevier homepage for books at http://www.elsevier.com; Central Storage: This license does not include permission for a scanned version of the material to be stored in a central repository such as that provided by Heron/XanEdu.

Licensing material from an Elsevier book: A hyper-text link must be included to the Elsevier homepage at http://www.elsevier.com . All content posted to the web site must maintain the copyright information line on the bottom of each image.

Posting licensed content on Electronic reserve: In addition to the above the following clauses are applicable: The web site must be password-protected and made available only to bona fide students registered on a relevant course. This permission is granted for 1 year only. You may obtain a new license for future website posting.

17. **For journal authors:** the following clauses are applicable in addition to the above:

Preprints:

A preprint is an author's own write-up of research results and analysis, it has not been peer-reviewed, nor has it had any other value added to it by a publisher (such as formatting, copyright, technical enhancement etc.).

Authors can share their preprints anywhere at any time. Preprints should not be added to or enhanced in any way in order to appear more like, or to substitute for, the final versions of articles however authors can update their preprints on arXiv or RePEc with their Accepted Author Manuscript (see below).

If accepted for publication, we encourage authors to link from the preprint to their formal publication via its DOI. Millions of researchers have access to the formal publications on ScienceDirect, and so links will help users to find, access, cite and use the best available version. Please note that Cell Press, The Lancet and some society-owned have different preprint policies. Information on these policies is available on the journal homepage.

Accepted Author Manuscripts: An accepted author manuscript is the manuscript of an article that has been accepted for publication and which typically includes author-incorporated changes suggested during submission, peer review and editor-author communications.

Authors can share their accepted author manuscript:

- immediately

  - via their non-commercial person homepage or blog
  - by updating a preprint in arXiv or RePEc with the accepted manuscript
  - via their research institute or institutional repository for internal institutional uses or as part of an invitation-only research collaboration work-group
  - directly by providing copies to their students or to research collaborators for their personal use
  - for private scholarly sharing as part of an invitation-only work group on commercial sites with which Elsevier has an agreement
- After the embargo period
  - via non-commercial hosting platforms such as their institutional repository
  - via commercial sites with which Elsevier has an agreement

In all cases accepted manuscripts should:

- link to the formal publication via its DOI
- bear a CC-BY-NC-ND license - this is easy to do
- if aggregated with other manuscripts, for example in a repository or other site, be shared in alignment with our hosting policy not be added to or enhanced in any way to appear more like, or to substitute for, the published journal article.

Published journal article (JPA): A published journal article (PJA) is the definitive final record of published research that appears or will appear in the journal and embodies all value-adding publishing activities including peer review co-ordination, copy-editing, formatting, (if relevant) pagination and online enrichment.
Policies for sharing publishing journal articles differ for subscription and gold open access articles:
Subscription Articles: If you are an author, please share a link to your article rather than the full-text. Millions of researchers have access to the formal publications on ScienceDirect, and so links will help your users to find, access, cite, and use the best available version.
Theses and dissertations which contain embedded PJAs as part of the formal submission can be posted publicly by the awarding institution with DOI links back to the formal publications on ScienceDirect.
If you are affiliated with a library that subscribes to ScienceDirect you have additional private sharing rights for others' research accessed under that agreement. This includes use for classroom teaching and internal training at the institution (including use in course packs and courseware programs), and inclusion of the article for grant funding purposes.
Gold Open Access Articles: May be shared according to the author-selected end-user license and should contain a CrossMark logo, the end user license, and a DOI link to the formal publication on ScienceDirect.
Please refer to Elsevier's posting policy for further information.
18. **For book authors** the following clauses are applicable in addition to the above: Authors are permitted to place a brief summary of their work online only. You are not allowed to download and post the published electronic version of your chapter, nor may you scan the printed edition to create an electronic version. **Posting to a repository:** Authors are permitted to post a summary of their chapter only in their institution's repository.
19. **Thesis/Dissertation**: If your license is for use in a thesis/dissertation your thesis may be submitted to your institution in either print or electronic form. Should your thesis be published commercially, please reapply for permission. These requirements include permission for the Library and Archives of Canada to supply single copies, on demand, of the complete thesis and include permission for Proquest/UMI to supply single copies, on demand, of the complete thesis. Should your thesis be published commercially, please reapply for permission. Theses and dissertations which contain embedded PJAs as part of the formal submission can be posted publicly by the awarding institution with DOI links back to the formal publications on ScienceDirect.

Elsevier Open Access Terms and Conditions
You can publish open access with Elsevier in hundreds of open access journals or in nearly 2000 established subscription journals that support open access publishing. Permitted third

party re-use of these open access articles is defined by the author's choice of Creative Commons user license. See our open access license policy for more information.

Terms & Conditions applicable to all Open Access articles published with Elsevier:

Any reuse of the article must not represent the author as endorsing the adaptation of the article nor should the article be modified in such a way as to damage the author's honour or reputation. If any changes have been made, such changes must be clearly indicated.

The author(s) must be appropriately credited and we ask that you include the end user license and a DOI link to the formal publication on ScienceDirect.

If any part of the material to be used (for example, figures) has appeared in our publication with credit or acknowledgement to another source it is the responsibility of the user to ensure their reuse complies with the terms and conditions determined by the rights holder.

Additional Terms & Conditions applicable to each Creative Commons user license:

CC BY: The CC-BY license allows users to copy, to create extracts, abstracts and new works from the Article, to alter and revise the Article and to make commercial use of the Article (including reuse and/or resale of the Article by commercial entities), provided the user gives appropriate credit (with a link to the formal publication through the relevant DOI), provides a link to the license, indicates if changes were made and the licensor is not represented as endorsing the use made of the work. The full details of the license are available at http://creativecommons.org/licenses/by/4.0.

CC BY NC SA: The CC BY-NC-SA license allows users to copy, to create extracts, abstracts and new works from the Article, to alter and revise the Article, provided this is not done for commercial purposes, and that the user gives appropriate credit (with a link to the formal publication through the relevant DOI), provides a link to the license, indicates if changes were made and the licensor is not represented as endorsing the use made of the work. Further, any new works must be made available on the same conditions. The full details of the license are available at http://creativecommons.org/licenses/by-nc-sa/4.0.

CC BY NC ND: The CC BY-NC-ND license allows users to copy and distribute the Article, provided this is not done for commercial purposes and further does not permit distribution of the Article if it is changed or edited in any way, and provided the user gives appropriate credit (with a link to the formal publication through the relevant DOI), provides a link to the license, and that the licensor is not represented as endorsing the use made of the work. The full details of the license are available at http://creativecommons.org/licenses/by-nc-nd/4.0.

Any commercial reuse of Open Access articles published with a CC BY NC SA or CC BY NC ND license requires permission from Elsevier and will be subject to a fee.

Commercial reuse includes:

- Associating advertising with the full text of the Article
- Charging fees for document delivery or access
- Article aggregation
- Systematic distribution via e-mail lists or share buttons

Posting or linking by commercial companies for use by customers of those companies.

20. **Other Conditions**:

v1.9

Questions? customercare@copyright.com or +1-855-239-3415 (toll free in the US) or +1-978-646-2777.

ELSEVIER LICENSE
TERMS AND CONDITIONS

Jul 22, 2018

This Agreement between Curtin University ("You") and Elsevier ("Elsevier") consists of your license details and the terms and conditions provided by Elsevier and Copyright Clearance Center.

License Number	4394290715187
License date	Jul 22, 2018
Licensed Content Publisher	Elsevier
Licensed Content Publication	Construction and Building Materials
Licensed Content Title	Investigation of buried full-scale SFRC pipes under live loads
Licensed Content Author	Moncef L. Nehdi,Nedal Mohamed,Ahmed M. Soliman
Licensed Content Date	Jan 15, 2016
Licensed Content Volume	102
Licensed Content Issue	n/a
Licensed Content Pages	10
Start Page	733
End Page	742
Type of Use	reuse in a thesis/dissertation
Intended publisher of new work	other
Portion	figures/tables/illustrations
Number of figures/tables/illustrations	1
Format	both print and electronic
Are you the author of this Elsevier article?	No
Will you be translating?	No
Original figure numbers	Figure 1
Title of your thesis/dissertation	Experimental and Numerical Investigations to Assess the Performance of a Buried Pipe Subjected to Traffic Load / Non-Treated and Cement-Treated Trench
Expected completion date	Aug 2018
Estimated size (number of pages)	300
Requestor Location	Curtin University 24 Everingham Street Clarkson, Western Australia 6030 Australia Attn: Curtin University
Publisher Tax ID	GB 494 6272 12
Total	0.00 AUD
Terms and Conditions	

INTRODUCTION

1. The publisher for this copyrighted material is Elsevier. By clicking "accept" in connection with completing this licensing transaction, you agree that the following terms and conditions apply to this transaction (along with the Billing and Payment terms and conditions established by Copyright Clearance Center, Inc. ("CCC"), at the time that you opened your Rightslink account and that are available at any time at http://myaccount.copyright.com).

GENERAL TERMS

2. Elsevier hereby grants you permission to reproduce the aforementioned material subject to the terms and conditions indicated.

3. Acknowledgement: If any part of the material to be used (for example, figures) has appeared in our publication with credit or acknowledgement to another source, permission must also be sought from that source. If such permission is not obtained then that material may not be included in your publication/copies. Suitable acknowledgement to the source must be made, either as a footnote or in a reference list at the end of your publication, as follows:

"Reprinted from Publication title, Vol /edition number, Author(s), Title of article / title of chapter, Pages No., Copyright (Year), with permission from Elsevier [OR APPLICABLE SOCIETY COPYRIGHT OWNER]." Also Lancet special credit - "Reprinted from The Lancet, Vol. number, Author(s), Title of article, Pages No., Copyright (Year), with permission from Elsevier."

4. Reproduction of this material is confined to the purpose and/or media for which permission is hereby given.

5. Altering/Modifying Material: Not Permitted. However figures and illustrations may be altered/adapted minimally to serve your work. Any other abbreviations, additions, deletions and/or any other alterations shall be made only with prior written authorization of Elsevier Ltd. (Please contact Elsevier at permissions@elsevier.com). No modifications can be made to any Lancet figures/tables and they must be reproduced in full.

6. If the permission fee for the requested use of our material is waived in this instance, please be advised that your future requests for Elsevier materials may attract a fee.

7. Reservation of Rights: Publisher reserves all rights not specifically granted in the combination of (i) the license details provided by you and accepted in the course of this licensing transaction, (ii) these terms and conditions and (iii) CCC's Billing and Payment terms and conditions.

8. License Contingent Upon Payment: While you may exercise the rights licensed immediately upon issuance of the license at the end of the licensing process for the transaction, provided that you have disclosed complete and accurate details of your proposed use, no license is finally effective unless and until full payment is received from you (either by publisher or by CCC) as provided in CCC's Billing and Payment terms and conditions. If full payment is not received on a timely basis, then any license preliminarily granted shall be deemed automatically revoked and shall be void as if never granted. Further, in the event that you breach any of these terms and conditions or any of CCC's Billing and Payment terms and conditions, the license is automatically revoked and shall be void as if never granted. Use of materials as described in a revoked license, as well as any use of the materials beyond the scope of an unrevoked license, may constitute copyright infringement and publisher reserves the right to take any and all action to protect its copyright in the materials.

9. Warranties: Publisher makes no representations or warranties with respect to the licensed material.

10. Indemnity: You hereby indemnify and agree to hold harmless publisher and CCC, and their respective officers, directors, employees and agents, from and against any and all claims arising out of your use of the licensed material other than as specifically authorized pursuant to this license.

11. No Transfer of License: This license is personal to you and may not be sublicensed, assigned, or transferred by you to any other person without publisher's written permission.

12. No Amendment Except in Writing: This license may not be amended except in a writing signed by both parties (or, in the case of publisher, by CCC on publisher's behalf).

13. Objection to Contrary Terms: Publisher hereby objects to any terms contained in any purchase order, acknowledgment, check endorsement or other writing prepared by you, which terms are inconsistent with these terms and conditions or CCC's Billing and Payment

terms and conditions. These terms and conditions, together with CCC's Billing and Payment terms and conditions (which are incorporated herein), comprise the entire agreement between you and publisher (and CCC) concerning this licensing transaction. In the event of any conflict between your obligations established by these terms and conditions and those established by CCC's Billing and Payment terms and conditions, these terms and conditions shall control.

14. Revocation: Elsevier or Copyright Clearance Center may deny the permissions described in this License at their sole discretion, for any reason or no reason, with a full refund payable to you. Notice of such denial will be made using the contact information provided by you. Failure to receive such notice will not alter or invalidate the denial. In no event will Elsevier or Copyright Clearance Center be responsible or liable for any costs, expenses or damage incurred by you as a result of a denial of your permission request, other than a refund of the amount(s) paid by you to Elsevier and/or Copyright Clearance Center for denied permissions.

LIMITED LICENSE

The following terms and conditions apply only to specific license types:

15. **Translation**: This permission is granted for non-exclusive world **English** rights only unless your license was granted for translation rights. If you licensed translation rights you may only translate this content into the languages you requested. A professional translator must perform all translations and reproduce the content word for word preserving the integrity of the article.

16. **Posting licensed content on any Website**: The following terms and conditions apply as follows: Licensing material from an Elsevier journal: All content posted to the web site must maintain the copyright information line on the bottom of each image; A hyper-text must be included to the Homepage of the journal from which you are licensing at http://www.sciencedirect.com/science/journal/xxxxx or the Elsevier homepage for books at http://www.elsevier.com; Central Storage: This license does not include permission for a scanned version of the material to be stored in a central repository such as that provided by Heron/XanEdu.

Licensing material from an Elsevier book: A hyper-text link must be included to the Elsevier homepage at http://www.elsevier.com . All content posted to the web site must maintain the copyright information line on the bottom of each image.

Posting licensed content on Electronic reserve: In addition to the above the following clauses are applicable: The web site must be password-protected and made available only to bona fide students registered on a relevant course. This permission is granted for 1 year only. You may obtain a new license for future website posting.

17. **For journal authors:** the following clauses are applicable in addition to the above:

Preprints:

A preprint is an author's own write-up of research results and analysis, it has not been peer-reviewed, nor has it had any other value added to it by a publisher (such as formatting, copyright, technical enhancement etc.).

Authors can share their preprints anywhere at any time. Preprints should not be added to or enhanced in any way in order to appear more like, or to substitute for, the final versions of articles however authors can update their preprints on arXiv or RePEc with their Accepted Author Manuscript (see below).

If accepted for publication, we encourage authors to link from the preprint to their formal publication via its DOI. Millions of researchers have access to the formal publications on ScienceDirect, and so links will help users to find, access, cite and use the best available version. Please note that Cell Press, The Lancet and some society-owned have different preprint policies. Information on these policies is available on the journal homepage.

Accepted Author Manuscripts: An accepted author manuscript is the manuscript of an article that has been accepted for publication and which typically includes author-incorporated changes suggested during submission, peer review and editor-author communications.

Authors can share their accepted author manuscript:

- immediately

  - via their non-commercial person homepage or blog
  - by updating a preprint in arXiv or RePEc with the accepted manuscript
  - via their research institute or institutional repository for internal institutional uses or as part of an invitation-only research collaboration work-group
  - directly by providing copies to their students or to research collaborators for their personal use
  - for private scholarly sharing as part of an invitation-only work group on commercial sites with which Elsevier has an agreement
- After the embargo period
  - via non-commercial hosting platforms such as their institutional repository
  - via commercial sites with which Elsevier has an agreement

In all cases accepted manuscripts should:

- link to the formal publication via its DOI
- bear a CC-BY-NC-ND license - this is easy to do
- if aggregated with other manuscripts, for example in a repository or other site, be shared in alignment with our hosting policy not be added to or enhanced in any way to appear more like, or to substitute for, the published journal article.

Published journal article (JPA): A published journal article (PJA) is the definitive final record of published research that appears or will appear in the journal and embodies all value-adding publishing activities including peer review co-ordination, copy-editing, formatting, (if relevant) pagination and online enrichment.
Policies for sharing publishing journal articles differ for subscription and gold open access articles:
Subscription Articles: If you are an author, please share a link to your article rather than the full-text. Millions of researchers have access to the formal publications on ScienceDirect, and so links will help your users to find, access, cite, and use the best available version.
Theses and dissertations which contain embedded PJAs as part of the formal submission can be posted publicly by the awarding institution with DOI links back to the formal publications on ScienceDirect.
If you are affiliated with a library that subscribes to ScienceDirect you have additional private sharing rights for others' research accessed under that agreement. This includes use for classroom teaching and internal training at the institution (including use in course packs and courseware programs), and inclusion of the article for grant funding purposes.
Gold Open Access Articles: May be shared according to the author-selected end-user license and should contain a CrossMark logo, the end user license, and a DOI link to the formal publication on ScienceDirect.
Please refer to Elsevier's posting policy for further information.
18. **For book authors** the following clauses are applicable in addition to the above: Authors are permitted to place a brief summary of their work online only. You are not allowed to download and post the published electronic version of your chapter, nor may you scan the printed edition to create an electronic version. **Posting to a repository:** Authors are permitted to post a summary of their chapter only in their institution's repository.
19. **Thesis/Dissertation**: If your license is for use in a thesis/dissertation your thesis may be submitted to your institution in either print or electronic form. Should your thesis be published commercially, please reapply for permission. These requirements include permission for the Library and Archives of Canada to supply single copies, on demand, of the complete thesis and include permission for Proquest/UMI to supply single copies, on demand, of the complete thesis. Should your thesis be published commercially, please reapply for permission. Theses and dissertations which contain embedded PJAs as part of the formal submission can be posted publicly by the awarding institution with DOI links back to the formal publications on ScienceDirect.

Elsevier Open Access Terms and Conditions
You can publish open access with Elsevier in hundreds of open access journals or in nearly 2000 established subscription journals that support open access publishing. Permitted third

party re-use of these open access articles is defined by the author's choice of Creative Commons user license. See our open access license policy for more information.

Terms & Conditions applicable to all Open Access articles published with Elsevier:

Any reuse of the article must not represent the author as endorsing the adaptation of the article nor should the article be modified in such a way as to damage the author's honour or reputation. If any changes have been made, such changes must be clearly indicated.

The author(s) must be appropriately credited and we ask that you include the end user license and a DOI link to the formal publication on ScienceDirect.

If any part of the material to be used (for example, figures) has appeared in our publication with credit or acknowledgement to another source it is the responsibility of the user to ensure their reuse complies with the terms and conditions determined by the rights holder.

Additional Terms & Conditions applicable to each Creative Commons user license:

CC BY: The CC-BY license allows users to copy, to create extracts, abstracts and new works from the Article, to alter and revise the Article and to make commercial use of the Article (including reuse and/or resale of the Article by commercial entities), provided the user gives appropriate credit (with a link to the formal publication through the relevant DOI), provides a link to the license, indicates if changes were made and the licensor is not represented as endorsing the use made of the work. The full details of the license are available at http://creativecommons.org/licenses/by/4.0.

CC BY NC SA: The CC BY-NC-SA license allows users to copy, to create extracts, abstracts and new works from the Article, to alter and revise the Article, provided this is not done for commercial purposes, and that the user gives appropriate credit (with a link to the formal publication through the relevant DOI), provides a link to the license, indicates if changes were made and the licensor is not represented as endorsing the use made of the work. Further, any new works must be made available on the same conditions. The full details of the license are available at http://creativecommons.org/licenses/by-nc-sa/4.0.

CC BY NC ND: The CC BY-NC-ND license allows users to copy and distribute the Article, provided this is not done for commercial purposes and further does not permit distribution of the Article if it is changed or edited in any way, and provided the user gives appropriate credit (with a link to the formal publication through the relevant DOI), provides a link to the license, and that the licensor is not represented as endorsing the use made of the work. The full details of the license are available at http://creativecommons.org/licenses/by-nc-nd/4.0.

Any commercial reuse of Open Access articles published with a CC BY NC SA or CC BY NC ND license requires permission from Elsevier and will be subject to a fee.

Commercial reuse includes:

- Associating advertising with the full text of the Article
- Charging fees for document delivery or access
- Article aggregation
- Systematic distribution via e-mail lists or share buttons

Posting or linking by commercial companies for use by customers of those companies.

20. **Other Conditions**:

v1.9

Questions? customercare@copyright.com or +1-855-239-3415 (toll free in the US) or +1-978-646-2777.

ELSEVIER LICENSE
TERMS AND CONDITIONS

Jul 22, 2018

This Agreement between Curtin University ("You") and Elsevier ("Elsevier") consists of your license details and the terms and conditions provided by Elsevier and Copyright Clearance Center.

License Number	4394551162340
License date	Jul 22, 2018
Licensed Content Publisher	Elsevier
Licensed Content Publication	Journal of Archaeological Science
Licensed Content Title	A method for calculating soil pressure overlying human burials
Licensed Content Author	Glenys McGowan,Jonathan Prangnell
Licensed Content Date	Jan 1, 2015
Licensed Content Volume	53
Licensed Content Issue	n/a
Licensed Content Pages	7
Start Page	12
End Page	18
Type of Use	reuse in a thesis/dissertation
Portion	figures/tables/illustrations
Number of figures/tables/illustrations	1
Format	both print and electronic
Are you the author of this Elsevier article?	No
Will you be translating?	No
Original figure numbers	Figure 5
Title of your thesis/dissertation	Experimental and Numerical Investigations to Assess the Performance of a Buried Pipe Subjected to Traffic Load / Non-Treated and Cement-Treated Trench
Expected completion date	Aug 2018
Estimated size (number of pages)	300
Requestor Location	Curtin University 24 Everingham Street Clarkson, Western Australia 6030 Australia Attn: Curtin University
Publisher Tax ID	GB 494 6272 12
Total	0.00 AUD
Terms and Conditions	

INTRODUCTION

1. The publisher for this copyrighted material is Elsevier. By clicking "accept" in connection with completing this licensing transaction, you agree that the following terms and conditions apply to this transaction (along with the Billing and Payment terms and conditions

established by Copyright Clearance Center, Inc. ("CCC"), at the time that you opened your Rightslink account and that are available at any time at http://myaccount.copyright.com).

GENERAL TERMS

2. Elsevier hereby grants you permission to reproduce the aforementioned material subject to the terms and conditions indicated.

3. Acknowledgement: If any part of the material to be used (for example, figures) has appeared in our publication with credit or acknowledgement to another source, permission must also be sought from that source. If such permission is not obtained then that material may not be included in your publication/copies. Suitable acknowledgement to the source must be made, either as a footnote or in a reference list at the end of your publication, as follows:

"Reprinted from Publication title, Vol /edition number, Author(s), Title of article / title of chapter, Pages No., Copyright (Year), with permission from Elsevier [OR APPLICABLE SOCIETY COPYRIGHT OWNER]." Also Lancet special credit - "Reprinted from The Lancet, Vol. number, Author(s), Title of article, Pages No., Copyright (Year), with permission from Elsevier."

4. Reproduction of this material is confined to the purpose and/or media for which permission is hereby given.

5. Altering/Modifying Material: Not Permitted. However figures and illustrations may be altered/adapted minimally to serve your work. Any other abbreviations, additions, deletions and/or any other alterations shall be made only with prior written authorization of Elsevier Ltd. (Please contact Elsevier at permissions@elsevier.com). No modifications can be made to any Lancet figures/tables and they must be reproduced in full.

6. If the permission fee for the requested use of our material is waived in this instance, please be advised that your future requests for Elsevier materials may attract a fee.

7. Reservation of Rights: Publisher reserves all rights not specifically granted in the combination of (i) the license details provided by you and accepted in the course of this licensing transaction, (ii) these terms and conditions and (iii) CCC's Billing and Payment terms and conditions.

8. License Contingent Upon Payment: While you may exercise the rights licensed immediately upon issuance of the license at the end of the licensing process for the transaction, provided that you have disclosed complete and accurate details of your proposed use, no license is finally effective unless and until full payment is received from you (either by publisher or by CCC) as provided in CCC's Billing and Payment terms and conditions. If full payment is not received on a timely basis, then any license preliminarily granted shall be deemed automatically revoked and shall be void as if never granted. Further, in the event that you breach any of these terms and conditions or any of CCC's Billing and Payment terms and conditions, the license is automatically revoked and shall be void as if never granted. Use of materials as described in a revoked license, as well as any use of the materials beyond the scope of an unrevoked license, may constitute copyright infringement and publisher reserves the right to take any and all action to protect its copyright in the materials.

9. Warranties: Publisher makes no representations or warranties with respect to the licensed material.

10. Indemnity: You hereby indemnify and agree to hold harmless publisher and CCC, and their respective officers, directors, employees and agents, from and against any and all claims arising out of your use of the licensed material other than as specifically authorized pursuant to this license.

11. No Transfer of License: This license is personal to you and may not be sublicensed, assigned, or transferred by you to any other person without publisher's written permission.

12. No Amendment Except in Writing: This license may not be amended except in a writing signed by both parties (or, in the case of publisher, by CCC on publisher's behalf).

13. Objection to Contrary Terms: Publisher hereby objects to any terms contained in any purchase order, acknowledgment, check endorsement or other writing prepared by you, which terms are inconsistent with these terms and conditions or CCC's Billing and Payment terms and conditions. These terms and conditions, together with CCC's Billing and Payment terms and conditions (which are incorporated herein), comprise the entire agreement between you and publisher (and CCC) concerning this licensing transaction. In the event of

any conflict between your obligations established by these terms and conditions and those established by CCC's Billing and Payment terms and conditions, these terms and conditions shall control.

14. Revocation: Elsevier or Copyright Clearance Center may deny the permissions described in this License at their sole discretion, for any reason or no reason, with a full refund payable to you. Notice of such denial will be made using the contact information provided by you. Failure to receive such notice will not alter or invalidate the denial. In no event will Elsevier or Copyright Clearance Center be responsible or liable for any costs, expenses or damage incurred by you as a result of a denial of your permission request, other than a refund of the amount(s) paid by you to Elsevier and/or Copyright Clearance Center for denied permissions.

LIMITED LICENSE

The following terms and conditions apply only to specific license types:

15. **Translation**: This permission is granted for non-exclusive world **English** rights only unless your license was granted for translation rights. If you licensed translation rights you may only translate this content into the languages you requested. A professional translator must perform all translations and reproduce the content word for word preserving the integrity of the article.

16. **Posting licensed content on any Website**: The following terms and conditions apply as follows: Licensing material from an Elsevier journal: All content posted to the web site must maintain the copyright information line on the bottom of each image; A hyper-text must be included to the Homepage of the journal from which you are licensing at http://www.sciencedirect.com/science/journal/xxxxx or the Elsevier homepage for books at http://www.elsevier.com; Central Storage: This license does not include permission for a scanned version of the material to be stored in a central repository such as that provided by Heron/XanEdu.

Licensing material from an Elsevier book: A hyper-text link must be included to the Elsevier homepage at http://www.elsevier.com . All content posted to the web site must maintain the copyright information line on the bottom of each image.

Posting licensed content on Electronic reserve: In addition to the above the following clauses are applicable: The web site must be password-protected and made available only to bona fide students registered on a relevant course. This permission is granted for 1 year only. You may obtain a new license for future website posting.

17. **For journal authors:** the following clauses are applicable in addition to the above:

Preprints:

A preprint is an author's own write-up of research results and analysis, it has not been peer-reviewed, nor has it had any other value added to it by a publisher (such as formatting, copyright, technical enhancement etc.).

Authors can share their preprints anywhere at any time. Preprints should not be added to or enhanced in any way in order to appear more like, or to substitute for, the final versions of articles however authors can update their preprints on arXiv or RePEc with their Accepted Author Manuscript (see below).

If accepted for publication, we encourage authors to link from the preprint to their formal publication via its DOI. Millions of researchers have access to the formal publications on ScienceDirect, and so links will help users to find, access, cite and use the best available version. Please note that Cell Press, The Lancet and some society-owned have different preprint policies. Information on these policies is available on the journal homepage.

Accepted Author Manuscripts: An accepted author manuscript is the manuscript of an article that has been accepted for publication and which typically includes author-incorporated changes suggested during submission, peer review and editor-author communications.

Authors can share their accepted author manuscript:

- immediately
    - via their non-commercial person homepage or blog
    - by updating a preprint in arXiv or RePEc with the accepted manuscript

- via their research institute or institutional repository for internal institutional uses or as part of an invitation-only research collaboration work-group
- directly by providing copies to their students or to research collaborators for their personal use
- for private scholarly sharing as part of an invitation-only work group on commercial sites with which Elsevier has an agreement

- After the embargo period
  - via non-commercial hosting platforms such as their institutional repository
  - via commercial sites with which Elsevier has an agreement

In all cases accepted manuscripts should:

- link to the formal publication via its DOI
- bear a CC-BY-NC-ND license - this is easy to do
- if aggregated with other manuscripts, for example in a repository or other site, be shared in alignment with our hosting policy not be added to or enhanced in any way to appear more like, or to substitute for, the published journal article.

Published journal article (JPA): A published journal article (PJA) is the definitive final record of published research that appears or will appear in the journal and embodies all value-adding publishing activities including peer review co-ordination, copy-editing, formatting, (if relevant) pagination and online enrichment.
Policies for sharing publishing journal articles differ for subscription and gold open access articles:
Subscription Articles: If you are an author, please share a link to your article rather than the full-text. Millions of researchers have access to the formal publications on ScienceDirect, and so links will help your users to find, access, cite, and use the best available version.
Theses and dissertations which contain embedded PJAs as part of the formal submission can be posted publicly by the awarding institution with DOI links back to the formal publications on ScienceDirect.
If you are affiliated with a library that subscribes to ScienceDirect you have additional private sharing rights for others' research accessed under that agreement. This includes use for classroom teaching and internal training at the institution (including use in course packs and courseware programs), and inclusion of the article for grant funding purposes.
Gold Open Access Articles: May be shared according to the author-selected end-user license and should contain a CrossMark logo, the end user license, and a DOI link to the formal publication on ScienceDirect.
Please refer to Elsevier's posting policy for further information.
18. **For book authors** the following clauses are applicable in addition to the above:
Authors are permitted to place a brief summary of their work online only. You are not allowed to download and post the published electronic version of your chapter, nor may you scan the printed edition to create an electronic version. **Posting to a repository:** Authors are permitted to post a summary of their chapter only in their institution's repository.
19. **Thesis/Dissertation**: If your license is for use in a thesis/dissertation your thesis may be submitted to your institution in either print or electronic form. Should your thesis be published commercially, please reapply for permission. These requirements include permission for the Library and Archives of Canada to supply single copies, on demand, of the complete thesis and include permission for Proquest/UMI to supply single copies, on demand, of the complete thesis. Should your thesis be published commercially, please reapply for permission. Theses and dissertations which contain embedded PJAs as part of the formal submission can be posted publicly by the awarding institution with DOI links back to the formal publications on ScienceDirect.

Elsevier Open Access Terms and Conditions
You can publish open access with Elsevier in hundreds of open access journals or in nearly 2000 established subscription journals that support open access publishing. Permitted third party re-use of these open access articles is defined by the author's choice of Creative Commons user license. See our open access license policy for more information.

Terms & Conditions applicable to all Open Access articles published with Elsevier:
Any reuse of the article must not represent the author as endorsing the adaptation of the article nor should the article be modified in such a way as to damage the author's honour or reputation. If any changes have been made, such changes must be clearly indicated.
The author(s) must be appropriately credited and we ask that you include the end user license and a DOI link to the formal publication on ScienceDirect.
If any part of the material to be used (for example, figures) has appeared in our publication with credit or acknowledgement to another source it is the responsibility of the user to ensure their reuse complies with the terms and conditions determined by the rights holder.
Additional Terms & Conditions applicable to each Creative Commons user license:
CC BY: The CC-BY license allows users to copy, to create extracts, abstracts and new works from the Article, to alter and revise the Article and to make commercial use of the Article (including reuse and/or resale of the Article by commercial entities), provided the user gives appropriate credit (with a link to the formal publication through the relevant DOI), provides a link to the license, indicates if changes were made and the licensor is not represented as endorsing the use made of the work. The full details of the license are available at http://creativecommons.org/licenses/by/4.0.
CC BY NC SA: The CC BY-NC-SA license allows users to copy, to create extracts, abstracts and new works from the Article, to alter and revise the Article, provided this is not done for commercial purposes, and that the user gives appropriate credit (with a link to the formal publication through the relevant DOI), provides a link to the license, indicates if changes were made and the licensor is not represented as endorsing the use made of the work. Further, any new works must be made available on the same conditions. The full details of the license are available at http://creativecommons.org/licenses/by-nc-sa/4.0.
CC BY NC ND: The CC BY-NC-ND license allows users to copy and distribute the Article, provided this is not done for commercial purposes and further does not permit distribution of the Article if it is changed or edited in any way, and provided the user gives appropriate credit (with a link to the formal publication through the relevant DOI), provides a link to the license, and that the licensor is not represented as endorsing the use made of the work. The full details of the license are available at http://creativecommons.org/licenses/by-nc-nd/4.0.
Any commercial reuse of Open Access articles published with a CC BY NC SA or CC BY NC ND license requires permission from Elsevier and will be subject to a fee.
Commercial reuse includes:

- Associating advertising with the full text of the Article
- Charging fees for document delivery or access
- Article aggregation
- Systematic distribution via e-mail lists or share buttons

Posting or linking by commercial companies for use by customers of those companies.

20. **Other Conditions**:

v1.9

Questions? customercare@copyright.com or +1-855-239-3415 (toll free in the US) or +1-978-646-2777.

ELSEVIER LICENSE
TERMS AND CONDITIONS

Jul 22, 2018

This Agreement between Curtin University ("You") and Elsevier ("Elsevier") consists of your license details and the terms and conditions provided by Elsevier and Copyright Clearance Center.

License Number	4394320364144
License date	Jul 22, 2018
Licensed Content Publisher	Elsevier
Licensed Content Publication	Geotextiles and Geomembranes
Licensed Content Title	Combined use of geocell reinforcement and rubber–soil mixtures to improve performance of buried pipes
Licensed Content Author	Gh. Tavakoli Mehrjardi,S.N. Moghaddas Tafreshi,A.R. Dawson
Licensed Content Date	Oct 1, 2012
Licensed Content Volume	34
Licensed Content Issue	n/a
Licensed Content Pages	15
Start Page	116
End Page	130
Type of Use	reuse in a thesis/dissertation
Intended publisher of new work	other
Portion	figures/tables/illustrations
Number of figures/tables/illustrations	2
Format	both print and electronic
Are you the author of this Elsevier article?	No
Will you be translating?	No
Original figure numbers	Figure 2 Figure 3
Title of your thesis/dissertation	Experimental and Numerical Investigations to Assess the Performance of a Buried Pipe Subjected to Traffic Load / Non-Treated and Cement-Treated Trench
Expected completion date	Aug 2018
Estimated size (number of pages)	300
Requestor Location	Curtin University 24 Everingham Street Clarkson, Western Australia 6030 Australia Attn: Curtin University
Publisher Tax ID	GB 494 6272 12
Total	0.00 AUD
Terms and Conditions	

INTRODUCTION

1. The publisher for this copyrighted material is Elsevier. By clicking "accept" in connection with completing this licensing transaction, you agree that the following terms and conditions apply to this transaction (along with the Billing and Payment terms and conditions established by Copyright Clearance Center, Inc. ("CCC"), at the time that you opened your Rightslink account and that are available at any time at http://myaccount.copyright.com).

GENERAL TERMS

2. Elsevier hereby grants you permission to reproduce the aforementioned material subject to the terms and conditions indicated.

3. Acknowledgement: If any part of the material to be used (for example, figures) has appeared in our publication with credit or acknowledgement to another source, permission must also be sought from that source. If such permission is not obtained then that material may not be included in your publication/copies. Suitable acknowledgement to the source must be made, either as a footnote or in a reference list at the end of your publication, as follows:

"Reprinted from Publication title, Vol /edition number, Author(s), Title of article / title of chapter, Pages No., Copyright (Year), with permission from Elsevier [OR APPLICABLE SOCIETY COPYRIGHT OWNER]." Also Lancet special credit - "Reprinted from The Lancet, Vol. number, Author(s), Title of article, Pages No., Copyright (Year), with permission from Elsevier."

4. Reproduction of this material is confined to the purpose and/or media for which permission is hereby given.

5. Altering/Modifying Material: Not Permitted. However figures and illustrations may be altered/adapted minimally to serve your work. Any other abbreviations, additions, deletions and/or any other alterations shall be made only with prior written authorization of Elsevier Ltd. (Please contact Elsevier at permissions@elsevier.com). No modifications can be made to any Lancet figures/tables and they must be reproduced in full.

6. If the permission fee for the requested use of our material is waived in this instance, please be advised that your future requests for Elsevier materials may attract a fee.

7. Reservation of Rights: Publisher reserves all rights not specifically granted in the combination of (i) the license details provided by you and accepted in the course of this licensing transaction, (ii) these terms and conditions and (iii) CCC's Billing and Payment terms and conditions.

8. License Contingent Upon Payment: While you may exercise the rights licensed immediately upon issuance of the license at the end of the licensing process for the transaction, provided that you have disclosed complete and accurate details of your proposed use, no license is finally effective unless and until full payment is received from you (either by publisher or by CCC) as provided in CCC's Billing and Payment terms and conditions. If full payment is not received on a timely basis, then any license preliminarily granted shall be deemed automatically revoked and shall be void as if never granted. Further, in the event that you breach any of these terms and conditions or any of CCC's Billing and Payment terms and conditions, the license is automatically revoked and shall be void as if never granted. Use of materials as described in a revoked license, as well as any use of the materials beyond the scope of an unrevoked license, may constitute copyright infringement and publisher reserves the right to take any and all action to protect its copyright in the materials.

9. Warranties: Publisher makes no representations or warranties with respect to the licensed material.

10. Indemnity: You hereby indemnify and agree to hold harmless publisher and CCC, and their respective officers, directors, employees and agents, from and against any and all claims arising out of your use of the licensed material other than as specifically authorized pursuant to this license.

11. No Transfer of License: This license is personal to you and may not be sublicensed, assigned, or transferred by you to any other person without publisher's written permission.

12. No Amendment Except in Writing: This license may not be amended except in a writing signed by both parties (or, in the case of publisher, by CCC on publisher's behalf).

13. Objection to Contrary Terms: Publisher hereby objects to any terms contained in any purchase order, acknowledgment, check endorsement or other writing prepared by you, which terms are inconsistent with these terms and conditions or CCC's Billing and Payment

terms and conditions. These terms and conditions, together with CCC's Billing and Payment terms and conditions (which are incorporated herein), comprise the entire agreement between you and publisher (and CCC) concerning this licensing transaction. In the event of any conflict between your obligations established by these terms and conditions and those established by CCC's Billing and Payment terms and conditions, these terms and conditions shall control.

14. Revocation: Elsevier or Copyright Clearance Center may deny the permissions described in this License at their sole discretion, for any reason or no reason, with a full refund payable to you. Notice of such denial will be made using the contact information provided by you. Failure to receive such notice will not alter or invalidate the denial. In no event will Elsevier or Copyright Clearance Center be responsible or liable for any costs, expenses or damage incurred by you as a result of a denial of your permission request, other than a refund of the amount(s) paid by you to Elsevier and/or Copyright Clearance Center for denied permissions.

LIMITED LICENSE

The following terms and conditions apply only to specific license types:

15. **Translation**: This permission is granted for non-exclusive world **English** rights only unless your license was granted for translation rights. If you licensed translation rights you may only translate this content into the languages you requested. A professional translator must perform all translations and reproduce the content word for word preserving the integrity of the article.

16. **Posting licensed content on any Website**: The following terms and conditions apply as follows: Licensing material from an Elsevier journal: All content posted to the web site must maintain the copyright information line on the bottom of each image; A hyper-text must be included to the Homepage of the journal from which you are licensing at http://www.sciencedirect.com/science/journal/xxxxx or the Elsevier homepage for books at http://www.elsevier.com; Central Storage: This license does not include permission for a scanned version of the material to be stored in a central repository such as that provided by Heron/XanEdu.

Licensing material from an Elsevier book: A hyper-text link must be included to the Elsevier homepage at http://www.elsevier.com . All content posted to the web site must maintain the copyright information line on the bottom of each image.

Posting licensed content on Electronic reserve: In addition to the above the following clauses are applicable: The web site must be password-protected and made available only to bona fide students registered on a relevant course. This permission is granted for 1 year only. You may obtain a new license for future website posting.

17. **For journal authors:** the following clauses are applicable in addition to the above:

Preprints:

A preprint is an author's own write-up of research results and analysis, it has not been peer-reviewed, nor has it had any other value added to it by a publisher (such as formatting, copyright, technical enhancement etc.).

Authors can share their preprints anywhere at any time. Preprints should not be added to or enhanced in any way in order to appear more like, or to substitute for, the final versions of articles however authors can update their preprints on arXiv or RePEc with their Accepted Author Manuscript (see below).

If accepted for publication, we encourage authors to link from the preprint to their formal publication via its DOI. Millions of researchers have access to the formal publications on ScienceDirect, and so links will help users to find, access, cite and use the best available version. Please note that Cell Press, The Lancet and some society-owned have different preprint policies. Information on these policies is available on the journal homepage.

Accepted Author Manuscripts: An accepted author manuscript is the manuscript of an article that has been accepted for publication and which typically includes author-incorporated changes suggested during submission, peer review and editor-author communications.

Authors can share their accepted author manuscript:

- immediately

- via their non-commercial person homepage or blog
- by updating a preprint in arXiv or RePEc with the accepted manuscript
- via their research institute or institutional repository for internal institutional uses or as part of an invitation-only research collaboration work-group
- directly by providing copies to their students or to research collaborators for their personal use
- for private scholarly sharing as part of an invitation-only work group on commercial sites with which Elsevier has an agreement

- After the embargo period
  - via non-commercial hosting platforms such as their institutional repository
  - via commercial sites with which Elsevier has an agreement

In all cases accepted manuscripts should:

- link to the formal publication via its DOI
- bear a CC-BY-NC-ND license - this is easy to do
- if aggregated with other manuscripts, for example in a repository or other site, be shared in alignment with our hosting policy not be added to or enhanced in any way to appear more like, or to substitute for, the published journal article.

Published journal article (JPA): A published journal article (PJA) is the definitive final record of published research that appears or will appear in the journal and embodies all value-adding publishing activities including peer review co-ordination, copy-editing, formatting, (if relevant) pagination and online enrichment.
Policies for sharing publishing journal articles differ for subscription and gold open access articles:
Subscription Articles: If you are an author, please share a link to your article rather than the full-text. Millions of researchers have access to the formal publications on ScienceDirect, and so links will help your users to find, access, cite, and use the best available version.
Theses and dissertations which contain embedded PJAs as part of the formal submission can be posted publicly by the awarding institution with DOI links back to the formal publications on ScienceDirect.
If you are affiliated with a library that subscribes to ScienceDirect you have additional private sharing rights for others' research accessed under that agreement. This includes use for classroom teaching and internal training at the institution (including use in course packs and courseware programs), and inclusion of the article for grant funding purposes.
Gold Open Access Articles: May be shared according to the author-selected end-user license and should contain a CrossMark logo, the end user license, and a DOI link to the formal publication on ScienceDirect.
Please refer to Elsevier's posting policy for further information.
18. **For book authors** the following clauses are applicable in addition to the above: Authors are permitted to place a brief summary of their work online only. You are not allowed to download and post the published electronic version of your chapter, nor may you scan the printed edition to create an electronic version. **Posting to a repository:** Authors are permitted to post a summary of their chapter only in their institution's repository.
19. **Thesis/Dissertation**: If your license is for use in a thesis/dissertation your thesis may be submitted to your institution in either print or electronic form. Should your thesis be published commercially, please reapply for permission. These requirements include permission for the Library and Archives of Canada to supply single copies, on demand, of the complete thesis and include permission for Proquest/UMI to supply single copies, on demand, of the complete thesis. Should your thesis be published commercially, please reapply for permission. Theses and dissertations which contain embedded PJAs as part of the formal submission can be posted publicly by the awarding institution with DOI links back to the formal publications on ScienceDirect.

Elsevier Open Access Terms and Conditions
You can publish open access with Elsevier in hundreds of open access journals or in nearly 2000 established subscription journals that support open access publishing. Permitted third

party re-use of these open access articles is defined by the author's choice of Creative Commons user license. See our open access license policy for more information.

Terms & Conditions applicable to all Open Access articles published with Elsevier:

Any reuse of the article must not represent the author as endorsing the adaptation of the article nor should the article be modified in such a way as to damage the author's honour or reputation. If any changes have been made, such changes must be clearly indicated.

The author(s) must be appropriately credited and we ask that you include the end user license and a DOI link to the formal publication on ScienceDirect.

If any part of the material to be used (for example, figures) has appeared in our publication with credit or acknowledgement to another source it is the responsibility of the user to ensure their reuse complies with the terms and conditions determined by the rights holder.

Additional Terms & Conditions applicable to each Creative Commons user license:

CC BY: The CC-BY license allows users to copy, to create extracts, abstracts and new works from the Article, to alter and revise the Article and to make commercial use of the Article (including reuse and/or resale of the Article by commercial entities), provided the user gives appropriate credit (with a link to the formal publication through the relevant DOI), provides a link to the license, indicates if changes were made and the licensor is not represented as endorsing the use made of the work. The full details of the license are available at http://creativecommons.org/licenses/by/4.0.

CC BY NC SA: The CC BY-NC-SA license allows users to copy, to create extracts, abstracts and new works from the Article, to alter and revise the Article, provided this is not done for commercial purposes, and that the user gives appropriate credit (with a link to the formal publication through the relevant DOI), provides a link to the license, indicates if changes were made and the licensor is not represented as endorsing the use made of the work. Further, any new works must be made available on the same conditions. The full details of the license are available at http://creativecommons.org/licenses/by-nc-sa/4.0.

CC BY NC ND: The CC BY-NC-ND license allows users to copy and distribute the Article, provided this is not done for commercial purposes and further does not permit distribution of the Article if it is changed or edited in any way, and provided the user gives appropriate credit (with a link to the formal publication through the relevant DOI), provides a link to the license, and that the licensor is not represented as endorsing the use made of the work. The full details of the license are available at http://creativecommons.org/licenses/by-nc-nd/4.0.

Any commercial reuse of Open Access articles published with a CC BY NC SA or CC BY NC ND license requires permission from Elsevier and will be subject to a fee.

Commercial reuse includes:

- Associating advertising with the full text of the Article
- Charging fees for document delivery or access
- Article aggregation
- Systematic distribution via e-mail lists or share buttons

Posting or linking by commercial companies for use by customers of those companies.

20. **Other Conditions**:

v1.9

Questions? customercare@copyright.com or +1-855-239-3415 (toll free in the US) or +1-978-646-2777.

ELSEVIER LICENSE
TERMS AND CONDITIONS

Jul 22, 2018

This Agreement between Curtin University ("You") and Elsevier ("Elsevier") consists of your license details and the terms and conditions provided by Elsevier and Copyright Clearance Center.

License Number	4394101142887
License date	Jul 22, 2018
Licensed Content Publisher	Elsevier
Licensed Content Publication	Geotextiles and Geomembranes
Licensed Content Title	Laboratory tests of small-diameter HDPE pipes buried in reinforced sand under repeated-load
Licensed Content Author	S.N. Moghaddas Tafreshi,O. Khalaj
Licensed Content Date	Apr 1, 2008
Licensed Content Volume	26
Licensed Content Issue	2
Licensed Content Pages	19
Start Page	145
End Page	163
Type of Use	reuse in a thesis/dissertation
Portion	figures/tables/illustrations
Number of figures/tables/illustrations	2
Format	both print and electronic
Are you the author of this Elsevier article?	No
Will you be translating?	No
Original figure numbers	Figure 3 Figure 14
Title of your thesis/dissertation	Experimental and Numerical Investigations to Assess the Performance of a Buried Pipe Subjected to Traffic Load / Non-Treated and Cement-Treated Trench
Expected completion date	Aug 2018
Estimated size (number of pages)	300
Requestor Location	Curtin University 24 Everingham Street Clarkson, Western Australia 6030 Australia Attn: Curtin University
Publisher Tax ID	GB 494 6272 12
Total	0.00 AUD
Terms and Conditions	

INTRODUCTION

1. The publisher for this copyrighted material is Elsevier. By clicking "accept" in connection with completing this licensing transaction, you agree that the following terms and conditions

apply to this transaction (along with the Billing and Payment terms and conditions established by Copyright Clearance Center, Inc. ("CCC"), at the time that you opened your Rightslink account and that are available at any time at http://myaccount.copyright.com).

GENERAL TERMS

2. Elsevier hereby grants you permission to reproduce the aforementioned material subject to the terms and conditions indicated.

3. Acknowledgement: If any part of the material to be used (for example, figures) has appeared in our publication with credit or acknowledgement to another source, permission must also be sought from that source. If such permission is not obtained then that material may not be included in your publication/copies. Suitable acknowledgement to the source must be made, either as a footnote or in a reference list at the end of your publication, as follows:

"Reprinted from Publication title, Vol /edition number, Author(s), Title of article / title of chapter, Pages No., Copyright (Year), with permission from Elsevier [OR APPLICABLE SOCIETY COPYRIGHT OWNER]." Also Lancet special credit - "Reprinted from The Lancet, Vol. number, Author(s), Title of article, Pages No., Copyright (Year), with permission from Elsevier."

4. Reproduction of this material is confined to the purpose and/or media for which permission is hereby given.

5. Altering/Modifying Material: Not Permitted. However figures and illustrations may be altered/adapted minimally to serve your work. Any other abbreviations, additions, deletions and/or any other alterations shall be made only with prior written authorization of Elsevier Ltd. (Please contact Elsevier at permissions@elsevier.com). No modifications can be made to any Lancet figures/tables and they must be reproduced in full.

6. If the permission fee for the requested use of our material is waived in this instance, please be advised that your future requests for Elsevier materials may attract a fee.

7. Reservation of Rights: Publisher reserves all rights not specifically granted in the combination of (i) the license details provided by you and accepted in the course of this licensing transaction, (ii) these terms and conditions and (iii) CCC's Billing and Payment terms and conditions.

8. License Contingent Upon Payment: While you may exercise the rights licensed immediately upon issuance of the license at the end of the licensing process for the transaction, provided that you have disclosed complete and accurate details of your proposed use, no license is finally effective unless and until full payment is received from you (either by publisher or by CCC) as provided in CCC's Billing and Payment terms and conditions. If full payment is not received on a timely basis, then any license preliminarily granted shall be deemed automatically revoked and shall be void as if never granted. Further, in the event that you breach any of these terms and conditions or any of CCC's Billing and Payment terms and conditions, the license is automatically revoked and shall be void as if never granted. Use of materials as described in a revoked license, as well as any use of the materials beyond the scope of an unrevoked license, may constitute copyright infringement and publisher reserves the right to take any and all action to protect its copyright in the materials.

9. Warranties: Publisher makes no representations or warranties with respect to the licensed material.

10. Indemnity: You hereby indemnify and agree to hold harmless publisher and CCC, and their respective officers, directors, employees and agents, from and against any and all claims arising out of your use of the licensed material other than as specifically authorized pursuant to this license.

11. No Transfer of License: This license is personal to you and may not be sublicensed, assigned, or transferred by you to any other person without publisher's written permission.

12. No Amendment Except in Writing: This license may not be amended except in a writing signed by both parties (or, in the case of publisher, by CCC on publisher's behalf).

13. Objection to Contrary Terms: Publisher hereby objects to any terms contained in any purchase order, acknowledgment, check endorsement or other writing prepared by you, which terms are inconsistent with these terms and conditions or CCC's Billing and Payment terms and conditions. These terms and conditions, together with CCC's Billing and Payment terms and conditions (which are incorporated herein), comprise the entire agreement

between you and publisher (and CCC) concerning this licensing transaction. In the event of any conflict between your obligations established by these terms and conditions and those established by CCC's Billing and Payment terms and conditions, these terms and conditions shall control.

14. Revocation: Elsevier or Copyright Clearance Center may deny the permissions described in this License at their sole discretion, for any reason or no reason, with a full refund payable to you. Notice of such denial will be made using the contact information provided by you. Failure to receive such notice will not alter or invalidate the denial. In no event will Elsevier or Copyright Clearance Center be responsible or liable for any costs, expenses or damage incurred by you as a result of a denial of your permission request, other than a refund of the amount(s) paid by you to Elsevier and/or Copyright Clearance Center for denied permissions.

LIMITED LICENSE

The following terms and conditions apply only to specific license types:

15. **Translation**: This permission is granted for non-exclusive world **English** rights only unless your license was granted for translation rights. If you licensed translation rights you may only translate this content into the languages you requested. A professional translator must perform all translations and reproduce the content word for word preserving the integrity of the article.

16. **Posting licensed content on any Website**: The following terms and conditions apply as follows: Licensing material from an Elsevier journal: All content posted to the web site must maintain the copyright information line on the bottom of each image; A hyper-text must be included to the Homepage of the journal from which you are licensing at http://www.sciencedirect.com/science/journal/xxxxx or the Elsevier homepage for books at http://www.elsevier.com; Central Storage: This license does not include permission for a scanned version of the material to be stored in a central repository such as that provided by Heron/XanEdu.

Licensing material from an Elsevier book: A hyper-text link must be included to the Elsevier homepage at http://www.elsevier.com . All content posted to the web site must maintain the copyright information line on the bottom of each image.

Posting licensed content on Electronic reserve: In addition to the above the following clauses are applicable: The web site must be password-protected and made available only to bona fide students registered on a relevant course. This permission is granted for 1 year only. You may obtain a new license for future website posting.

17. **For journal authors:** the following clauses are applicable in addition to the above:

Preprints:

A preprint is an author's own write-up of research results and analysis, it has not been peer-reviewed, nor has it had any other value added to it by a publisher (such as formatting, copyright, technical enhancement etc.).

Authors can share their preprints anywhere at any time. Preprints should not be added to or enhanced in any way in order to appear more like, or to substitute for, the final versions of articles however authors can update their preprints on arXiv or RePEc with their Accepted Author Manuscript (see below).

If accepted for publication, we encourage authors to link from the preprint to their formal publication via its DOI. Millions of researchers have access to the formal publications on ScienceDirect, and so links will help users to find, access, cite and use the best available version. Please note that Cell Press, The Lancet and some society-owned have different preprint policies. Information on these policies is available on the journal homepage.

Accepted Author Manuscripts: An accepted author manuscript is the manuscript of an article that has been accepted for publication and which typically includes author-incorporated changes suggested during submission, peer review and editor-author communications.

Authors can share their accepted author manuscript:

- immediately
  - via their non-commercial person homepage or blog
  - by updating a preprint in arXiv or RePEc with the accepted manuscript

- via their research institute or institutional repository for internal institutional uses or as part of an invitation-only research collaboration work-group
- directly by providing copies to their students or to research collaborators for their personal use
- for private scholarly sharing as part of an invitation-only work group on commercial sites with which Elsevier has an agreement

- After the embargo period
  - via non-commercial hosting platforms such as their institutional repository
  - via commercial sites with which Elsevier has an agreement

In all cases accepted manuscripts should:

- link to the formal publication via its DOI
- bear a CC-BY-NC-ND license - this is easy to do
- if aggregated with other manuscripts, for example in a repository or other site, be shared in alignment with our hosting policy not be added to or enhanced in any way to appear more like, or to substitute for, the published journal article.

Published journal article (JPA): A published journal article (PJA) is the definitive final record of published research that appears or will appear in the journal and embodies all value-adding publishing activities including peer review co-ordination, copy-editing, formatting, (if relevant) pagination and online enrichment.
Policies for sharing publishing journal articles differ for subscription and gold open access articles:
Subscription Articles: If you are an author, please share a link to your article rather than the full-text. Millions of researchers have access to the formal publications on ScienceDirect, and so links will help your users to find, access, cite, and use the best available version.
Theses and dissertations which contain embedded PJAs as part of the formal submission can be posted publicly by the awarding institution with DOI links back to the formal publications on ScienceDirect.
If you are affiliated with a library that subscribes to ScienceDirect you have additional private sharing rights for others' research accessed under that agreement. This includes use for classroom teaching and internal training at the institution (including use in course packs and courseware programs), and inclusion of the article for grant funding purposes.
Gold Open Access Articles: May be shared according to the author-selected end-user license and should contain a CrossMark logo, the end user license, and a DOI link to the formal publication on ScienceDirect.
Please refer to Elsevier's posting policy for further information.
18. **For book authors** the following clauses are applicable in addition to the above:
Authors are permitted to place a brief summary of their work online only. You are not allowed to download and post the published electronic version of your chapter, nor may you scan the printed edition to create an electronic version. **Posting to a repository:** Authors are permitted to post a summary of their chapter only in their institution's repository.
19. **Thesis/Dissertation**: If your license is for use in a thesis/dissertation your thesis may be submitted to your institution in either print or electronic form. Should your thesis be published commercially, please reapply for permission. These requirements include permission for the Library and Archives of Canada to supply single copies, on demand, of the complete thesis and include permission for Proquest/UMI to supply single copies, on demand, of the complete thesis. Should your thesis be published commercially, please reapply for permission. Theses and dissertations which contain embedded PJAs as part of the formal submission can be posted publicly by the awarding institution with DOI links back to the formal publications on ScienceDirect.

Elsevier Open Access Terms and Conditions
You can publish open access with Elsevier in hundreds of open access journals or in nearly 2000 established subscription journals that support open access publishing. Permitted third party re-use of these open access articles is defined by the author's choice of Creative Commons user license. See our open access license policy for more information.

Terms & Conditions applicable to all Open Access articles published with Elsevier:
Any reuse of the article must not represent the author as endorsing the adaptation of the article nor should the article be modified in such a way as to damage the author's honour or reputation. If any changes have been made, such changes must be clearly indicated.
The author(s) must be appropriately credited and we ask that you include the end user license and a DOI link to the formal publication on ScienceDirect.
If any part of the material to be used (for example, figures) has appeared in our publication with credit or acknowledgement to another source it is the responsibility of the user to ensure their reuse complies with the terms and conditions determined by the rights holder.
Additional Terms & Conditions applicable to each Creative Commons user license:
CC BY: The CC-BY license allows users to copy, to create extracts, abstracts and new works from the Article, to alter and revise the Article and to make commercial use of the Article (including reuse and/or resale of the Article by commercial entities), provided the user gives appropriate credit (with a link to the formal publication through the relevant DOI), provides a link to the license, indicates if changes were made and the licensor is not represented as endorsing the use made of the work. The full details of the license are available at http://creativecommons.org/licenses/by/4.0.
CC BY NC SA: The CC BY-NC-SA license allows users to copy, to create extracts, abstracts and new works from the Article, to alter and revise the Article, provided this is not done for commercial purposes, and that the user gives appropriate credit (with a link to the formal publication through the relevant DOI), provides a link to the license, indicates if changes were made and the licensor is not represented as endorsing the use made of the work. Further, any new works must be made available on the same conditions. The full details of the license are available at http://creativecommons.org/licenses/by-nc-sa/4.0.
CC BY NC ND: The CC BY-NC-ND license allows users to copy and distribute the Article, provided this is not done for commercial purposes and further does not permit distribution of the Article if it is changed or edited in any way, and provided the user gives appropriate credit (with a link to the formal publication through the relevant DOI), provides a link to the license, and that the licensor is not represented as endorsing the use made of the work. The full details of the license are available at http://creativecommons.org/licenses/by-nc-nd/4.0.
Any commercial reuse of Open Access articles published with a CC BY NC SA or CC BY NC ND license requires permission from Elsevier and will be subject to a fee.
Commercial reuse includes:

- Associating advertising with the full text of the Article
- Charging fees for document delivery or access
- Article aggregation
- Systematic distribution via e-mail lists or share buttons

Posting or linking by commercial companies for use by customers of those companies.

20. **Other Conditions**:

v1.9

Questions? customercare@copyright.com or +1-855-239-3415 (toll free in the US) or +1-978-646-2777.

Copyright Clearance Center

Note: Copyright.com supplies permissions but not the copyrighted content itself.

1 PAYMENT 2 REVIEW 3 CONFIRMATION

Step 3: Order Confirmation

Thank you for your order! A confirmation for your order will be sent to your account email address. If you have questions about your order, you can call us 24 hrs/day, M-F at +1.855.239.3415 Toll Free, or write to us at info@copyright.com. This is not an invoice.

Confirmation Number: 11732496
Order Date: 07/22/2018

If you paid by credit card, your order will be finalized and your card will be charged within 24 hours. If you choose to be invoiced, you can change or cancel your order until the invoice is generated.

Payment Information

Ahdyeh Mosadegh
ahdyeh.mosadegh@postgrad.curtin.edu.au
+61 (4)52502080
Payment Method: invoice

Billing address:

24 Everingham Street
Clarkson, Western Australia 6030
AU

Order Details

Special Orders

Journal of transportation engineering

Order detail ID:	71325433
Job Ticket:	501415681
ISSN:	0733-947X
Publication Type:	Journal
Volume:	
Issue:	
Start page:	
Publisher:	AMERICAN SOCIETY OF CIVIL ENGINEERS
Author/Editor:	AMERICAN SOCIETY OF CIVIL ENGINEERS

Permission Status: **Special Order**
Special Order Update: Checking availability

Permission type:
Republish or display content

Type of use:
Thesis/Dissertation

Requestor type	Academic institution
Format	Print, Electronic
Portion	image/photo
Number of images/photos requested	1
The requesting person/organization	Curtin University
Title or numeric reference of the portion(s)	Experimental and Numerical Investigations to Assess the Performance of a Buried Pipe Subjected to Traffic Load / Non-Treated and Cement-Treated Trench
Title of the article or chapter the portion is from	N/N

Editor of portion(s)	N/A
Author of portion(s)	N/A
Volume of serial or monograph	N/A
Issue, if republishing an article from a serial	N/A
Page range of portion	300
Publication date of portion	August 2018
Rights for	Main product
Duration of use	Life of current edition
Creation of copies for the disabled	no
With minor editing privileges	no
For distribution to	Worldwide
In the following language(s)	Original language of publication
With incidental promotional use	no
Lifetime unit quantity of new product	Up to 499
Title	Experimental and Numerical Investigations to Assess the Performance of a Buried Pipe Subjected to Traffic Load / Non-Treated and Cement-Treated Trench
Instructor name	n/a
Institution name	n/a
Expected presentation date	Aug 2018

Note: This item will be managed through CCC's **RightsLink service.**More info **TBD**

This is not an invoice.

Total order items: 1

Order Total: TBD

Confirmation Number: 11732496

Special Rightsholder Terms & Conditions

The following terms & conditions apply to the specific publication under which they are listed

Journal of transportation engineering
Permission type: Republish or display content
Type of use: Thesis/Dissertation

TERMS AND CONDITIONS

The following terms are individual to this publisher:

Per Page limit should be set at 1-12 pages.

Per Image/Photo/Illustration limit should be set at 1-8 images, photos, etc.

Per Chart/Graph/Table/Figure limit should be set at 1-8 charts, graphs, etc.

Per Cartoon limit should be set at 1-8 cartoons.

Other Terms and Conditions:

STANDARD TERMS AND CONDITIONS

1. Description of Service; Defined Terms. This Republication License enables the User to obtain licenses for republication of one or more copyrighted works as described in detail on the relevant Order Confirmation (the "Work(s)"). Copyright Clearance Center, Inc. ("CCC") grants licenses through the Service on behalf of the rightsholder identified on the Order Confirmation (the "Rightsholder"). "Republication", as used herein, generally means the inclusion of a Work, in whole or in part, in a new work or works, also as described on the Order Confirmation. "User", as used herein, means the person or entity making such republication.

2. The terms set forth in the relevant Order Confirmation, and any terms set by the Rightsholder with respect to a particular Work, govern the terms of use of Works in connection with the Service. By using the Service, the person transacting for a republication license on behalf of the User represents and warrants that he/she/it (a) has been duly authorized by the User to accept, and hereby does accept, all such terms and conditions on behalf of User, and (b) shall inform User of all such terms and conditions. In the event such person is a "freelancer" or other third party independent of User and CCC, such party shall be deemed jointly a "User" for purposes of these terms and conditions. In any event, User shall be deemed to have accepted and agreed to all such terms and conditions if User republishes the Work in any fashion.

3. Scope of License; Limitations and Obligations.

3.1 All Works and all rights therein, including copyright rights, remain the sole and exclusive property of the Rightsholder. The license created by the exchange of an Order Confirmation (and/or any invoice) and payment by User of the full amount set forth on that document includes only those rights expressly set forth in the Order Confirmation and in these terms and conditions, and conveys no other rights in the Work(s) to User. All rights not expressly granted are hereby reserved.

3.2 General Payment Terms: You may pay by credit card or through an account with us payable at the end of the month. If you and we agree that you may establish a standing account with CCC, then the following terms apply: Remit Payment to: Copyright Clearance Center, 29118 Network Place, Chicago, IL 60673-1291. Payments Due: Invoices are payable upon their delivery to you (or upon our notice to you that they are available to you for downloading). After 30 days, outstanding amounts will be subject to a service charge of 1-1/2% per month or, if less, the maximum rate allowed by applicable law. Unless otherwise specifically set forth in the Order Confirmation or in a separate written agreement signed by CCC, invoices are due and payable on "net 30" terms. While User may exercise the rights licensed immediately upon issuance of the Order Confirmation, the license is automatically revoked and is null and void, as if it had never been issued, if complete payment for the license is not received on a timely basis either from User directly or through a payment agent, such as a credit card company.

3.3 Unless otherwise provided in the Order Confirmation, any grant of rights to User (i) is "one-time" (including the editions and product family specified in the license), (ii) is non-exclusive and non-transferable and (iii) is subject to any and all limitations and restrictions (such as, but not limited to, limitations on duration of use or circulation) included in the Order Confirmation or invoice and/or in these terms and conditions. Upon completion of the licensed use, User shall either secure a new permission for further use of the Work(s) or immediately cease any new use of the Work(s) and shall render inaccessible (such as by deleting or by removing or severing links or other locators) any further copies of the Work (except for copies printed on paper in accordance with this license and still in User's stock at the end of such period).

3.4 In the event that the material for which a republication license is sought includes third party materials (such as photographs, illustrations, graphs, inserts and similar materials) which are identified in such material as having been used by permission, User is responsible for identifying, and seeking separate licenses (under this Service or otherwise) for, any of such third party materials; without a separate license, such third party materials may not be used.

3.5 Use of proper copyright notice for a Work is required as a condition of any license granted under the Service. Unless otherwise provided in the Order Confirmation, a proper copyright notice will read substantially as follows: "Republished with permission of [Rightsholder's name], from [Work's title, author, volume, edition number and year of copyright]; permission conveyed through Copyright Clearance Center, Inc. " Such notice must be provided in a reasonably legible font size and must be placed either immediately adjacent to the Work as used (for example, as part of a by-line or footnote but not as a separate electronic link) or in the place where substantially all other credits or notices for the new work containing the republished Work are located. Failure to include the required notice results in loss to the Rightsholder and

CCC, and the User shall be liable to pay liquidated damages for each such failure equal to twice the use fee specified in the Order Confirmation, in addition to the use fee itself and any other fees and charges specified.

3.6 User may only make alterations to the Work if and as expressly set forth in the Order Confirmation. No Work may be used in any way that is defamatory, violates the rights of third parties (including such third parties' rights of copyright, privacy, publicity, or other tangible or intangible property), or is otherwise illegal, sexually explicit or obscene. In addition, User may not conjoin a Work with any other material that may result in damage to the reputation of the Rightsholder. User agrees to inform CCC if it becomes aware of any infringement of any rights in a Work and to cooperate with any reasonable request of CCC or the Rightsholder in connection therewith.

4. Indemnity. User hereby indemnifies and agrees to defend the Rightsholder and CCC, and their respective employees and directors, against all claims, liability, damages, costs and expenses, including legal fees and expenses, arising out of any use of a Work beyond the scope of the rights granted herein, or any use of a Work which has been altered in any unauthorized way by User, including claims of defamation or infringement of rights of copyright, publicity, privacy or other tangible or intangible property.

5. Limitation of Liability. UNDER NO CIRCUMSTANCES WILL CCC OR THE RIGHTSHOLDER BE LIABLE FOR ANY DIRECT, INDIRECT, CONSEQUENTIAL OR INCIDENTAL DAMAGES (INCLUDING WITHOUT LIMITATION DAMAGES FOR LOSS OF BUSINESS PROFITS OR INFORMATION, OR FOR BUSINESS INTERRUPTION) ARISING OUT OF THE USE OR INABILITY TO USE A WORK, EVEN IF ONE OF THEM HAS BEEN ADVISED OF THE POSSIBILITY OF SUCH DAMAGES. In any event, the total liability of the Rightsholder and CCC (including their respective employees and directors) shall not exceed the total amount actually paid by User for this license. User assumes full liability for the actions and omissions of its principals, employees, agents, affiliates, successors and assigns.

6. Limited Warranties. THE WORK(S) AND RIGHT(S) ARE PROVIDED "AS IS". CCC HAS THE RIGHT TO GRANT TO USER THE RIGHTS GRANTED IN THE ORDER CONFIRMATION DOCUMENT. CCC AND THE RIGHTSHOLDER DISCLAIM ALL OTHER WARRANTIES RELATING TO THE WORK(S) AND RIGHT(S), EITHER EXPRESS OR IMPLIED, INCLUDING WITHOUT LIMITATION IMPLIED WARRANTIES OF MERCHANTABILITY OR FITNESS FOR A PARTICULAR PURPOSE. ADDITIONAL RIGHTS MAY BE REQUIRED TO USE ILLUSTRATIONS, GRAPHS, PHOTOGRAPHS, ABSTRACTS, INSERTS OR OTHER PORTIONS OF THE WORK (AS OPPOSED TO THE ENTIRE WORK) IN A MANNER CONTEMPLATED BY USER; USER UNDERSTANDS AND AGREES THAT NEITHER CCC NOR THE RIGHTSHOLDER MAY HAVE SUCH ADDITIONAL RIGHTS TO GRANT.

7. Effect of Breach. Any failure by User to pay any amount when due, or any use by User of a Work beyond the scope of the license set forth in the Order Confirmation and/or these terms and conditions, shall be a material breach of the license created by the Order Confirmation and these terms and conditions. Any breach not cured within 30 days of written notice thereof shall result in immediate termination of such license without further notice. Any unauthorized (but licensable) use of a Work that is terminated immediately upon notice thereof may be liquidated by payment of the Rightsholder's ordinary license price therefor; any unauthorized (and unlicensable) use that is not terminated immediately for any reason (including, for example, because materials containing the Work cannot reasonably be recalled) will be subject to all remedies available at law or in equity, but in no event to a payment of less than three times the Rightsholder's ordinary license price for the most closely analogous licensable use plus Rightsholder's and/or CCC's costs and expenses incurred in collecting such payment.

8. **Miscellaneous.**

8.1 User acknowledges that CCC may, from time to time, make changes or additions to the Service or to these terms and conditions, and CCC reserves the right to send notice to the User by electronic mail or otherwise for the purposes of notifying User of such changes or additions; provided that any such changes or additions shall not apply to permissions already secured and paid for.

8.2 Use of User-related information collected through the Service is governed by CCC's privacy policy, available online here: http://www.copyright.com/content/cc3/en/tools/footer/privacypolicy.html.

8.3 The licensing transaction described in the Order Confirmation is personal to User. Therefore, User may not assign or transfer to any other person (whether a natural person or an organization of any kind) the license created by the Order Confirmation and these terms and conditions or any rights granted hereunder; provided, however, that User may assign such license in its entirety on written notice to CCC in the event of a transfer of all or substantially all of User's rights in the new material which includes the Work(s) licensed under this Service.

8.4 No amendment or waiver of any terms is binding unless set forth in writing and signed by the parties. The Rightsholder and CCC hereby object to any terms contained in any writing prepared by the User or its principals, employees, agents or affiliates and purporting to govern or otherwise relate to the licensing transaction described in the Order Confirmation, which terms are in any way inconsistent with any terms set forth in the Order Confirmation and/or in these terms and conditions or CCC's standard operating procedures, whether such writing is prepared prior to, simultaneously with or subsequent to the Order Confirmation, and whether such writing appears on a copy of the Order Confirmation or in a separate instrument.

8.5 The licensing transaction described in the Order Confirmation document shall be governed by and construed under the law of the State of New York, USA, without regard to the principles thereof of conflicts of law. Any case, controversy, suit, action, or proceeding arising out of, in connection with, or related to such licensing transaction shall be brought, at CCC's sole discretion, in any federal or state court located in the County of New York, State of New York, USA, or in any federal or state court whose geographical jurisdiction covers the location of the Rightsholder set forth in the Order Confirmation. The parties expressly submit to the personal jurisdiction and venue of each such federal or state court.If you have any comments or questions about the Service or Copyright Clearance Center, please contact us at 978-750-8400 or send an e-mail to info@copyright.com.

v 1.1

Close

Confirmation Number: 11732496

Citation Information

Order Detail ID: 71325433

Journal of transportation engineering by AMERICAN SOCIETY OF CIVIL ENGINEERS Reproduced with permission of AMERICAN SOCIETY OF CIVIL ENGINEERS in the format Thesis/Dissertation via Copyright Clearance Center.

Close

ELSEVIER LICENSE
TERMS AND CONDITIONS

Jul 22, 2018

This Agreement between Curtin University ("You") and Elsevier ("Elsevier") consists of your license details and the terms and conditions provided by Elsevier and Copyright Clearance Center.

License Number	4394301406454
License date	Jul 22, 2018
Licensed Content Publisher	Elsevier
Licensed Content Publication	Construction and Building Materials
Licensed Content Title	Thin-walled thermoplastic pipes
Licensed Content Author	J.J. Järvenkylä
Licensed Content Date	Dec 1, 1989
Licensed Content Volume	3
Licensed Content Issue	4
Licensed Content Pages	10
Start Page	191
End Page	200
Type of Use	reuse in a thesis/dissertation
Intended publisher of new work	other
Portion	figures/tables/illustrations
Number of figures/tables/illustrations	1
Format	both print and electronic
Are you the author of this Elsevier article?	No
Will you be translating?	No
Original figure numbers	Figure 7
Title of your thesis/dissertation	Experimental and Numerical Investigations to Assess the Performance of a Buried Pipe Subjected to Traffic Load / Non-Treated and Cement-Treated Trench
Expected completion date	Aug 2018
Estimated size (number of pages)	300
Requestor Location	Curtin University 24 Everingham Street Clarkson, Western Australia 6030 Australia Attn: Curtin University
Publisher Tax ID	GB 494 6272 12
Total	0.00 AUD
Terms and Conditions	

INTRODUCTION

1. The publisher for this copyrighted material is Elsevier. By clicking "accept" in connection with completing this licensing transaction, you agree that the following terms and conditions apply to this transaction (along with the Billing and Payment terms and conditions established by Copyright Clearance Center, Inc. ("CCC"), at the time that you opened your Rightslink account and that are available at any time at http://myaccount.copyright.com).

GENERAL TERMS

2. Elsevier hereby grants you permission to reproduce the aforementioned material subject to the terms and conditions indicated.

3. Acknowledgement: If any part of the material to be used (for example, figures) has appeared in our publication with credit or acknowledgement to another source, permission must also be sought from that source. If such permission is not obtained then that material may not be included in your publication/copies. Suitable acknowledgement to the source must be made, either as a footnote or in a reference list at the end of your publication, as follows:

"Reprinted from Publication title, Vol /edition number, Author(s), Title of article / title of chapter, Pages No., Copyright (Year), with permission from Elsevier [OR APPLICABLE SOCIETY COPYRIGHT OWNER]." Also Lancet special credit - "Reprinted from The Lancet, Vol. number, Author(s), Title of article, Pages No., Copyright (Year), with permission from Elsevier."

4. Reproduction of this material is confined to the purpose and/or media for which permission is hereby given.

5. Altering/Modifying Material: Not Permitted. However figures and illustrations may be altered/adapted minimally to serve your work. Any other abbreviations, additions, deletions and/or any other alterations shall be made only with prior written authorization of Elsevier Ltd. (Please contact Elsevier at permissions@elsevier.com). No modifications can be made to any Lancet figures/tables and they must be reproduced in full.

6. If the permission fee for the requested use of our material is waived in this instance, please be advised that your future requests for Elsevier materials may attract a fee.

7. Reservation of Rights: Publisher reserves all rights not specifically granted in the combination of (i) the license details provided by you and accepted in the course of this licensing transaction, (ii) these terms and conditions and (iii) CCC's Billing and Payment terms and conditions.

8. License Contingent Upon Payment: While you may exercise the rights licensed immediately upon issuance of the license at the end of the licensing process for the transaction, provided that you have disclosed complete and accurate details of your proposed use, no license is finally effective unless and until full payment is received from you (either by publisher or by CCC) as provided in CCC's Billing and Payment terms and conditions. If full payment is not received on a timely basis, then any license preliminarily granted shall be deemed automatically revoked and shall be void as if never granted. Further, in the event that you breach any of these terms and conditions or any of CCC's Billing and Payment terms and conditions, the license is automatically revoked and shall be void as if never granted. Use of materials as described in a revoked license, as well as any use of the materials beyond the scope of an unrevoked license, may constitute copyright infringement and publisher reserves the right to take any and all action to protect its copyright in the materials.

9. Warranties: Publisher makes no representations or warranties with respect to the licensed material.

10. Indemnity: You hereby indemnify and agree to hold harmless publisher and CCC, and their respective officers, directors, employees and agents, from and against any and all claims arising out of your use of the licensed material other than as specifically authorized pursuant to this license.

11. No Transfer of License: This license is personal to you and may not be sublicensed, assigned, or transferred by you to any other person without publisher's written permission.

12. No Amendment Except in Writing: This license may not be amended except in a writing signed by both parties (or, in the case of publisher, by CCC on publisher's behalf).

13. Objection to Contrary Terms: Publisher hereby objects to any terms contained in any purchase order, acknowledgment, check endorsement or other writing prepared by you, which terms are inconsistent with these terms and conditions or CCC's Billing and Payment

terms and conditions. These terms and conditions, together with CCC's Billing and Payment terms and conditions (which are incorporated herein), comprise the entire agreement between you and publisher (and CCC) concerning this licensing transaction. In the event of any conflict between your obligations established by these terms and conditions and those established by CCC's Billing and Payment terms and conditions, these terms and conditions shall control.

14. Revocation: Elsevier or Copyright Clearance Center may deny the permissions described in this License at their sole discretion, for any reason or no reason, with a full refund payable to you. Notice of such denial will be made using the contact information provided by you. Failure to receive such notice will not alter or invalidate the denial. In no event will Elsevier or Copyright Clearance Center be responsible or liable for any costs, expenses or damage incurred by you as a result of a denial of your permission request, other than a refund of the amount(s) paid by you to Elsevier and/or Copyright Clearance Center for denied permissions.

LIMITED LICENSE

The following terms and conditions apply only to specific license types:

15. **Translation**: This permission is granted for non-exclusive world **English** rights only unless your license was granted for translation rights. If you licensed translation rights you may only translate this content into the languages you requested. A professional translator must perform all translations and reproduce the content word for word preserving the integrity of the article.

16. **Posting licensed content on any Website**: The following terms and conditions apply as follows: Licensing material from an Elsevier journal: All content posted to the web site must maintain the copyright information line on the bottom of each image; A hyper-text must be included to the Homepage of the journal from which you are licensing at http://www.sciencedirect.com/science/journal/xxxxx or the Elsevier homepage for books at http://www.elsevier.com; Central Storage: This license does not include permission for a scanned version of the material to be stored in a central repository such as that provided by Heron/XanEdu.

Licensing material from an Elsevier book: A hyper-text link must be included to the Elsevier homepage at http://www.elsevier.com . All content posted to the web site must maintain the copyright information line on the bottom of each image.

Posting licensed content on Electronic reserve: In addition to the above the following clauses are applicable: The web site must be password-protected and made available only to bona fide students registered on a relevant course. This permission is granted for 1 year only. You may obtain a new license for future website posting.

17. **For journal authors:** the following clauses are applicable in addition to the above:

Preprints:

A preprint is an author's own write-up of research results and analysis, it has not been peer-reviewed, nor has it had any other value added to it by a publisher (such as formatting, copyright, technical enhancement etc.).

Authors can share their preprints anywhere at any time. Preprints should not be added to or enhanced in any way in order to appear more like, or to substitute for, the final versions of articles however authors can update their preprints on arXiv or RePEc with their Accepted Author Manuscript (see below).

If accepted for publication, we encourage authors to link from the preprint to their formal publication via its DOI. Millions of researchers have access to the formal publications on ScienceDirect, and so links will help users to find, access, cite and use the best available version. Please note that Cell Press, The Lancet and some society-owned have different preprint policies. Information on these policies is available on the journal homepage.

Accepted Author Manuscripts: An accepted author manuscript is the manuscript of an article that has been accepted for publication and which typically includes author-incorporated changes suggested during submission, peer review and editor-author communications.

Authors can share their accepted author manuscript:

- immediately

  - via their non-commercial person homepage or blog
  - by updating a preprint in arXiv or RePEc with the accepted manuscript
  - via their research institute or institutional repository for internal institutional uses or as part of an invitation-only research collaboration work-group
  - directly by providing copies to their students or to research collaborators for their personal use
  - for private scholarly sharing as part of an invitation-only work group on commercial sites with which Elsevier has an agreement
- After the embargo period
  - via non-commercial hosting platforms such as their institutional repository
  - via commercial sites with which Elsevier has an agreement

In all cases accepted manuscripts should:

- link to the formal publication via its DOI
- bear a CC-BY-NC-ND license - this is easy to do
- if aggregated with other manuscripts, for example in a repository or other site, be shared in alignment with our hosting policy not be added to or enhanced in any way to appear more like, or to substitute for, the published journal article.

Published journal article (JPA): A published journal article (PJA) is the definitive final record of published research that appears or will appear in the journal and embodies all value-adding publishing activities including peer review co-ordination, copy-editing, formatting, (if relevant) pagination and online enrichment.
Policies for sharing publishing journal articles differ for subscription and gold open access articles:
Subscription Articles: If you are an author, please share a link to your article rather than the full-text. Millions of researchers have access to the formal publications on ScienceDirect, and so links will help your users to find, access, cite, and use the best available version.
Theses and dissertations which contain embedded PJAs as part of the formal submission can be posted publicly by the awarding institution with DOI links back to the formal publications on ScienceDirect.
If you are affiliated with a library that subscribes to ScienceDirect you have additional private sharing rights for others' research accessed under that agreement. This includes use for classroom teaching and internal training at the institution (including use in course packs and courseware programs), and inclusion of the article for grant funding purposes.
Gold Open Access Articles: May be shared according to the author-selected end-user license and should contain a CrossMark logo, the end user license, and a DOI link to the formal publication on ScienceDirect.
Please refer to Elsevier's posting policy for further information.
18. **For book authors** the following clauses are applicable in addition to the above: Authors are permitted to place a brief summary of their work online only. You are not allowed to download and post the published electronic version of your chapter, nor may you scan the printed edition to create an electronic version. **Posting to a repository:** Authors are permitted to post a summary of their chapter only in their institution's repository.
19. **Thesis/Dissertation**: If your license is for use in a thesis/dissertation your thesis may be submitted to your institution in either print or electronic form. Should your thesis be published commercially, please reapply for permission. These requirements include permission for the Library and Archives of Canada to supply single copies, on demand, of the complete thesis and include permission for Proquest/UMI to supply single copies, on demand, of the complete thesis. Should your thesis be published commercially, please reapply for permission. Theses and dissertations which contain embedded PJAs as part of the formal submission can be posted publicly by the awarding institution with DOI links back to the formal publications on ScienceDirect.

Elsevier Open Access Terms and Conditions
You can publish open access with Elsevier in hundreds of open access journals or in nearly 2000 established subscription journals that support open access publishing. Permitted third

party re-use of these open access articles is defined by the author's choice of Creative Commons user license. See our open access license policy for more information.

Terms & Conditions applicable to all Open Access articles published with Elsevier:

Any reuse of the article must not represent the author as endorsing the adaptation of the article nor should the article be modified in such a way as to damage the author's honour or reputation. If any changes have been made, such changes must be clearly indicated.

The author(s) must be appropriately credited and we ask that you include the end user license and a DOI link to the formal publication on ScienceDirect.

If any part of the material to be used (for example, figures) has appeared in our publication with credit or acknowledgement to another source it is the responsibility of the user to ensure their reuse complies with the terms and conditions determined by the rights holder.

Additional Terms & Conditions applicable to each Creative Commons user license:

CC BY: The CC-BY license allows users to copy, to create extracts, abstracts and new works from the Article, to alter and revise the Article and to make commercial use of the Article (including reuse and/or resale of the Article by commercial entities), provided the user gives appropriate credit (with a link to the formal publication through the relevant DOI), provides a link to the license, indicates if changes were made and the licensor is not represented as endorsing the use made of the work. The full details of the license are available at http://creativecommons.org/licenses/by/4.0.

CC BY NC SA: The CC BY-NC-SA license allows users to copy, to create extracts, abstracts and new works from the Article, to alter and revise the Article, provided this is not done for commercial purposes, and that the user gives appropriate credit (with a link to the formal publication through the relevant DOI), provides a link to the license, indicates if changes were made and the licensor is not represented as endorsing the use made of the work. Further, any new works must be made available on the same conditions. The full details of the license are available at http://creativecommons.org/licenses/by-nc-sa/4.0.

CC BY NC ND: The CC BY-NC-ND license allows users to copy and distribute the Article, provided this is not done for commercial purposes and further does not permit distribution of the Article if it is changed or edited in any way, and provided the user gives appropriate credit (with a link to the formal publication through the relevant DOI), provides a link to the license, and that the licensor is not represented as endorsing the use made of the work. The full details of the license are available at http://creativecommons.org/licenses/by-nc-nd/4.0.

Any commercial reuse of Open Access articles published with a CC BY NC SA or CC BY NC ND license requires permission from Elsevier and will be subject to a fee.

Commercial reuse includes:

- Associating advertising with the full text of the Article
- Charging fees for document delivery or access
- Article aggregation
- Systematic distribution via e-mail lists or share buttons

Posting or linking by commercial companies for use by customers of those companies.

20. **Other Conditions**:

v1.9

Questions? customercare@copyright.com or +1-855-239-3415 (toll free in the US) or +1-978-646-2777.

Copyright Clearance Center

Note: Copyright.com supplies permissions but not the copyrighted content itself.

1 PAYMENT 2 REVIEW 3 CONFIRMATION

Step 3: Order Confirmation

Thank you for your order! A confirmation for your order will be sent to your account email address. If you have questions about your order, you can call us 24 hrs/day, M-F at +1.855.239.3415 Toll Free, or write to us at info@copyright.com. This is not an invoice.

Confirmation Number: 11732494
Order Date: 07/22/2018

If you paid by credit card, your order will be finalized and your card will be charged within 24 hours. If you choose to be invoiced, you can change or cancel your order until the invoice is generated.

Payment Information

Ahdyeh Mosadegh
ahdyeh.mosadegh@postgrad.curtin.edu.au
+61 (4)52502080
Payment Method: n/a

Order Details

GEOSYNTHETICS INTERNATIONAL

Order detail ID:	71325431
Order License Id:	4394121033918
ISSN:	1072-6349
Publication Type:	Journal
Volume:	
Issue:	
Start page:	
Publisher:	THOMAS/TELFORD LTD.
Author/Editor:	Industrial Fabrics Association International

Permission Status: Granted
Permission type: Republish or display content
Type of use: Republish in a thesis/dissertation

Requestor type	Academic institution
Format	Print, Electronic
Portion	chart/graph/table/figure
Number of charts/graphs/tables/figures	1
The requesting person/organization	Curtin University
Title or numeric reference of the portion(s)	Experimental and Numerical Investigations to Assess the Performance of a Buried Pipe Subjected to Traffic Load / Non-Treated and Cement-Treated Trench
Title of the article or chapter the portion is from	N/A
Editor of portion(s)	N/A
Author of portion(s)	N/A

Volume of serial or monograph	N/A
Issue, if republishing an article from a serial	N/A
Page range of portion	300
Publication date of portion	August 2018
Rights for	Main product
Duration of use	Life of current and all future editions
Creation of copies for the disabled	no
With minor editing privileges	no
For distribution to	Worldwide
In the following language(s)	Original language of publication
With incidental promotional use	no
Lifetime unit quantity of new product	Up to 499
Title	Experimental and Numerical Investigations to Assess the Performance of a Buried Pipe Subjected to Traffic Load / Non-Treated and Cement-Treated Trench
Instructor name	n/a
Institution name	n/a
Expected presentation date	Aug 2018

Note: This item will be invoiced or charged separately through CCC's **RightsLink** service. More info **$ 0.00**

Total order items: 1

This is not an invoice.

Order Total: 0.00 USD

Confirmation Number: 11732494

Special Rightsholder Terms & Conditions

The following terms & conditions apply to the specific publication under which they are listed

GEOSYNTHETICS INTERNATIONAL
Permission type: Republish or display content
Type of use: Republish in a thesis/dissertation

TERMS AND CONDITIONS

The following terms are individual to this publisher:

None

Other Terms and Conditions:

STANDARD TERMS AND CONDITIONS

1. Description of Service; Defined Terms. This Republication License enables the User to obtain licenses for republication of one or more copyrighted works as described in detail on the relevant Order Confirmation (the "Work(s)"). Copyright Clearance Center, Inc. ("CCC") grants licenses through the Service on behalf of the rightsholder identified on the Order Confirmation (the "Rightsholder"). "Republication", as used herein, generally means the inclusion of a Work, in whole or in part, in a new work or works, also as described on the Order Confirmation. "User", as used herein, means the person or entity making such republication.

2. The terms set forth in the relevant Order Confirmation, and any terms set by the Rightsholder with respect to a particular Work, govern the terms of use of Works in connection with the Service. By using the Service, the person transacting for a republication license on behalf of the User represents and warrants that he/she/it (a) has been duly authorized by the User to accept, and hereby does accept, all such terms and conditions on behalf of User, and (b) shall inform User of all such terms and conditions. In the event such person is a "freelancer" or other third party independent of User and CCC, such party shall be deemed jointly a "User" for purposes of these terms and conditions. In any event, User shall be deemed to have accepted and agreed to all such terms and conditions if User republishes the Work in any fashion.

3. Scope of License; Limitations and Obligations.

3.1 All Works and all rights therein, including copyright rights, remain the sole and exclusive property of the Rightsholder. The license created by the exchange of an Order Confirmation (and/or any invoice) and payment by User of the full amount set forth on that document includes only those rights expressly set forth in the Order Confirmation and in these terms and conditions, and conveys no other rights in the Work(s) to User. All rights not expressly granted are hereby reserved.

3.2 General Payment Terms: You may pay by credit card or through an account with us payable at the end of the month. If you and we agree that you may establish a standing account with CCC, then the following terms apply: Remit Payment to: Copyright Clearance Center, 29118 Network Place, Chicago, IL 60673-1291. Payments Due: Invoices are payable upon their delivery to you (or upon our notice to you that they are available to you for downloading). After 30 days, outstanding amounts will be subject to a service charge of 1-1/2% per month or, if less, the maximum rate allowed by applicable law. Unless otherwise specifically set forth in the Order Confirmation or in a separate written agreement signed by CCC, invoices are due and payable on "net 30" terms. While User may exercise the rights licensed immediately upon issuance of the Order Confirmation, the license is automatically revoked and is null and void, as if it had never been issued, if complete payment for the license is not received on a timely basis either from User directly or through a payment agent, such as a credit card company.

3.3 Unless otherwise provided in the Order Confirmation, any grant of rights to User (i) is "one-time" (including the editions and product family specified in the license), (ii) is non-exclusive and non-transferable and (iii) is subject to any and all limitations and restrictions (such as, but not limited to, limitations on duration of use or circulation) included in the Order Confirmation or invoice and/or in these terms and conditions. Upon completion of the licensed use, User shall either secure a new permission for further use of the Work(s) or immediately cease any new use of the Work(s) and shall render inaccessible (such as by deleting or by removing or severing links or other locators) any further copies of the Work (except for copies printed on paper in accordance with this license and still in User's stock at the end of such period).

3.4 In the event that the material for which a republication license is sought includes third party materials (such as photographs, illustrations, graphs, inserts and similar materials) which are identified in such material as having been used by permission, User is responsible for identifying, and seeking separate licenses (under this Service or otherwise) for, any of such third party materials; without a separate license, such third party materials may not be used.

3.5 Use of proper copyright notice for a Work is required as a condition of any license granted under the Service. Unless otherwise provided in the Order Confirmation, a proper copyright notice will read substantially as follows: "Republished with permission of [Rightsholder's name], from [Work's title, author, volume, edition number and year of copyright]; permission conveyed through Copyright Clearance Center, Inc. " Such notice must be provided in a reasonably legible font size and must be placed either immediately adjacent to the Work as used (for example, as part of a by-line or footnote but not as a separate electronic link) or in the place where substantially all other credits or notices for the new work containing the republished Work are located. Failure to include the required notice results in loss to the Rightsholder and CCC, and the User shall be liable to pay liquidated damages for each such failure equal to twice the use fee specified in the Order Confirmation, in addition to the use fee itself and any other fees and charges specified.

3.6 User may only make alterations to the Work if and as expressly set forth in the Order Confirmation. No Work may be used in any way that is defamatory, violates the rights of third parties (including such third parties' rights of copyright, privacy, publicity, or other tangible or intangible property), or is otherwise illegal, sexually explicit or obscene. In

addition, User may not conjoin a Work with any other material that may result in damage to the reputation of the Rightsholder. User agrees to inform CCC if it becomes aware of any infringement of any rights in a Work and to cooperate with any reasonable request of CCC or the Rightsholder in connection therewith.

4. Indemnity. User hereby indemnifies and agrees to defend the Rightsholder and CCC, and their respective employees and directors, against all claims, liability, damages, costs and expenses, including legal fees and expenses, arising out of any use of a Work beyond the scope of the rights granted herein, or any use of a Work which has been altered in any unauthorized way by User, including claims of defamation or infringement of rights of copyright, publicity, privacy or other tangible or intangible property.

5. Limitation of Liability. UNDER NO CIRCUMSTANCES WILL CCC OR THE RIGHTSHOLDER BE LIABLE FOR ANY DIRECT, INDIRECT, CONSEQUENTIAL OR INCIDENTAL DAMAGES (INCLUDING WITHOUT LIMITATION DAMAGES FOR LOSS OF BUSINESS PROFITS OR INFORMATION, OR FOR BUSINESS INTERRUPTION) ARISING OUT OF THE USE OR INABILITY TO USE A WORK, EVEN IF ONE OF THEM HAS BEEN ADVISED OF THE POSSIBILITY OF SUCH DAMAGES. In any event, the total liability of the Rightsholder and CCC (including their respective employees and directors) shall not exceed the total amount actually paid by User for this license. User assumes full liability for the actions and omissions of its principals, employees, agents, affiliates, successors and assigns.

6. Limited Warranties. THE WORK(S) AND RIGHT(S) ARE PROVIDED "AS IS". CCC HAS THE RIGHT TO GRANT TO USER THE RIGHTS GRANTED IN THE ORDER CONFIRMATION DOCUMENT. CCC AND THE RIGHTSHOLDER DISCLAIM ALL OTHER WARRANTIES RELATING TO THE WORK(S) AND RIGHT(S), EITHER EXPRESS OR IMPLIED, INCLUDING WITHOUT LIMITATION IMPLIED WARRANTIES OF MERCHANTABILITY OR FITNESS FOR A PARTICULAR PURPOSE. ADDITIONAL RIGHTS MAY BE REQUIRED TO USE ILLUSTRATIONS, GRAPHS, PHOTOGRAPHS, ABSTRACTS, INSERTS OR OTHER PORTIONS OF THE WORK (AS OPPOSED TO THE ENTIRE WORK) IN A MANNER CONTEMPLATED BY USER; USER UNDERSTANDS AND AGREES THAT NEITHER CCC NOR THE RIGHTSHOLDER MAY HAVE SUCH ADDITIONAL RIGHTS TO GRANT.

7. Effect of Breach. Any failure by User to pay any amount when due, or any use by User of a Work beyond the scope of the license set forth in the Order Confirmation and/or these terms and conditions, shall be a material breach of the license created by the Order Confirmation and these terms and conditions. Any breach not cured within 30 days of written notice thereof shall result in immediate termination of such license without further notice. Any unauthorized (but licensable) use of a Work that is terminated immediately upon notice thereof may be liquidated by payment of the Rightsholder's ordinary license price therefor; any unauthorized (and unlicensable) use that is not terminated immediately for any reason (including, for example, because materials containing the Work cannot reasonably be recalled) will be subject to all remedies available at law or in equity, but in no event to a payment of less than three times the Rightsholder's ordinary license price for the most closely analogous licensable use plus Rightsholder's and/or CCC's costs and expenses incurred in collecting such payment.

8. **Miscellaneous.**

8.1 User acknowledges that CCC may, from time to time, make changes or additions to the Service or to these terms and conditions, and CCC reserves the right to send notice to the User by electronic mail or otherwise for the purposes of notifying User of such changes or additions; provided that any such changes or additions shall not apply to permissions already secured and paid for.

8.2 Use of User-related information collected through the Service is governed by CCC's privacy policy, available online here: http://www.copyright.com/content/cc3/en/tools/footer/privacypolicy.html.

8.3 The licensing transaction described in the Order Confirmation is personal to User. Therefore, User may not assign or transfer to any other person (whether a natural person or an organization of any kind) the license created by the Order Confirmation and these terms and conditions or any rights granted hereunder; provided, however, that User may assign such license in its entirety on written notice to CCC in the event of a transfer of all or substantially all of User's rights in the new material which includes the Work(s) licensed under this Service.

8.4 No amendment or waiver of any terms is binding unless set forth in writing and signed by the parties. The Rightsholder and CCC hereby object to any terms contained in any writing prepared by the User or its principals, employees, agents or affiliates and purporting to govern or otherwise relate to the licensing transaction described in the Order Confirmation, which terms are in any way inconsistent with any terms set forth in the Order Confirmation and/or in these terms and conditions or CCC's standard operating procedures, whether such writing is prepared prior to, simultaneously with or subsequent to the Order Confirmation, and whether such writing appears on a copy of the Order Confirmation or in a separate instrument.

8.5 The licensing transaction described in the Order Confirmation document shall be governed by and construed under the law of the State of New York, USA, without regard to the principles thereof of conflicts of law. Any case, controversy, suit, action, or proceeding arising out of, in connection with, or related to such licensing transaction shall be brought, at CCC's sole discretion, in any federal or state court located in the County of New York, State of New York, USA, or in any federal or state court whose geographical jurisdiction covers the location of the Rightsholder set forth in the Order Confirmation. The parties expressly submit to the personal jurisdiction and venue of each such federal or state court.If you have any comments or questions about the Service or Copyright Clearance Center, please contact us at 978-750-8400 or send an e-mail to info@copyright.com.

v 1.1

Close

Confirmation Number: 11732494

Citation Information

Order Detail ID: 71325431

GEOSYNTHETICS INTERNATIONAL by Industrial Fabrics Association International Reproduced with permission of THOMAS/TELFORD LTD. in the format Republish in a thesis/dissertation via Copyright Clearance Center.

Close

ELSEVIER LICENSE
TERMS AND CONDITIONS

Jul 22, 2018

This Agreement between Curtin University ("You") and Elsevier ("Elsevier") consists of your license details and the terms and conditions provided by Elsevier and Copyright Clearance Center.

License Number	4394320273105
License date	Jul 22, 2018
Licensed Content Publisher	Elsevier
Licensed Content Publication	Geotextiles and Geomembranes
Licensed Content Title	Combined use of geocell reinforcement and rubber–soil mixtures to improve performance of buried pipes
Licensed Content Author	Gh. Tavakoli Mehrjardi,S.N. Moghaddas Tafreshi,A.R. Dawson
Licensed Content Date	Oct 1, 2012
Licensed Content Volume	34
Licensed Content Issue	n/a
Licensed Content Pages	15
Start Page	116
End Page	130
Type of Use	reuse in a thesis/dissertation
Intended publisher of new work	other
Portion	figures/tables/illustrations
Number of figures/tables/illustrations	1
Format	both print and electronic
Are you the author of this Elsevier article?	No
Will you be translating?	No
Original figure numbers	Figure 2
Title of your thesis/dissertation	Experimental and Numerical Investigations to Assess the Performance of a Buried Pipe Subjected to Traffic Load / Non-Treated and Cement-Treated Trench
Expected completion date	Aug 2018
Estimated size (number of pages)	300
Requestor Location	Curtin University 24 Everingham Street Clarkson, Western Australia 6030 Australia Attn: Curtin University
Publisher Tax ID	GB 494 6272 12
Total	0.00 AUD
Terms and Conditions	

INTRODUCTION

1. The publisher for this copyrighted material is Elsevier. By clicking "accept" in connection with completing this licensing transaction, you agree that the following terms and conditions apply to this transaction (along with the Billing and Payment terms and conditions established by Copyright Clearance Center, Inc. ("CCC"), at the time that you opened your Rightslink account and that are available at any time at http://myaccount.copyright.com).

GENERAL TERMS

2. Elsevier hereby grants you permission to reproduce the aforementioned material subject to the terms and conditions indicated.

3. Acknowledgement: If any part of the material to be used (for example, figures) has appeared in our publication with credit or acknowledgement to another source, permission must also be sought from that source. If such permission is not obtained then that material may not be included in your publication/copies. Suitable acknowledgement to the source must be made, either as a footnote or in a reference list at the end of your publication, as follows:

"Reprinted from Publication title, Vol /edition number, Author(s), Title of article / title of chapter, Pages No., Copyright (Year), with permission from Elsevier [OR APPLICABLE SOCIETY COPYRIGHT OWNER]." Also Lancet special credit - "Reprinted from The Lancet, Vol. number, Author(s), Title of article, Pages No., Copyright (Year), with permission from Elsevier."

4. Reproduction of this material is confined to the purpose and/or media for which permission is hereby given.

5. Altering/Modifying Material: Not Permitted. However figures and illustrations may be altered/adapted minimally to serve your work. Any other abbreviations, additions, deletions and/or any other alterations shall be made only with prior written authorization of Elsevier Ltd. (Please contact Elsevier at permissions@elsevier.com). No modifications can be made to any Lancet figures/tables and they must be reproduced in full.

6. If the permission fee for the requested use of our material is waived in this instance, please be advised that your future requests for Elsevier materials may attract a fee.

7. Reservation of Rights: Publisher reserves all rights not specifically granted in the combination of (i) the license details provided by you and accepted in the course of this licensing transaction, (ii) these terms and conditions and (iii) CCC's Billing and Payment terms and conditions.

8. License Contingent Upon Payment: While you may exercise the rights licensed immediately upon issuance of the license at the end of the licensing process for the transaction, provided that you have disclosed complete and accurate details of your proposed use, no license is finally effective unless and until full payment is received from you (either by publisher or by CCC) as provided in CCC's Billing and Payment terms and conditions. If full payment is not received on a timely basis, then any license preliminarily granted shall be deemed automatically revoked and shall be void as if never granted. Further, in the event that you breach any of these terms and conditions or any of CCC's Billing and Payment terms and conditions, the license is automatically revoked and shall be void as if never granted. Use of materials as described in a revoked license, as well as any use of the materials beyond the scope of an unrevoked license, may constitute copyright infringement and publisher reserves the right to take any and all action to protect its copyright in the materials.

9. Warranties: Publisher makes no representations or warranties with respect to the licensed material.

10. Indemnity: You hereby indemnify and agree to hold harmless publisher and CCC, and their respective officers, directors, employees and agents, from and against any and all claims arising out of your use of the licensed material other than as specifically authorized pursuant to this license.

11. No Transfer of License: This license is personal to you and may not be sublicensed, assigned, or transferred by you to any other person without publisher's written permission.

12. No Amendment Except in Writing: This license may not be amended except in a writing signed by both parties (or, in the case of publisher, by CCC on publisher's behalf).

13. Objection to Contrary Terms: Publisher hereby objects to any terms contained in any purchase order, acknowledgment, check endorsement or other writing prepared by you, which terms are inconsistent with these terms and conditions or CCC's Billing and Payment

terms and conditions. These terms and conditions, together with CCC's Billing and Payment terms and conditions (which are incorporated herein), comprise the entire agreement between you and publisher (and CCC) concerning this licensing transaction. In the event of any conflict between your obligations established by these terms and conditions and those established by CCC's Billing and Payment terms and conditions, these terms and conditions shall control.

14. Revocation: Elsevier or Copyright Clearance Center may deny the permissions described in this License at their sole discretion, for any reason or no reason, with a full refund payable to you. Notice of such denial will be made using the contact information provided by you. Failure to receive such notice will not alter or invalidate the denial. In no event will Elsevier or Copyright Clearance Center be responsible or liable for any costs, expenses or damage incurred by you as a result of a denial of your permission request, other than a refund of the amount(s) paid by you to Elsevier and/or Copyright Clearance Center for denied permissions.

LIMITED LICENSE

The following terms and conditions apply only to specific license types:

15. **Translation**: This permission is granted for non-exclusive world **English** rights only unless your license was granted for translation rights. If you licensed translation rights you may only translate this content into the languages you requested. A professional translator must perform all translations and reproduce the content word for word preserving the integrity of the article.

16. **Posting licensed content on any Website**: The following terms and conditions apply as follows: Licensing material from an Elsevier journal: All content posted to the web site must maintain the copyright information line on the bottom of each image; A hyper-text must be included to the Homepage of the journal from which you are licensing at http://www.sciencedirect.com/science/journal/xxxxx or the Elsevier homepage for books at http://www.elsevier.com; Central Storage: This license does not include permission for a scanned version of the material to be stored in a central repository such as that provided by Heron/XanEdu.

Licensing material from an Elsevier book: A hyper-text link must be included to the Elsevier homepage at http://www.elsevier.com . All content posted to the web site must maintain the copyright information line on the bottom of each image.

Posting licensed content on Electronic reserve: In addition to the above the following clauses are applicable: The web site must be password-protected and made available only to bona fide students registered on a relevant course. This permission is granted for 1 year only. You may obtain a new license for future website posting.

17. **For journal authors:** the following clauses are applicable in addition to the above:

Preprints:

A preprint is an author's own write-up of research results and analysis, it has not been peer-reviewed, nor has it had any other value added to it by a publisher (such as formatting, copyright, technical enhancement etc.).

Authors can share their preprints anywhere at any time. Preprints should not be added to or enhanced in any way in order to appear more like, or to substitute for, the final versions of articles however authors can update their preprints on arXiv or RePEc with their Accepted Author Manuscript (see below).

If accepted for publication, we encourage authors to link from the preprint to their formal publication via its DOI. Millions of researchers have access to the formal publications on ScienceDirect, and so links will help users to find, access, cite and use the best available version. Please note that Cell Press, The Lancet and some society-owned have different preprint policies. Information on these policies is available on the journal homepage.

Accepted Author Manuscripts: An accepted author manuscript is the manuscript of an article that has been accepted for publication and which typically includes author-incorporated changes suggested during submission, peer review and editor-author communications.

Authors can share their accepted author manuscript:

- immediately

- via their non-commercial person homepage or blog
- by updating a preprint in arXiv or RePEc with the accepted manuscript
- via their research institute or institutional repository for internal institutional uses or as part of an invitation-only research collaboration work-group
- directly by providing copies to their students or to research collaborators for their personal use
- for private scholarly sharing as part of an invitation-only work group on commercial sites with which Elsevier has an agreement

- After the embargo period
  - via non-commercial hosting platforms such as their institutional repository
  - via commercial sites with which Elsevier has an agreement

In all cases accepted manuscripts should:

- link to the formal publication via its DOI
- bear a CC-BY-NC-ND license - this is easy to do
- if aggregated with other manuscripts, for example in a repository or other site, be shared in alignment with our hosting policy not be added to or enhanced in any way to appear more like, or to substitute for, the published journal article.

Published journal article (JPA): A published journal article (PJA) is the definitive final record of published research that appears or will appear in the journal and embodies all value-adding publishing activities including peer review co-ordination, copy-editing, formatting, (if relevant) pagination and online enrichment.
Policies for sharing publishing journal articles differ for subscription and gold open access articles:
Subscription Articles: If you are an author, please share a link to your article rather than the full-text. Millions of researchers have access to the formal publications on ScienceDirect, and so links will help your users to find, access, cite, and use the best available version.
Theses and dissertations which contain embedded PJAs as part of the formal submission can be posted publicly by the awarding institution with DOI links back to the formal publications on ScienceDirect.
If you are affiliated with a library that subscribes to ScienceDirect you have additional private sharing rights for others' research accessed under that agreement. This includes use for classroom teaching and internal training at the institution (including use in course packs and courseware programs), and inclusion of the article for grant funding purposes.
Gold Open Access Articles: May be shared according to the author-selected end-user license and should contain a CrossMark logo, the end user license, and a DOI link to the formal publication on ScienceDirect.
Please refer to Elsevier's posting policy for further information.
18. **For book authors** the following clauses are applicable in addition to the above: Authors are permitted to place a brief summary of their work online only. You are not allowed to download and post the published electronic version of your chapter, nor may you scan the printed edition to create an electronic version. **Posting to a repository:** Authors are permitted to post a summary of their chapter only in their institution's repository.
19. **Thesis/Dissertation**: If your license is for use in a thesis/dissertation your thesis may be submitted to your institution in either print or electronic form. Should your thesis be published commercially, please reapply for permission. These requirements include permission for the Library and Archives of Canada to supply single copies, on demand, of the complete thesis and include permission for Proquest/UMI to supply single copies, on demand, of the complete thesis. Should your thesis be published commercially, please reapply for permission. Theses and dissertations which contain embedded PJAs as part of the formal submission can be posted publicly by the awarding institution with DOI links back to the formal publications on ScienceDirect.

Elsevier Open Access Terms and Conditions
You can publish open access with Elsevier in hundreds of open access journals or in nearly 2000 established subscription journals that support open access publishing. Permitted third

party re-use of these open access articles is defined by the author's choice of Creative Commons user license. See our open access license policy for more information.

Terms & Conditions applicable to all Open Access articles published with Elsevier:

Any reuse of the article must not represent the author as endorsing the adaptation of the article nor should the article be modified in such a way as to damage the author's honour or reputation. If any changes have been made, such changes must be clearly indicated.

The author(s) must be appropriately credited and we ask that you include the end user license and a DOI link to the formal publication on ScienceDirect.

If any part of the material to be used (for example, figures) has appeared in our publication with credit or acknowledgement to another source it is the responsibility of the user to ensure their reuse complies with the terms and conditions determined by the rights holder.

Additional Terms & Conditions applicable to each Creative Commons user license:

CC BY: The CC-BY license allows users to copy, to create extracts, abstracts and new works from the Article, to alter and revise the Article and to make commercial use of the Article (including reuse and/or resale of the Article by commercial entities), provided the user gives appropriate credit (with a link to the formal publication through the relevant DOI), provides a link to the license, indicates if changes were made and the licensor is not represented as endorsing the use made of the work. The full details of the license are available at http://creativecommons.org/licenses/by/4.0.

CC BY NC SA: The CC BY-NC-SA license allows users to copy, to create extracts, abstracts and new works from the Article, to alter and revise the Article, provided this is not done for commercial purposes, and that the user gives appropriate credit (with a link to the formal publication through the relevant DOI), provides a link to the license, indicates if changes were made and the licensor is not represented as endorsing the use made of the work. Further, any new works must be made available on the same conditions. The full details of the license are available at http://creativecommons.org/licenses/by-nc-sa/4.0.

CC BY NC ND: The CC BY-NC-ND license allows users to copy and distribute the Article, provided this is not done for commercial purposes and further does not permit distribution of the Article if it is changed or edited in any way, and provided the user gives appropriate credit (with a link to the formal publication through the relevant DOI), provides a link to the license, and that the licensor is not represented as endorsing the use made of the work. The full details of the license are available at http://creativecommons.org/licenses/by-nc-nd/4.0.

Any commercial reuse of Open Access articles published with a CC BY NC SA or CC BY NC ND license requires permission from Elsevier and will be subject to a fee.

Commercial reuse includes:

- Associating advertising with the full text of the Article
- Charging fees for document delivery or access
- Article aggregation
- Systematic distribution via e-mail lists or share buttons

Posting or linking by commercial companies for use by customers of those companies.

20. **Other Conditions**:

v1.9

Questions? customercare@copyright.com or +1-855-239-3415 (toll free in the US) or +1-978-646-2777.

ELSEVIER LICENSE
TERMS AND CONDITIONS

Jul 29, 2018

This Agreement between Curtin University ("You") and Elsevier ("Elsevier") consists of your license details and the terms and conditions provided by Elsevier and Copyright Clearance Center.

License Number	4398360786207
License date	Jul 29, 2018
Licensed Content Publisher	Elsevier
Licensed Content Publication	Computers & Structures
Licensed Content Title	Bearing capacity of surface footings by finite elements
Licensed Content Author	N. Manoharan,S.P. Dasgupta
Licensed Content Date	Feb 17, 1995
Licensed Content Volume	54
Licensed Content Issue	4
Licensed Content Pages	24
Start Page	563
End Page	586
Type of Use	reuse in a thesis/dissertation
Portion	figures/tables/illustrations
Number of figures/tables/illustrations	1
Format	both print and electronic
Are you the author of this Elsevier article?	No
Will you be translating?	No
Original figure numbers	Figure 1
Title of your thesis/dissertation	Experimental and Numerical Investigations to Assess the Performance of a Buried Pipe Subjected to Traffic Load / Non-Treated and Cement-Treated Trench
Expected completion date	Aug 2018
Estimated size (number of pages)	300
Requestor Location	Curtin University 24 Everingham Street Clarkson, Western Australia 6030 Australia Attn: Curtin University
Publisher Tax ID	GB 494 6272 12
Total	0.00 AUD
Terms and Conditions	

INTRODUCTION

1. The publisher for this copyrighted material is Elsevier. By clicking "accept" in connection with completing this licensing transaction, you agree that the following terms and conditions apply to this transaction (along with the Billing and Payment terms and conditions

established by Copyright Clearance Center, Inc. ("CCC"), at the time that you opened your Rightslink account and that are available at any time at http://myaccount.copyright.com).

GENERAL TERMS

2. Elsevier hereby grants you permission to reproduce the aforementioned material subject to the terms and conditions indicated.

3. Acknowledgement: If any part of the material to be used (for example, figures) has appeared in our publication with credit or acknowledgement to another source, permission must also be sought from that source. If such permission is not obtained then that material may not be included in your publication/copies. Suitable acknowledgement to the source must be made, either as a footnote or in a reference list at the end of your publication, as follows:

"Reprinted from Publication title, Vol /edition number, Author(s), Title of article / title of chapter, Pages No., Copyright (Year), with permission from Elsevier [OR APPLICABLE SOCIETY COPYRIGHT OWNER]." Also Lancet special credit - "Reprinted from The Lancet, Vol. number, Author(s), Title of article, Pages No., Copyright (Year), with permission from Elsevier."

4. Reproduction of this material is confined to the purpose and/or media for which permission is hereby given.

5. Altering/Modifying Material: Not Permitted. However figures and illustrations may be altered/adapted minimally to serve your work. Any other abbreviations, additions, deletions and/or any other alterations shall be made only with prior written authorization of Elsevier Ltd. (Please contact Elsevier at permissions@elsevier.com). No modifications can be made to any Lancet figures/tables and they must be reproduced in full.

6. If the permission fee for the requested use of our material is waived in this instance, please be advised that your future requests for Elsevier materials may attract a fee.

7. Reservation of Rights: Publisher reserves all rights not specifically granted in the combination of (i) the license details provided by you and accepted in the course of this licensing transaction, (ii) these terms and conditions and (iii) CCC's Billing and Payment terms and conditions.

8. License Contingent Upon Payment: While you may exercise the rights licensed immediately upon issuance of the license at the end of the licensing process for the transaction, provided that you have disclosed complete and accurate details of your proposed use, no license is finally effective unless and until full payment is received from you (either by publisher or by CCC) as provided in CCC's Billing and Payment terms and conditions. If full payment is not received on a timely basis, then any license preliminarily granted shall be deemed automatically revoked and shall be void as if never granted. Further, in the event that you breach any of these terms and conditions or any of CCC's Billing and Payment terms and conditions, the license is automatically revoked and shall be void as if never granted. Use of materials as described in a revoked license, as well as any use of the materials beyond the scope of an unrevoked license, may constitute copyright infringement and publisher reserves the right to take any and all action to protect its copyright in the materials.

9. Warranties: Publisher makes no representations or warranties with respect to the licensed material.

10. Indemnity: You hereby indemnify and agree to hold harmless publisher and CCC, and their respective officers, directors, employees and agents, from and against any and all claims arising out of your use of the licensed material other than as specifically authorized pursuant to this license.

11. No Transfer of License: This license is personal to you and may not be sublicensed, assigned, or transferred by you to any other person without publisher's written permission.

12. No Amendment Except in Writing: This license may not be amended except in a writing signed by both parties (or, in the case of publisher, by CCC on publisher's behalf).

13. Objection to Contrary Terms: Publisher hereby objects to any terms contained in any purchase order, acknowledgment, check endorsement or other writing prepared by you, which terms are inconsistent with these terms and conditions or CCC's Billing and Payment terms and conditions. These terms and conditions, together with CCC's Billing and Payment terms and conditions (which are incorporated herein), comprise the entire agreement between you and publisher (and CCC) concerning this licensing transaction. In the event of

any conflict between your obligations established by these terms and conditions and those established by CCC's Billing and Payment terms and conditions, these terms and conditions shall control.

14. Revocation: Elsevier or Copyright Clearance Center may deny the permissions described in this License at their sole discretion, for any reason or no reason, with a full refund payable to you. Notice of such denial will be made using the contact information provided by you. Failure to receive such notice will not alter or invalidate the denial. In no event will Elsevier or Copyright Clearance Center be responsible or liable for any costs, expenses or damage incurred by you as a result of a denial of your permission request, other than a refund of the amount(s) paid by you to Elsevier and/or Copyright Clearance Center for denied permissions.

LIMITED LICENSE

The following terms and conditions apply only to specific license types:

15. **Translation**: This permission is granted for non-exclusive world **English** rights only unless your license was granted for translation rights. If you licensed translation rights you may only translate this content into the languages you requested. A professional translator must perform all translations and reproduce the content word for word preserving the integrity of the article.

16. **Posting licensed content on any Website**: The following terms and conditions apply as follows: Licensing material from an Elsevier journal: All content posted to the web site must maintain the copyright information line on the bottom of each image; A hyper-text must be included to the Homepage of the journal from which you are licensing at http://www.sciencedirect.com/science/journal/xxxxx or the Elsevier homepage for books at http://www.elsevier.com; Central Storage: This license does not include permission for a scanned version of the material to be stored in a central repository such as that provided by Heron/XanEdu.

Licensing material from an Elsevier book: A hyper-text link must be included to the Elsevier homepage at http://www.elsevier.com . All content posted to the web site must maintain the copyright information line on the bottom of each image.

Posting licensed content on Electronic reserve: In addition to the above the following clauses are applicable: The web site must be password-protected and made available only to bona fide students registered on a relevant course. This permission is granted for 1 year only. You may obtain a new license for future website posting.

17. **For journal authors:** the following clauses are applicable in addition to the above:

Preprints:

A preprint is an author's own write-up of research results and analysis, it has not been peer-reviewed, nor has it had any other value added to it by a publisher (such as formatting, copyright, technical enhancement etc.).

Authors can share their preprints anywhere at any time. Preprints should not be added to or enhanced in any way in order to appear more like, or to substitute for, the final versions of articles however authors can update their preprints on arXiv or RePEc with their Accepted Author Manuscript (see below).

If accepted for publication, we encourage authors to link from the preprint to their formal publication via its DOI. Millions of researchers have access to the formal publications on ScienceDirect, and so links will help users to find, access, cite and use the best available version. Please note that Cell Press, The Lancet and some society-owned have different preprint policies. Information on these policies is available on the journal homepage.

Accepted Author Manuscripts: An accepted author manuscript is the manuscript of an article that has been accepted for publication and which typically includes author-incorporated changes suggested during submission, peer review and editor-author communications.

Authors can share their accepted author manuscript:

- immediately
    - via their non-commercial person homepage or blog
    - by updating a preprint in arXiv or RePEc with the accepted manuscript

- via their research institute or institutional repository for internal institutional uses or as part of an invitation-only research collaboration work-group
- directly by providing copies to their students or to research collaborators for their personal use
- for private scholarly sharing as part of an invitation-only work group on commercial sites with which Elsevier has an agreement

- After the embargo period
  - via non-commercial hosting platforms such as their institutional repository
  - via commercial sites with which Elsevier has an agreement

In all cases accepted manuscripts should:

- link to the formal publication via its DOI
- bear a CC-BY-NC-ND license - this is easy to do
- if aggregated with other manuscripts, for example in a repository or other site, be shared in alignment with our hosting policy not be added to or enhanced in any way to appear more like, or to substitute for, the published journal article.

Published journal article (JPA): A published journal article (PJA) is the definitive final record of published research that appears or will appear in the journal and embodies all value-adding publishing activities including peer review co-ordination, copy-editing, formatting, (if relevant) pagination and online enrichment.
Policies for sharing publishing journal articles differ for subscription and gold open access articles:
Subscription Articles: If you are an author, please share a link to your article rather than the full-text. Millions of researchers have access to the formal publications on ScienceDirect, and so links will help your users to find, access, cite, and use the best available version.
Theses and dissertations which contain embedded PJAs as part of the formal submission can be posted publicly by the awarding institution with DOI links back to the formal publications on ScienceDirect.
If you are affiliated with a library that subscribes to ScienceDirect you have additional private sharing rights for others' research accessed under that agreement. This includes use for classroom teaching and internal training at the institution (including use in course packs and courseware programs), and inclusion of the article for grant funding purposes.
Gold Open Access Articles: May be shared according to the author-selected end-user license and should contain a CrossMark logo, the end user license, and a DOI link to the formal publication on ScienceDirect.
Please refer to Elsevier's posting policy for further information.
18. **For book authors** the following clauses are applicable in addition to the above:
Authors are permitted to place a brief summary of their work online only. You are not allowed to download and post the published electronic version of your chapter, nor may you scan the printed edition to create an electronic version. **Posting to a repository:** Authors are permitted to post a summary of their chapter only in their institution's repository.
19. **Thesis/Dissertation**: If your license is for use in a thesis/dissertation your thesis may be submitted to your institution in either print or electronic form. Should your thesis be published commercially, please reapply for permission. These requirements include permission for the Library and Archives of Canada to supply single copies, on demand, of the complete thesis and include permission for Proquest/UMI to supply single copies, on demand, of the complete thesis. Should your thesis be published commercially, please reapply for permission. Theses and dissertations which contain embedded PJAs as part of the formal submission can be posted publicly by the awarding institution with DOI links back to the formal publications on ScienceDirect.

Elsevier Open Access Terms and Conditions
You can publish open access with Elsevier in hundreds of open access journals or in nearly 2000 established subscription journals that support open access publishing. Permitted third party re-use of these open access articles is defined by the author's choice of Creative Commons user license. See our open access license policy for more information.

Terms & Conditions applicable to all Open Access articles published with Elsevier:
Any reuse of the article must not represent the author as endorsing the adaptation of the article nor should the article be modified in such a way as to damage the author's honour or reputation. If any changes have been made, such changes must be clearly indicated.
The author(s) must be appropriately credited and we ask that you include the end user license and a DOI link to the formal publication on ScienceDirect.
If any part of the material to be used (for example, figures) has appeared in our publication with credit or acknowledgement to another source it is the responsibility of the user to ensure their reuse complies with the terms and conditions determined by the rights holder.
Additional Terms & Conditions applicable to each Creative Commons user license:
CC BY: The CC-BY license allows users to copy, to create extracts, abstracts and new works from the Article, to alter and revise the Article and to make commercial use of the Article (including reuse and/or resale of the Article by commercial entities), provided the user gives appropriate credit (with a link to the formal publication through the relevant DOI), provides a link to the license, indicates if changes were made and the licensor is not represented as endorsing the use made of the work. The full details of the license are available at http://creativecommons.org/licenses/by/4.0.
CC BY NC SA: The CC BY-NC-SA license allows users to copy, to create extracts, abstracts and new works from the Article, to alter and revise the Article, provided this is not done for commercial purposes, and that the user gives appropriate credit (with a link to the formal publication through the relevant DOI), provides a link to the license, indicates if changes were made and the licensor is not represented as endorsing the use made of the work. Further, any new works must be made available on the same conditions. The full details of the license are available at http://creativecommons.org/licenses/by-nc-sa/4.0.
CC BY NC ND: The CC BY-NC-ND license allows users to copy and distribute the Article, provided this is not done for commercial purposes and further does not permit distribution of the Article if it is changed or edited in any way, and provided the user gives appropriate credit (with a link to the formal publication through the relevant DOI), provides a link to the license, and that the licensor is not represented as endorsing the use made of the work. The full details of the license are available at http://creativecommons.org/licenses/by-nc-nd/4.0.
Any commercial reuse of Open Access articles published with a CC BY NC SA or CC BY NC ND license requires permission from Elsevier and will be subject to a fee.
Commercial reuse includes:

- Associating advertising with the full text of the Article
- Charging fees for document delivery or access
- Article aggregation
- Systematic distribution via e-mail lists or share buttons

Posting or linking by commercial companies for use by customers of those companies.

20. **Other Conditions**:

v1.9

Questions? customercare@copyright.com or +1-855-239-3415 (toll free in the US) or +1-978-646-2777.

Physical Modelling in Geotechnics – Springman, Laue & Seward (eds)
© 2010 Taylor & Francis Group, London, ISBN 978-0-415-59288-8

Model tests on behaviour of buried pipes in a large soil chamber under cyclic loading

D.H. Ko & R. Kuwano
The University of Tokyo, Tokyo, Japan

ABSTRACT: In order to investigate behaviour of buried single flexible pipes under cyclic loading, a series of model tests were performed in a large soil chamber. The distribution of acting stress on the pipe was measured by eight two-way load cells installed in the PVC pipe, while the pipe deformation was investigated by strain gauges attached in the outer and inner surfaces of the pipe and vertical and horizontal potential transducers. The effect of the surrounding soil was investigated using tests with backfill soil of different densities. The behaviour of a liner in a double-layered pipe subjected to cyclic loading was investigated by using a four-segment model host pipe which can deform or keep its shape during the test to model the effects of host pipe deterioration and PVC pipe as the CIPP liner.

1 INTRODUCTION

An underground conduit laid under different environments exhibits various behaviours according to the ground and external load as well as the loading time and conditions. The design of buried pipes usually demands ensuring good compaction of backfill soil, as it is well known that their behaviour is largely governed by the properties of surrounding backfill. However, in practice, it does not seem to be always easy to ensure good compaction, due to the congested and limited surrounding space.

The structural response of flexible buried pipes has been long investigated since the pioneering work by Marston & Anderson (1913); Spanglar (1941) and others. Extensive and systematic studies have been recently carried out by Yoshimura et al. (1997) and Yoshimura & Tohda (1998), based on centrifuge testing. They were summarised as proposed design charts constructed by the elastic FEM analysis in which the relative stiffness of pipe to the surrounding soil was taken into account (Tohda & Yoshimura 1999). Most of the previous studies mainly focused on the response of flexible pipe under static loading. The behaviour of buried pipe subjected to cyclic loading and the effects of different densities in the backfill soil have not been fully understood. Recently authors have studied the behaviour of flexible pipes under cyclic loading using a small soil chamber (Ko et al. 2008). But it is considered that there may be boundary effects due to close distance between the wall of the chamber and the model pipe. In this research pipes under cyclic loading. In addition to single pipe tests, model tests of double-layered pipes (CIPP) used often as a rehabilitation method were performed to investigate the effects of host pipe deterioration. The aim of double-layered pipe tests is to know about magnitude of transfer of soil and traffic loads to flexible liner pipes.

2 APPARATUS AND TEST METHOD

2.1 *Model ground*

A model ground was constructed in a soil chamber 98 cm wide, 40 cm long and 45 cm high as schematically shown in Figure 1. The backfill material used was Toyoura sand, a uniform fine sand with a mean particle size of 0.16 mm and a specific gravity G_s of 2.65. The maximum void ratio e_{max} was 0.709 and the minimum void ratio e_{min} was 0.480. A model pipe

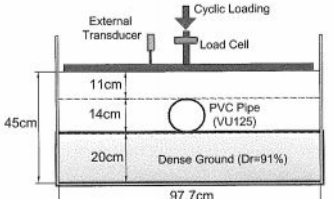

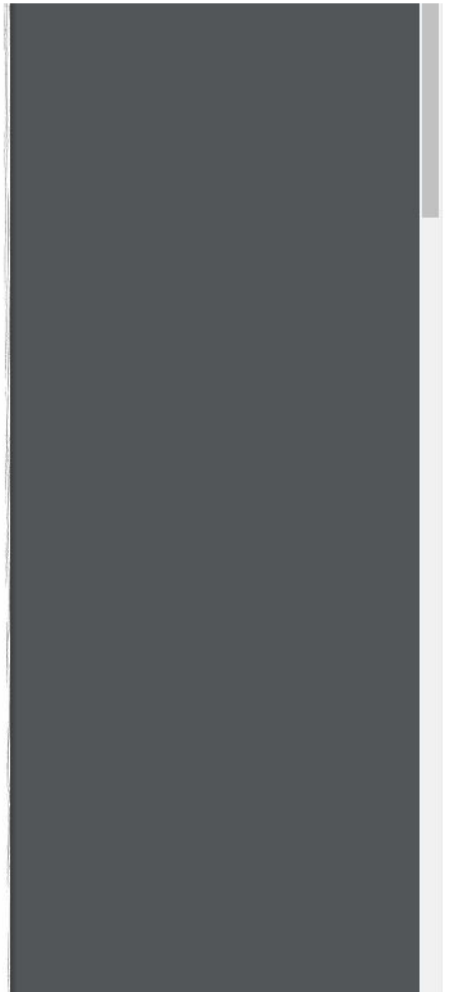

Permission given to use material in the thesis

DA

Day, Annette <Annette.Day@tandf.co.uk>
Yesterday, 23:19
Noosha Mosadegh

61CUR0007798 (1).pdf
2 MB

Download

Dear Noosha

9780415592888 | Physical Modelling in Geotechnics, 2V Set | Edn. 1 | Hardback | 2 x figures

I have received a positive response more quickly than I expected!

Further to your email, permission is granted for use of the above material in your forthcoming thesis, subject to the following conditions:

1. The material to be quoted/produced was published without credit to another source. If another source is acknowledged, please apply directly to that source for permission clearance.

2. Permission is for non-exclusive, English language rights, and covers **use in your thesis only**. Any further use (including storage, transmission or reproduction by electronic means) shall be the subject of a separate application for permission.

3. Full acknowledgement must be given to the original source, with full details of figure/page numbers, title, author(s), publisher and year of publication.

Kind regards

Annette
UK Books Permissions